NBSIR 73-339

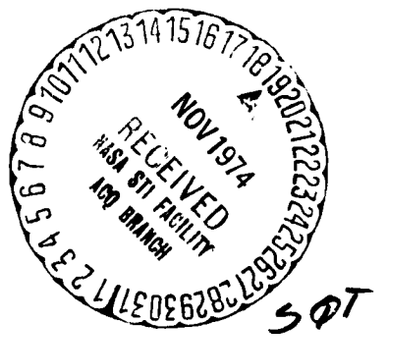

SQT

PRELIMINARY HYDROGEN FREEZING STUDIES

D. E. Daney
W. G. Steward
R. O. Voth

Cryogenics Division
Institute for Basic Standards
National Bureau of Standards
Boulder, Colorado 80302

October 1973
Final Report

Prepared for
NASA Headquarters
Washington, D. C.

NBSIR 73-339

PRELIMINARY HYDROGEN FREEZING STUDIES

D. E. Daney
W. G. Steward
R. O. Voth

Cryogenics Division
Institute for Basic Standards
National Bureau of Standards
Boulder, Colorado 80302

October 1973
Final Report

Prepared for
NASA Headquarters
Washington, D. C.

U.S. DEPARTMENT OF COMMERCE, Frederick B. Dent, Secretary

NATIONAL BUREAU OF STANDARDS Richard W. Roberts, Director

CONTENTS

LIST OF FIGURES

Preliminary Hydrogen Freezing Studies

D. E. Daney, W. G. Steward, and R. O. Voth

The study summarized in this report is aimed at developing the technology required to fill space vehicle propellant tanks with solid hydrogen by in-place freezing. Planned continuation of this work was terminated with the loss of NERVA funding by the NASA. Therefore, progress to-date is summarized but substantial experimental results have not yet been obtained.

The program was to have been carried out in two phases: a mathematical analysis and experimental verification of the analysis. Freezing times and heat flux have been calculated for four geometrical shapes, and a range of sizes, refrigerant temperatures, ortho-para concentrations, and heat transfer coefficients. The results of these calculations are presented in generalized graphical form, in a total of 240 graphs.

The freezing experimental apparatus has been built and a preliminary test performed which generally demonstrates the validity of the analytical and experimental approaches. With only minor modifications the apparatus is ready for a full test program of hydrogen freezing and melting techniques.

1.0 Introduction

This study is aimed at developing the technology required to fill space vehicle propellant tanks with solid hydrogen by in-place freezing. The specific goals of this phase of the study are, first, to calculate the freezing and melting rates of hydrogen for various geometries, refrigerant temperatures, and refrigerant heat transfer coefficients, secondly, to measure hydrogen freezing and melting rates for a simple geometry such as a cylinder, and finally and most important, to develop techniques which yield a uniform and high density solid.

At this time, only the freezing rate calculations and the experimental apparatus have been completed. One preliminary hydrogen freezing experiment has been performed which generally demonstrates the validity of both the analytical and experimental approaches. With only minor modifications, the apparatus is ready for a full test program to study hydrogen freezing and melting techniques.

Termination of funding has temporarily halted this program, so this report is a summary of our progress rather than a final report of the completed study.

2.0 Freezing Calculations

2.1 Introduction

The choice of a mathematical model for the freezing of solid hydrogen was governed by several considerations which indicated the desirability of a relatively simple model of modest accuracy. First, we are interested in a large number of combinations of geometry, heat transfer coefficient, refrigerant temperature, and ortho-para composition. Second, we are interested more in approximate answers which might indicate the feasibility of a scheme, rather than precise answers for a specific geometry and set of conditions. Third, even detailed approximate solutions of the freezing problem are extremely complex, and finally, the accuracy of the thermal conductivity data for solid hydrogen is so poor that high accuracy in the mathematical formulation is not justified at this time.

In general, the problem of calculating freezing rates is a difficult one. The boundary conditions are non-linear, and only a few exact solutions exist for one-dimensional problems with constant thermal properties [Carslaw and Jaeger, 1959]. Numerical methods, or approximate methods such as the integral technique, are generally required for the solution of the freezing problem, and even then, the calculations are usually complex. When we consider the calculation of

hydrogen freezing rates, the situation is complicated even further by the strong variation of the solid thermal conductivity with temperature and ortho-para composition. As indicated in figure 2.1, this variation exceeds two orders of magnitude over the range of 4K to 14K.

What effect does this temperature dependence of the thermal conductivity have on freezing rates? The freezing rate is proportional to $\int_{T_w}^{T_f} k\,dT$ where k is the thermal conductivity of the solid, T_f is the freezing-point temperature, and T_w is the temperature of the refrigerated wall. For substances with constant k the freezing rate is then proportional to the temperature difference $T_f - T_w$. For hydrogen, however, a relatively small change in the temperature difference $(T_f - T_w)$ can cause a large change in the value of the integral. For example, if T_w is lowered from 6.8K to 4.8K (T_f is 13.8K), ΔT increases by 28 percent while $\int_{T_w}^{T_f} k\,dT$ increases by over 300 percent for parahydrogen. Thus, relatively small reductions in the refrigerant temperature can result in substantially reduced freezing times.

2.2 Thermal Conductivity of Solid Hydrogen

Because the accuracy of the freezing calculations can be no better than the accuracy of the thermal conductivity data, a discussion of the thermal conductivity of solid hydrogen is in order. The two salient features of the thermal conductivity curves (figure 2.1) are the strong dependence of the thermal conductivity on the temperature and on the ortho-para composition.

The temperature dependence of the thermal conductivity is typical of dielectric solids (see, for example, Rosenberg, 1963). At the high temperature end of the curve, the thermal resistance (1/k) is dominated by Umklapp (U) processes (phonon-phonon scattering). For $T \leq \theta/10$ but T greater than where the conductivity is maximum, U processes require

$k \sim \exp(\theta/gT)$ where θ is the Debye temperature (θ = 116K for H_2 [Rosenberg, 1963]) and g is a numerical factor whose value is about 2. Thus at sufficiently low T the conductivity should undergo an exponential rise with decreasing temperature. At higher temperatures $T \geq \theta$, U processes require $k \sim 1/T$, and in the range in between θ and $\theta/10$, one would expect a gradual change from a 1/T behavior to an exp (θ/gT) behavior in k.

The complete disapearance of the thermal resistance as the temperature is decreased is prevented by other phonon scattering processes, such as grain boundary scattering ($1/k \sim T^{-3}$), which increase with decreasing temperature. The characteristic humped thermal conductivity curve is thus a result of the interplay of these different phonon scattering mechanisms.

The dependence of the thermal conductivity of solid hydrogen on the ortho-para composition, is believed to arise from a process not generally encountered with dielectric solids. We quote from Hill and Schneidmesser [1958] who first measured the thermal conductivity of solid hydrogen. "A process which may also contribute appreciably to thermal resistance arises when molecules can make transitions between states of different energy. In the simple case when the molecules can exist in two states separated by an energy E, transitions can be excited between these states by the absorption or emission of phonons of energy sufficiently close to E. Since this scattering process is effective in only a small part of the phonon spectrum, the contribution to the total thermal resistance will be small; comparatively little importance has therefore been attached to it. However, in a substance whose molecules can make transitions corresponding to a wide range of values of E, an important contribution to the thermal resistance is possible at suitable temperatures. Solid hydrogen is believed to be a substance of this type."

In figure 2. 1 the dashed lines represent extrapolations of the data beyond the range of measurements. The extrapolated curves are anchored to the thermal conductivity for solid deuterium measured by Daney [1971] rather than the measurements of Dwyer, Cook, and Berwaldt [1966] for solid parahydrogen. There are several reasons for this choice. The measurements of Dwyer, Cook, and Berwaldt were at elevated pressure (88-201 atm), and the relatively high compressibility of solid hydrogen [Lander, et al., 1966] might give rise to a strong pressure dependence in the thermal conductivity similar to that observed by Webb, Wilkinson, and Wilks [1952] in solid helium. In addition, the measurements appear to be of rather low accuracy, since measurements on liquid H_2 made in the same apparatus [Dwyer, et al., 1966] are about 200% higher than recent measurements reported by Roder and Diller [1970]. All of the curves should converge at high temperature since the ortho-para phonon scattering disappears at higher temperatures [Daney, 1971; Hill and Schneidmesser, 1958]. A curious set of high temperature curves results if the Hill and Schneidmesser curves are extrapolated to the Dwyer, Cook, and Berwaldt points.

Hill and Schneidmesser [1956] note that their conductivity curve for normal deuterium (33% para) was very similar to the corresponding curve of hydrogen (33% ortho). On the basis of this information, we chose the deuterium measurements of Daney [1971] as the anchor for the higher temperature curves. A smooth and natural appearing extension of the thermal conductivity curves results.

Contreras and Lee [1972] have recently reported values for the thermal conductivity of solid hydrogen based on a transient measurement scheme. At higher temperatures near the triple point their measurements fall considerably below the values selected here, but at lower temperatures their measurements and our selected values are in much better agreement. They attribute this discrepancy primarily to hairline cracks which were observed in their solid. Although cracks would cause an additional thermal resistance, this resistance should remain approximately constant over a range of temperatures. Because thermal resistances are additive, the thermal conductivity curve for cracked solid hydrogen should deviate from the uncracked curve most where the conductivity is the highest. A much flatter conductivity curve would result. This predicted behavior is opposite to the behavior of the Contreras and Lee data. Excessive radiation heat leak into their solid sample seems a more likely explanation for this discrepancy.

The uncertainty in the Hill and Schneidmesser data is estimated to be no greater than 10 percent, with less uncertainty for the higher conductivities. The uncertainty in the deuterium measurements is estimated to be less than 5 percent. The uncertainty in the extrapolation is no more than an educated guess, but we estimate it to be on the order of 20 percent. The agreement between the Hill and Schneidmesser data and the Bohn and Mate data is excellent along the right hand portion of the curves before the bend over to the conductivity maximum occurs. The maximums of the curves, however, differ by a factor of 3 for nearly the same composition. This discrepancy is probably due to different impurity levels or sample preparation techniques, and it should be considered as a variation that may be encountered in practice. It should be noted that for hydrogen with an ortho content less than 1 percent, this variation in the thermal conductivity will only become significant below 6K.

2.3 Analytical

Only one-dimensional or radially symmetric cases are treated because of the considerations discussed previously. Those cases chosen were: freezing a one-dimensional slab, freezing an infinitely long cylinder from the outside, freezing an infinitely long cylinder from the inside, and freezing a sphere from the outside. Expressions are presented for both freezing with constant wall temperature, and freezing with constant refrigerant temperature and heat transfer coefficient. Calculations were performed for only the latter case, since in practice it is almost impossible to freeze with constant wall temperature; however, as the heat transfer coefficient increases, the solution to the constant heat transfer coefficient problem approaches that of the constant wall temperature problem.

The physical model assumed for the constant heat transfer coefficient calculations is shown in figure 2.2. Heat is removed from the freezing hydrogen by a stream of cold helium gas with a constant temperature, T_o, and a constant heat transfer coefficient, h. The wall temperature, T_w, is allowed to float at whatever value is required by the process. The heat capacity of the solid is neglected and the liquid temperature is fixed at the melting point.

The error introduced into the calculations by neglecting the heat capacity is approximately equal to $C_p \frac{T_f - T_w}{2\ell}$ where C_p is the specific heat of the solid hydrogen. For hydrogen, this error should never exceed 10 percent, and the resulting simplification of the calculations is enormous. The overall accuracy of the calculations is estimated to be about 20 percent, when the accuracy of the thermal property data is considered also. For refrigerant temperatures below 5 K or ortho contents above one percent, the disagreement with experiment could be larger than 20 percent due to the variability from sample to sample in the thermal conductivity of solid hydrogen in this region.

To illustrate the method, we will derive the expression for one-dimensional linear freezing with constant heat transfer coefficient. The results for the other cases will then be summarized.

Case I. Linear one-dimensional freezing with constant heat transfer coefficient and constant refrigerant temperature.

Refer to figure 2.2 for the physical model. The heat transferred in the various zones is

$$Q = -kA\frac{dT}{dx} \tag{1}$$

in the solid,

$$Q = -\rho\ell A\frac{dX}{dt} \tag{2}$$

at the liquid-solid interface, and

$$Q = -hA\,(T_w - T_o) \tag{3}$$

at the helium side of the wall. The upper case X refers to the position of the liquid-solid interface, whereas the lower case x refers to any position in the solid.

Equating (1) and (2) we obtain

$$kdT = \rho\ell\frac{dX}{dt}\,dx. \tag{4}$$

If we now integrate (4) from the wall to the liquid-solid interface, we obtain

$$\int_{T_w}^{T_f} kdT = \int_{o}^{X} \rho\ell\frac{dX}{dt}\,dx, \quad \text{or}$$

$$dt = \frac{\rho\ell\, X\, dX}{\int_{T_w}^{T_f} kdT}\,. \tag{5}$$

Since T_w varies with time or position of the interface, $\int_{T_w}^{T_f} k\,dT$ also varies and equation (5) cannot be integrated.

In order to evaluate $\int_{T_w}^{T_f} k\,dT$, we must find T_w. Equating (1) and (3) we obtain

$$h(T_w - T_o) = k \frac{dT}{dx}. \tag{6}$$

Integrating (6) from the wall to the liquid-solid interface yields

$$\int_0^X h\,(T_w - T_o)\,dx = \int_{T_w}^{T_f} k\,dT,$$

or solving for T_w,

$$T_w = T_o + \frac{1}{hX} \int_{T_w}^{T_f} k\,dT. \tag{7}$$

In equation (7) T_w is obtained as a function of the liquid-solid interface position, X, and not as an explicit function of time.

Equations (2), (3), (5), and (7) can now be used to numerically obtain the time history of the liquid-solid interface, and the time history of the heat transfer rate Q. The procedure is as follows:

1. Divide the length to be frozen into a number of even intervals (100 in this work).

2. Obtain the initial heat transfer rate from (3) by assuming the wall to be at the freezing temperature, i.e.,

$$(Q/A)_1 = h\,(T_f - T_o)$$

(values of h are assumed).

3. Calculate the initial value of $(\Delta t/\Delta X)$ from equation (2)

$$(\Delta t/\Delta X)_1 = \frac{\rho \ell}{(Q/A)_1}.$$

4. Obtain the wall temperature, T_w, at the remaining positions by iteration from equation (7).

5. Calculate $(\Delta t/\Delta X)$ for the remaining positions using equation (5) and T_w obtained in step 4.

6. Calculate the heat transfer rate at each position using equation (3).

7. Obtain the total elapsed time at any position by integrating the values of $\Delta t/\Delta X$ calculated from steps 2 and 5.

Case II. <u>Freezing an infinite cylinder from the outside with constant heat transfer coefficient and constant refrigerant temperature.</u>

A derivation in cylindrical coordinates analogous to that of case I yields:

$$\frac{dt}{d\left(\frac{R}{R_o}\right)} = \frac{\rho\ell\, R_o^2}{\int_{T_w}^{T_f} k\,dT} \left[\frac{R}{R_o} \ln \frac{R}{R_o}\right]$$

$$T_w = T_o - \frac{1}{h R_o \ln \frac{R}{R_o}} \int_{T_w}^{T_f} k\,dT \qquad (7a)$$

$$\frac{Q}{L} = -h P_o (T_w - T_o) \qquad (3a)$$

$$Q/L = -2\pi \rho\ell\, R \frac{dR}{dt} \qquad (2a)$$

Case III. <u>Freezing an infinite cylinder from the inside with constant heat transfer coefficient and constant refrigerant temperature.</u>

$$\frac{dt}{d\left(\frac{R}{R_o}\right)} = \frac{\rho\ell\, R_o^2}{\int_{T_w}^{T_f} k\,dT} \left[\frac{R}{R_o} \ln \frac{R}{R_o}\right] \qquad (5b)$$

$$T_w = T_o + \frac{1}{h R_o \ln \frac{R}{R_o}} \int_{T_w}^{T_f} k\,dT \qquad (7b)$$

$$Q/L = -2\pi R_o h (T_w - T_o) \qquad (3b)$$

$$Q/L = -2\pi \rho \ell R \frac{dR}{dt} \qquad (2b)$$

Case IV. <u>Freezing a sphere from the outside with constant heat transfer coefficient and constant refrigerant temperature.</u>

An analogous derivation in spherical coordinates yields:

$$\frac{dt}{d\left(\frac{R}{R_o}\right)} = \frac{-\rho \ell R_o^2}{\int_{T_w}^{T_f} k\,dT} \left[\left(\frac{R}{R_o}\right)\left(1 - \left(\frac{R}{R_o}\right)\right)\right] \qquad (5c)$$

$$T_w = T_o + \frac{1}{h R_o\left[\frac{R_o}{R} - 1\right]} \int_{T_w}^{T_f} k\,dT \qquad (7c)$$

$$\frac{Q}{R_o} = 4\pi R_o h (T_w - T_o) \qquad (3c)$$

$$Q = -4\pi \rho \ell R^2 \frac{dR}{dt} \qquad (2c)$$

The following three cases are for constant wall temperature, T_w. When T_w is held constant, equation (5) (or the corresponding equation for cylindrical or spherical coordinates) can be integrated analytically, because $\int_{T_w}^{T_f} k\,dT$ is also constant. The resulting expression for the time, t, required to freeze a thickness of solid, X, is as follows:

Case V. Linear one-dimensional freezing with constant wall temperature.

$$t = \frac{\rho \ell X^2}{2 \int_{T_w}^{T_f} k dT} \tag{5d}$$

Case VI. Freezing on infinitely long cylinder with constant wall temperature from the inside or outside.

$$t = \frac{\rho \ell R_o^2}{\int_{T_w}^{T_f} k dT} \left\{ \frac{1}{2} \left(\frac{R}{R_o}\right) \ln \frac{R}{R_o} + \frac{1}{4} \left[1 - \left(\frac{R}{R_o}\right)^2 \right] \right\} \tag{5e}$$

Case VII. Freezing in sphere from the outside with constant wall temperature.

$$t = \frac{\rho \ell R_o^2}{\int_{T_w}^{T_f} k dT} \left[\frac{1}{3} \left(\frac{R}{R_o}\right)^3 - \frac{1}{2} \left(\frac{R}{R_o}\right)^2 + \frac{1}{6} \right] \tag{5f}$$

The results of a typical set of calculations are shown in figures 2.3, 2.4, and 2.5. Because of the choice of parameters, the results are independent of size and may thus be applied to any size cylinder, sphere, or flat plate. Figures 2.3 and 2.4 are self explanatory; they merely give the dimensionless position of the liquid solid interface and the heat transfer rate as a function of the time parameter for various heat transfer coefficient parameters.

Figure 2.5 requires some explanation. When consideration is given to sizing a refrigerator for a particular solid hydrogen freezing application, one observes that the refrigeration requirements are initially very high. Rather than sizing a refrigerator to these high

initial requirements, a more reasonable approach would be to size the refrigerator as small as is consistent with freezing the hydrogen in the required time. The curves in figure 2.5 show the time required for complete freezing of a cylinder if the maximum refrigeration available is limited to QM. The nearly vertical portions of the curves are a region where large reductions in refrigeration capacity may be achieved with insignificant increases in the freezing time. A refrigeration capacity lying in this region would be oversize. The common asymptote is a refrigeration limited region, i.e., the freezing time depends only on the refrigeration rate and not on the heat transfer coefficient.

The complete set of calculated freezing curves for the various combinations of geometry, ortho-para composition, and refrigerant temperature are given in the appendices. It should be noted, that if the wall of the vessel has a significant thermal resistance, then the overall heat transfer coefficient, U, should be used in place of the film or surface heat transfer coefficient h.

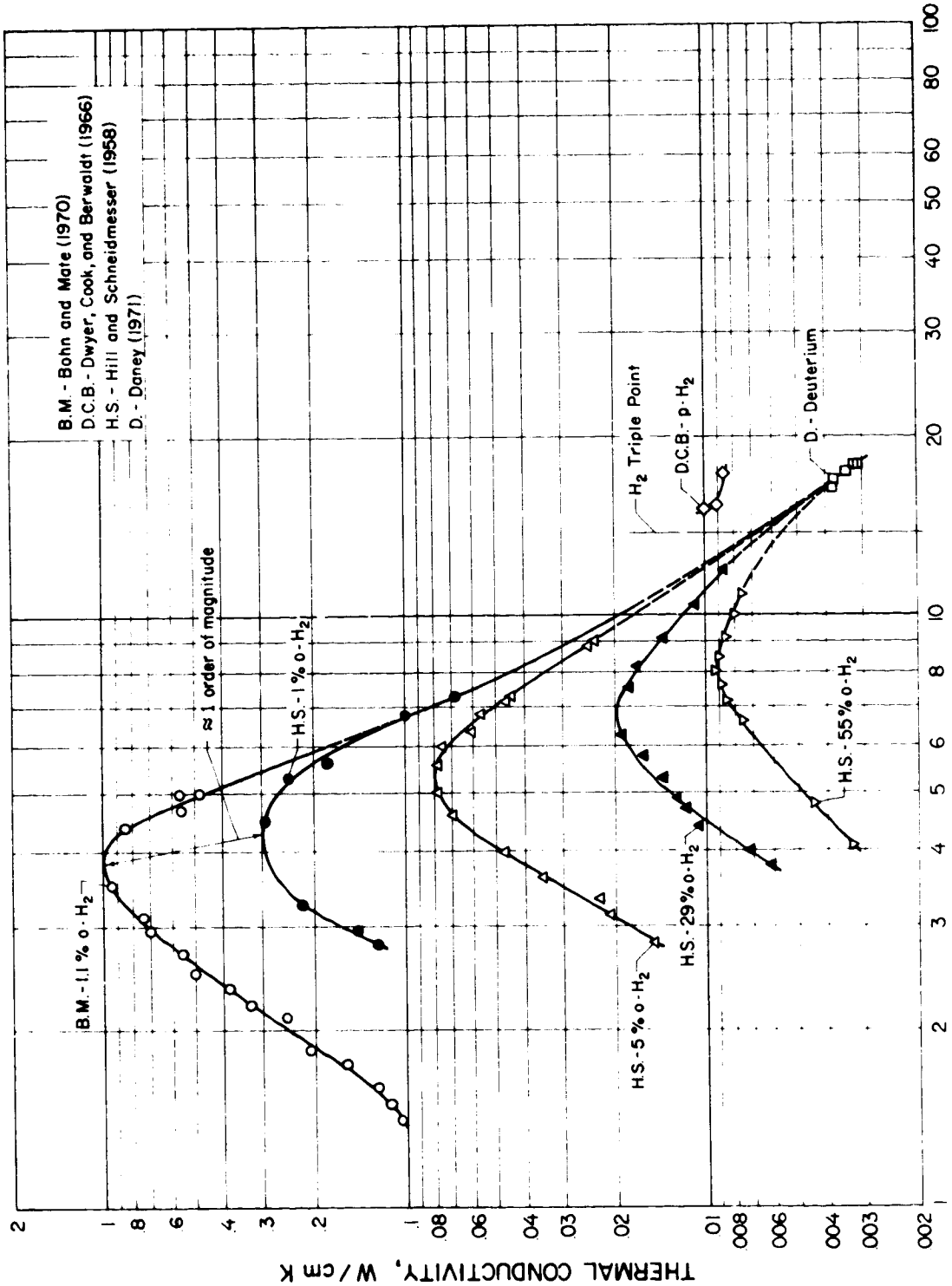

Figure 2.1. Thermal Conductivity of Solid Hydrogen.

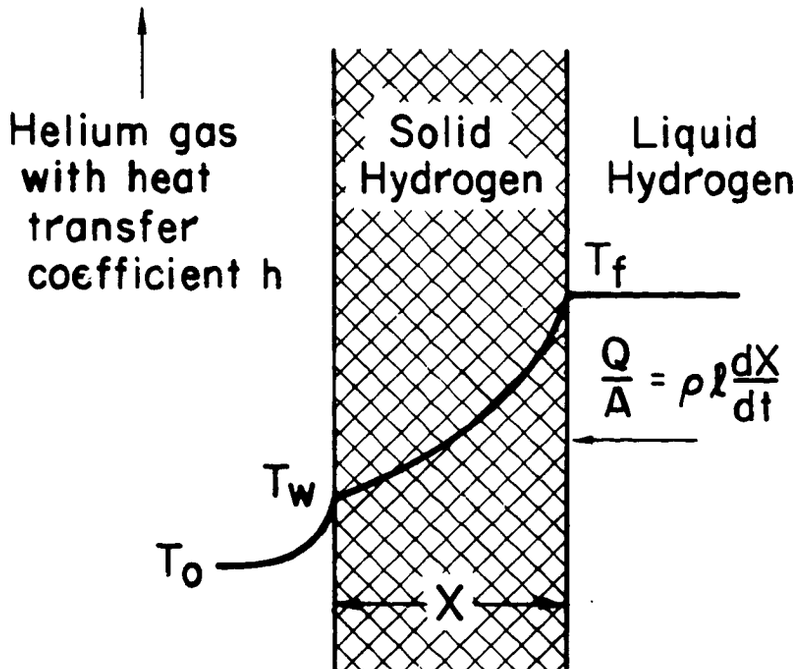

Figure 2.2 Schematic Temperature Distribution during One-Dimensional Freezing.

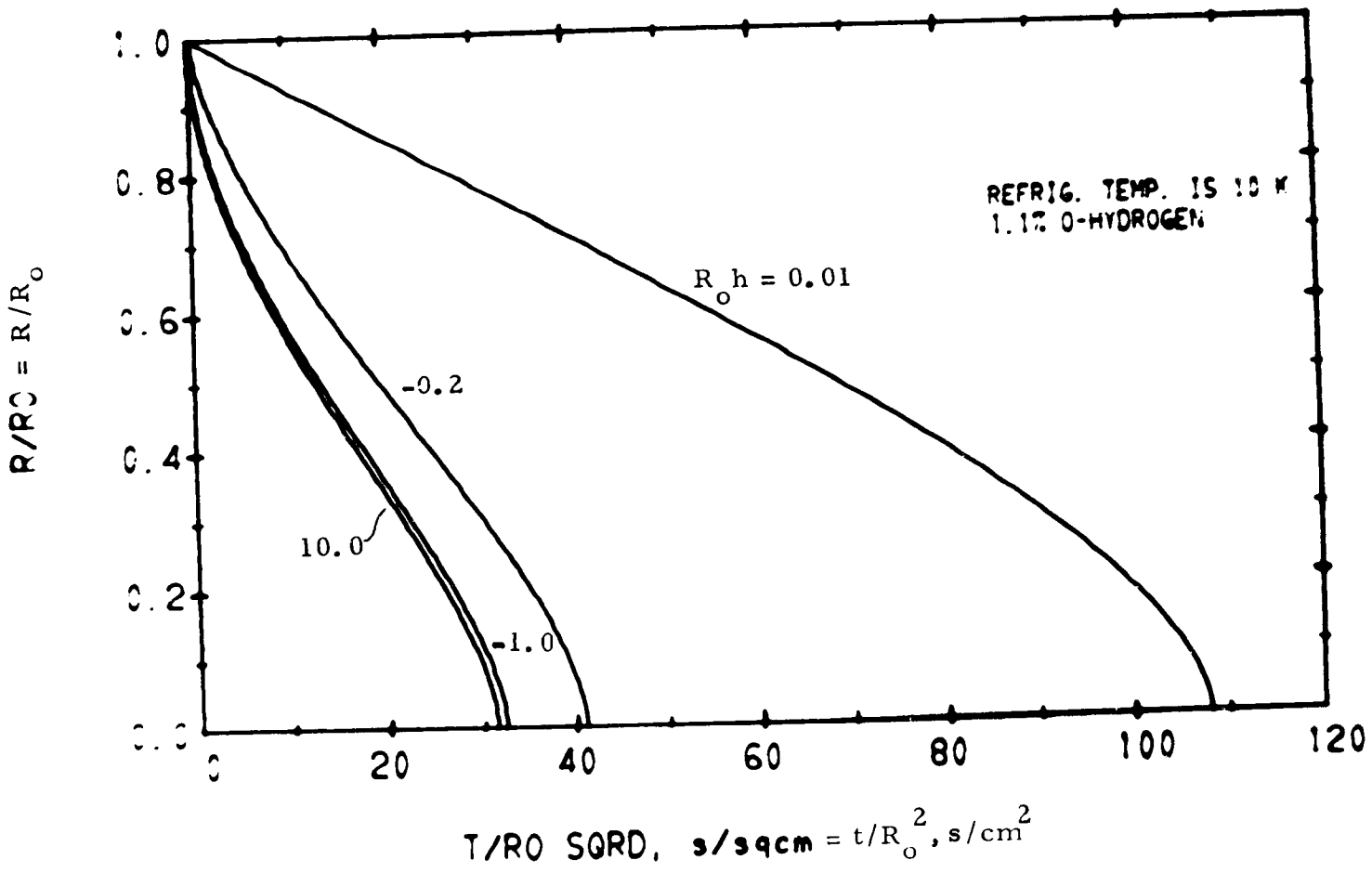
1.0
0.8
0.6
0.4
0.2
0.0
0
20
40
60
80
100
120
R/RO = R/R$_o$
REFRIG. TEMP. IS 1.0 K
1.1% O-HYDROGEN
R$_o$h = 0.01
-0.2
10.0
-1.0
T/RO SQRD, s/sqcm = t/R$_o^2$, s/cm^2
CYLINDER, FREEZING FROM OUTSIDE

Figure 2.3

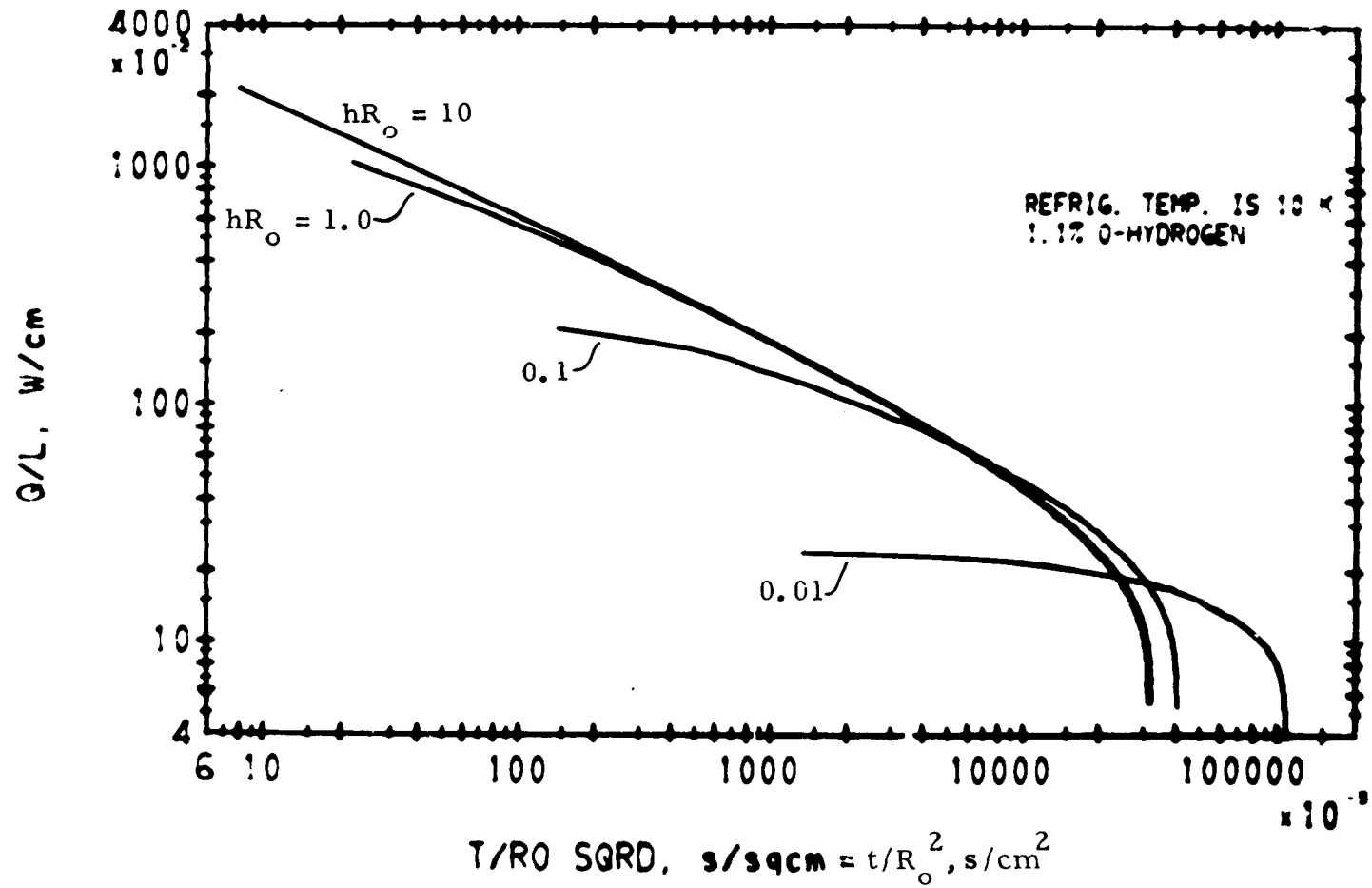
4000
x10⁻²
1000
100
10
4
Q/L, W/cm
hR_o = 10
hR_o = 1.0
0.1
0.01
REFRIG. TEMP. IS 1
1.1% O-HYDROGEN
6 10
100
1000
10000
100000
x10⁻⁸
T/RO SQRD, s/sqcm = t/R_o², s/cm²
CYLINDER, FREEZING FROM OUTSIDE

Figure 2.4

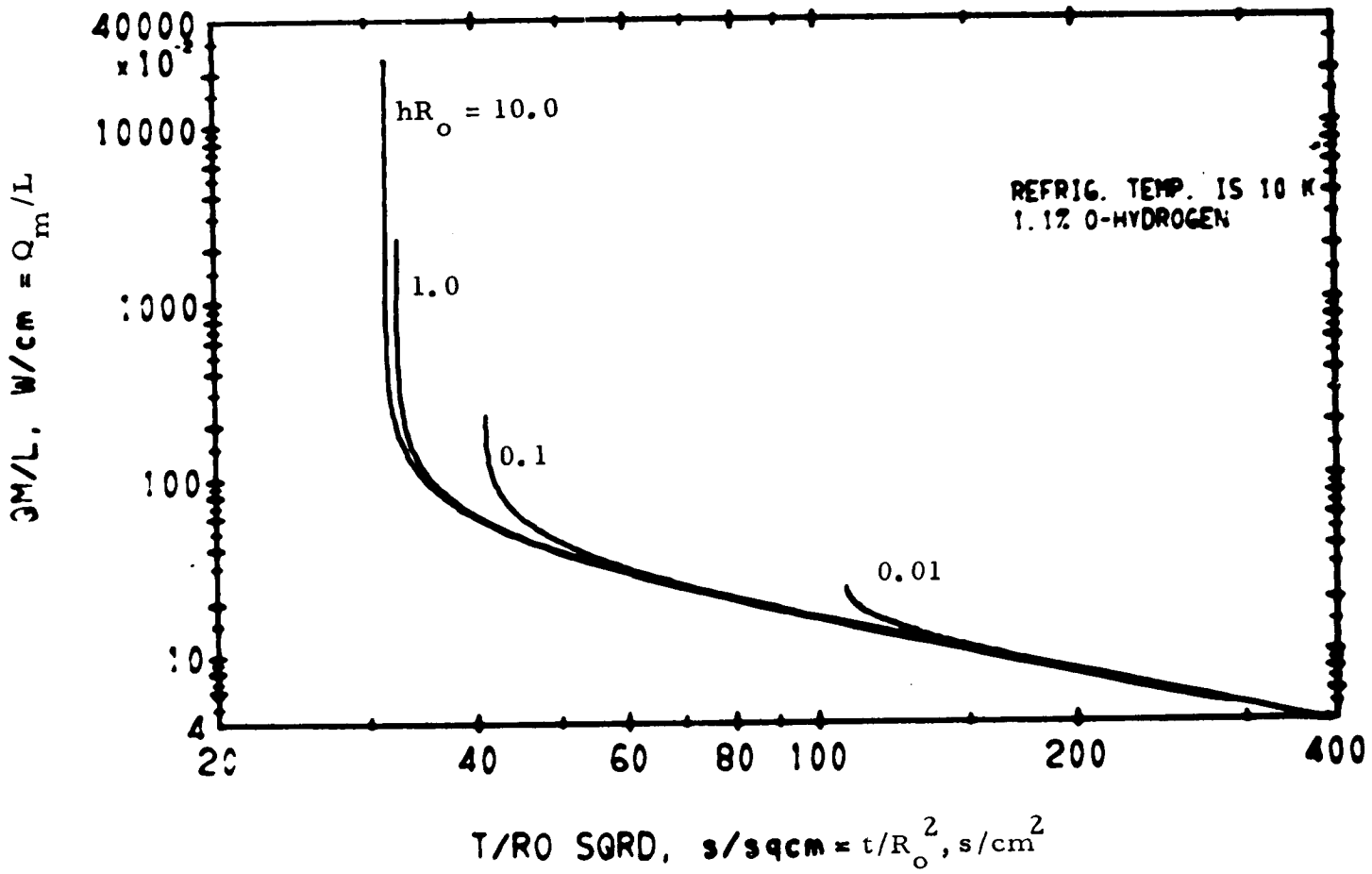
40000
x10⁻²
10000
1000
100
10
4
20
40
60
80
100
200
400
hR_o = 10.0
1.0
0.1
0.01
REFRIG. TEMP. IS 10 K
1.1% O-HYDROGEN
QM/L, W/cm = Q_m/L
T/RO SQRD, s/sqcm = t/R_o², s/cm²
CYLINDER, FREEZING FROM OUTSIDE

Figure 2.5

3.0 Experimental Program

3.1 Introduction

The experimental apparatus for freezing of hydrogen has been completed and tested. The assembly drawing (figure 3.1) and description of the apparatus are presented here. All the basic features are shown in figure 3.1 with the exception of the liquid nitrogen shield dewar and external instrumentation. The instrumentation and piping are shown schematically in figure 3.2. In section 3.1.1 the numbers in parentheses refer to the legend of figure 3.1.

3.1.1 Hydrogen System

1. A hydrogen freezing chamber (27) has walls made of 0.127 mm (0.005 inch) plastic (polyethylene terephthalate film) to minimize thermal resistance while allowing a clear view of the freezing hydrogen.

2. A standpipe (18) is located above (and connected to) the freezing chamber, to serve as a liquid hydrogen reservoir during freezing. The fall in liquid level, as indicated by the capacitance level gage, provides an indication of the reduction in volume of the hydrogen in the freezing chamber. From this liquid level reading, the mass of hydrogen solidified and the rate of freezing at a given time can be determined. The freezing rate provides one indication of the heat flux. A heater (21) on the standpipe prevents solid hydrogen blockage of the passageway leading into the freezing chamber.

3. A hydrogen chamber (3) at the upper end of the apparatus acts as a radiation shield and source of precooling refrigerant.

3.1.2 Helium Refrigerant System

1. The liquid helium bath (7) provides the refrigeration for freezing the hydrogen.

2. The variable speed blower (4) circulates helium heat exchange gas by variable paths as indicated by the arrows in figure 3.1.

3. A rotary valve (16) at the blower discharge allows a choice or combination of two possible paths for the helium gas, thus controlling the helium gas temperature and the freezing rate. For maximum refrigeration, all of the flow may be diverted through the ribbon packed heat exchanger (13) communicating with the liquid helium bath. For minimum refrigeration, the flow may be routed through the inner passage which is insulated from the liquid helium bath. This passage is also provided with a heater (9) to enable thawing the hydrogen. Intermediate degrees of refrigeration may be obtained by splitting the helium gas stream in any proportions desired.

3.1.3 Hydrogen-to-Helium Gas Heat Exchange System

Cold helium gas is routed around the outside of the pyrex baffle (24), then upward next to the freezing chamber. Refrigeration is restricted, as far as possible, to the vertical walls of the freezing chamber by means of the foam insulating blocks (23) and vacuum jackets surrounding the liquid and gaseous hydrogen containers.

3.2 Preliminary Experiment

3.2.1 Procedure

A preliminary experiment was performed to test the apparatus, instrumentation, and operating procedure. The procedure was as follows:

1. The freezing cylinder was purged, first with helium, then with hydrogen gas. The helium system was purged with helium gas.

2. Hydrogen gas for condensation into the freezing chamber was supplied by evaporation from liquid to ensure the composition being nearly equilibrium para-hydrogen. The freezing chamber was pressurized to 9 psig.

3. The pre-cooling chamber above the blower housing was temporarily filled with liquid nitrogen. (Liquid hydrogen would normally be used for pre-cooling). The liquid nitrogen shield dewar surrounding the liquid helium dewar was filled, and the system was allowed to pre-cool to 76K with the blower operating at low speed. The pre-cooling chamber was then purged and pressurized with helium gas.

4. The vacuum space in the hydrogen standpipe was pressurized with helium gas to provide heat transfer from the hydrogen gas entering the freezing chamber.

5. The liquid helium dewar was filled to the top of the heat exchanger, the blower speed was increased, and the freezing chamber and standpipe were condensed full of liquid hydrogen. (Unintentionally, some freezing occurred simultaneously with condensation).

6. The standpipe vacuum space was evacuated to prevent further heat transfer in the area of the capacitance liquid level sensor.

7. The temperature of the helium gas refrigerant was lowered and the remainder of the hydrogen was frozen.

8. Thawing was initiated at the top of the cylinder by means of the standpipe heater. After a liquid pool had formed, the helium gas temperature was raised above the thawing point. A problem connected with this thawing procedure is discussed in Section 3.3.2.

3.3 Results

The primary purpose of this experiment was to test the apparatus, instrumentation and operating procedure, and to assess the need for changes. Additional recording equipment and refinements of the procedure will be required in order to obtain accurate and complete data; however, the following preliminary data were obtained:

(1) Helium gas flow rates ranging from 0 to 1960 cm^3/s were measured.

(2) Helium gas temperatures down to 6.2K were obtained. This was achieved with a pump speed of only 5,500 RPM (rated speed is 10,700 RPM). Thus, even lower temperatures can easily be attained by increasing the pump speed. Control of the temperature through any desired range for condensing, freezing, or thawing was possible through variation of the liquid helium level, pump speed (gas flow rate), helium gas flow splitter valve position, heater current, or combination of these factors.

During this test we experimented with variation of all the control factors in order to gain experience with the operating characterisitics and capabilities of the apparatus. As a result, the conditions were unsteady and heat transfer calculations are only estimates based on averages. Further, we found that helium gas temperature was quite sensitive to the liquid helium bath level; therefore, in future tests it will be necessary to maintain a constant bath level through continuous

replenishing rather than periodic replenishing of the bath. Because of temperature fluctuation, some undesirable freezing and thawing took place during condensation. The formation of solid hydrogen during condensation interferes with the intended use of the standpipe liquid level sensor as an indicator of the fraction of volume solidified. The freezing must begin only after the entire freezing chamber and standpipe volume have been filled with liquid in order to approach a radial progression of the solid-liquid boundary. This pattern would allow comparison with freezing calculations for cylinders. Therefore, maintenance of a constant coolant temperature during condensation just above the hydrogen freezing point (13.8K) will be an objective in future tests.

(3) An average heat transfer rate during condensation was calculated from the rate of condensation and this was compared with a prediction based on a correlation for the outside convection coefficient. (Verification of heat transfer correlations will be essential to the design of large scale equipment for solidification of hydrogen.)

(a) 14.7 grams of hydrogen were condensed in 1620 seconds from initially room temperature gas. Approximately 60% was solidified simultaneously. The resulting average heat transfer rate was approximately,

$$Q = 37.4 \text{ W.}$$

(b) A heat transfer coefficient was calculated from forced convection correlation for double pipe heat exchangers with heat transferred through the inner wall only (Grober, Erk, Grigull, (1961), p. 263).

$$Nu = 0.021\,(Re)^{0.8}\,(Pr)^{\frac{1}{3}}\left(\frac{D_o}{D_i}\right)^{0.45}\left(\frac{\mu_b}{\mu_w}\right)^{0.14} \qquad (3.1)$$

For an average helium flow rate of $\bar{V} = 704\ cm^3/s$, hydraulic diameter $D_e = D_o - D_i = 0.2$ cm, flow area $A_f = 2.67\ cm^2$, and helium bulk temperature $T_{bHe} = 10.8K$, the heat transfer coefficient resulting from equation (3.1) is

$$h = 0.024\ \frac{W}{cm^2 K}\ .$$

Temperature T_w was measured on the inner wall of the plastic (polyethylene terephthalate film) cylinder. Allowing for temperature drop through the wall, we obtain,

$$Q = A_s\ \frac{h\,(T_w - T_{bHe})}{1 + h\,\frac{\delta}{k_w}}\ .$$

Heat transfer surface area A_s was assumed to be the area of the unfilled portion of the cylinder.

Average T_w during condensation = 20K.

A_{so} (cylinder empty) = $398\ cm^2$.

δ thickness of cylinder wall = 0.005 in = 0.0127 cm.

k_w thermal conductivity of the wall material $\tilde{=} 0.001\ \frac{W}{cm \cdot K}$.

Then

$Q_o = 67.1$ W (cylinder empty)

$Q_1 = 22.4$ W (at the end of measurement period).

Due to the dependence of q on A_s, the time averaged Q is:

$$Q = \frac{Q_o - Q_1}{\ln \frac{Q_o}{Q_1}} = 40.7\ W$$

(as compared to 37.4 watts calculated from condensation rate).

(4) Comparison of experimental radial freezing rate with prediction:

The rate at which the solid-liquid boundary progressed inward was observed at one axial location in the cylinder. The time required for the boundary to move from the wall to the center was

Δt = 15 min or 900 seconds

R_o (radius of the cylinder) = 4.13 cm .

During the freezing period h as calculated from eq. (3.1) was

$$h = 0.028 \frac{W}{cm^2 K}$$

$hR_o = 0.116$.

From Appendix A for a cylinder freezing from the outside with a refrigerant at 10K, 1 percent ortho-hydrogen and $hR_o = 0.116$ we find

$$\frac{\Delta t_f}{R_o^2} = 41,$$

from which

$$\Delta t_f = 699 \text{ s or } 11.6 \text{ min.}$$

(as compared to 15 min observed).

(5) The thawing procedure as outlined above resulted in a broken plastic test cylinder. Even though thawing was initiated from the top by means of an electrical resistance heater and a pool of liquid had formed, the cylinder cracked when the helium gas temperature was raised above the thawing point. Since the warmer gas passed upward over the cylinder, thawing began at the bottom where no path was open for the expanding liquid to discharge.

As a possible remedy for this problem an electrical resistance heater could be installed along the cylinder axis. The heater would extend into the standpipe reservoir so that melting would begin along a line leading into the discharge tube and progress outward from that line.

3.4 Conclusions and Recommendations

A preliminary test indicates that the hydrogen apparatus may be used to obtain heat transfer and phase transition data which will pertain to the design of large scale solidification equipment. Control of the amount of refrigeration or heating over a wide range was possible through variation of the helium heat exchange gas flow rate, or by routing the gas through or away from a liquid helium heat exchanger. Therefore, data could be obtained for a wide range of conditions.

For one set of conditions approximate calculations indicate that a standard heat transfer correlation adequately predicts the heat transfer coefficient between the freezing chamber and the refrigerant gas. (Conditions were not sufficiently steady during this preliminary test to obtain accurate heat transfer data, however.) The rate of freezing as calculated from one of the graphs discussed in the preceding section predicted a freezing time within 25% of the observed time. These tentative results indicate the freezing rate calculations will be applicable to the design of hydrogen solidification equipment.

The results of the preliminary test have led to the following proposed changes to be made in the apparatus and operating procedure for future tests:

(1) Liquid helium should be replenished continuously in order to provide constant rate of heat transfer. This will enable refrigerant conditions to be held steady and controlled more precisely to prevent freezing and thawing during condensation.

(2) Data acquisition should be automated -- this will permit the operator's attention to be focused on controlling the apparatus.

(3) An electrical resistance heater should be installed along the axis of the freezing cylinder extending into the discharge tube. A broken test cylinder resulted from attempts to thaw from the outside wall. The central heater would create a path through which the expanding liquid could escape through the discharge tube.

Legend for Figure 3.1

1. Helium Blower Motor.
2. Helium Blower Shaft.
3. Liquid Hydrogen Radiation Shield.
4. Helium Blower Impeller.
5. Internal Gear.
6. Helium Flow Control Valve.
7. Liquid Helium Bath.
8. Direction of Helium Gas Flow.
9. Heater.
10. 6-Inch I. D. Pyrex Dewar.
11. Flow Meter (Venturi in Final Design).
12. Dewar Vacuum Space.
13. Heat Exchanger (4-1/8 O. D. x 0. 095 inch wall copper tube with 3/8 inch fins at 1/4 inch spacing outside, ribbon packing inside).
14. Fill Line Heater.
15. Co-Axial Capacitor Leads.
16. Vacuum or He Transfer Gas.
17. Fill Line.
18. Standpipe with Concentric Tube Capacitor for Liquid Level Meas.
19. Vacuum.
20. Liquid Hydrogen.
21. Heater.
22. 4-Inch Pyrex Dewar With Stainless Steel-to-Pyrex Joint.
23. Foam.
24. Pyrex Baffle.
25. Germanium Thermometer.
26. Gold Iron vs. Copper Differential Thermocouple (Typical).
27. Freezing Hydrogen.
28. 82 mm O. D. x 0. 005 Inch Plastic (polyethylene terephthalate film) Cylinder.

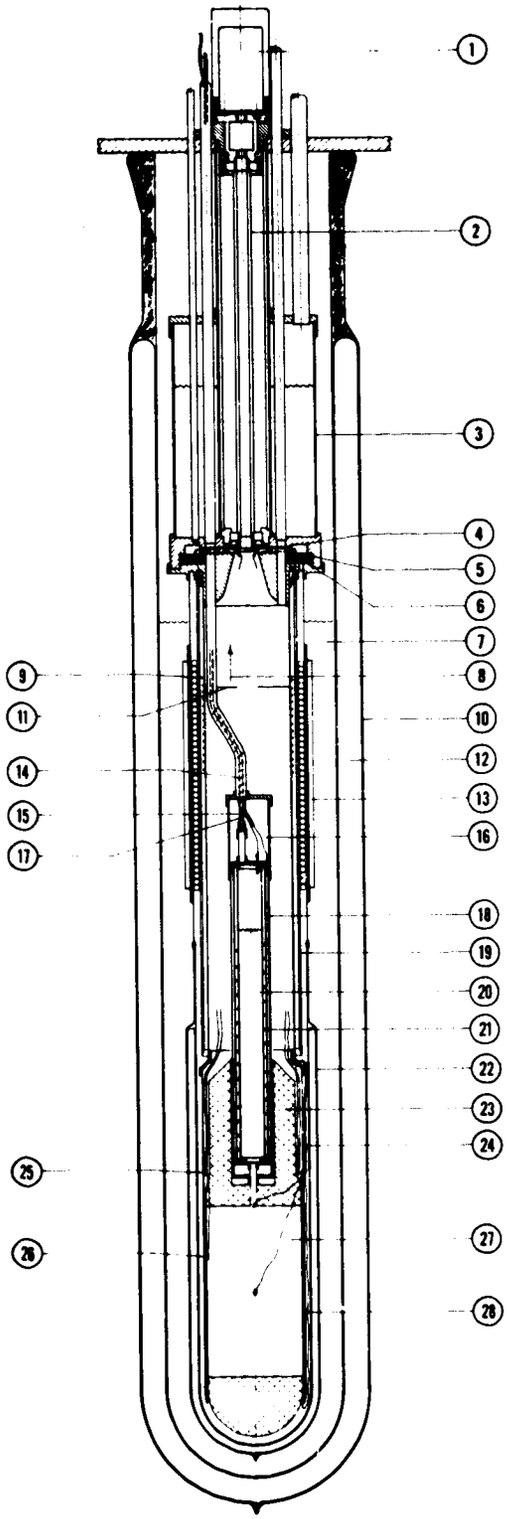

Figure 3.1 Hydrogen Freezing Apparatus

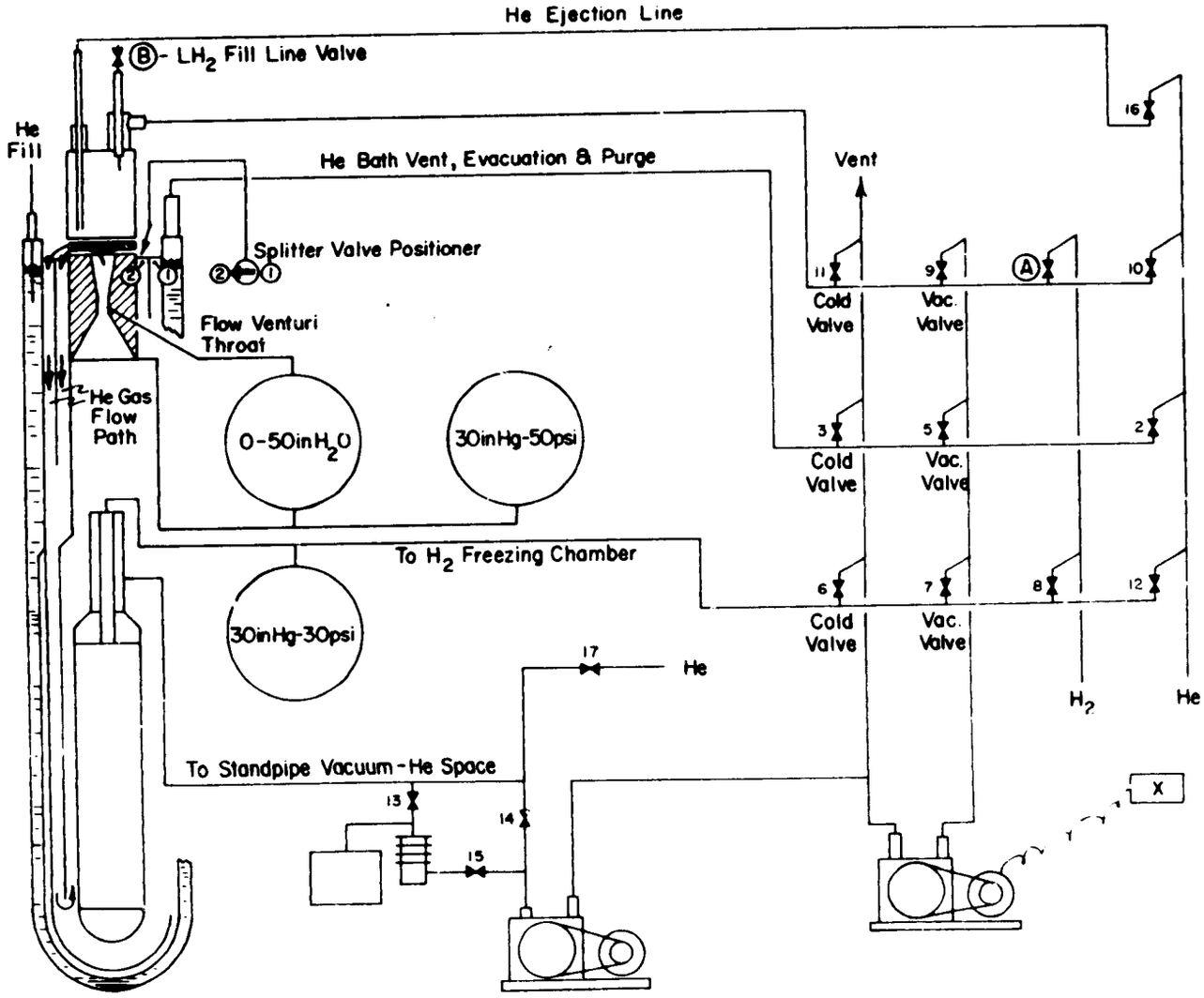

Figure 3.2 Instrumentation Schematic

4. References

1. Bohn, R. G., and Mate, C. F., Phys. Rev. B2, 2121 (1970).

2. Carslaw, H. S., and Jaeger, J. C., Conduction of heat in solids, 2nd Edn., 283 (Oxford University Press, London, 1959).

3. Contreras, W., and Lee, M., Melting characteristics and bulk thermophysical properties, Technical Report AFRPL-TR-72-48, Grumman Aerospace Corp. (1972).

4. Daney, D. E., Cryogenics, 11, 290 (1971).

5. Dwyer, R. F., Cook, G. A., and Berwaldt, O. E., J. Chem. Eng. Data, 11, 351 (1966).

6. Grober, H., Erk, S., and Grigull, U., Fundamentals of heat transfer, 3rd Edn., McGraw-Hill Book Co., Inc., New York, N. Y., (1961).

7. Hill, R. W., and Schneidmesser, B., Bull. IIF, Annexe 2, 115 (1956).

8. Hill, R. W., and Schneidmesser, B. Z., Physik. Chem. Neue Folge, 16, 17 (1958).

9. Lander, H. R., Dwyer, R. F., and Cook, G. A., Advances in Cryogenic Engineering, 11, 261 (Plenum Press, New York, N. Y., 1966).

10. Roder, H. M., and Diller, D. E., J. Chem. Phys., 52, 5928 (1970).

11. Rosenberg, H. M., Low temperature solid state physics (Oxford University Press, London, 1963).

12. Webb, F. J. Wilkinson, K. R., and Wilks, J., Proc. Roy. Soc., A214, 546:63 (1952).

NOMENCLATURE

Text Symbol	Figure Symbol	
A		area, cm
A_f		fluid flow cross sectional area, cm
A_s		surface area, cm^2
C_p		specific heat, j/g
D_e		hydraulic diameter = $D_o - D_i$, cm
D_i		inner diameter of annulus, cm
D_o		outer diameter of annulus, cm
E		energy, j
g		numerical factor
h	h	convective heat transfer coefficient, $W/cm^2 \cdot K$
k		thermal conductivity, $W/cm \cdot K$
ℓ		latent heat of fusion, j/g
L	L	cylinder length, cm
N_u		Nusselt number = hD_e/k_b
P_r		Prandtl number = $C_p\mu/k_b$
Q	Q	heat transfer rate, W
QM	QM	maximum heat transfer rate, W
r		radius, cm
R	R	radial position of the liquid-solid interface, cm
Re		Reynolds number = $\rho VD/\mu$
	RI	radius of refrigerated wall for cylinder freezing from inside, outward, cm
R_o		radius of refrigerated wall, cm
	RO	radius of refrigerated wall for cylinder freezing from outside, inward, cm
t	T	time, s
T		temperature, K

NOMENCLATURE (continued)

T_f	melting-point temperature, K
T_o	refrigerant temperature, K
T_w	wall temperature, K
U	overall heat transfer coefficient, $W/cm^2 \cdot K$
v	fluid velocity, cm/s
$\dot{V}$	volume flow rate, cm^3/s
x	distance from wall, cm
X	distance of liquid-solid interface from wall, cm
δ	wall thickness, cm
μ	viscosity, g/cm·s
θ	Debye temperature, K
ρ	density, g/cm^3

SUBSCRIPTS

b	bulk fluid property
w	fluid property at wall or property of the wall material

APPENDIX A

CYLINDER FREEZING FROM THE OUTSIDE

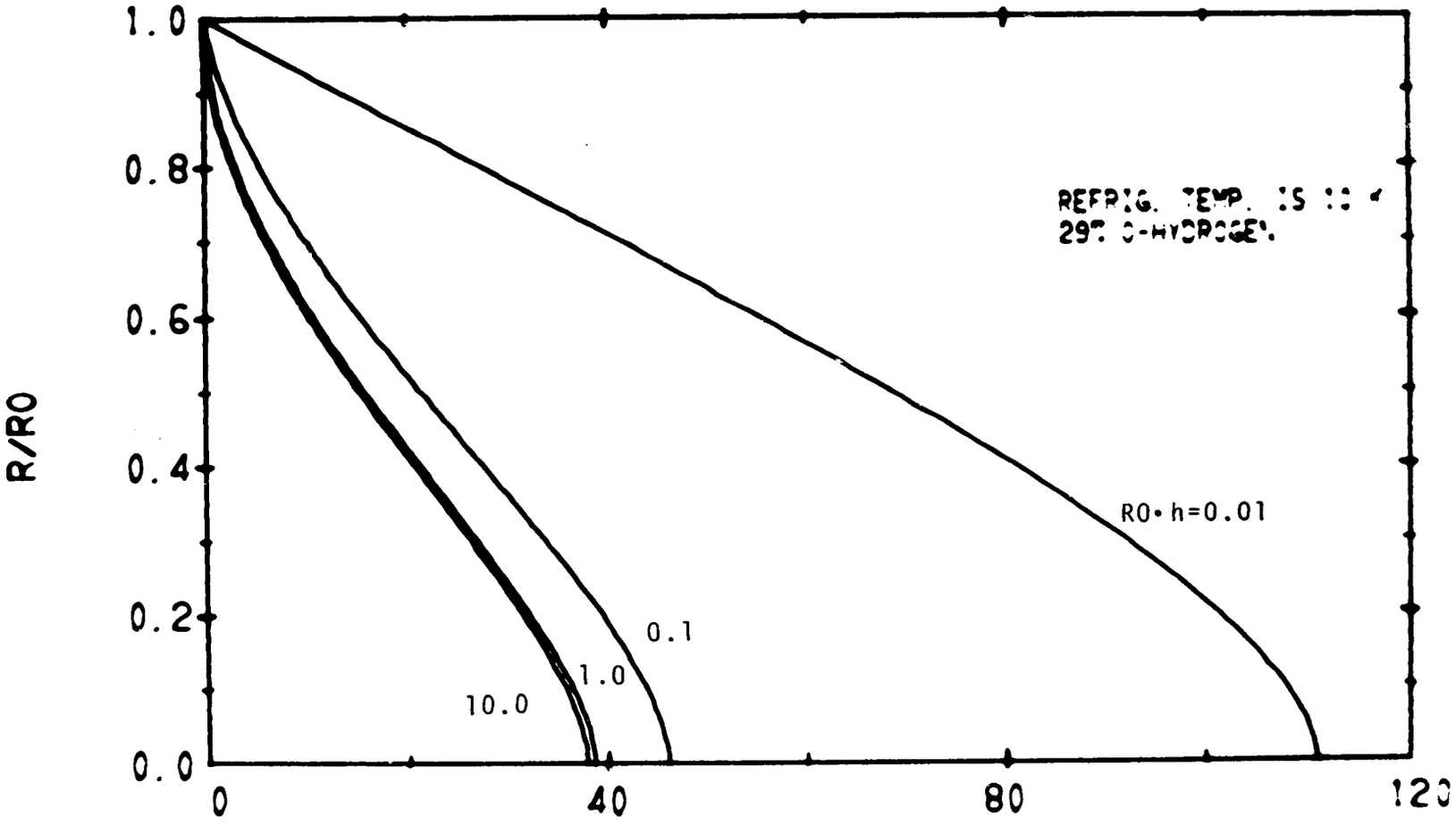

CYLINDER, FREEZING FROM OUTSIDE

12/29/71

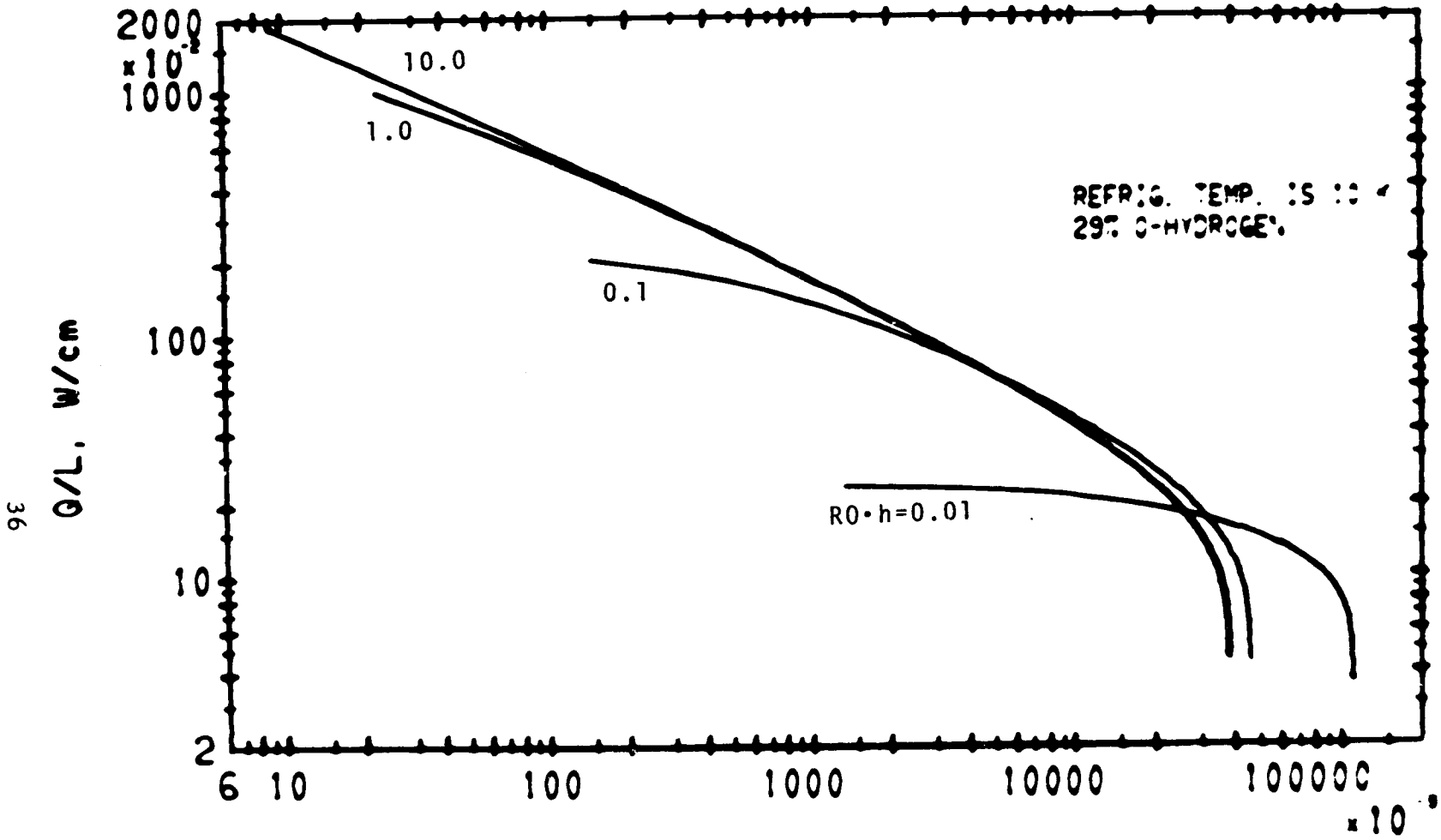

12/28/71

CYLINDER, FREEZING FROM OUTSIDE

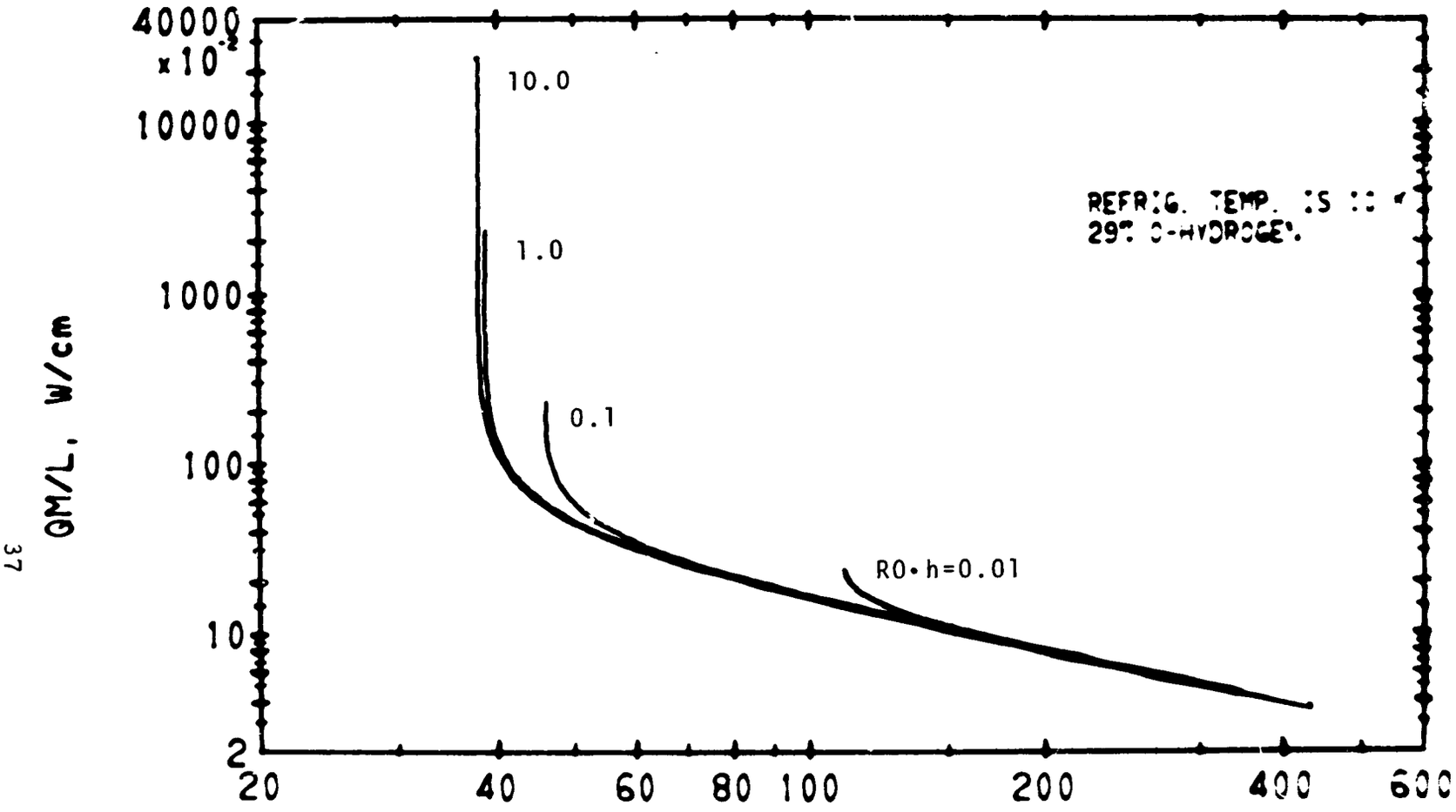

12/29/71

CYLINDER, FREEZING FROM OUTSIDE

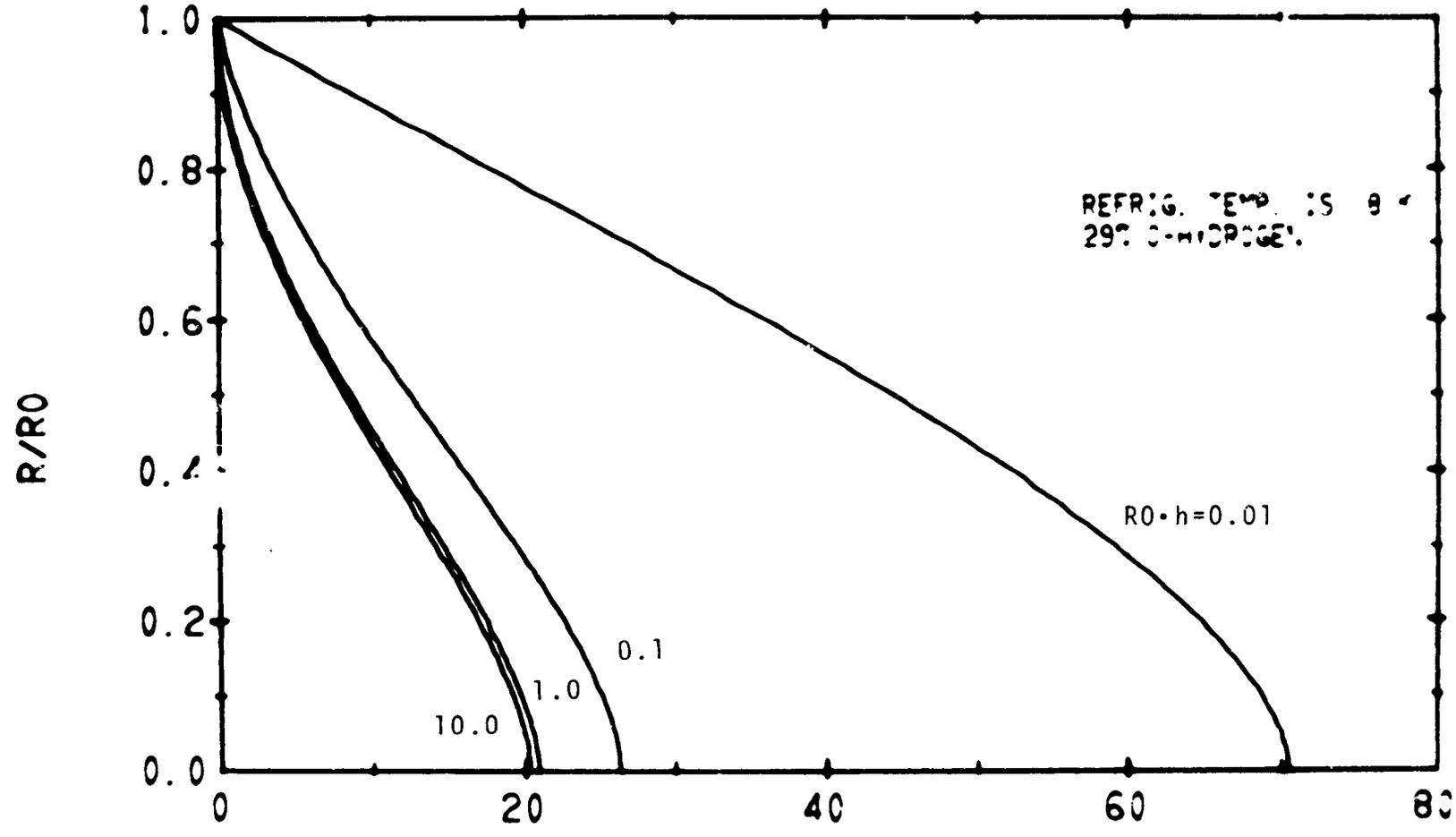

12/29/71

CYLINDER, FREEZING FROM OUTSIDE

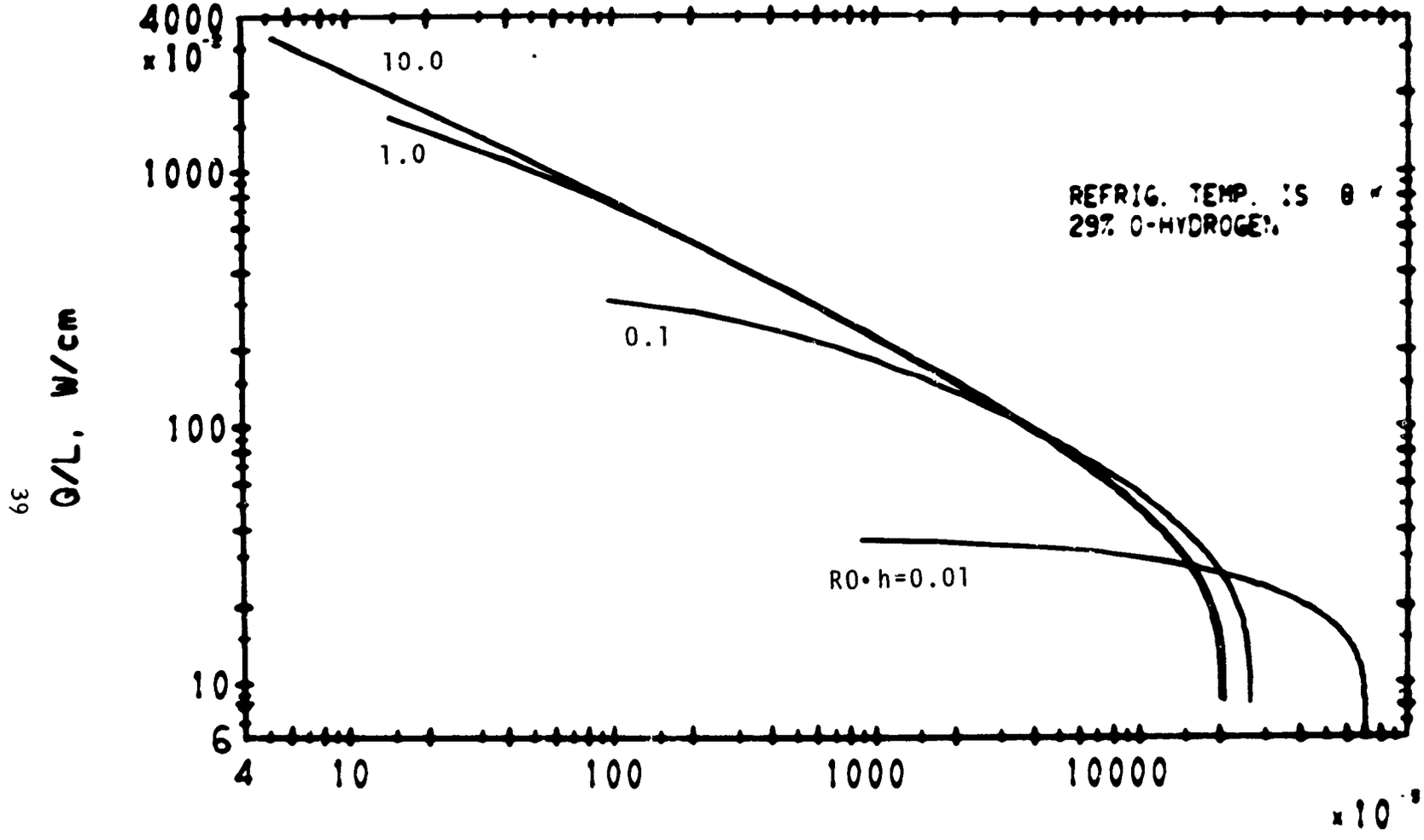

12/20/71

CYLINDER, FREEZING FROM OUTSIDE

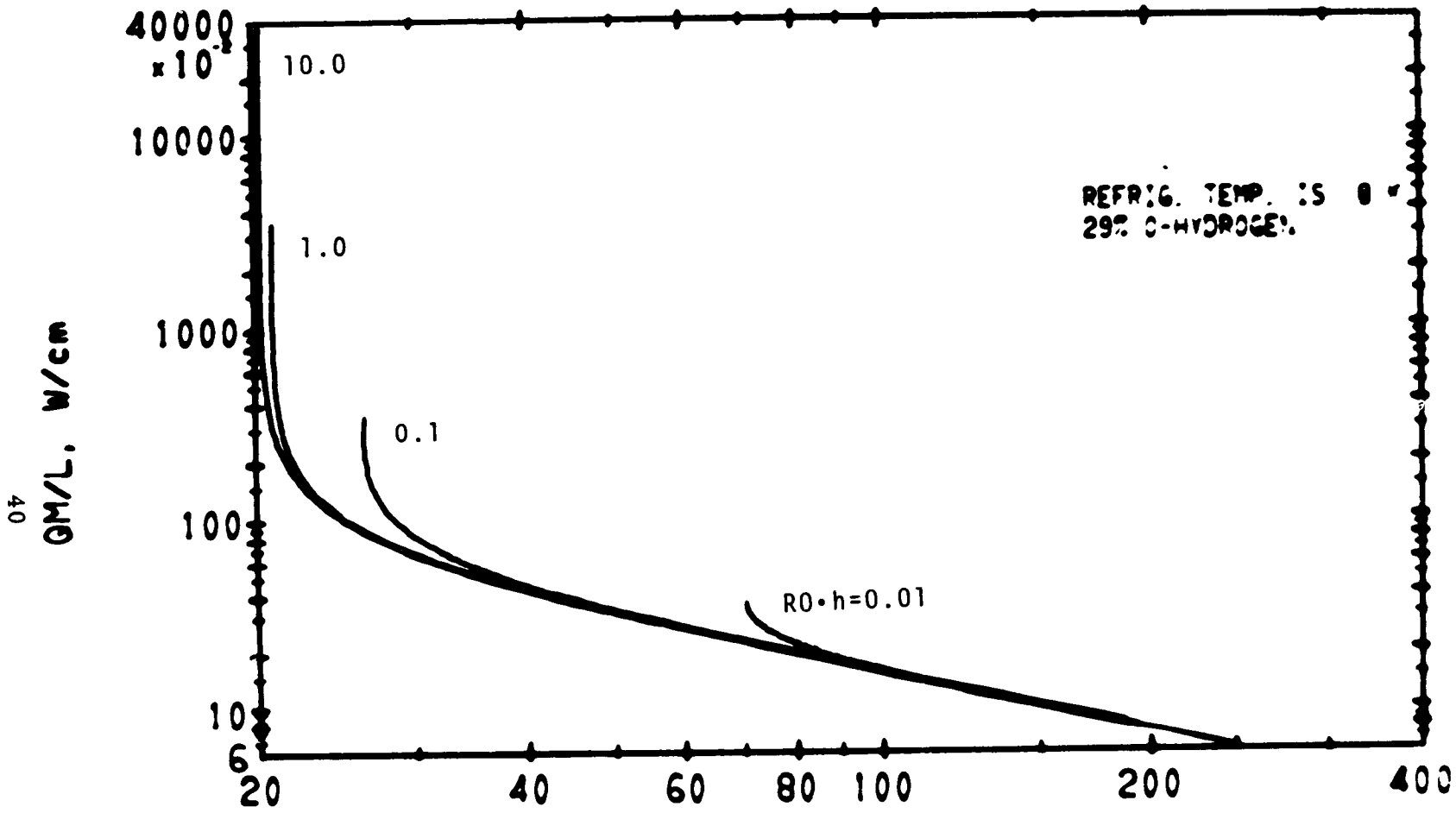

12/30/71

CYLINDER, FREEZING FROM OUTSIDE

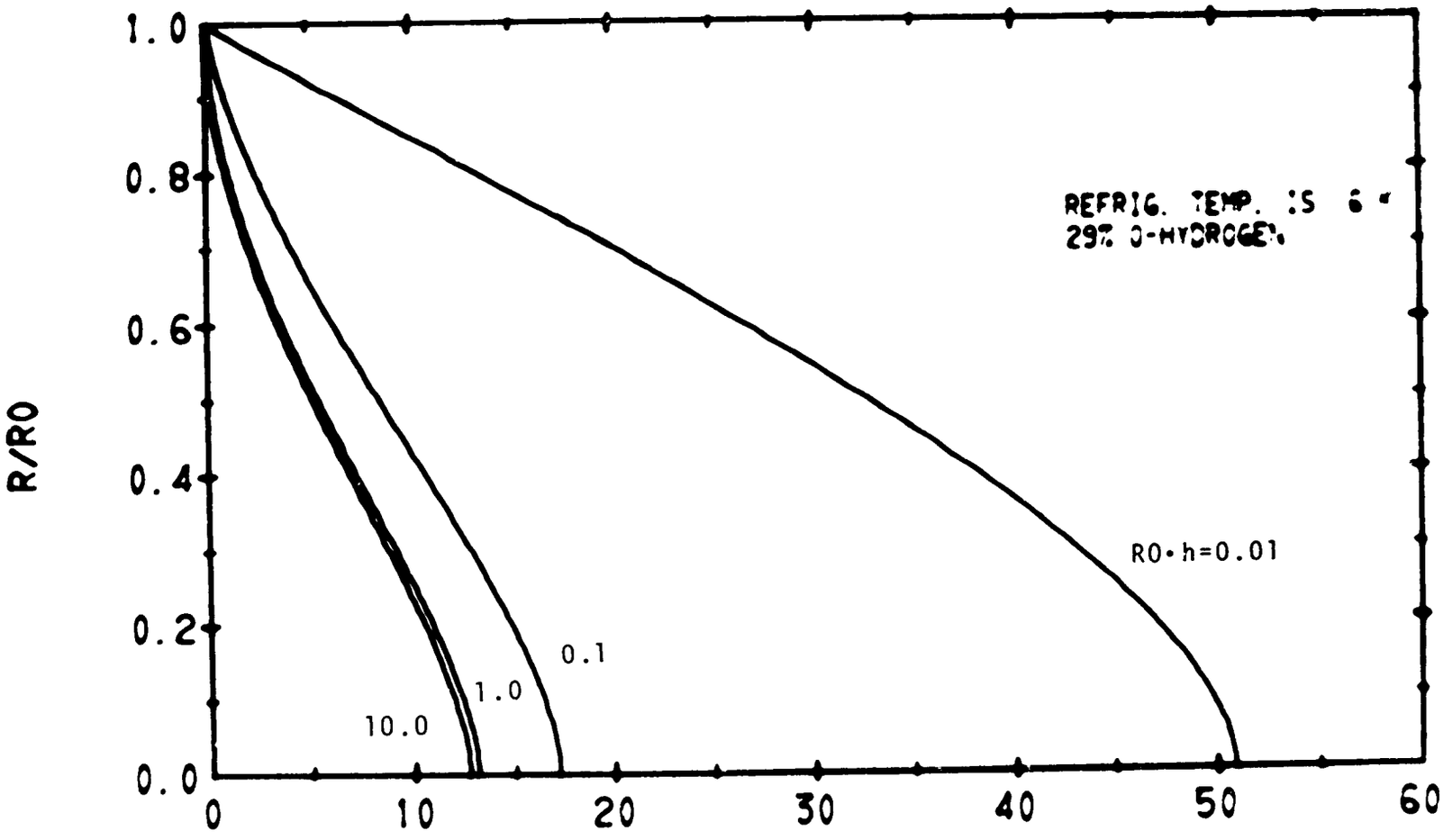

CYLINDER, FREEZING FROM OUTSIDE

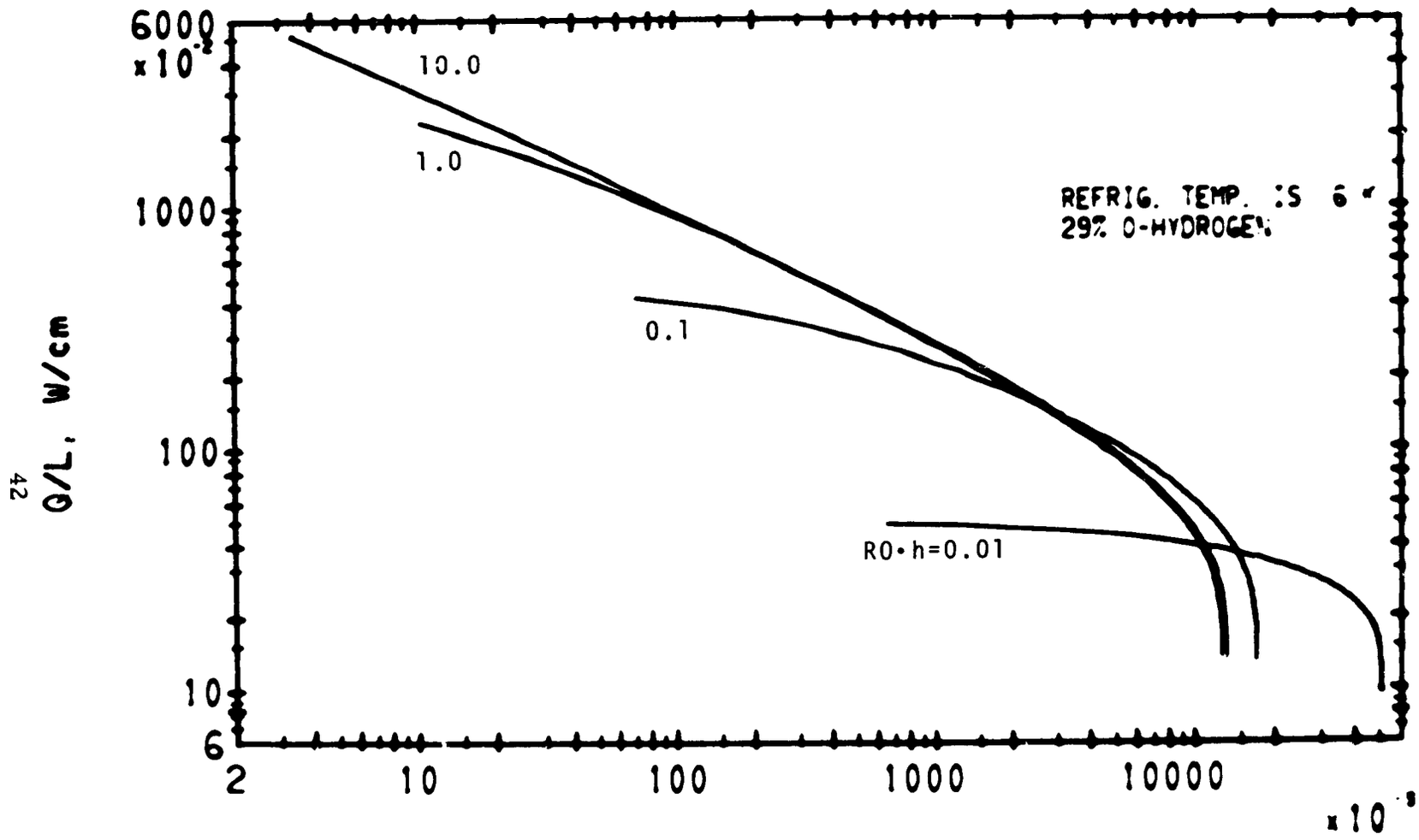

12/20/71

CYLINDER, FREEZING FROM OUTSIDE

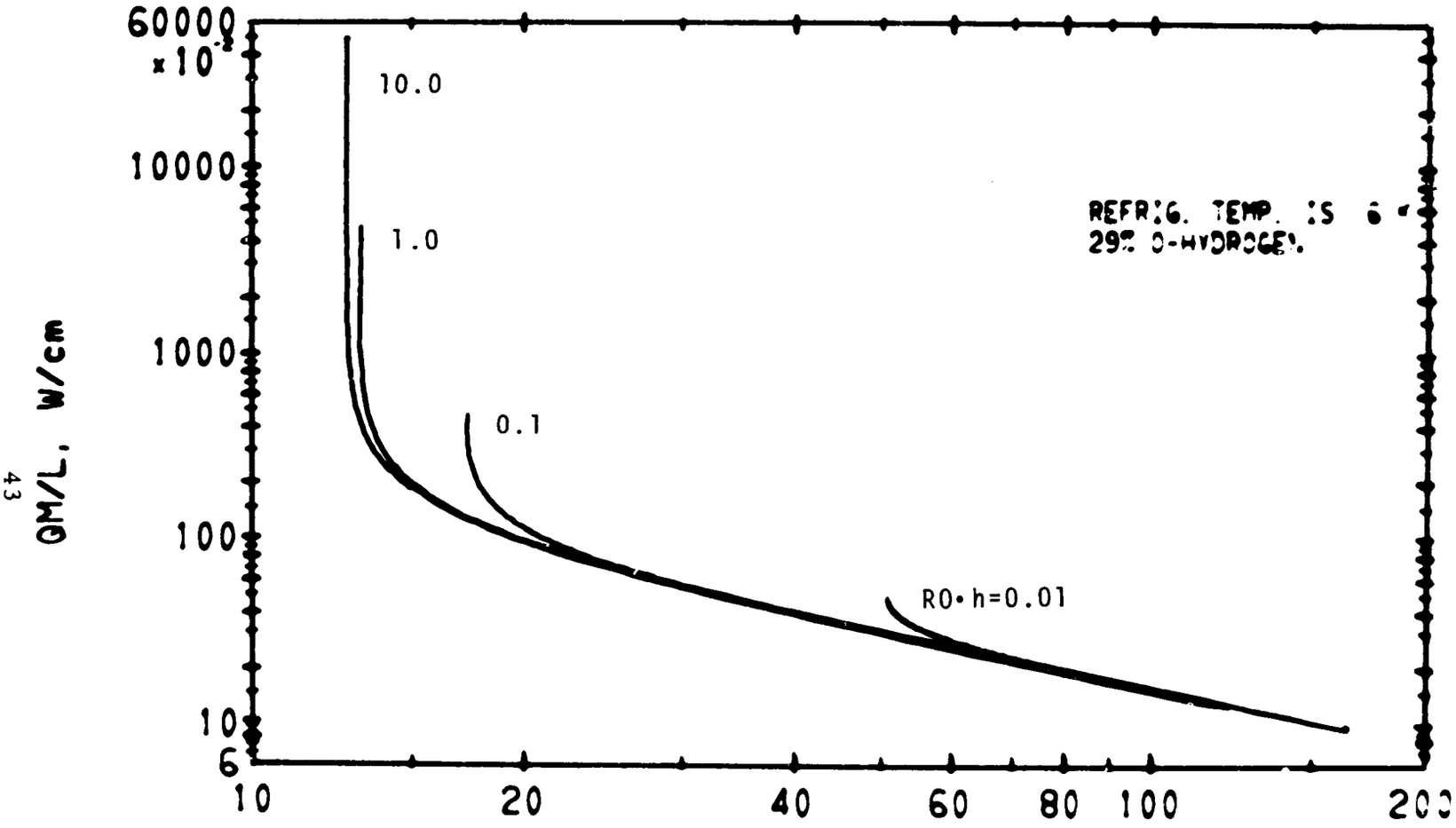

12/20/71

CYLINDER, FREEZING FROM OUTSIDE

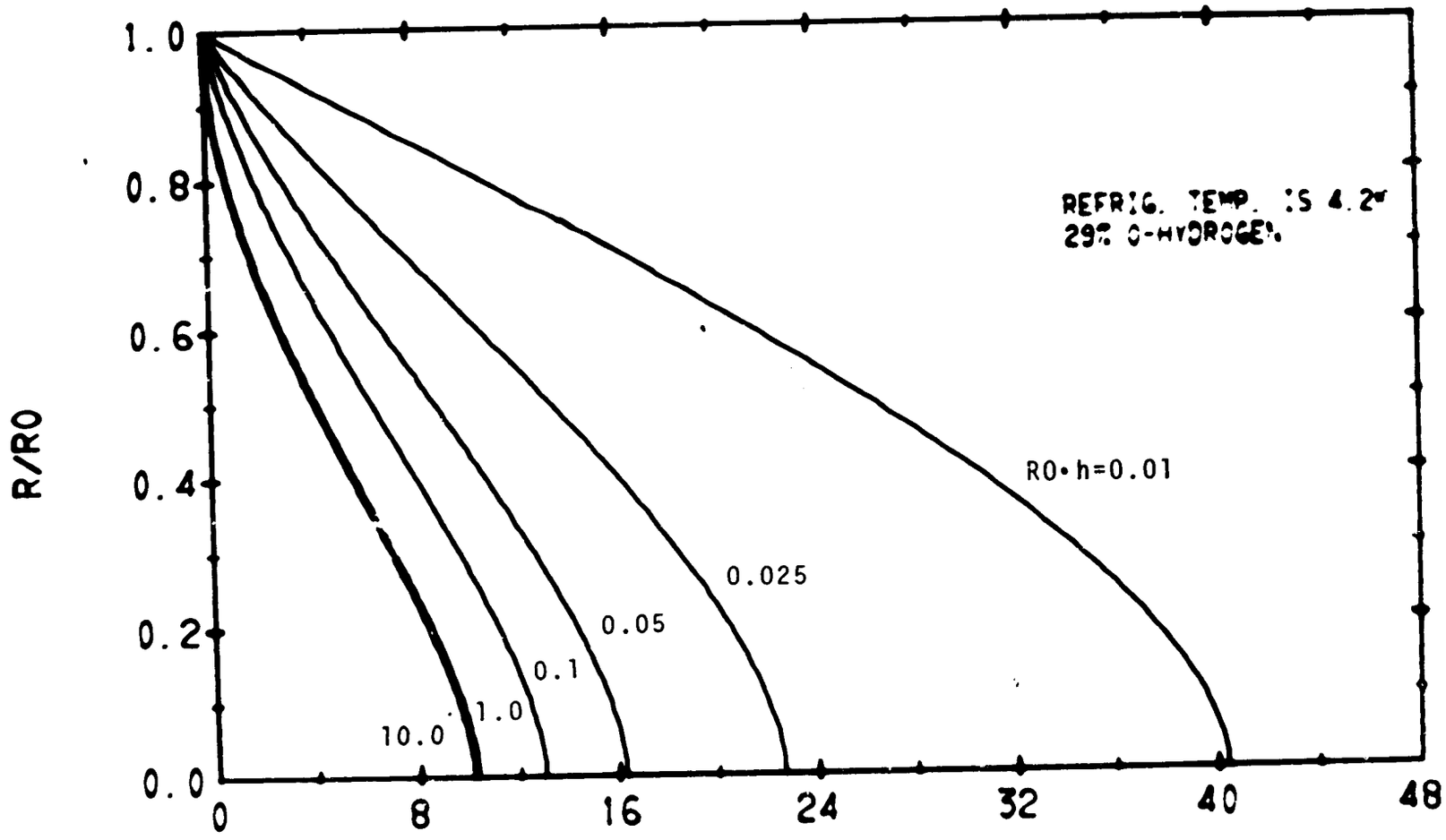

CYLINDER, FREEZING FROM OUTSIDE

12/29/71

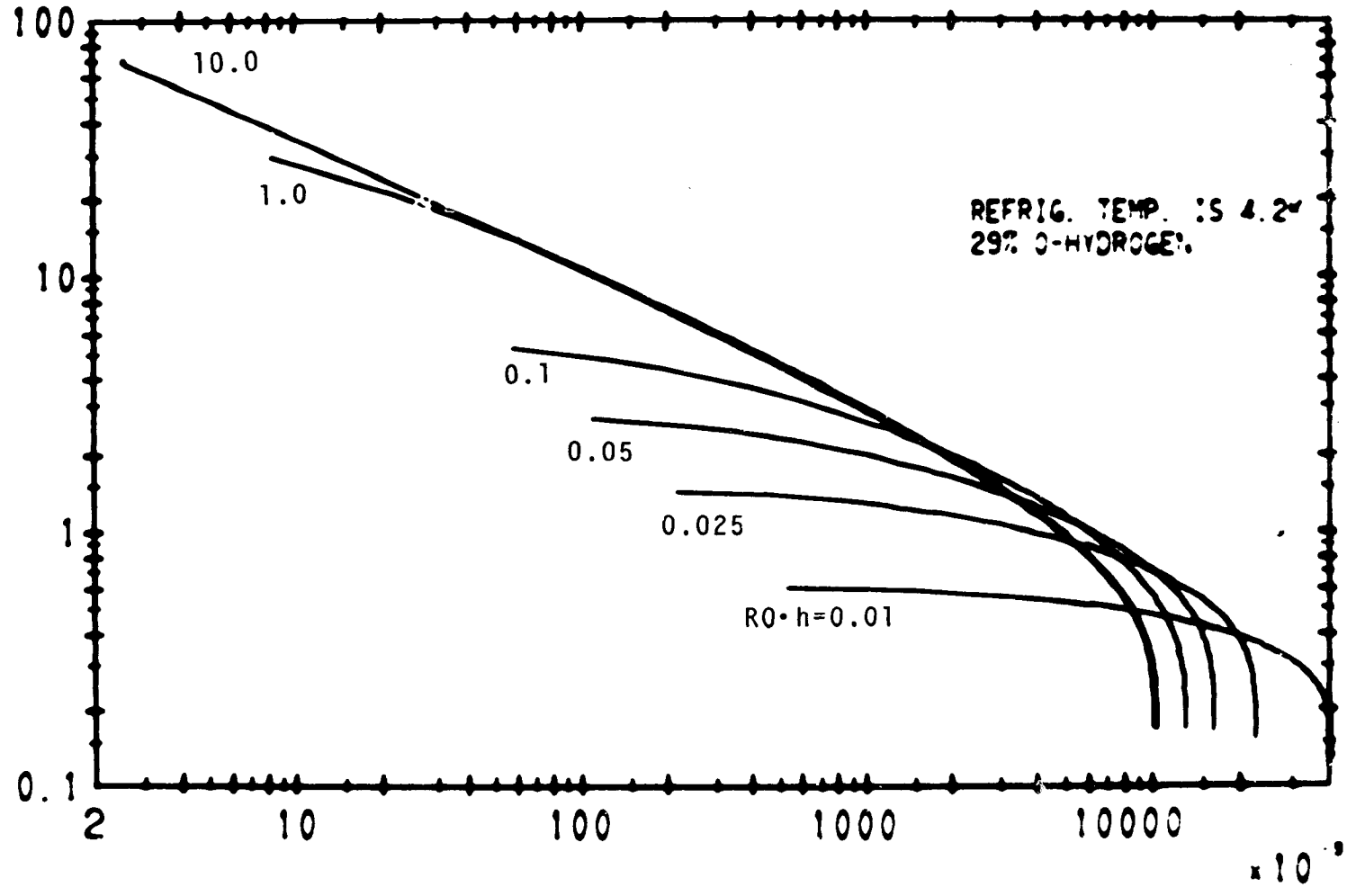

CYLINDER, FREEZING FROM OUTSIDE

12/29/71

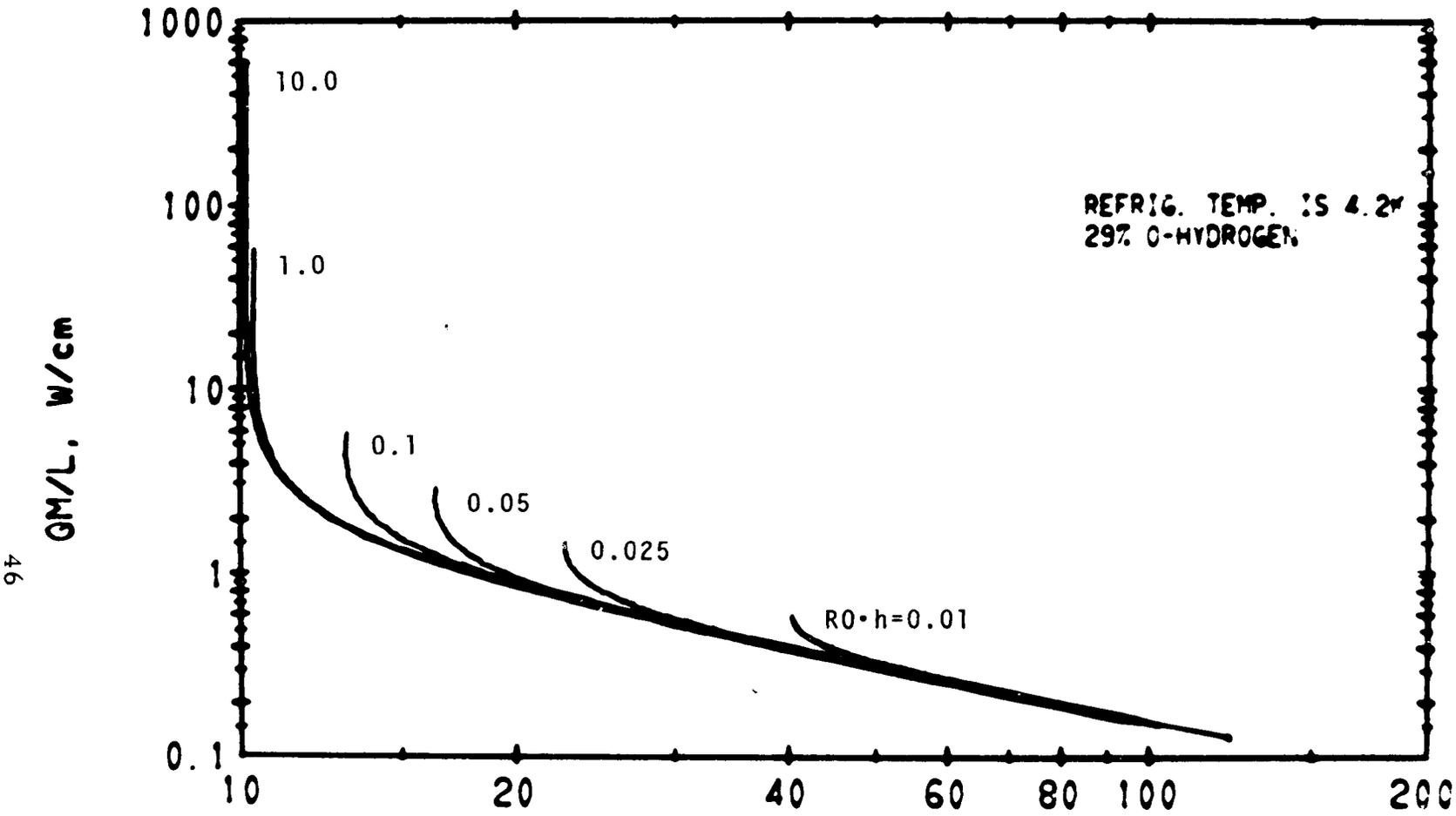

CYLINDER, FREEZING FROM OUTSIDE

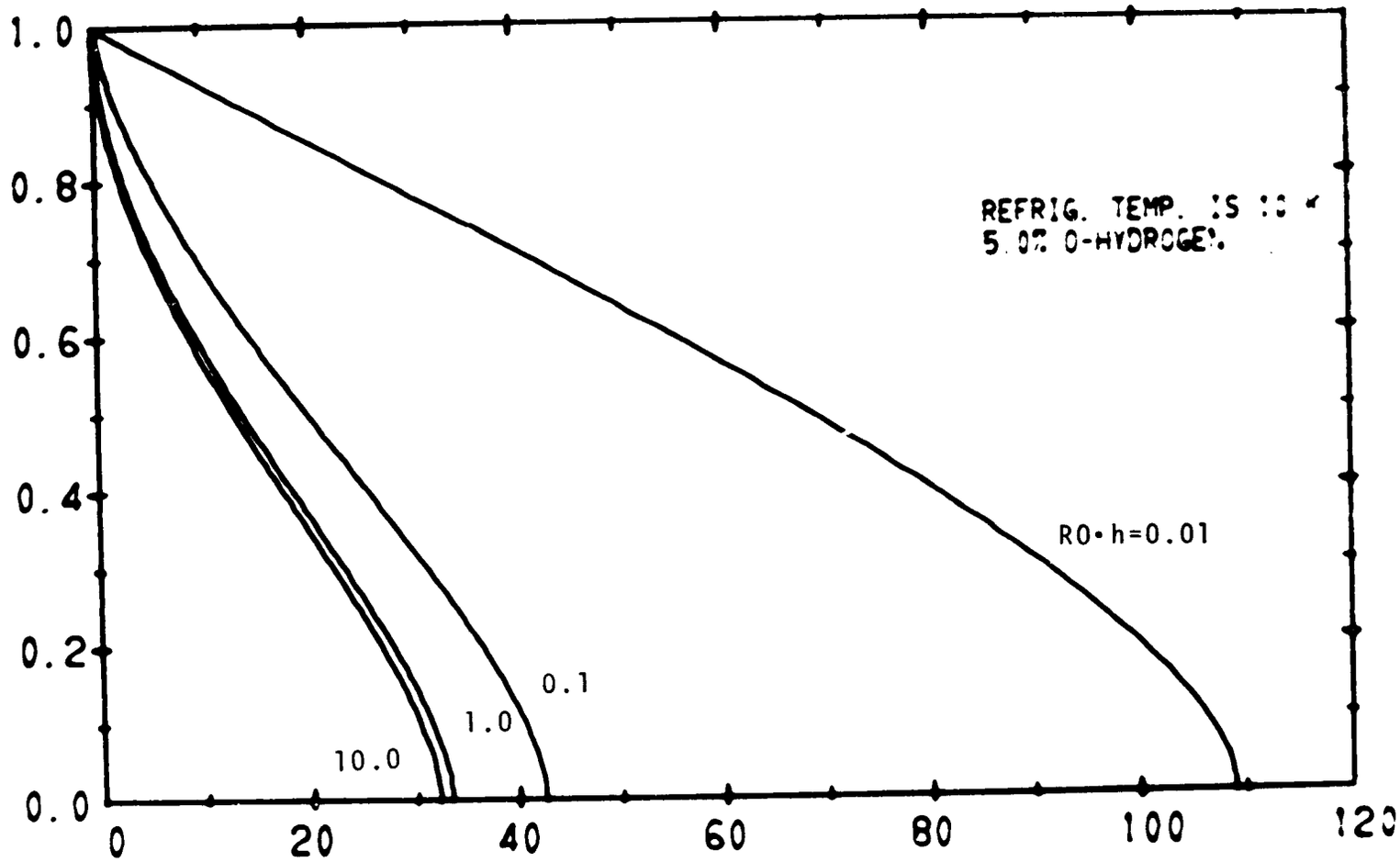

12/29/71

CYLINDER, FREEZING FROM OUTSIDE

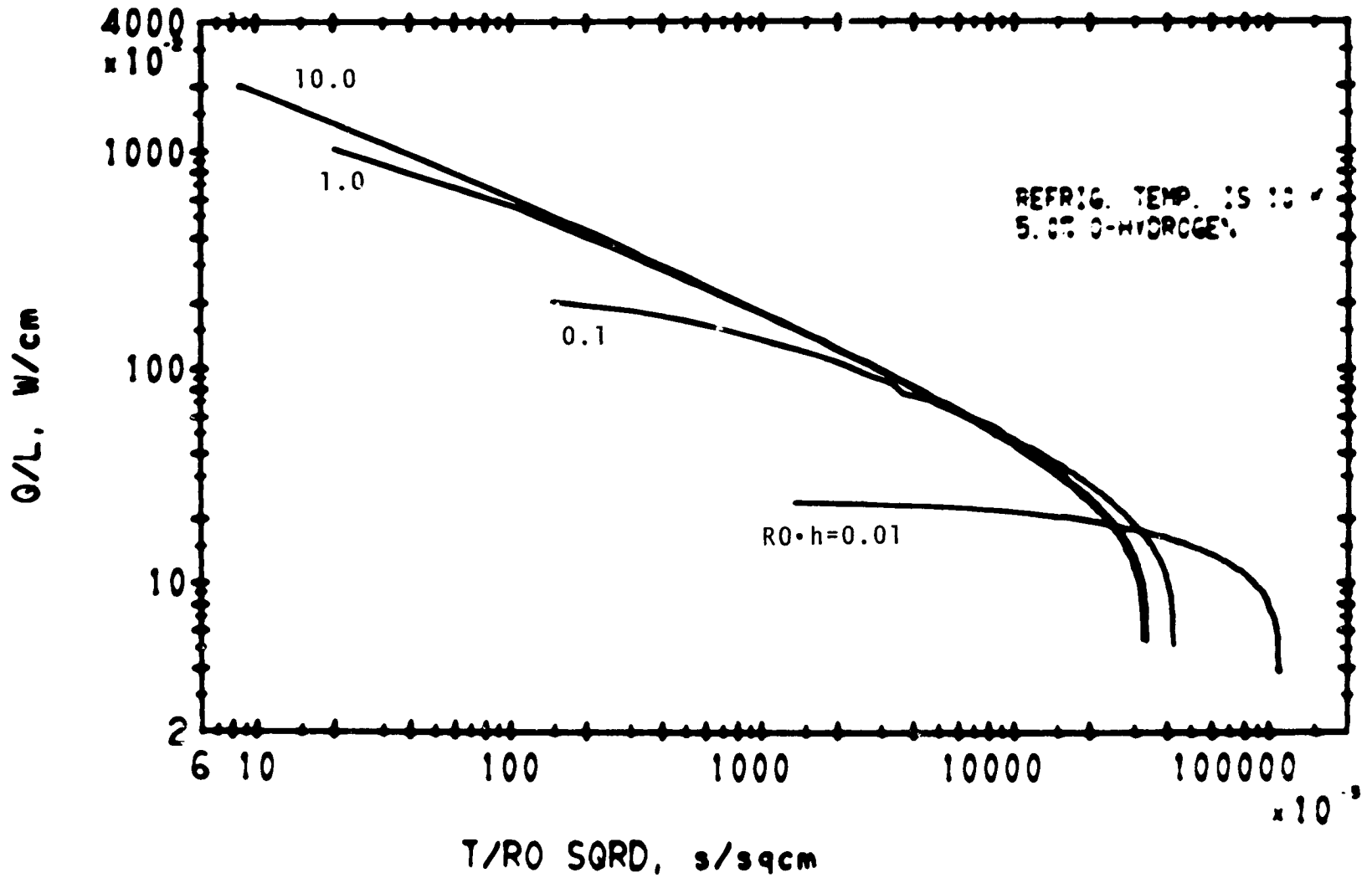

CYLINDER, FREEZING FROM OUTSIDE

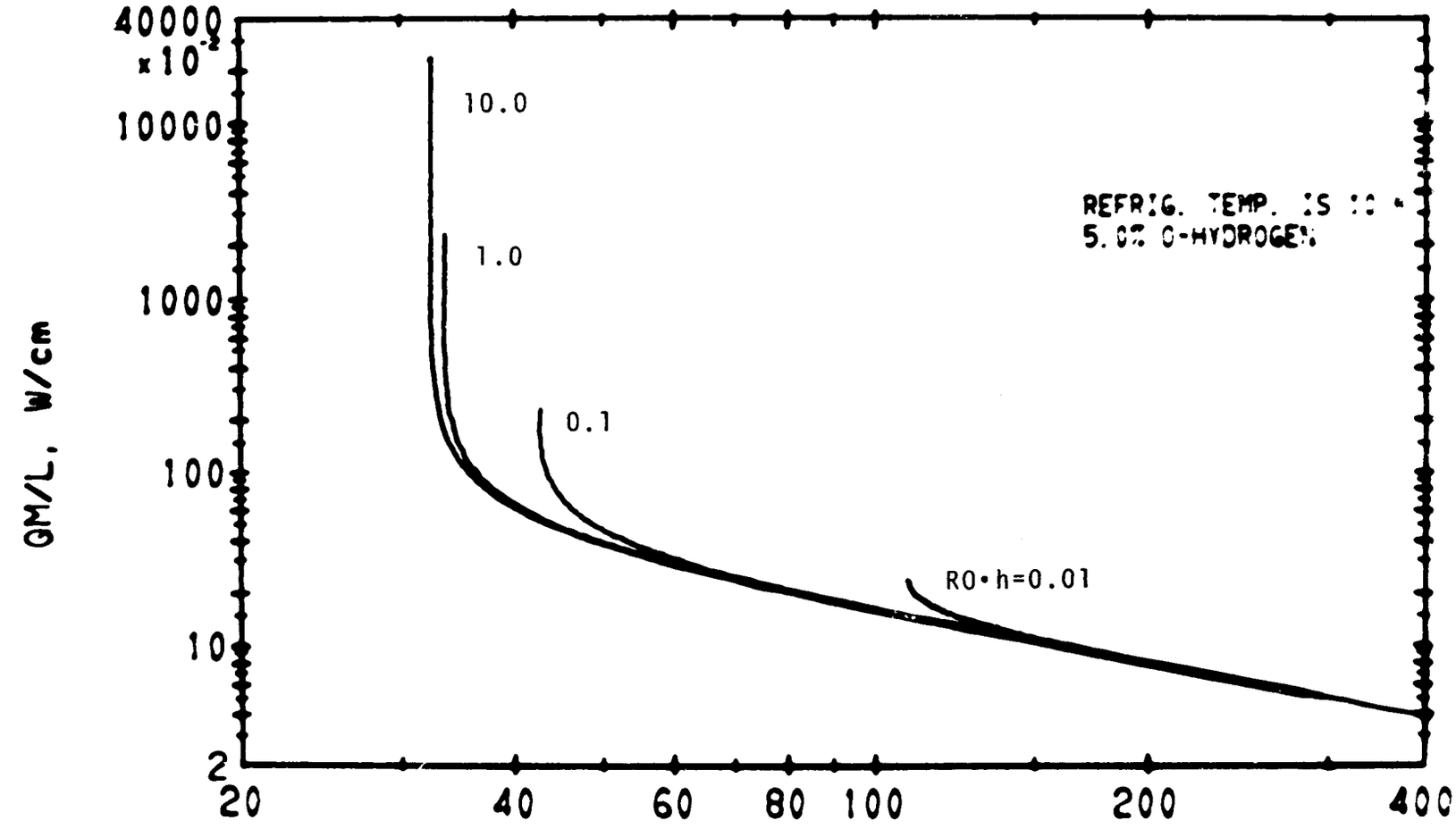

12/29/71

CYLINDER, FREEZING FROM OUTSIDE

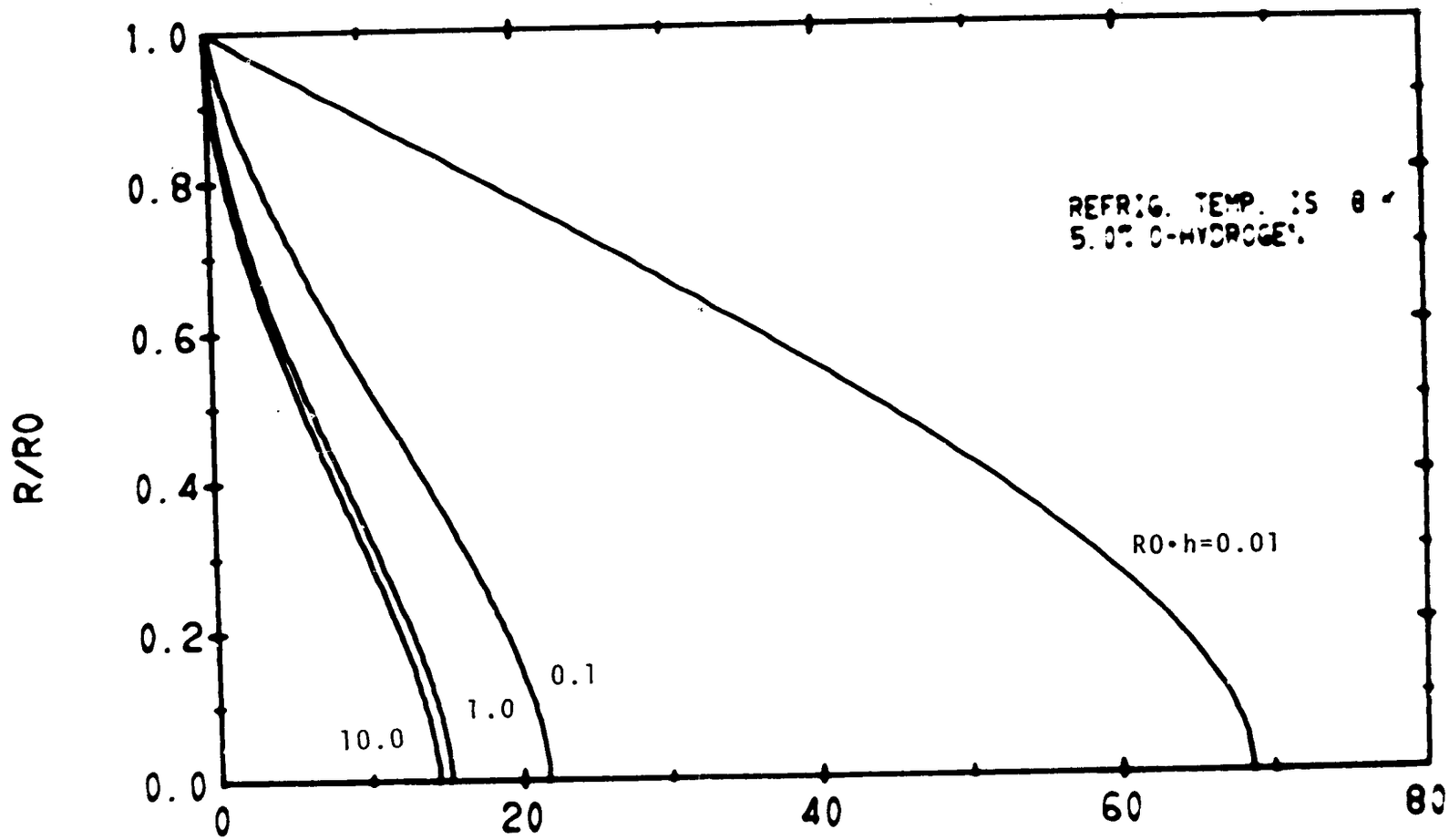

50

12/29/71

CYLINDER, FREEZING FROM OUTSIDE

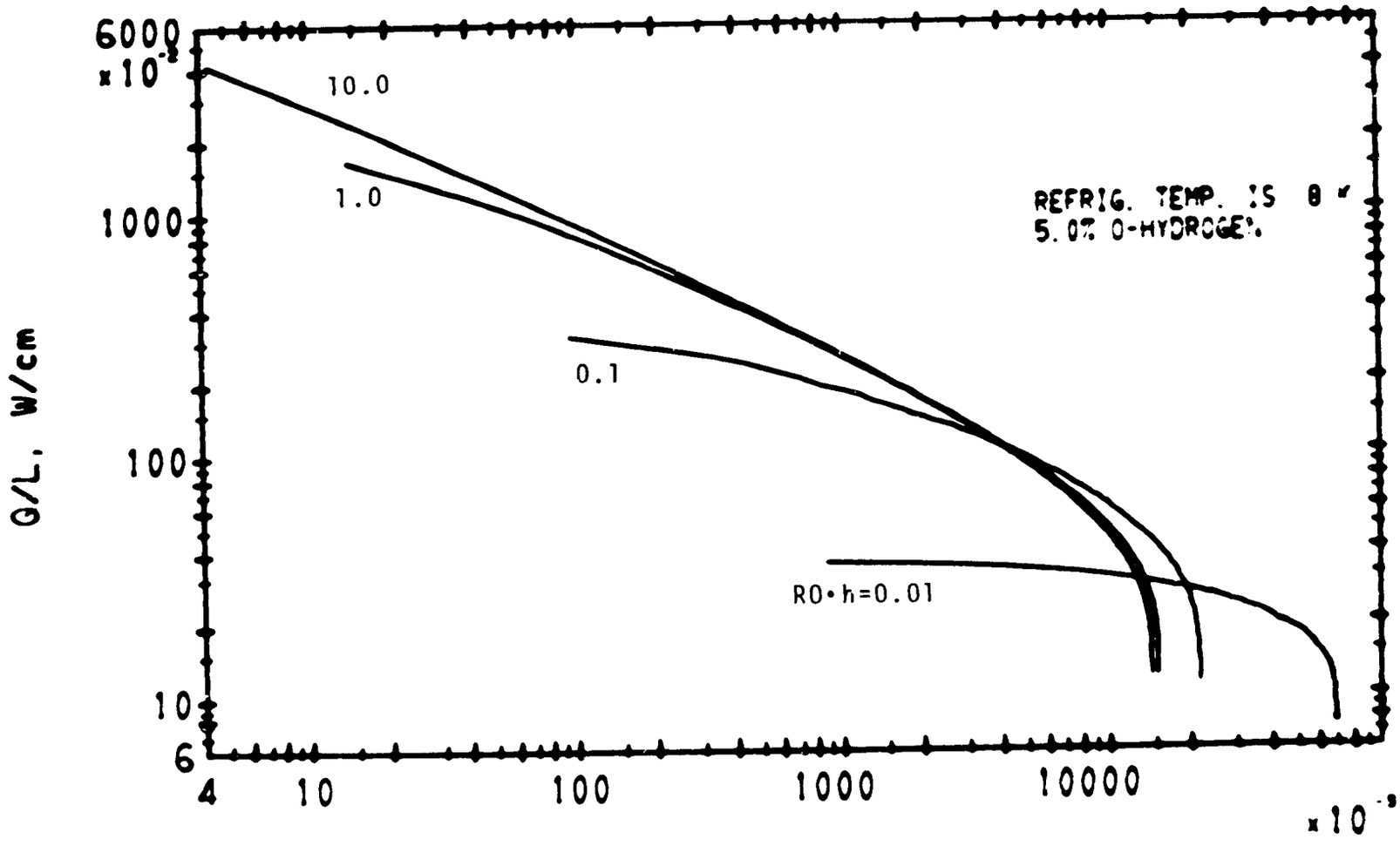

12/20/71

CYLINDER, FREEZING FROM OUTSIDE

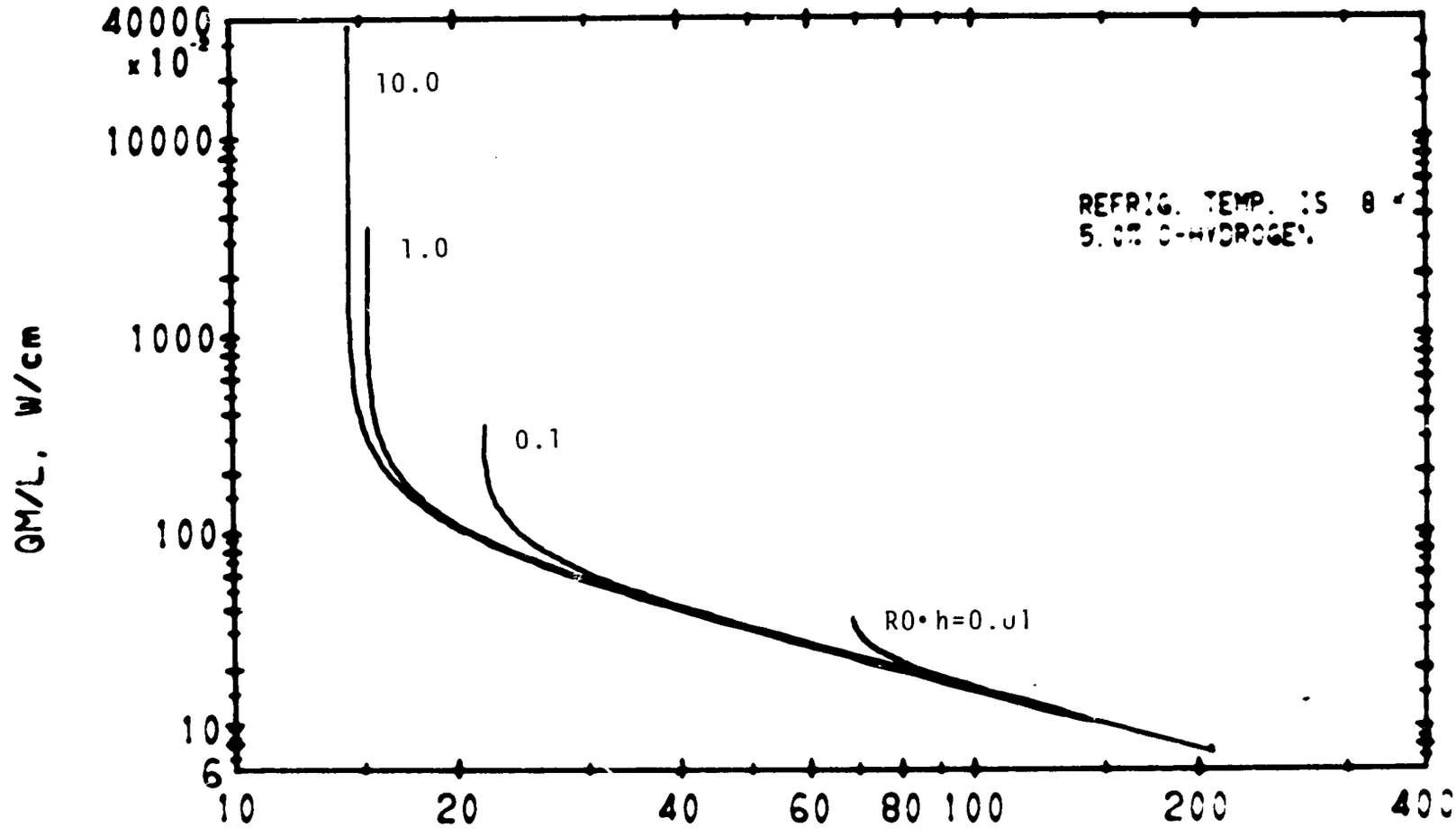

CYLINDER, FREEZING FROM OUTSIDE

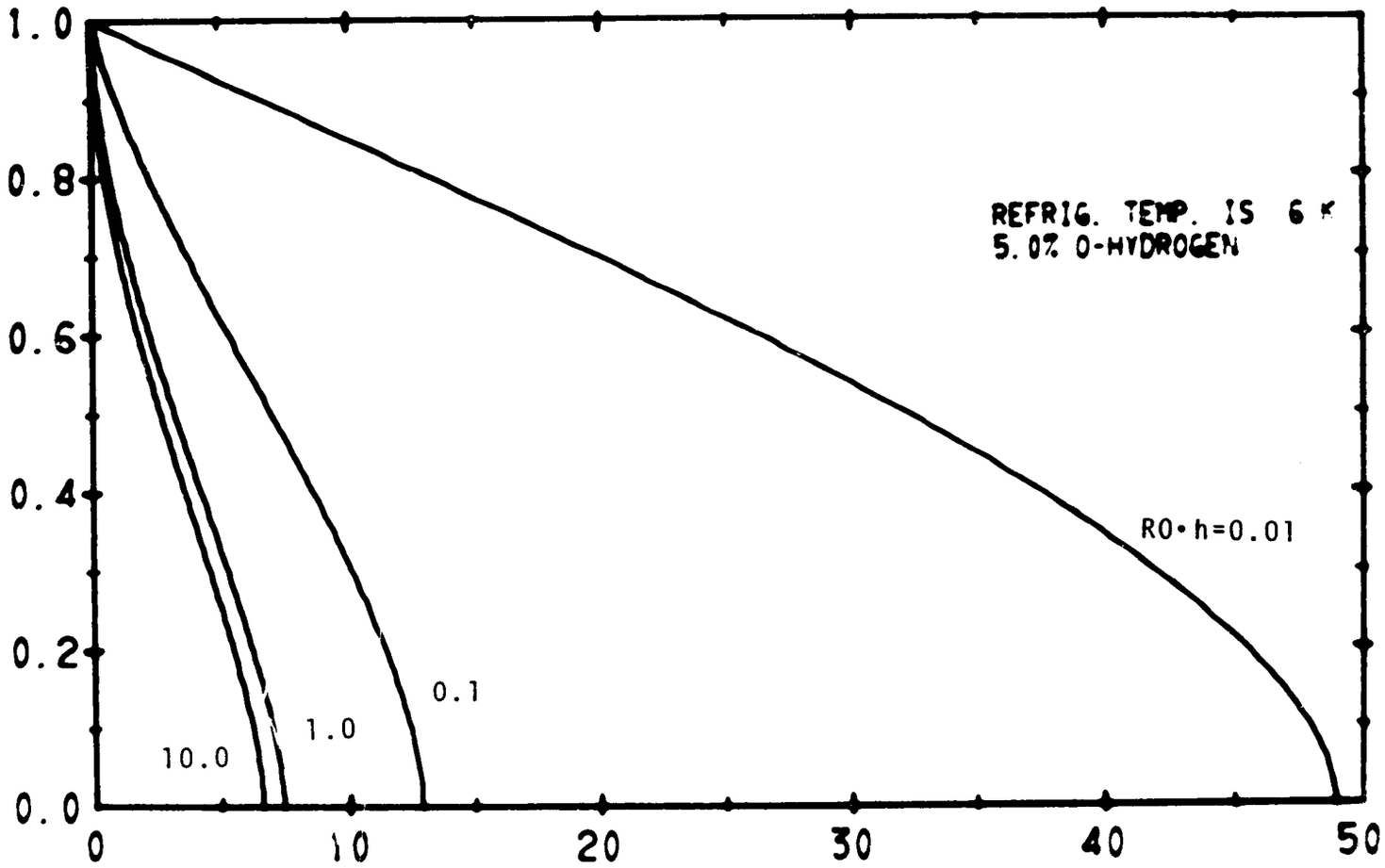

12/20/71

CYLINDER, FREEZING FROM OUTSIDE

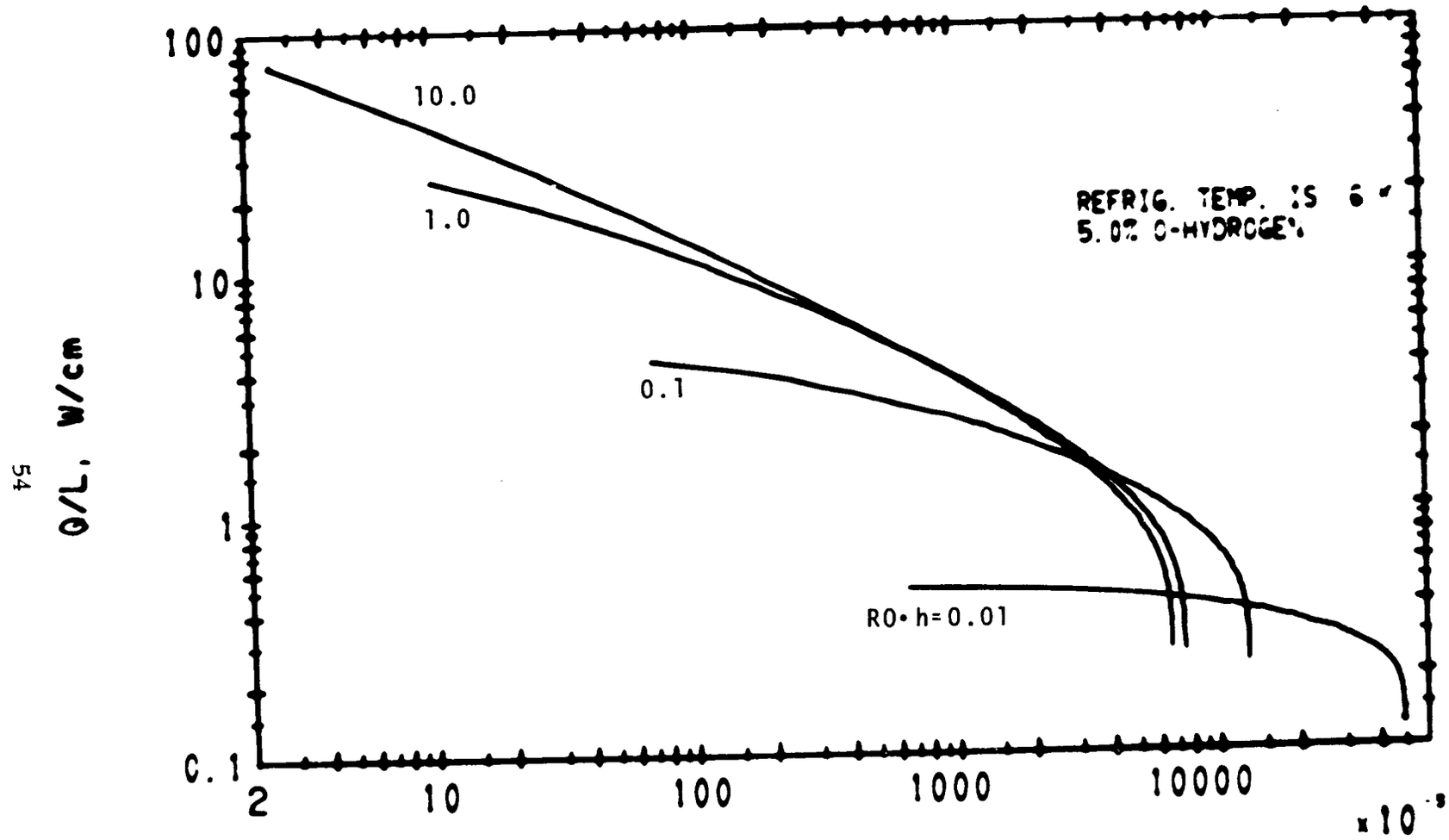

CYLINDER, FREEZING FROM OUTSIDE

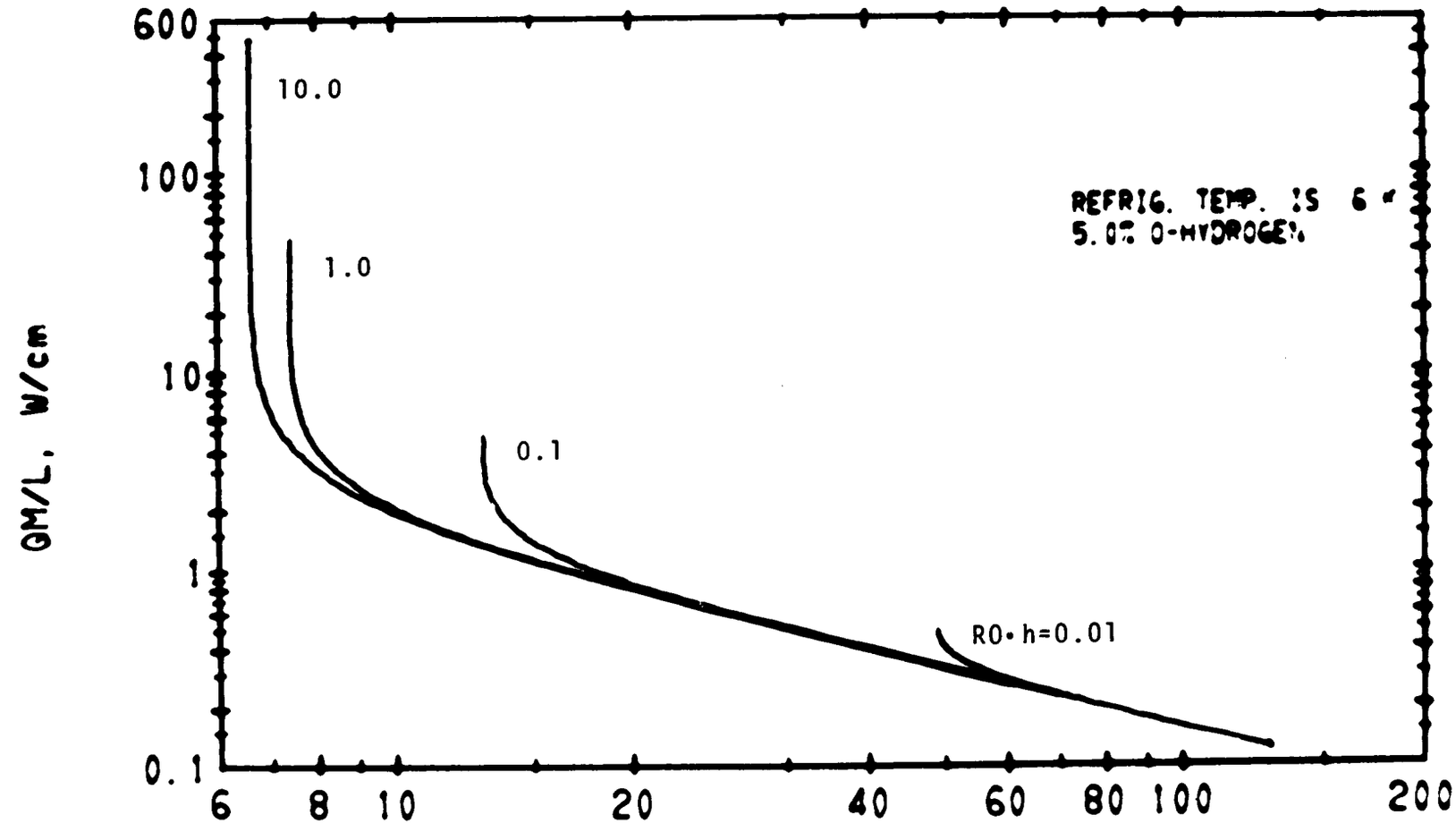

12/20/71

CYLINDER, FREEZING FROM OUTSIDE

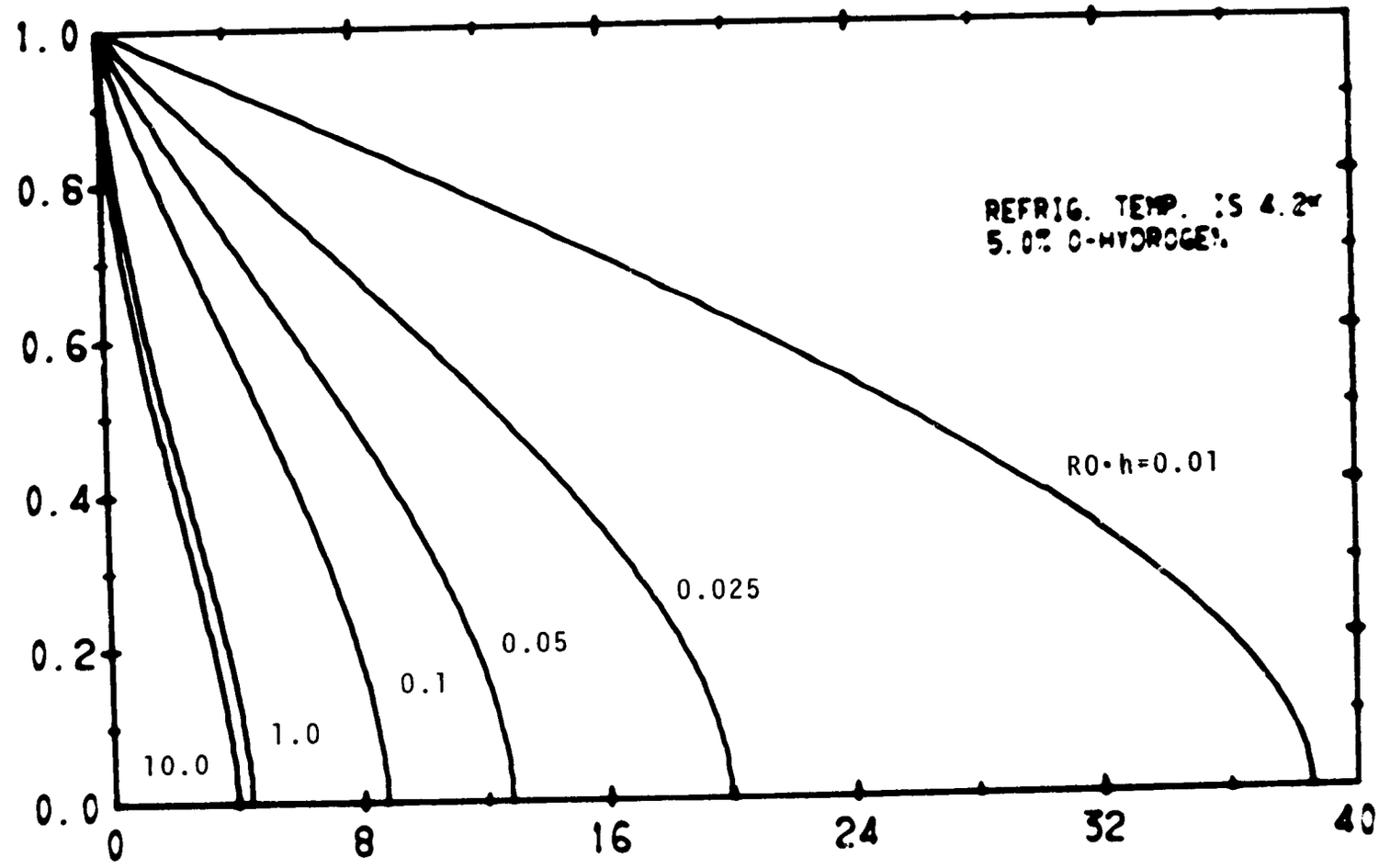

CYLINDER, FREEZING FROM OUTSIDE

12/20/71

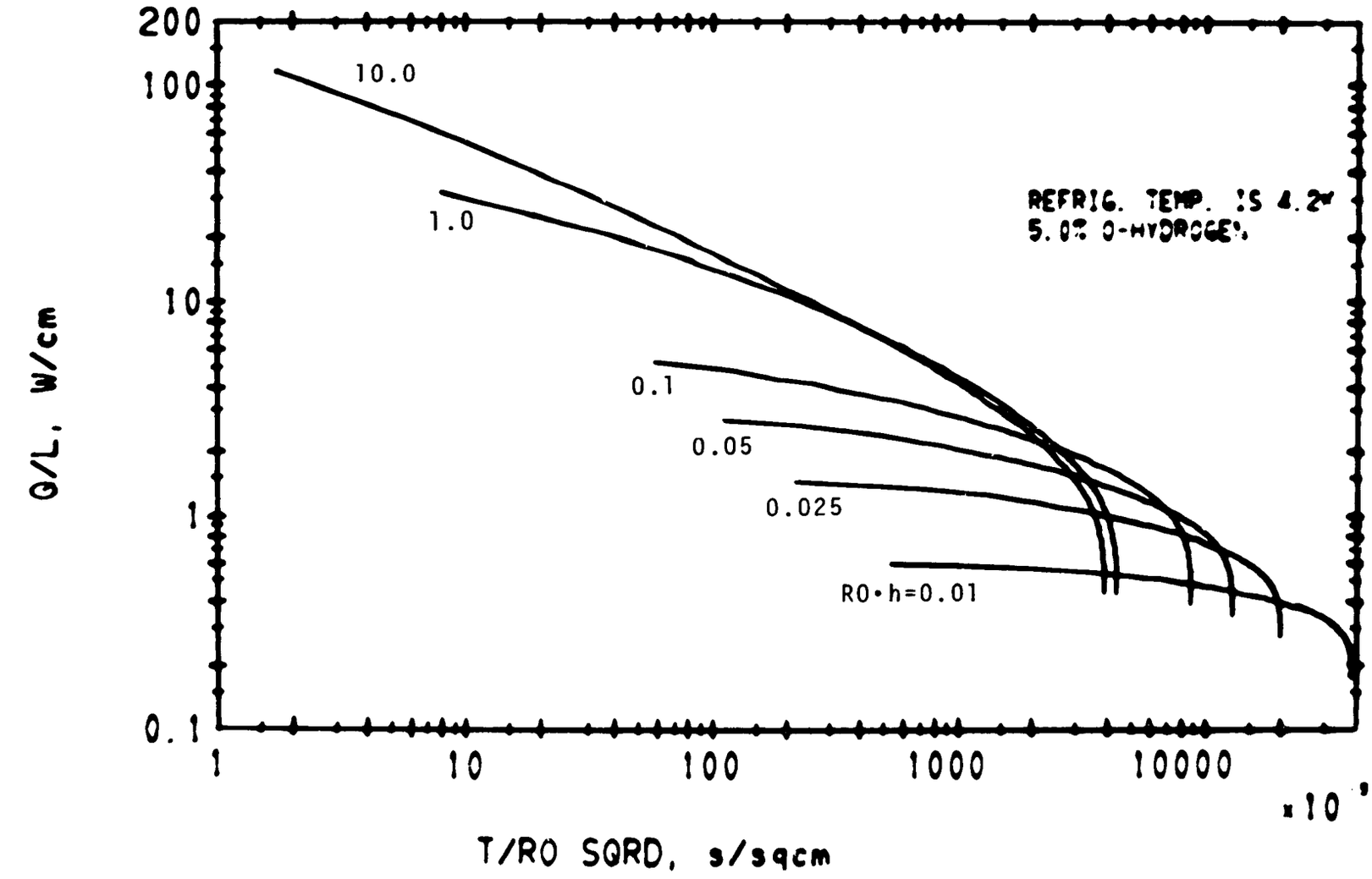

57

12/29/71

CYLINDER, FREEZING FROM OUTSIDE

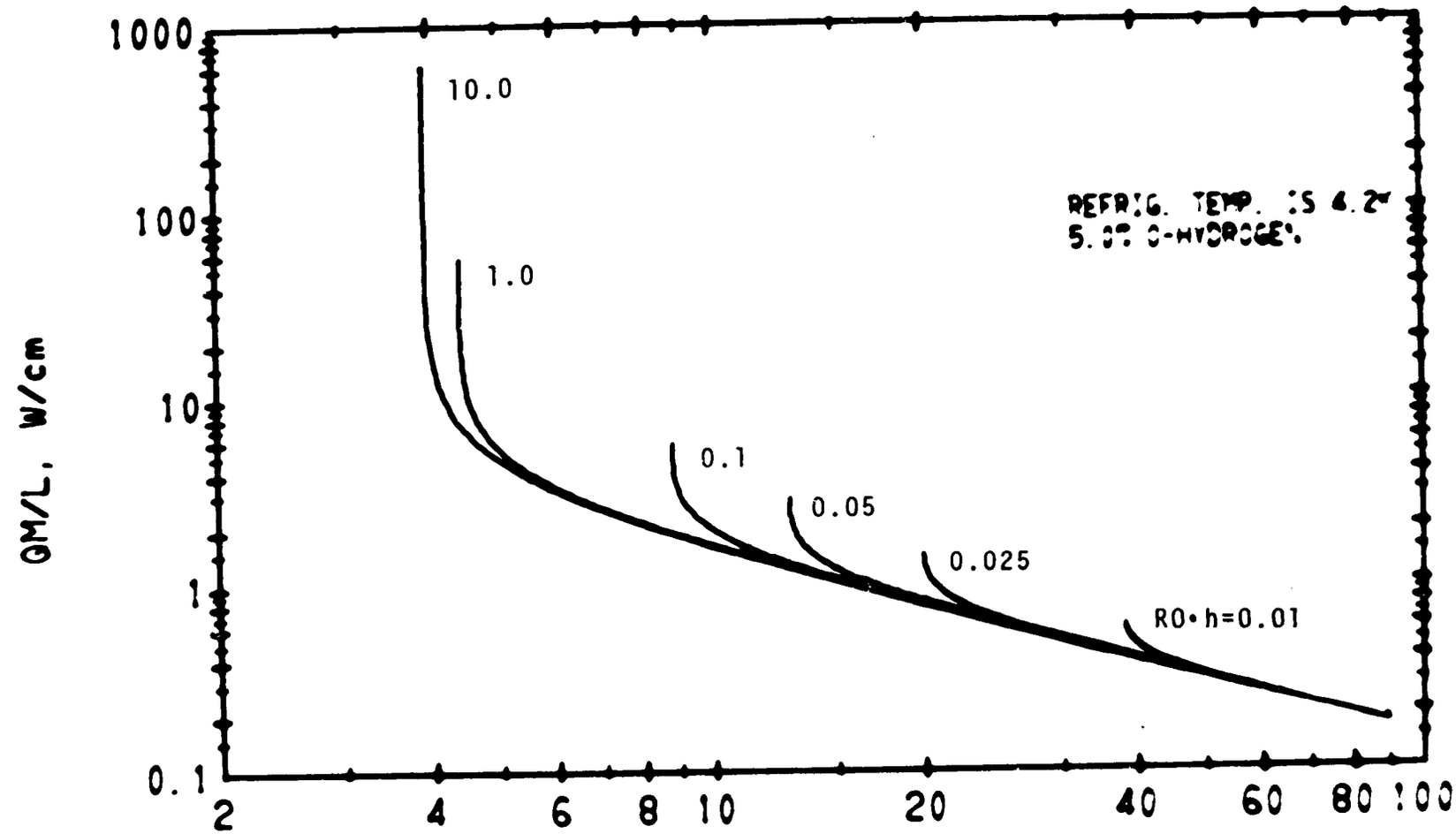

CYLINDER, FREEZING FROM OUTSIDE

12/20/71

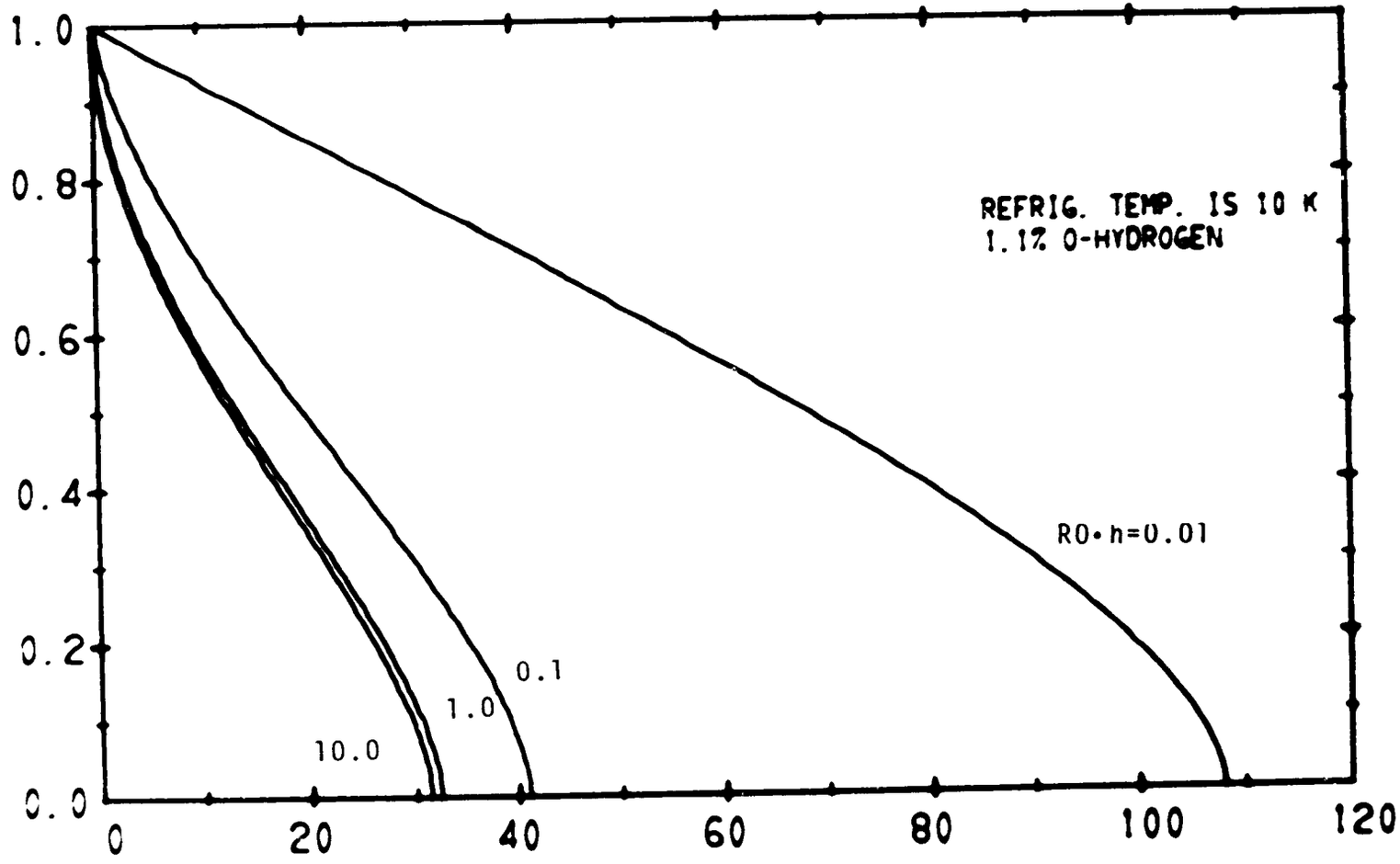

CYLINDER, FREEZING FROM OUTSIDE

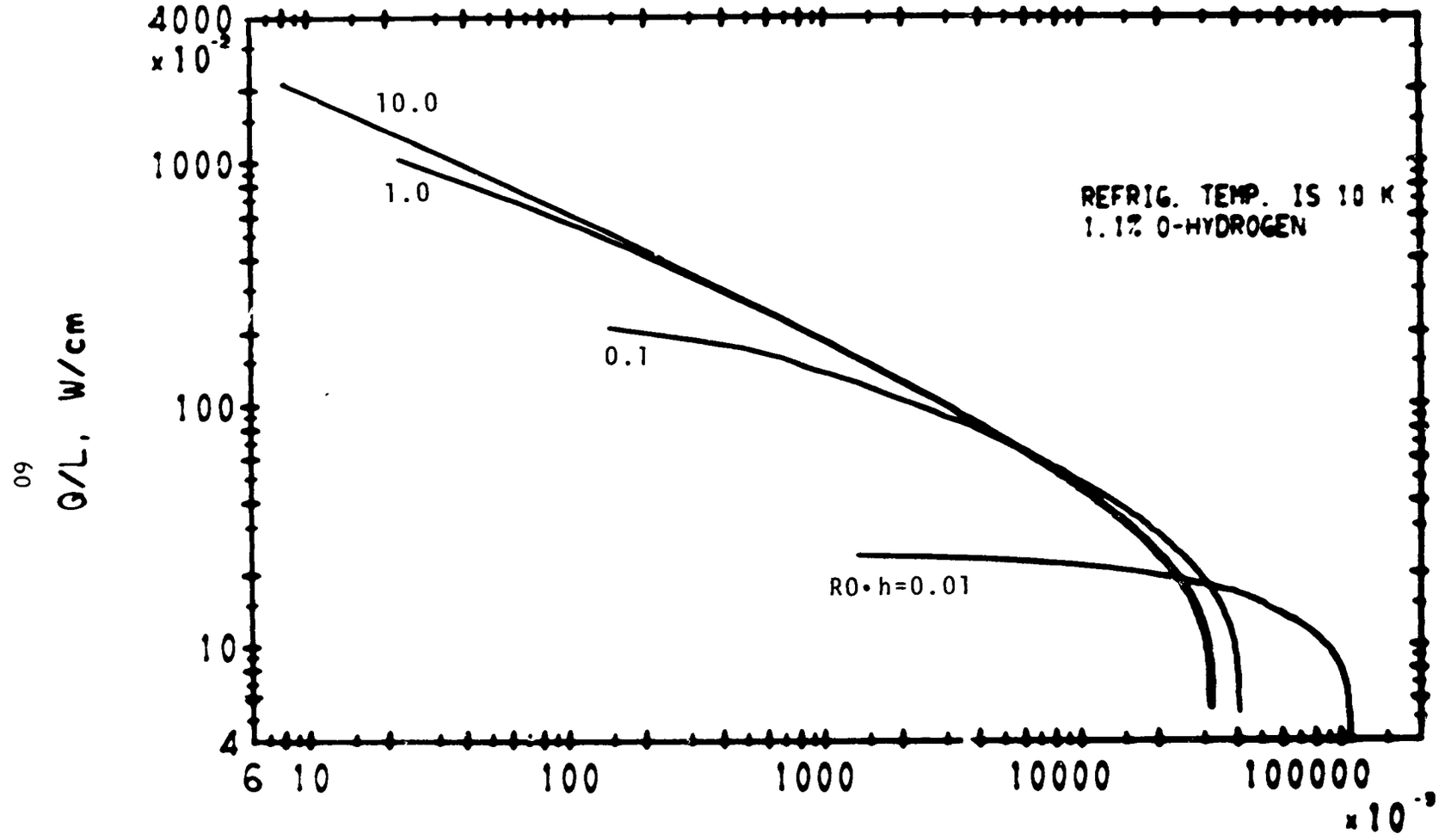

CYLINDER, FREEZING FROM OUTSIDE

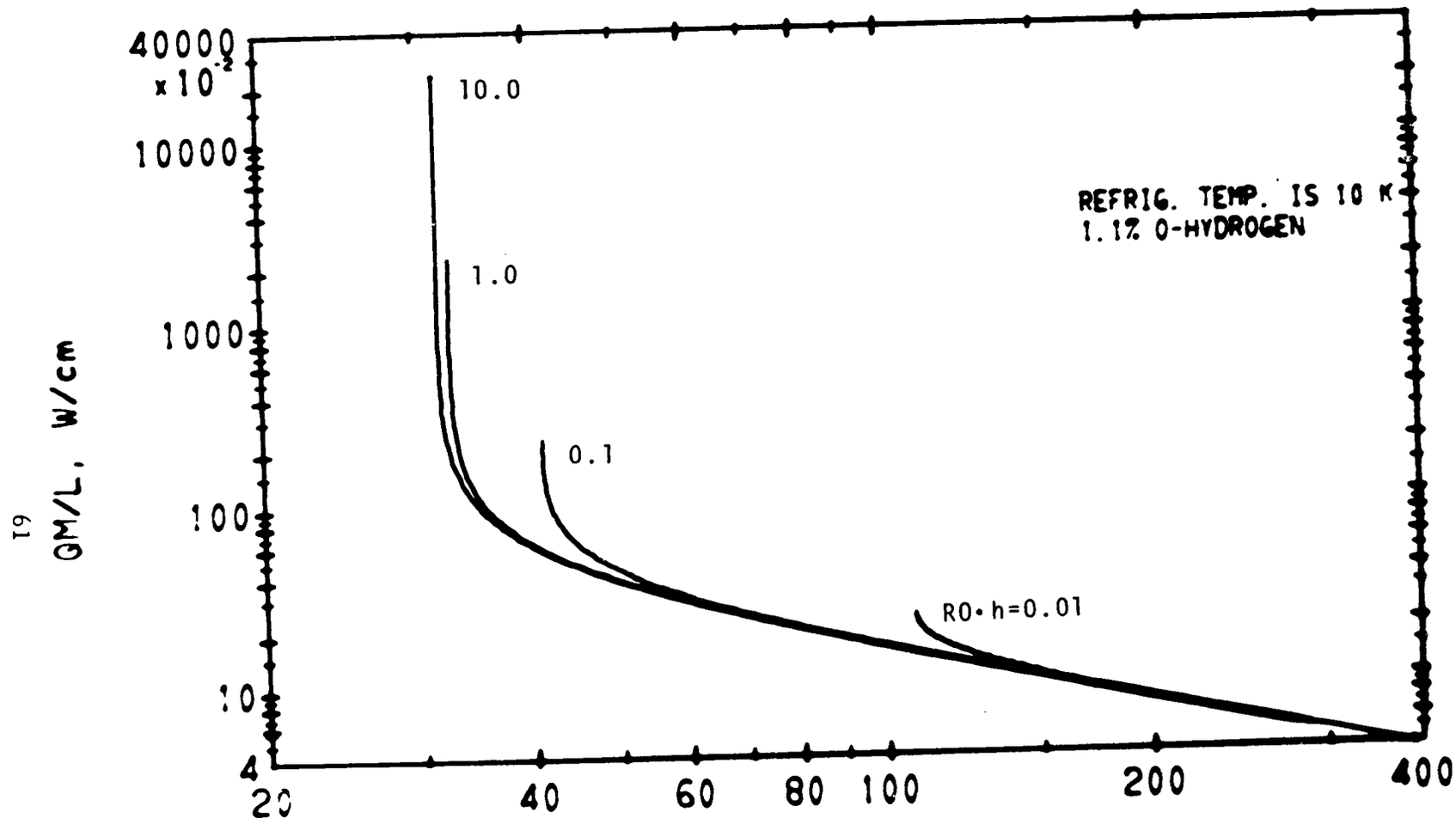

CYLINDER, FREEZING FROM OUTSIDE

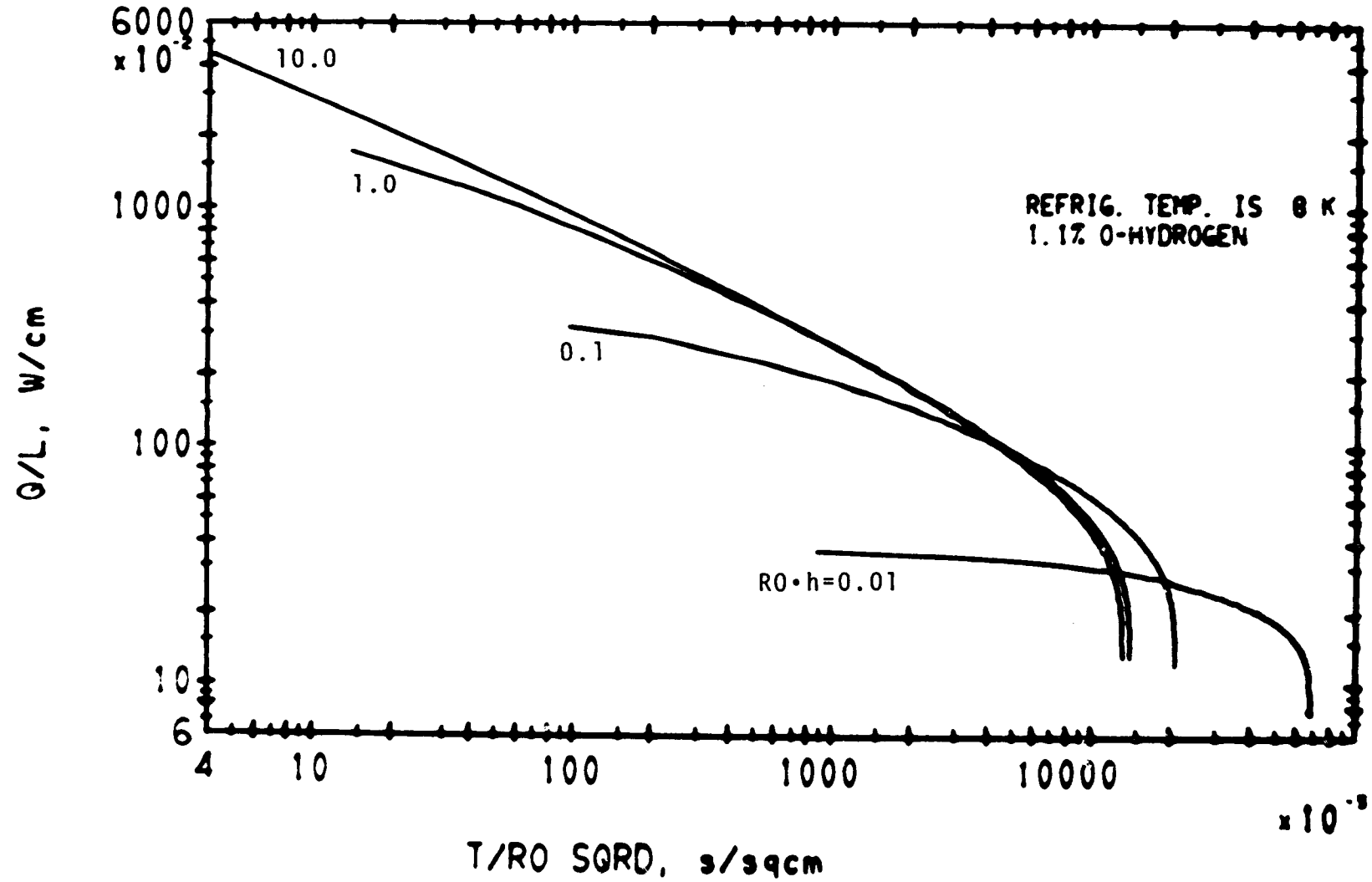

29

CYLINDER, FREEZING FROM OUTSIDE

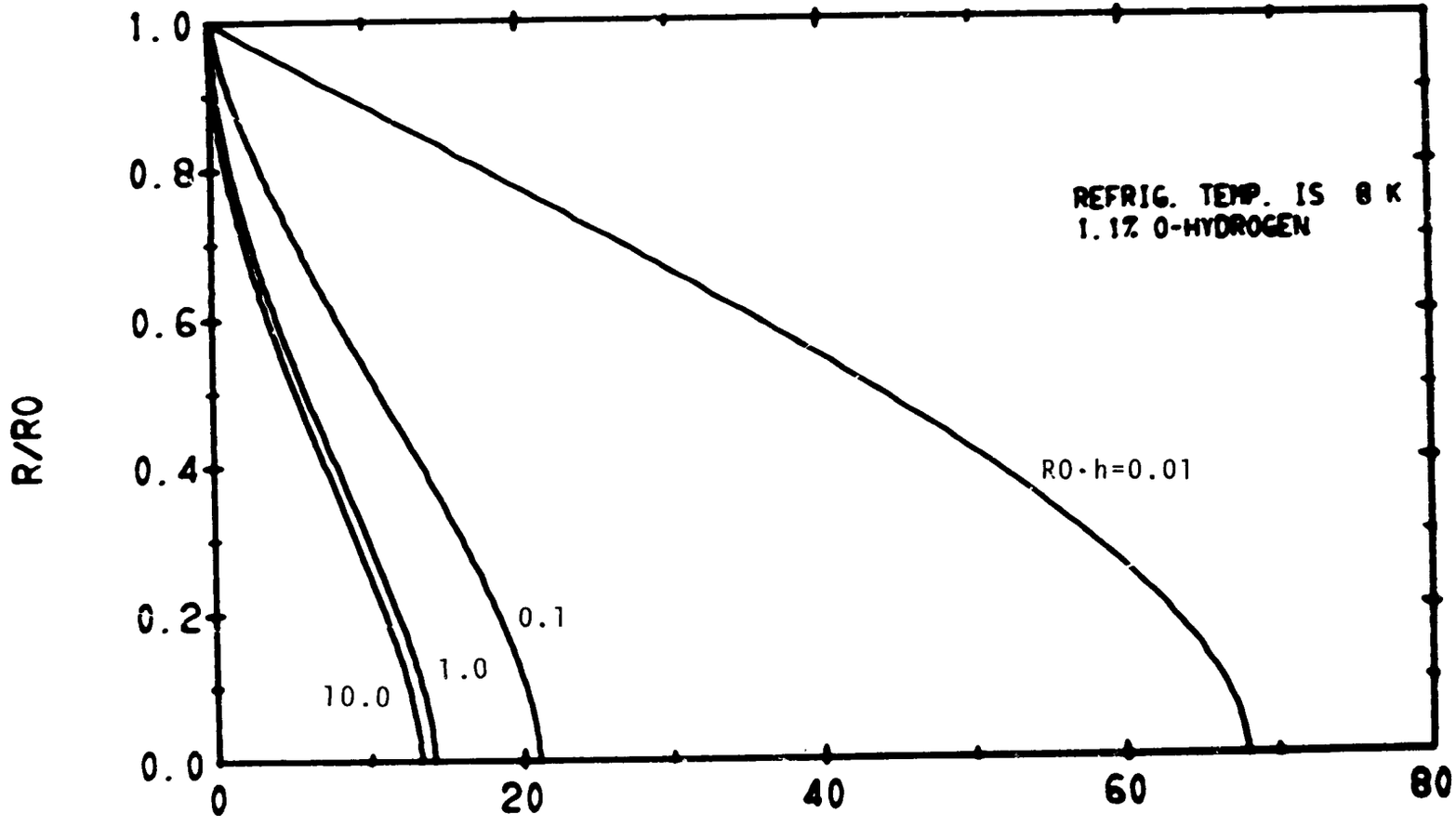

12/17/71

CYLINDER, FREEZING FROM OUTSIDE

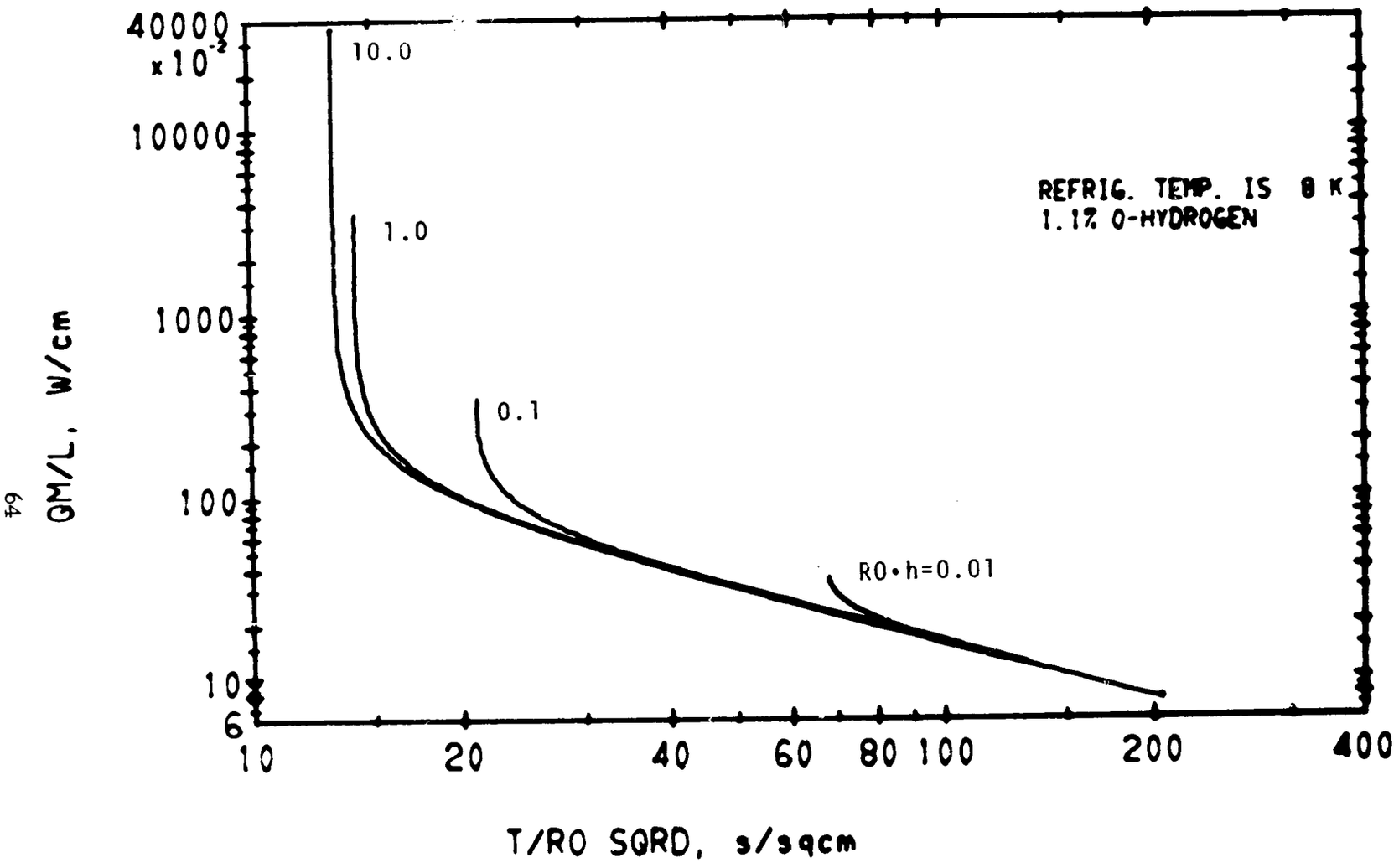

CYLINDER, FREEZING FROM OUTSIDE

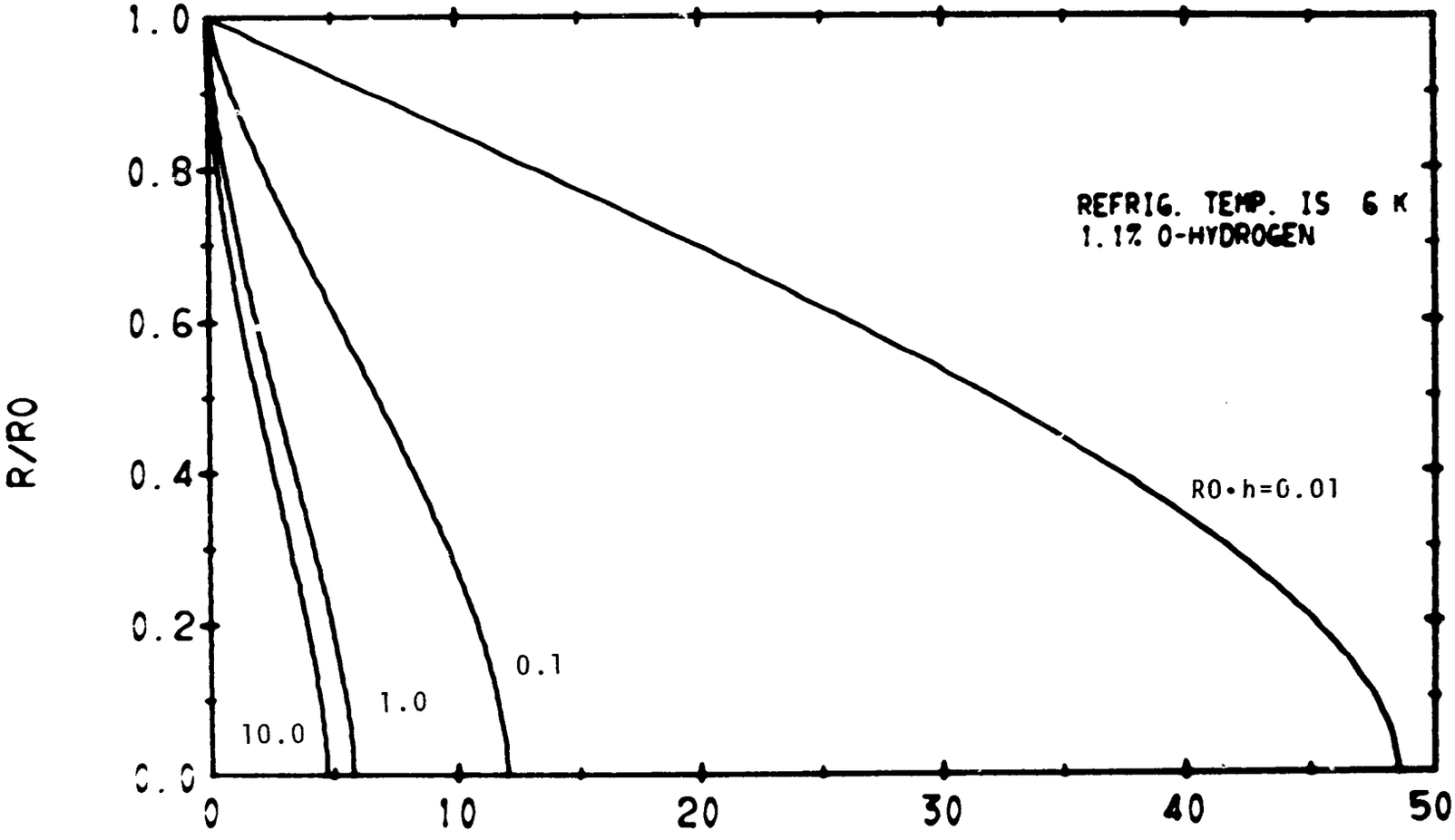

CYLINDER, FREEZING FROM OUTSIDE

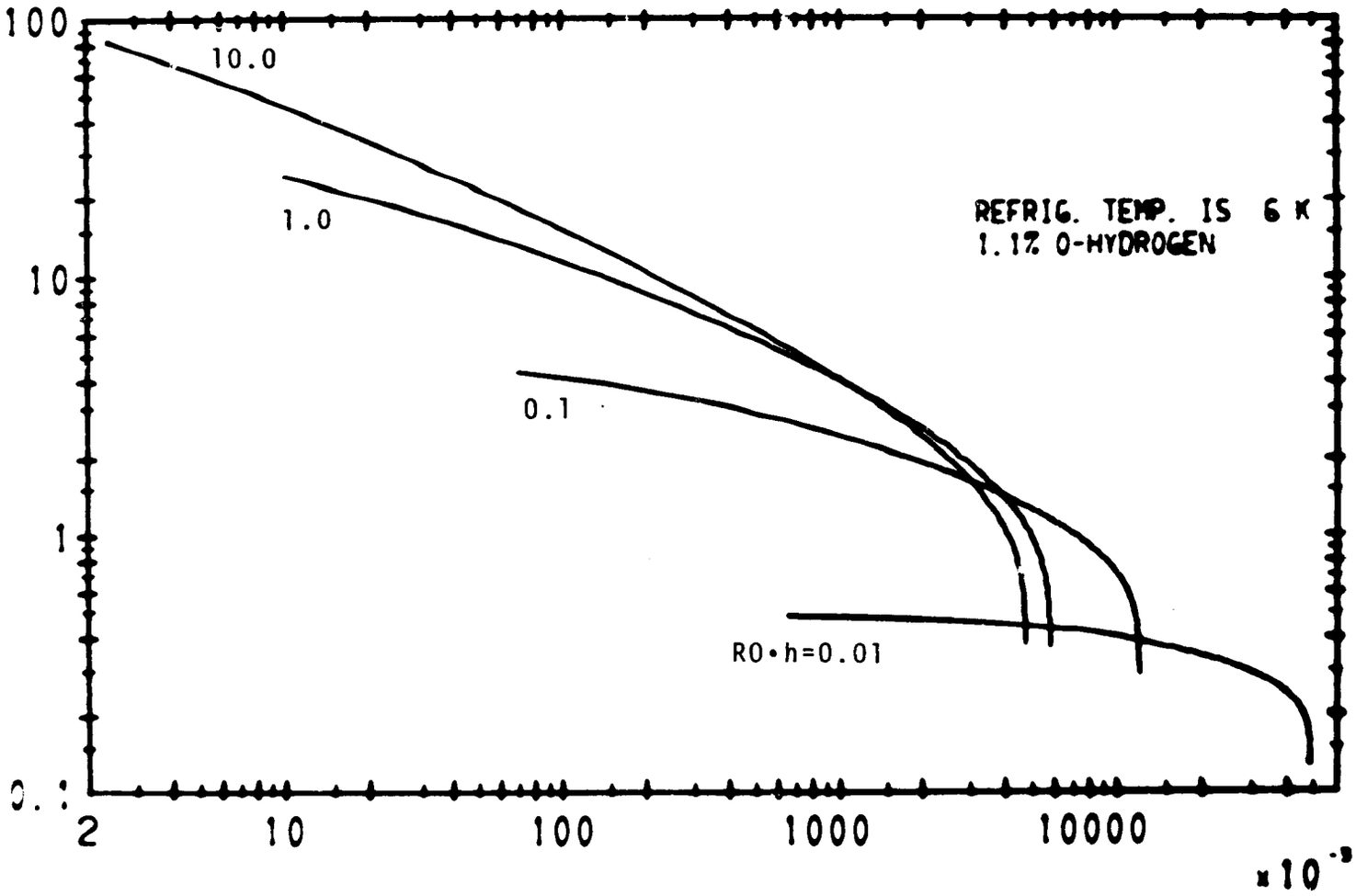

CYLINDER, FREEZING FROM OUTSIDE

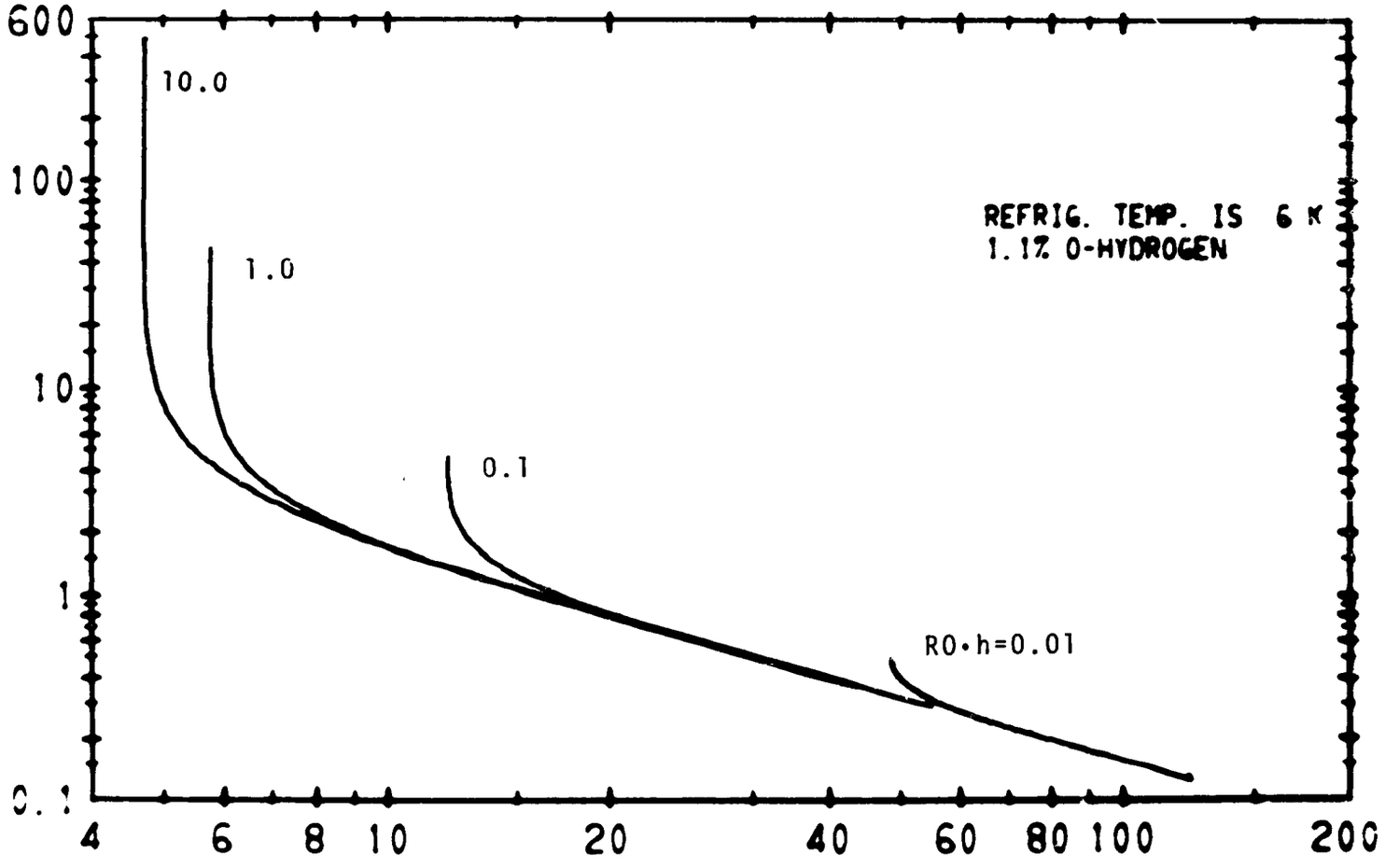

CYLINDER, FREEZING FROM OUTSIDE

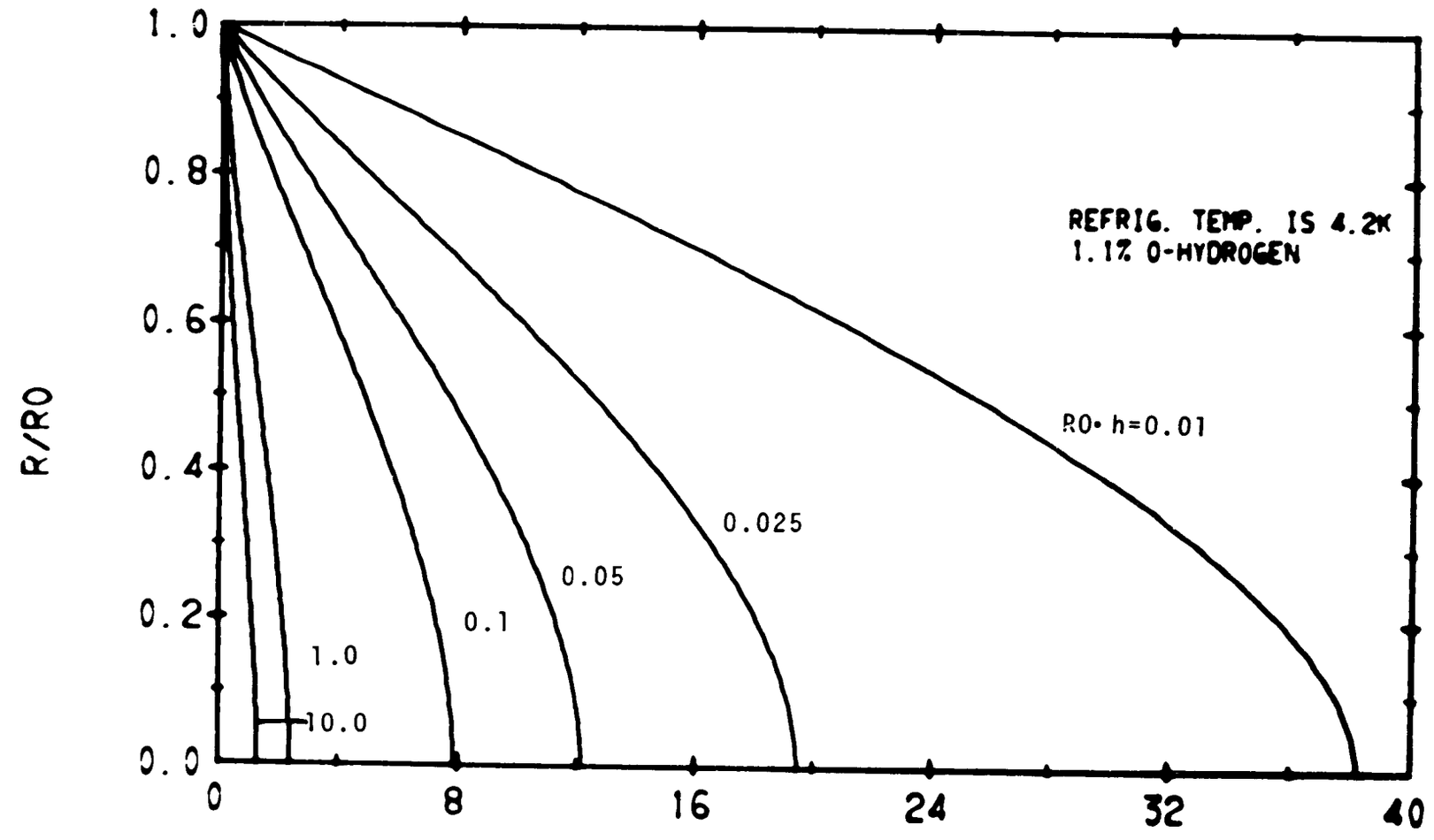

CYLINDER, FREEZING FROM OUTSIDE

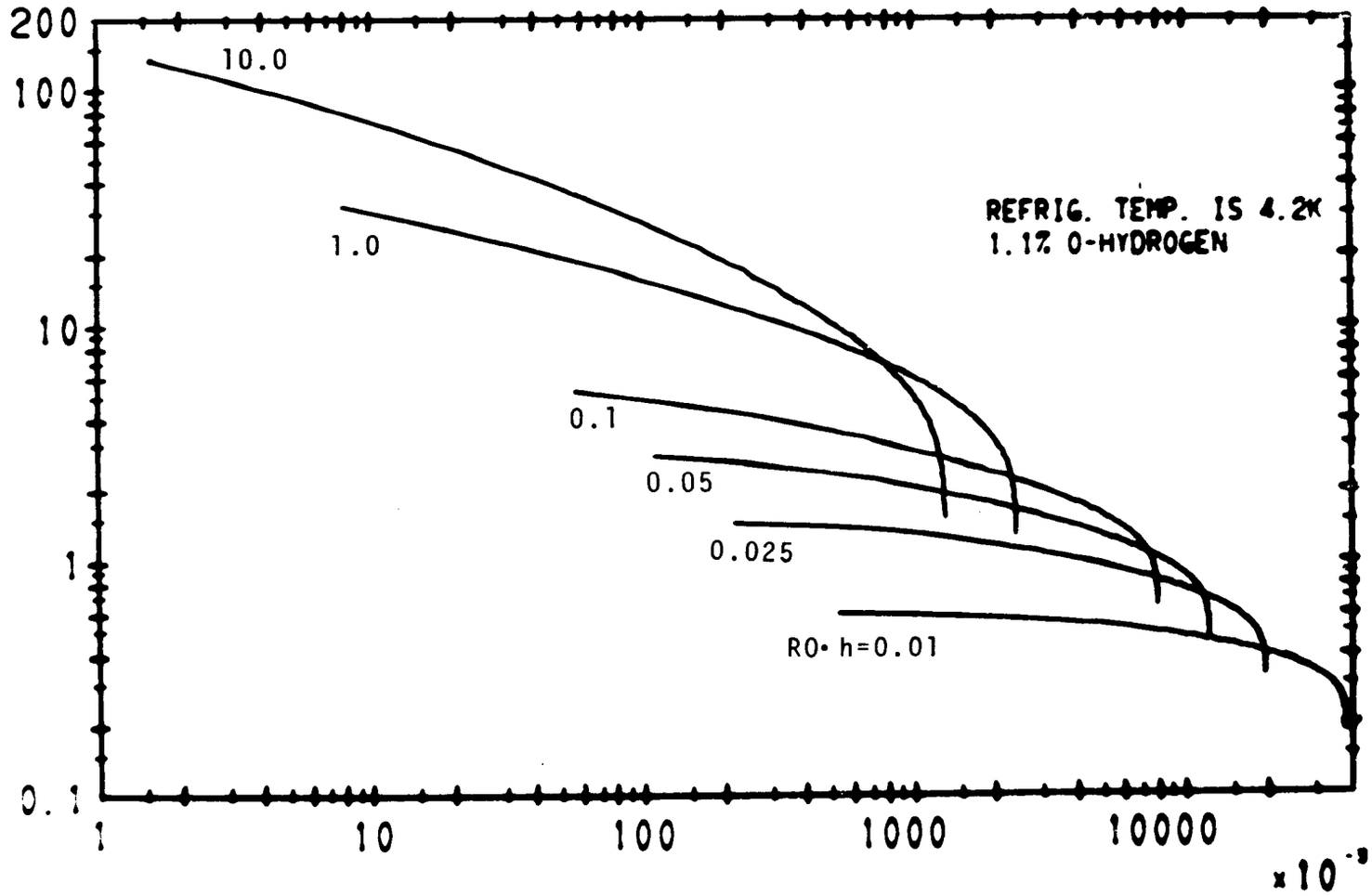

CYLINDER, FREEZING FROM OUTSIDE

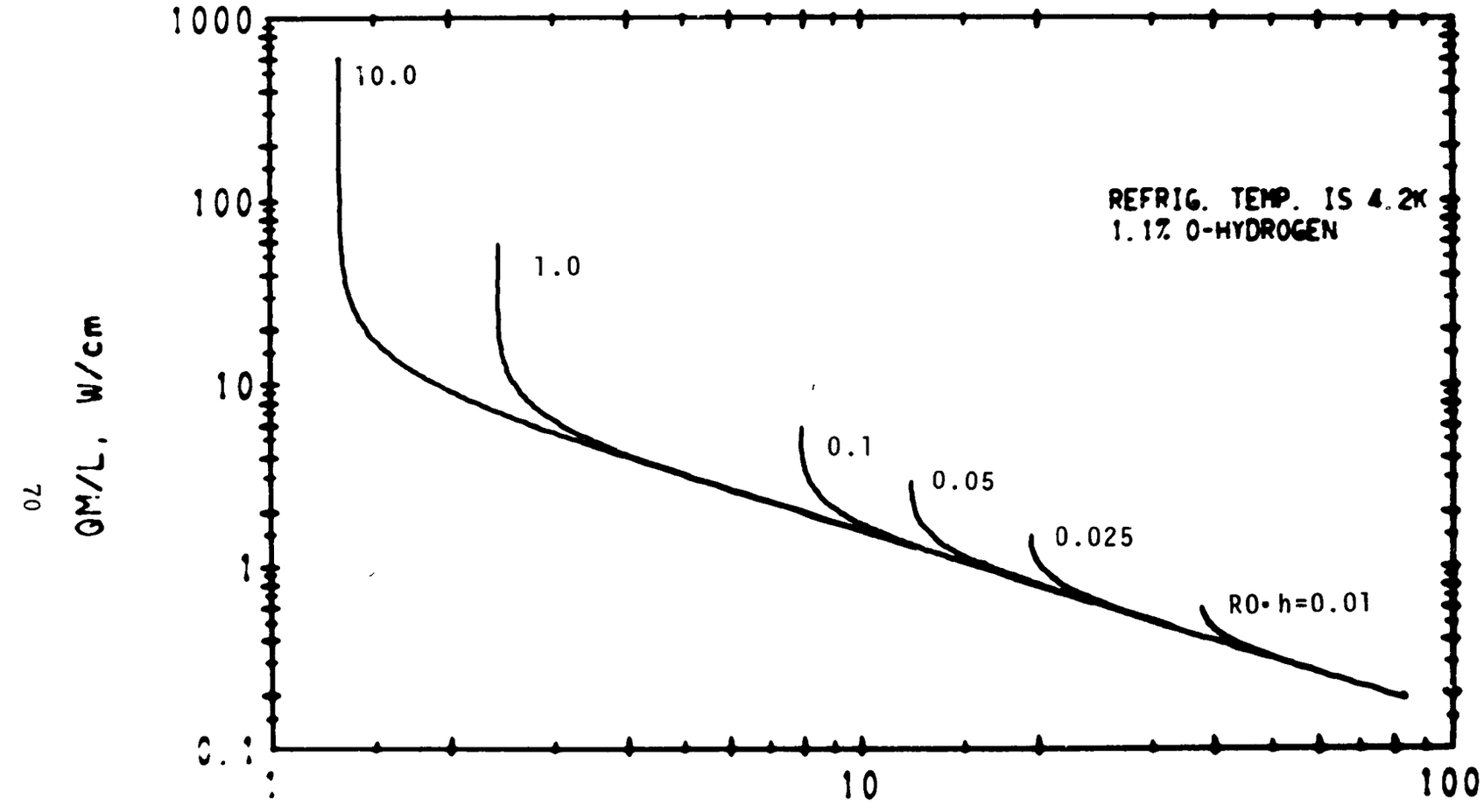

CYLINDER, FREEZING FROM OUTSIDE

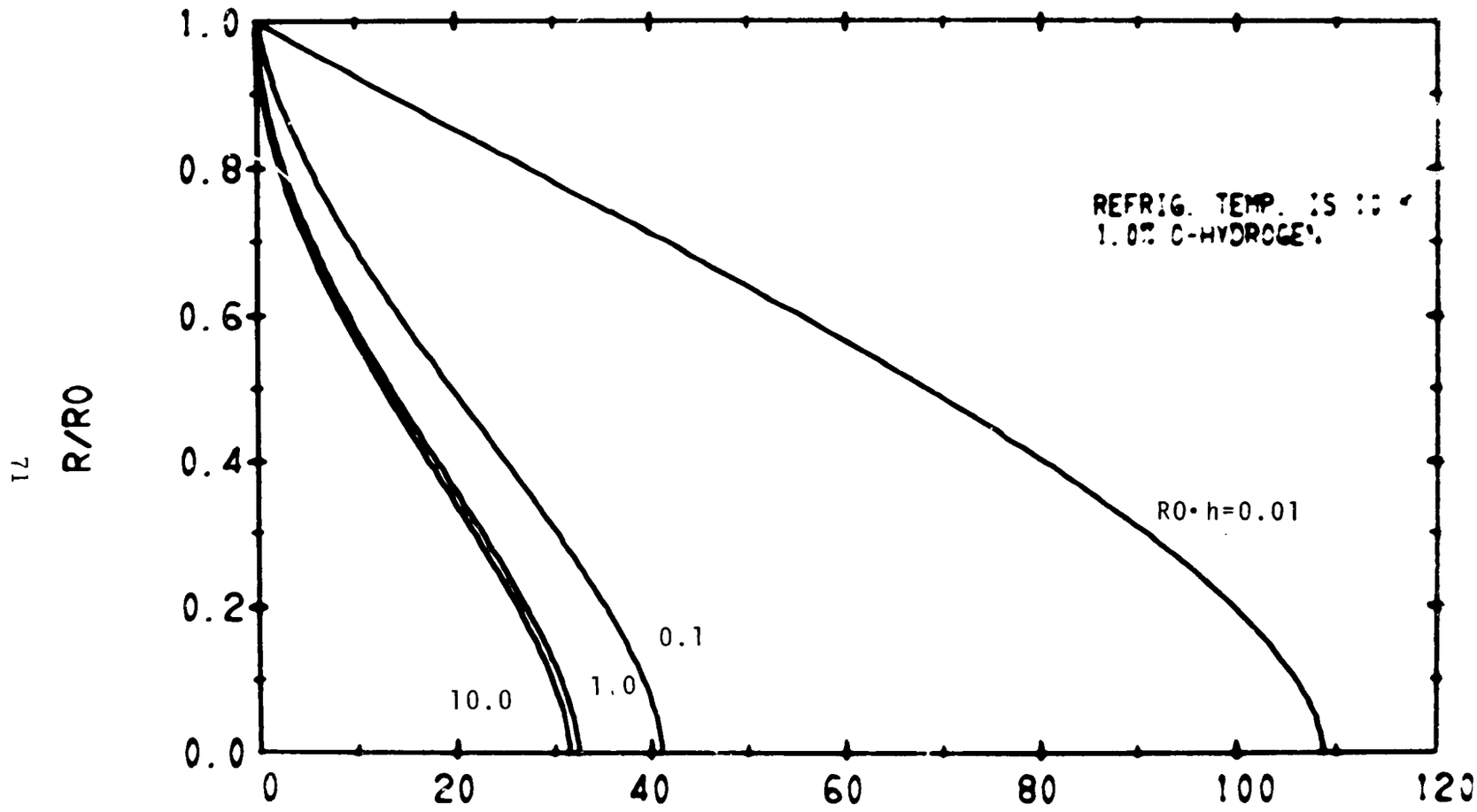

12/28/71

CYLINDER, FREEZING FROM OUTSIDE

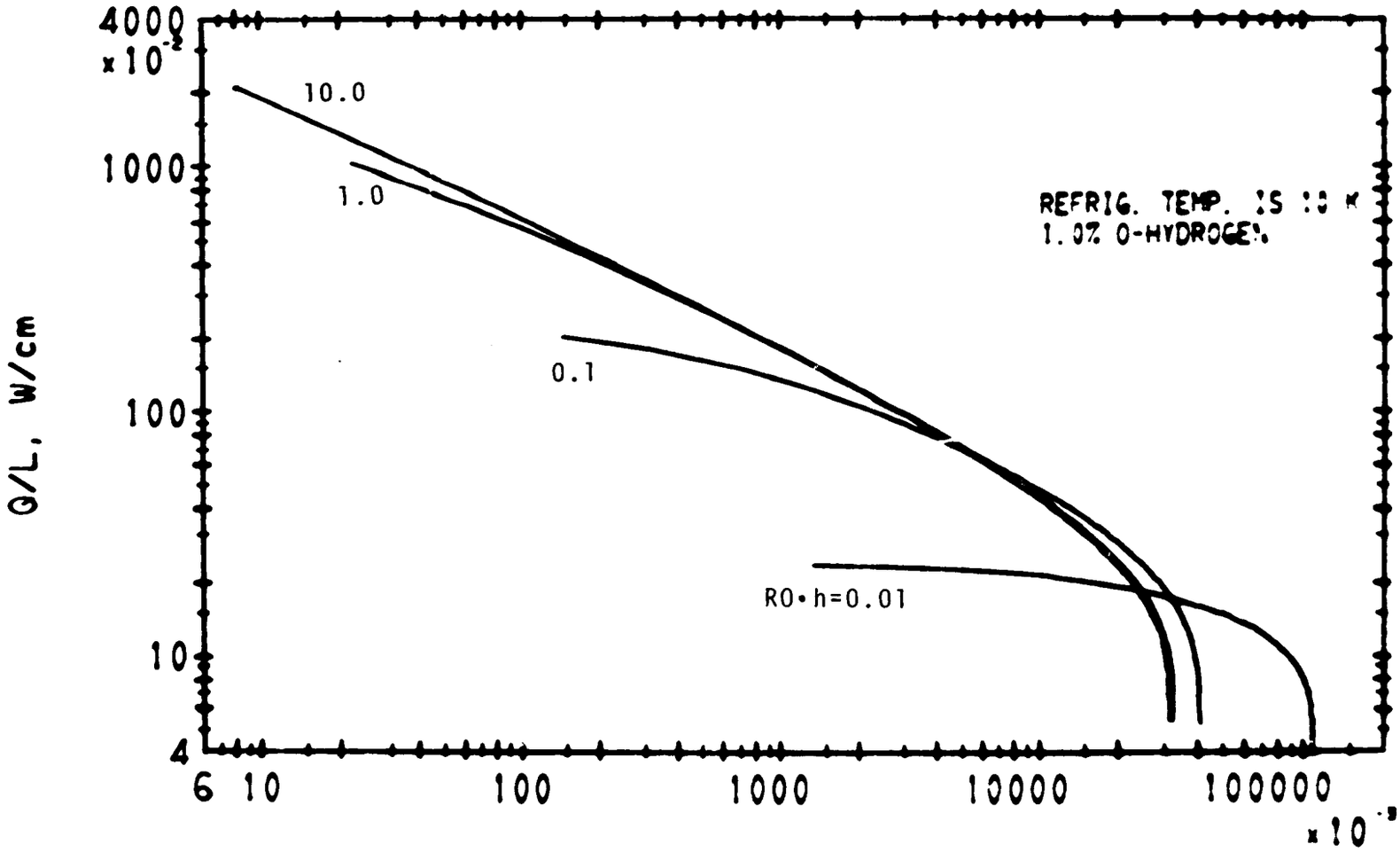

72

12/20/71

CYLINDER, FREEZING FROM OUTSIDE

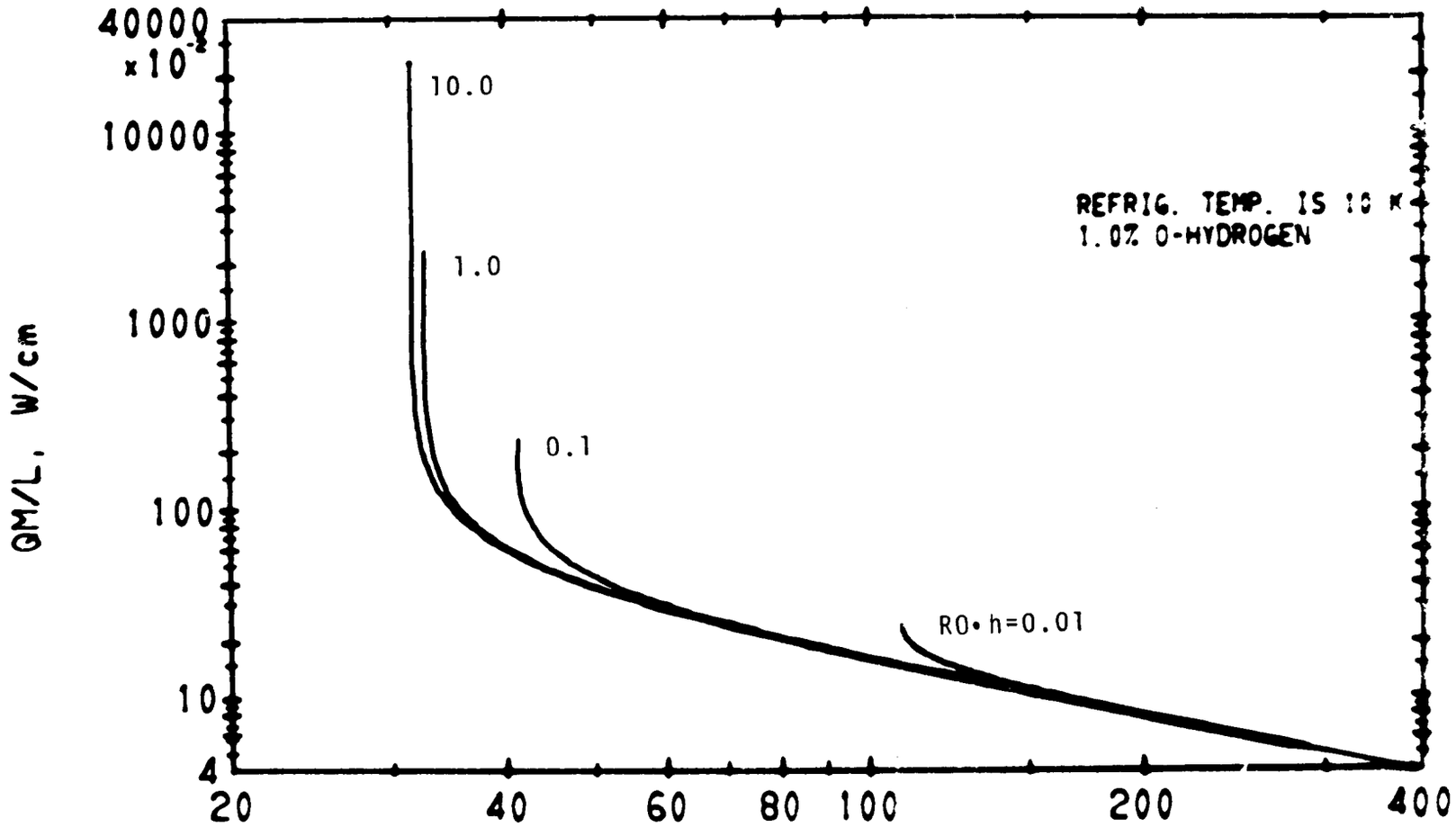

12/20/71

CYLINDER, FREEZING FROM OUTSIDE

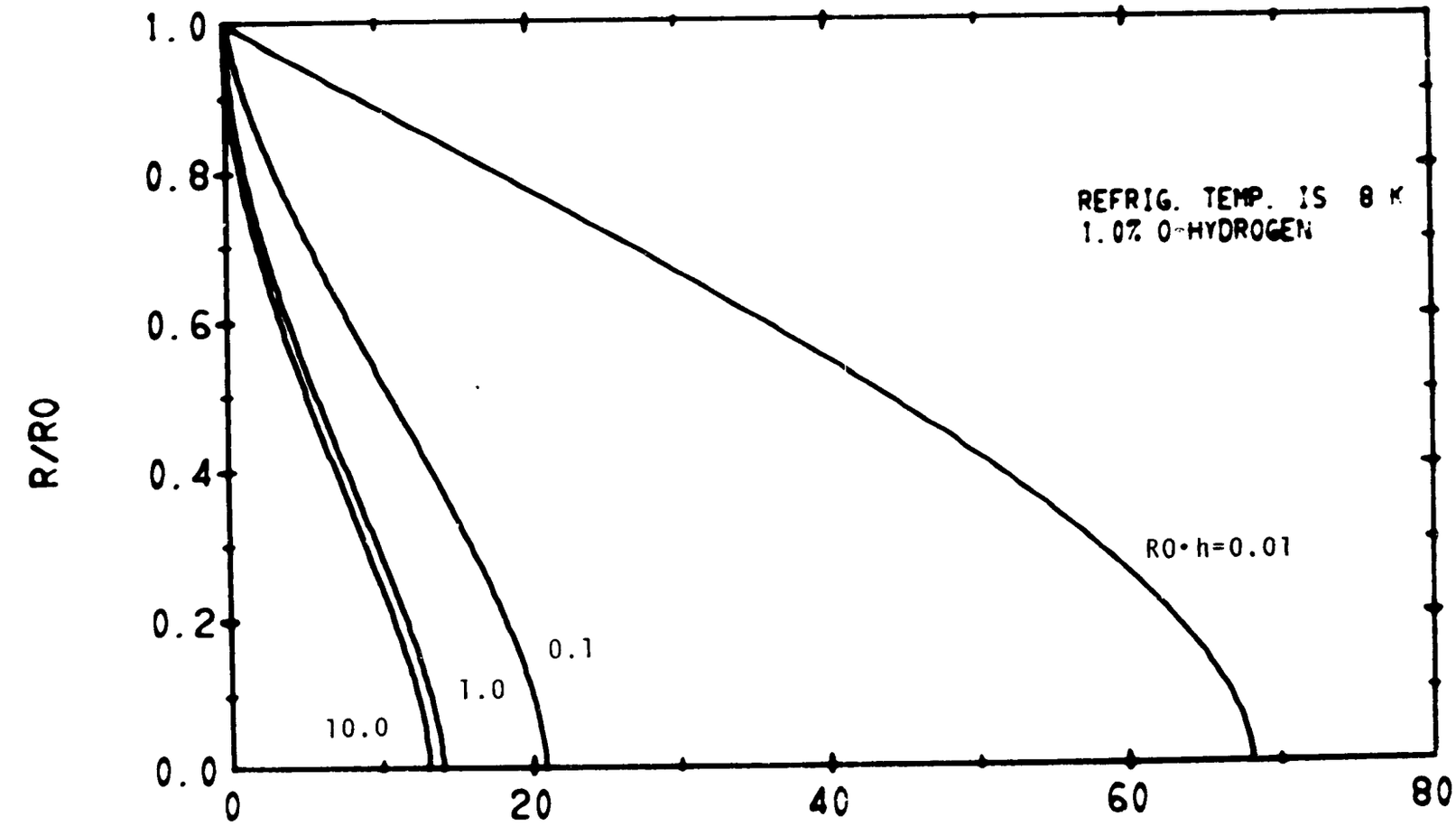

12/20/71

CYLINDER, FREEZING FROM OUTSIDE

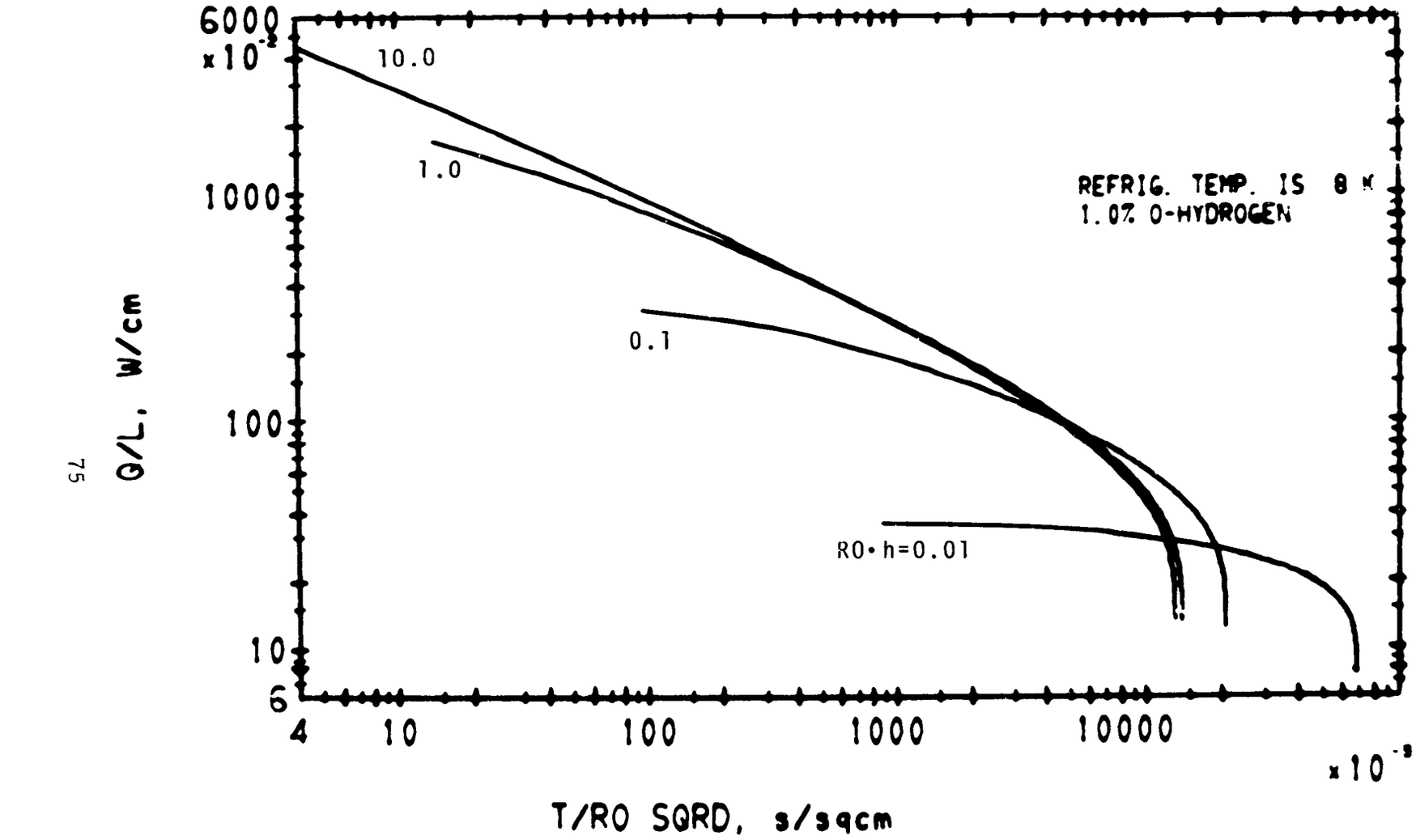

12/20/71

CYLINDER, FREEZING FROM OUTSIDE

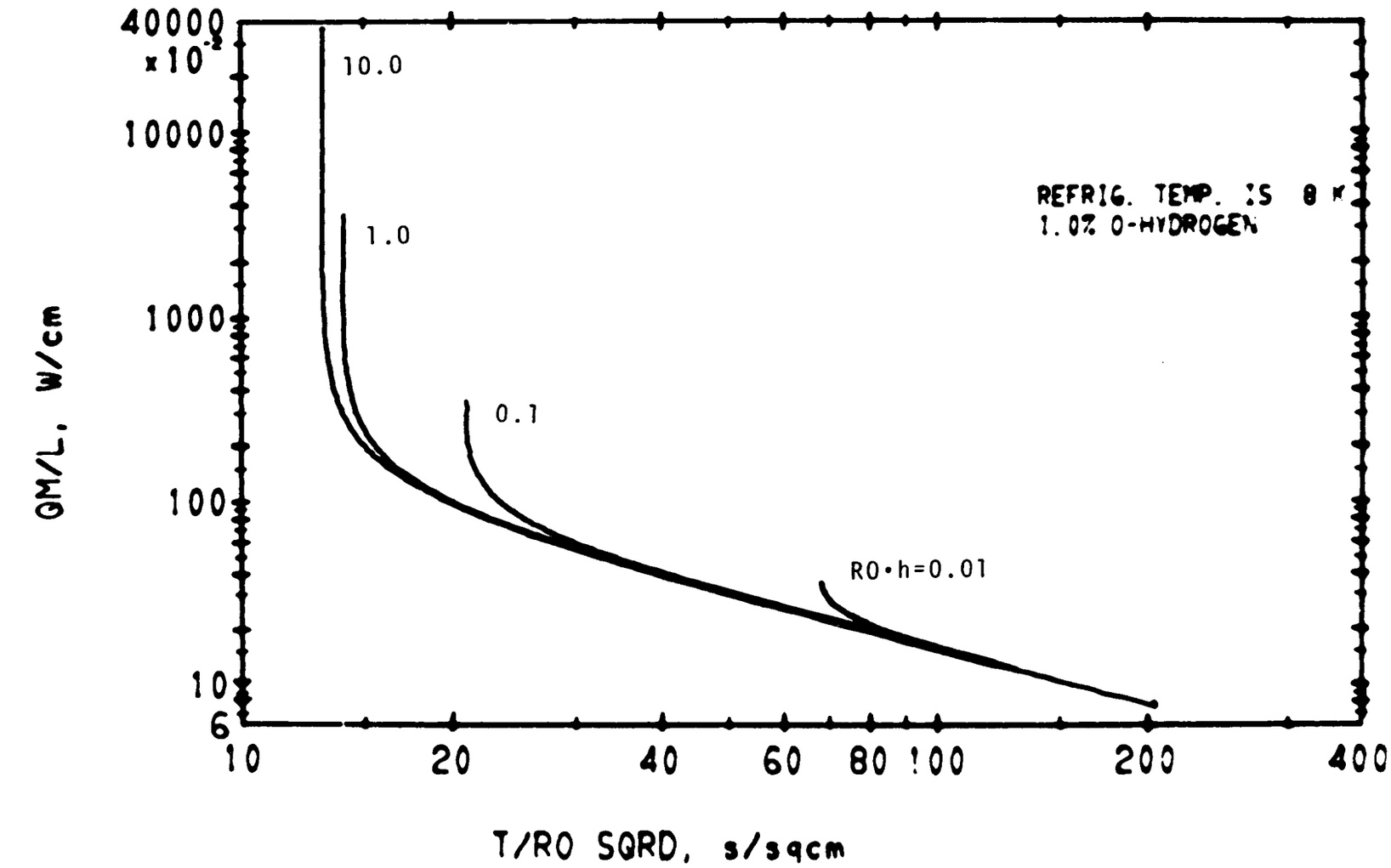

12/20/71

CYLINDER, FREEZING FROM OUTSIDE

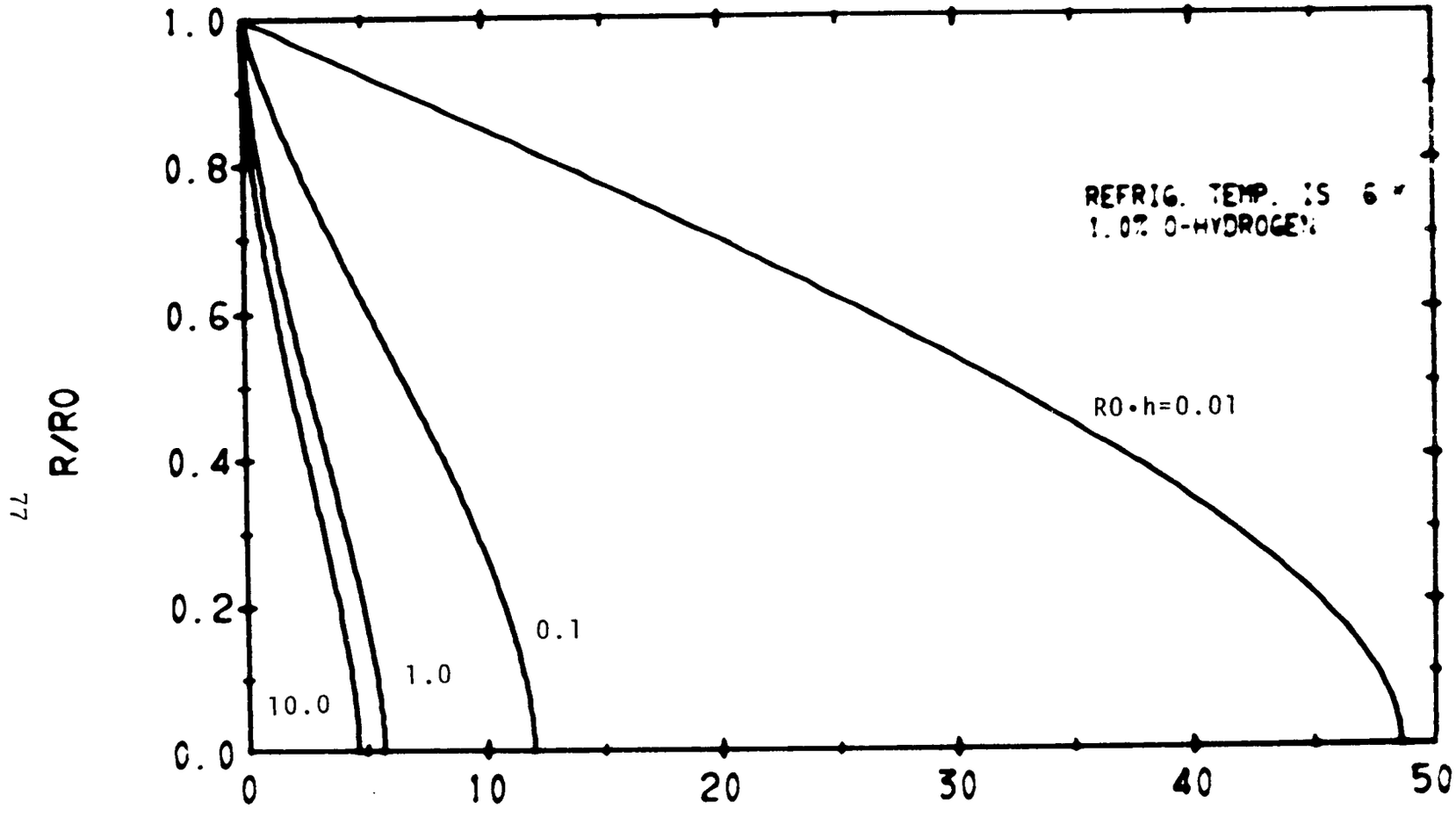

77

12/20/71

CYLINDER, FREEZING FROM OUTSIDE

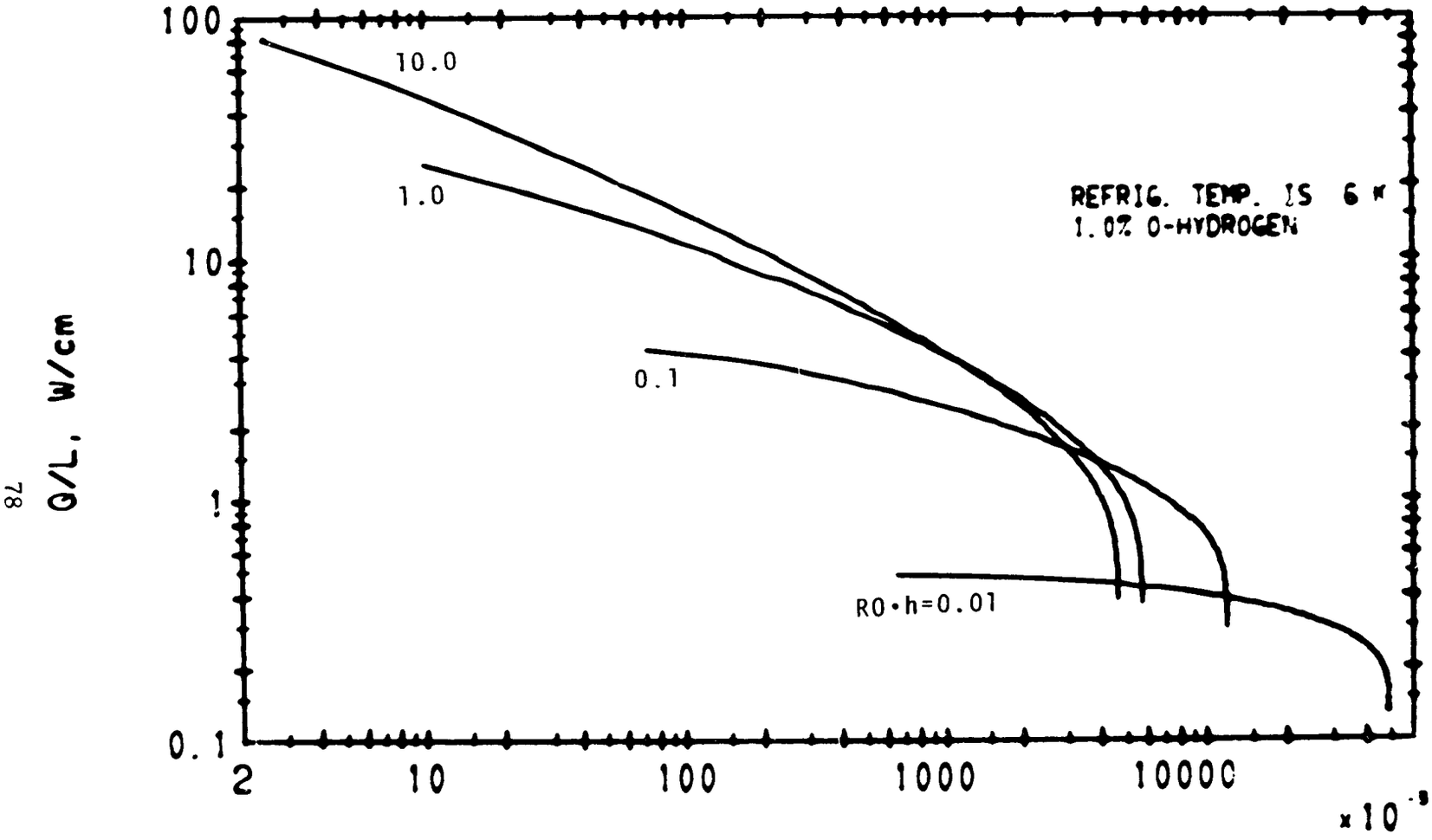

78

12/20/71

CYLINDER, FREEZING FROM OUTSIDE

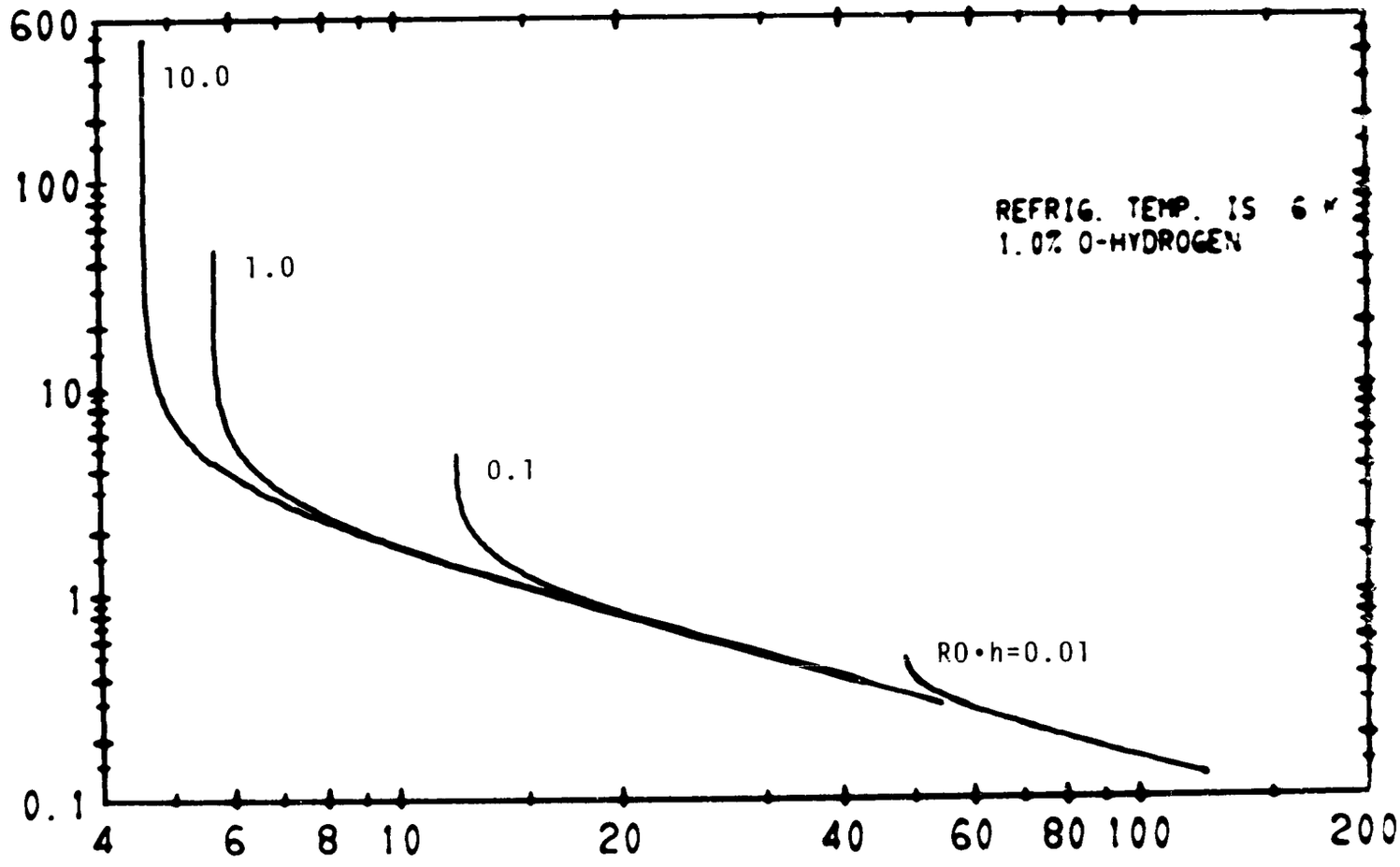

CYLINDER, FREEZING FROM OUTSIDE

12/28/71

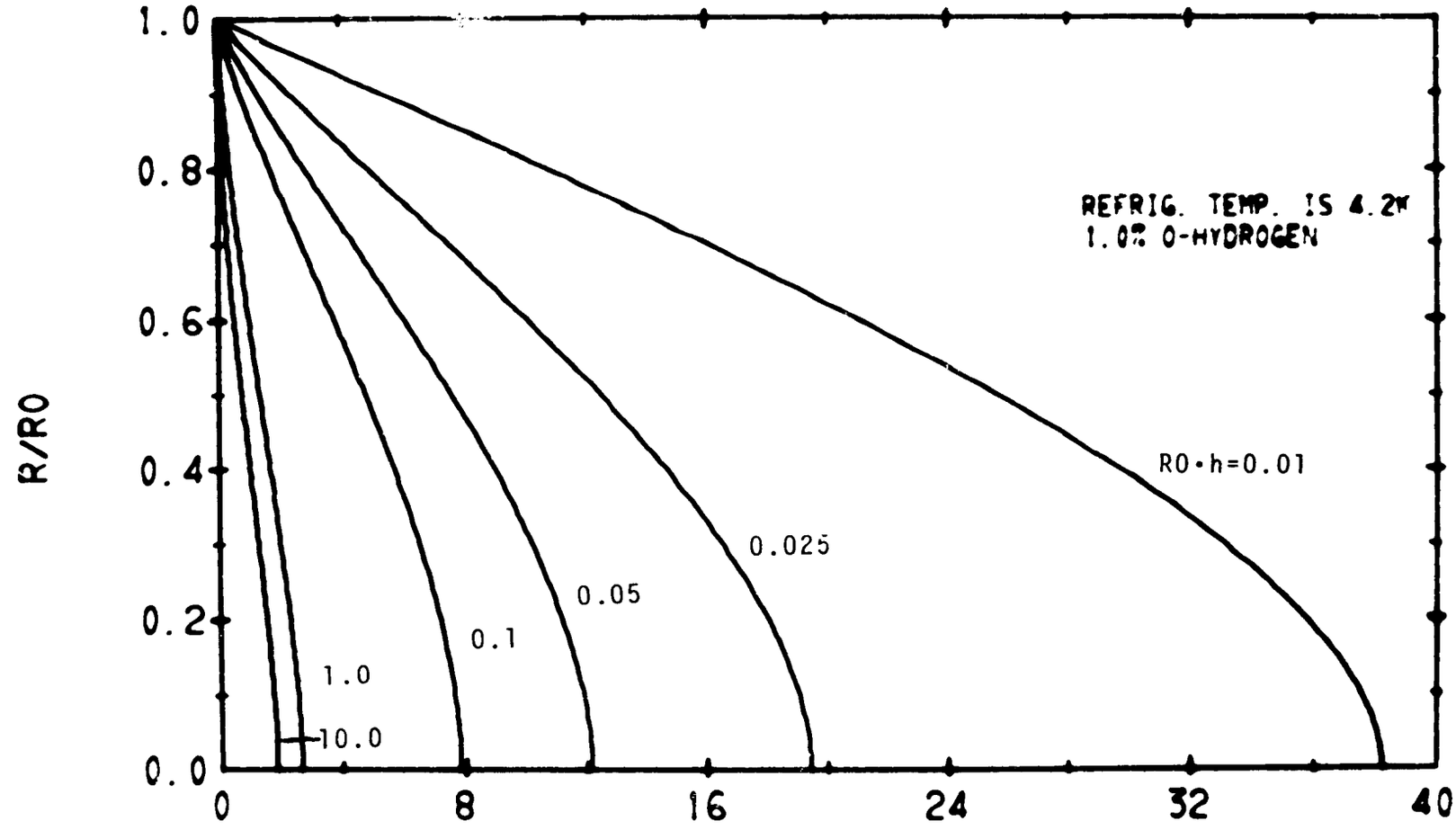

CYLINDER, FREEZING FROM OUTSIDE

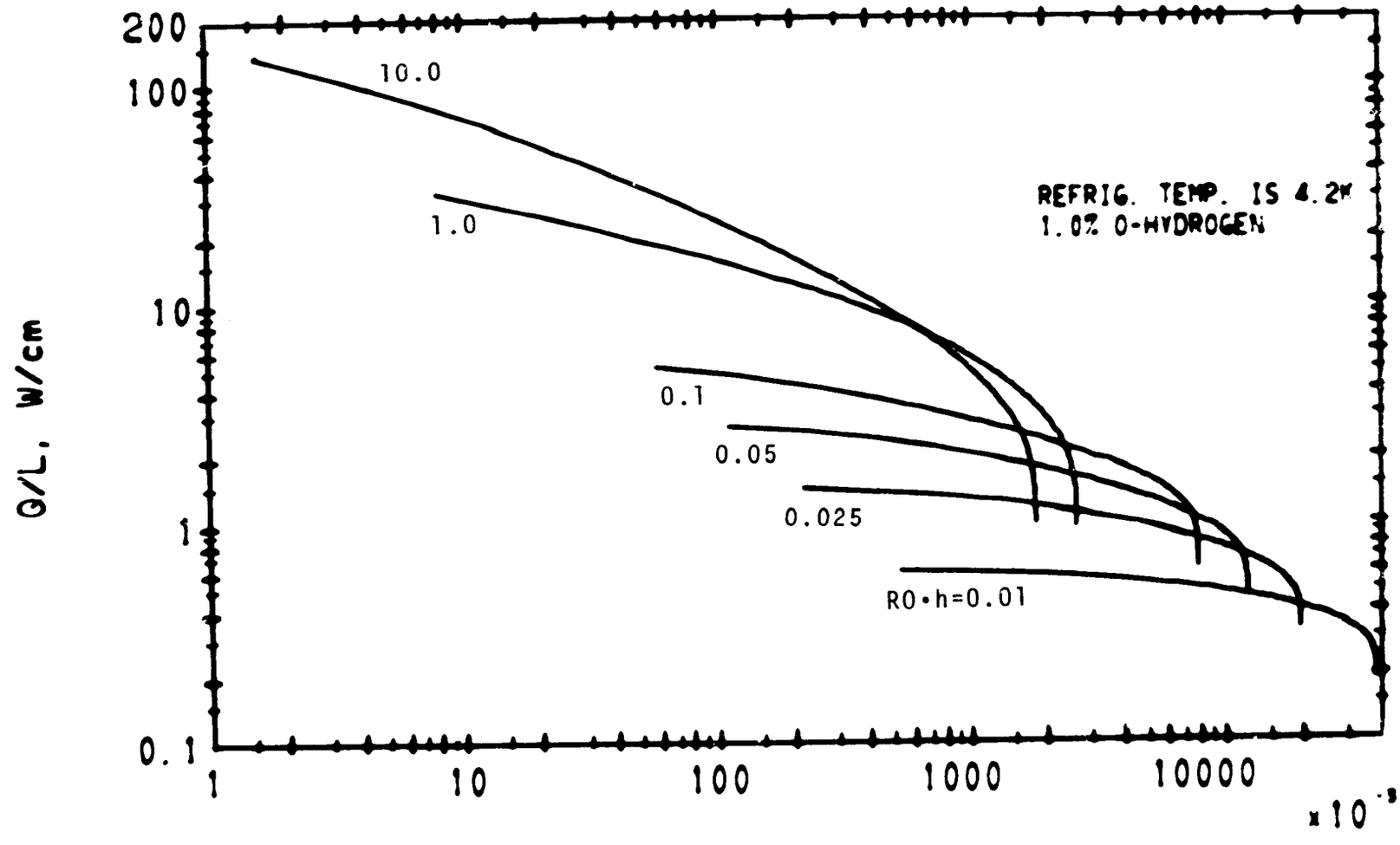

12/28/71

CYLINDER, FREEZING FROM OUTSIDE

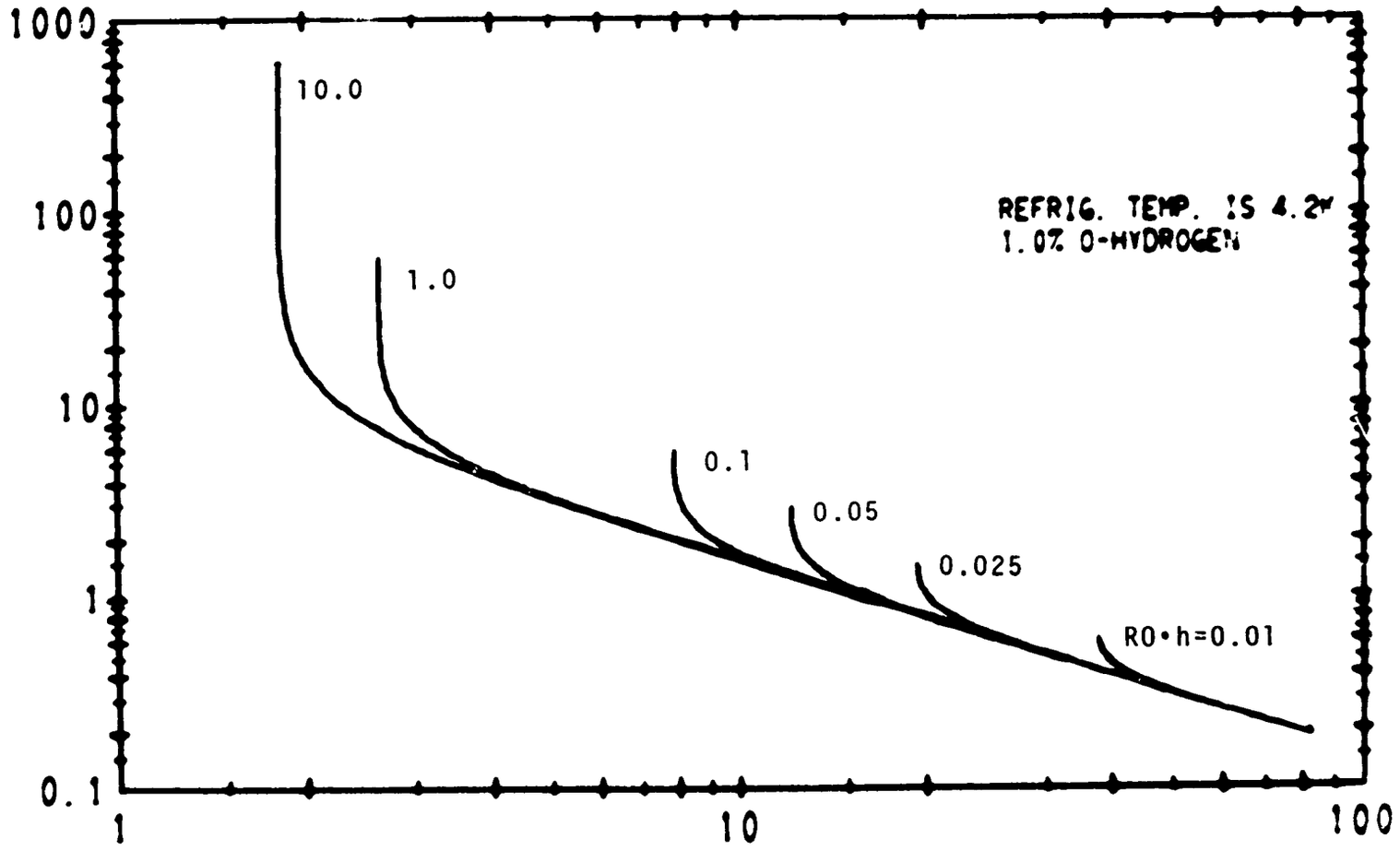

12/20/71

CYLINDER, FREEZING FROM OUTSIDE

APPENDIX B

CYLINDER FREEZING FROM THE INSIDE

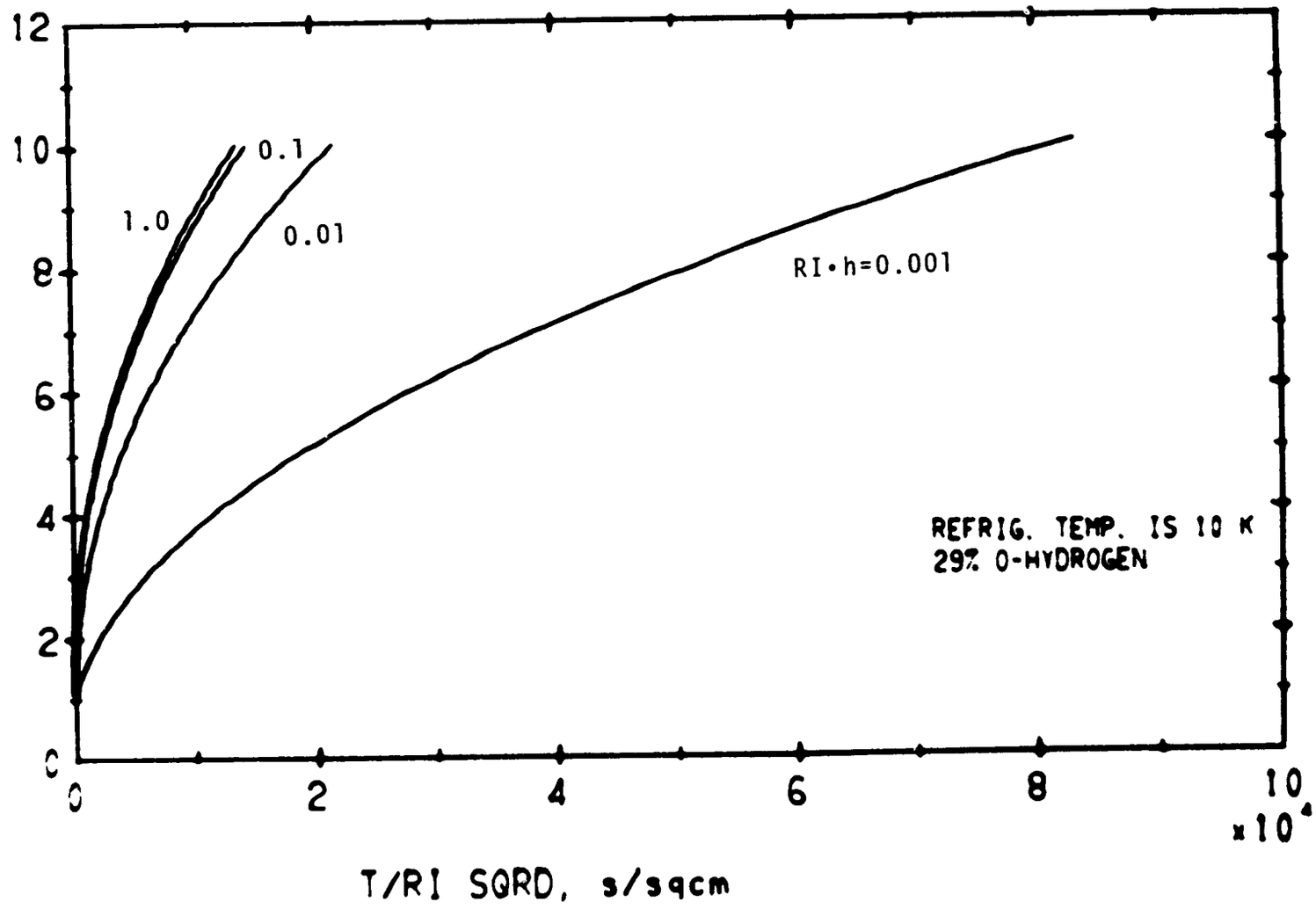

CYLINDER, FREEZING FROM INSIDE

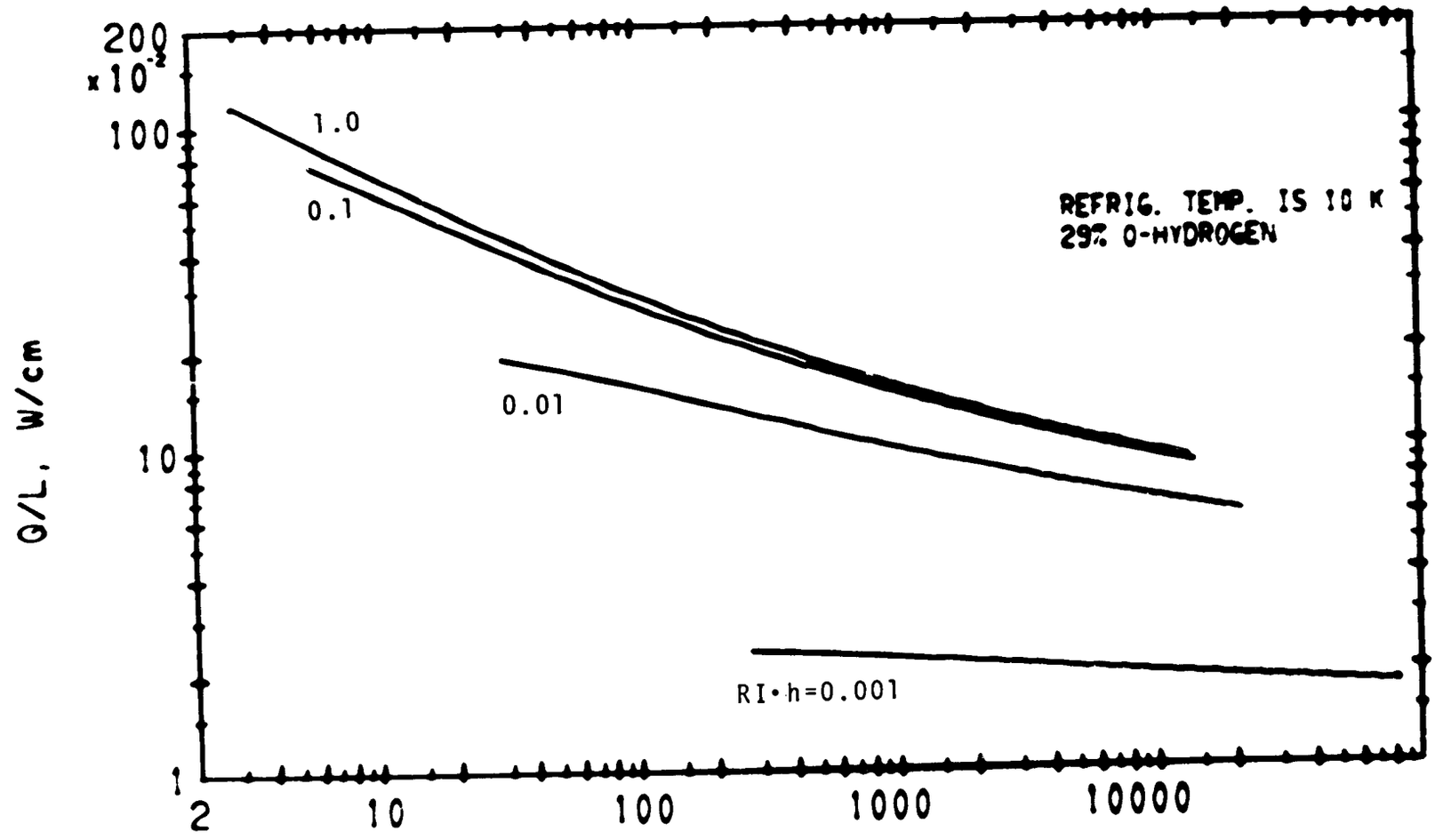

CYLINDER, FREEZING FROM INSIDE

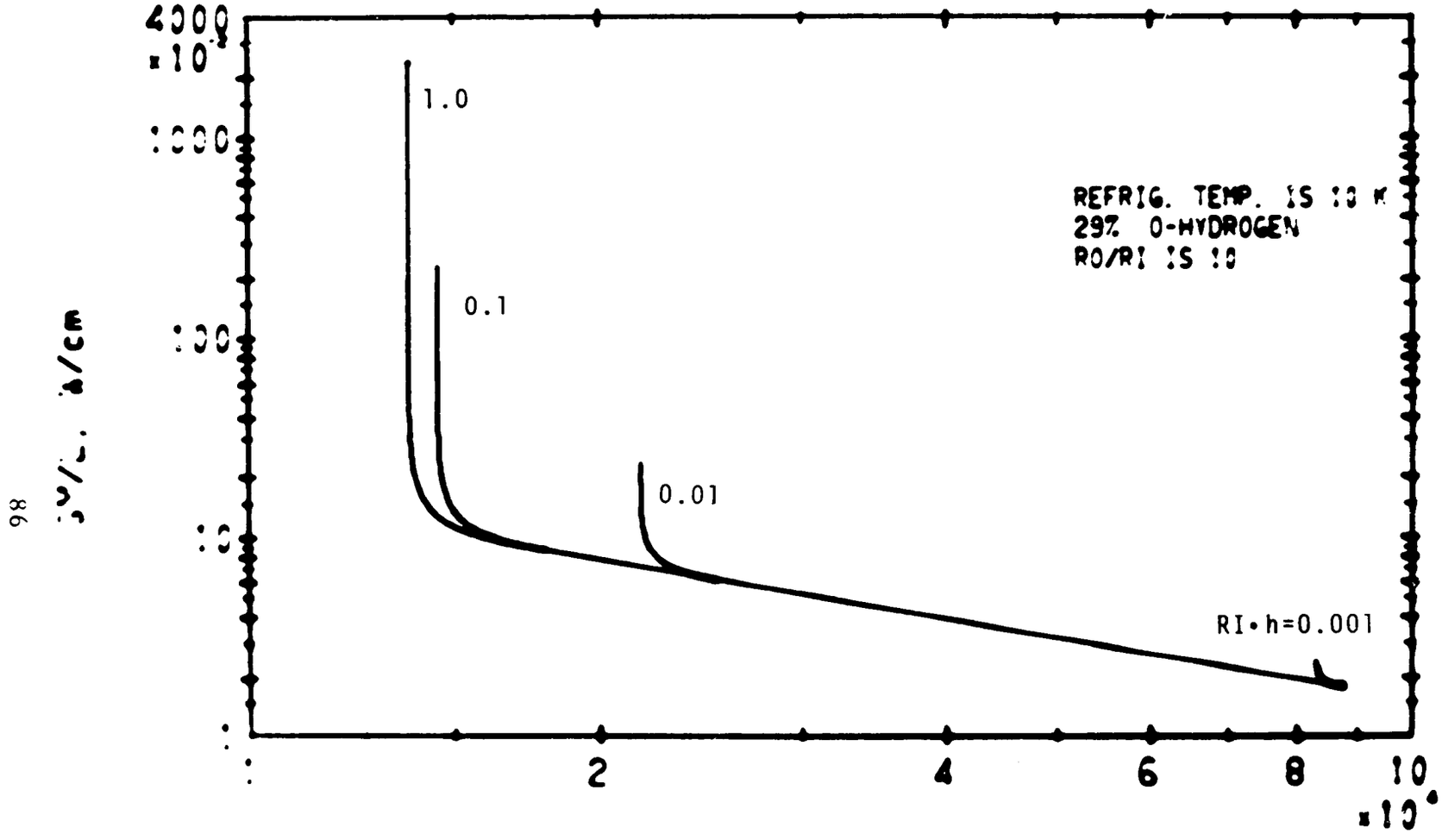

CYLINDER, FREEZING FROM INSIDE

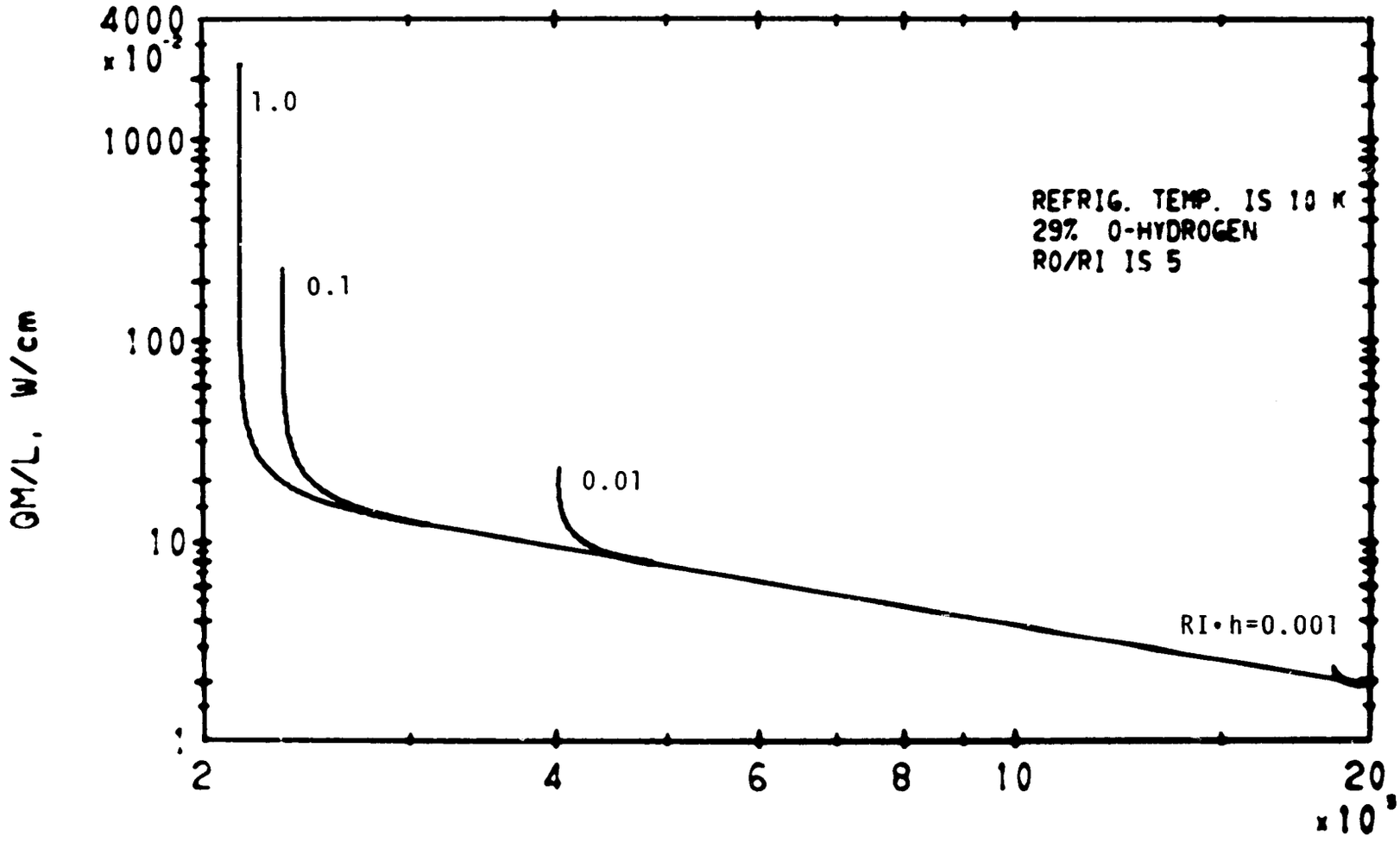

CYLINDER, FREEZING FROM INSIDE

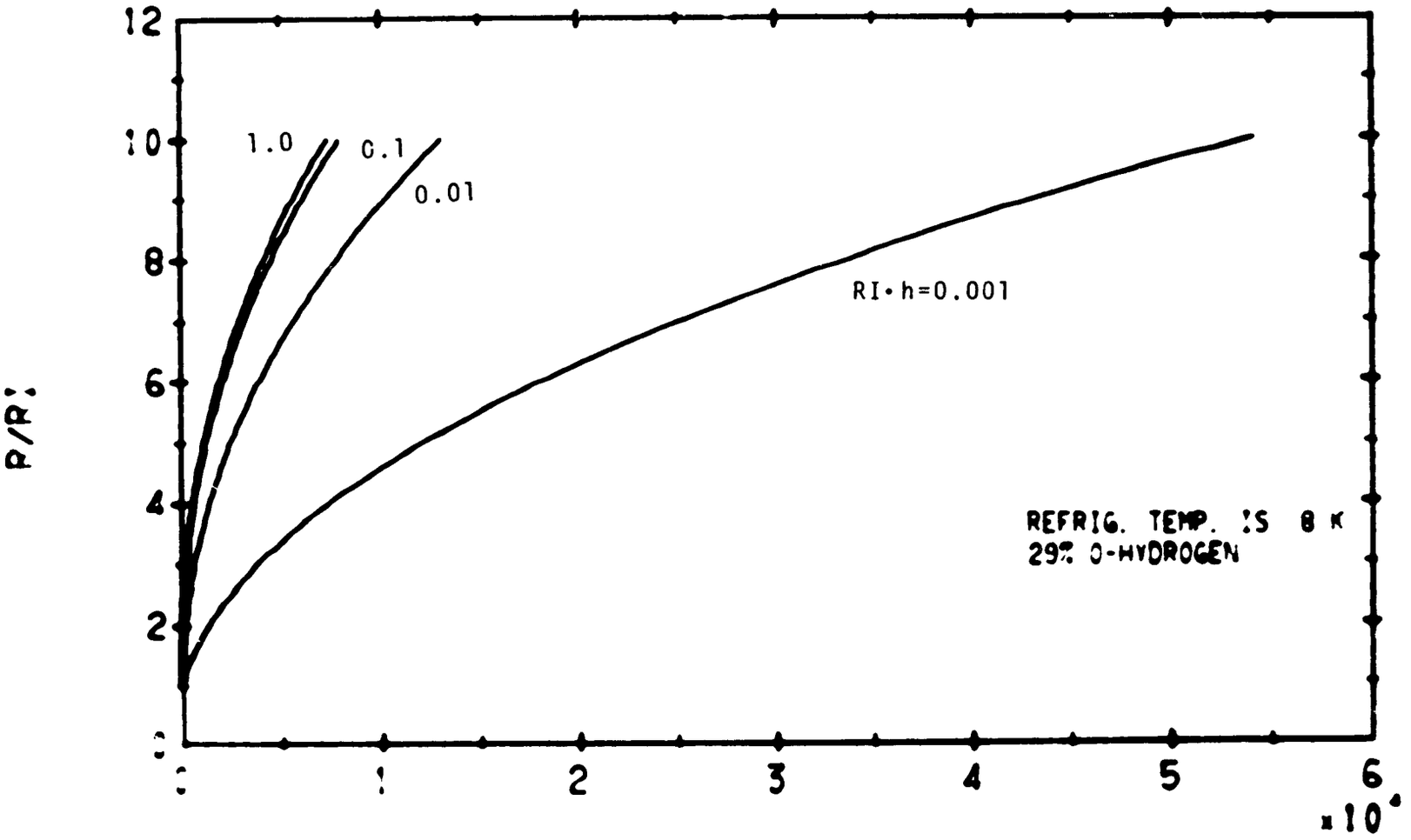

CYLINDER, FREEZING FROM INSIDE

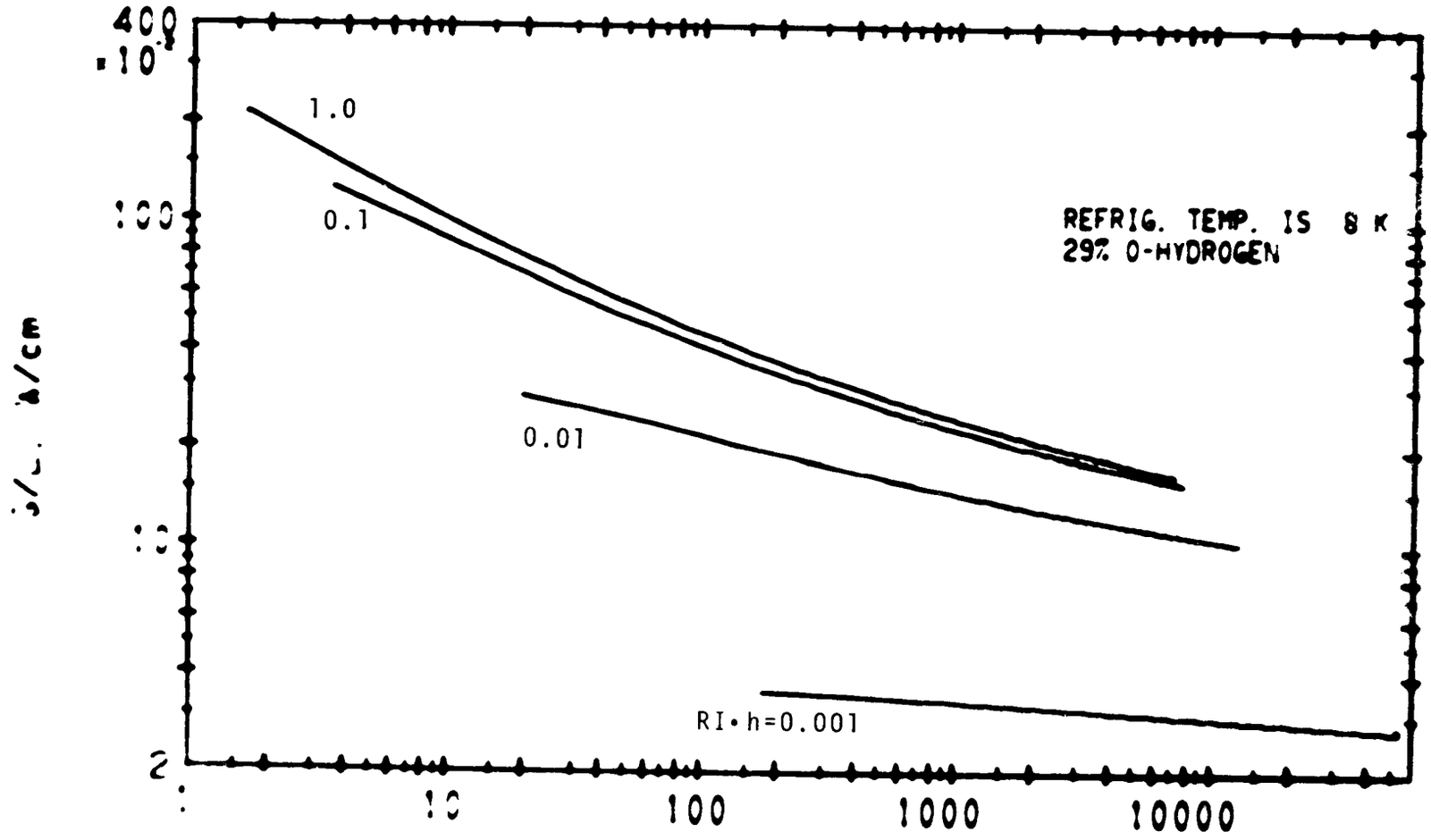

CYLINDER, FREEZING FROM INSIDE

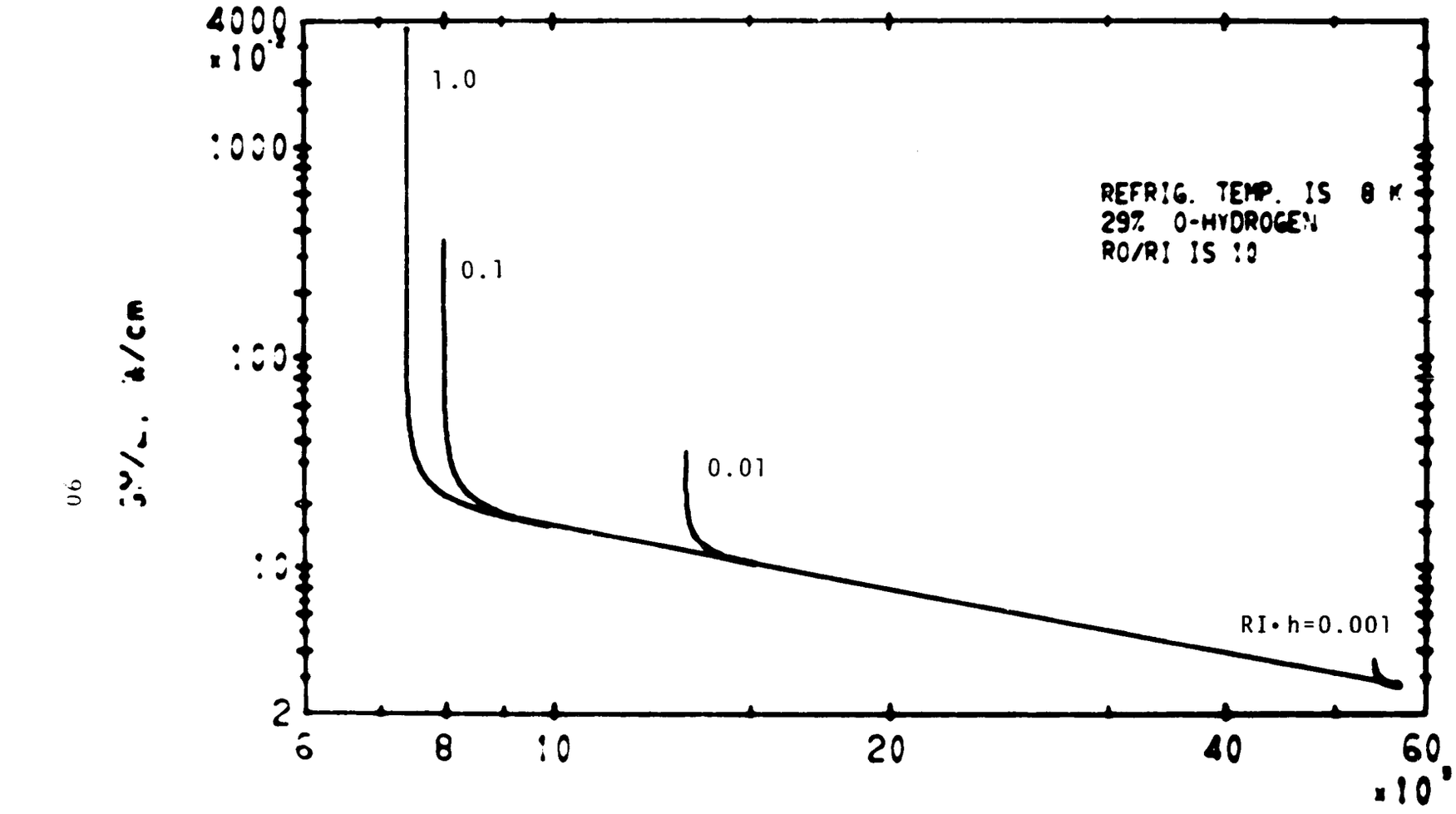

CYLINDER, FREEZING FROM INSIDE

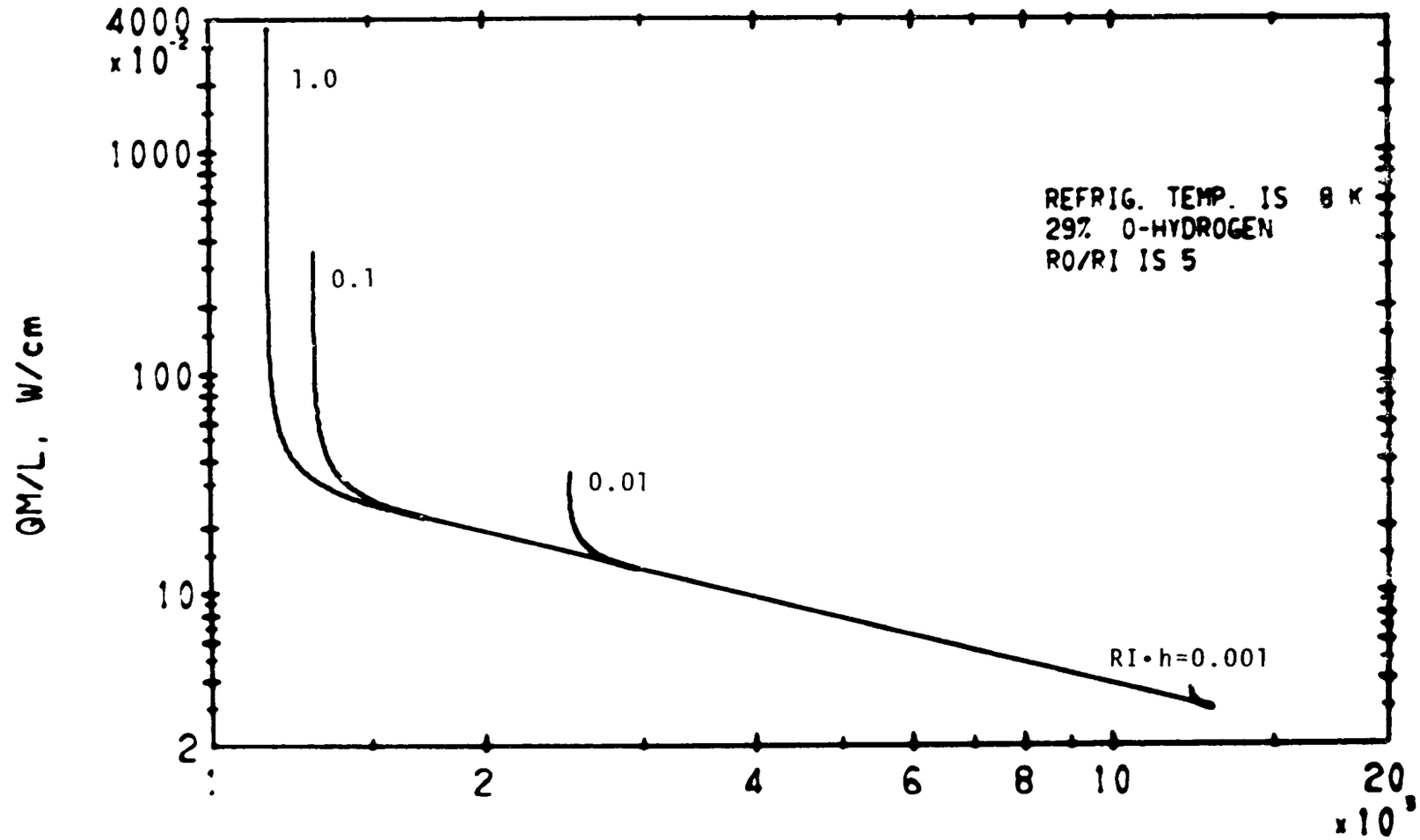

CYLINDER, FREEZING FROM INSIDE

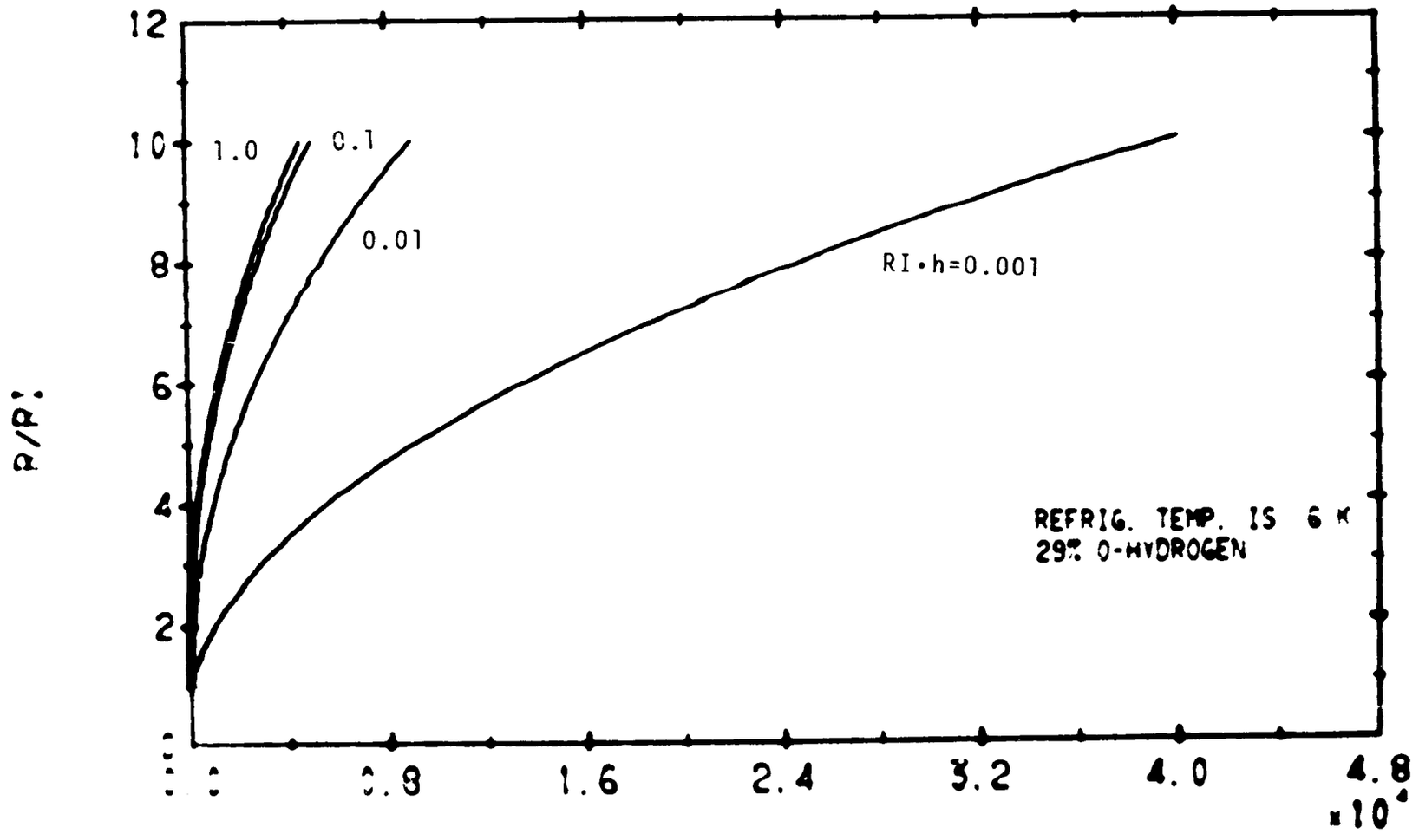

CYLINDER, FREEZING FROM INSIDE

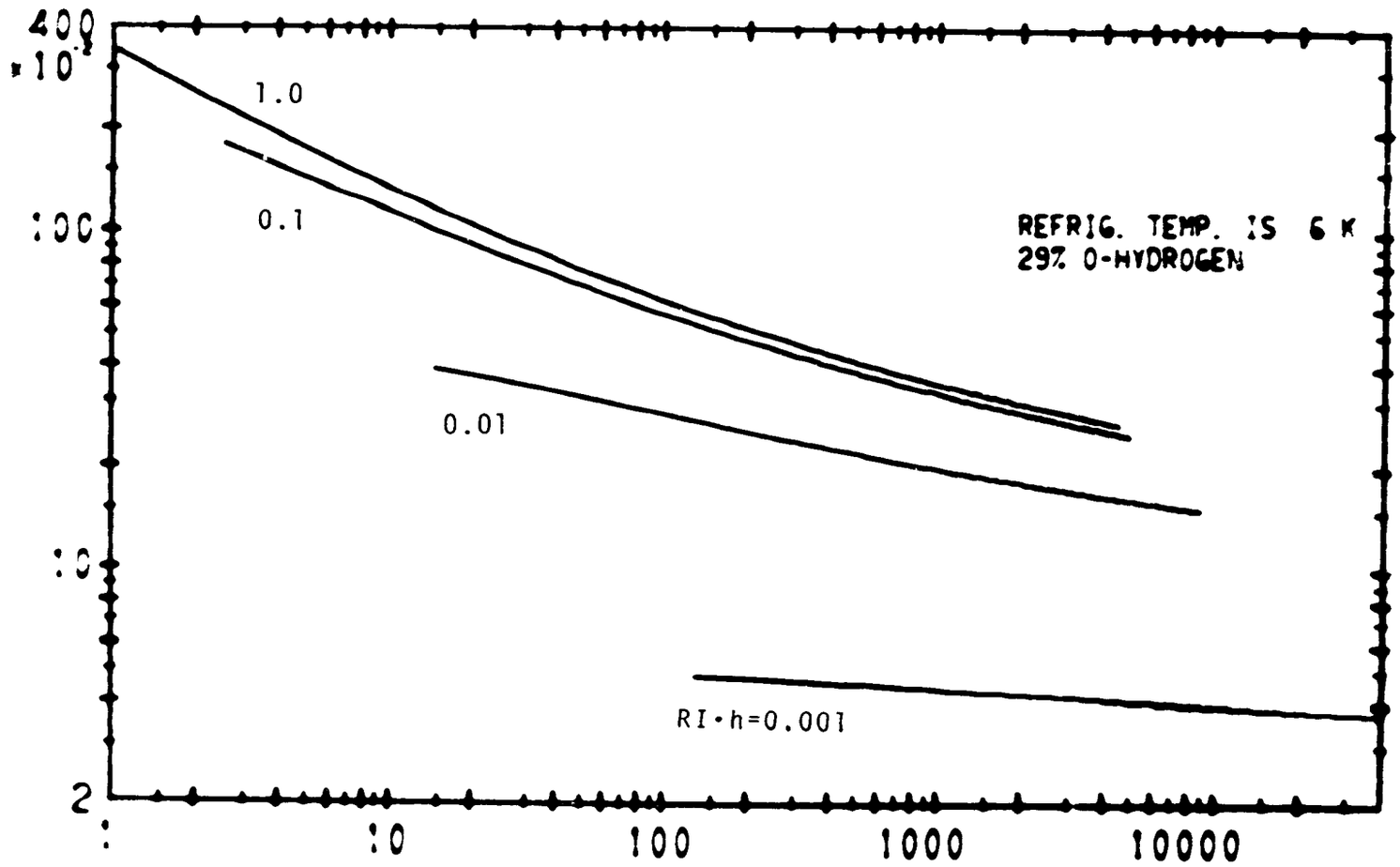

CYLINDER, FREEZING FROM INSIDE

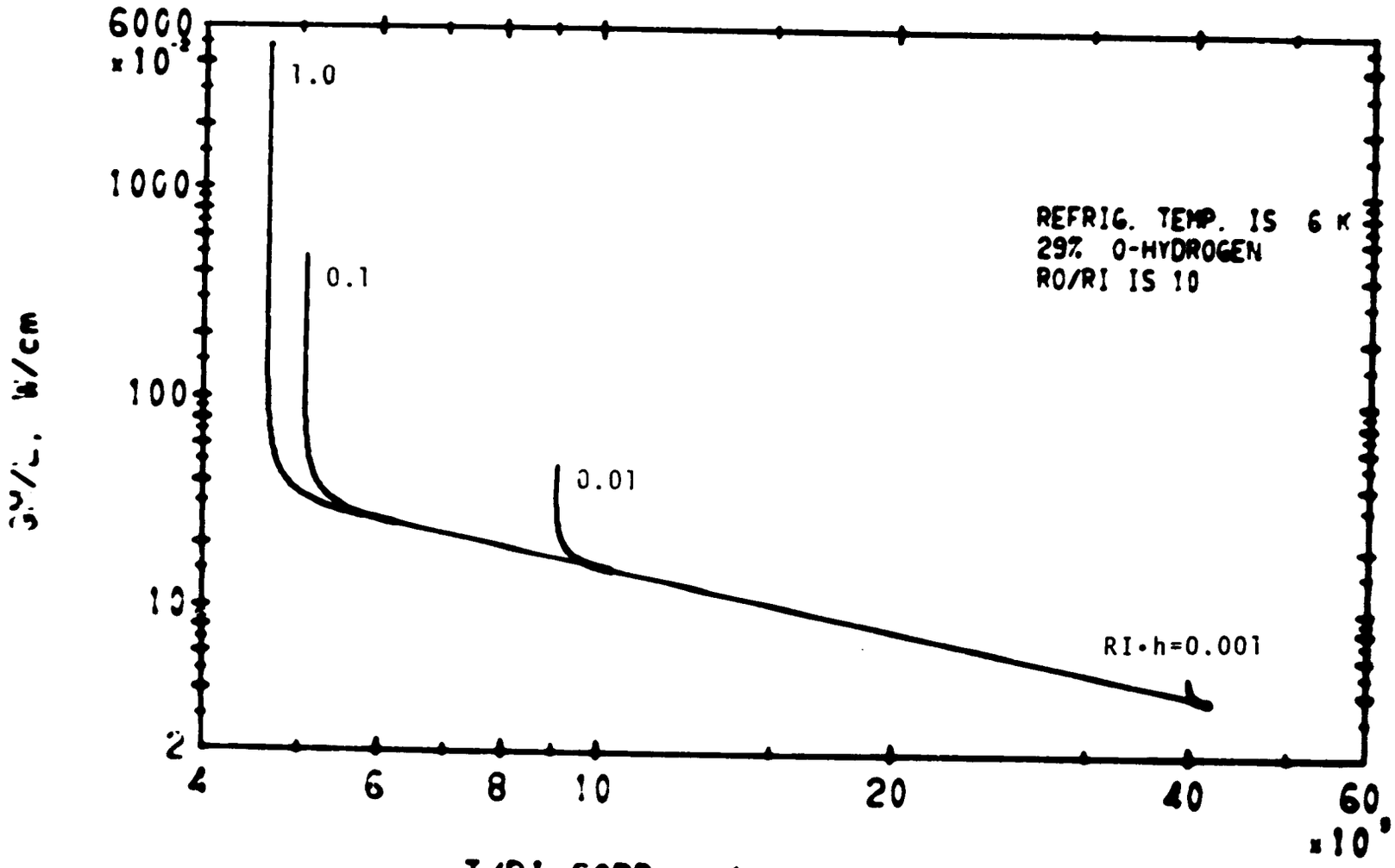

CYLINDER, FREEZING FROM INSIDE

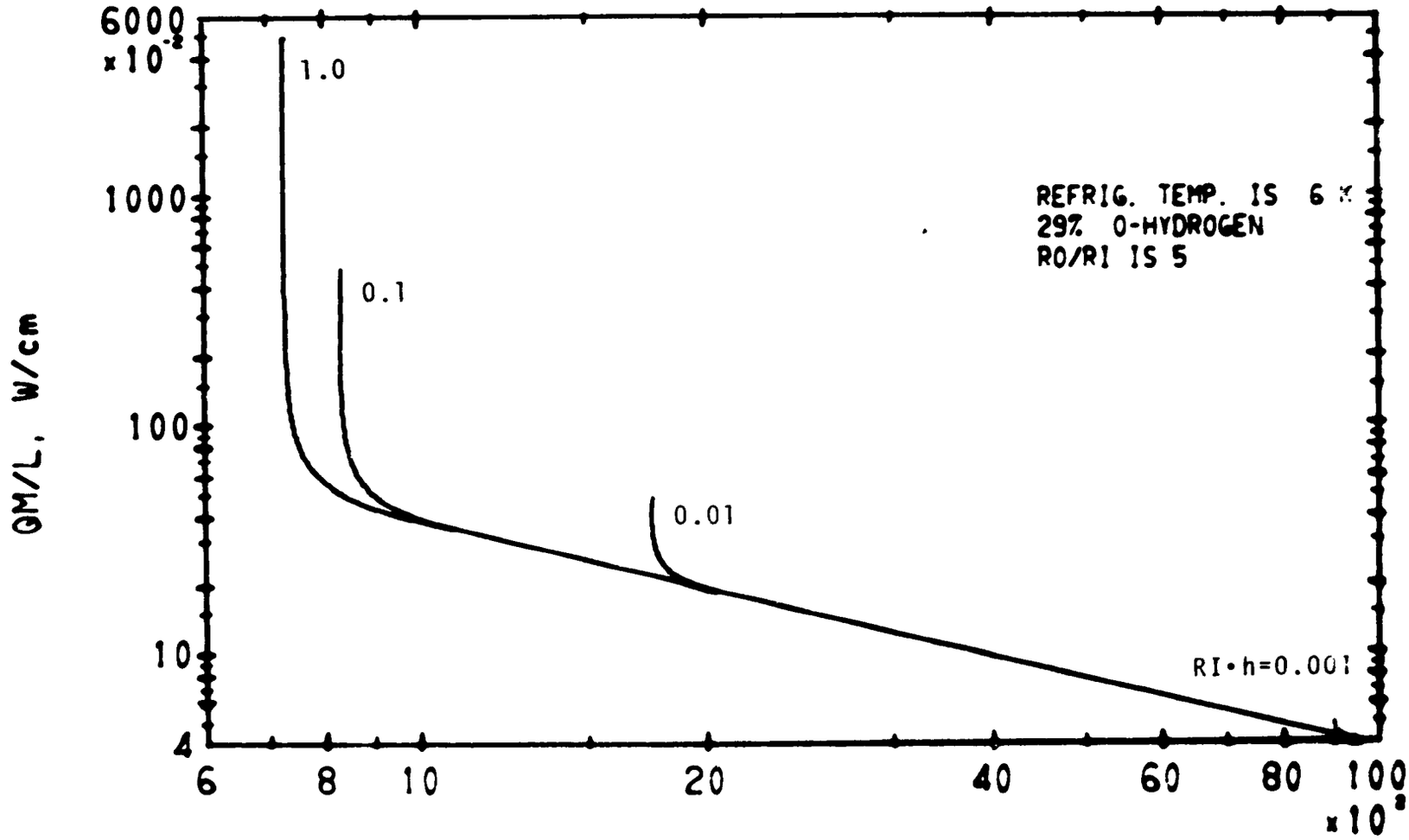

CYLINDER, FREEZING FROM INSIDE

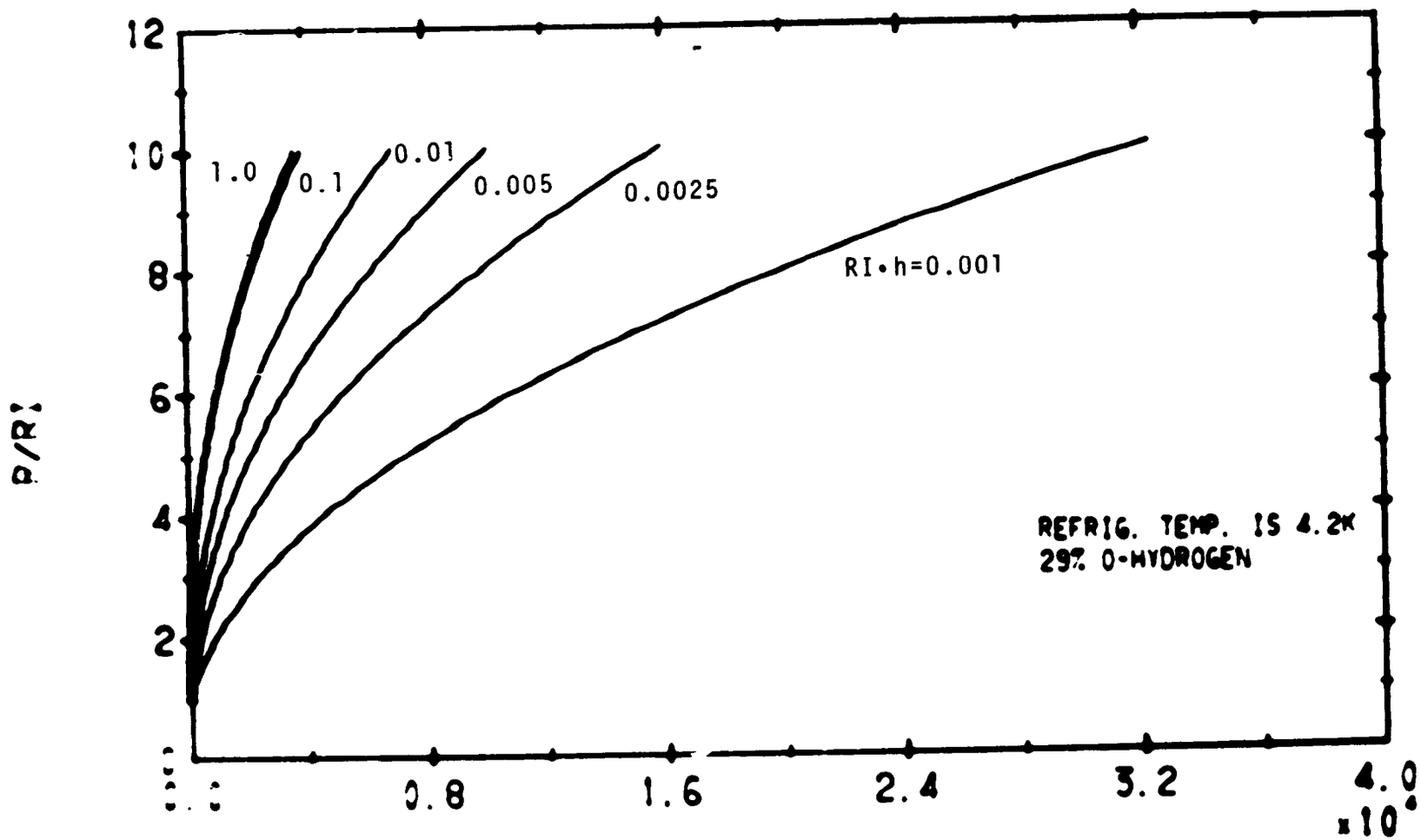

CYLINDER, FREEZING FROM INSIDE

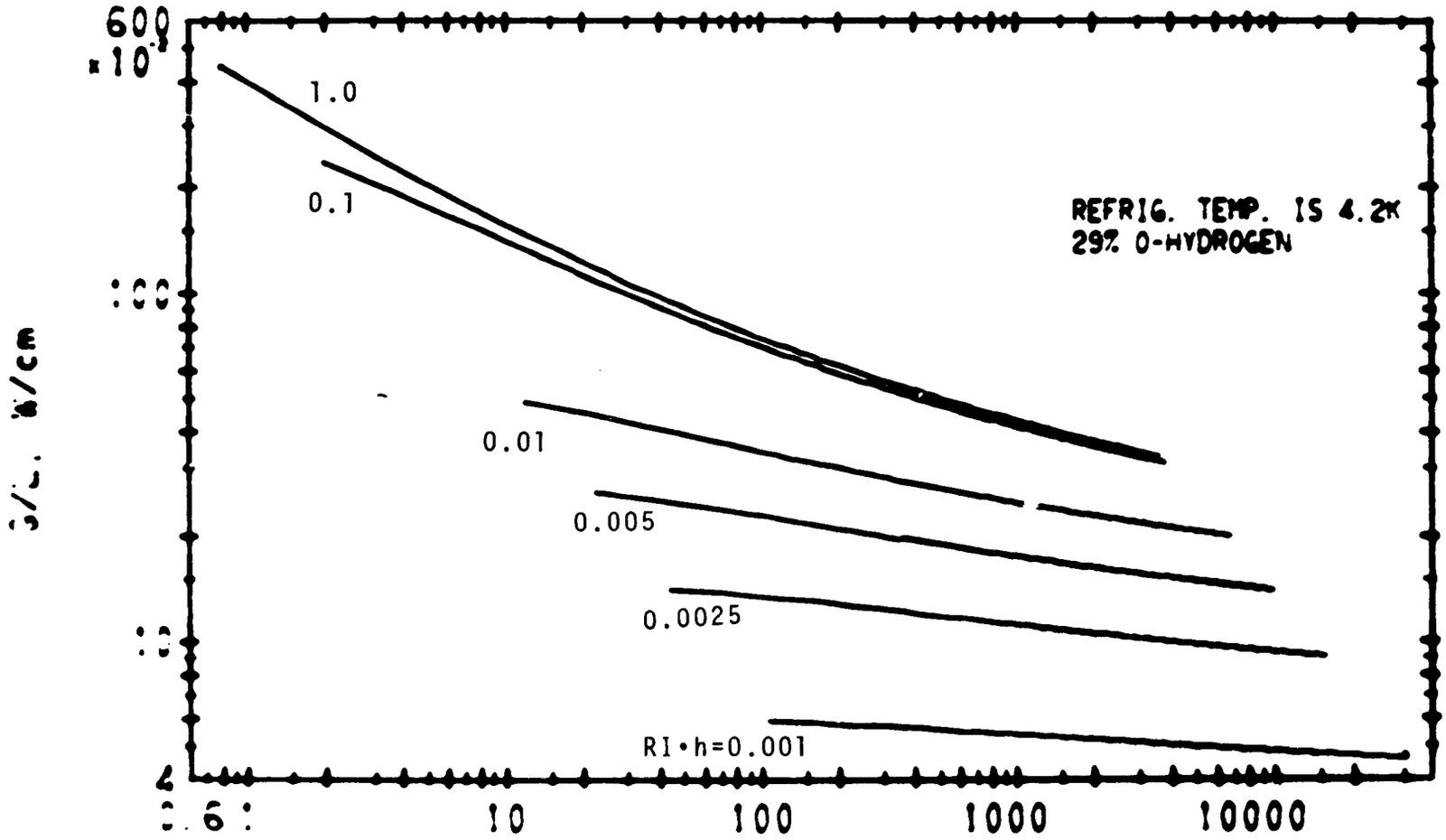

CYLINDER, FREEZING FROM INSIDE

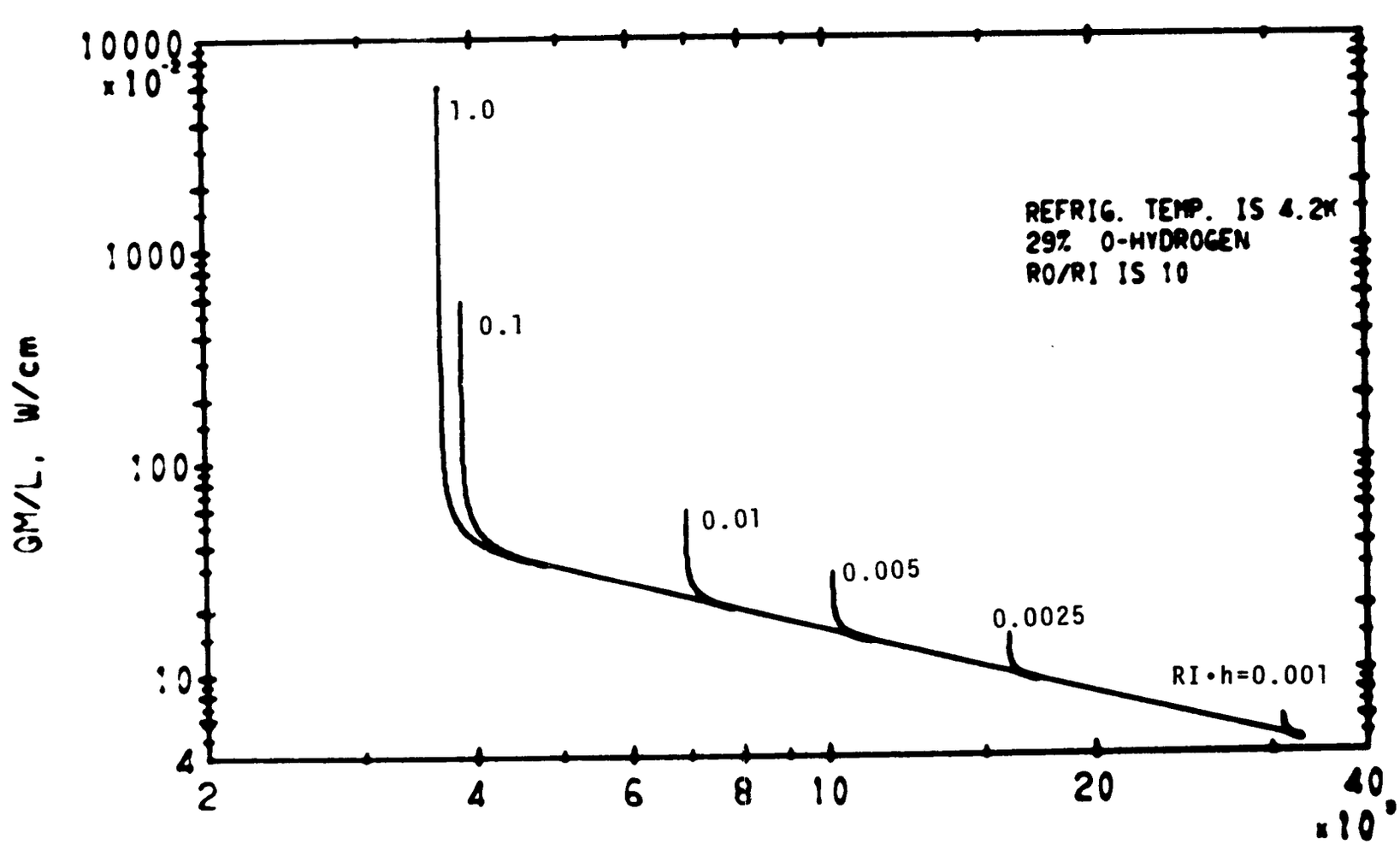

CYLINDER, FREEZING FROM INSIDE

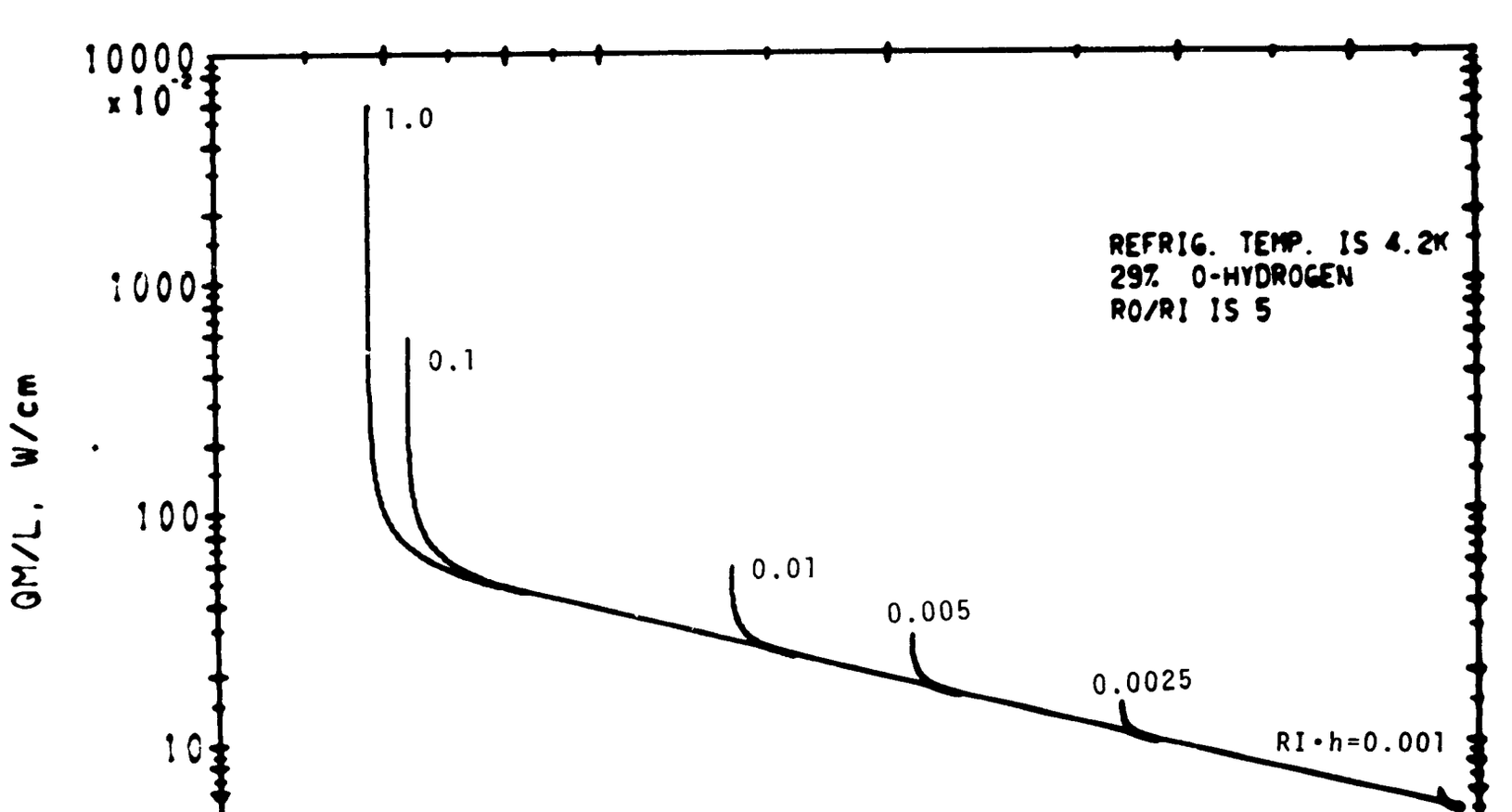

CYLINDER, FREEZING FROM INSIDE

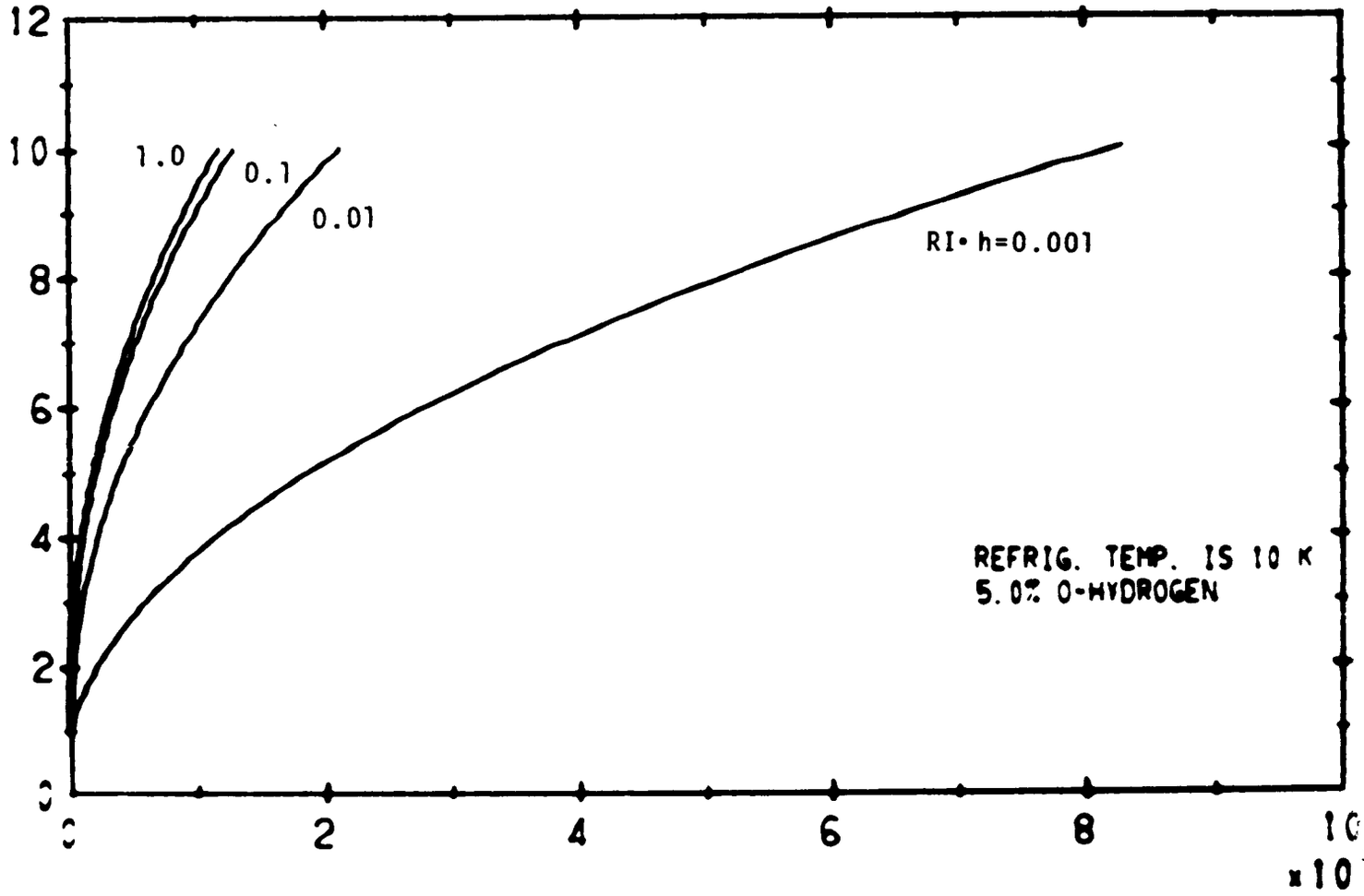

CYLINDER, FREEZING FROM INSIDE

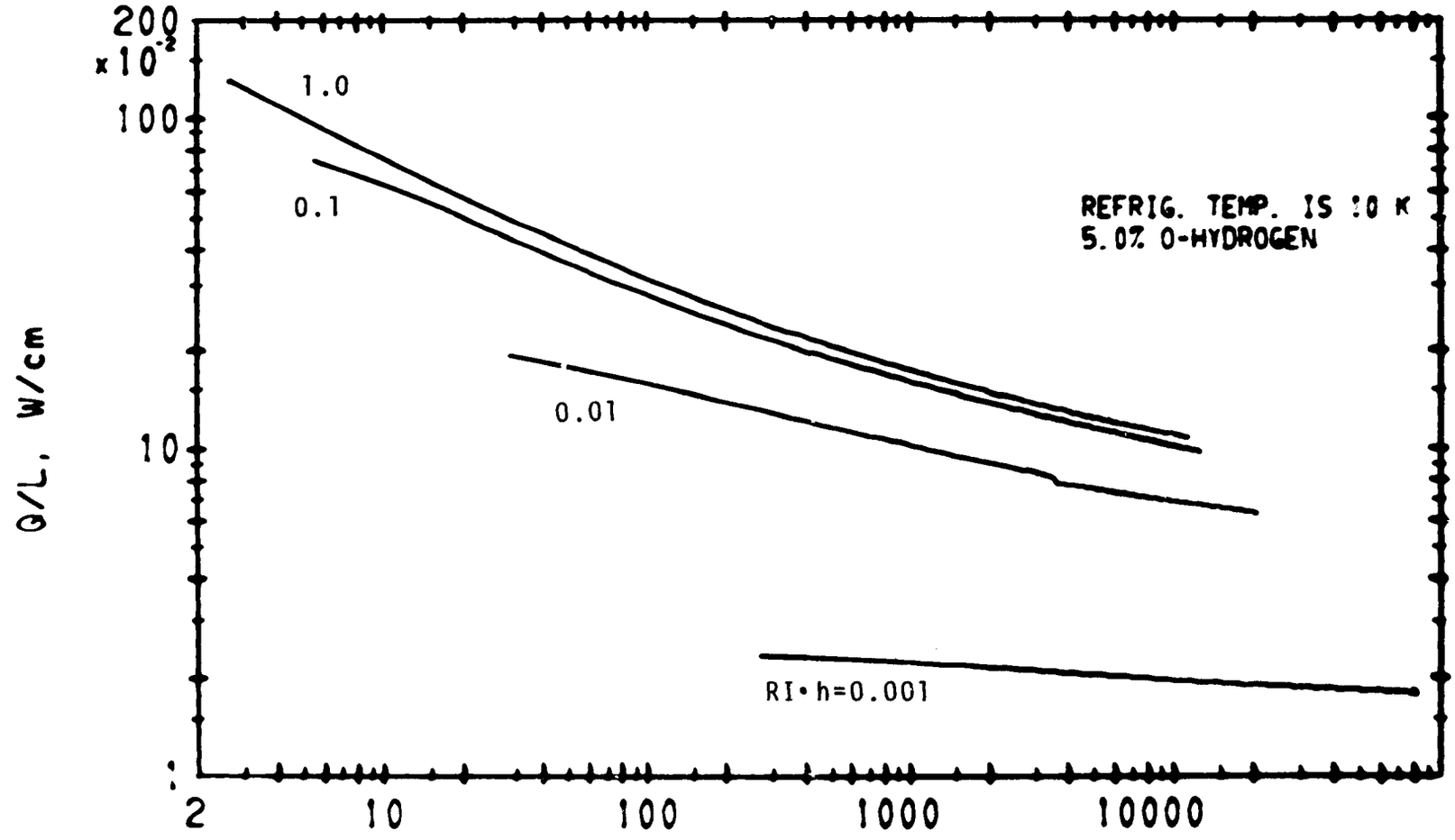

CYLINDER, FREEZING FROM INSIDE

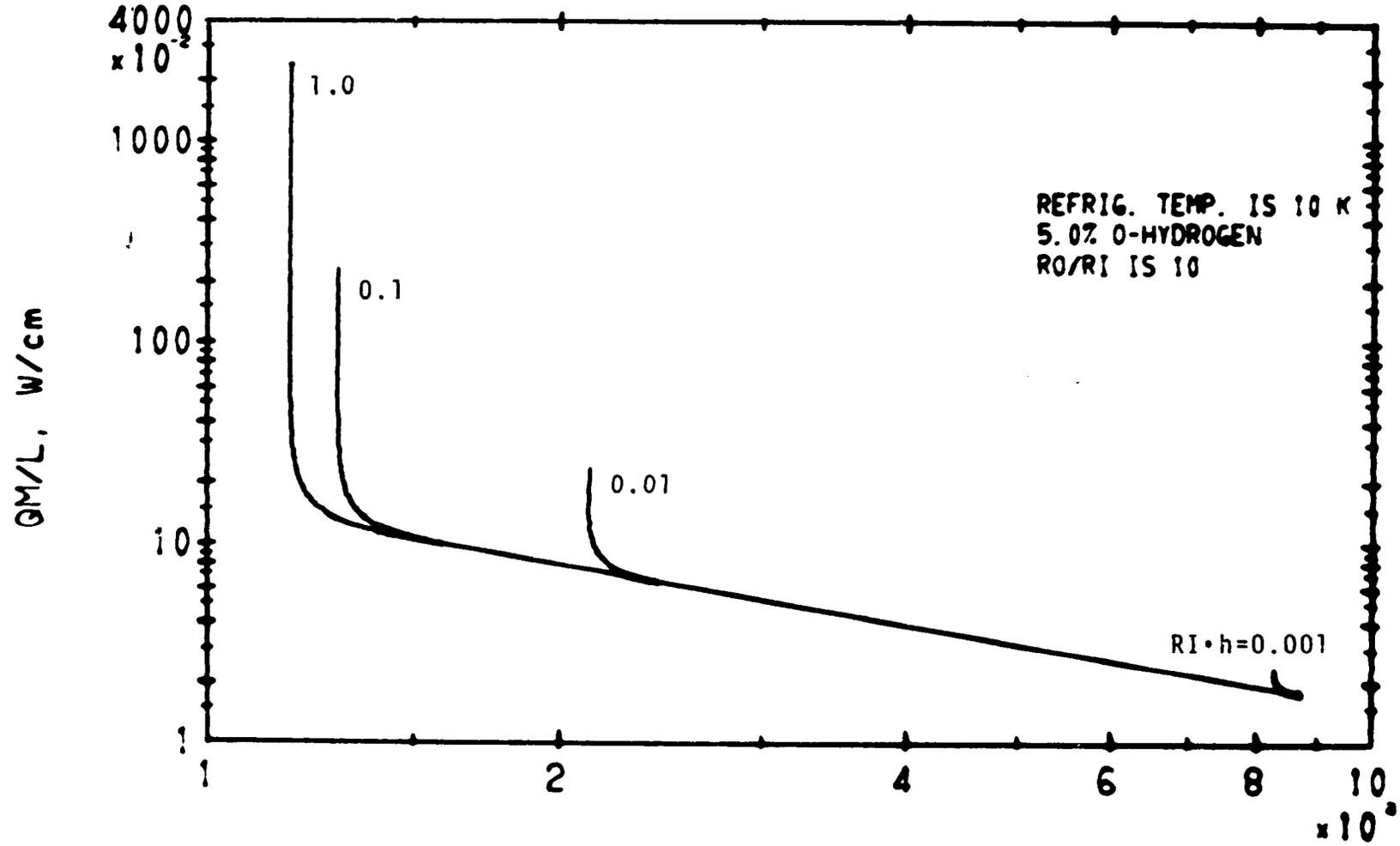

CYLINDER, FREEZING FROM INSIDE

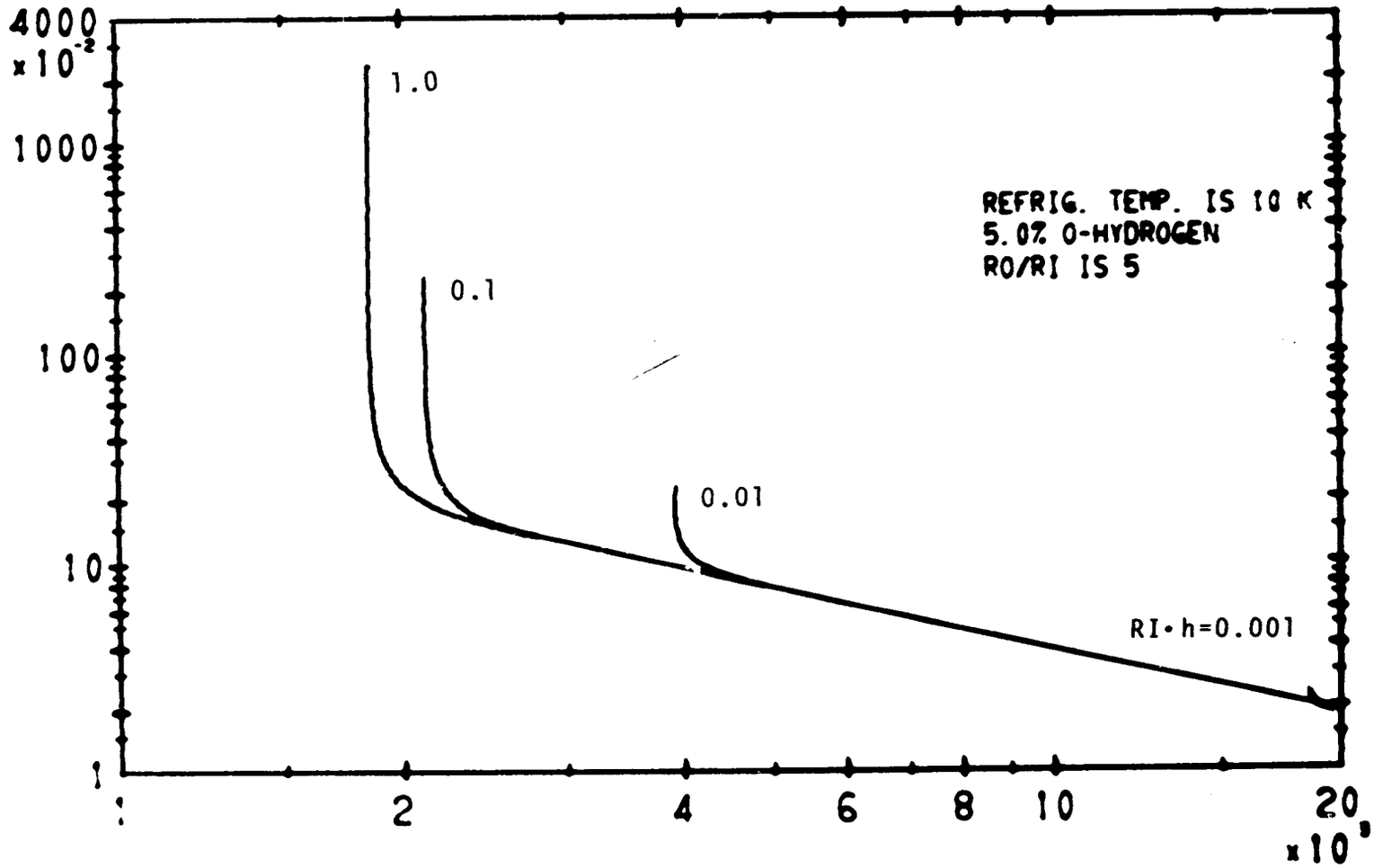

103

CYLINDER, FREEZING FROM INSIDE

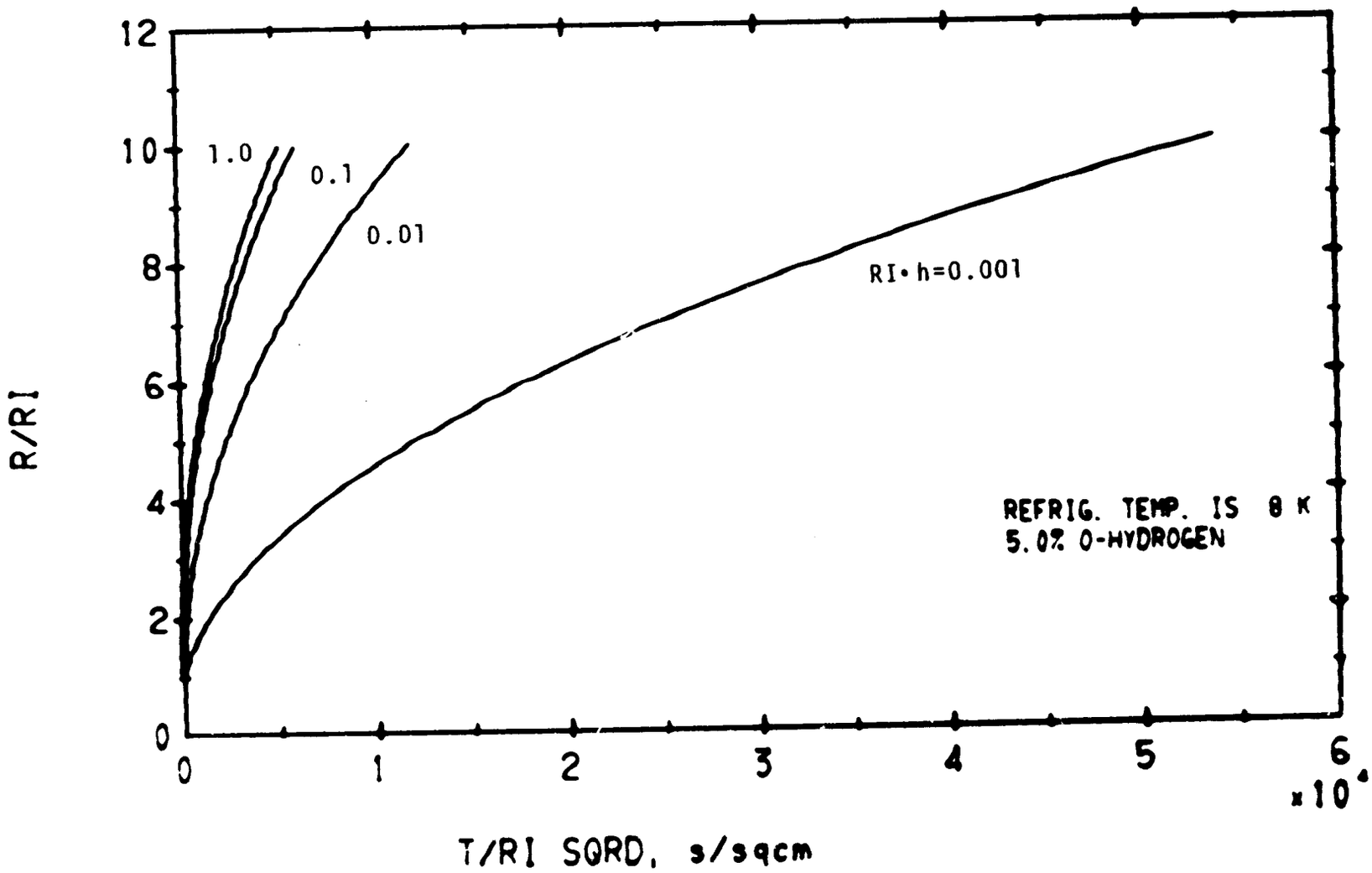

CYLINDER, FREEZING FROM INSIDE

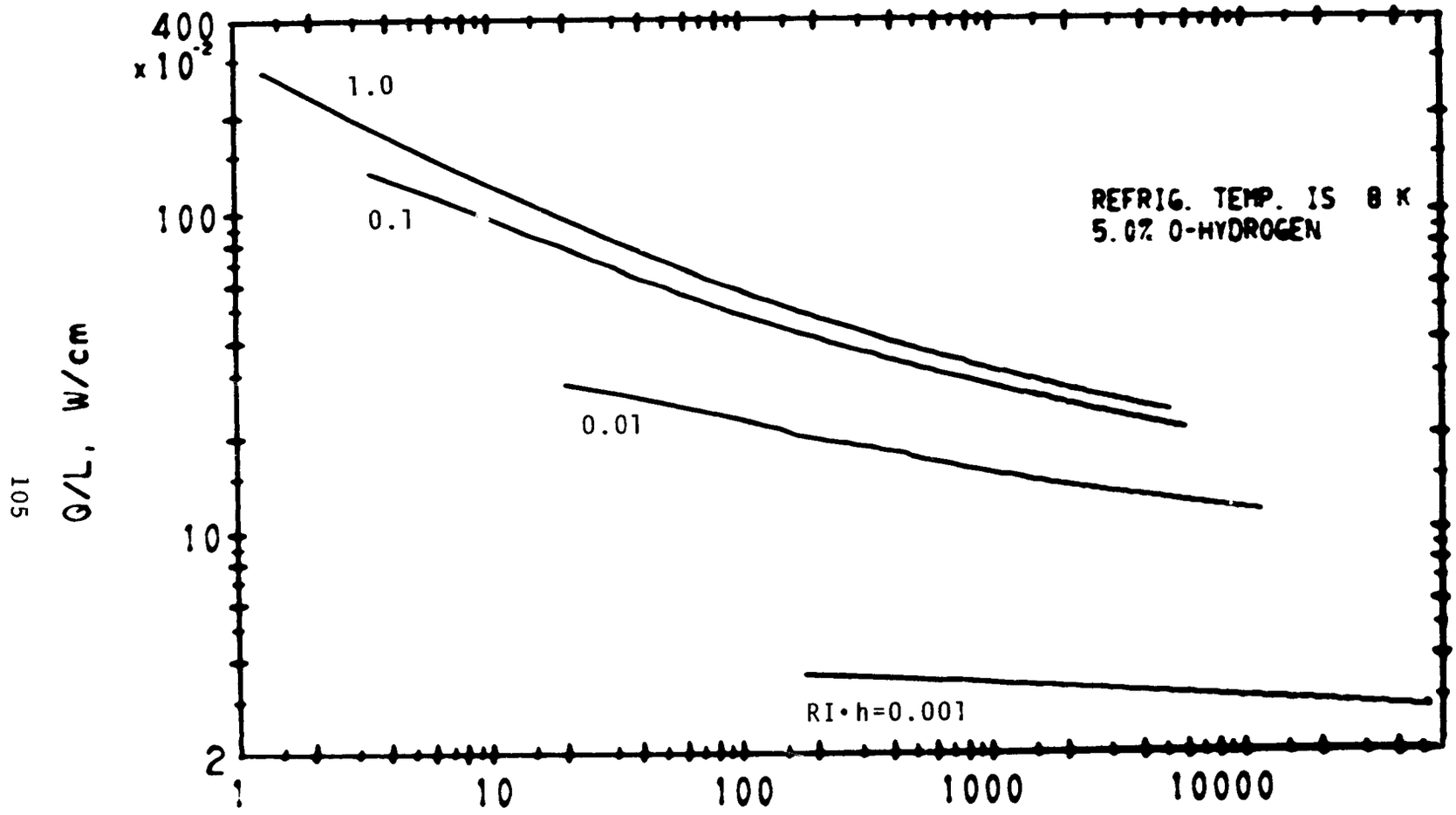

105

CYLINDER, FREEZING FROM INSIDE

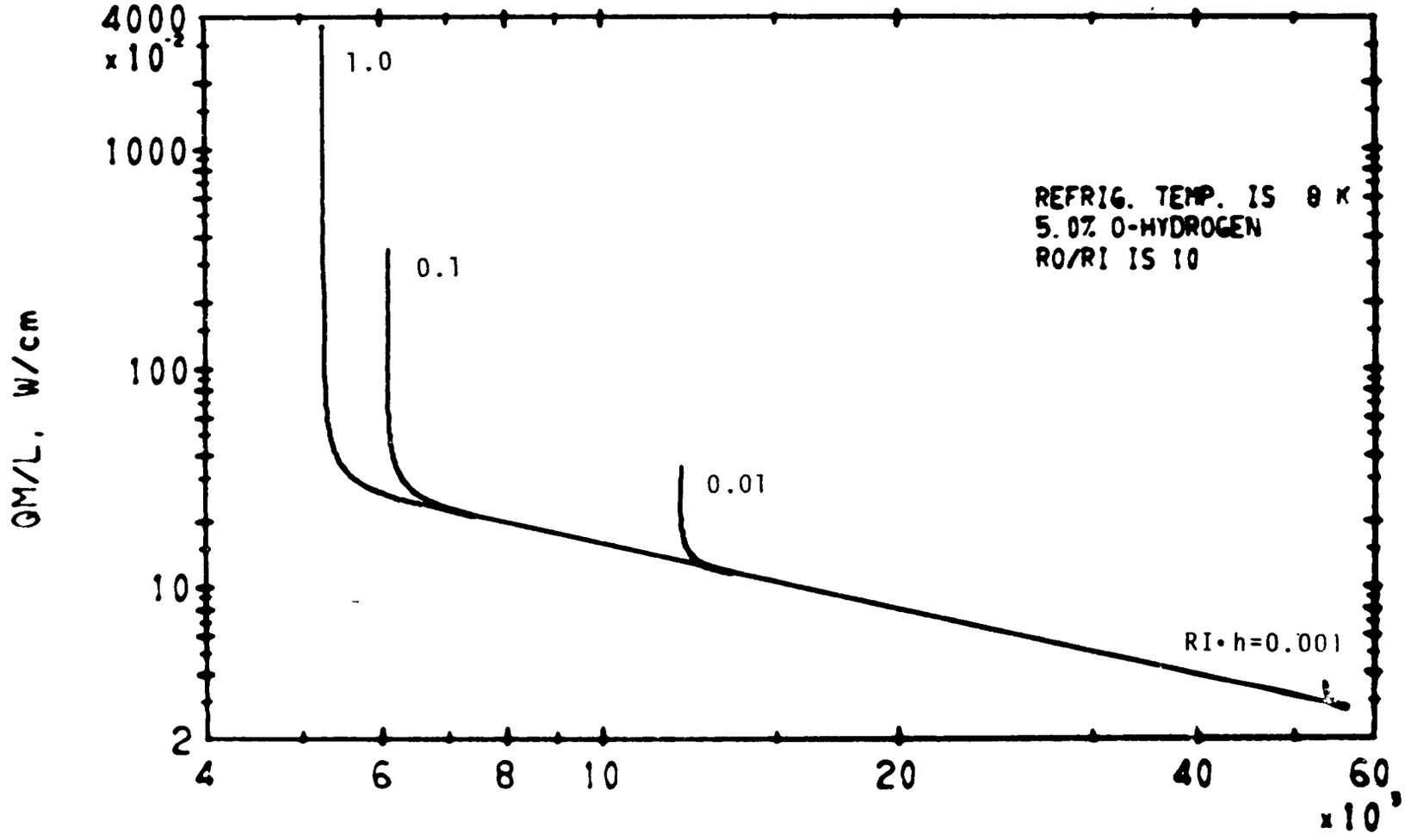

CYLINDER, FREEZING FROM INSIDE

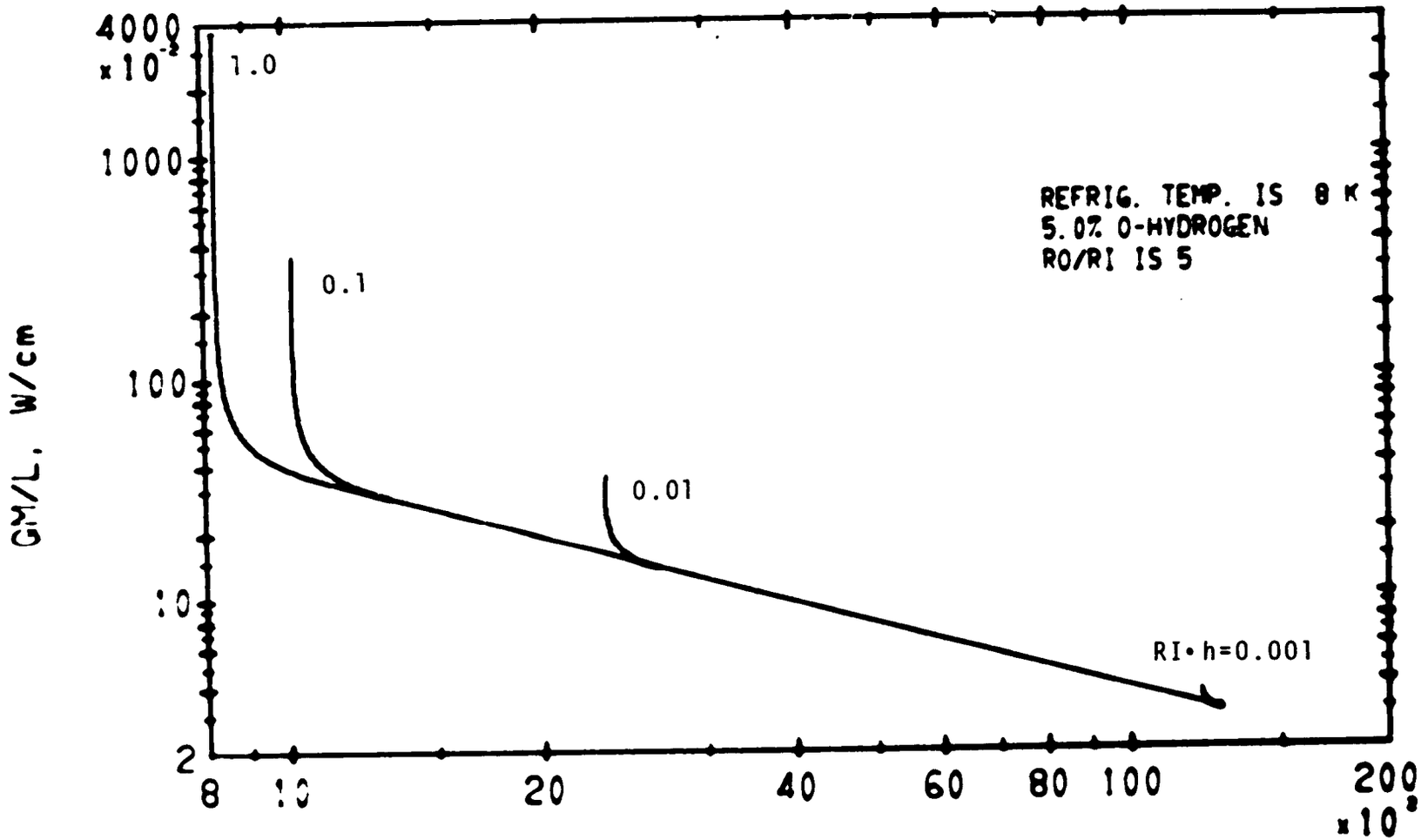

CYLINDER, FREEZING FROM INSIDE

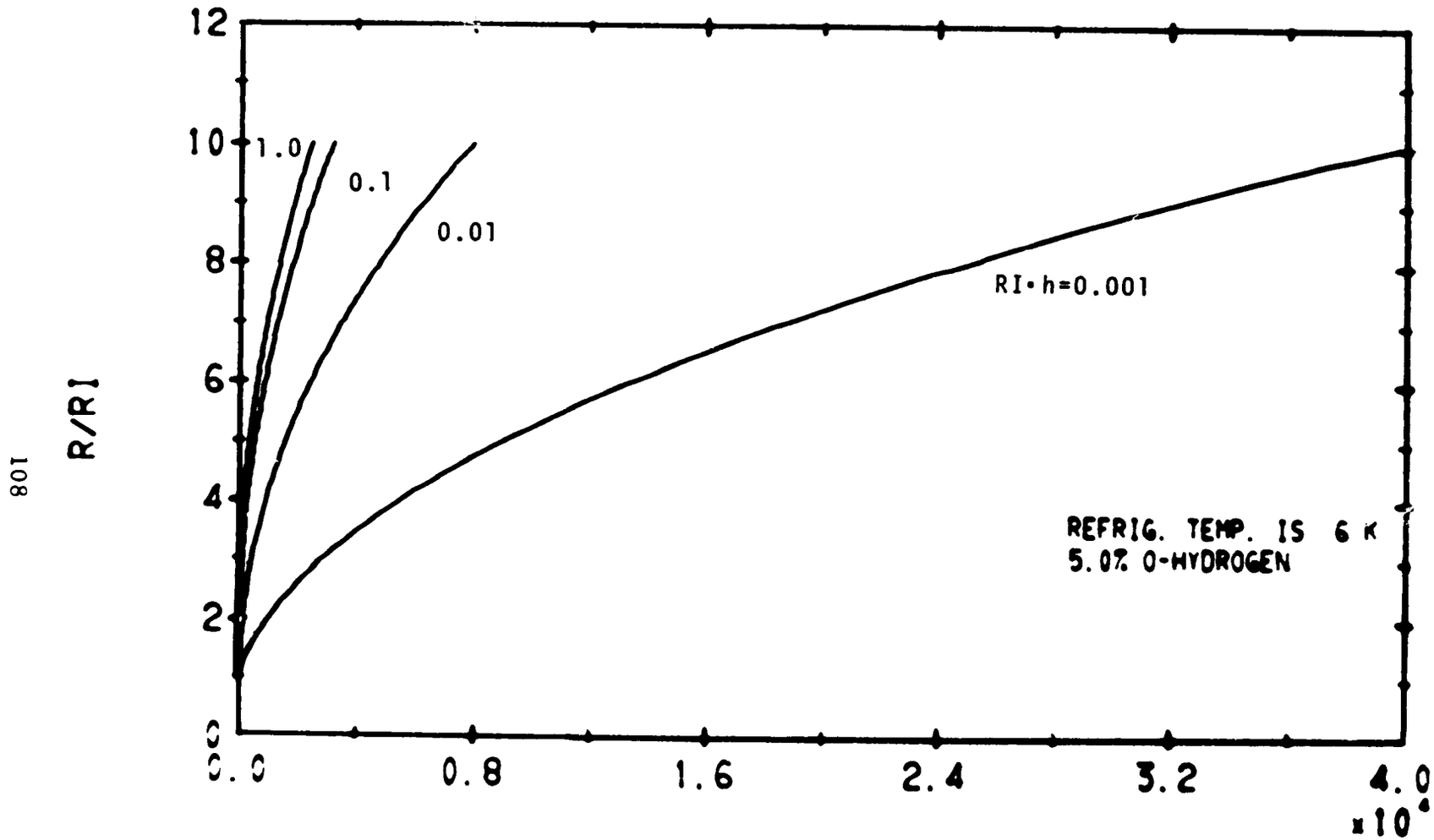

CYLINDER, FREEZING FROM INSIDE

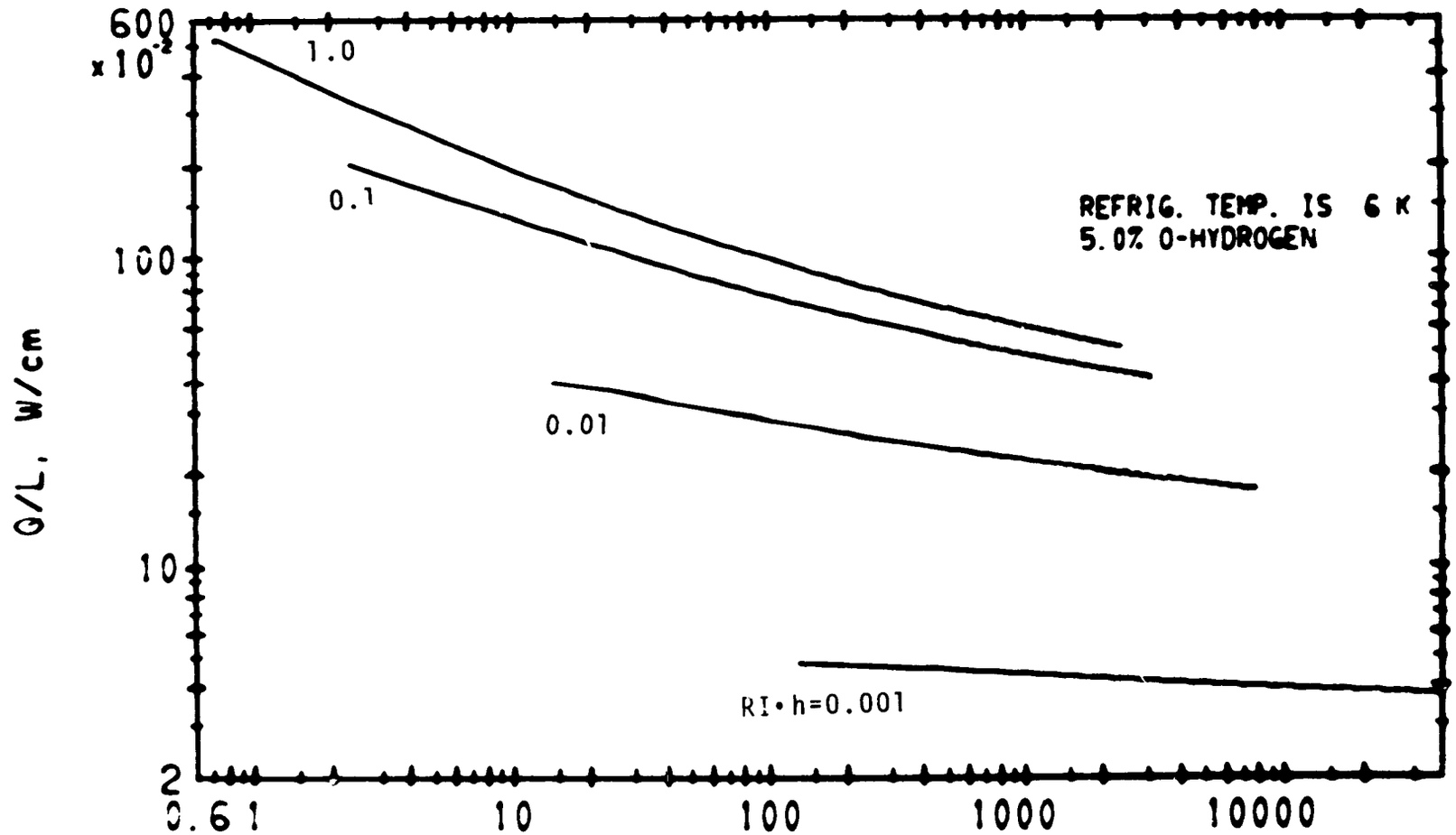

CYLINDER, FREEZING FROM INSIDE

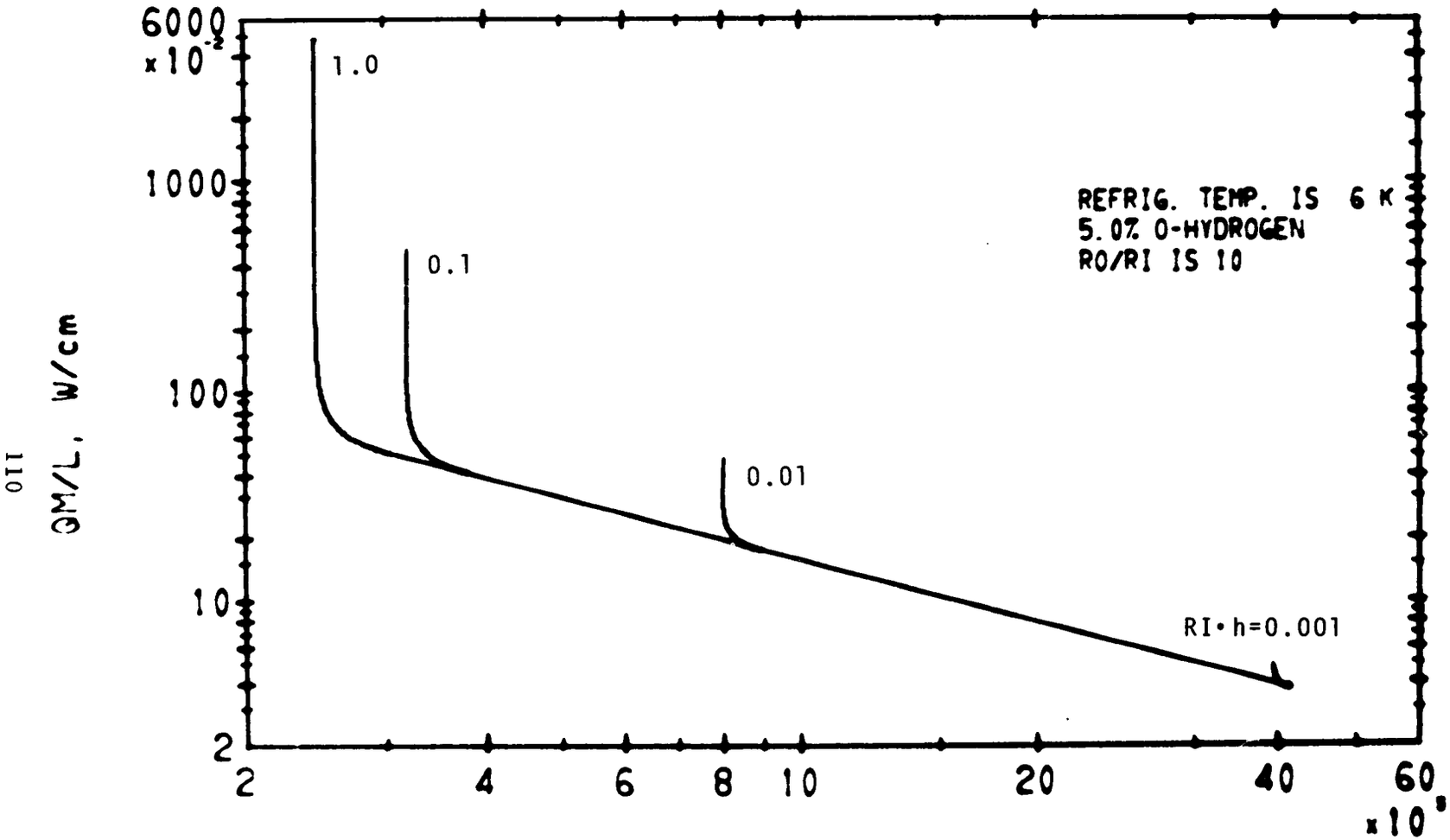

CYLINDER, FREEZING FROM INSIDE

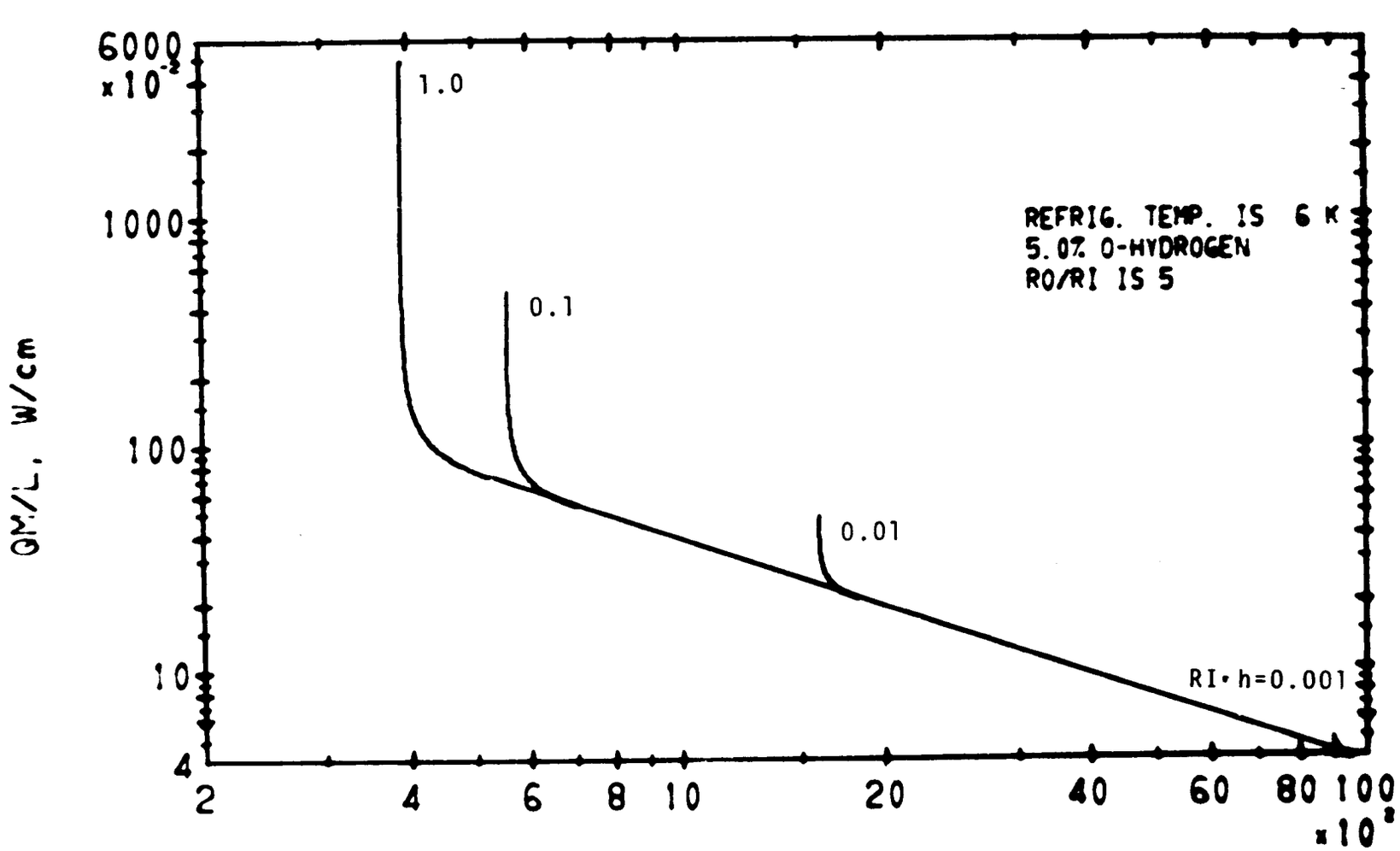

CYLINDER, FREEZING FROM INSIDE

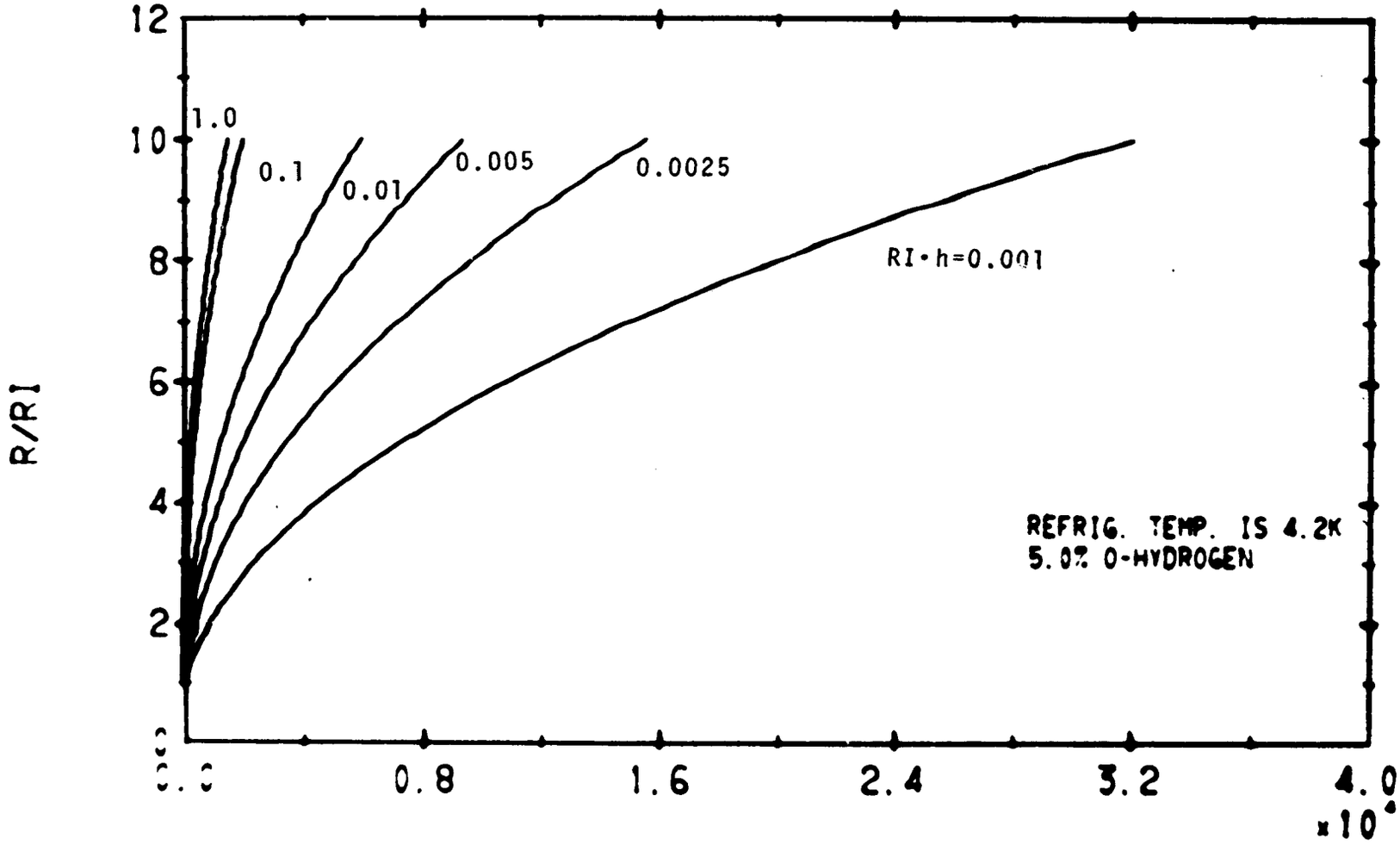

CYLINDER, FREEZING FROM INSIDE

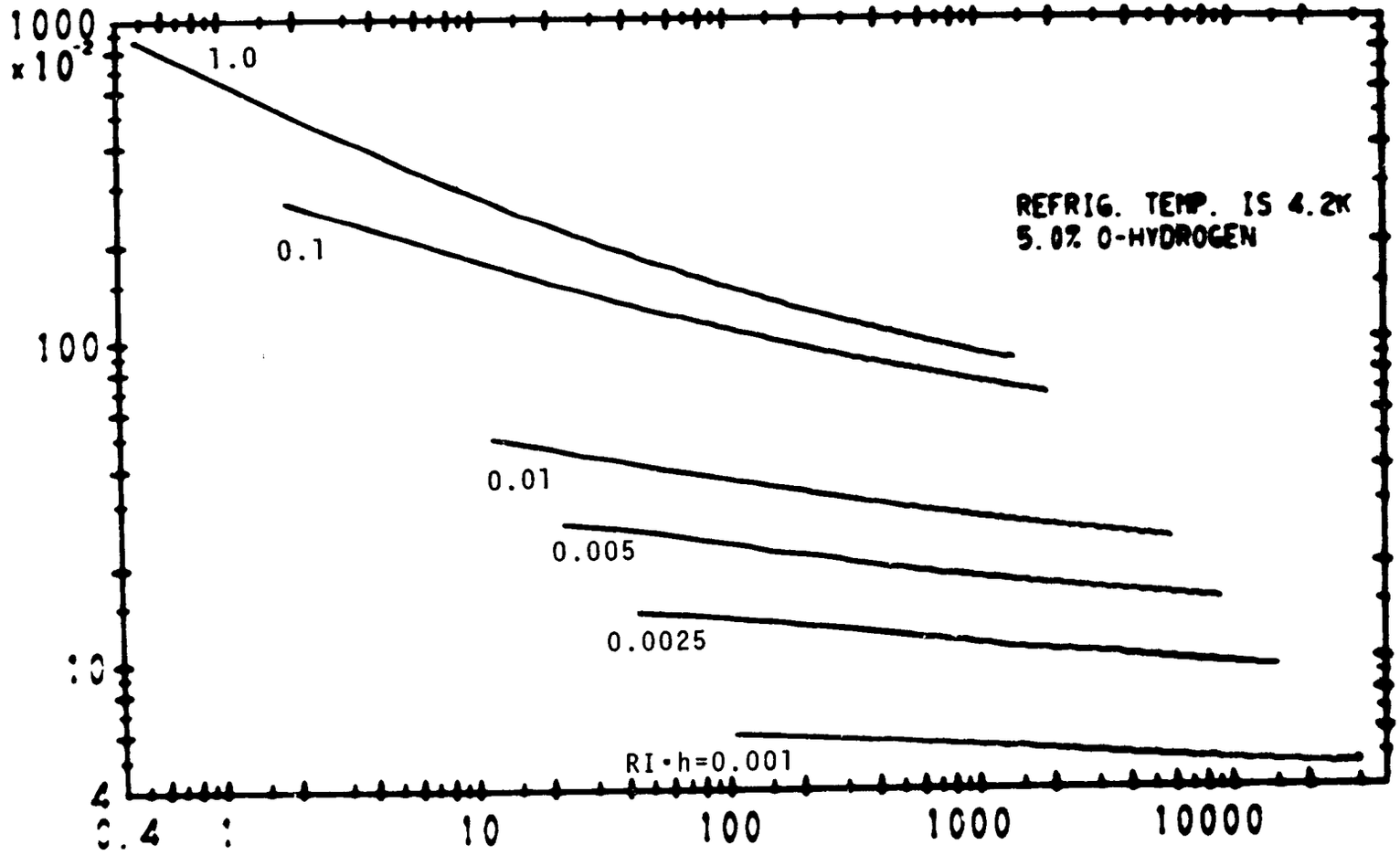

CYLINDER, FREEZING FROM INSIDE

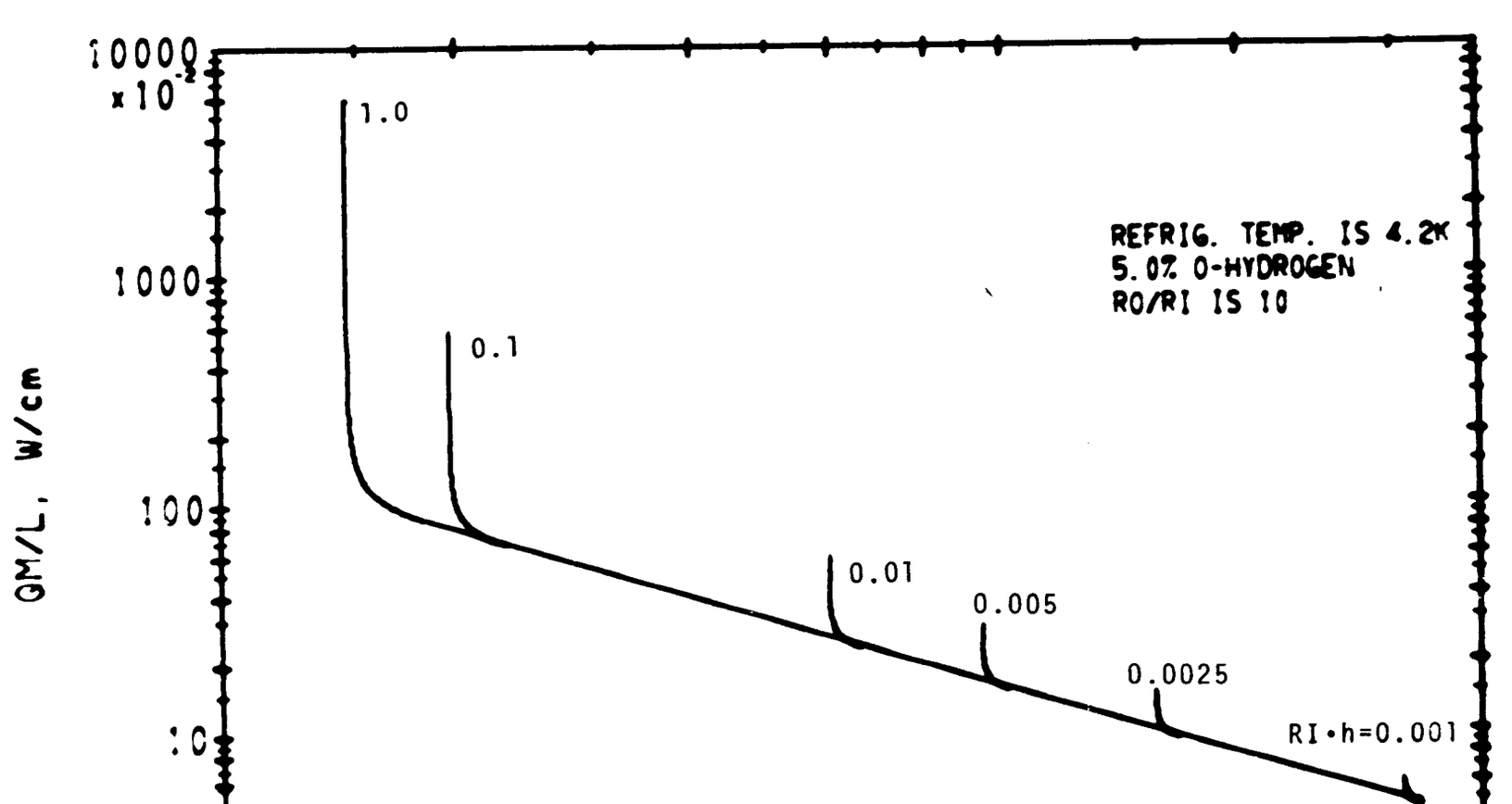

CYLINDER, FREEZING FROM INSIDE

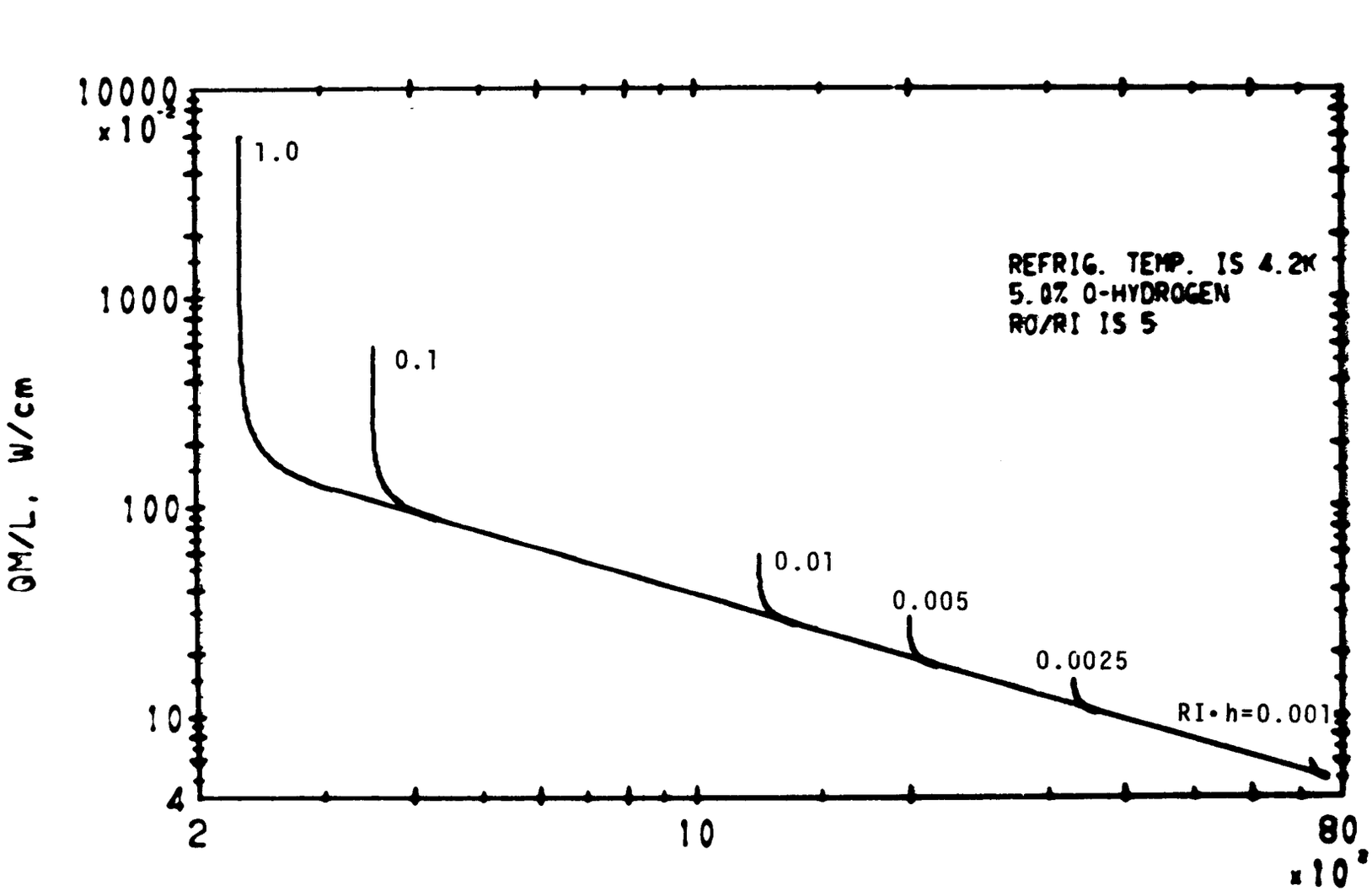

CYLINDER, FREEZING FROM INSIDE

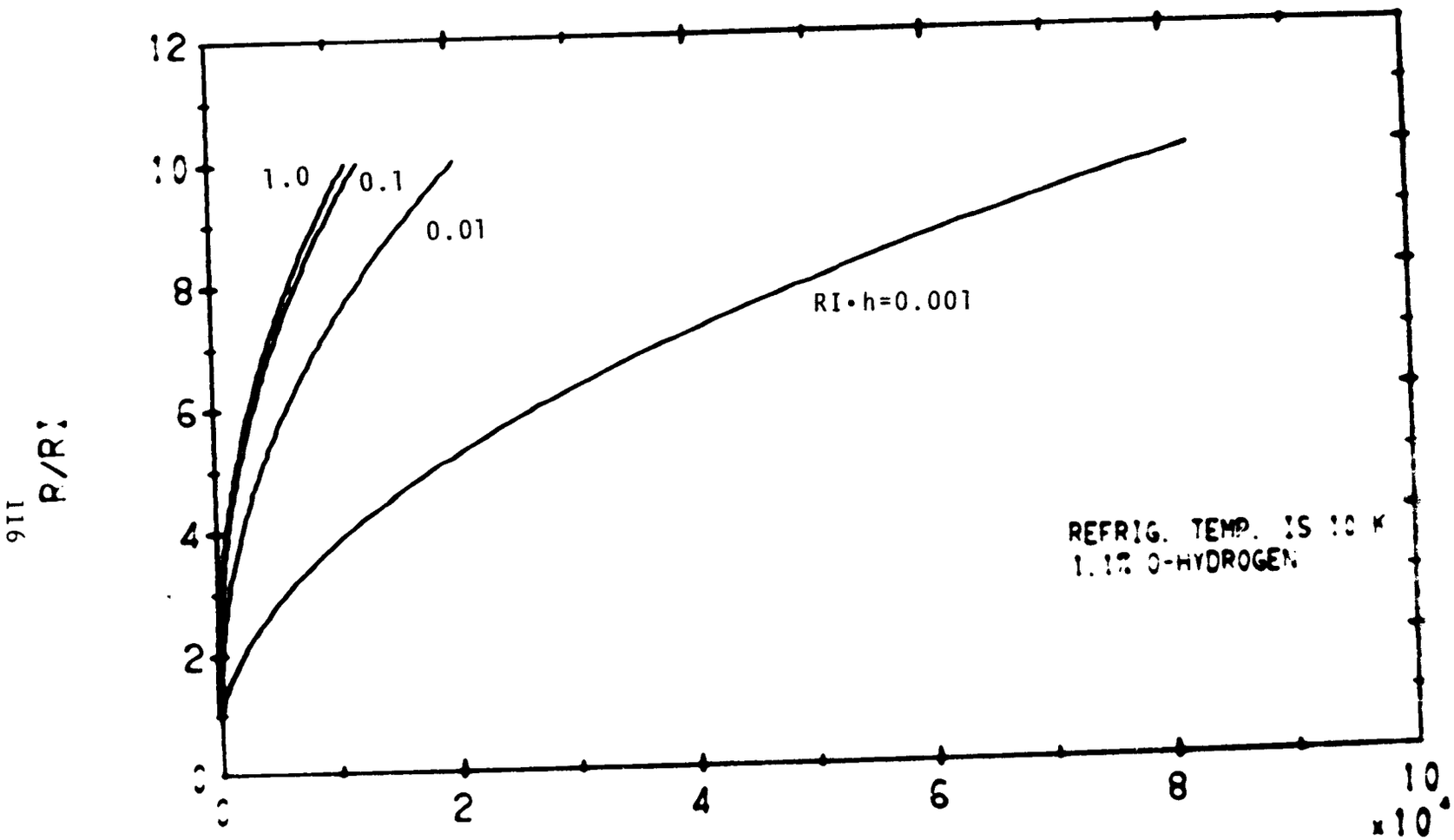

CYLINDER, FREEZING FROM INSIDE

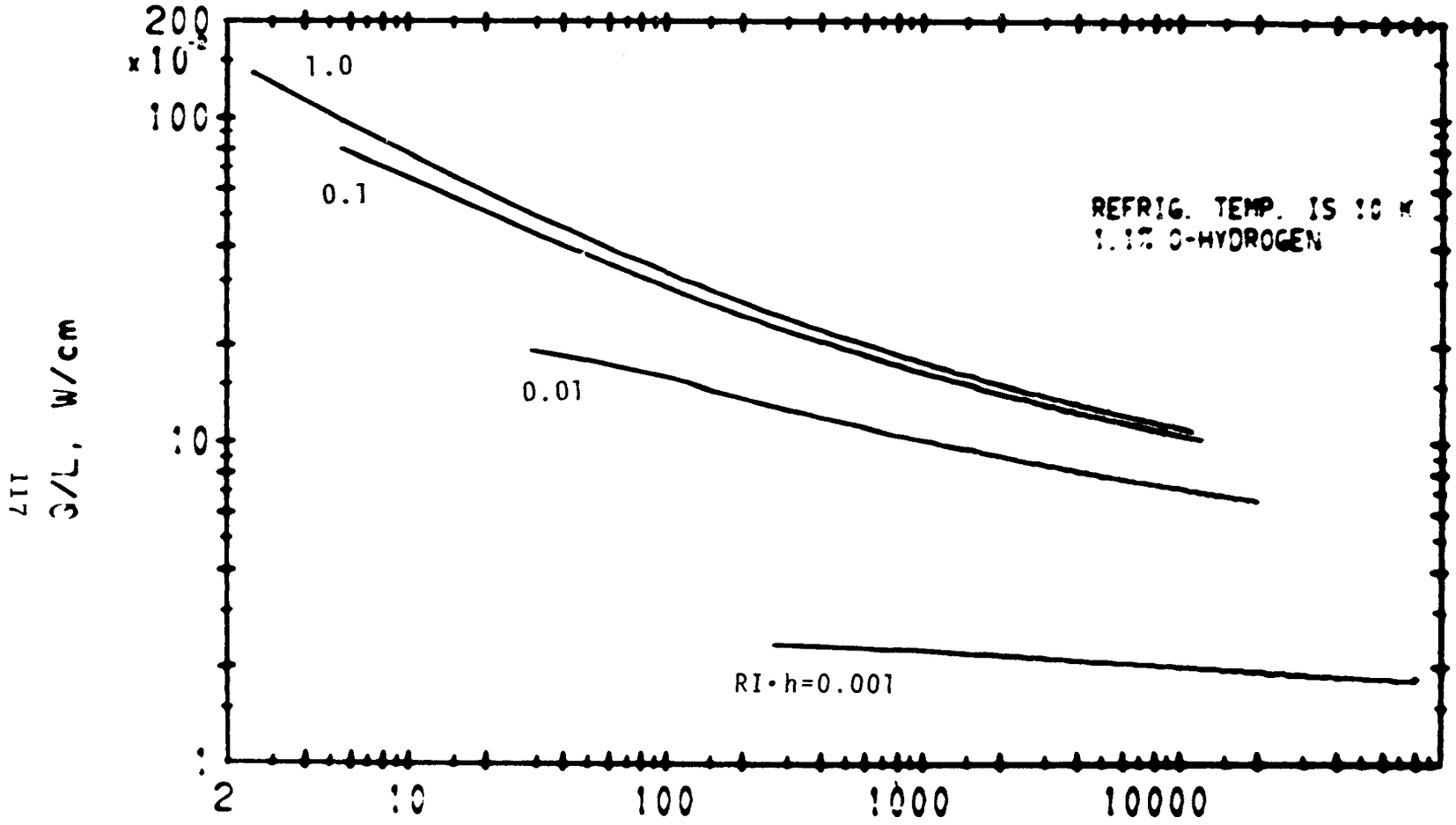

CYLINDER, FREEZING FROM INSIDE

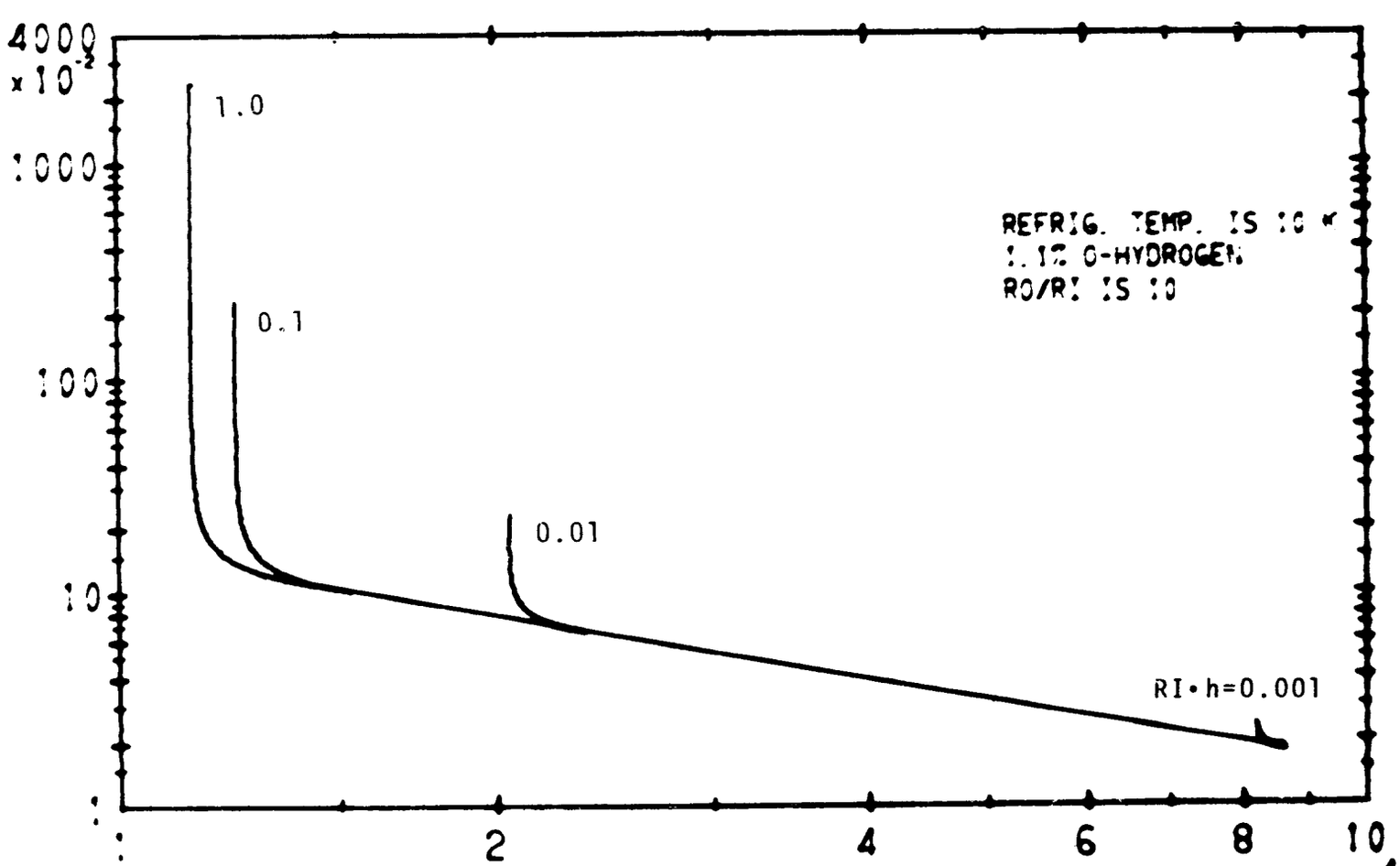

CYLINDER, FREEZING FROM INSIDE

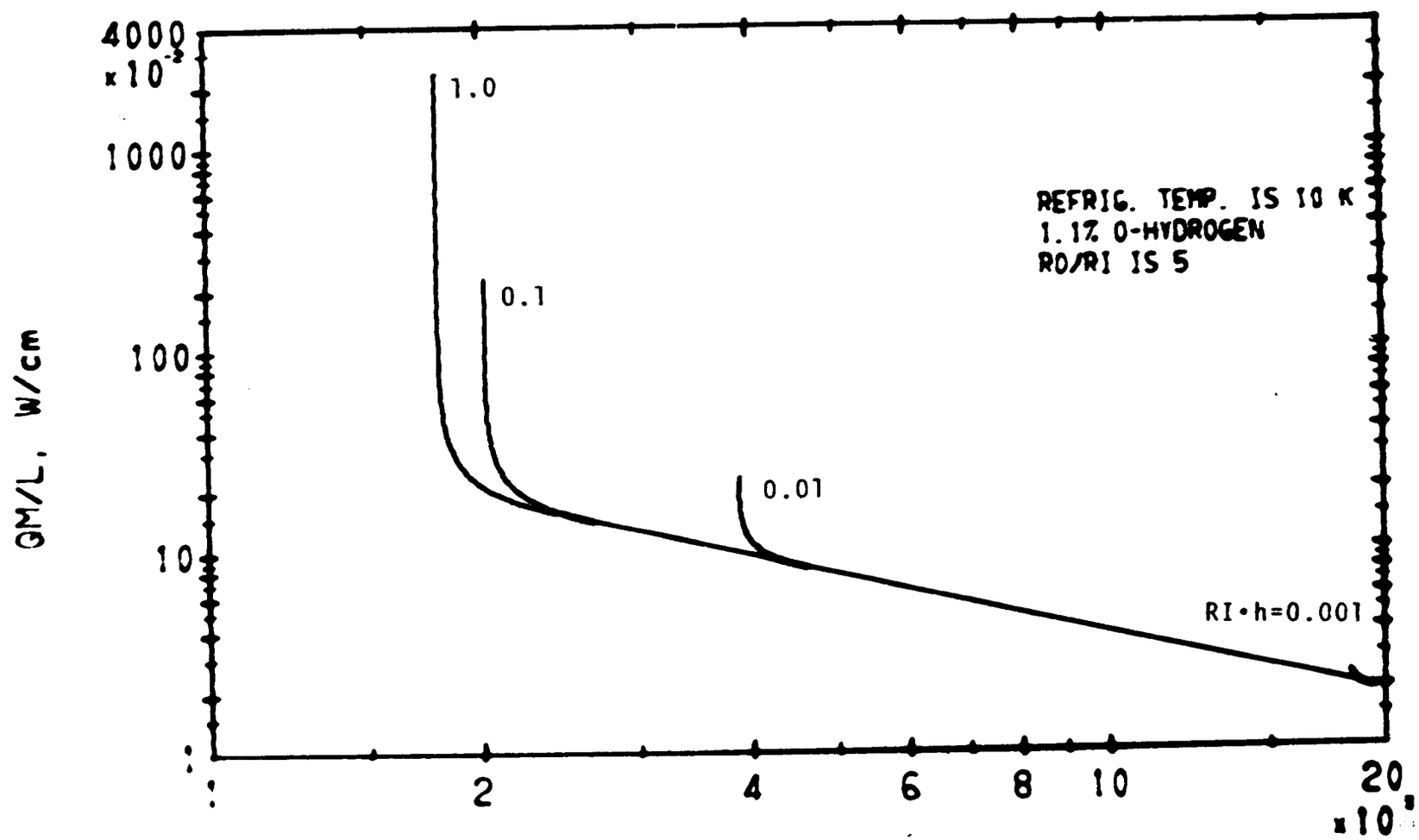

CYLINDER, FREEZING FROM INSIDE

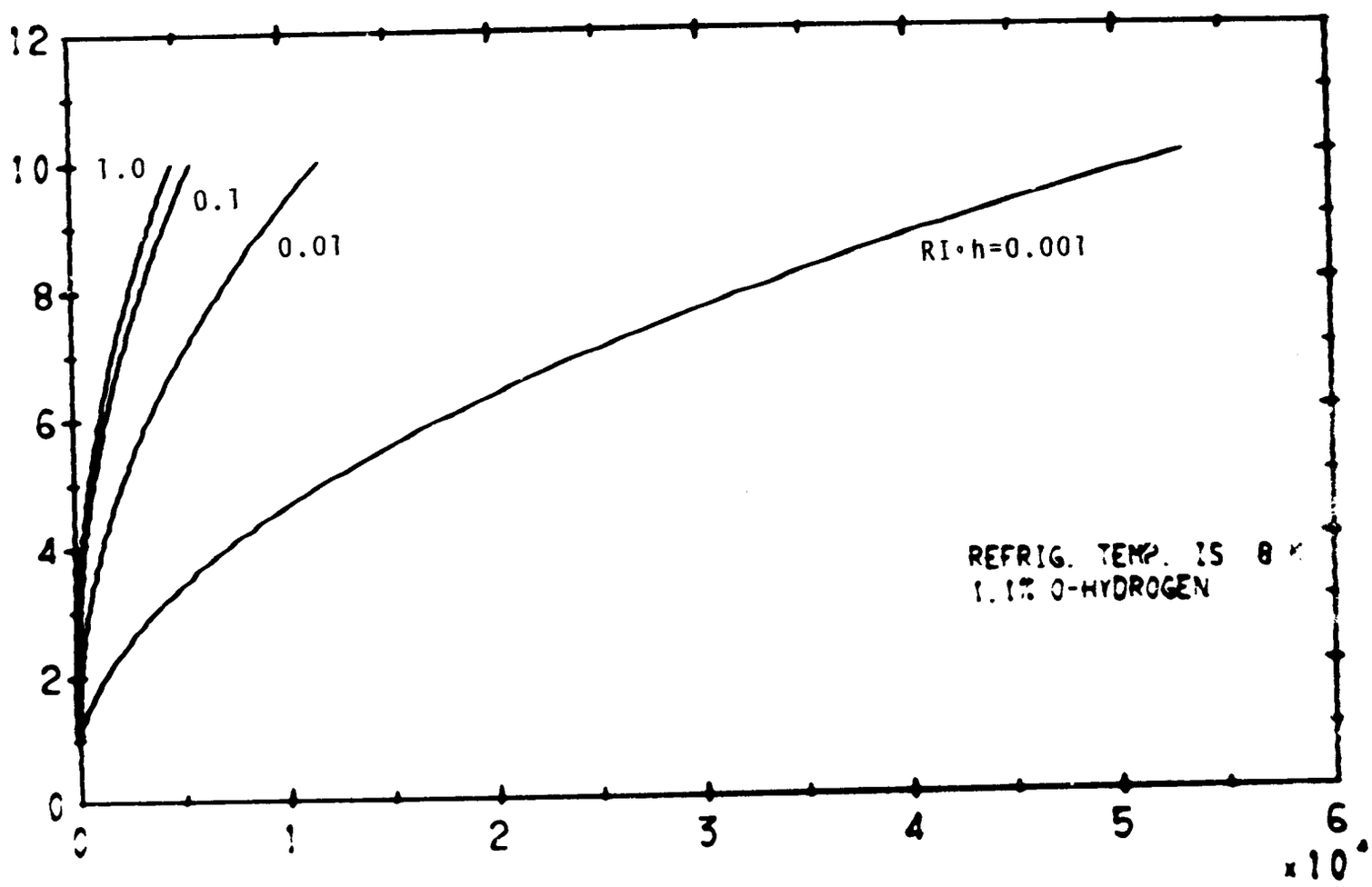

CYLINDER, FREEZING FROM INSIDE

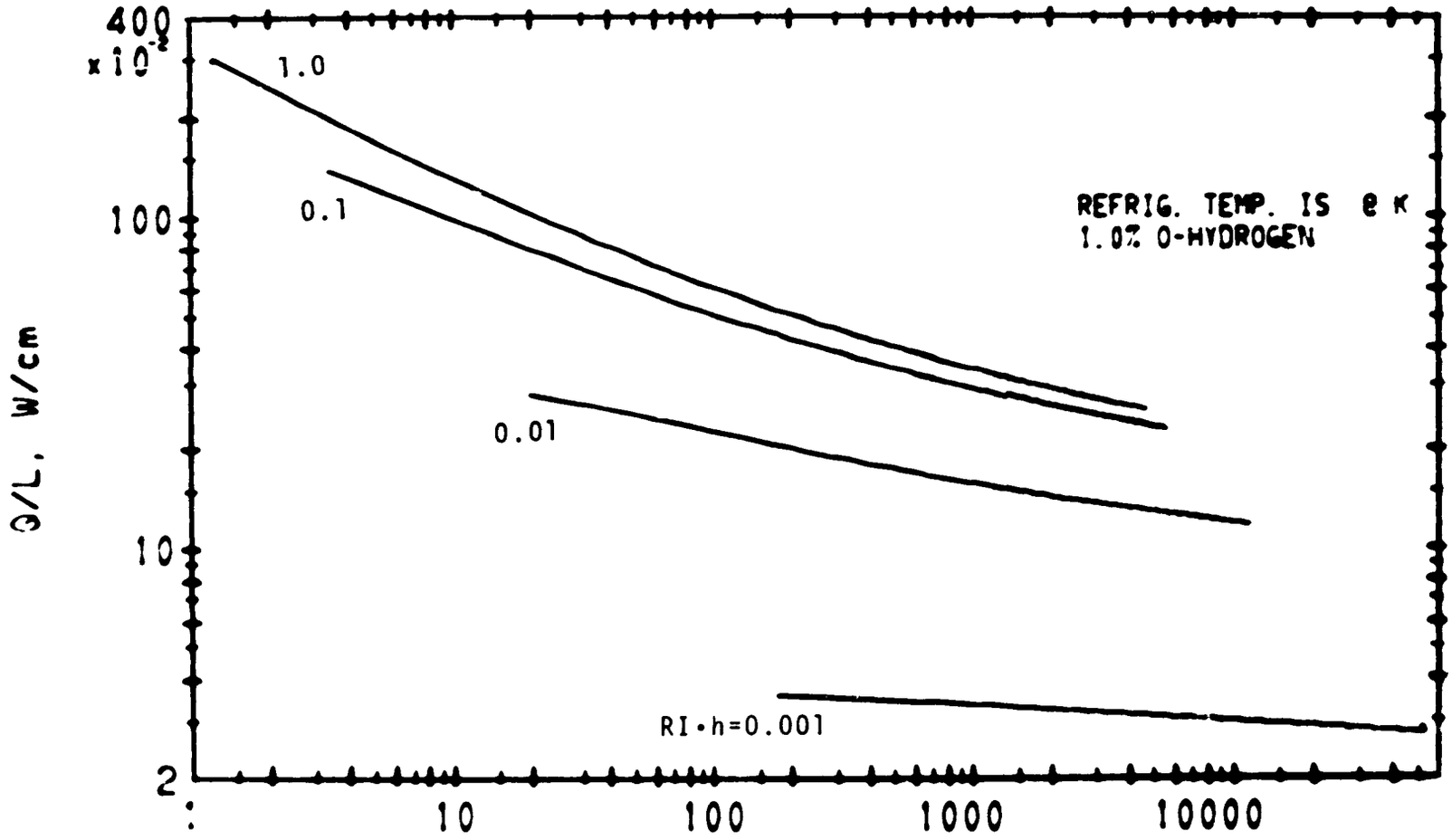

121

CYLINDER, FREEZING FROM INSIDE

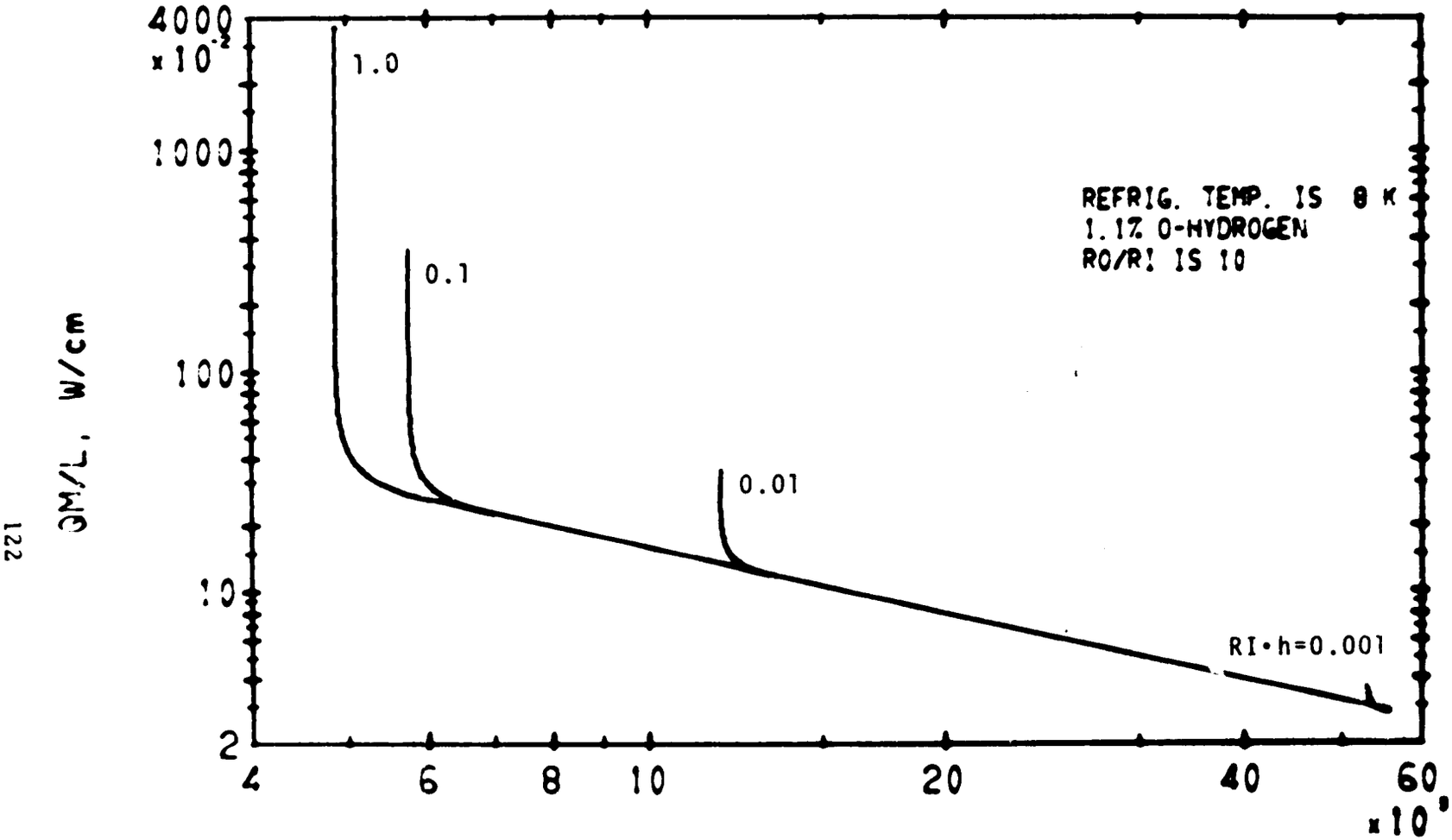

CYLINDER, FREEZING FROM INSIDE

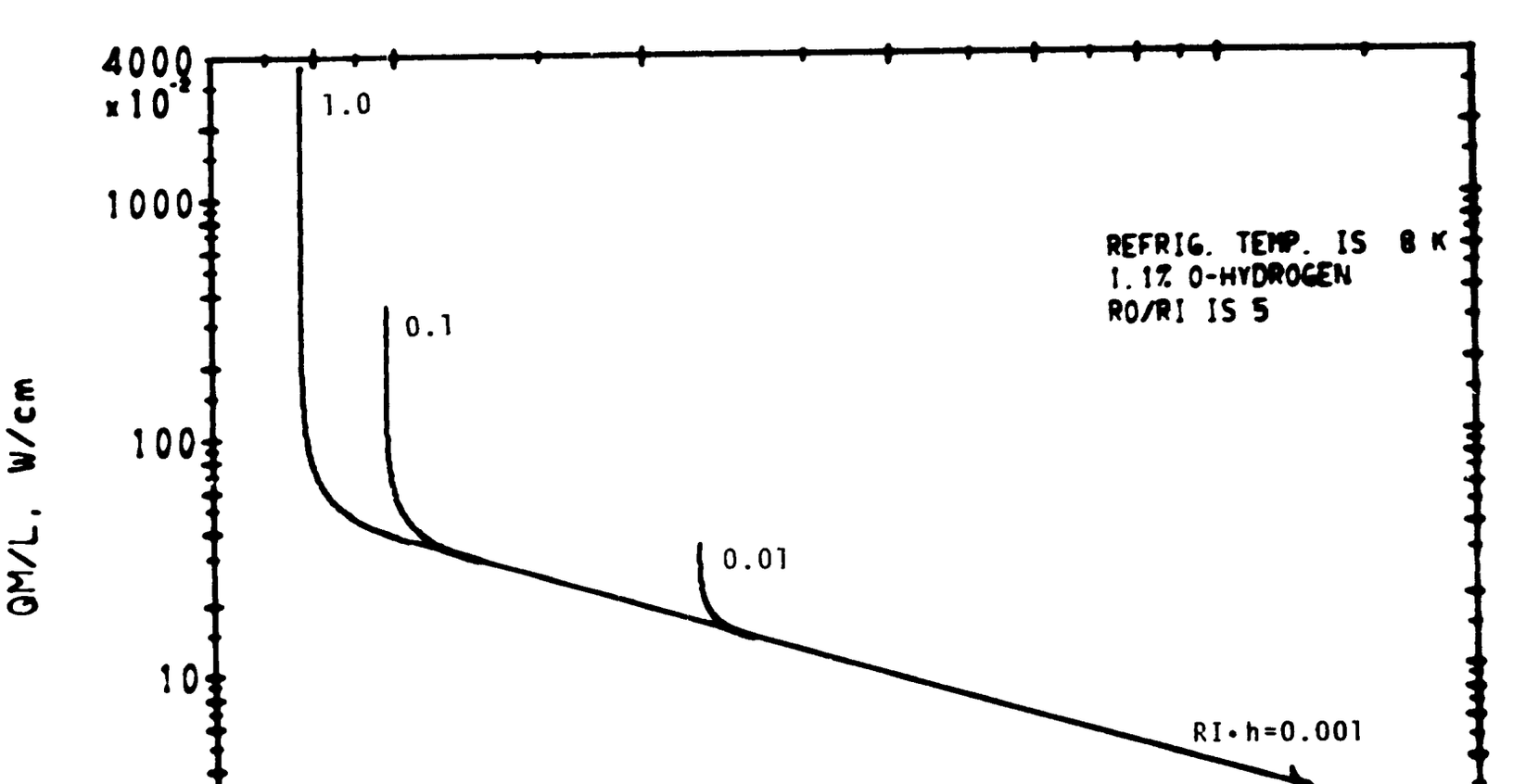

CYLINDER, FREEZING FROM INSIDE

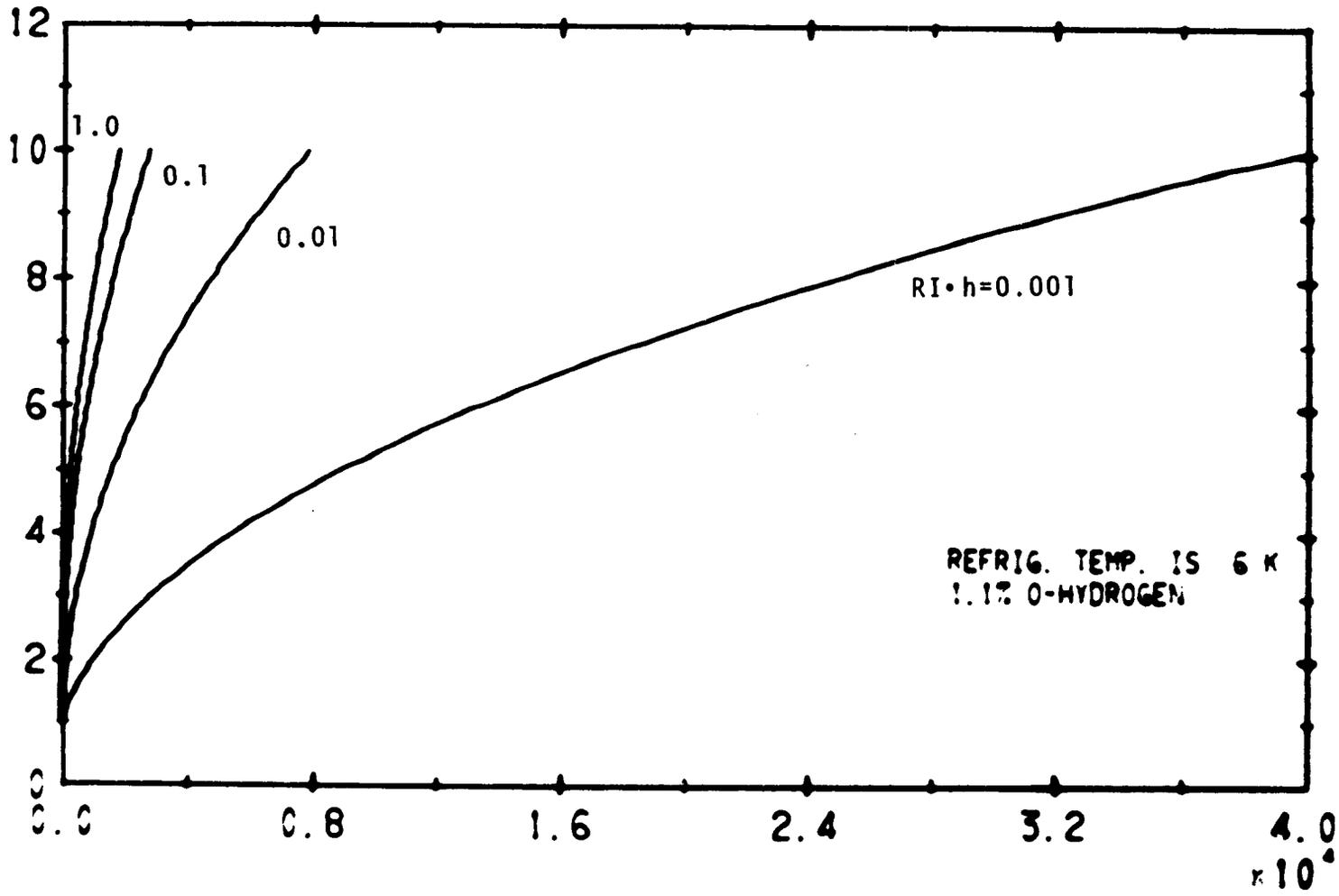

CYLINDER, FREEZING FROM INSIDE

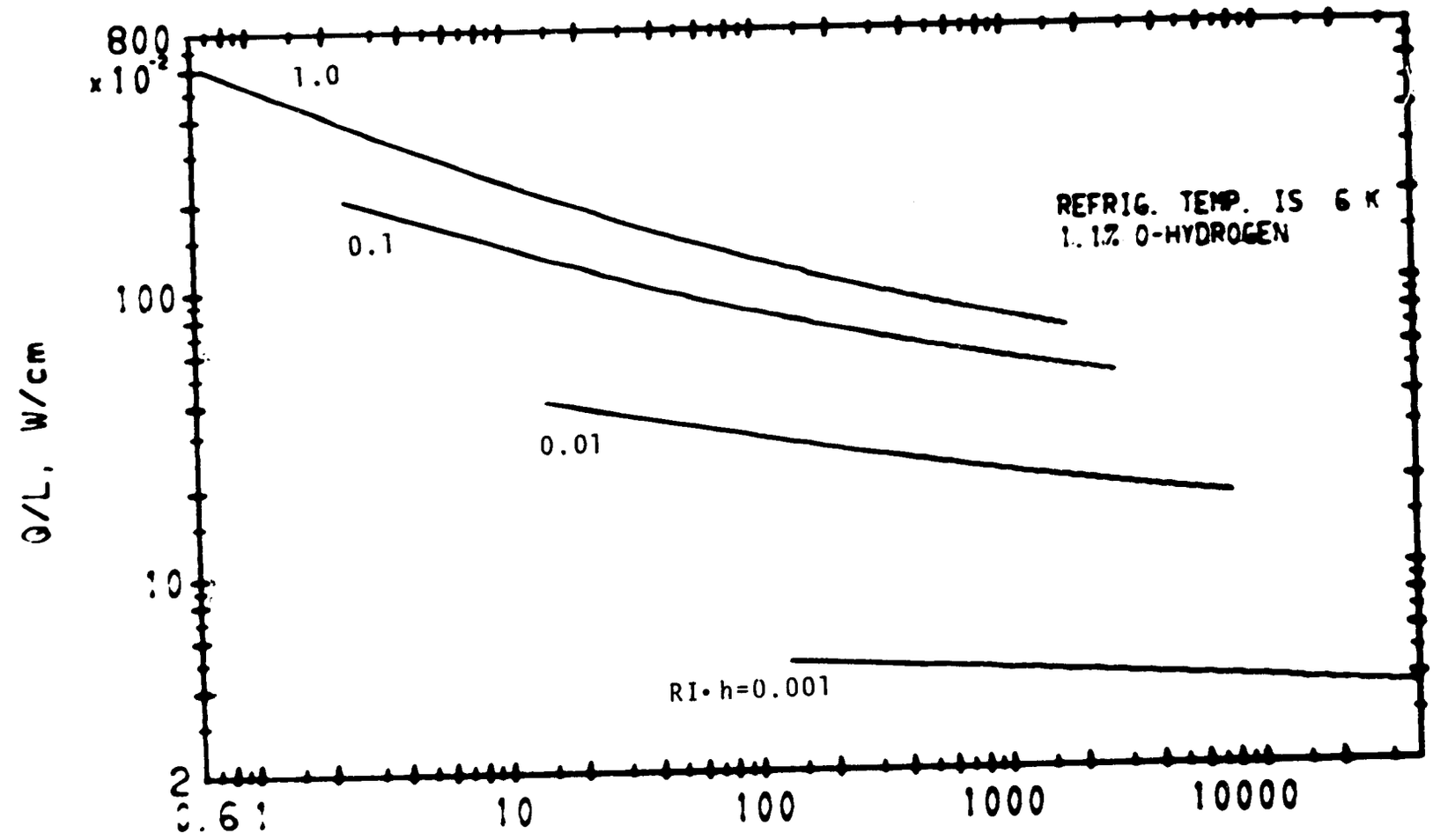

CYLINDER, FREEZING FROM INSIDE

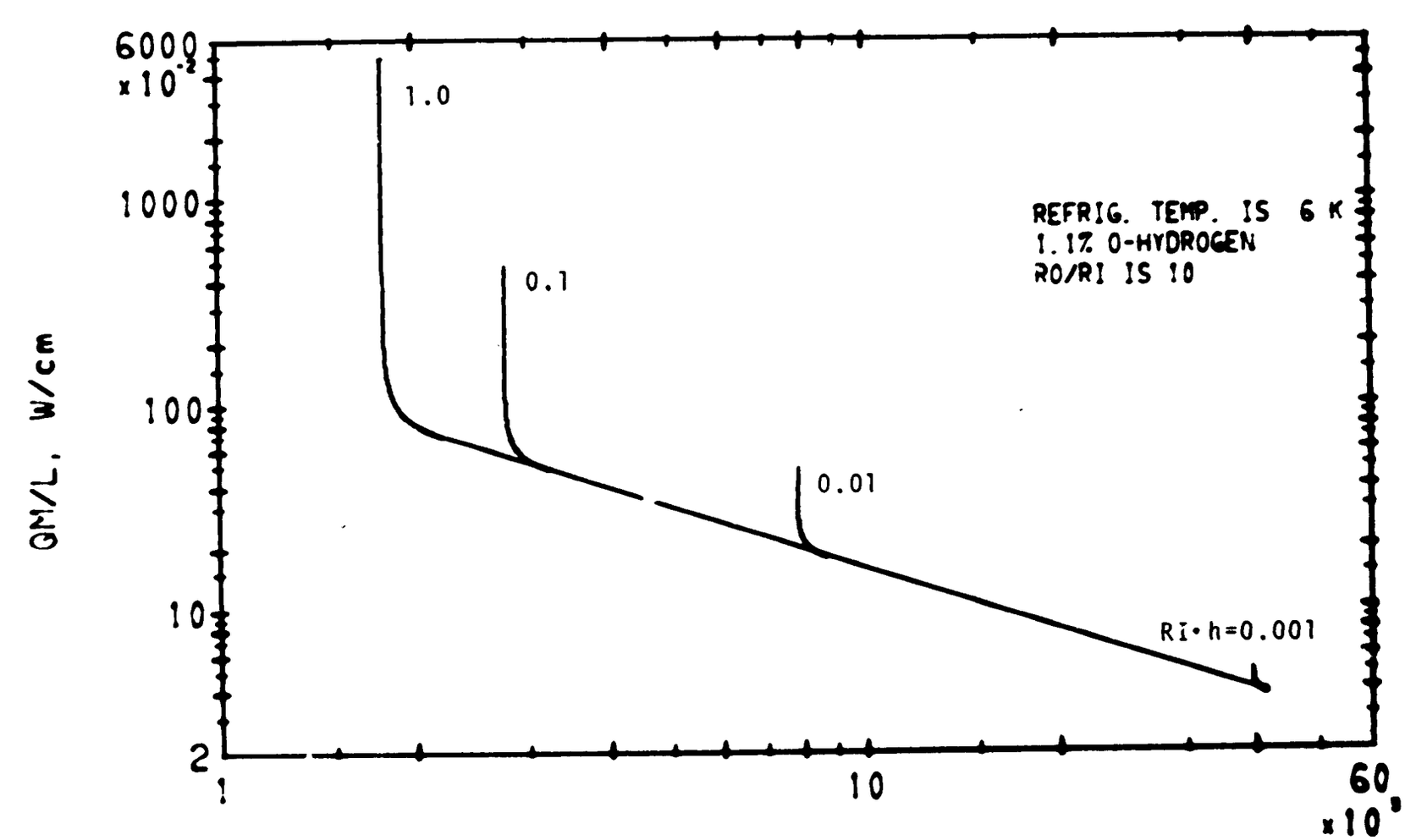

126

CYLINDER, FREEZING FROM INSIDE

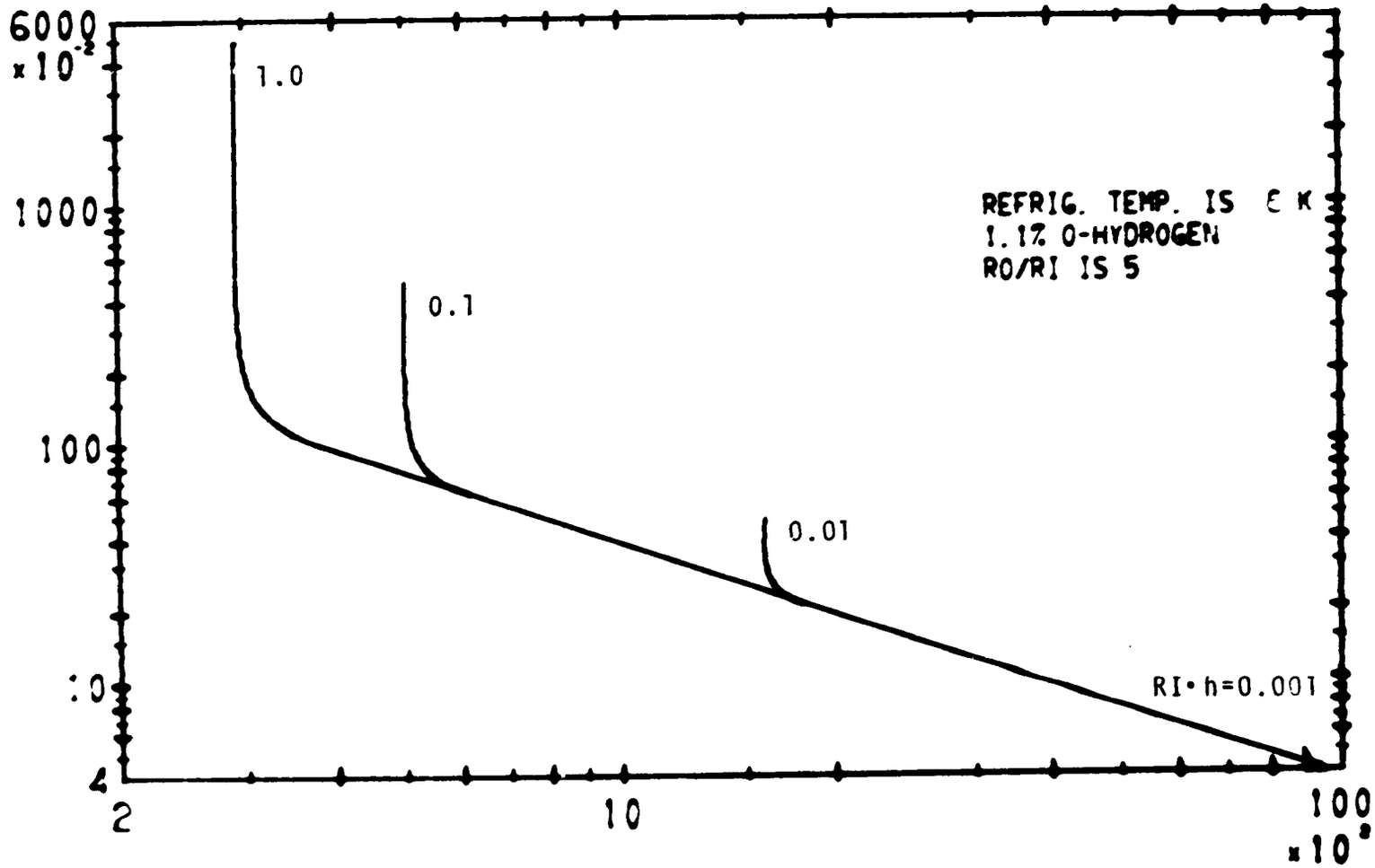

127

CYLINDER, FREEZING FROM INSIDE

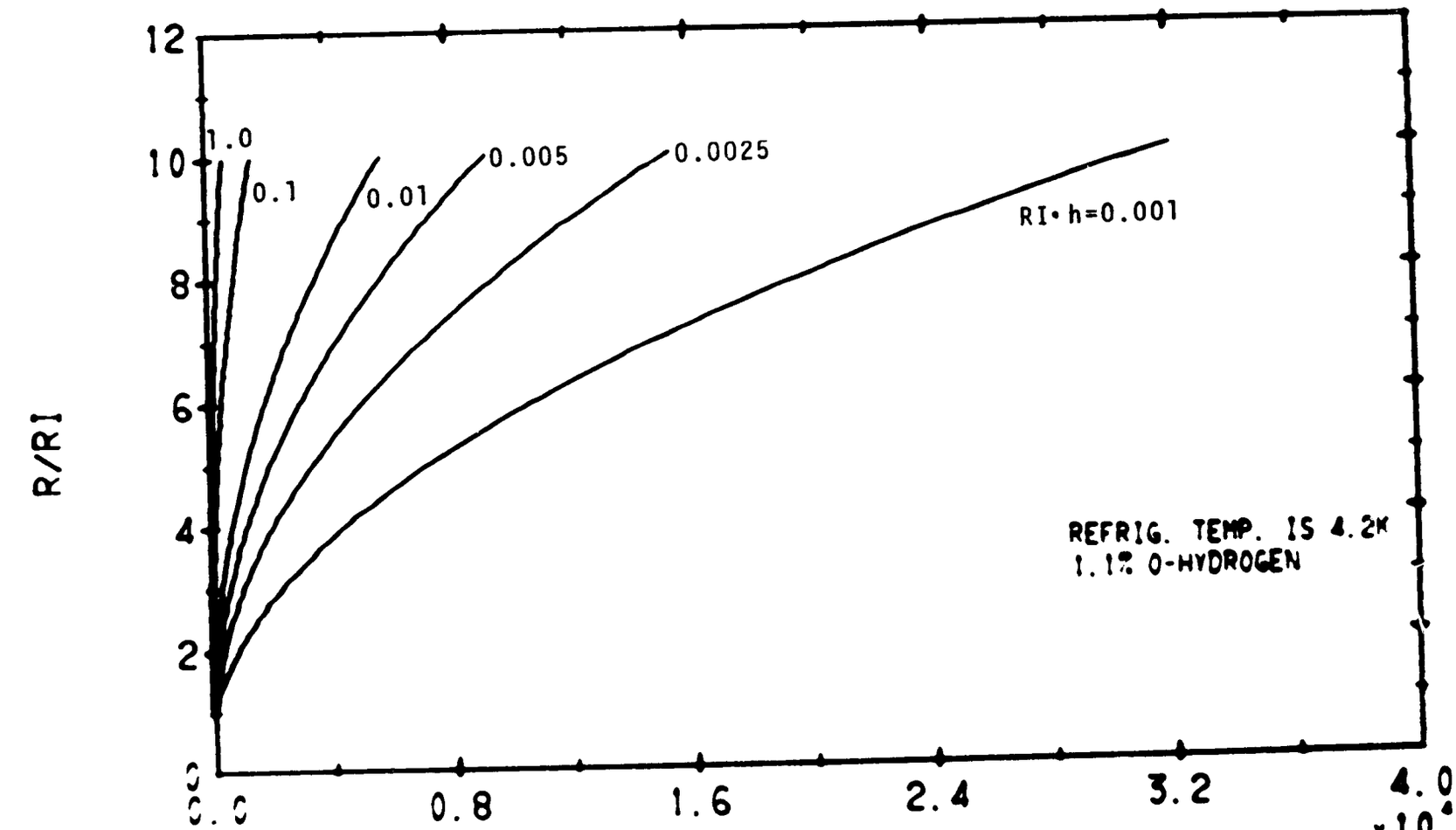

CYLINDER, FREEZING FROM INSIDE

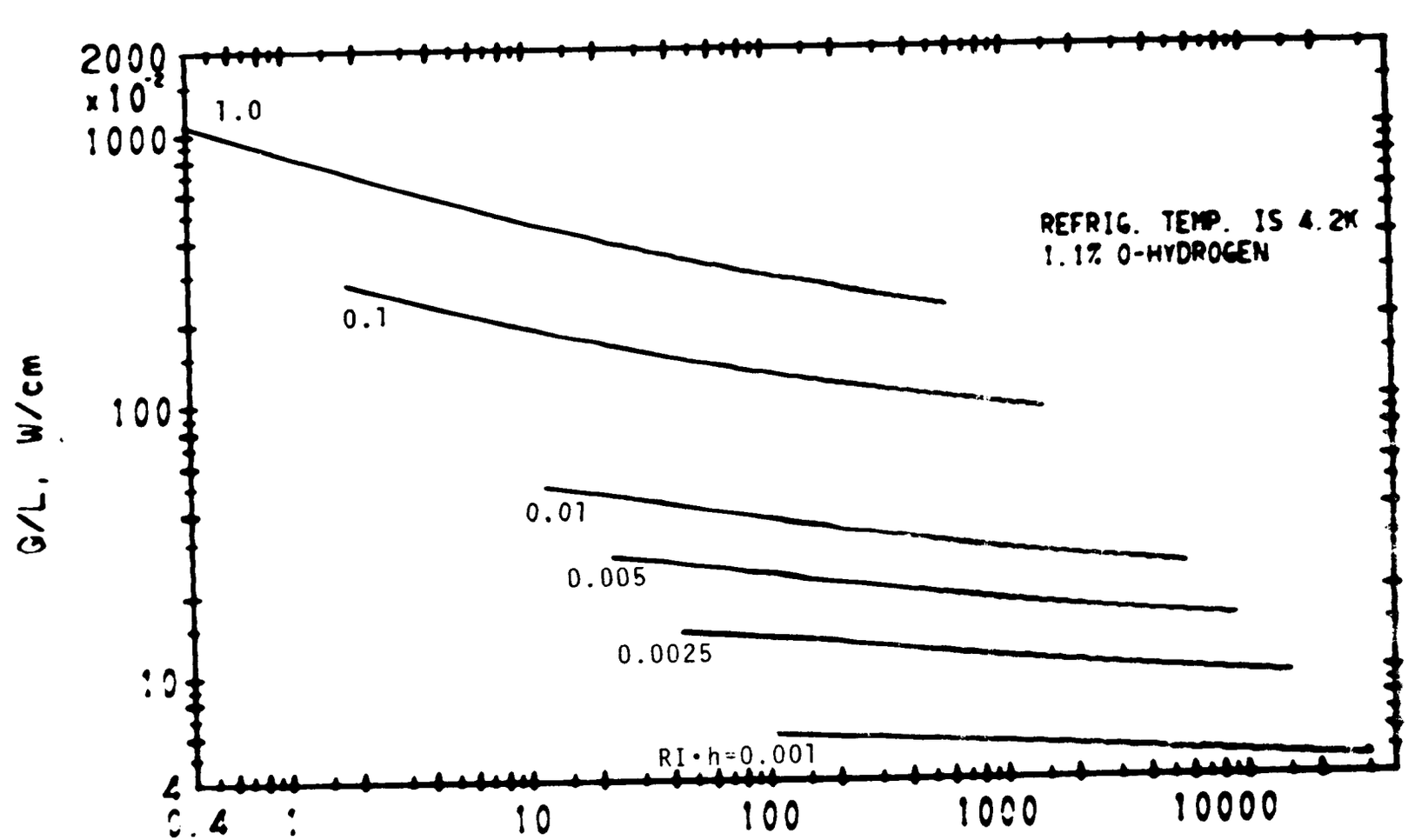

CYLINDER, FREEZING FROM INSIDE

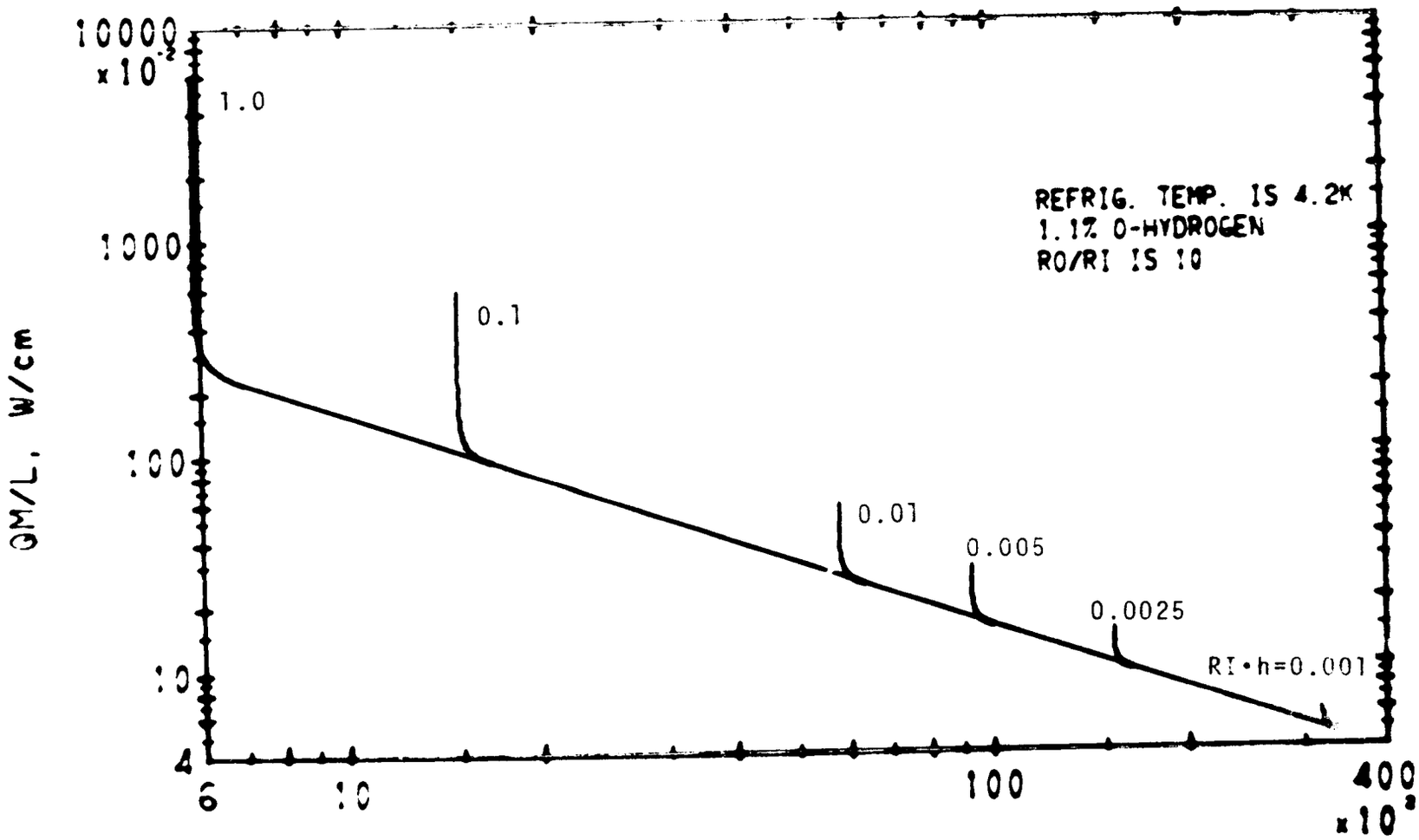

CYLINDER, FREEZING FROM INSIDE

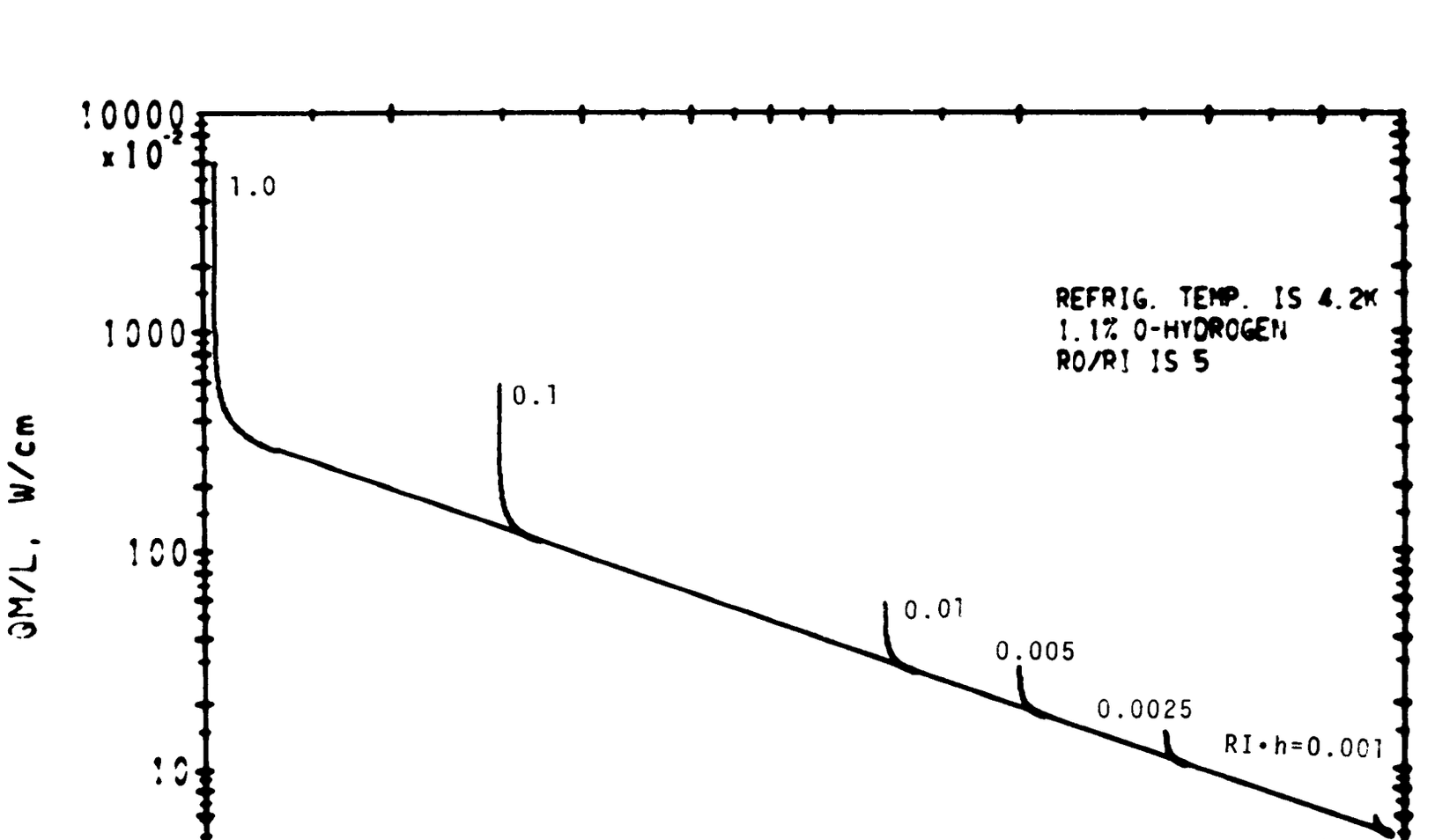

CYLINDER, FREEZING FROM INSIDE

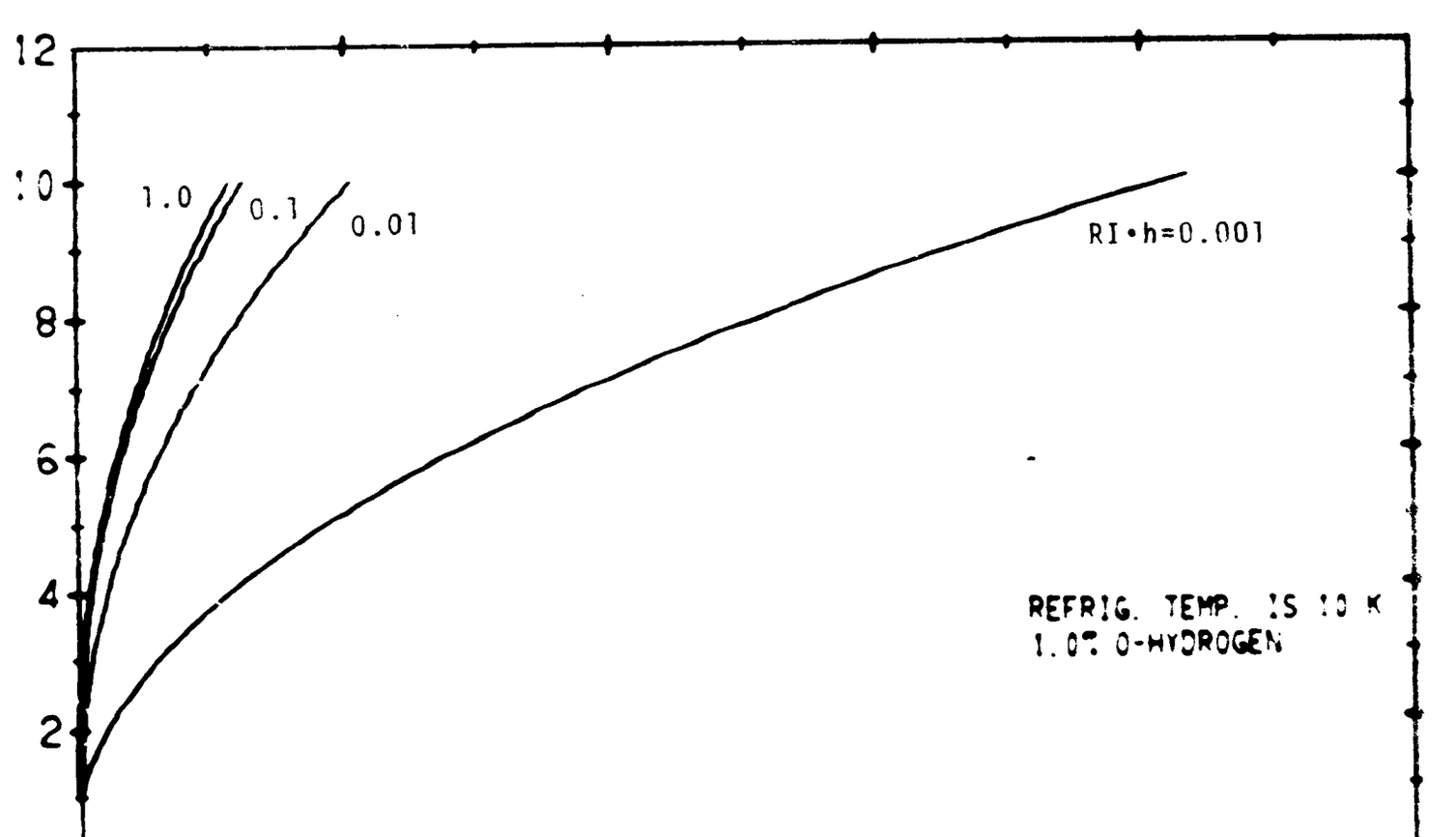

CYLINDER, FREEZING FROM INSIDE

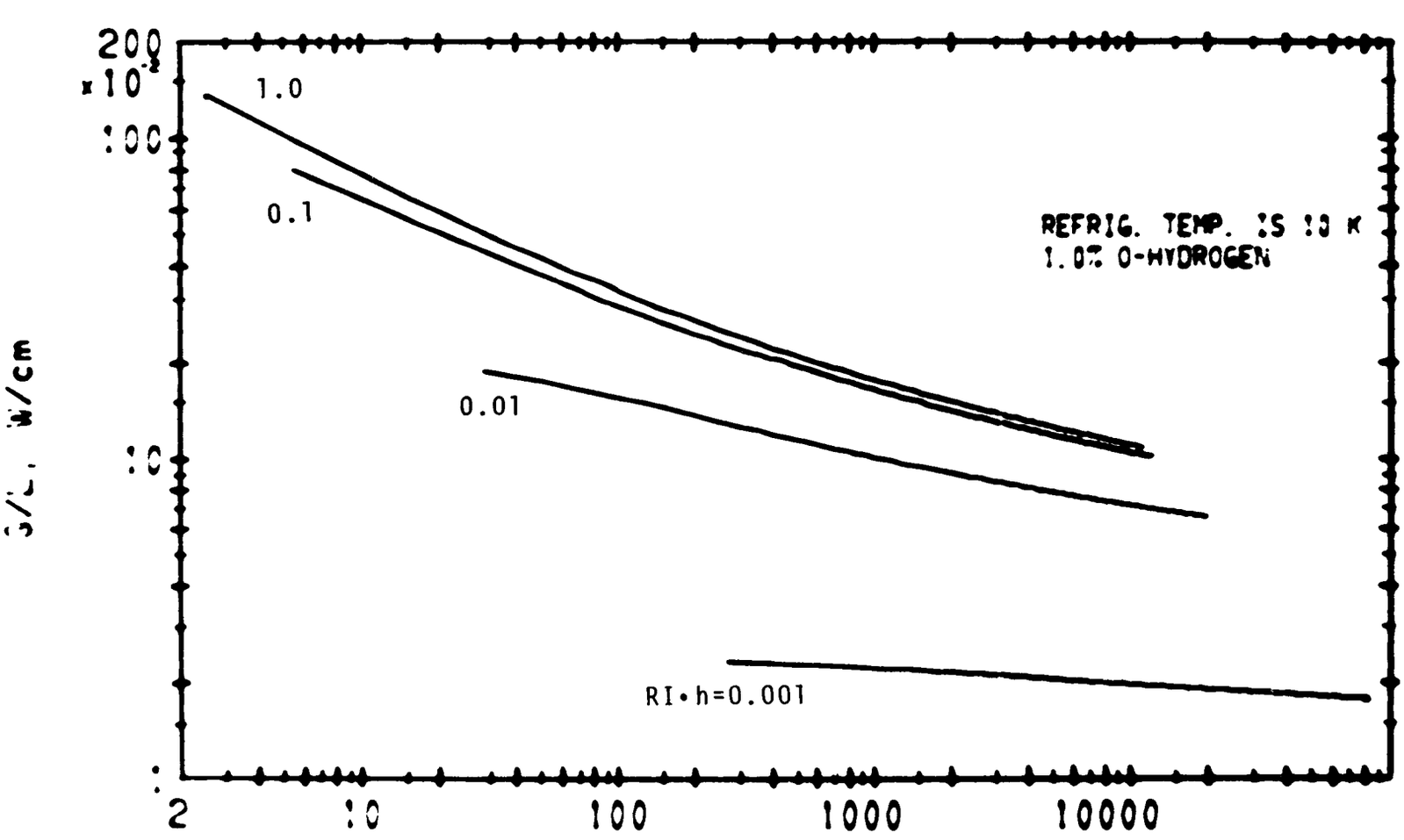

CYLINDER, FREEZING FROM INSIDE

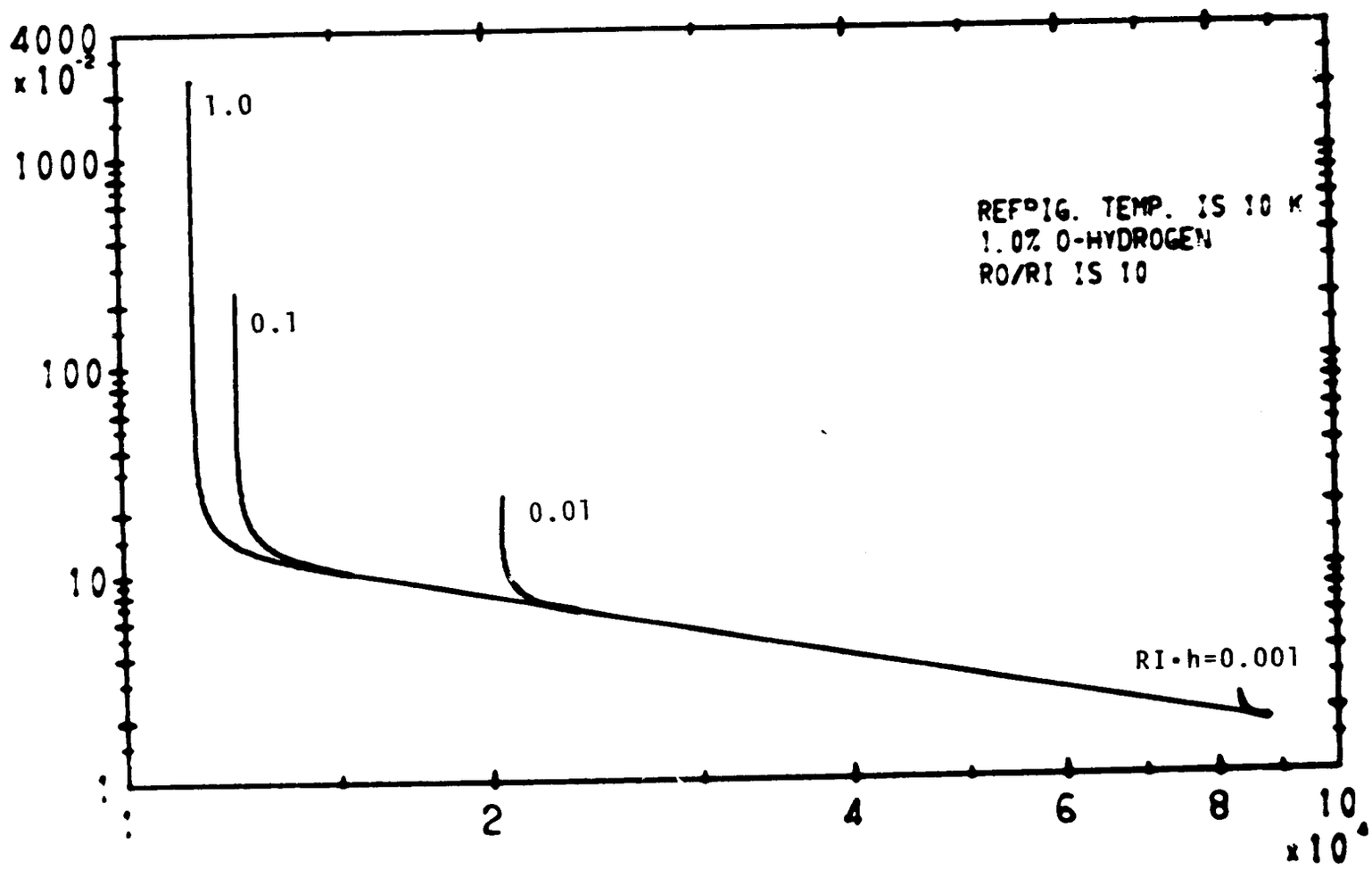

CYLINDER, FREEZING FROM INSIDE

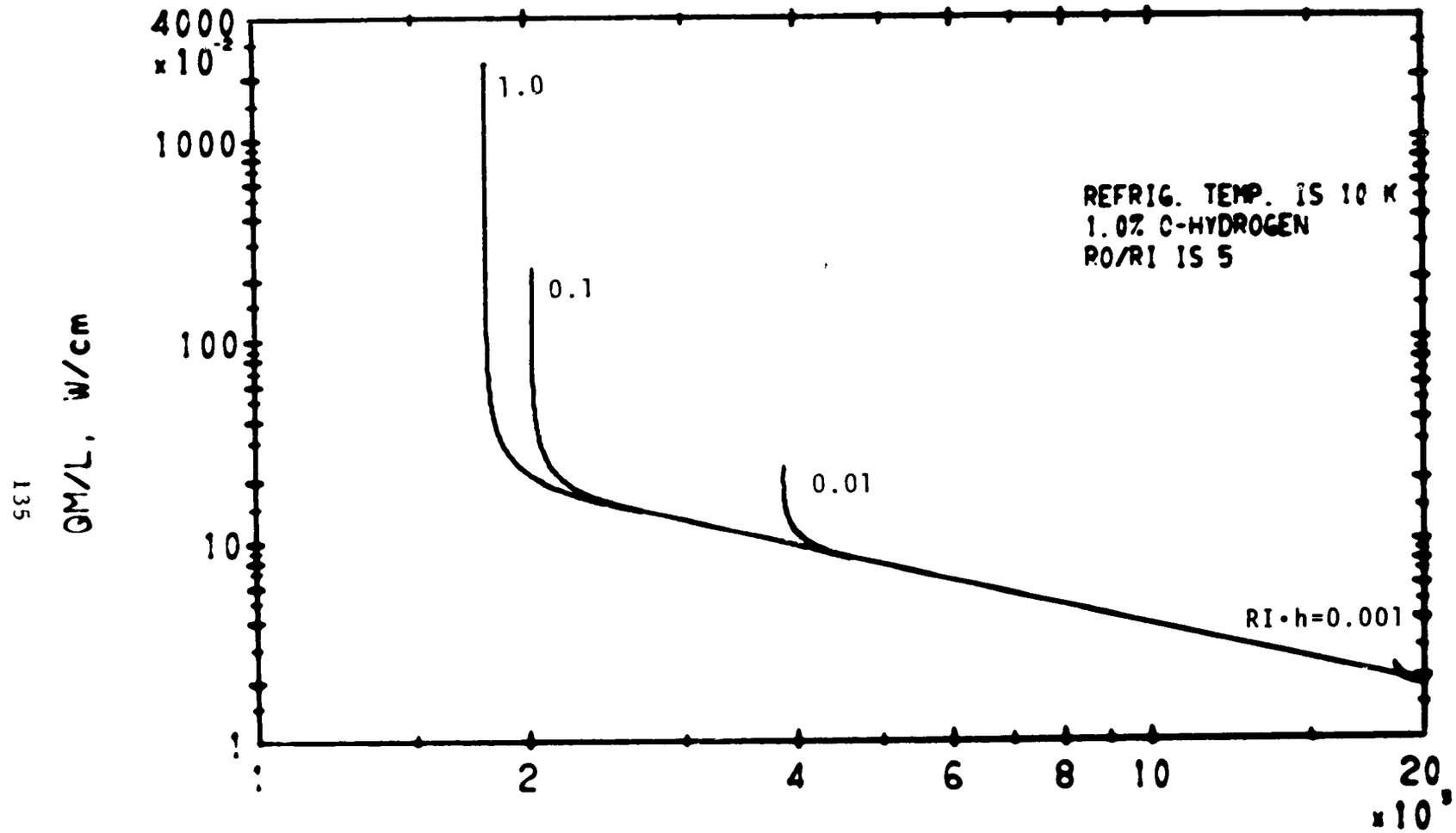

CYLINDER, FREEZING FROM INSIDE

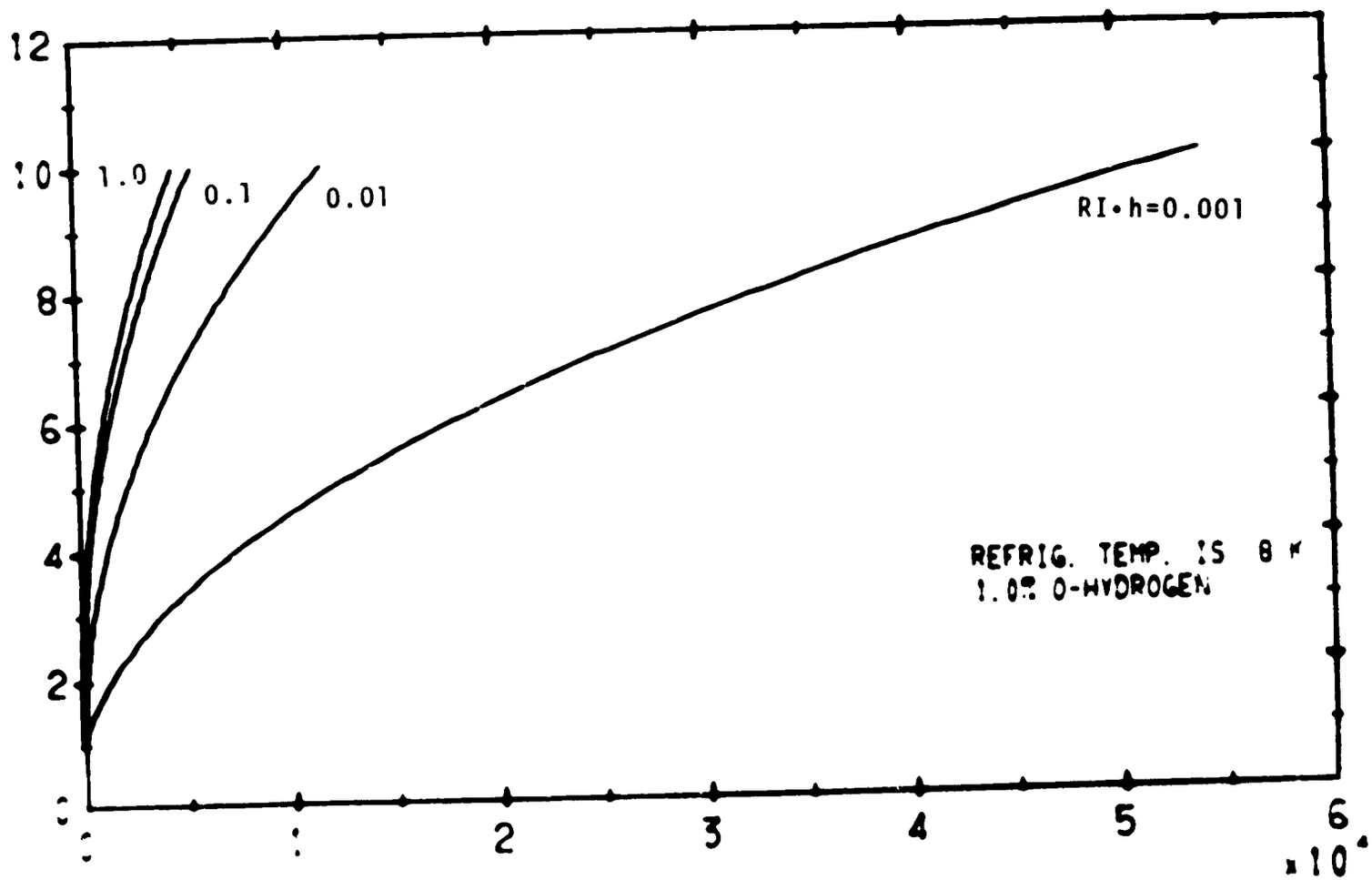

CYLINDER, FREEZING FROM INSIDE

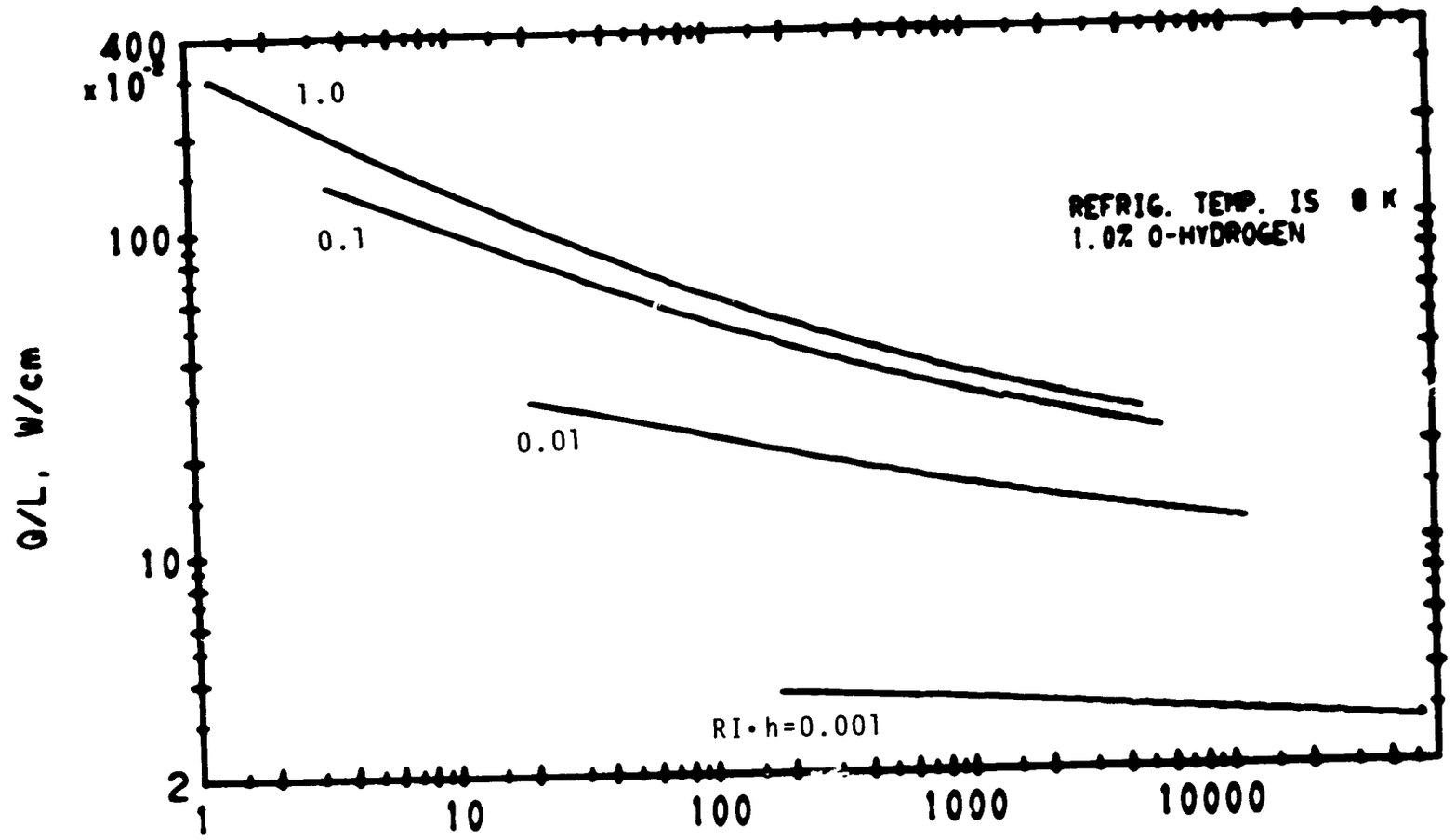

CYLINDER, FREEZING FROM INSIDE

12/27/71

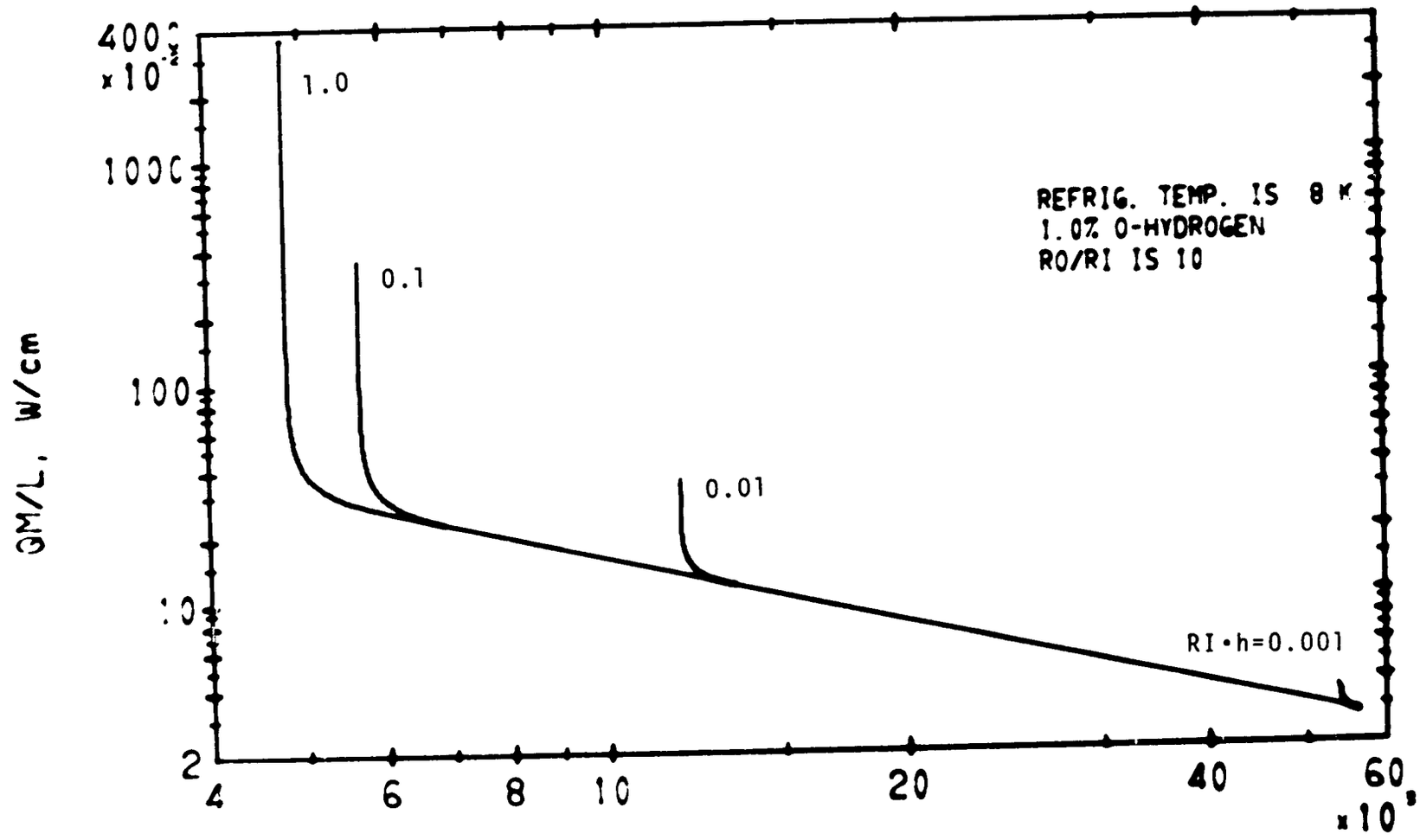

CYLINDER, FREEZING FROM INSIDE

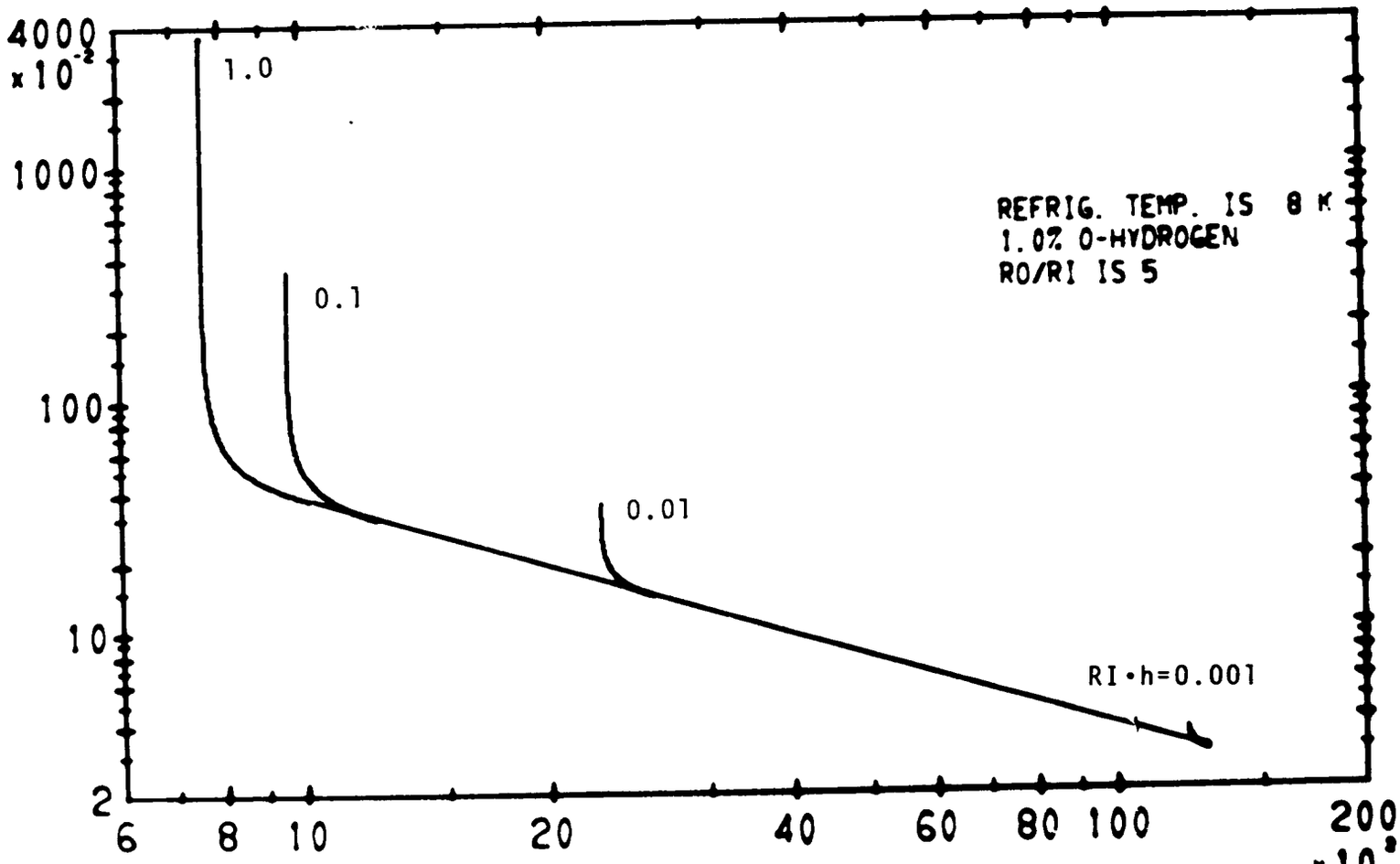

CYLINDER, FREEZING FROM INSIDE

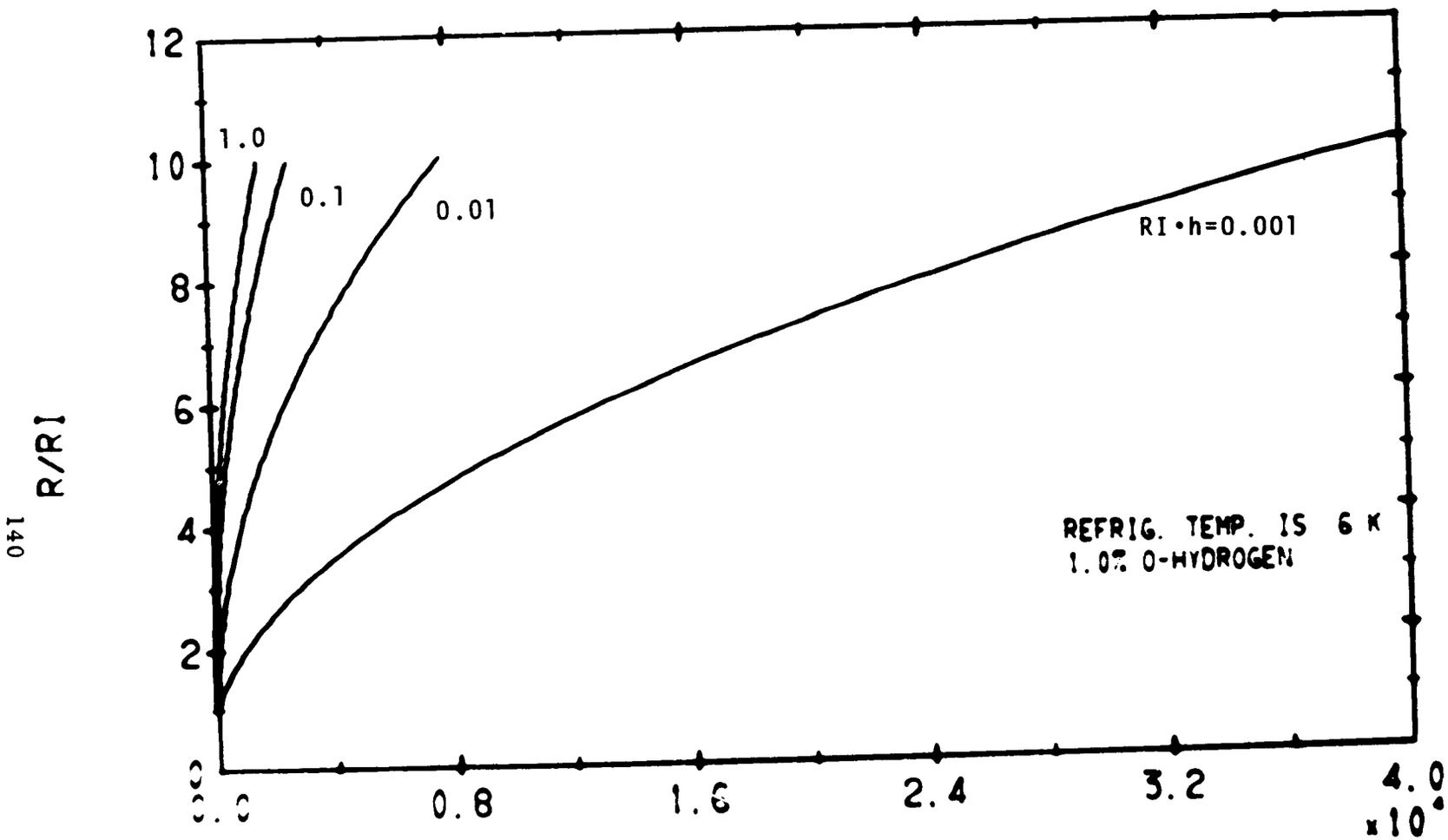

CYLINDER, FREEZING FROM INSIDE

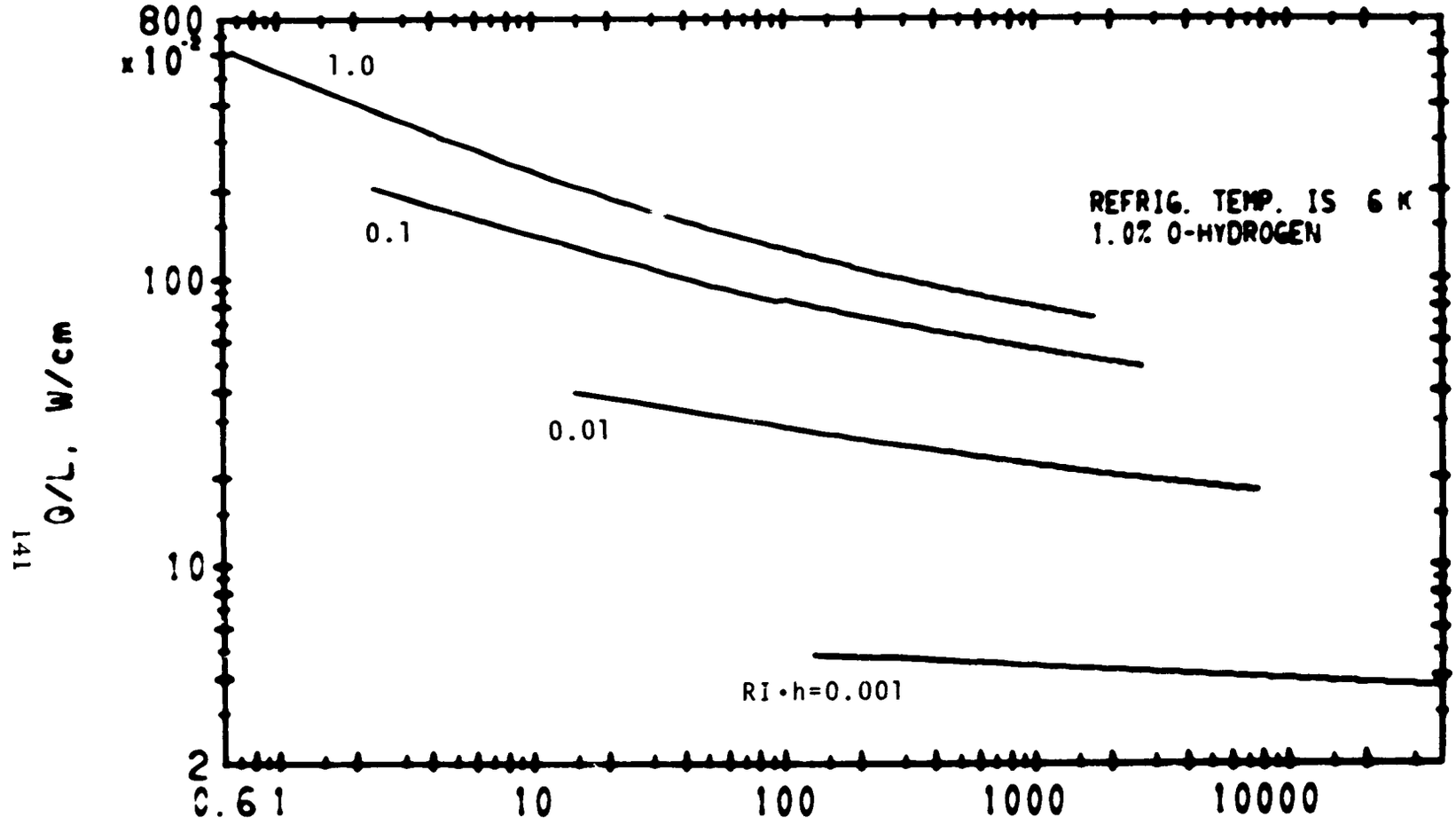

CYLINDER, FREEZING FROM INSIDE

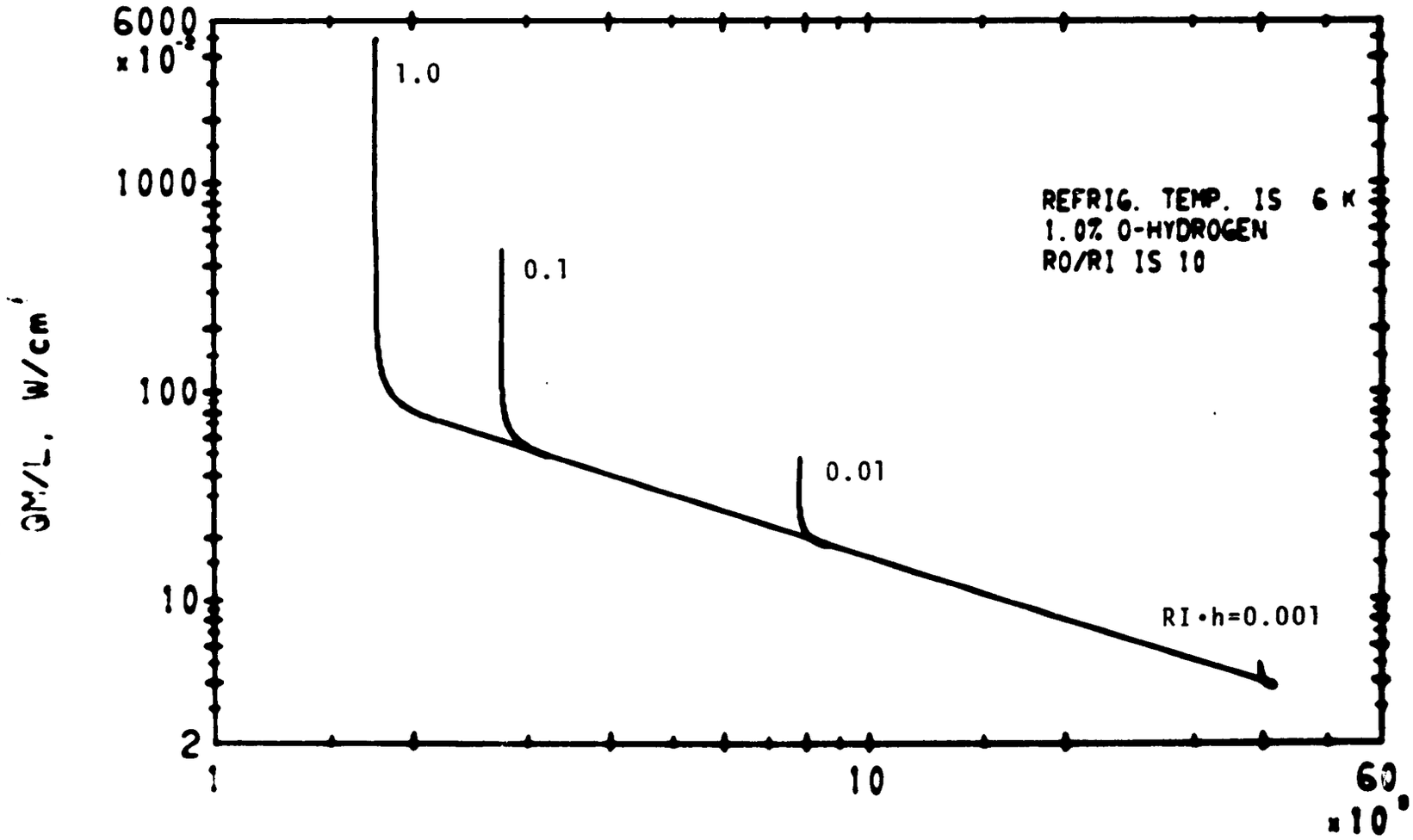

CYLINDER, FREEZING FROM INSIDE

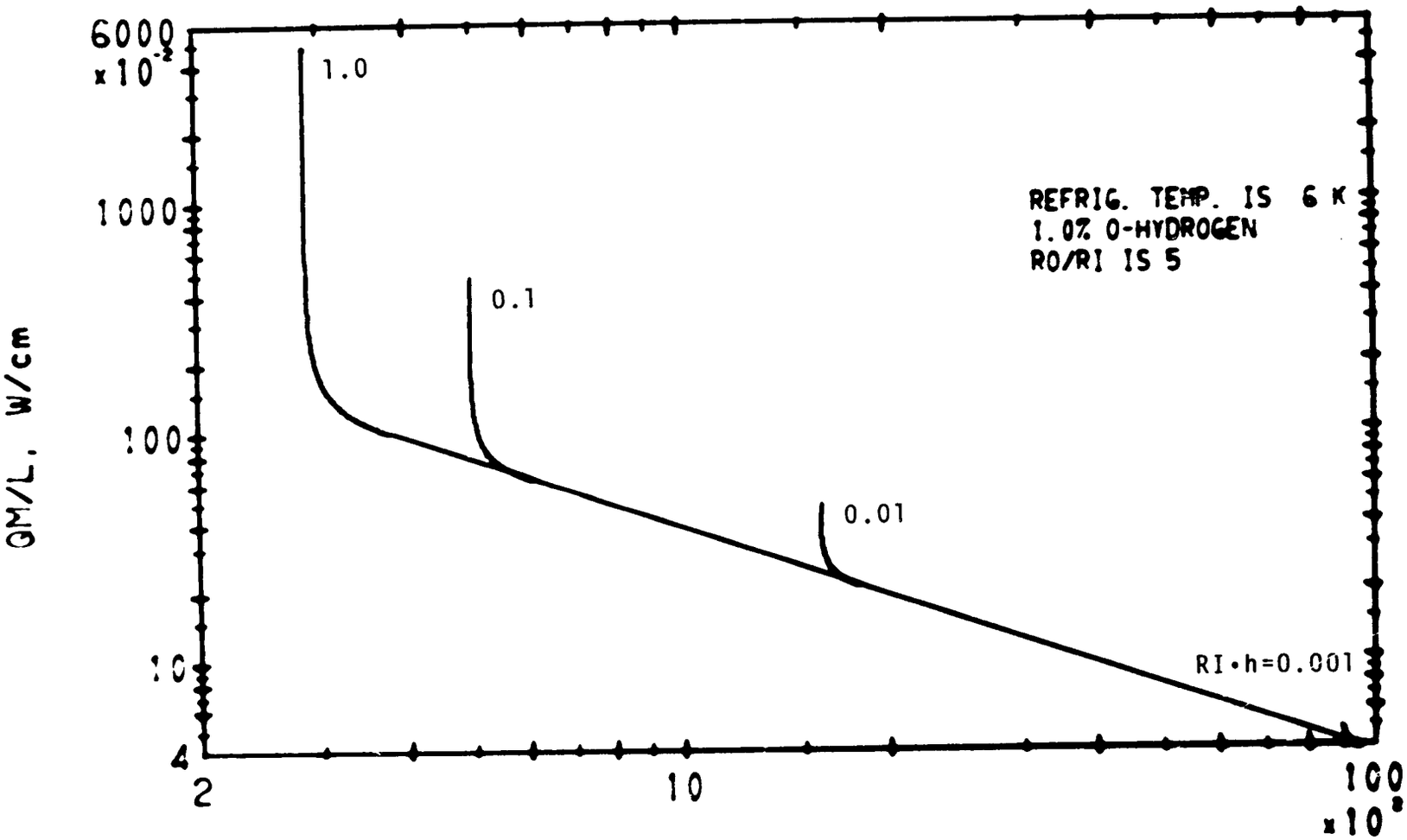

CYLINDER, FREEZING FROM INSIDE

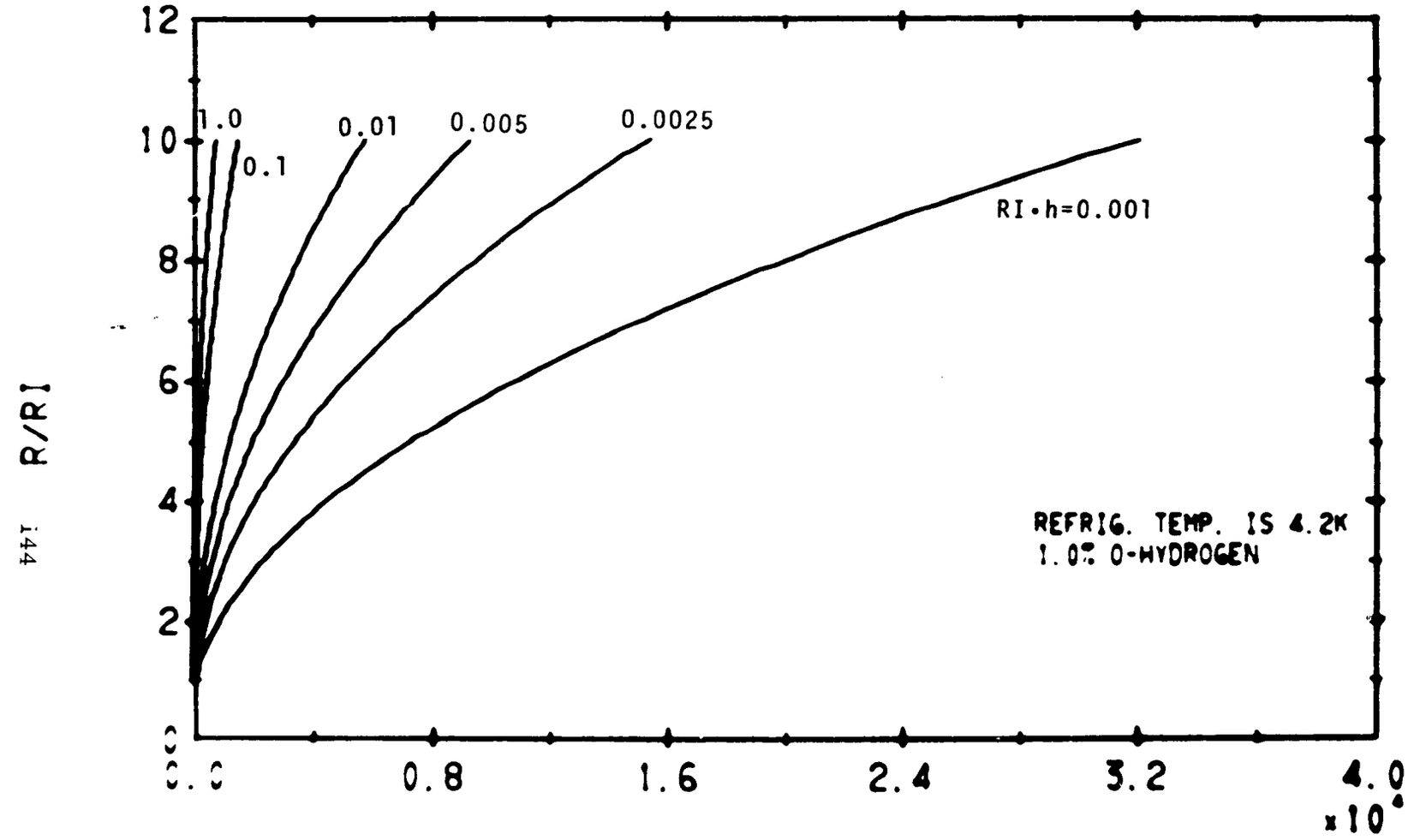

CYLINDER, FREEZING FROM INSIDE

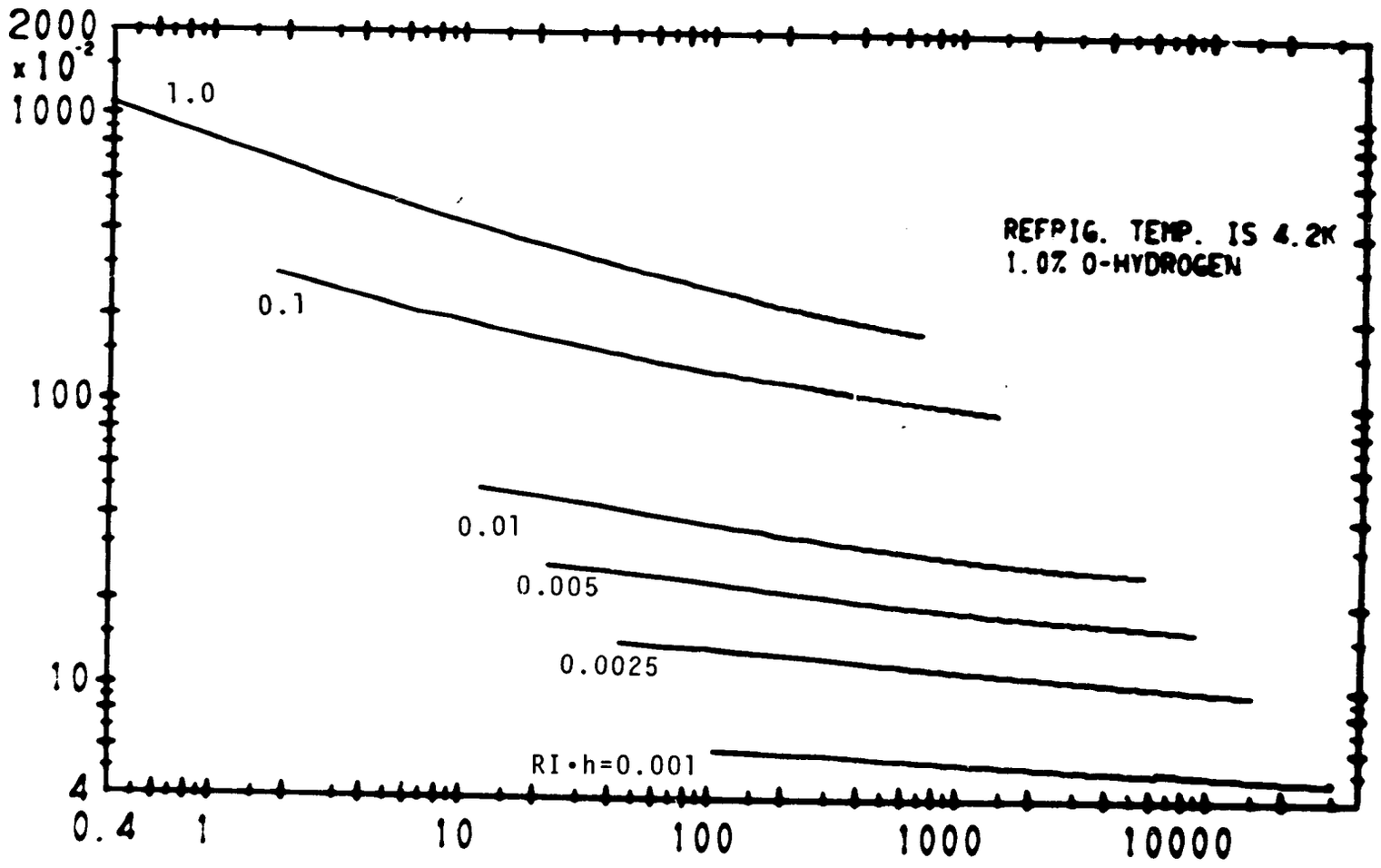

CYLINDER, FREEZING FROM INSIDE

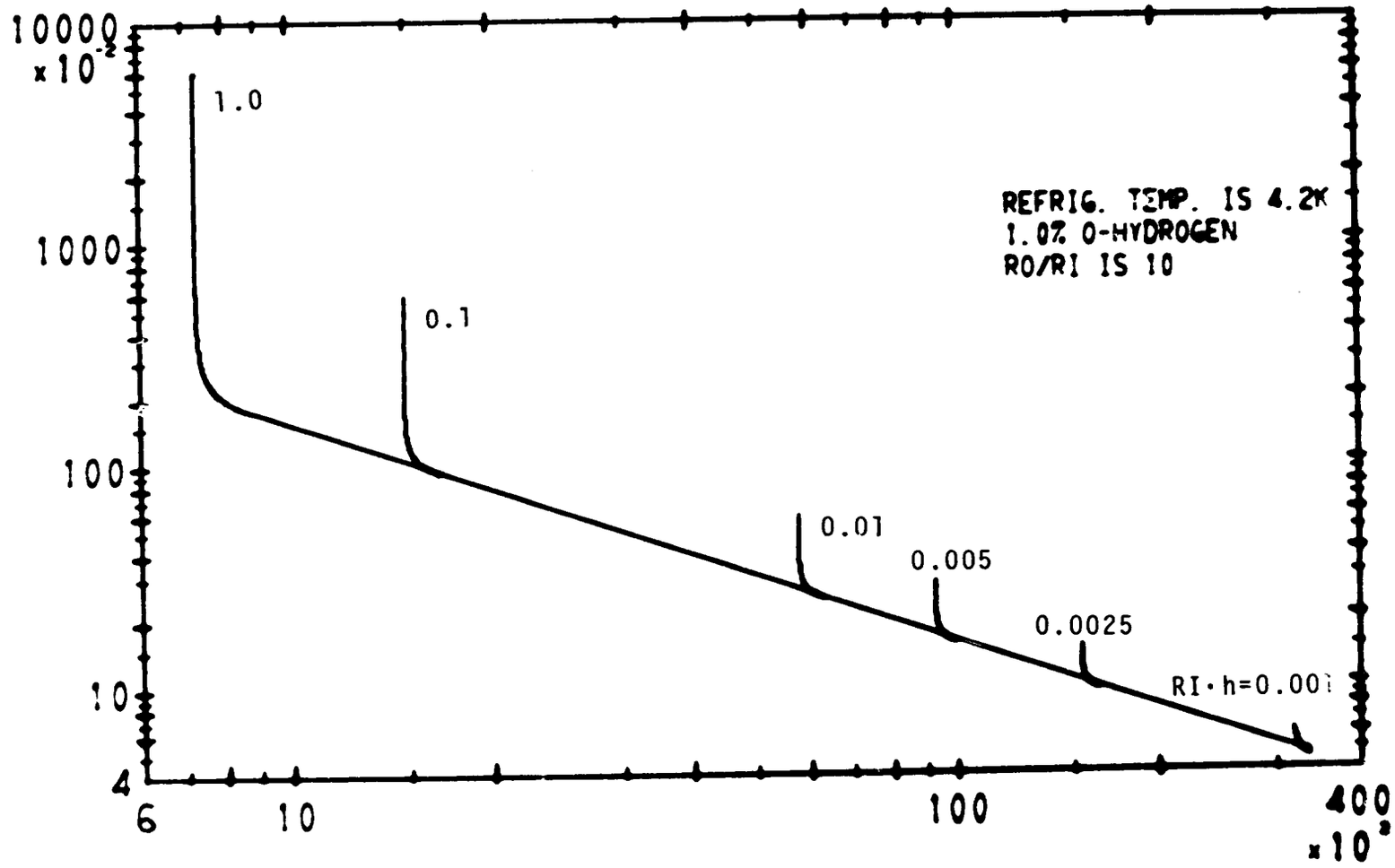

CYLINDER, FREEZING FROM INSIDE

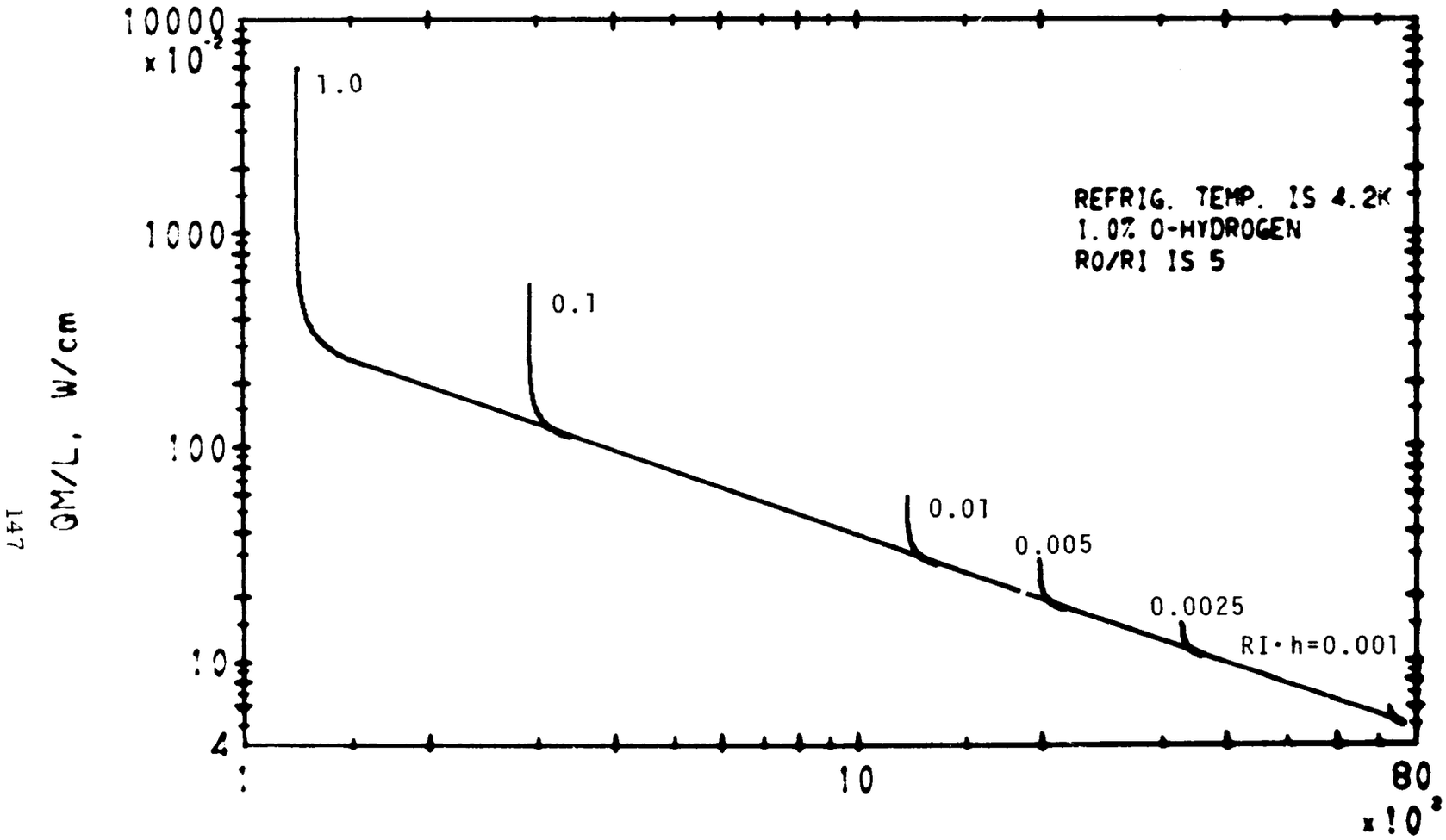

147

CYLINDER, FREEZING FROM INSIDE

APPENDIX C

SPHERE FREEZING FROM THE OUTSIDE

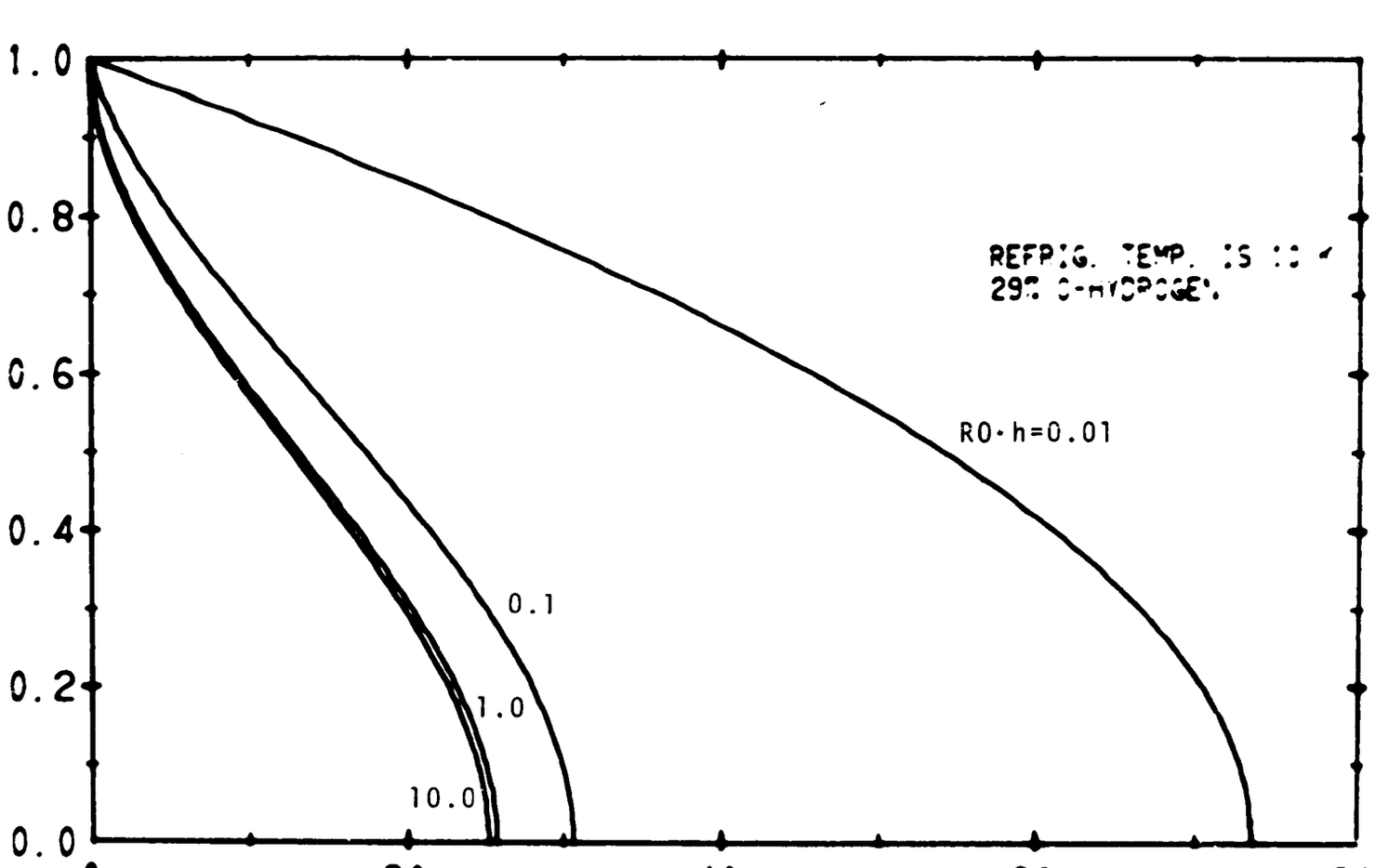

01/04/72

SPHERE, FREEZING FROM OUTSIDE

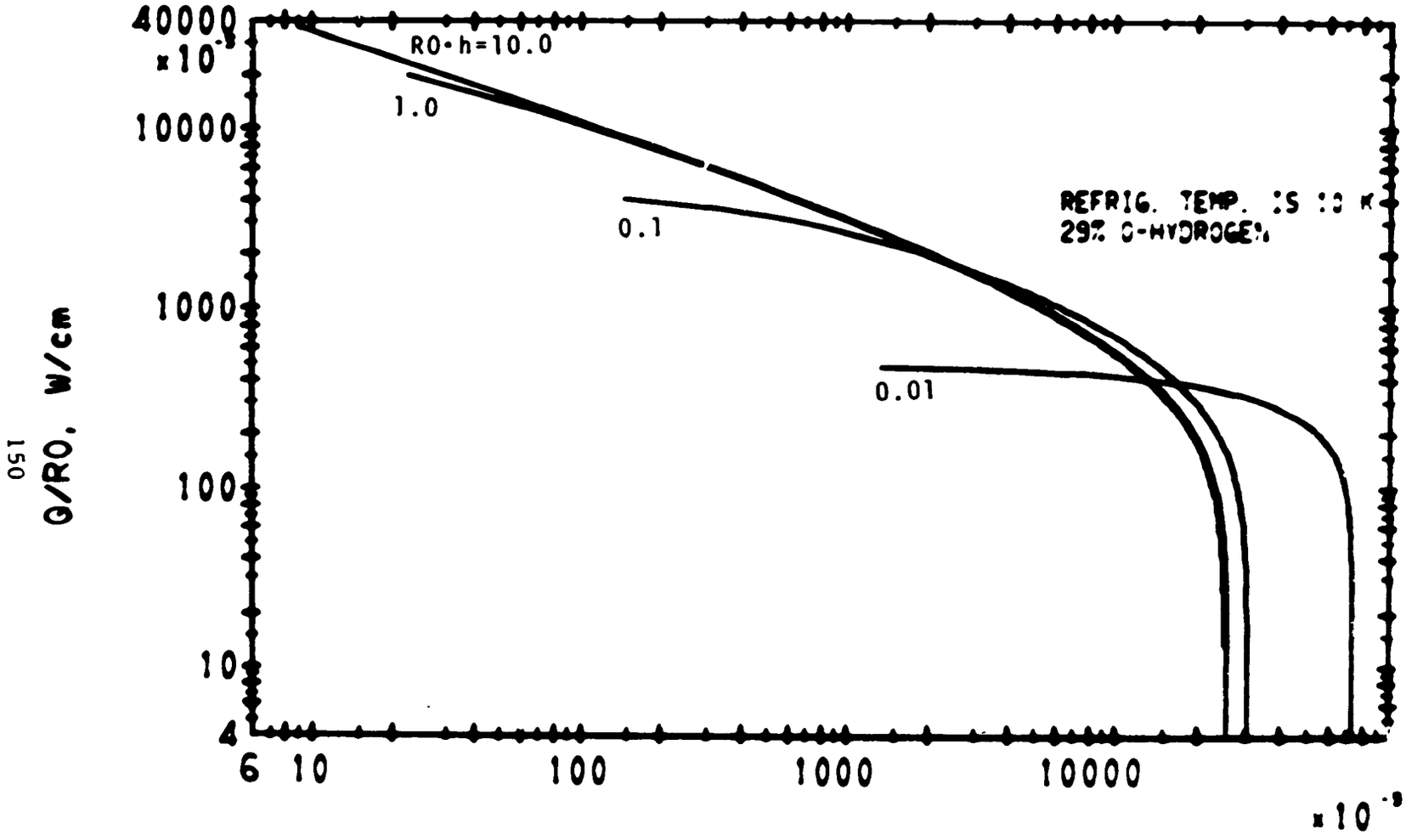

01/08/72

SPHERE, FREEZING FROM OUTSIDE

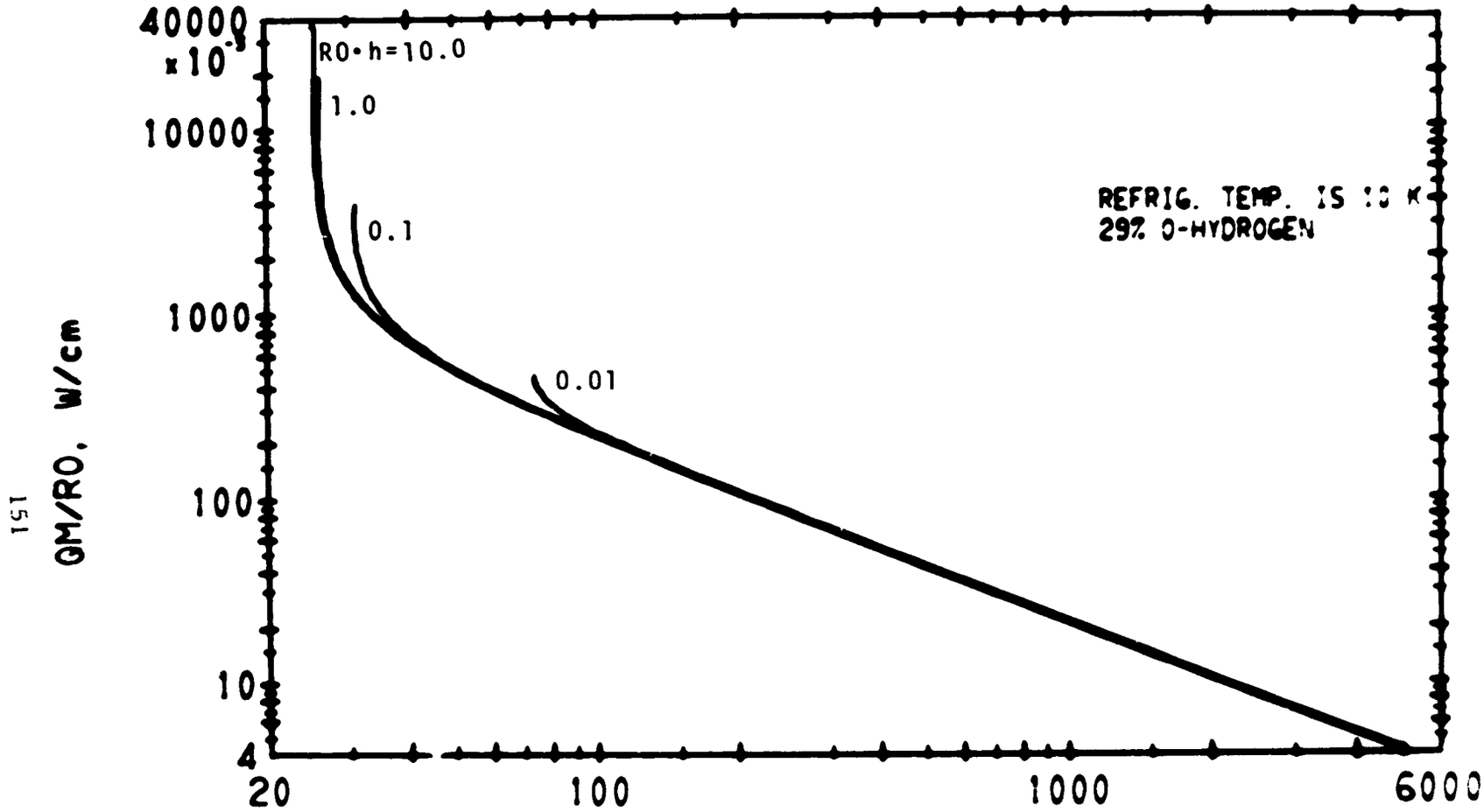

151

01/04/72

SPHERE, FREEZING FROM OUTSIDE

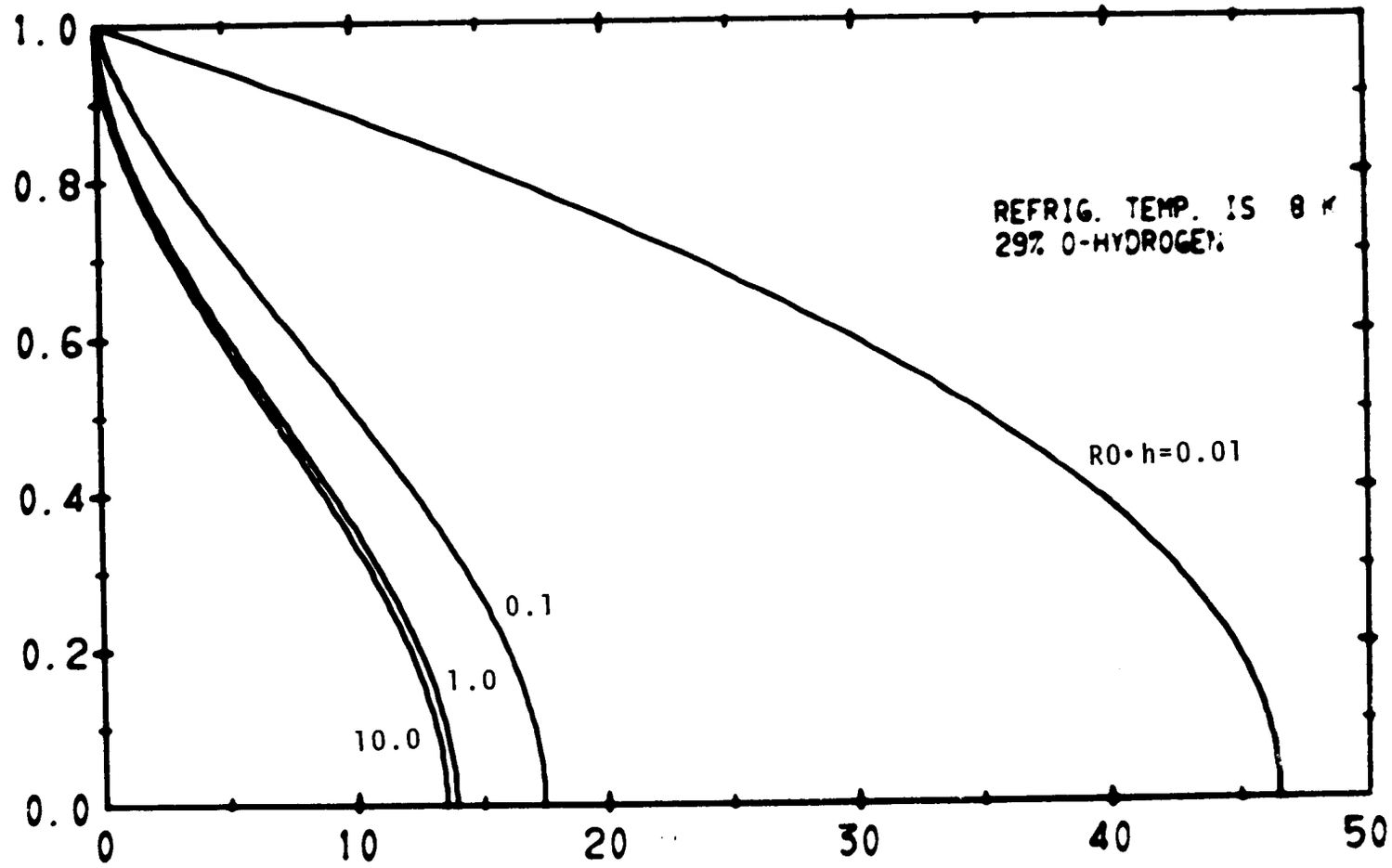

01/06/72

SPHERE, FREEZING FROM OUTSIDE

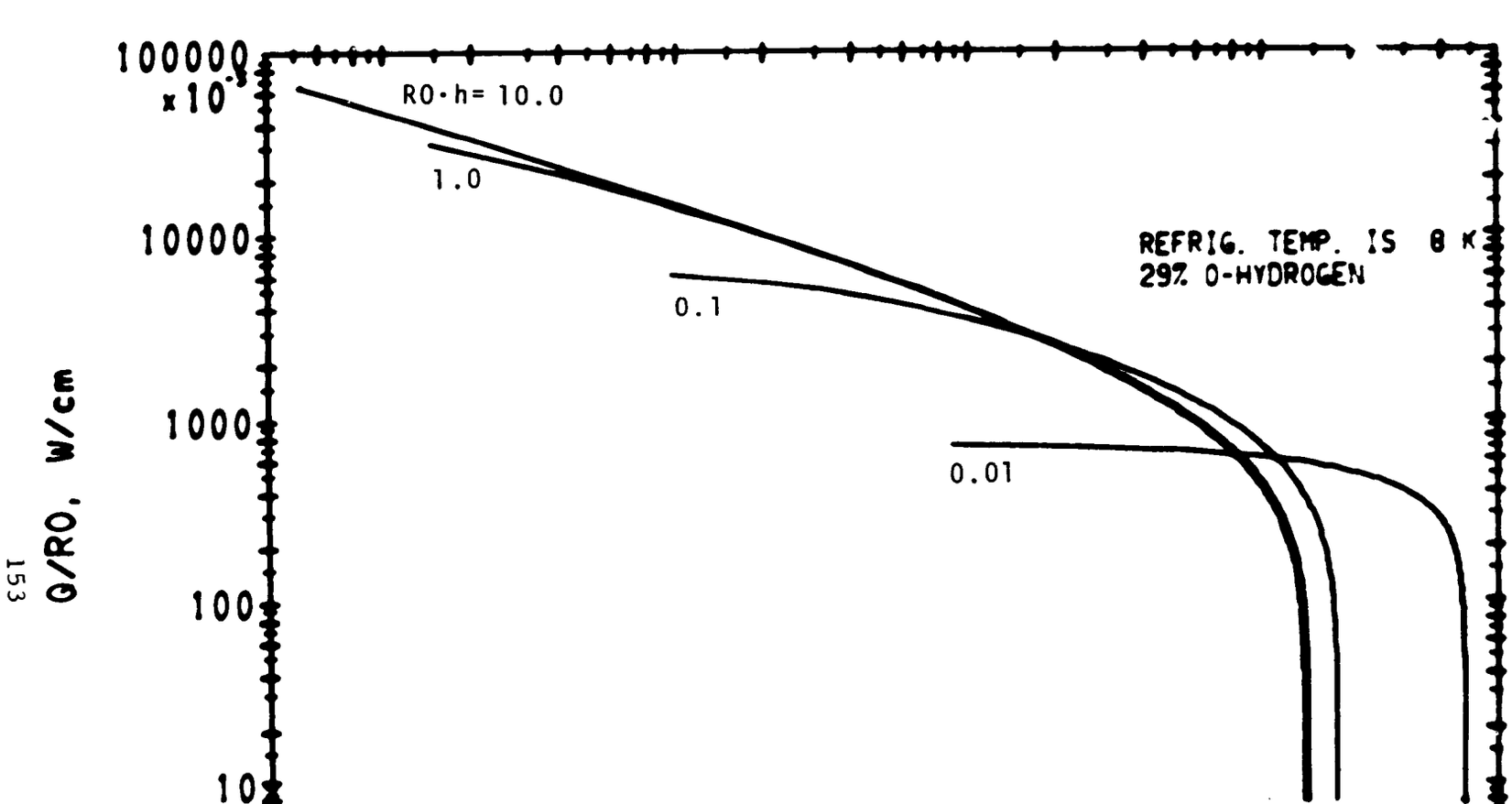

SPHERE, FREEZING FROM OUTSIDE

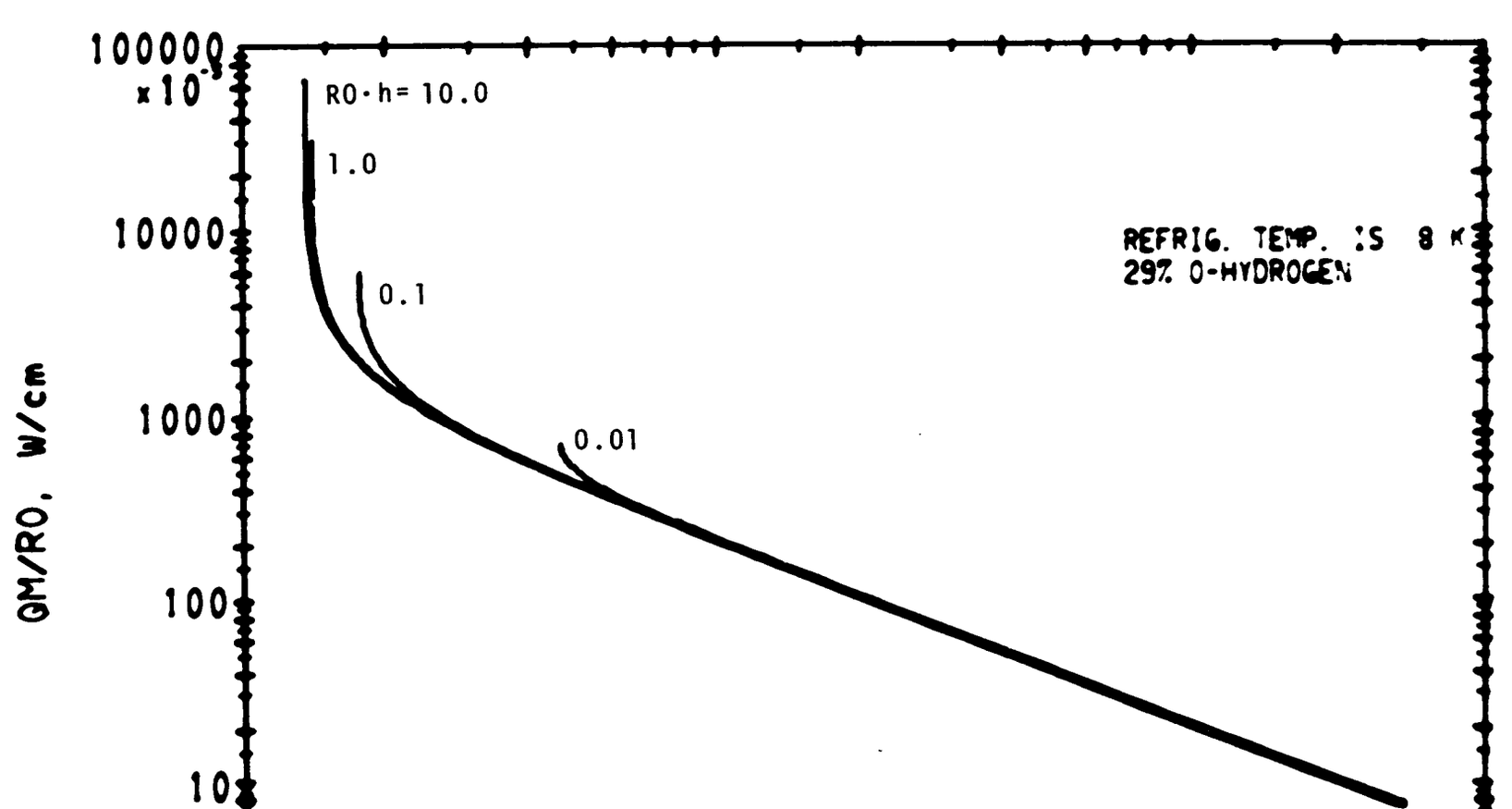

01/04/72

SPHERE, FREEZING FROM OUTSIDE

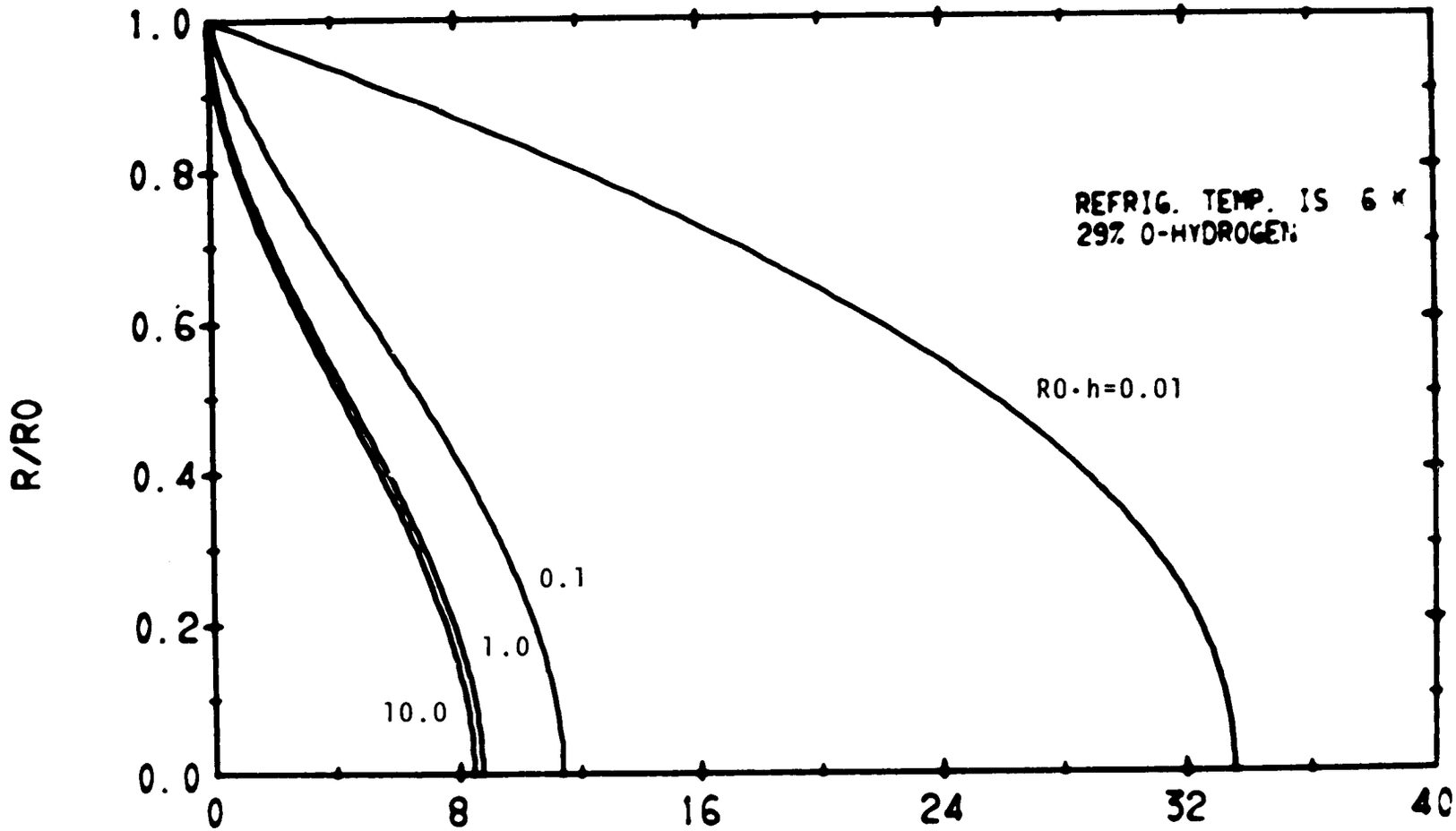

SPHERE, FREEZING FROM OUTSIDE

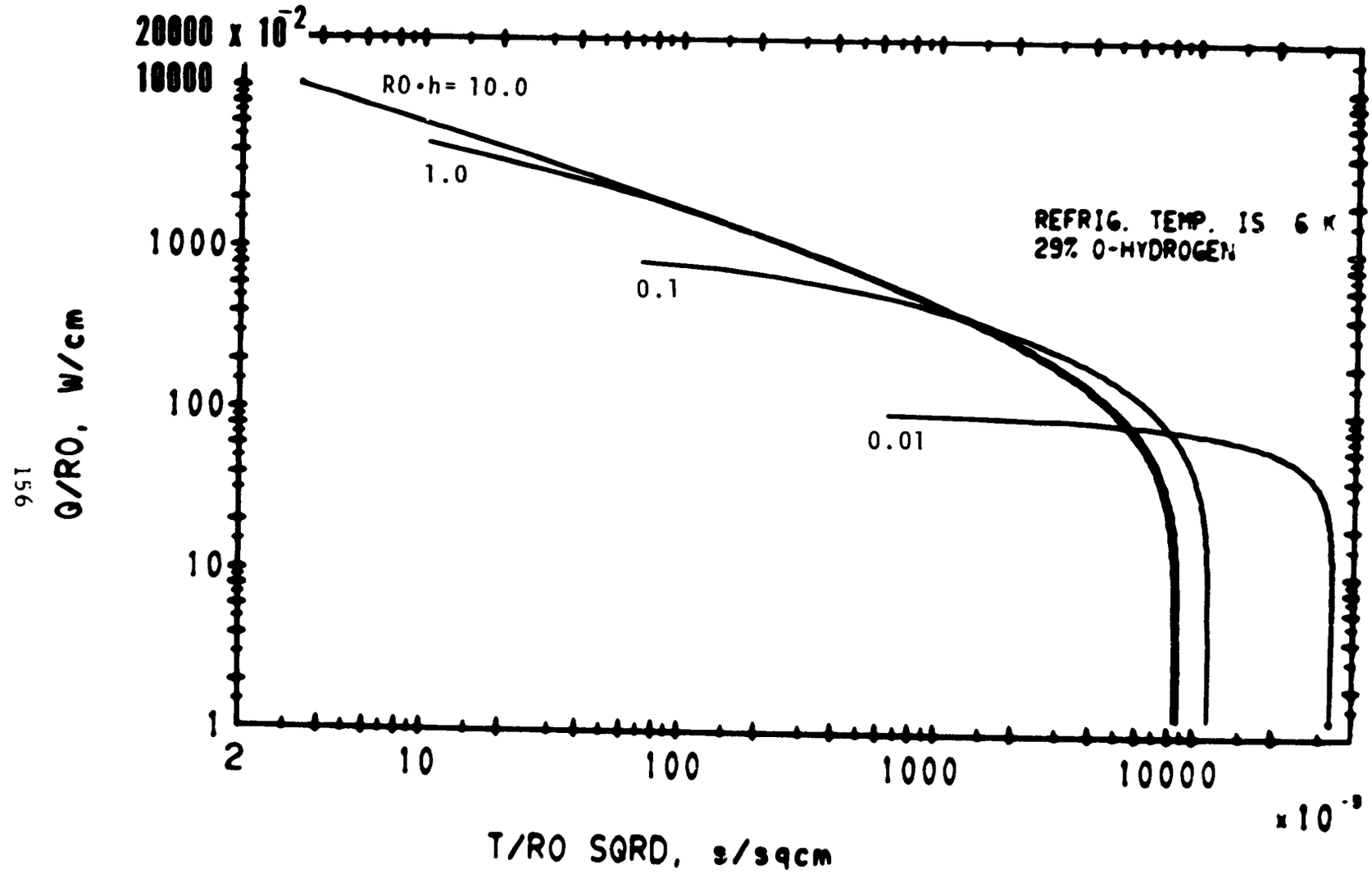

156

01/06/72

SPHERE, FREEZING FROM OUTSIDE

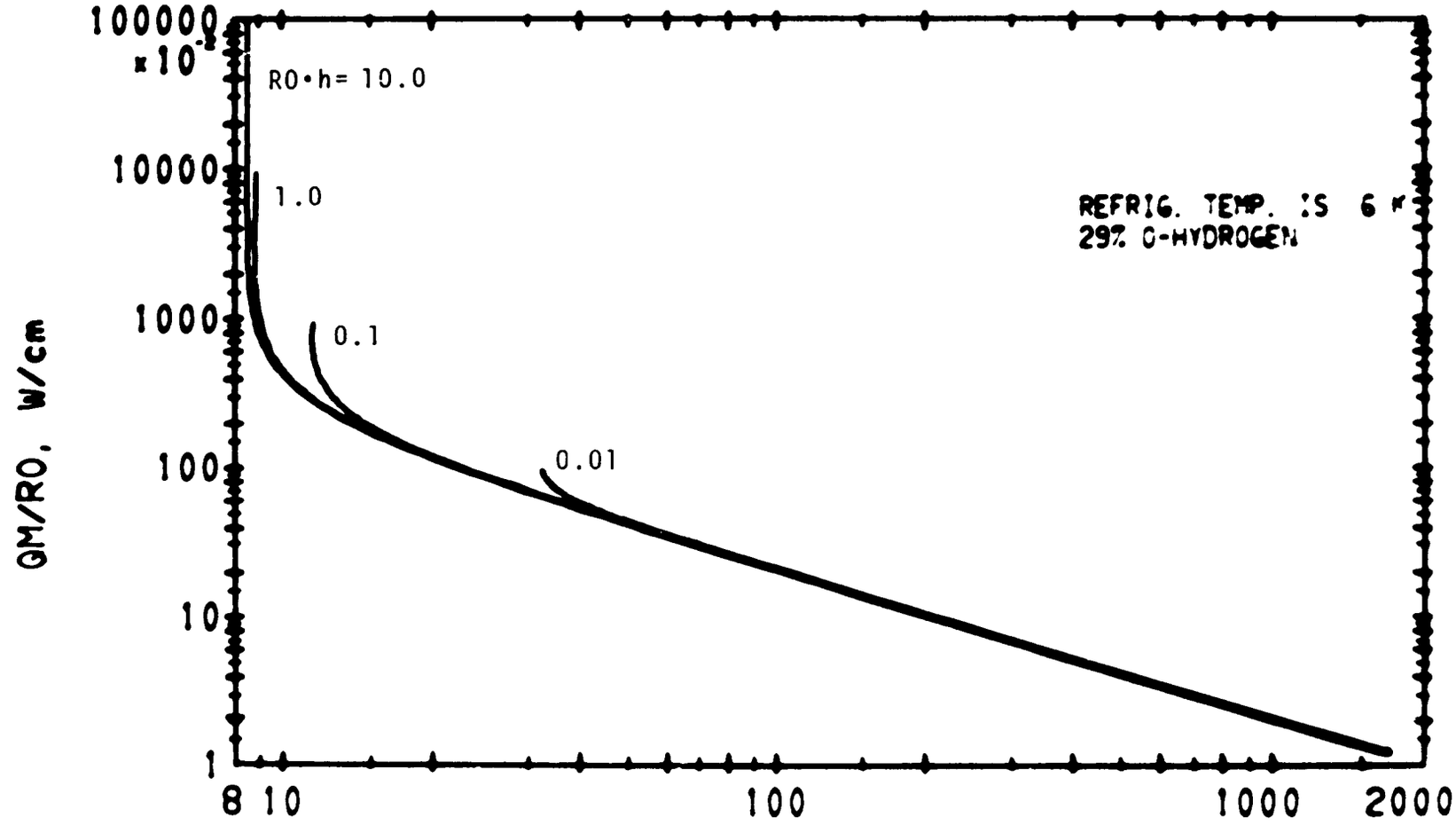

157

01/04/78

SPHERE, FREEZING FROM OUTSIDE

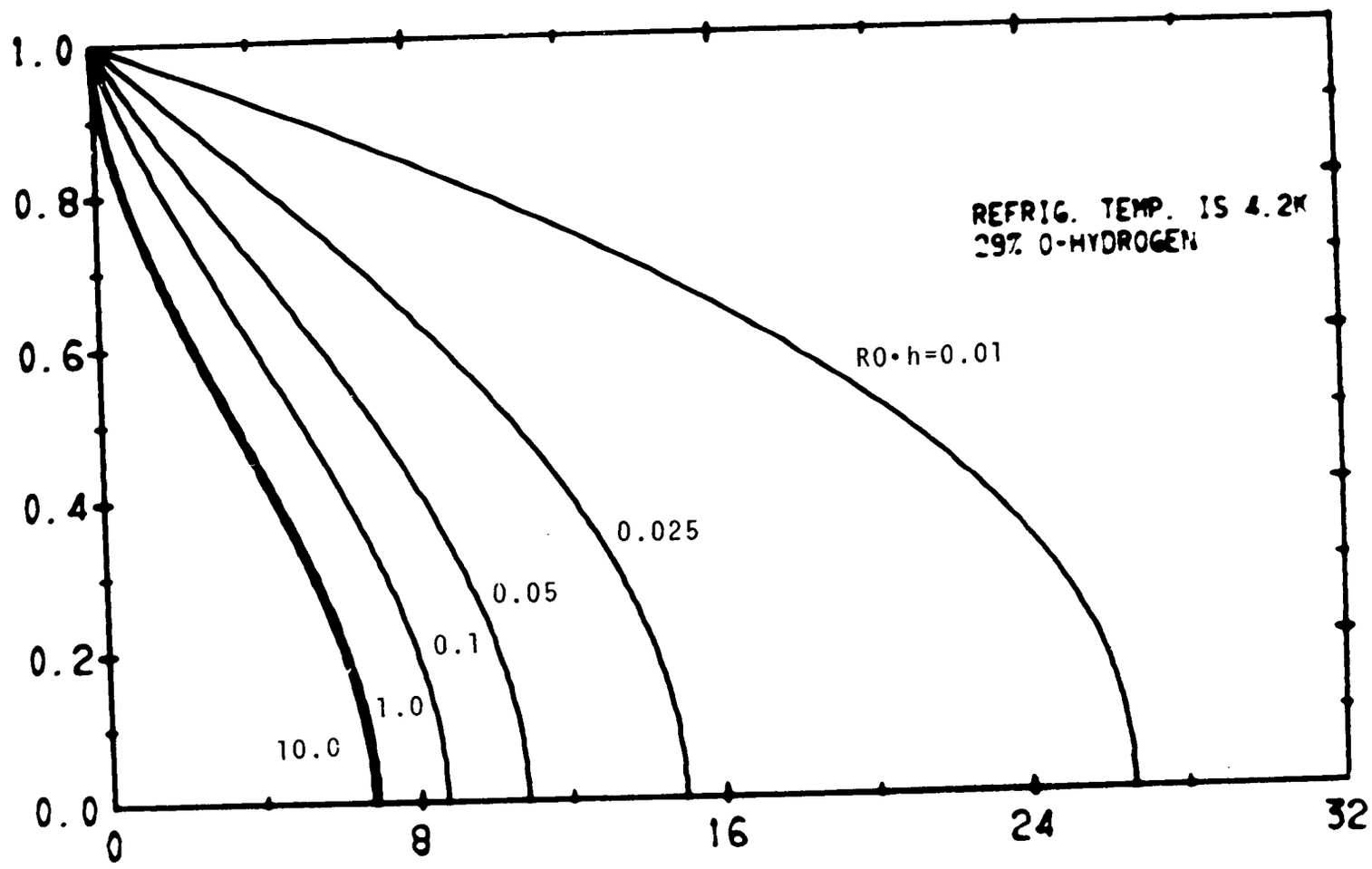

SPHERE, FREEZING FROM OUTSIDE

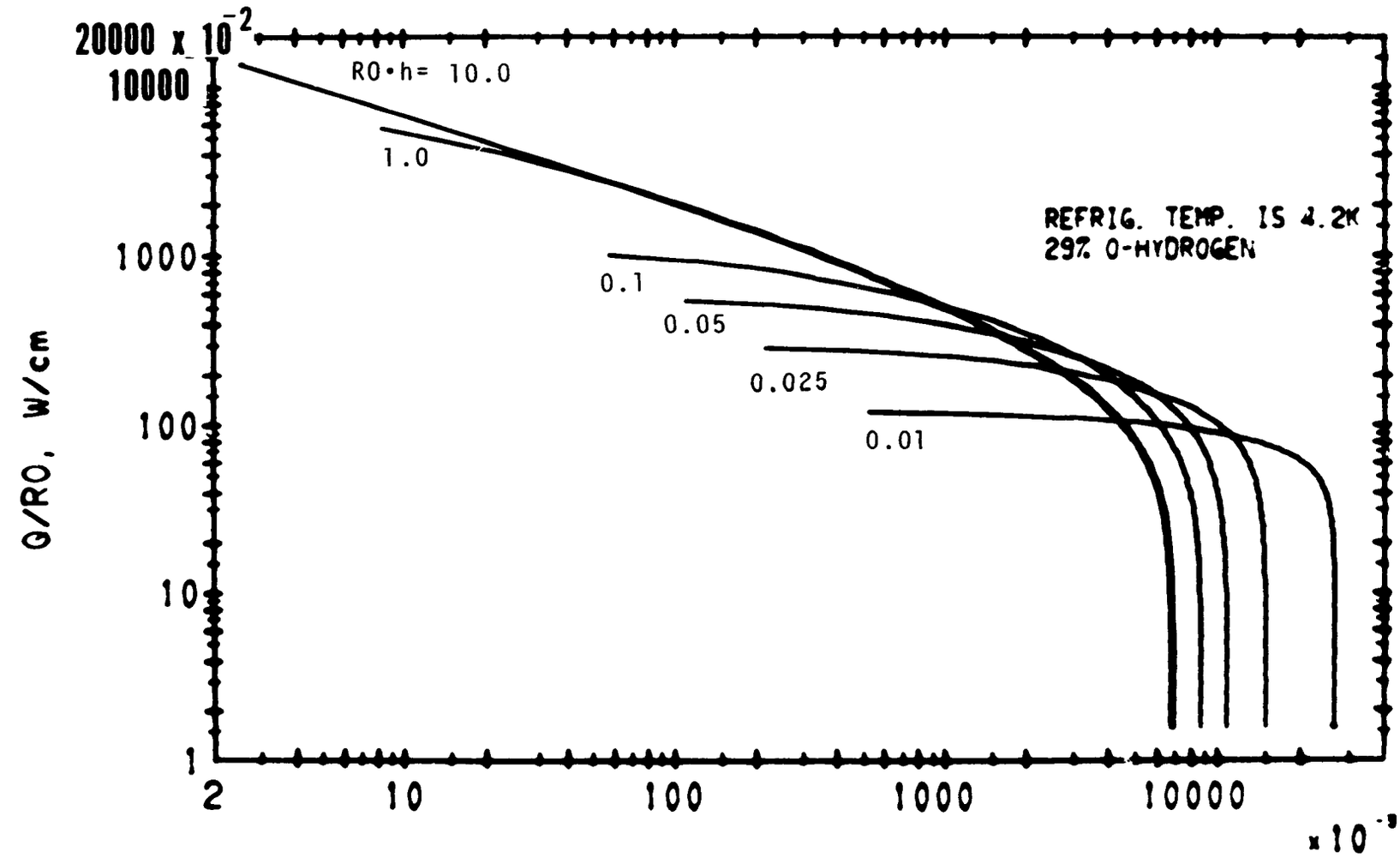

01/06/72

SPHERE, FREEZING FROM OUTSIDE

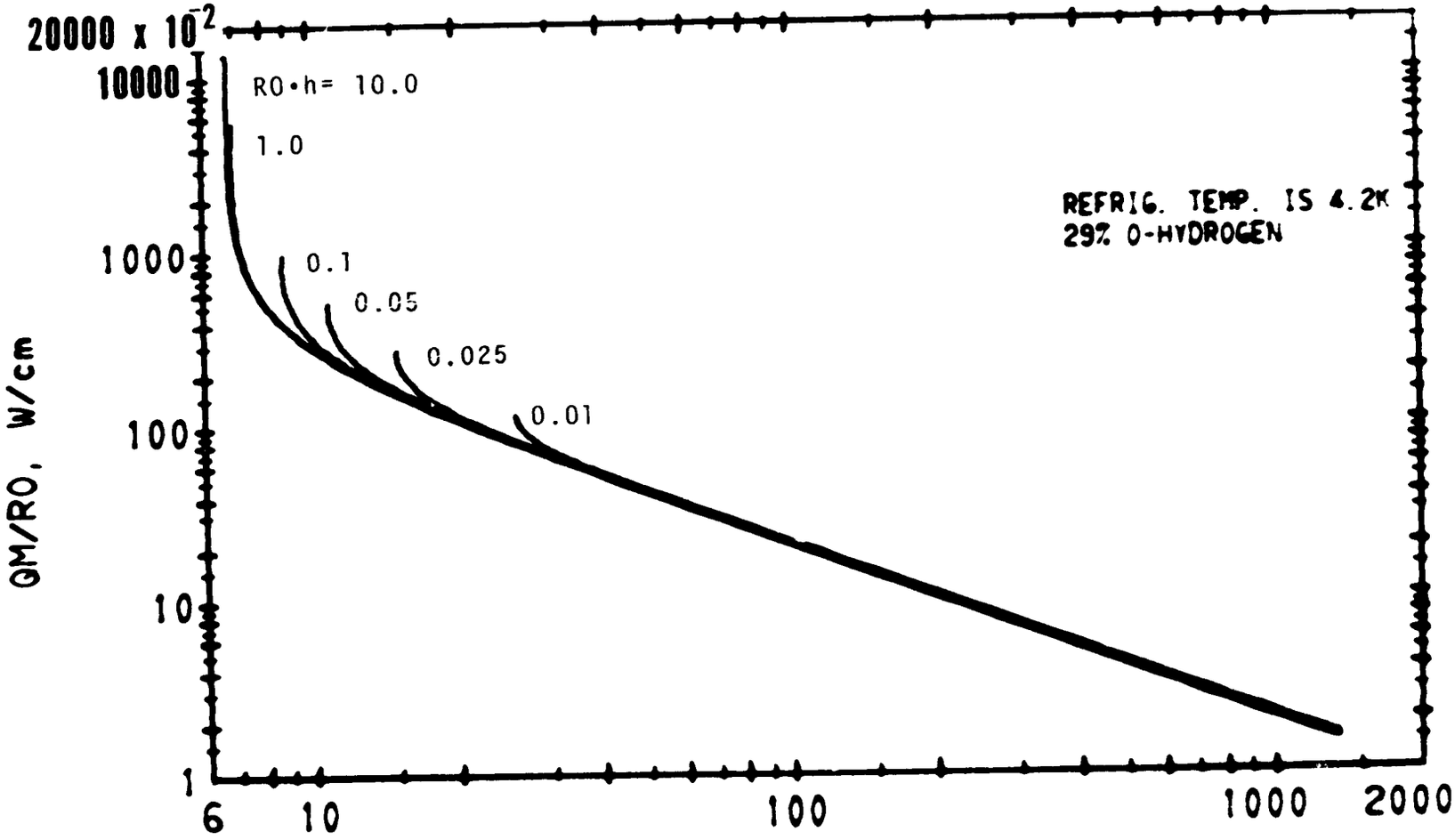

160

01/07/72

SPHERE, FREEZING FROM OUTSIDE

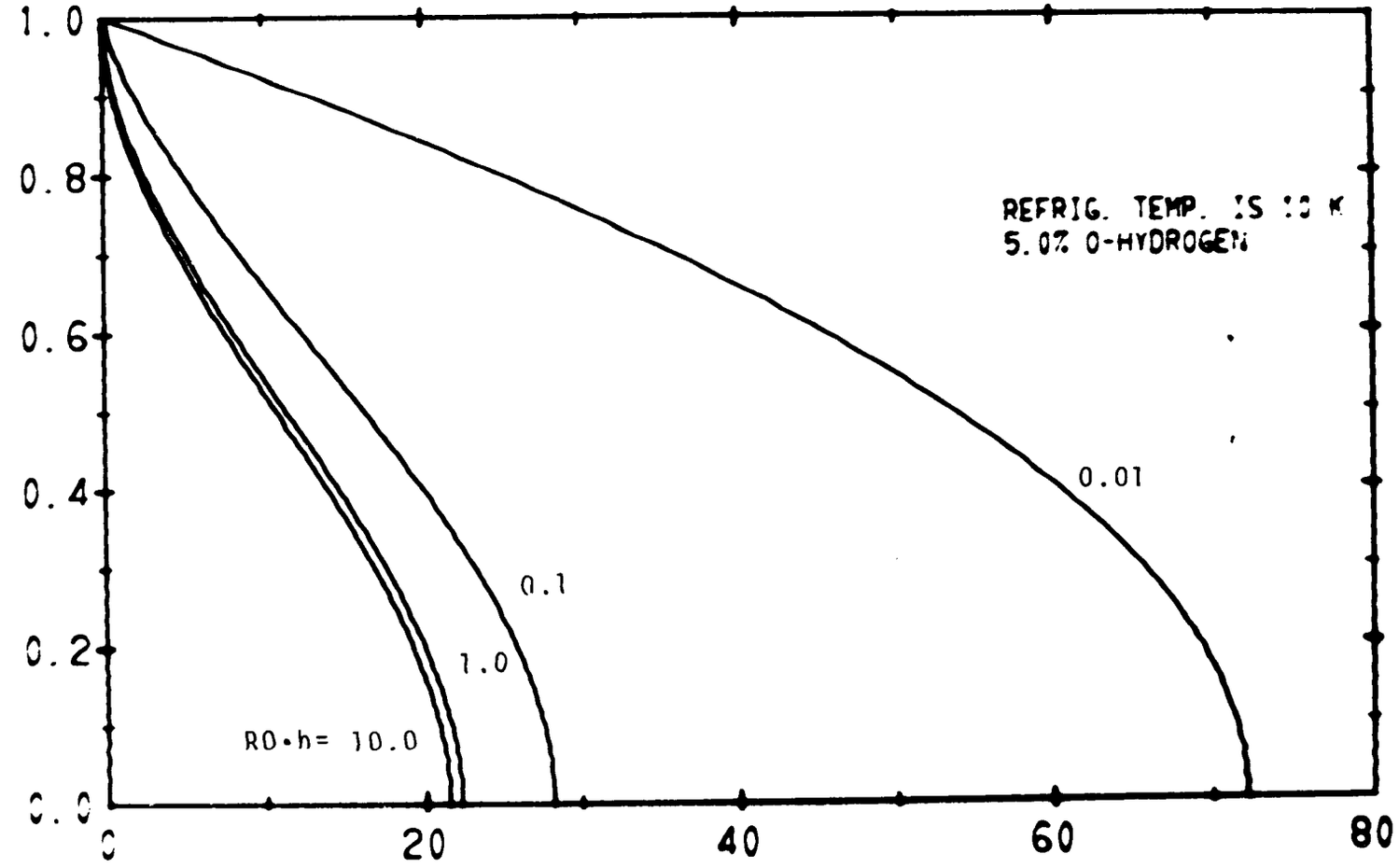

SPHERE, FREEZING FROM OUTSIDE

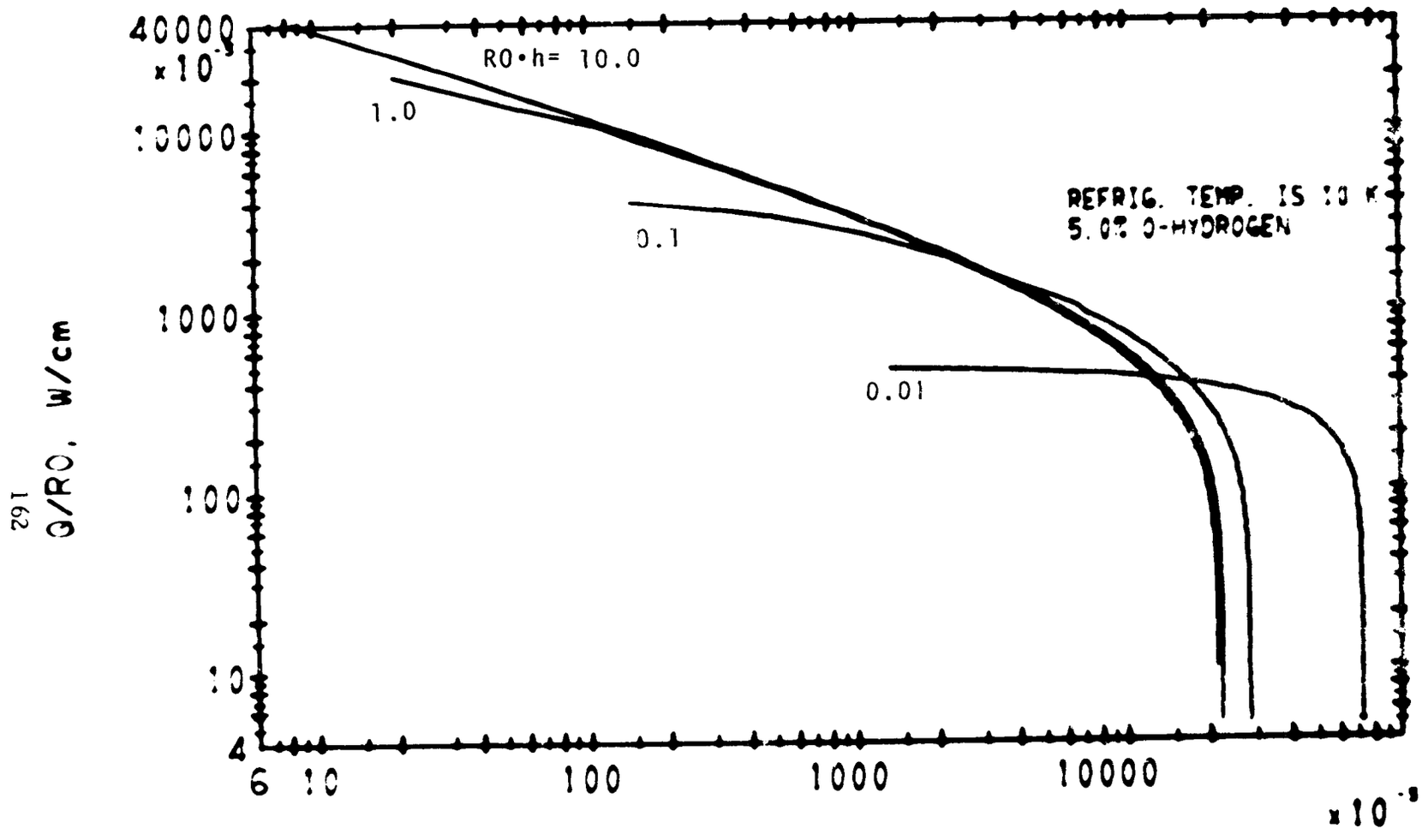

SPHERE, FREEZING FROM OUTSIDE

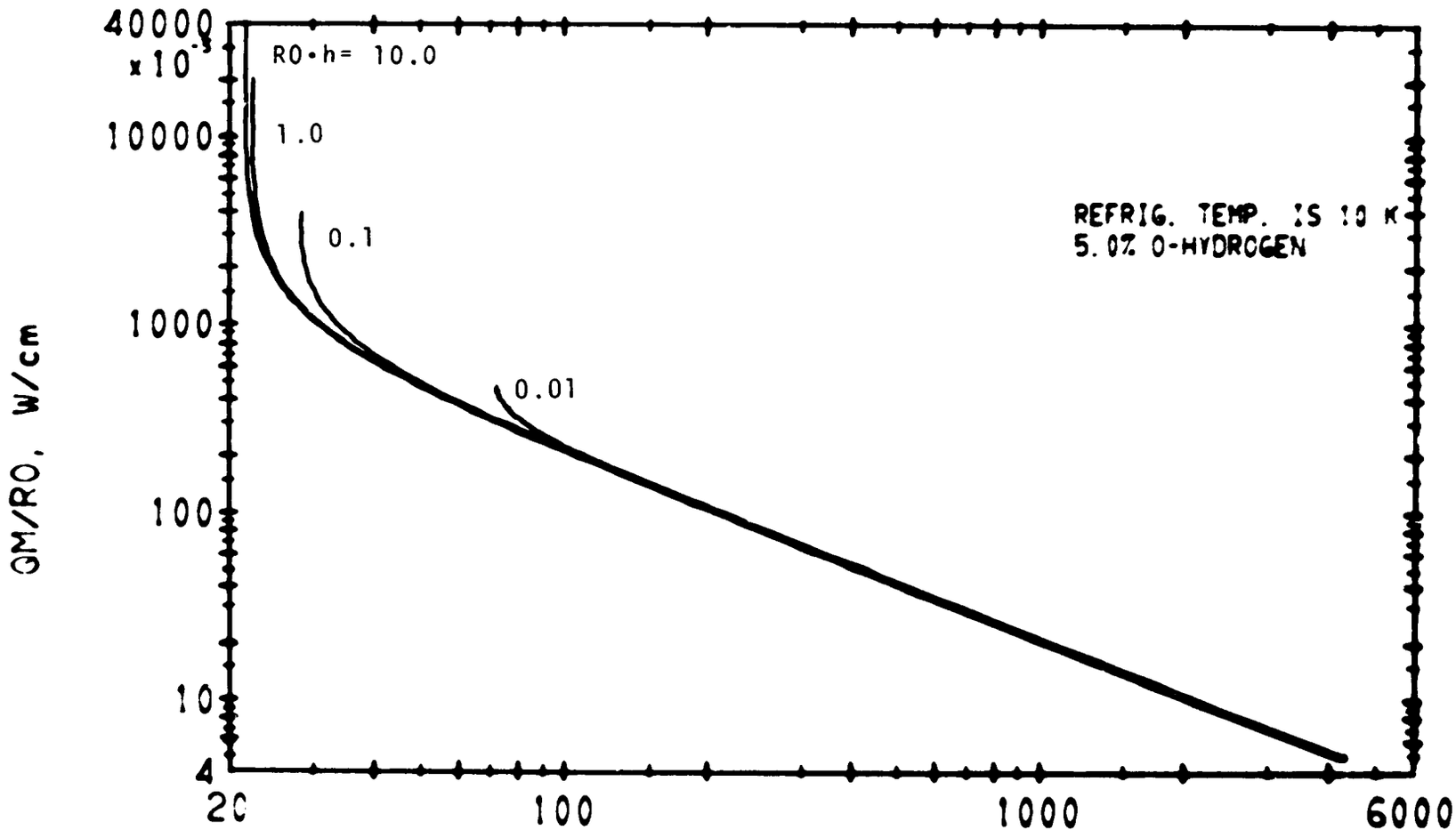

SPHERE, FREEZING FROM OUTSIDE

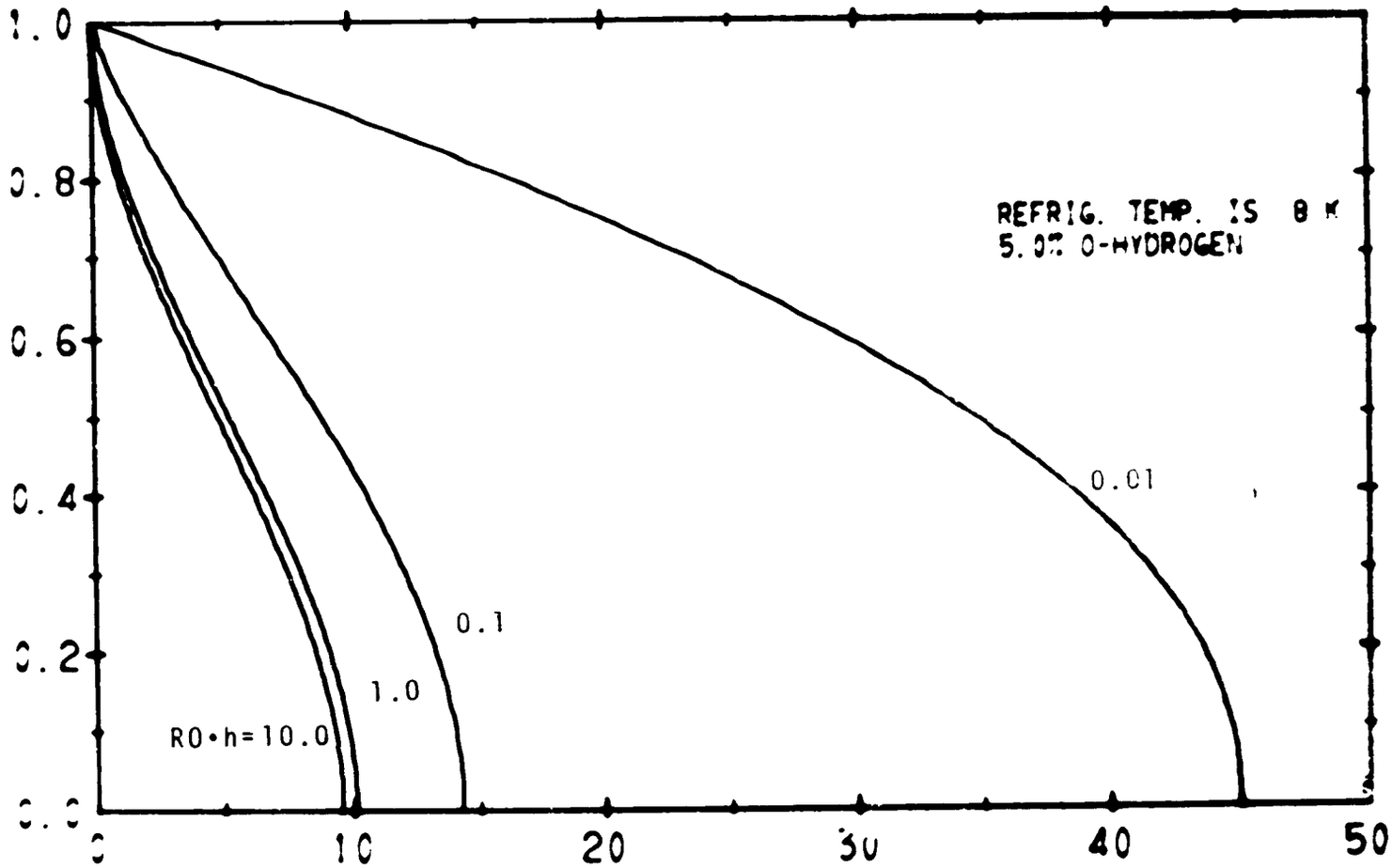

SPHERE, FREEZING FROM OUTSIDE

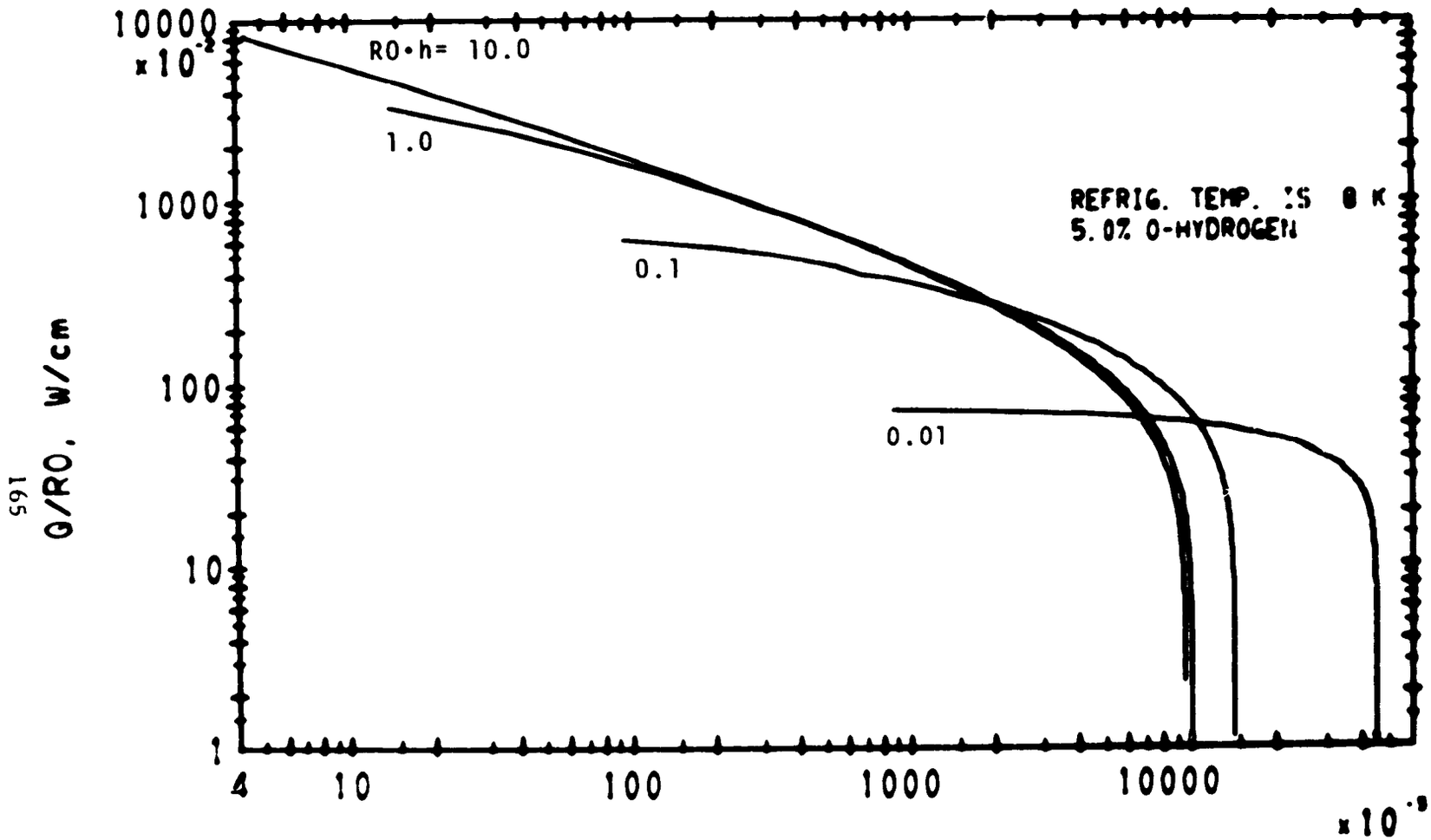

SPHERE, FREEZING FROM OUTSIDE

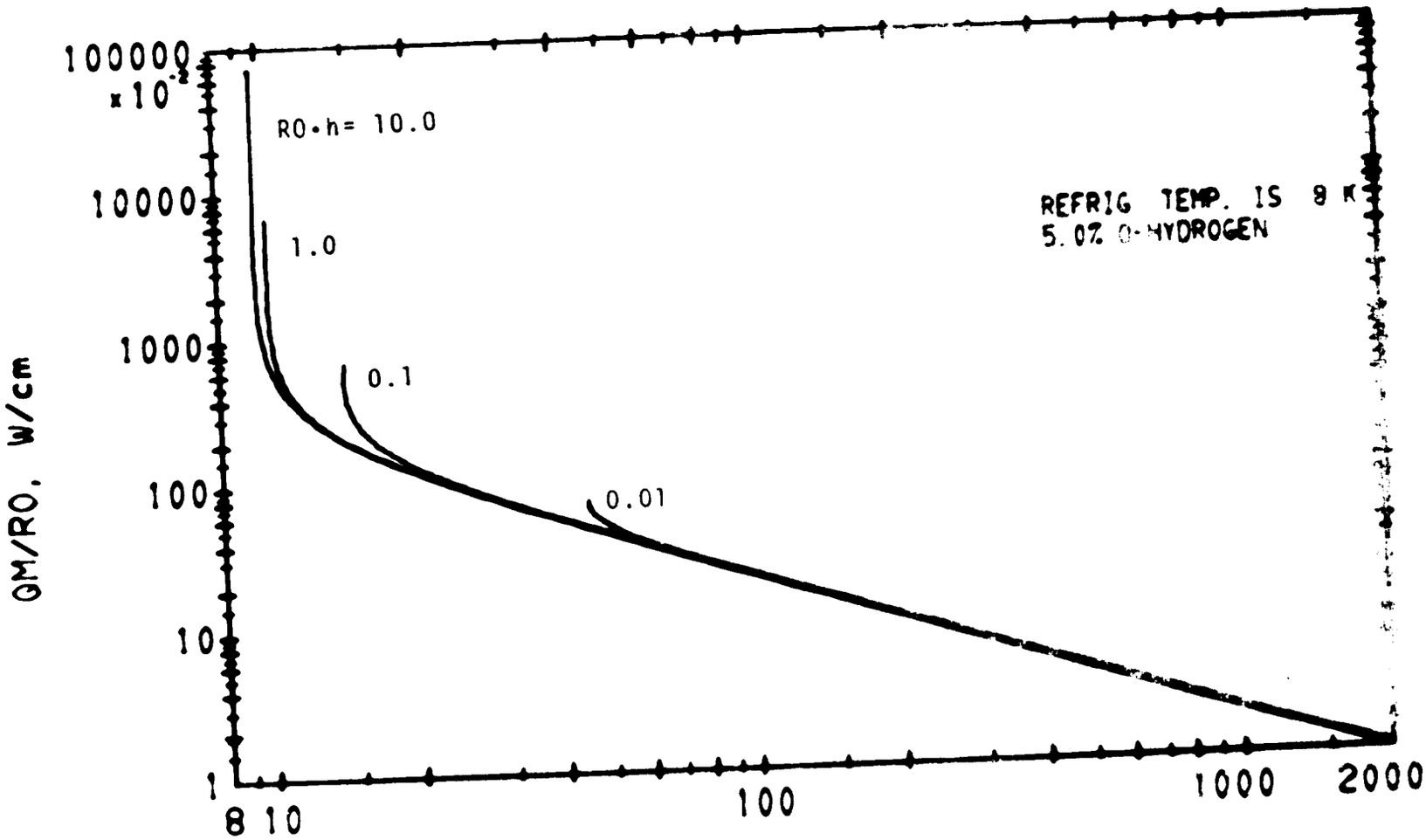

SPHERE, FREEZING FROM OUTSIDE

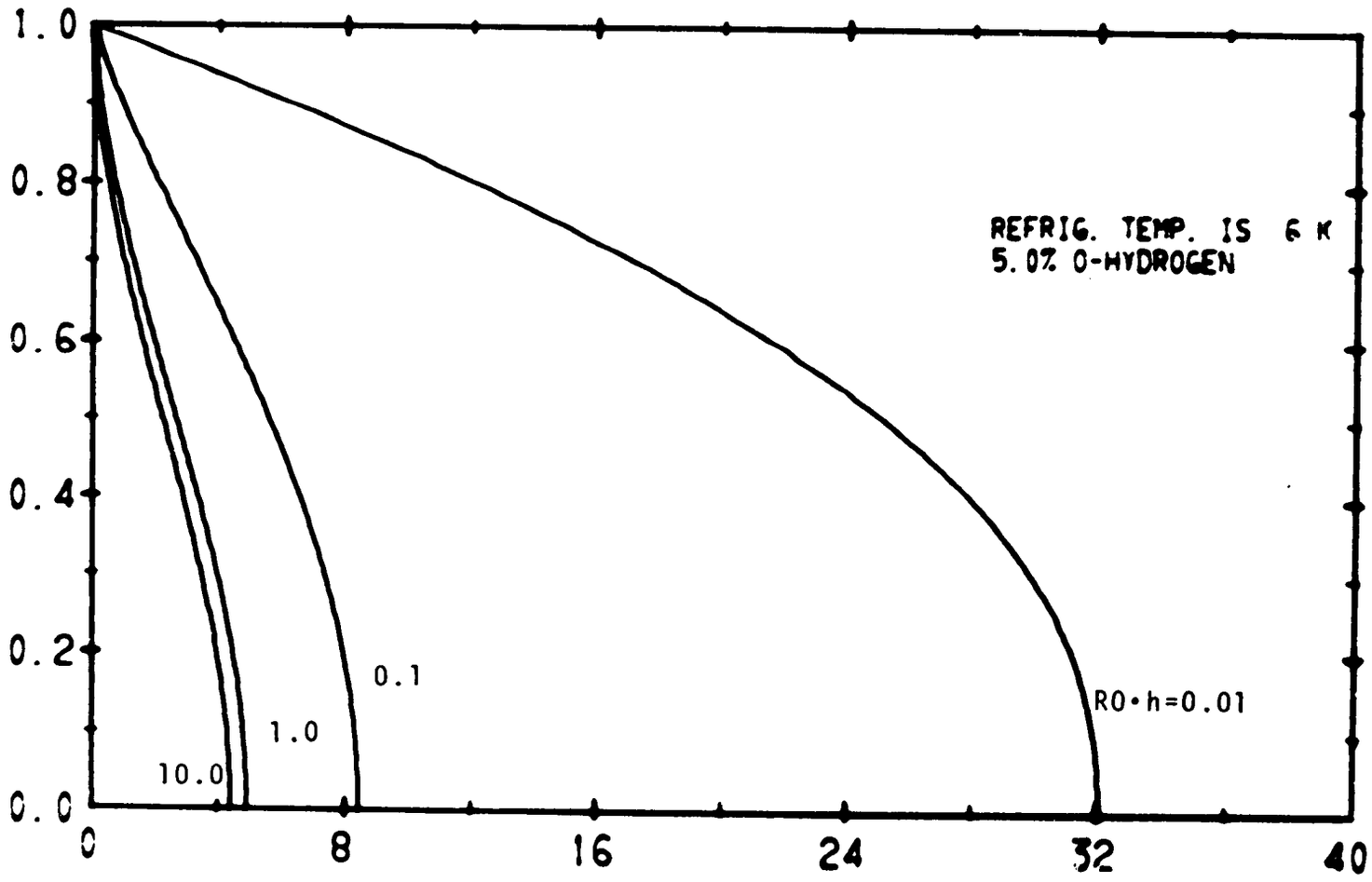

SPHERE, FREEZING FROM OUTSIDE

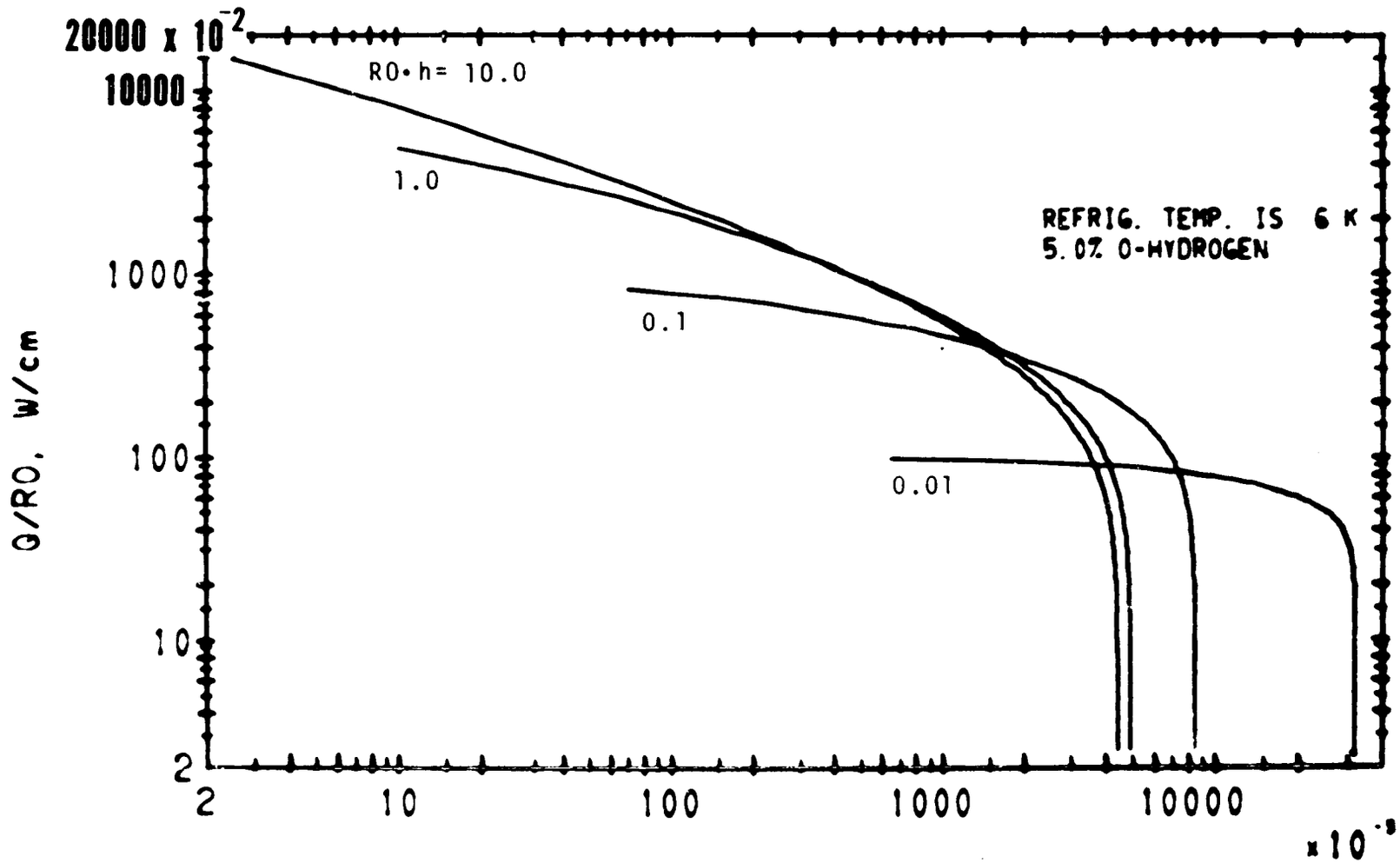

891

SPHERE, FREEZING FROM OUTSIDE

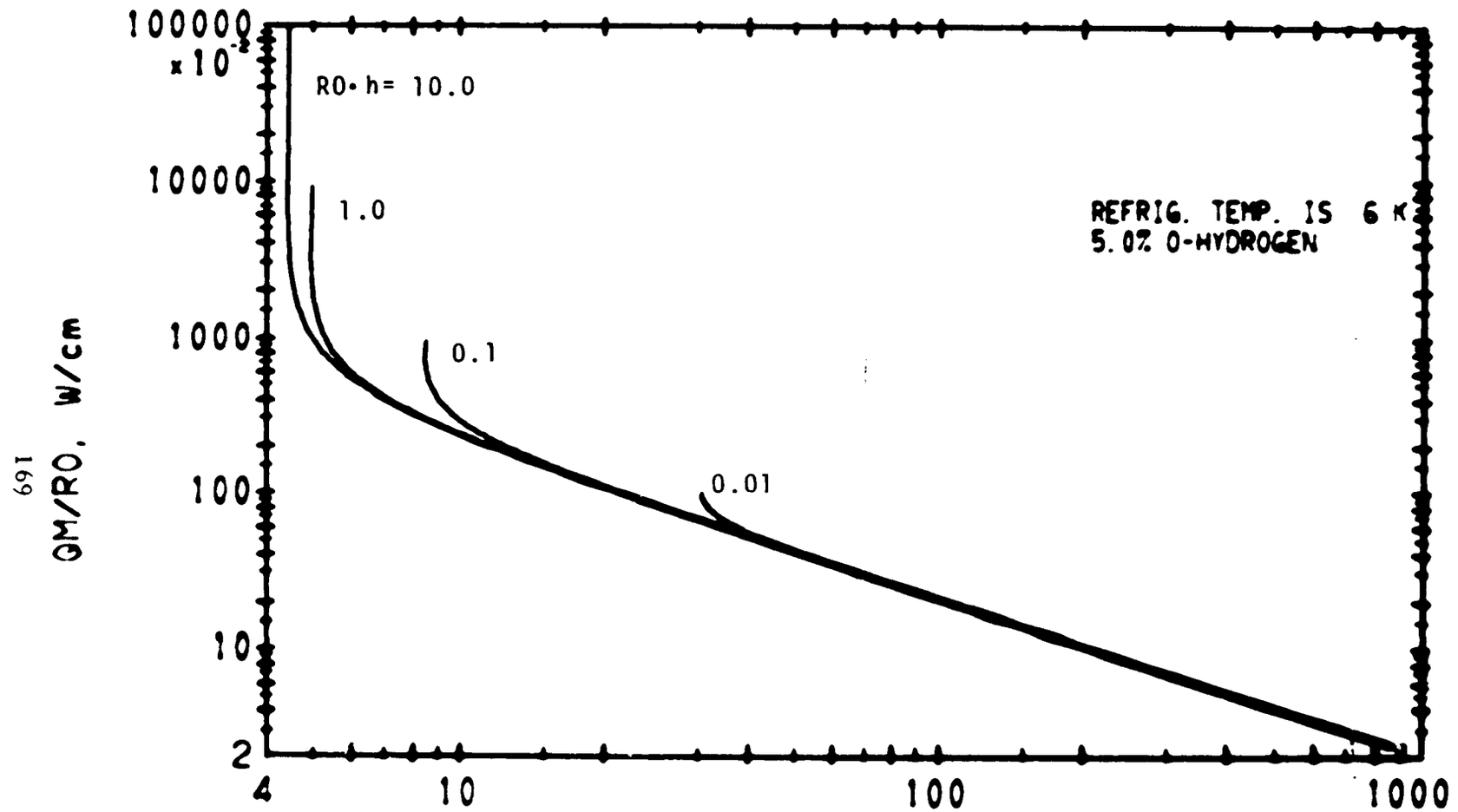

SPHERE, FREEZING FROM OUTSIDE

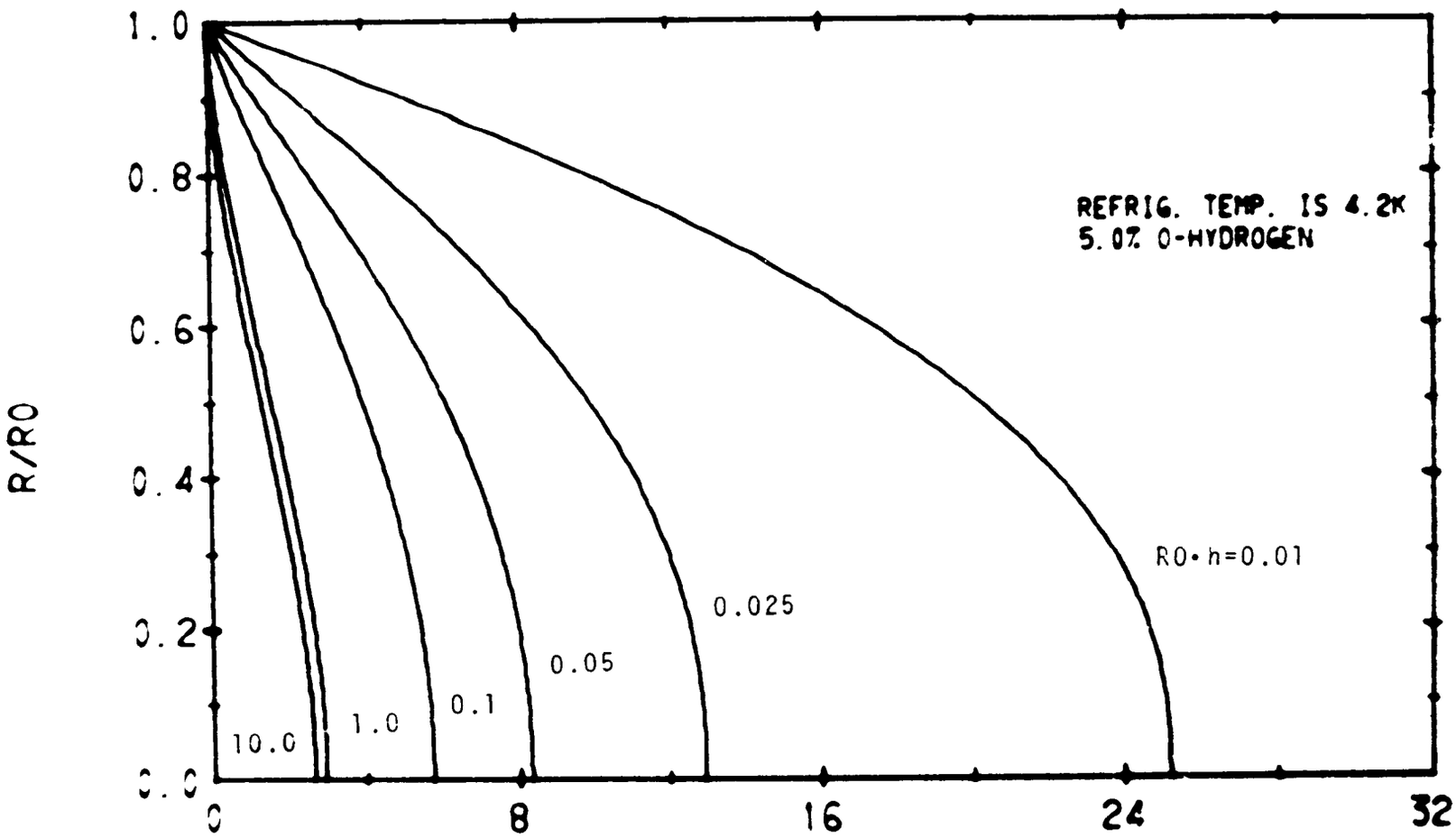

SPHERE, FREEZING FROM OUTSIDE

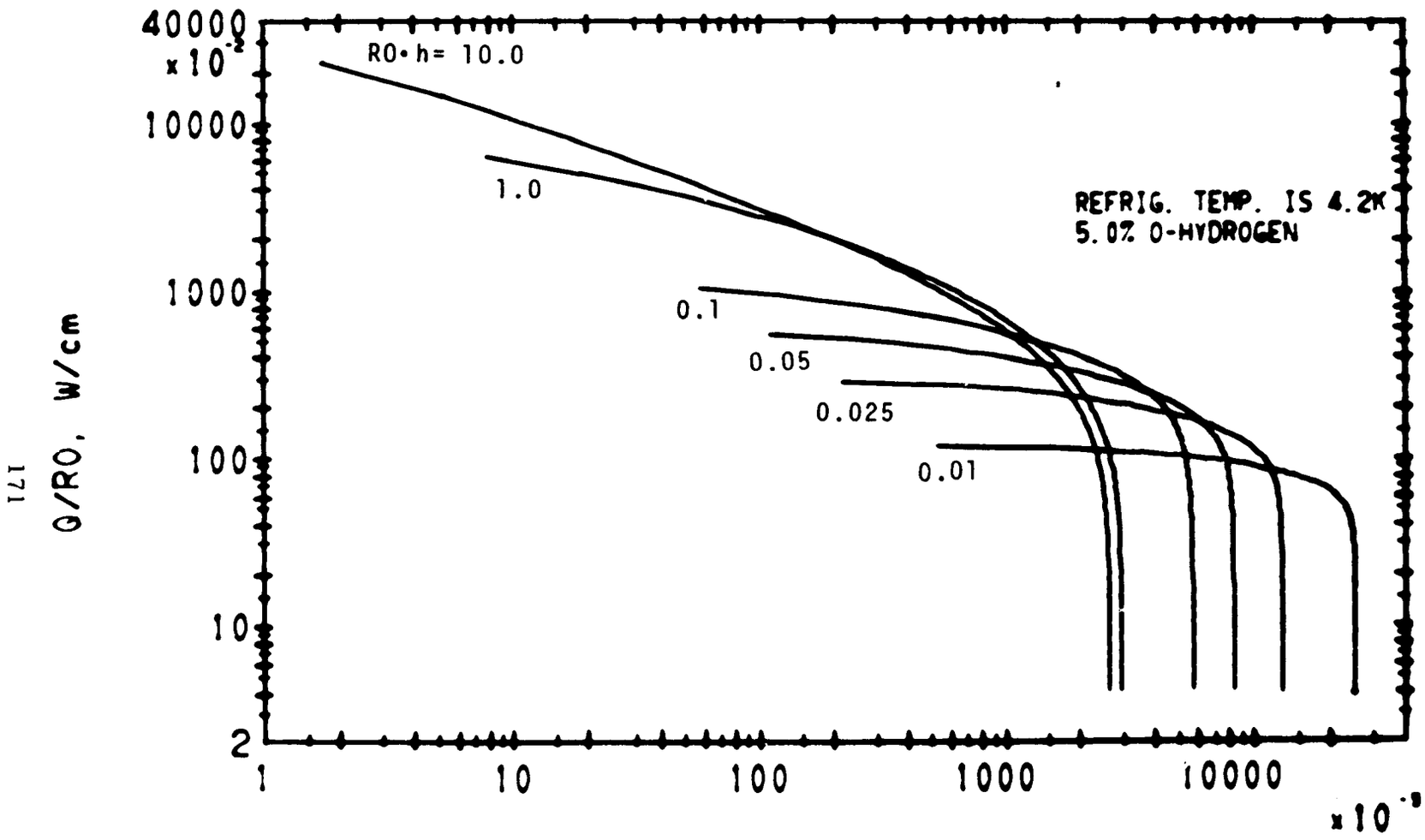

SPHERE, FREEZING FROM OUTSIDE

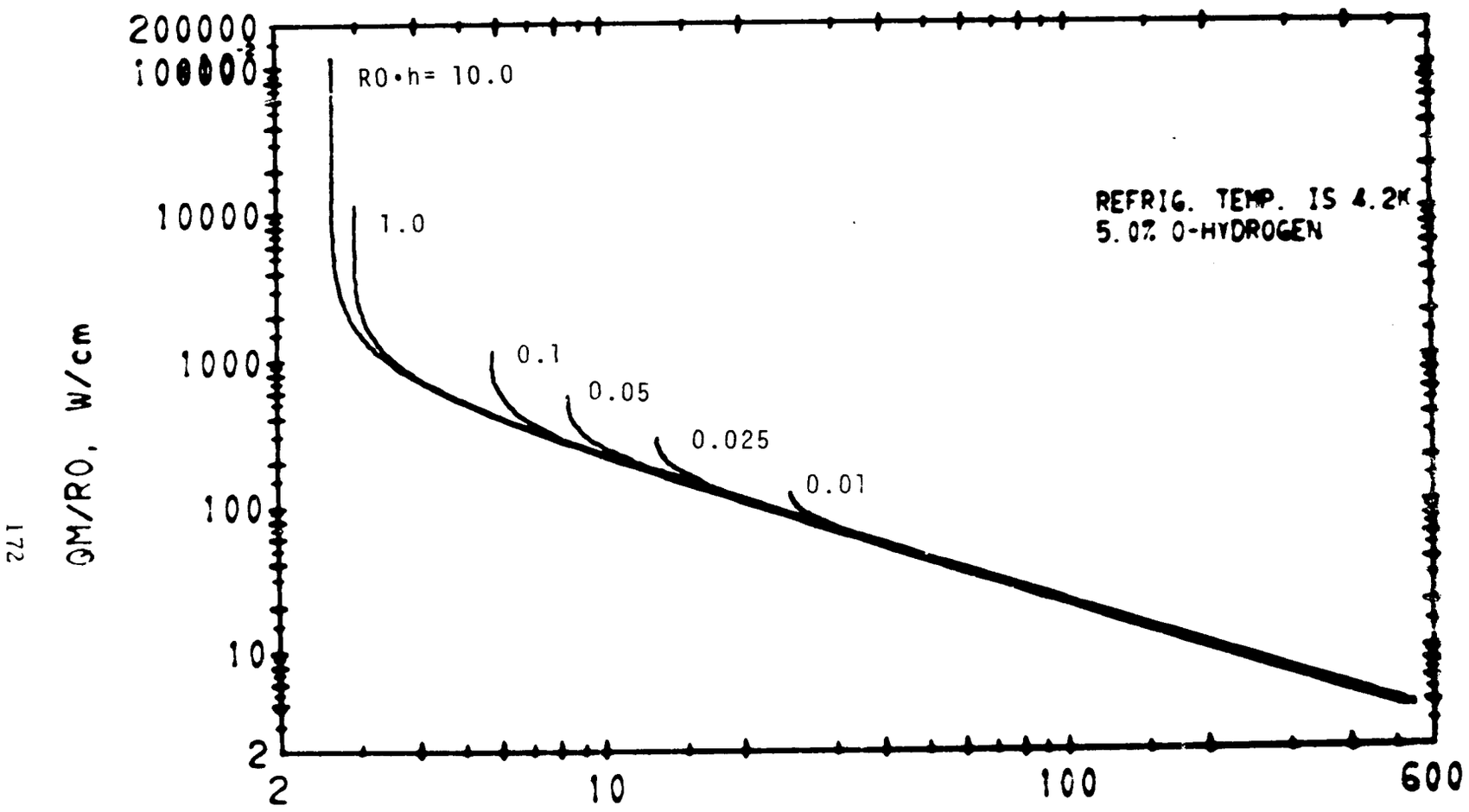

SPHERE, FREEZING FROM OUTSIDE

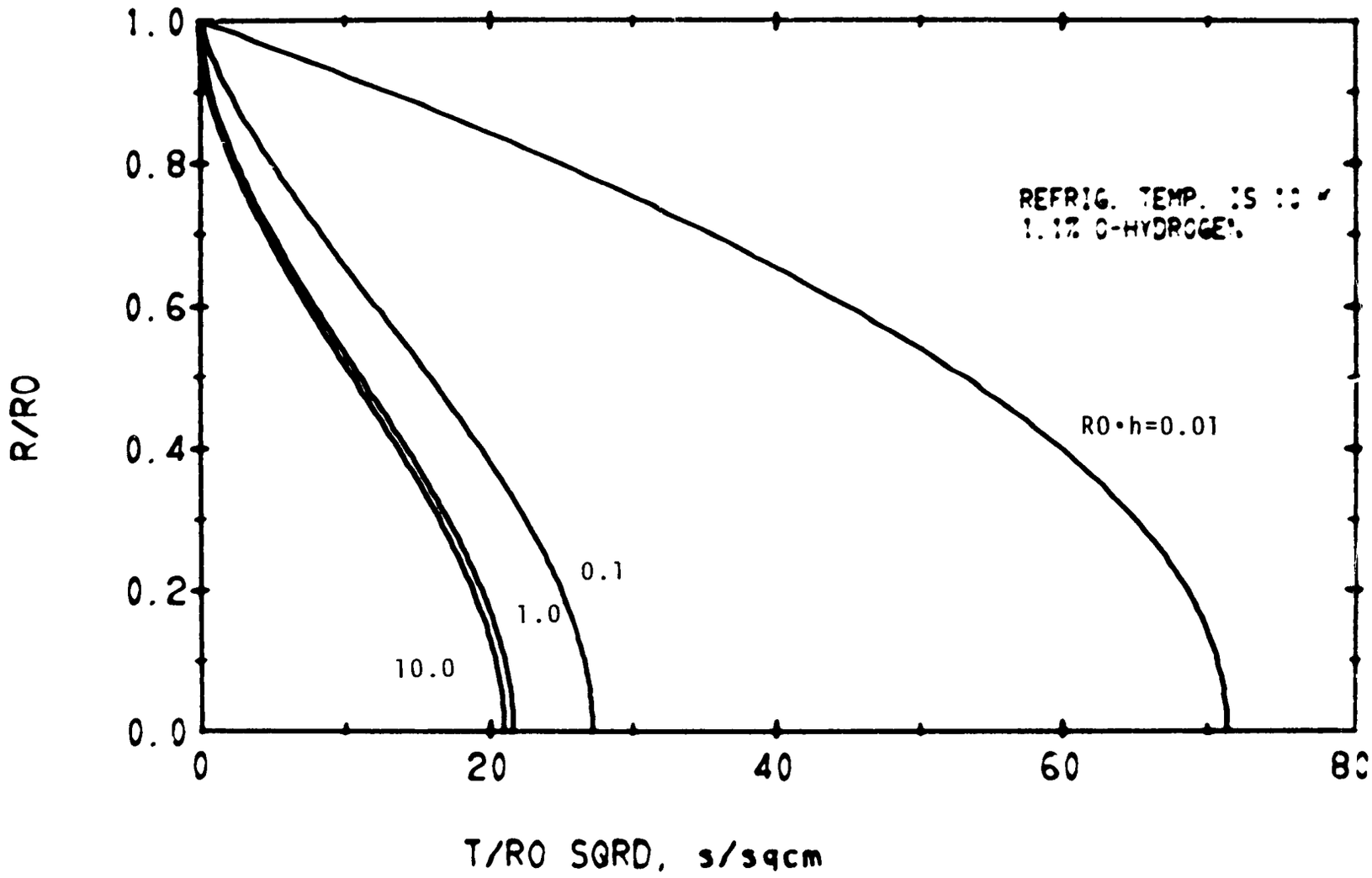

12/20/71

SPHERE, FREEZING FROM OUTSIDE

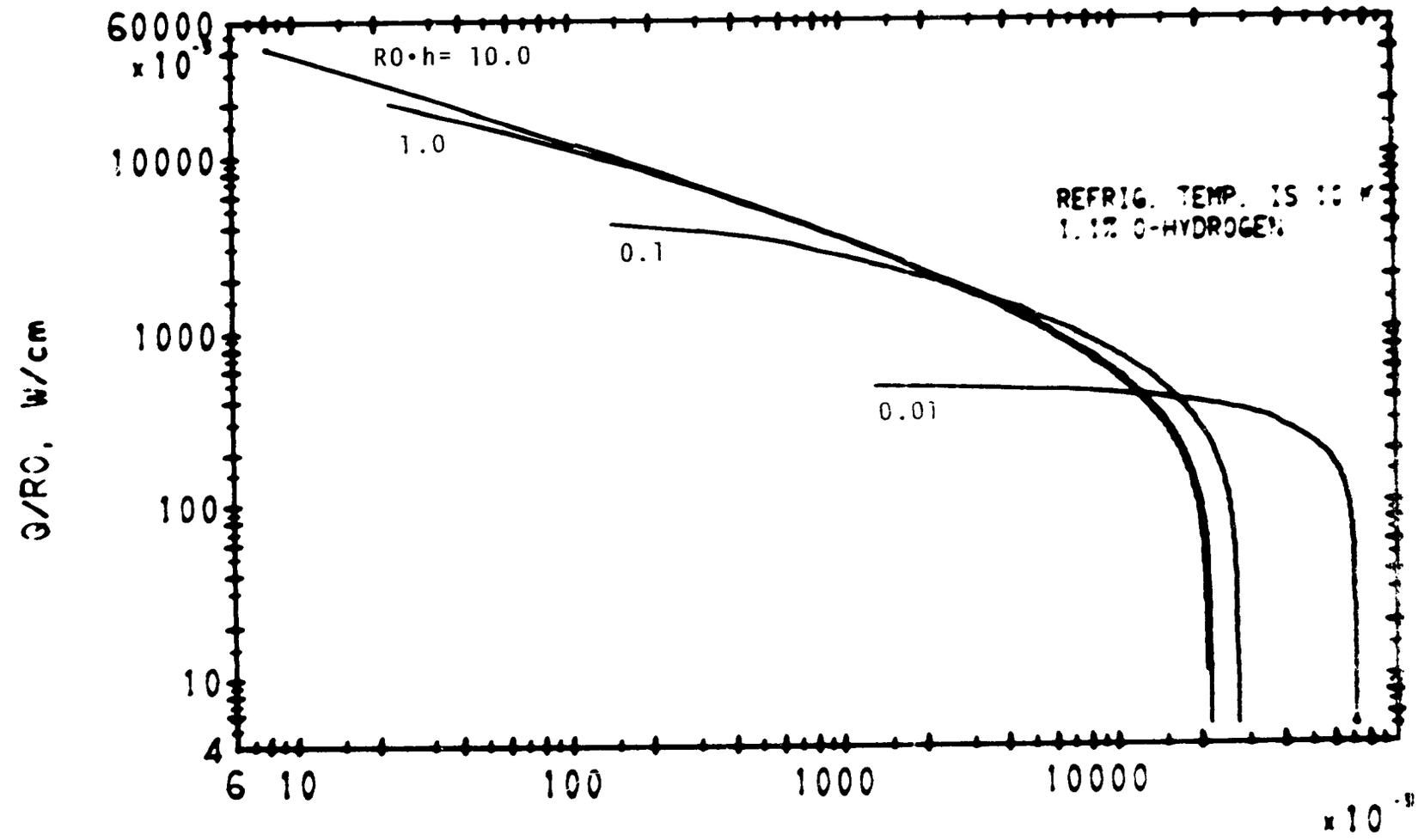

SPHERE, FREEZING FROM OUTSIDE

12/20/71

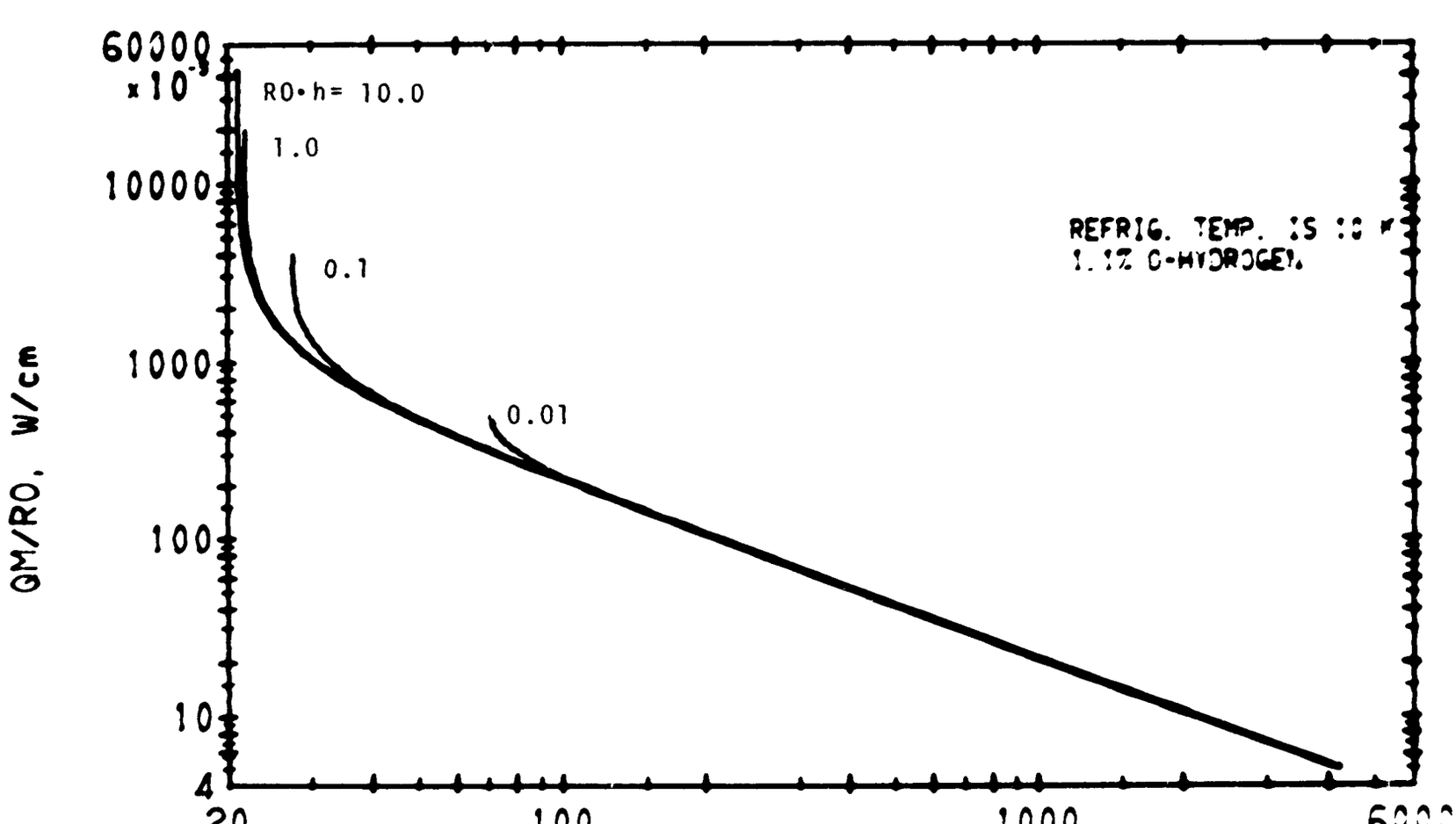

12/20/71

SPHERE, FREEZING FROM OUTSIDE

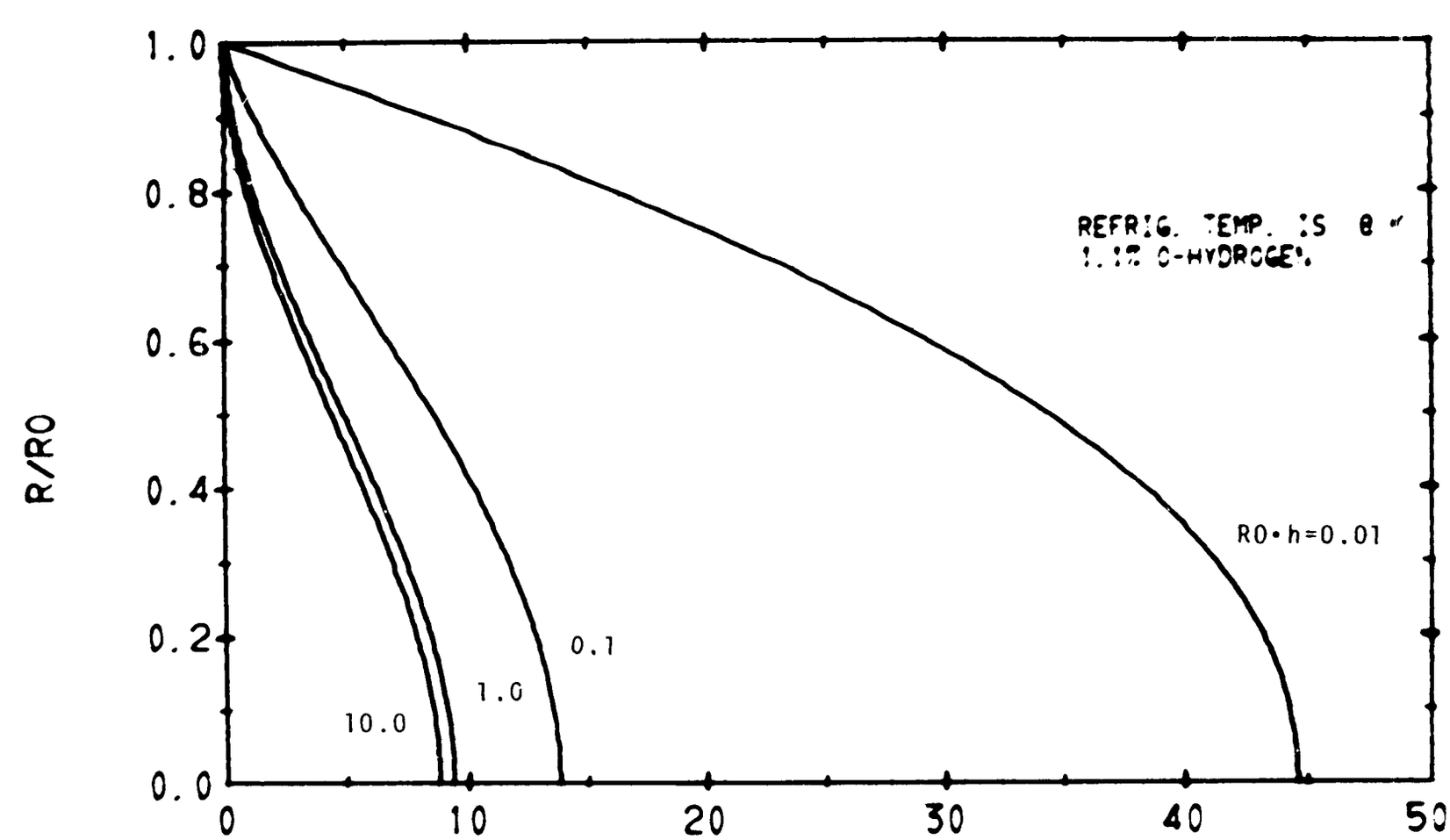

12/28/71

SPHERE, FREEZING FROM OUTSIDE

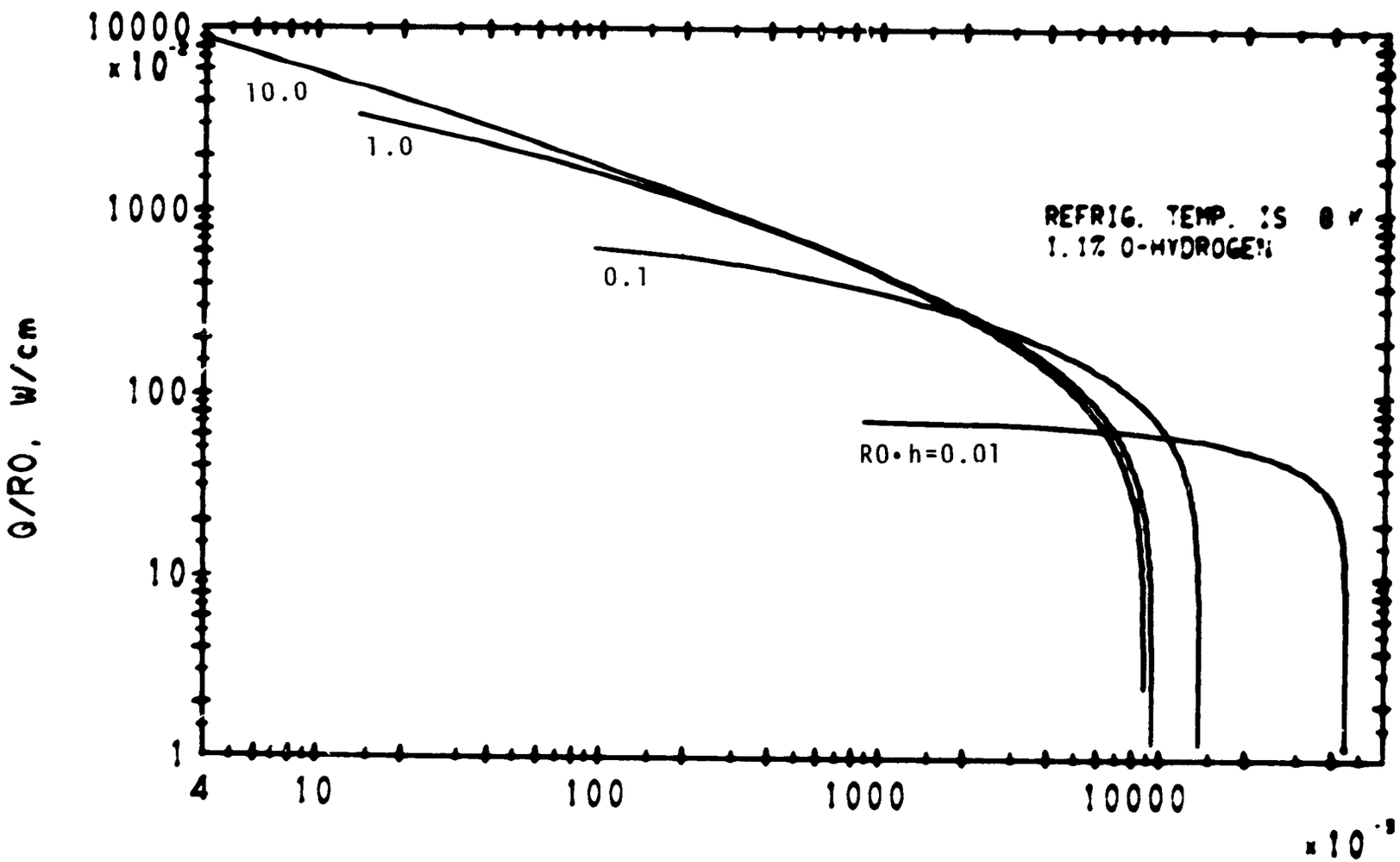

177

12/28/71

SPHERE, FREEZING FROM OUTSIDE

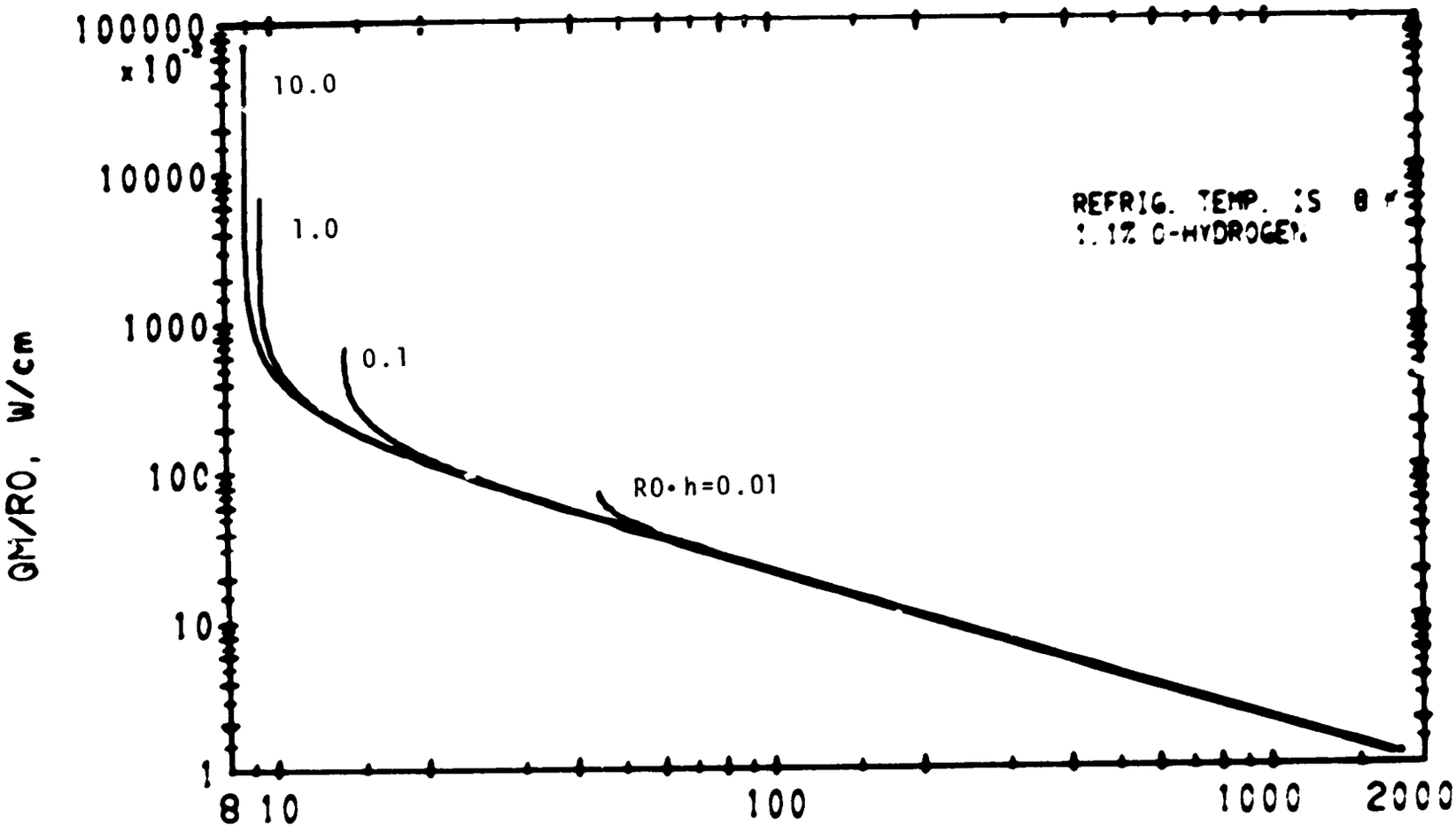

178

18/20/71

SPHERE, FREEZING FROM OUTSIDE

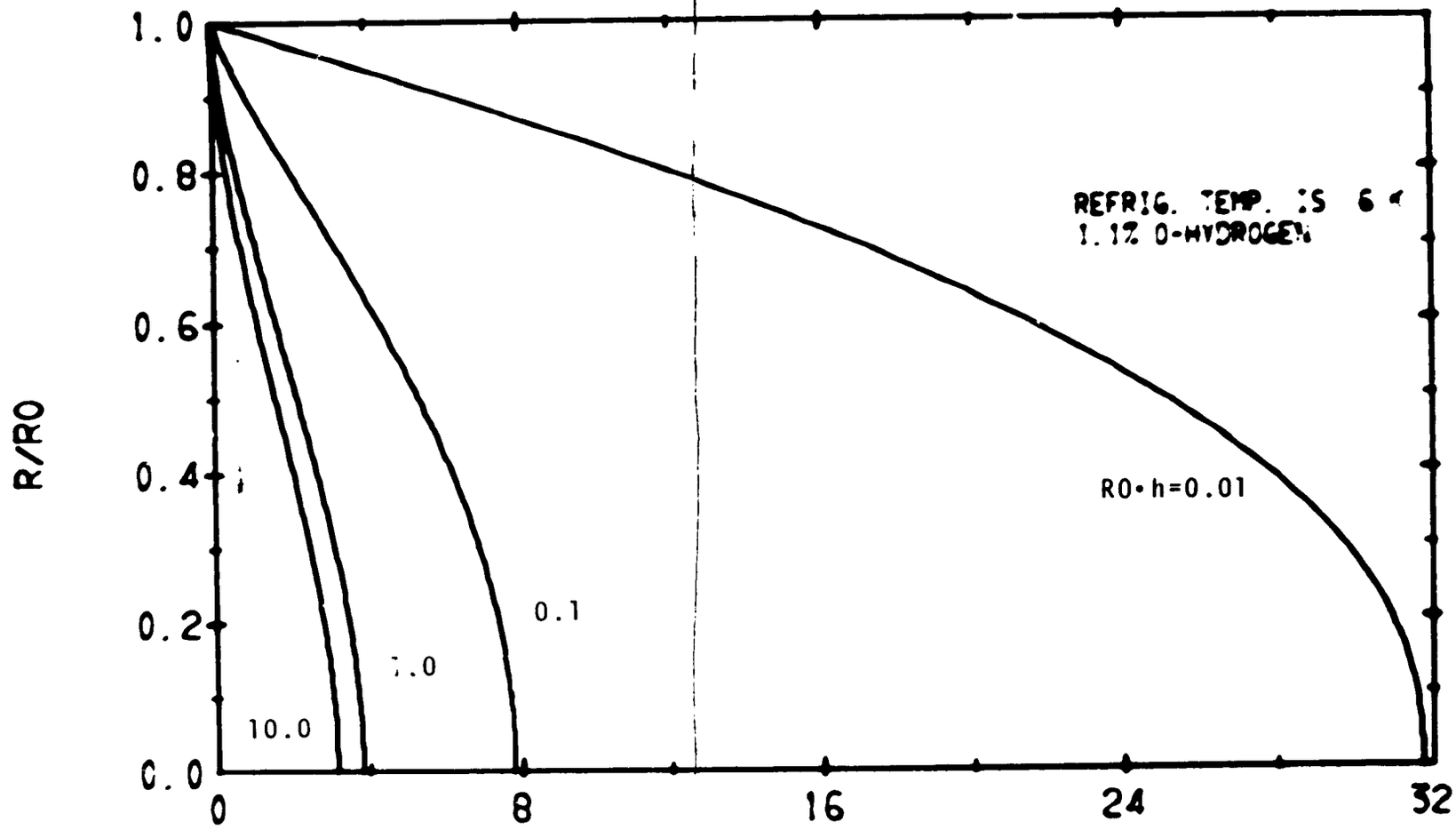

12/20/71

SPHERE, FREEZING FROM OUTSIDE

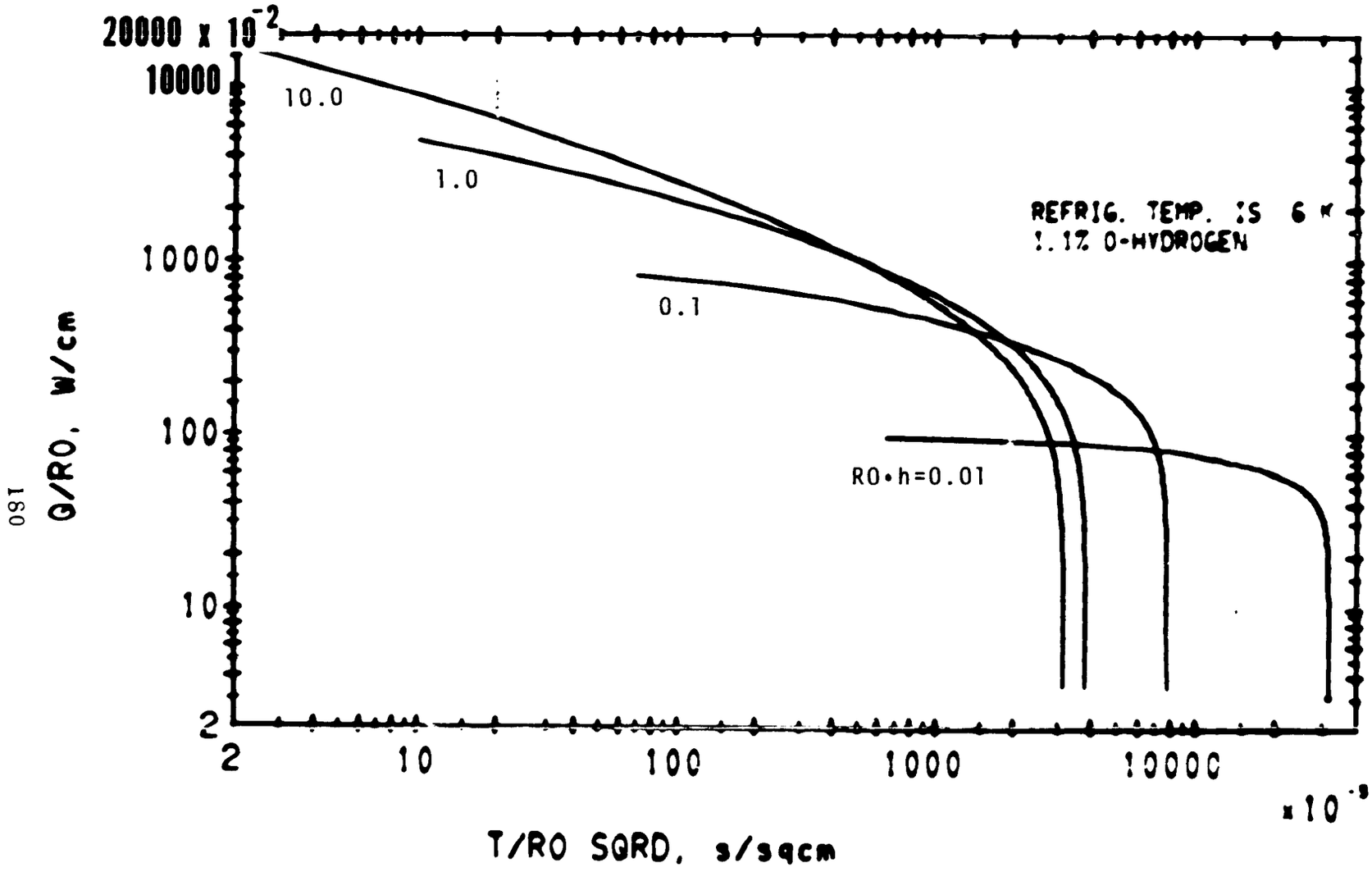

12/20/71

SPHERE, FREEZING FROM OUTSIDE

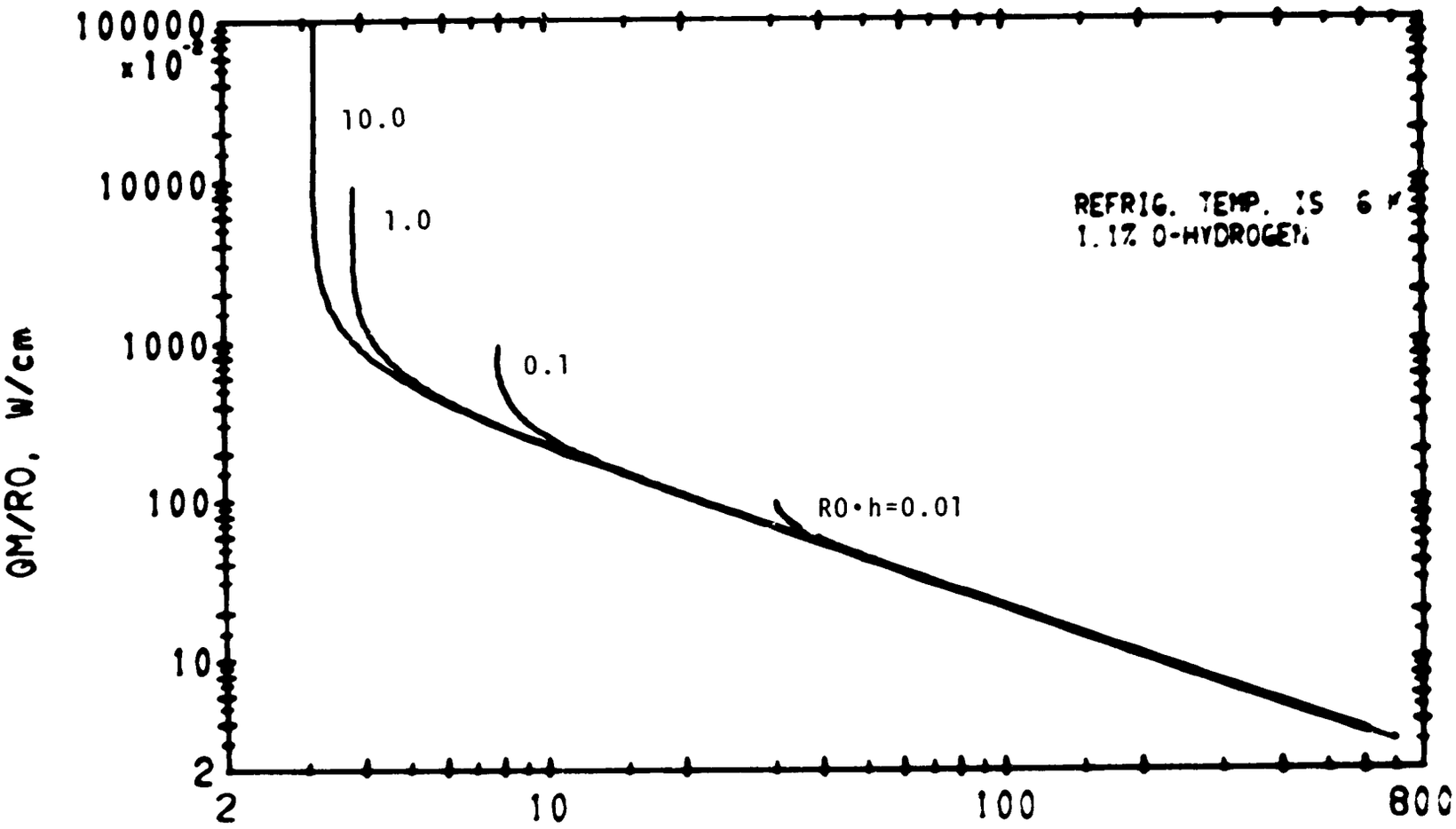

12/20/71

SPHERE, FREEZING FROM OUTSIDE

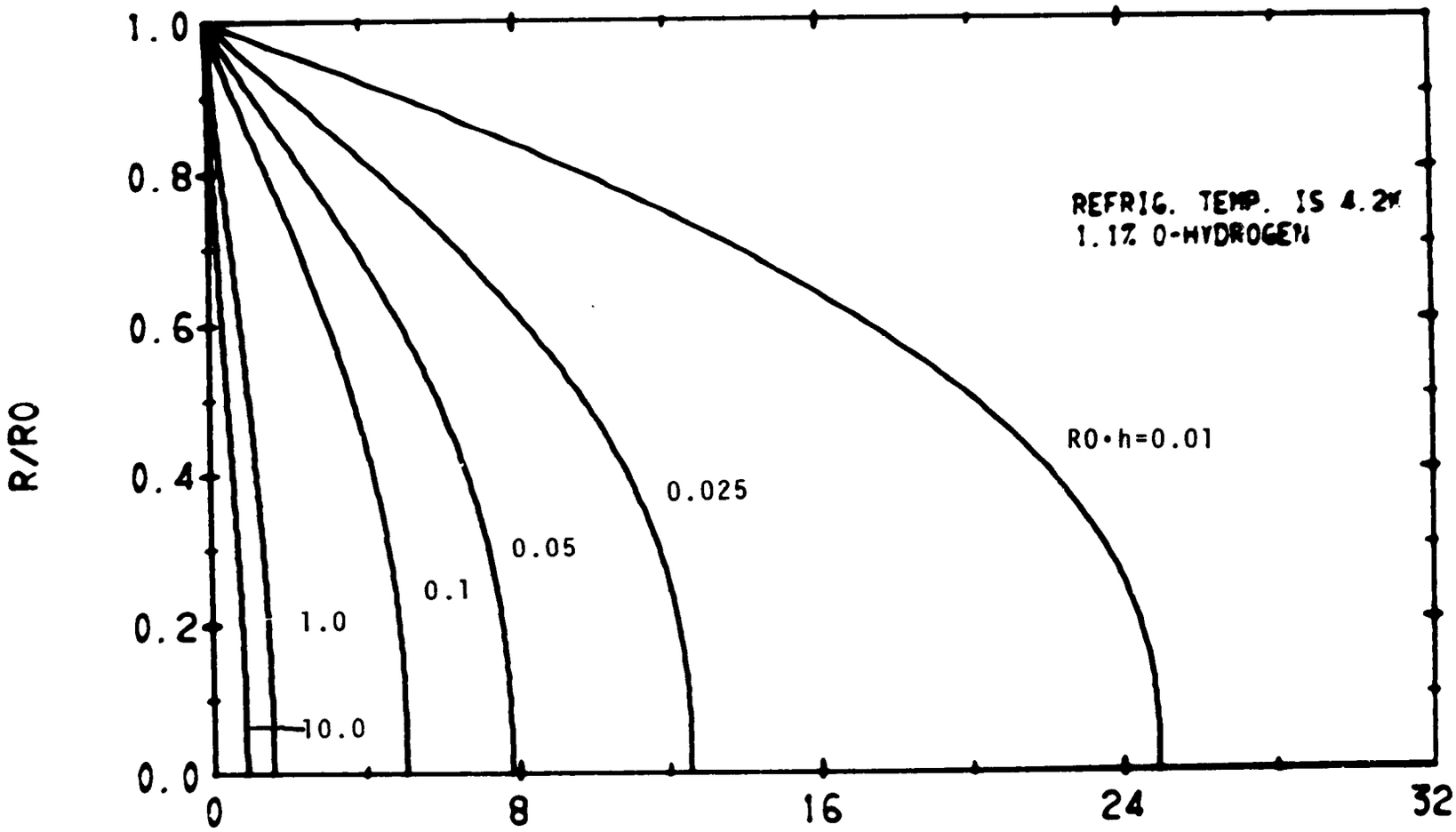

12/20/71

SPHERE, FREEZING FROM OUTSIDE

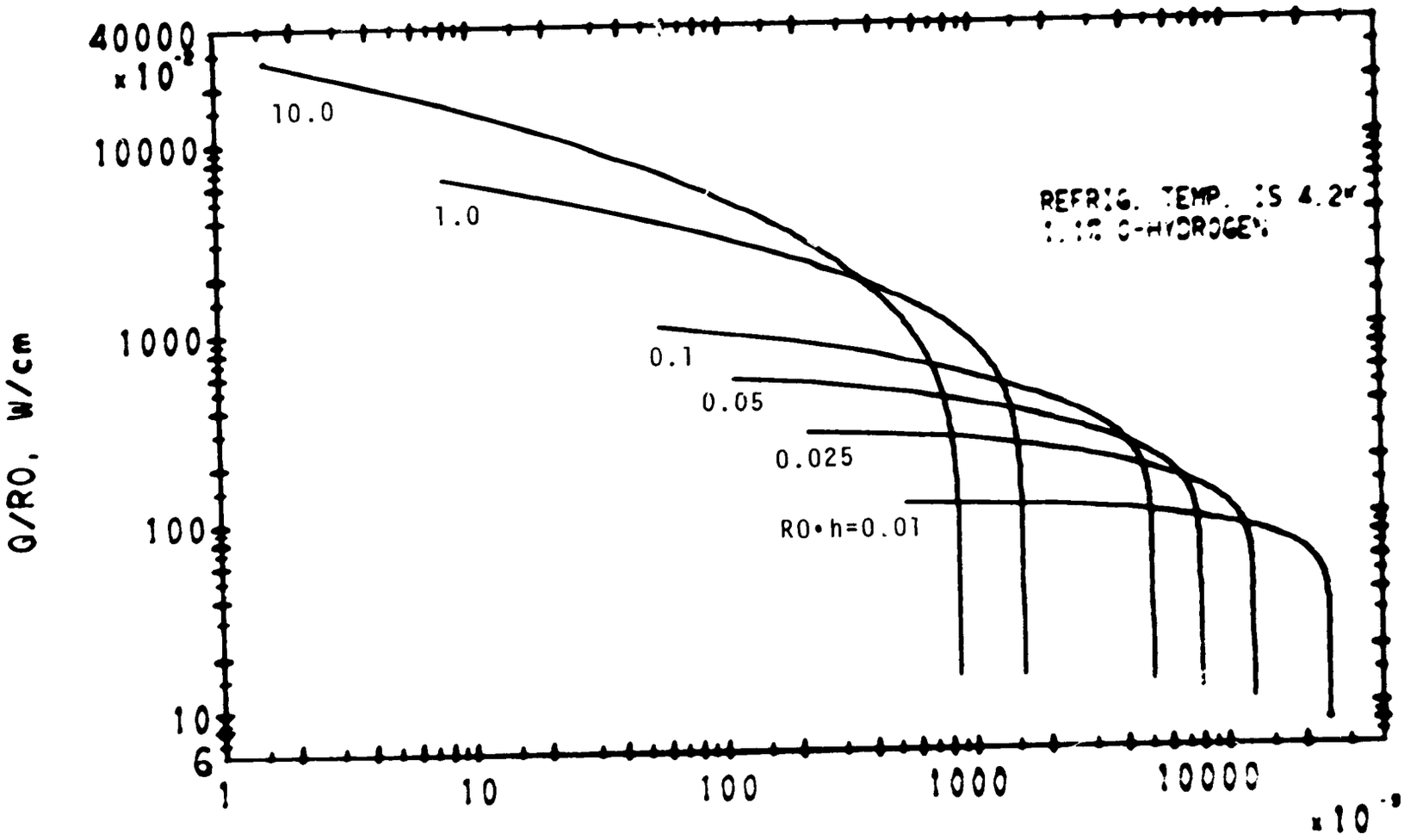

12/20/7

SPHERE, FREEZING FROM OUTSIDE

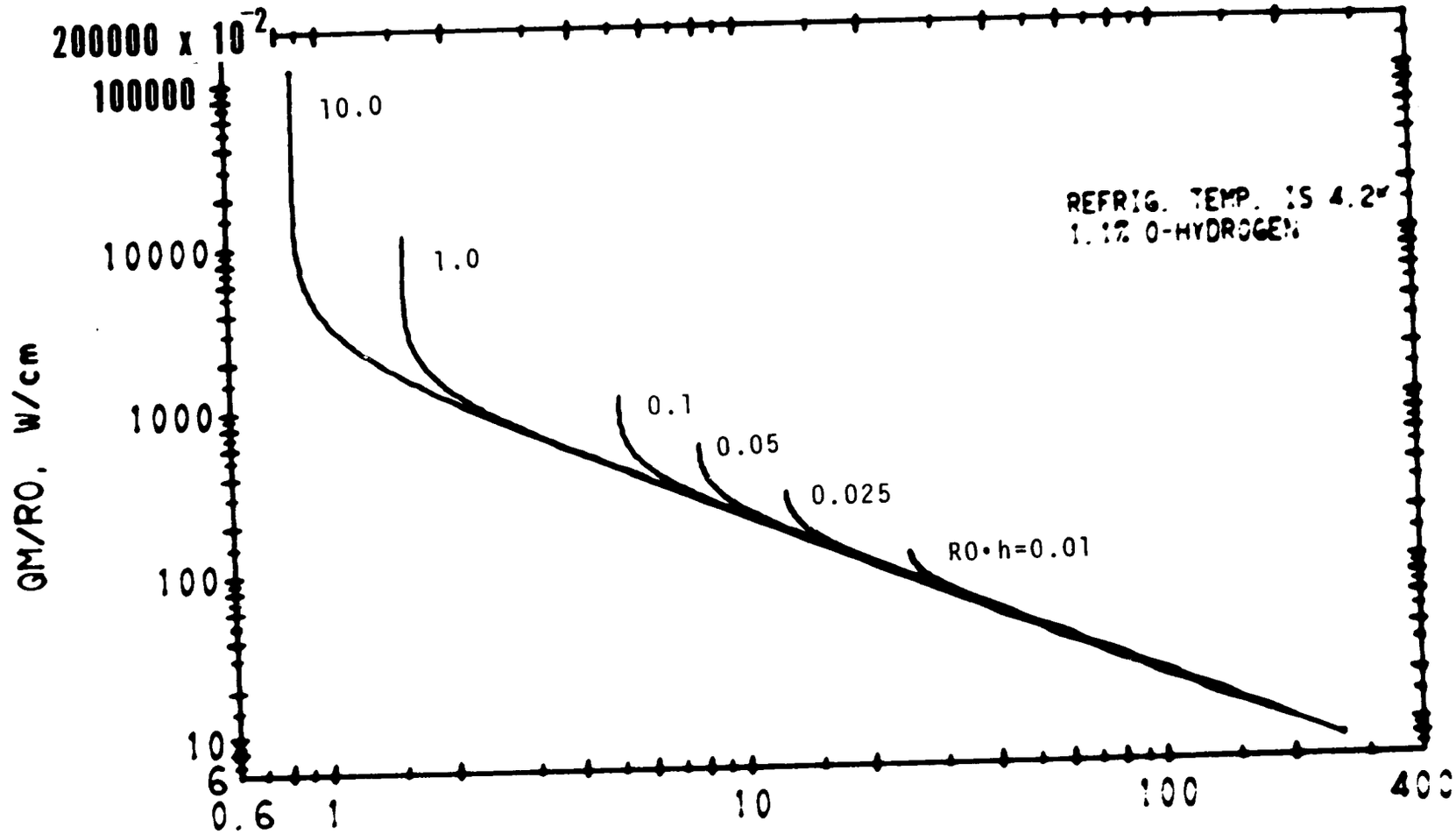

SPHERE, FREEZING FROM OUTSIDE

12/20/71

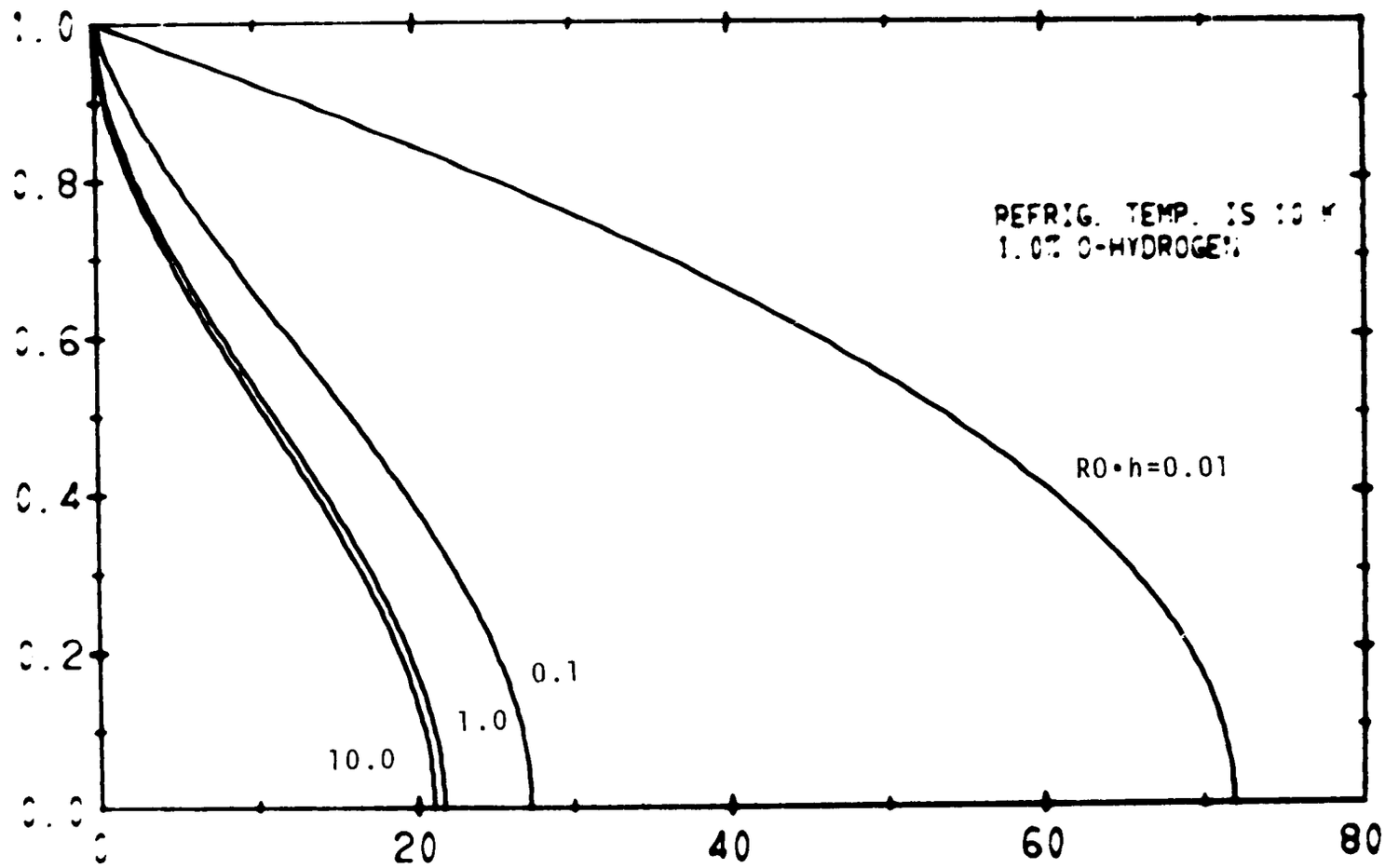

SPHERE, FREEZING FROM OUTSIDE

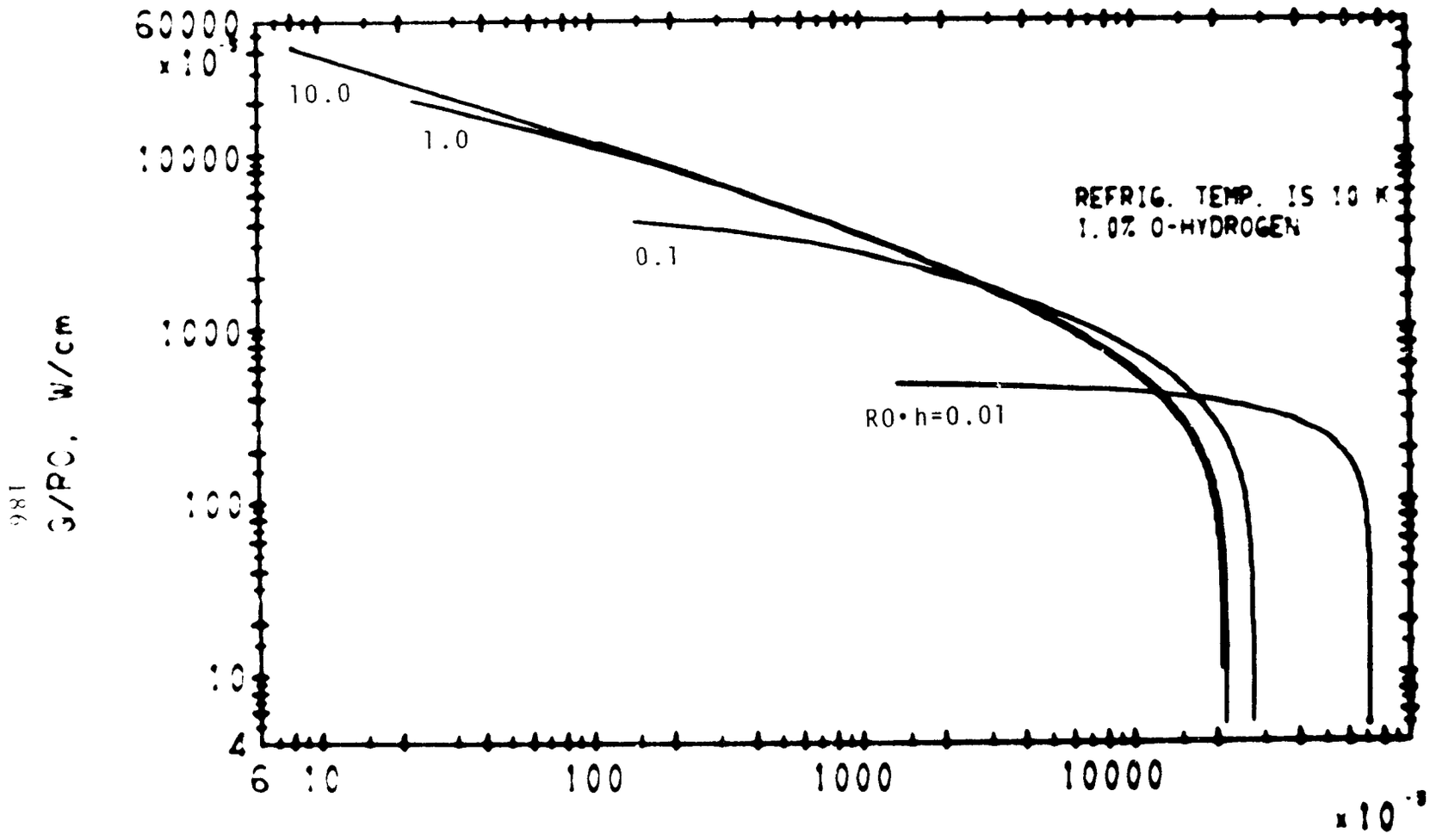

SPHERE, FREEZING FROM OUTSIDE

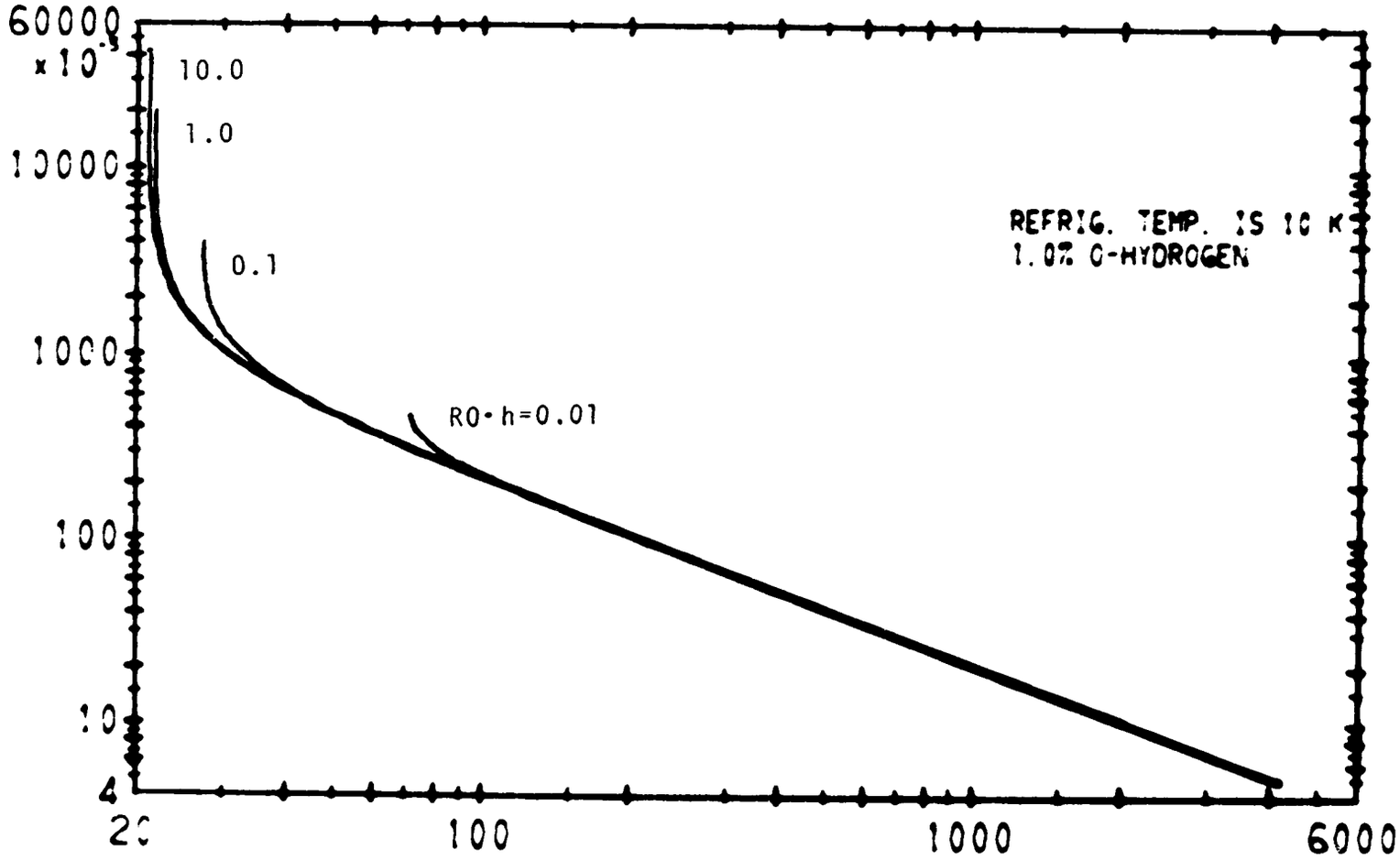

187

SPHERE, FREEZING FROM OUTSIDE

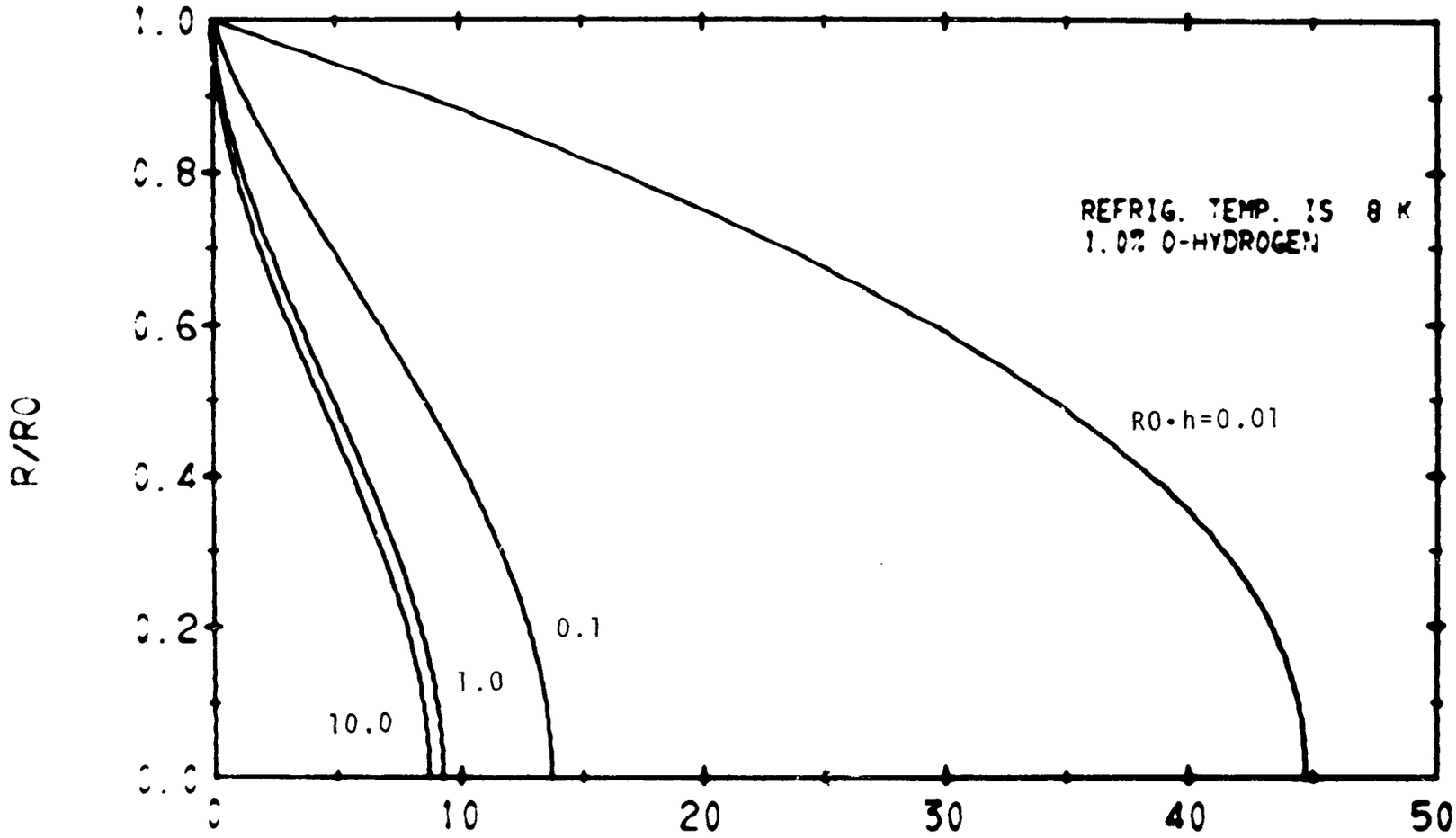

SPHERE, FREEZING FROM OUTSIDE

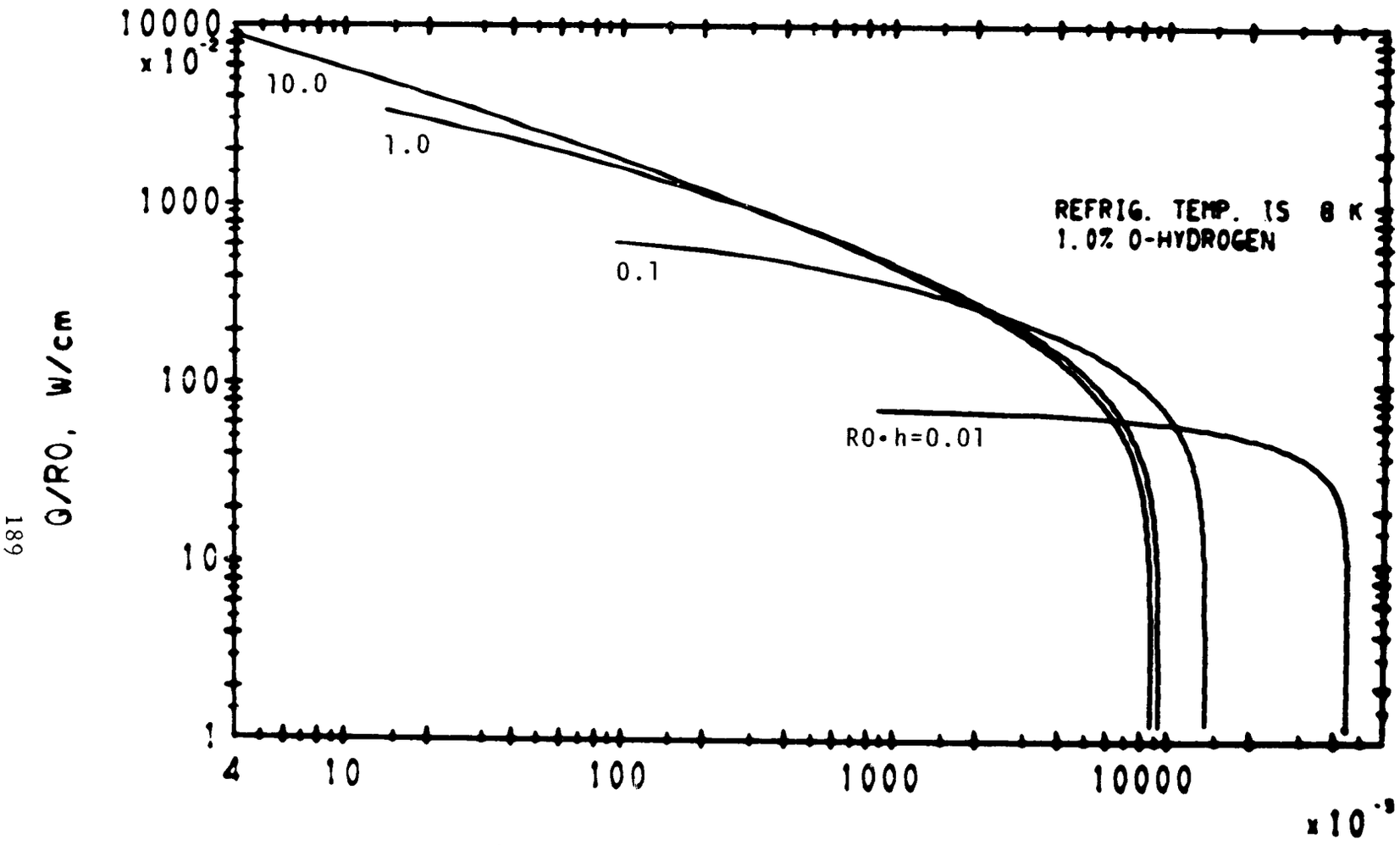

SPHERE, FREEZING FROM OUTSIDE

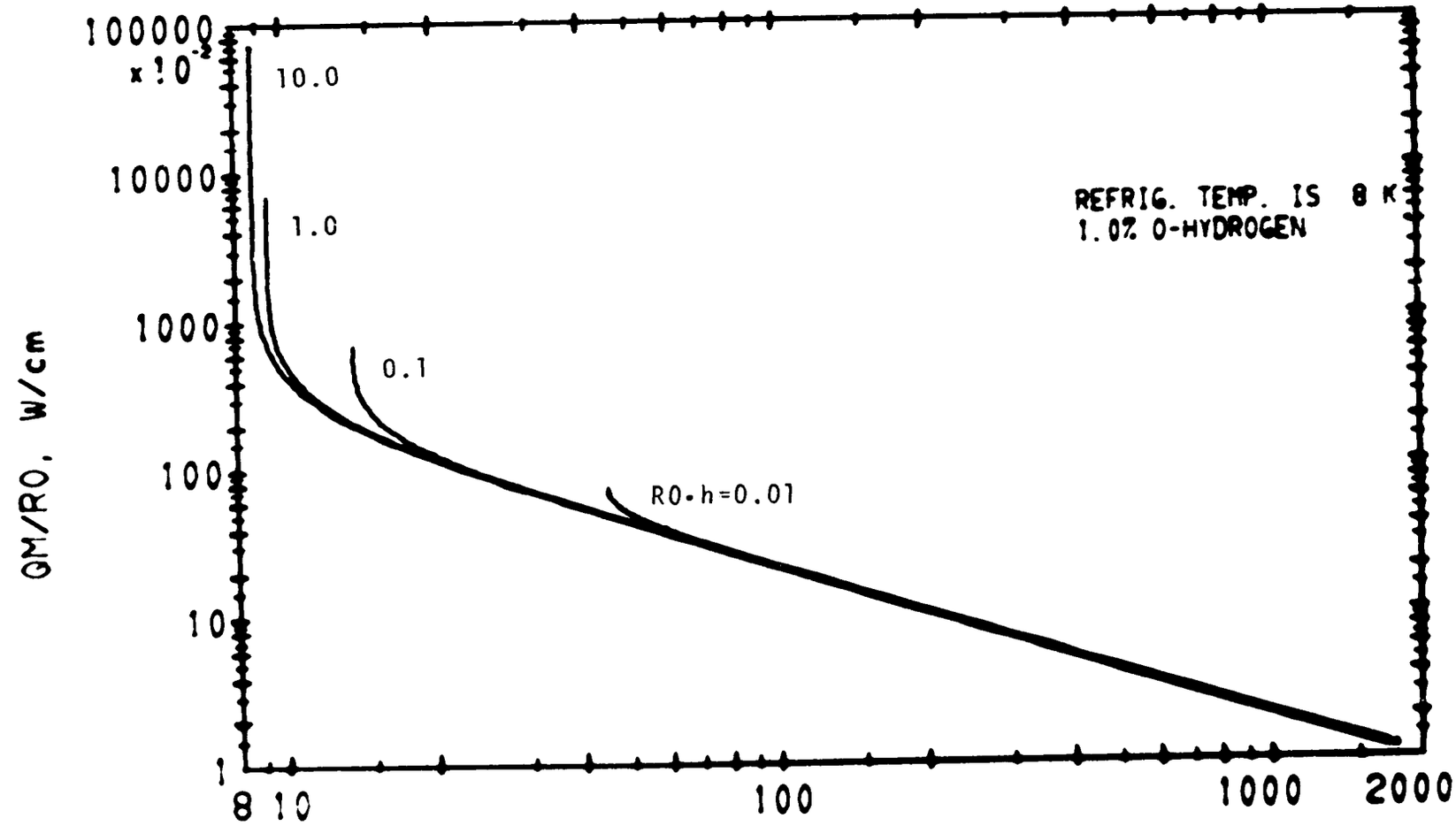

SPHERE, FREEZING FROM OUTSIDE

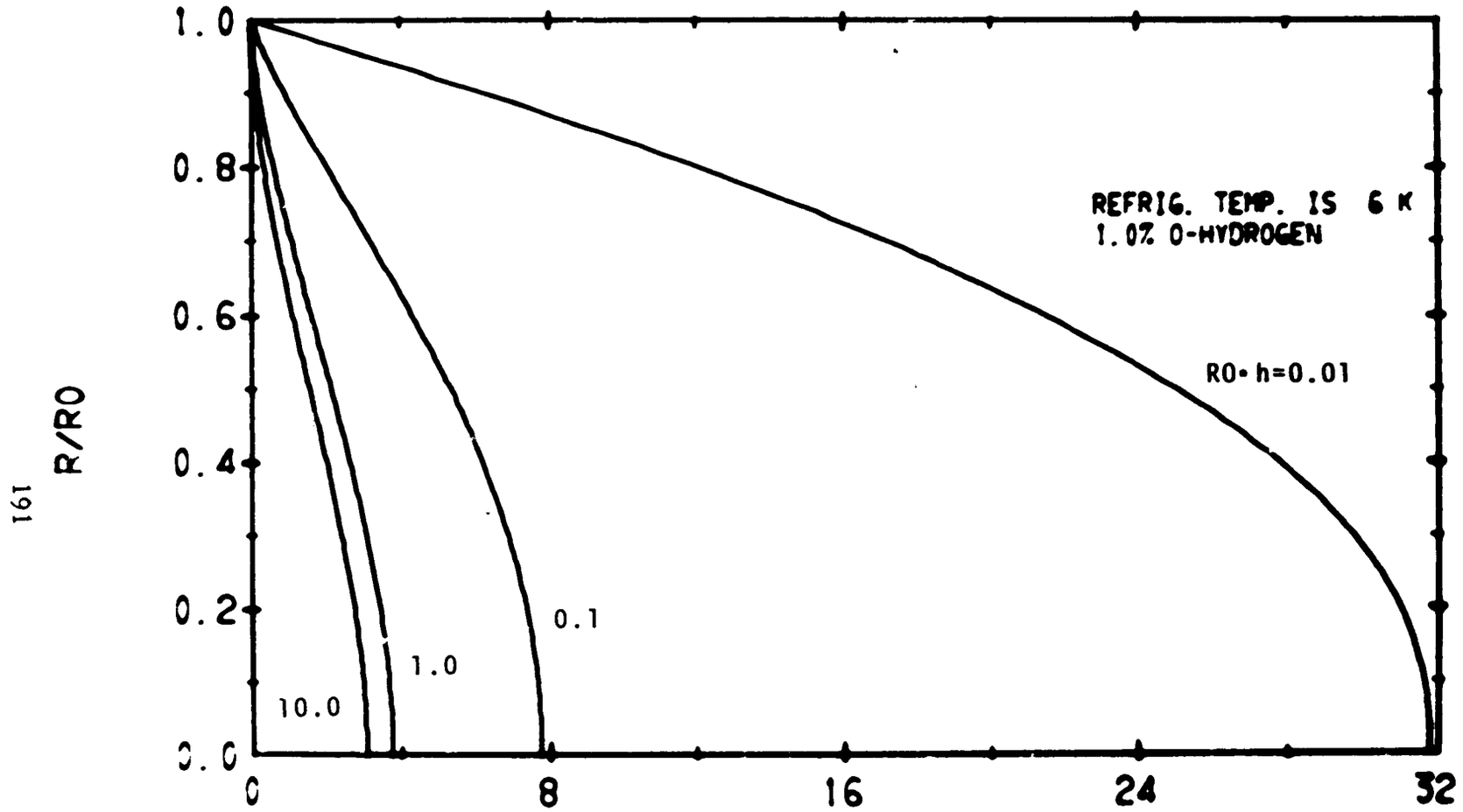

SPHERE, FREEZING FROM OUTSIDE

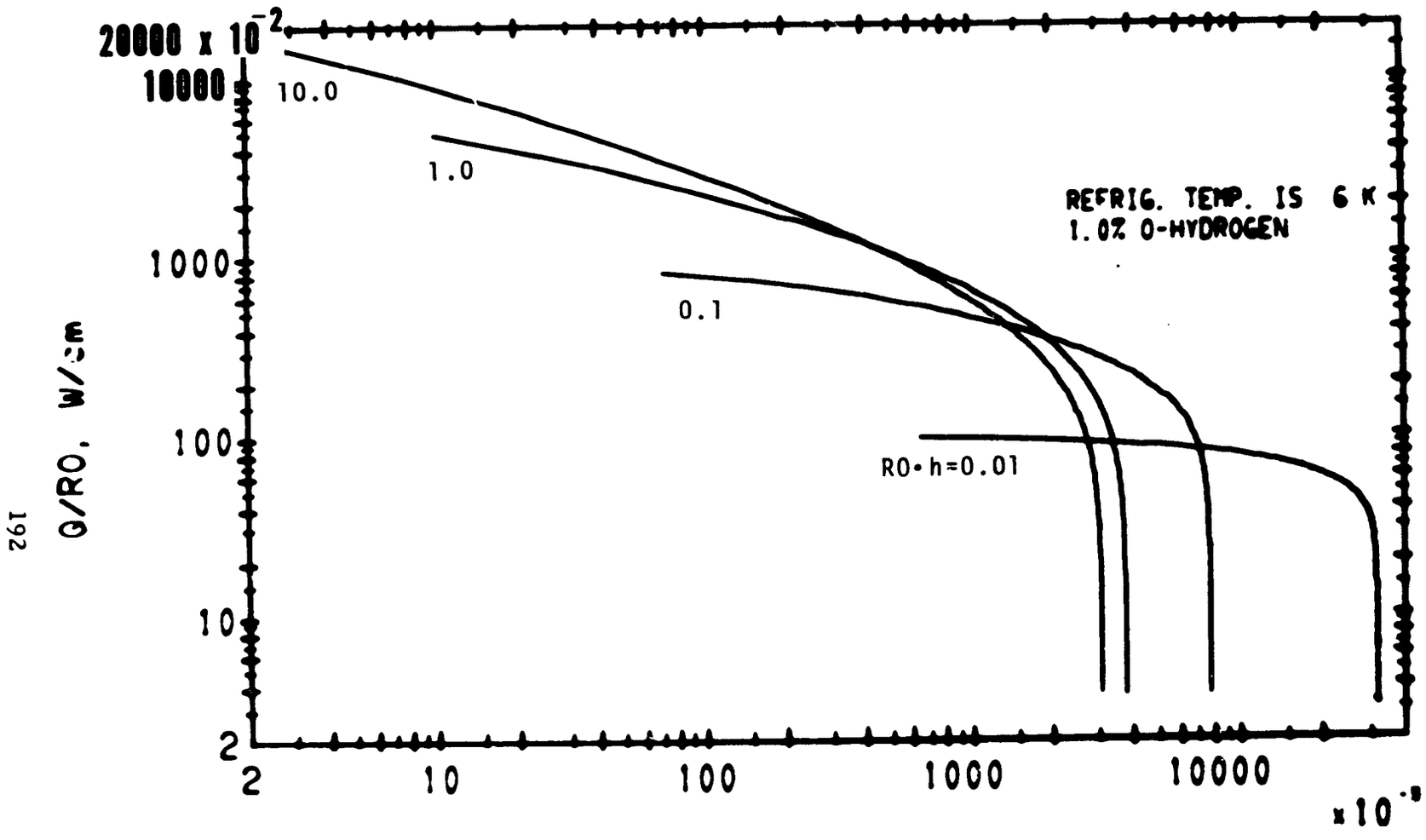

SPHERE, FREEZING FROM OUTSIDE

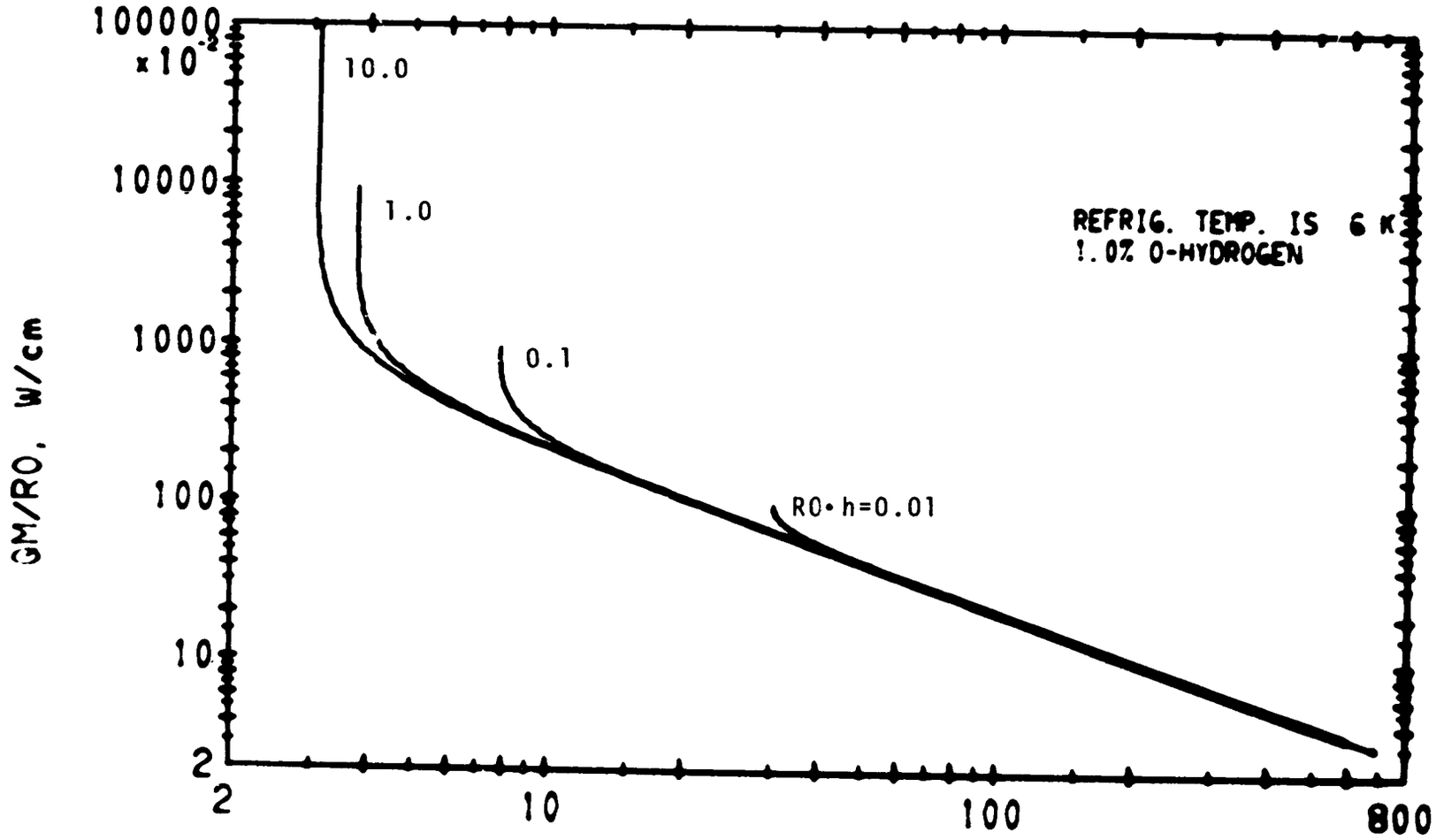

SPHERE, FREEZING FROM OUTSIDE

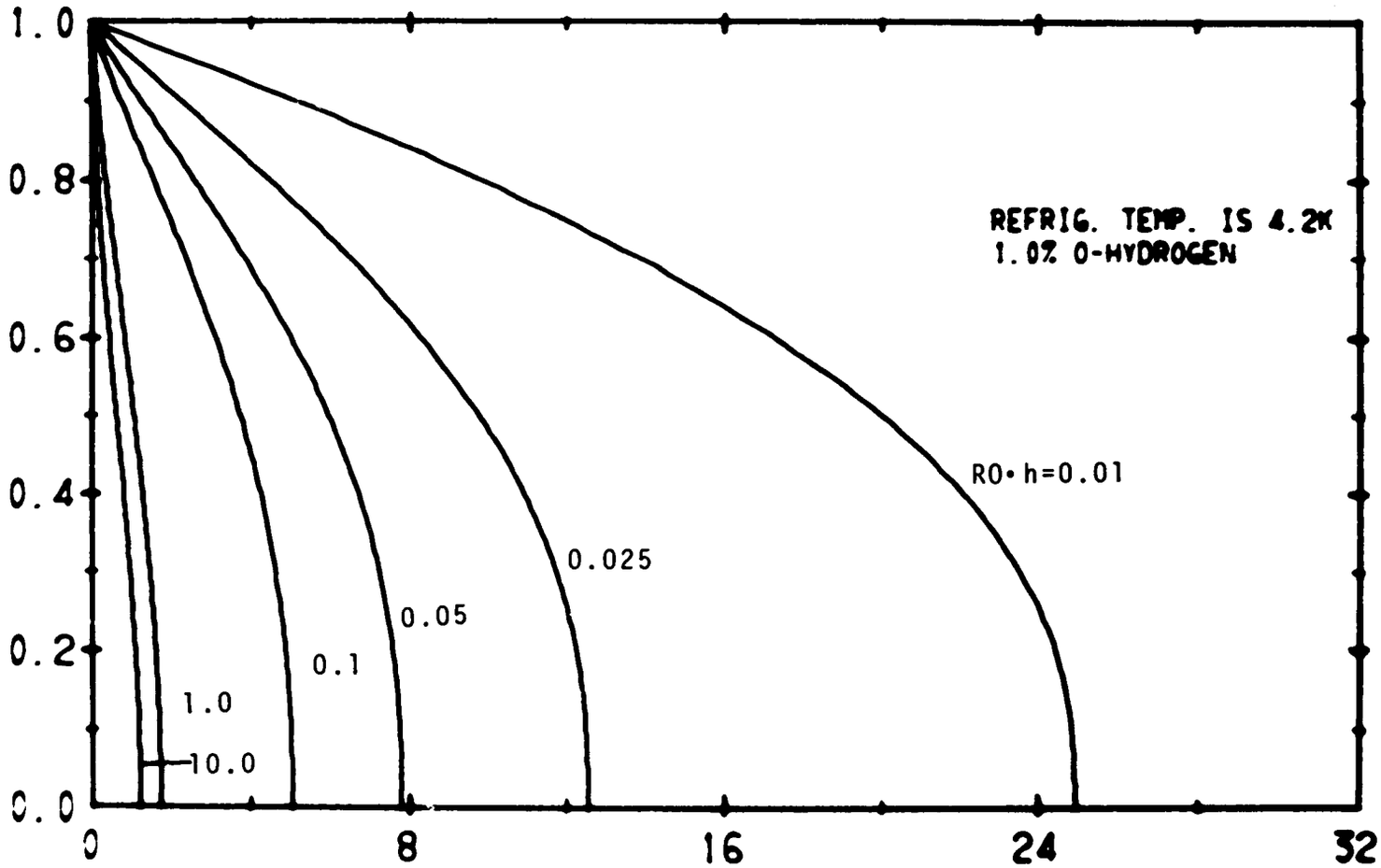

SPHERE, FREEZING FROM OUTSIDE

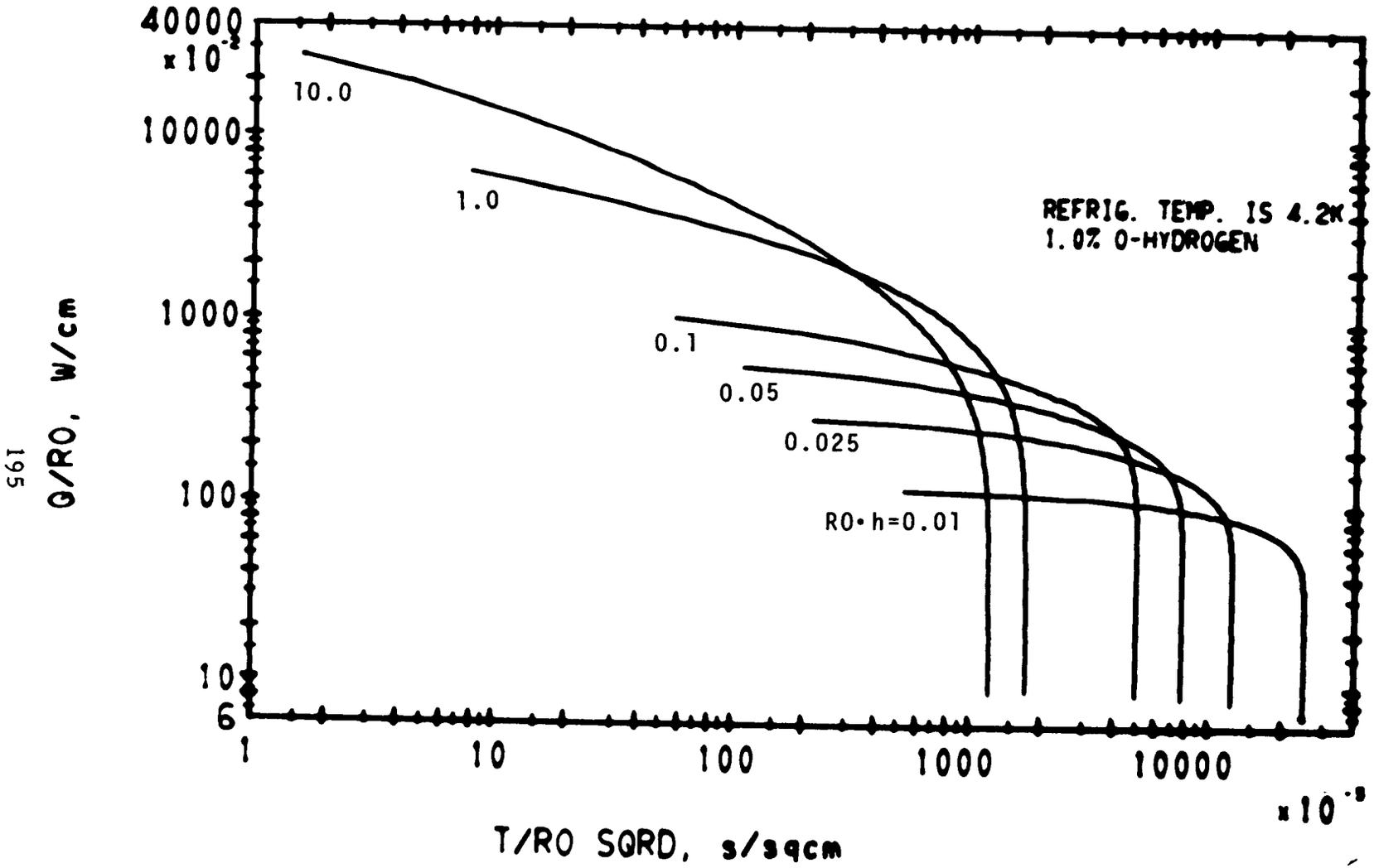

195

SPHERE, FREEZING FROM OUTSIDE

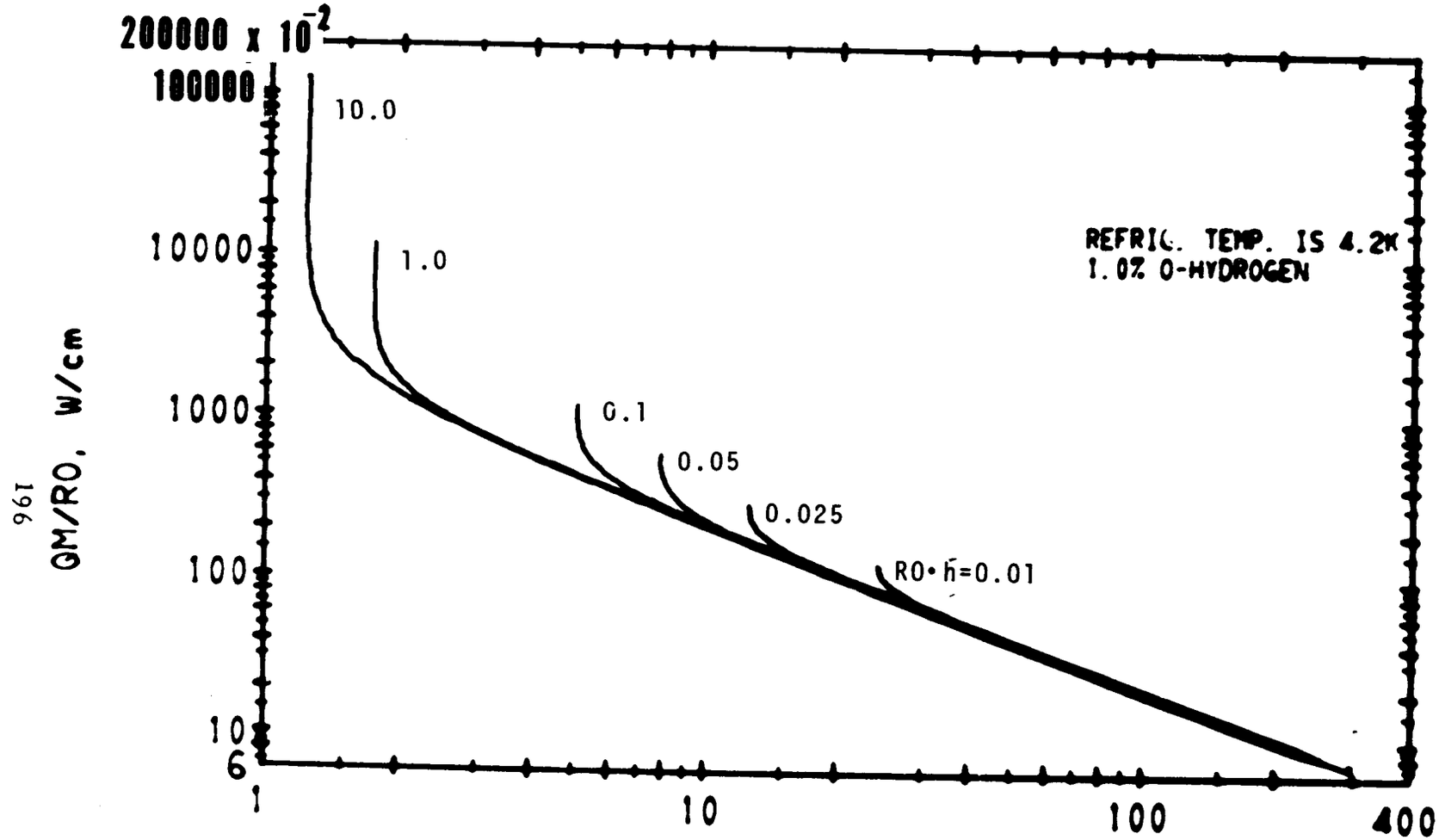

SPHERE, FREEZING FROM OUTSIDE

APPENDIX C

LINEAR FREEZING

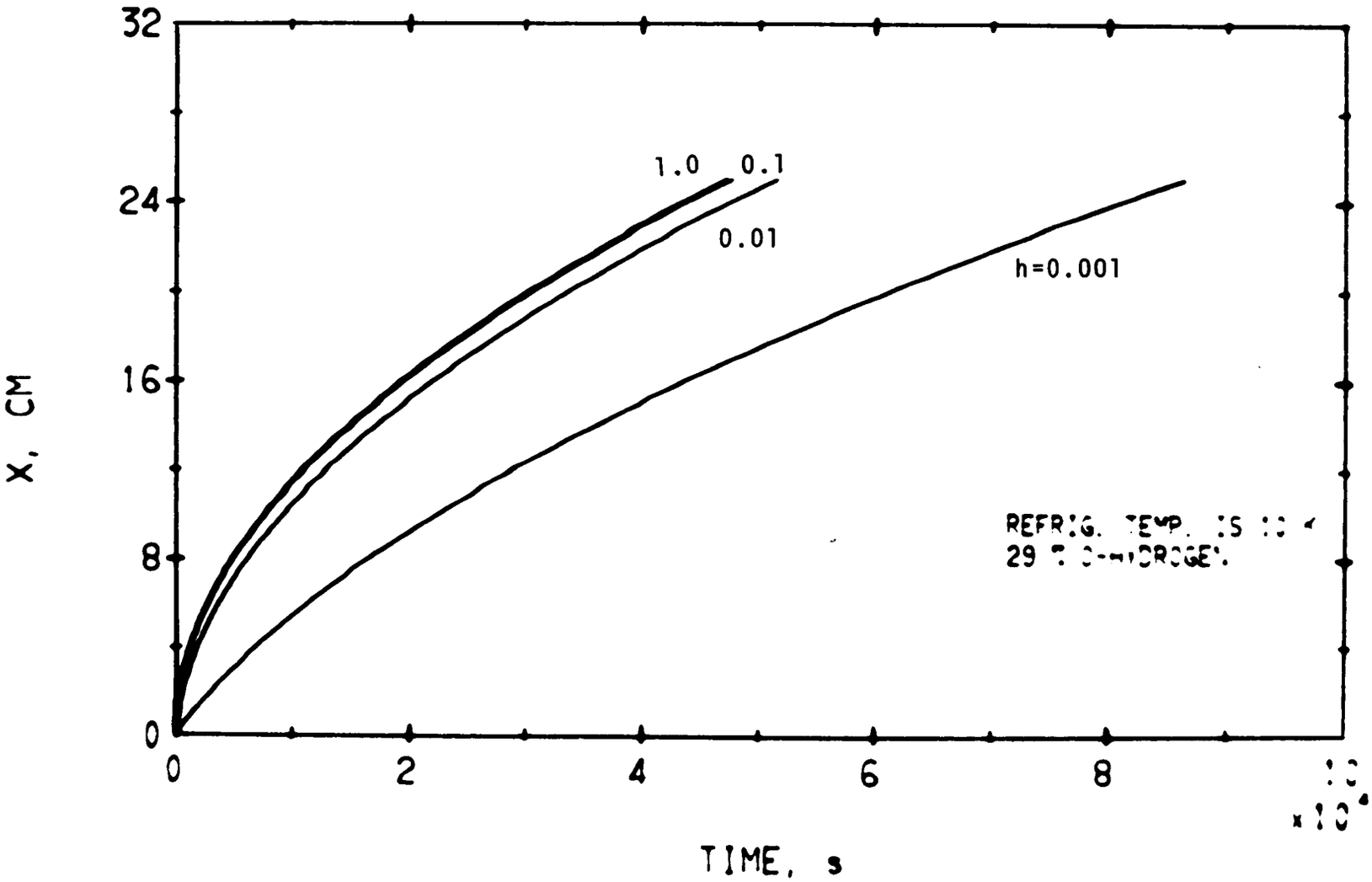

01/14/72

LINEAR FREEZING

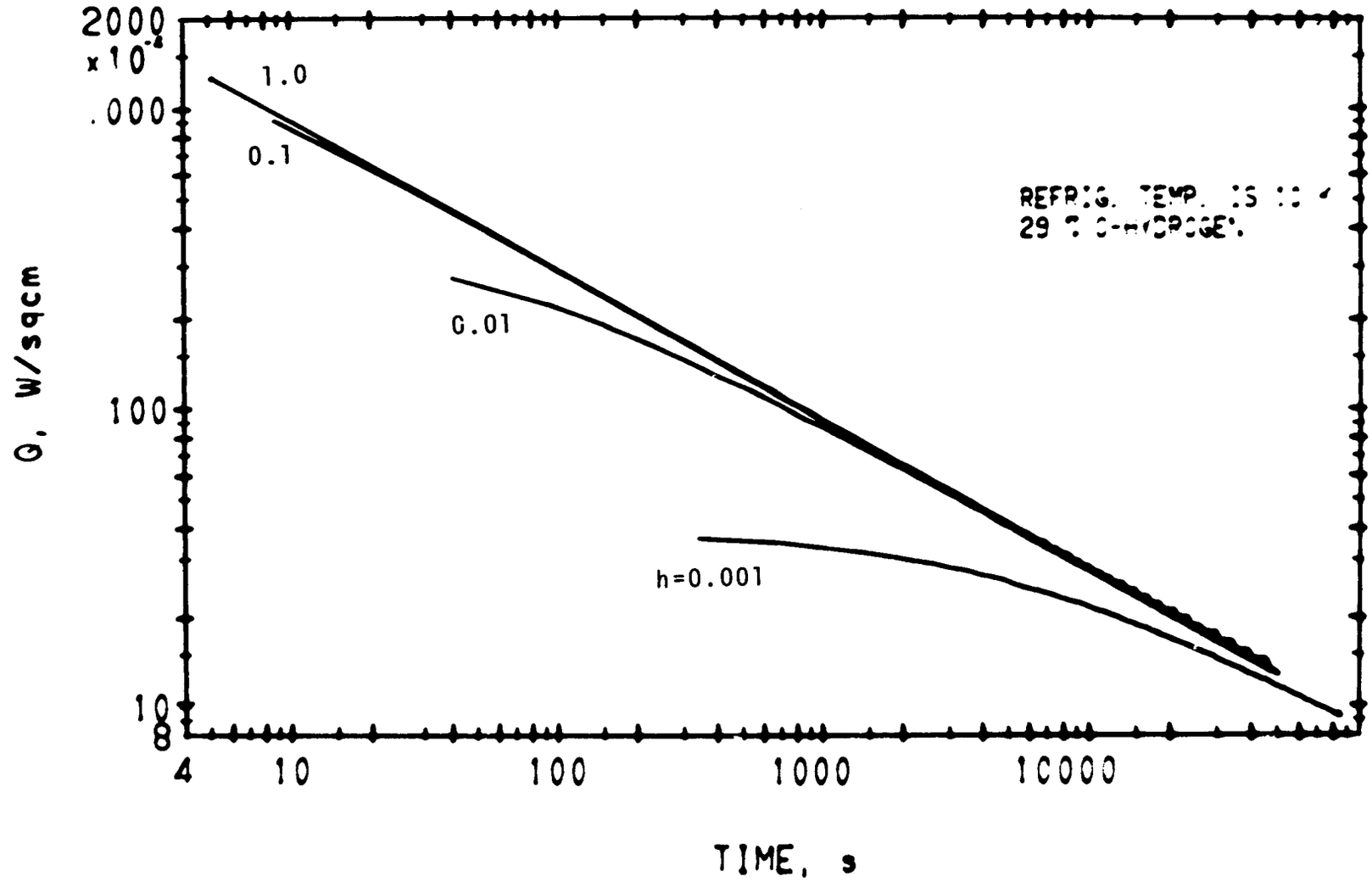

01/16/72

LINEAR FREEZING

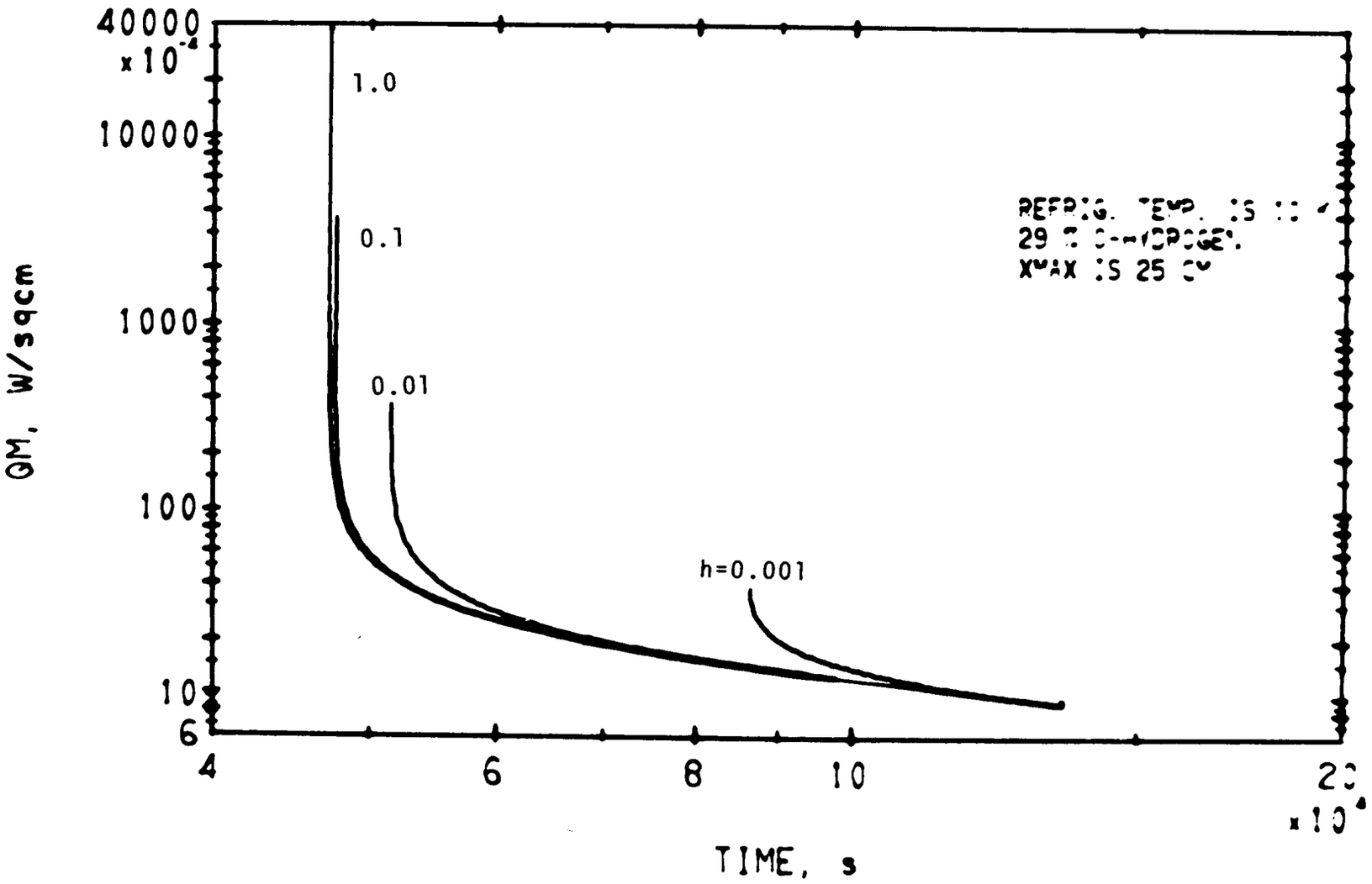

200

01/16/72

LINEAR FREEZING

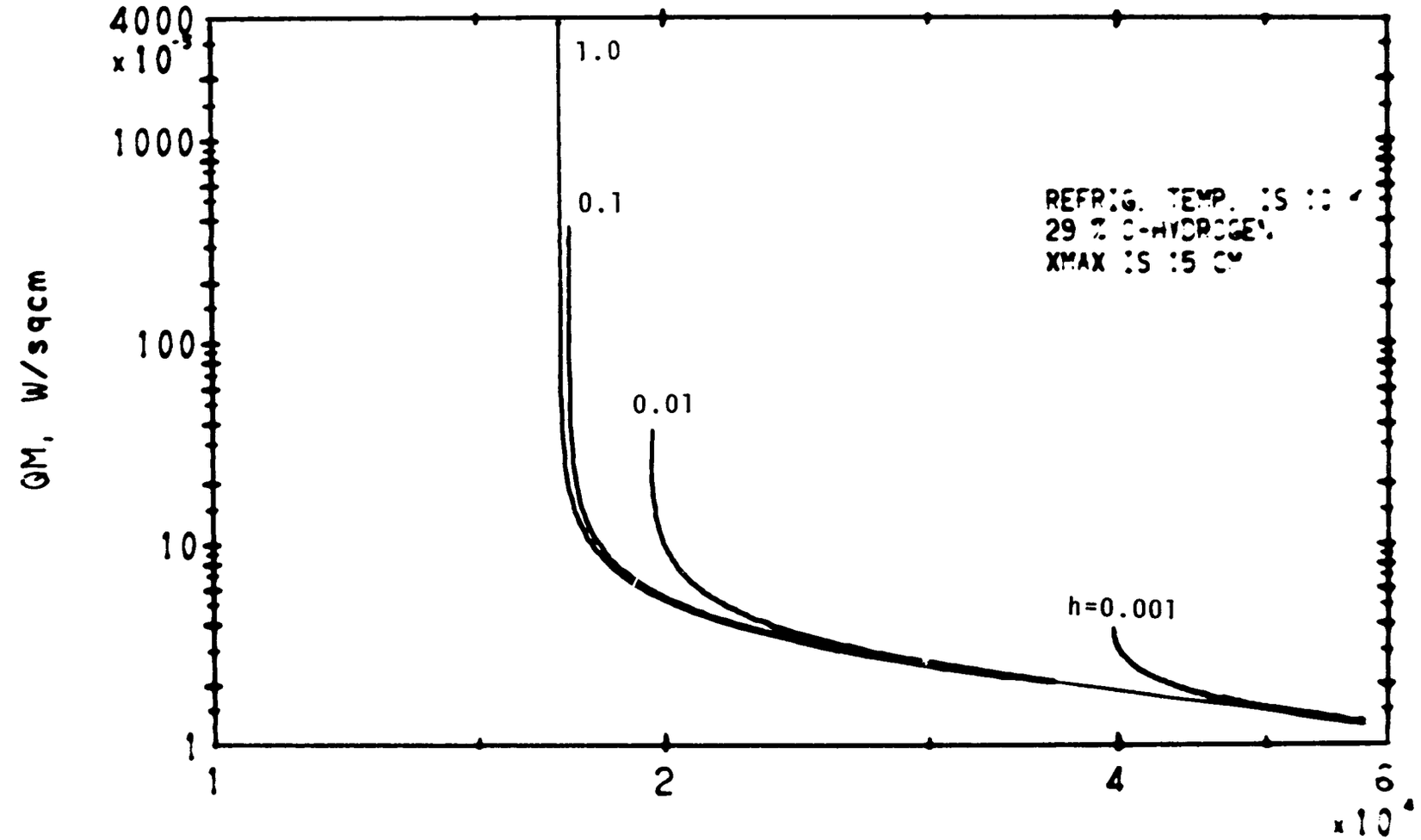

01/14/72

LINEAR FREEZING

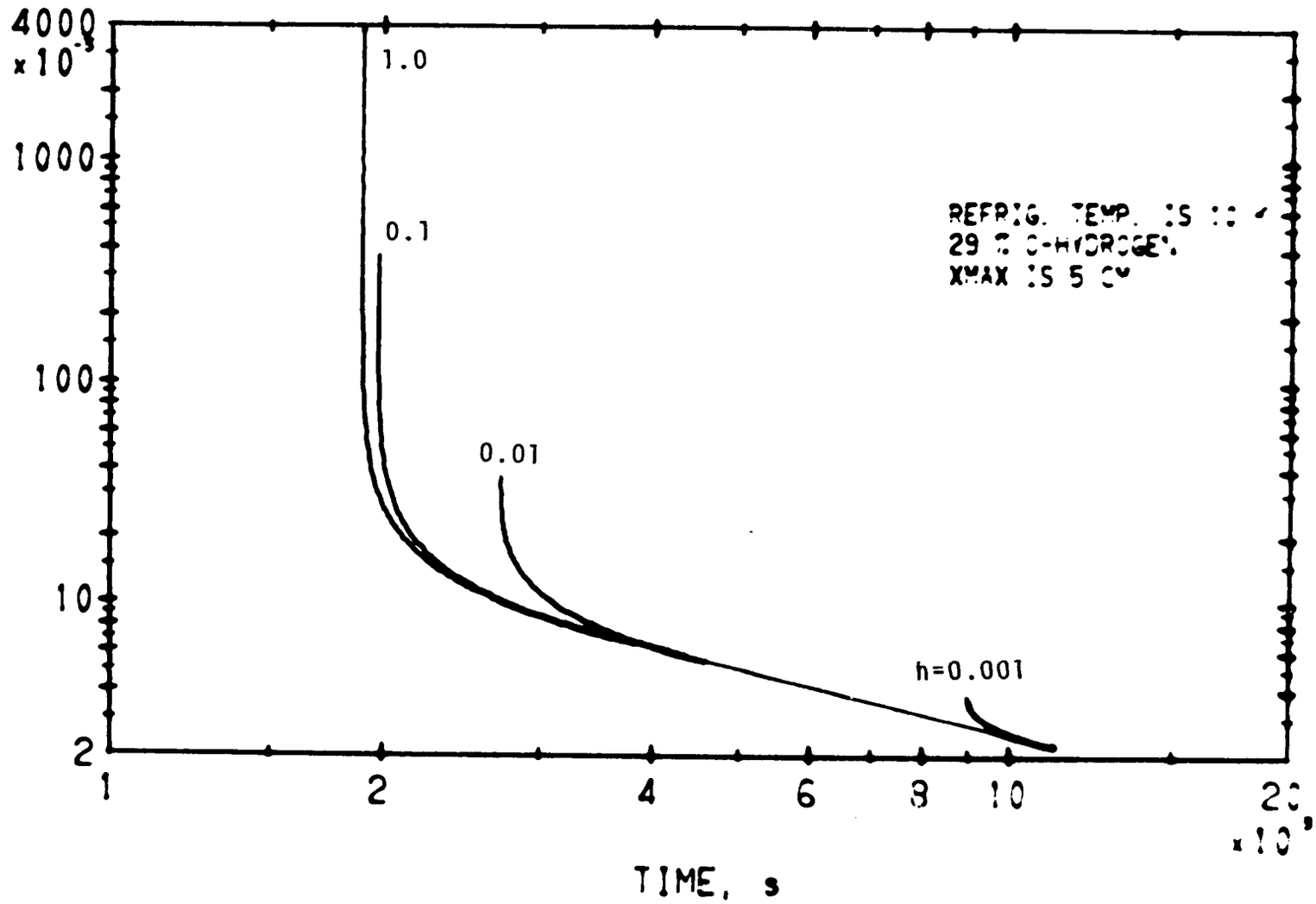

01/14/72

LINEAR FREEZING

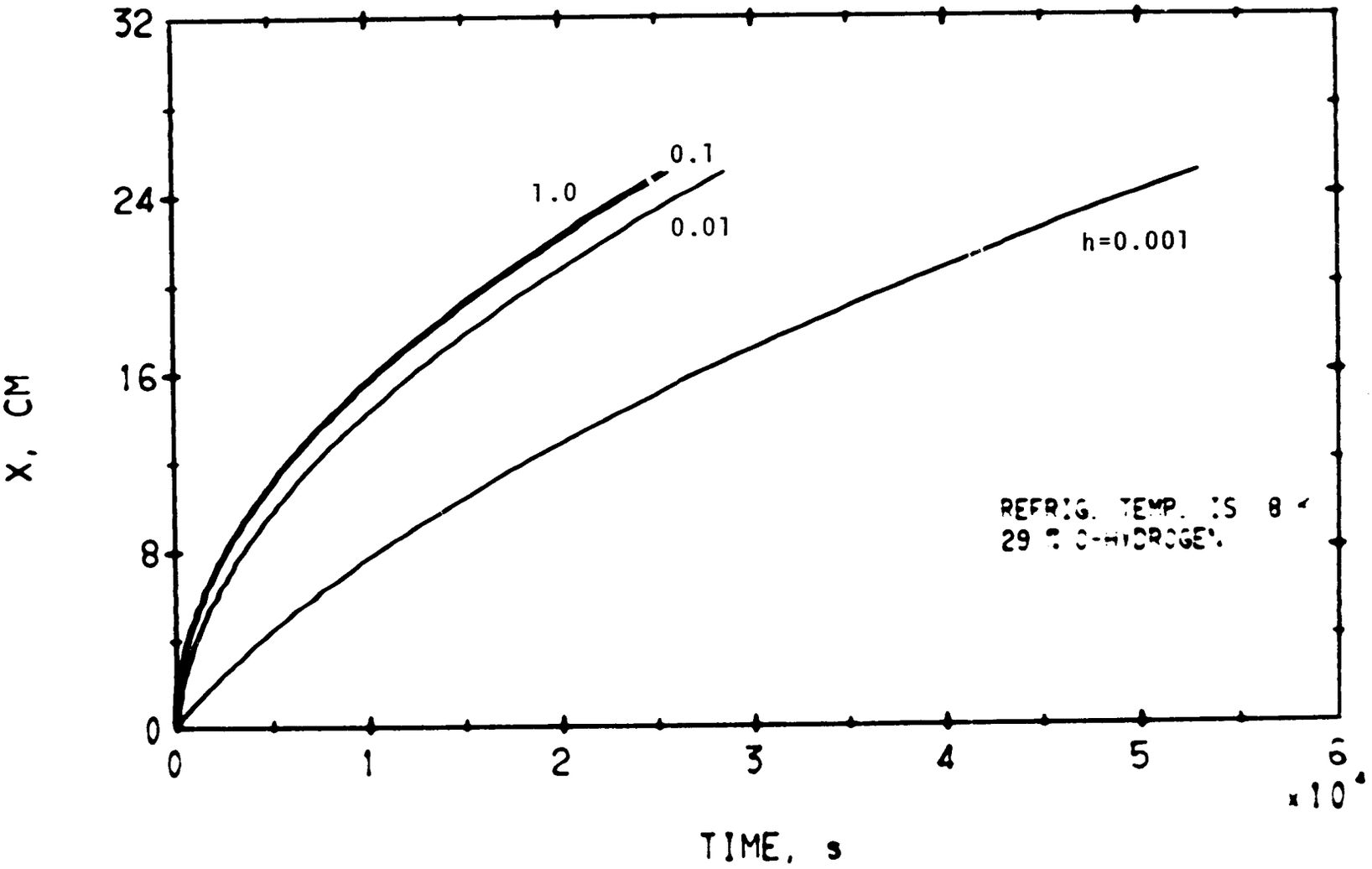

01/16/72

LINEAR FREEZING

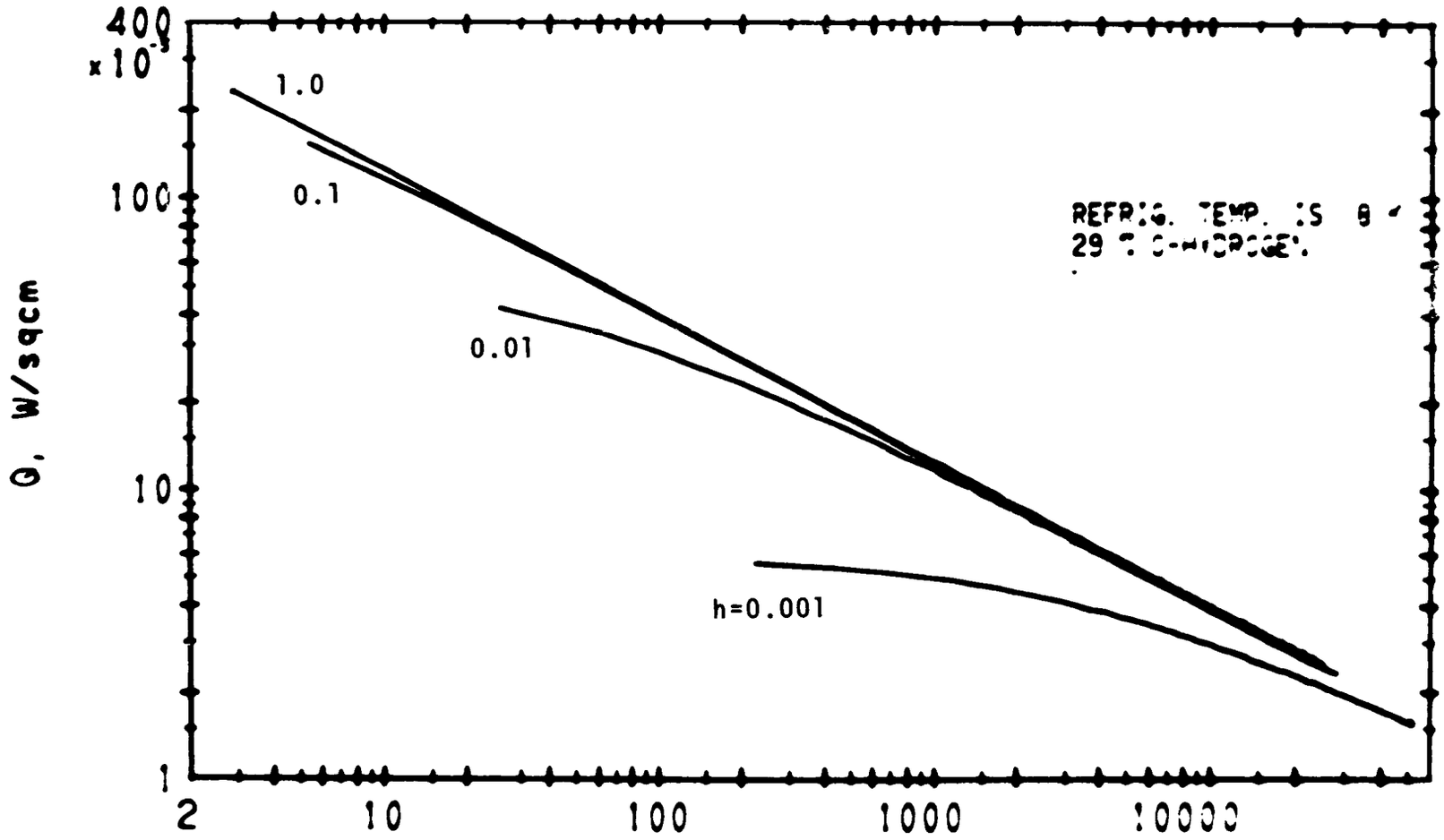

01/16/72

LINEAR FREEZING

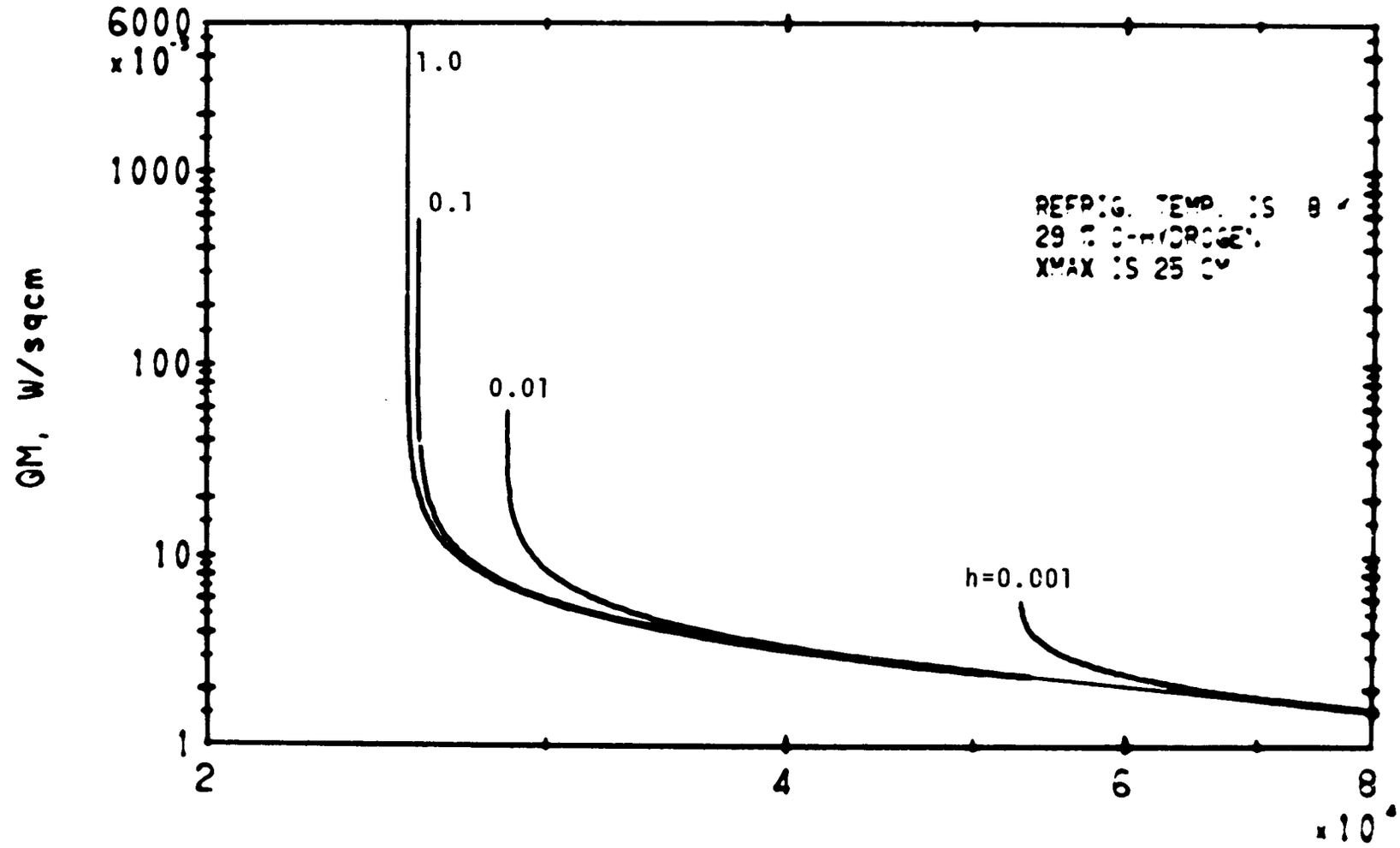

01/16/72

LINEAR FREEZING

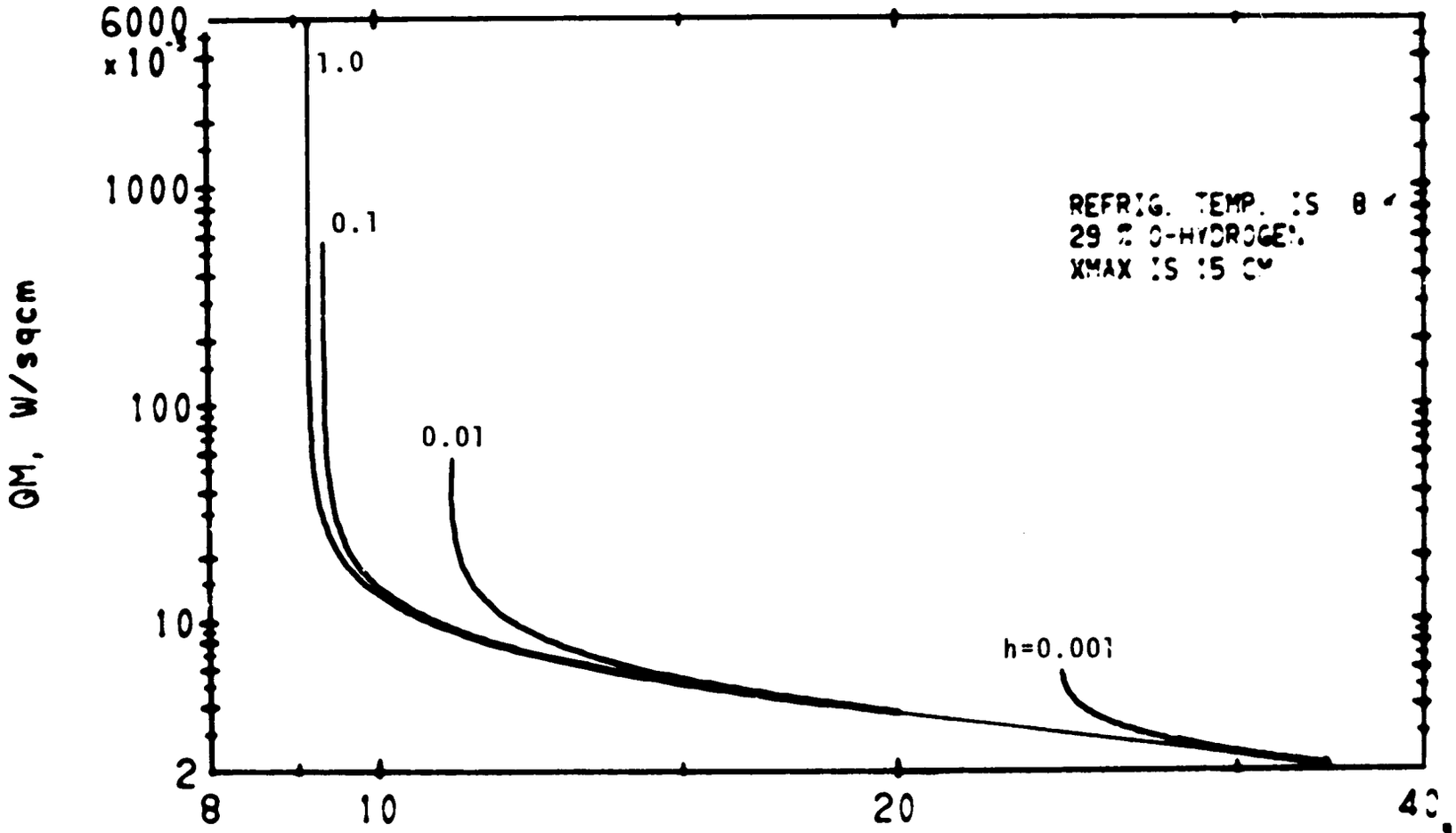

01/16/72

LINEAR FREEZING

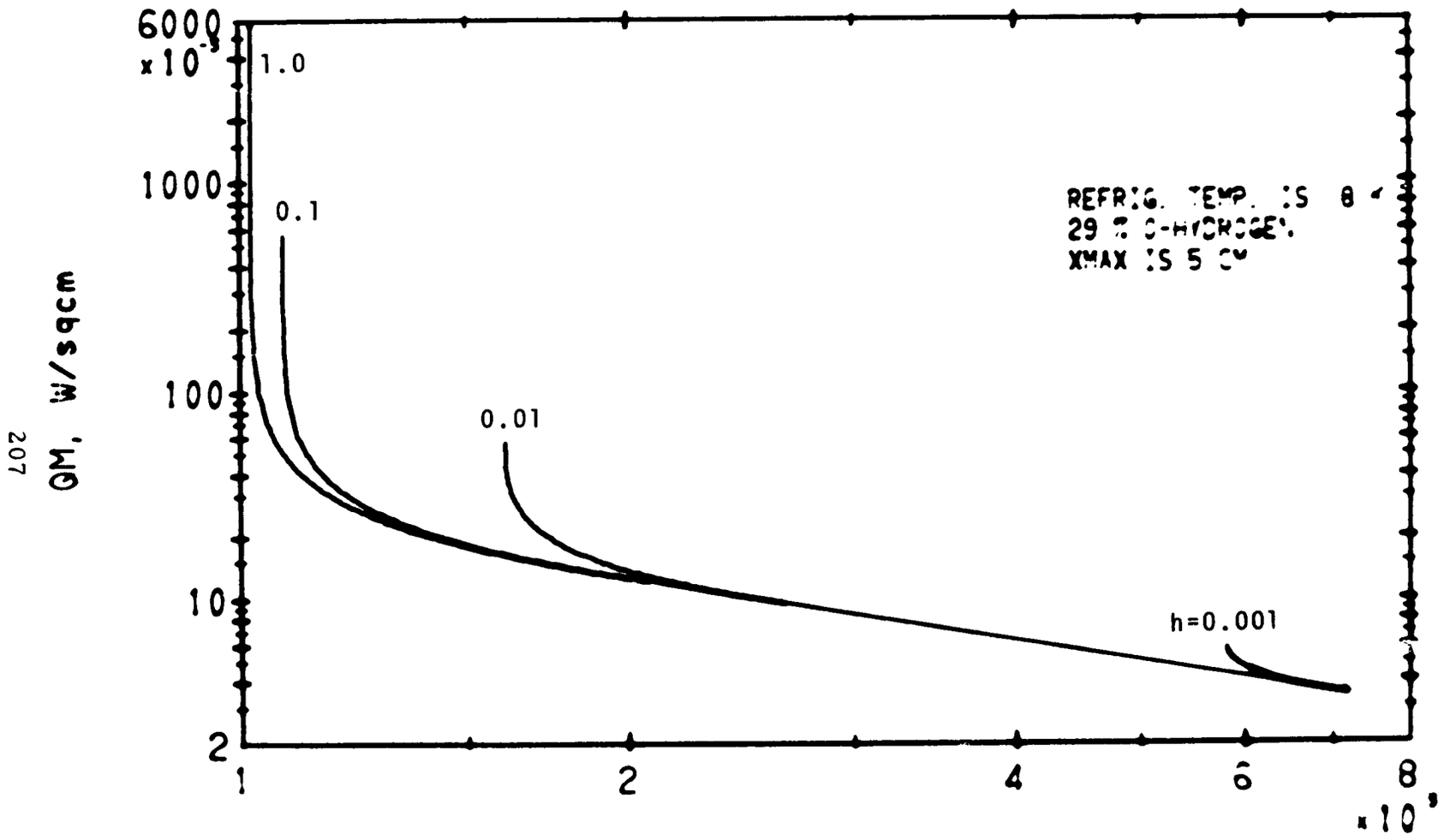

207

01/16/72

LINEAR FREEZING

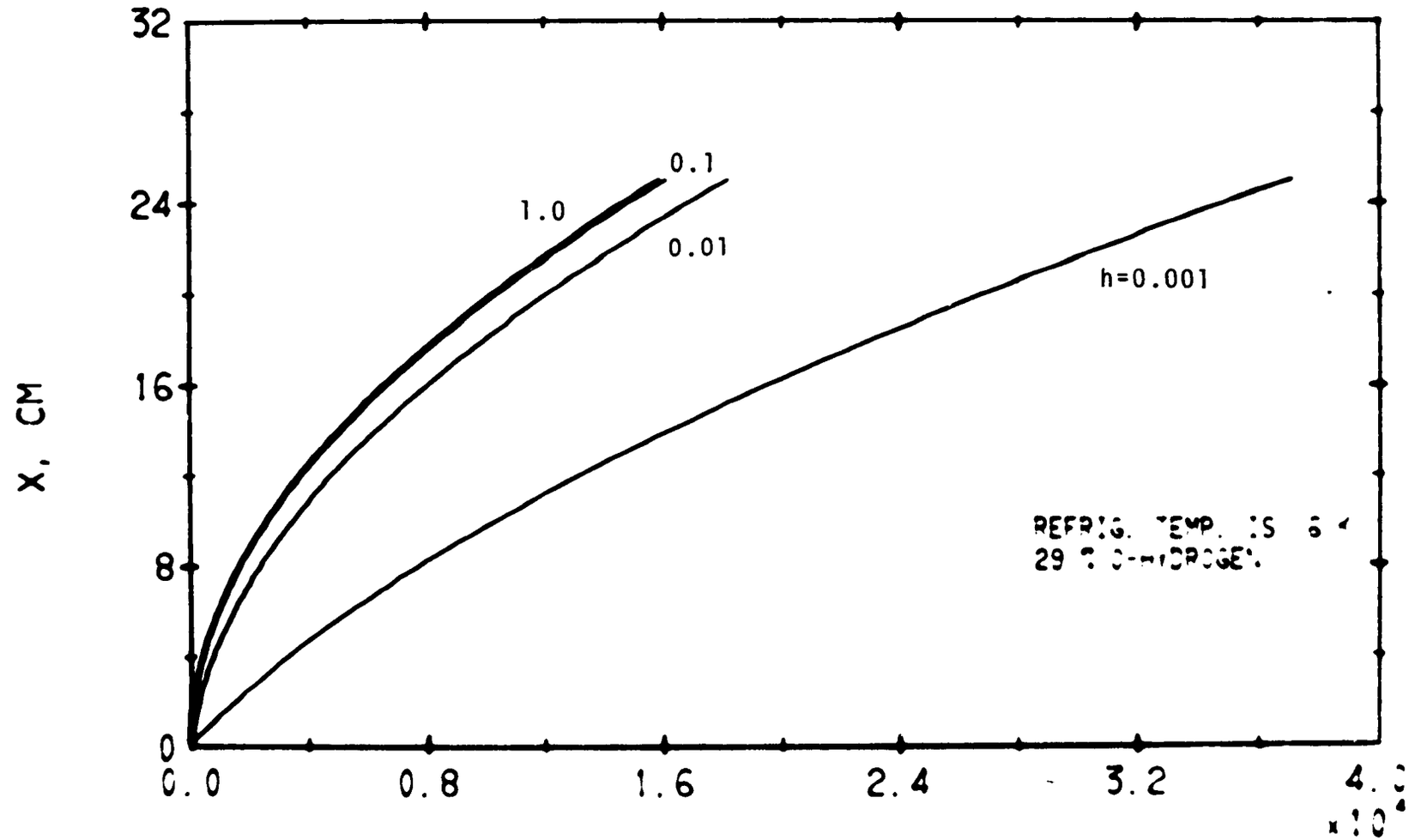

208

01/14/72

LINEAR FREEZING

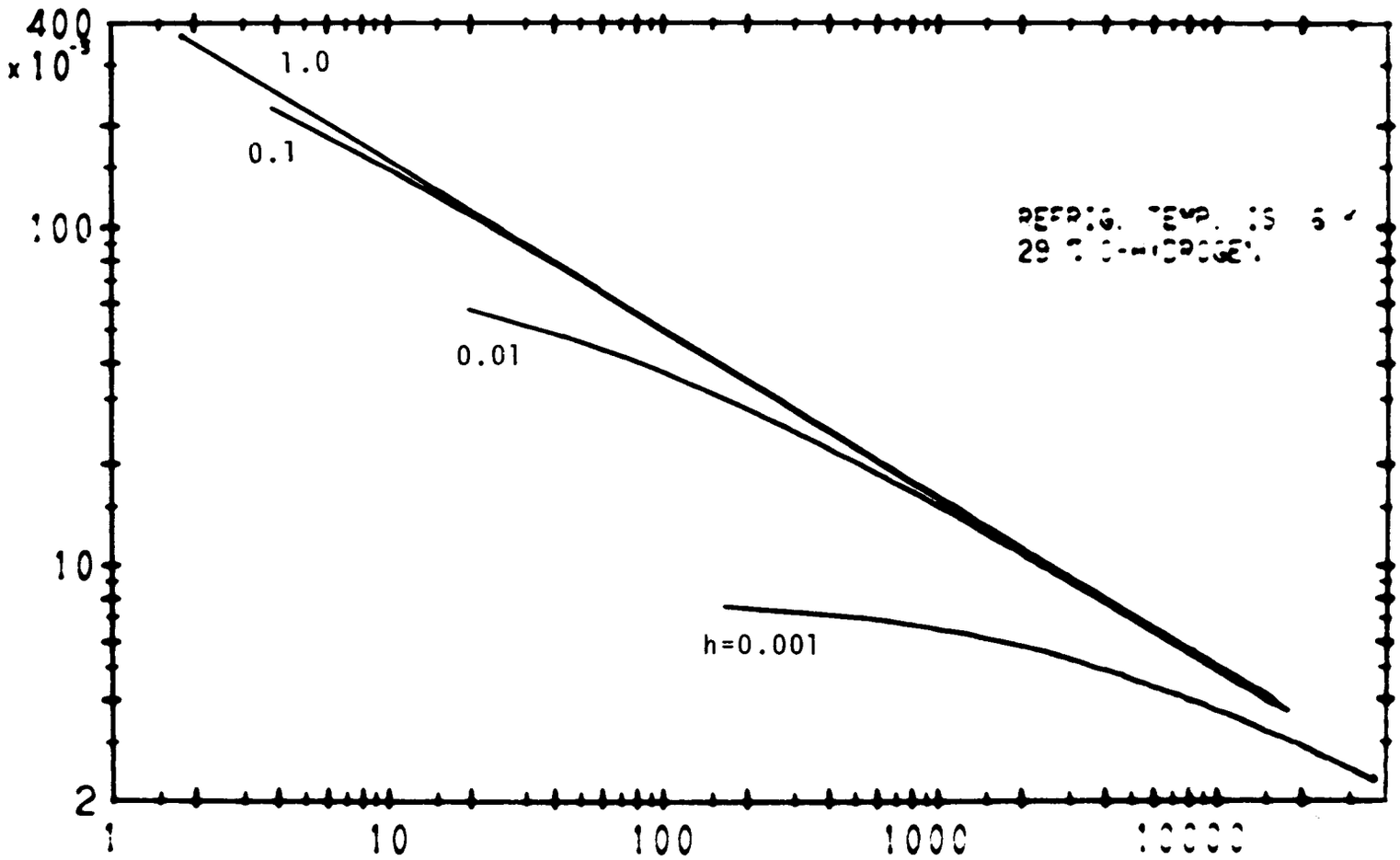

8/16/72

LINEAR FREEZING

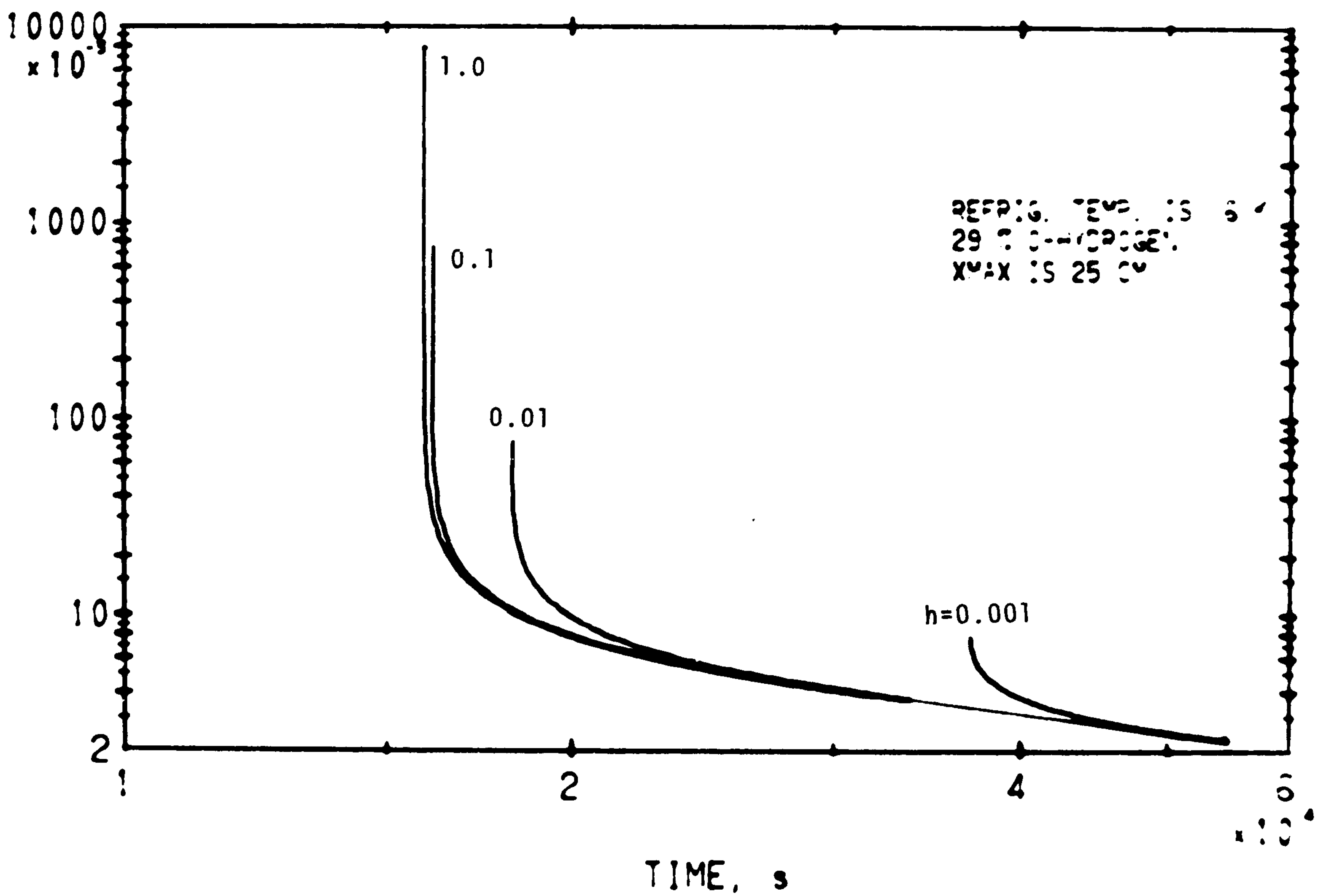

LINEAR FREEZING

01/14/72

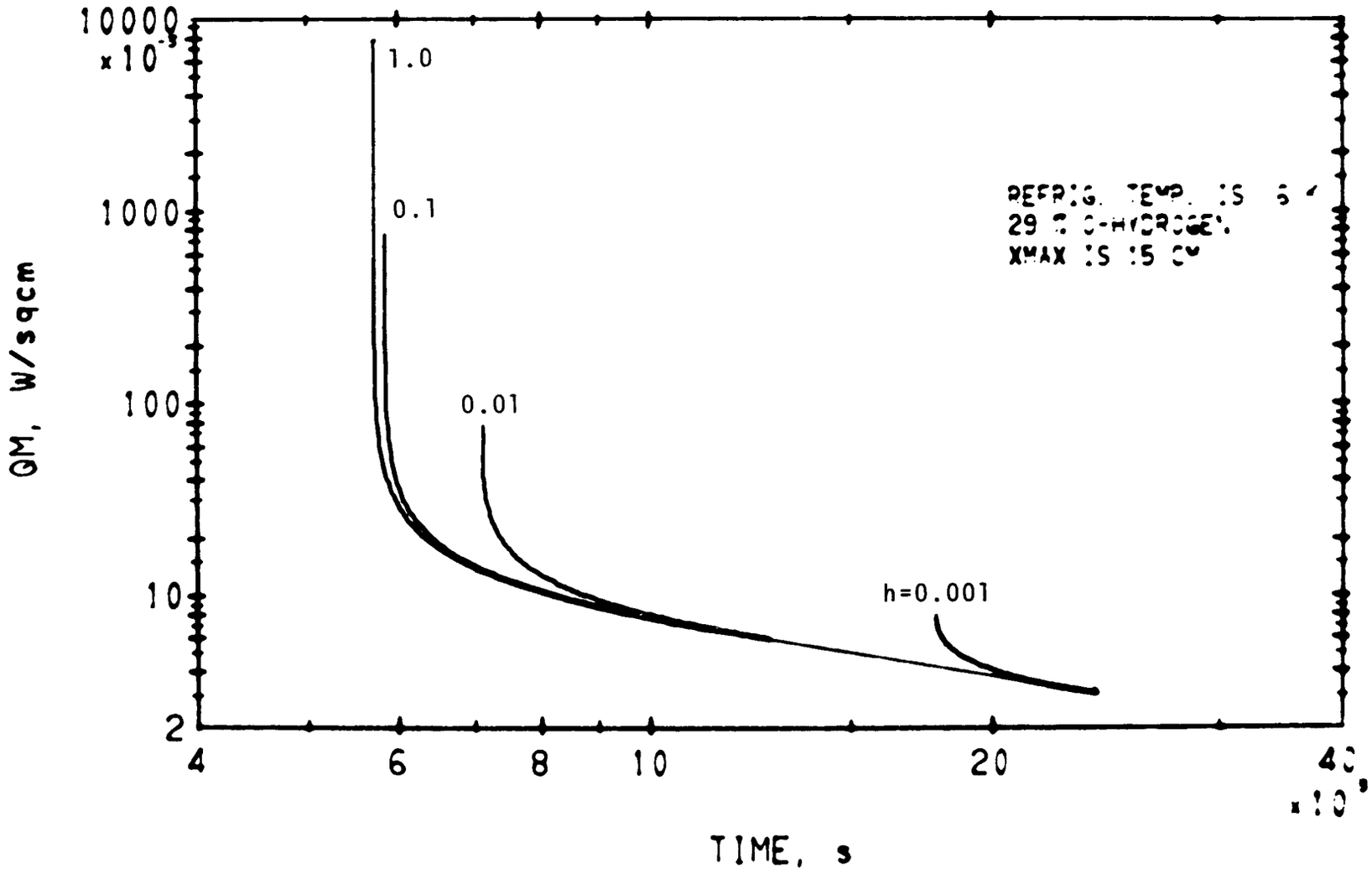

01/16/72

LINEAR FREEZING

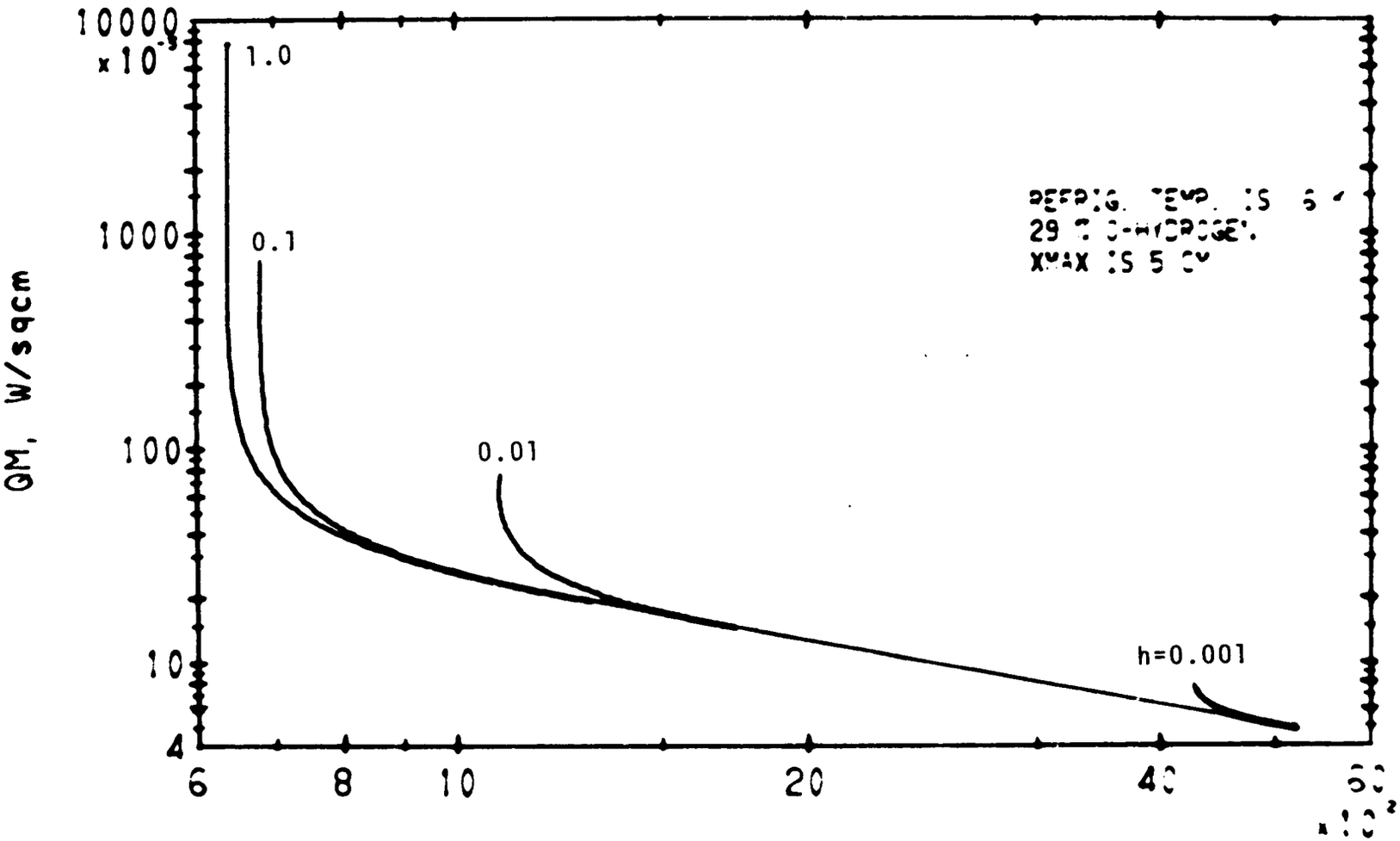

01/16/72

LINEAR FREEZING

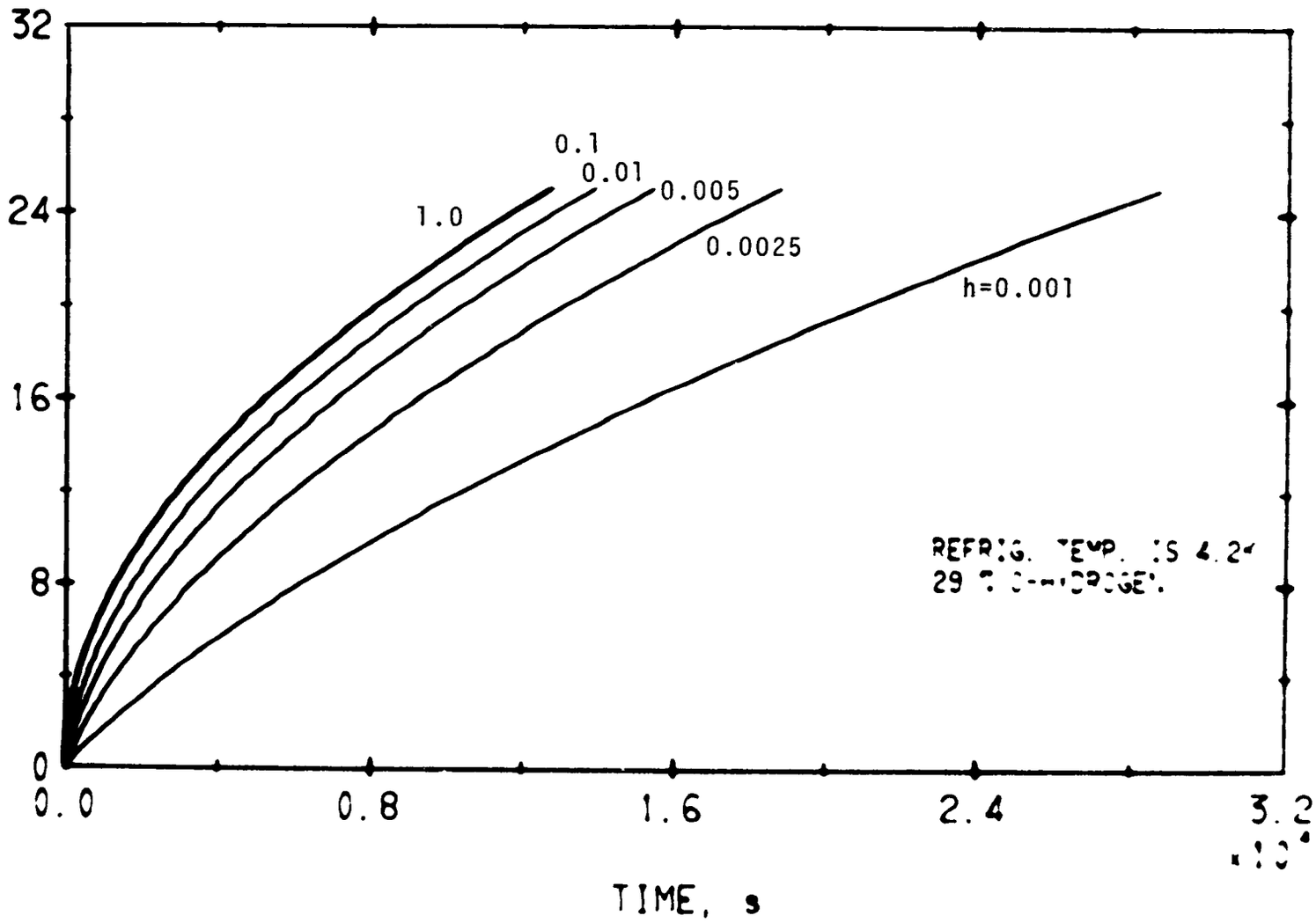

01/14/72

LINEAR FREEZING

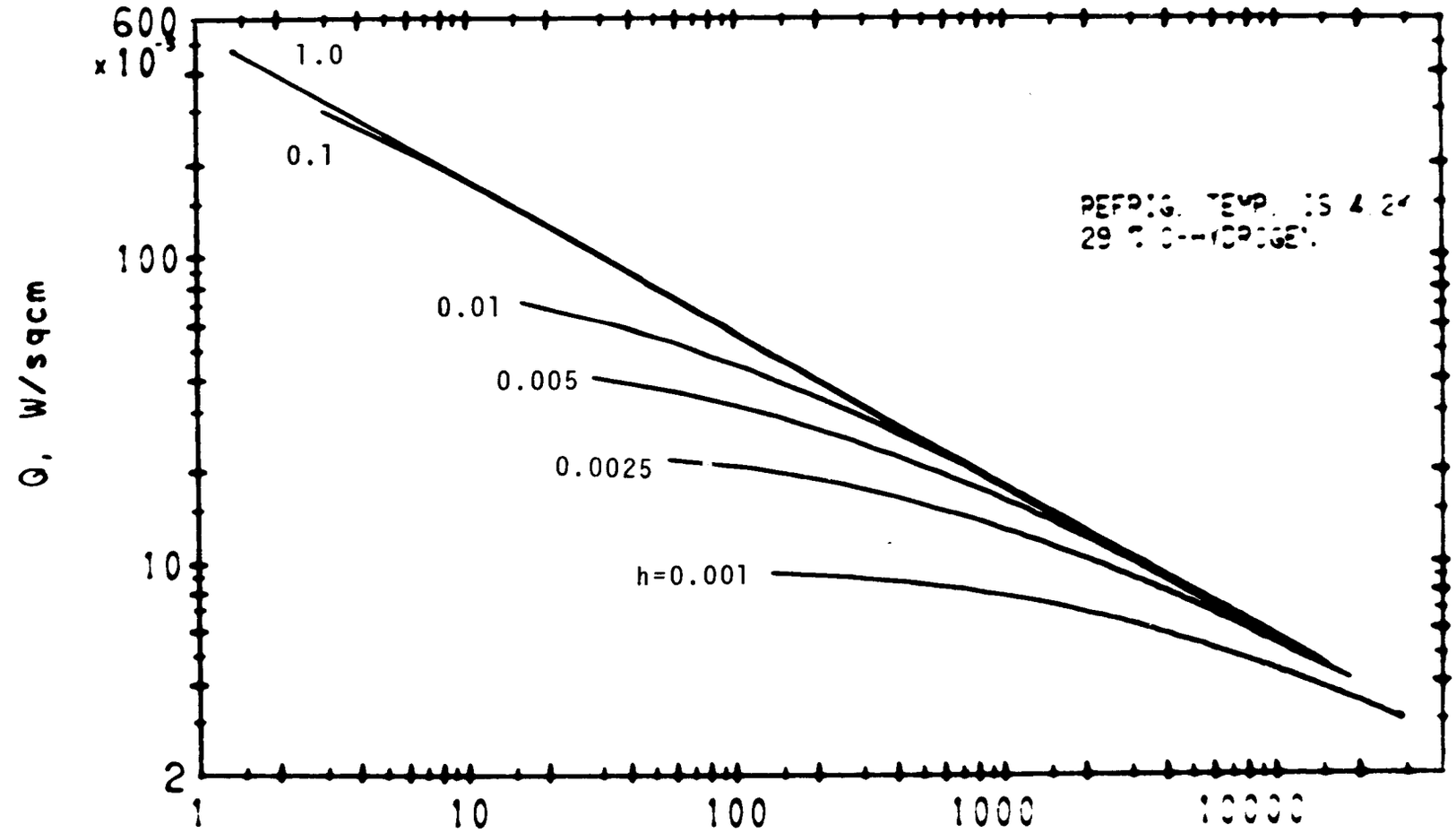

01/14/72

LINEAR FREEZING

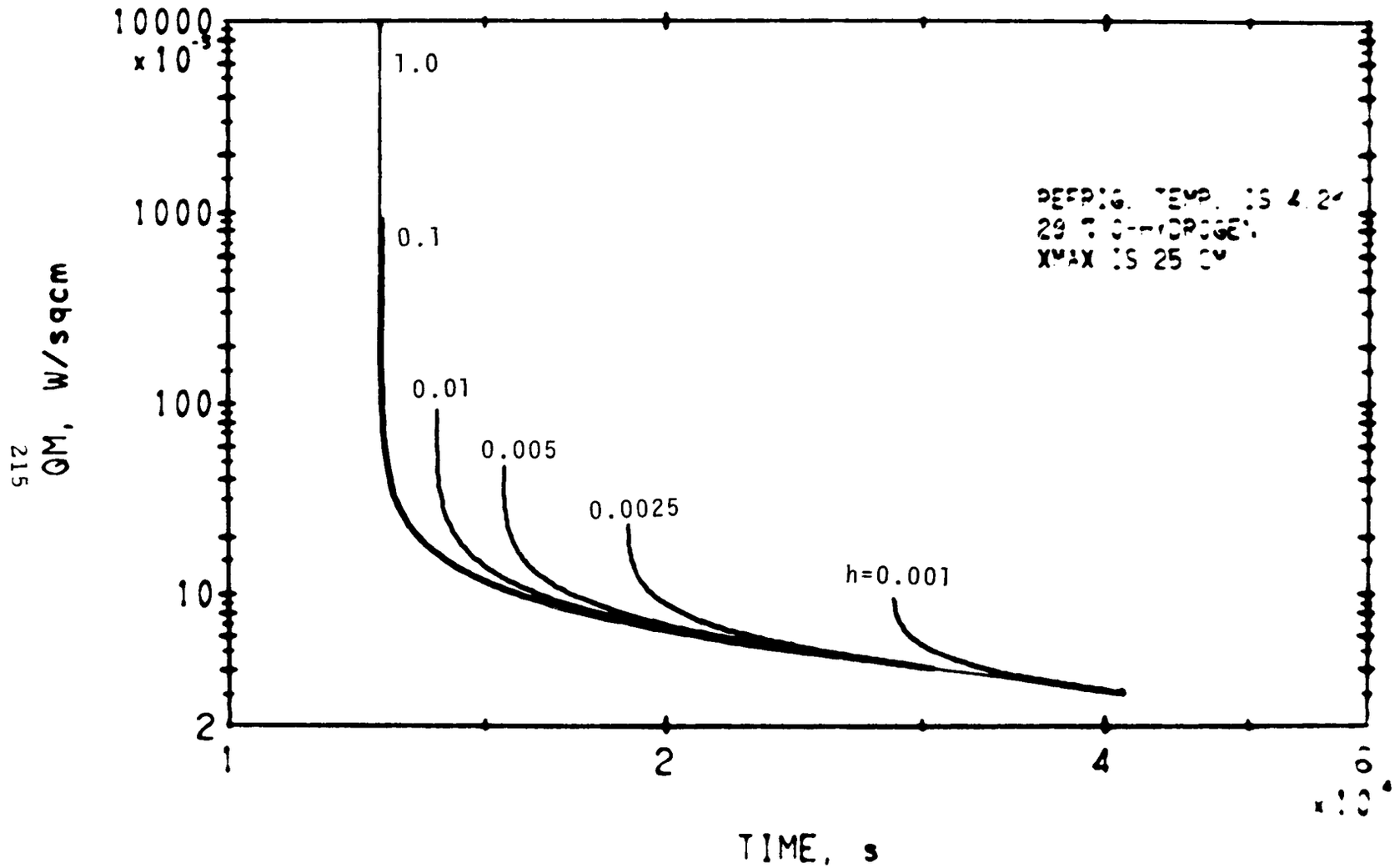

215

01/14/72

LINEAR FREEZING

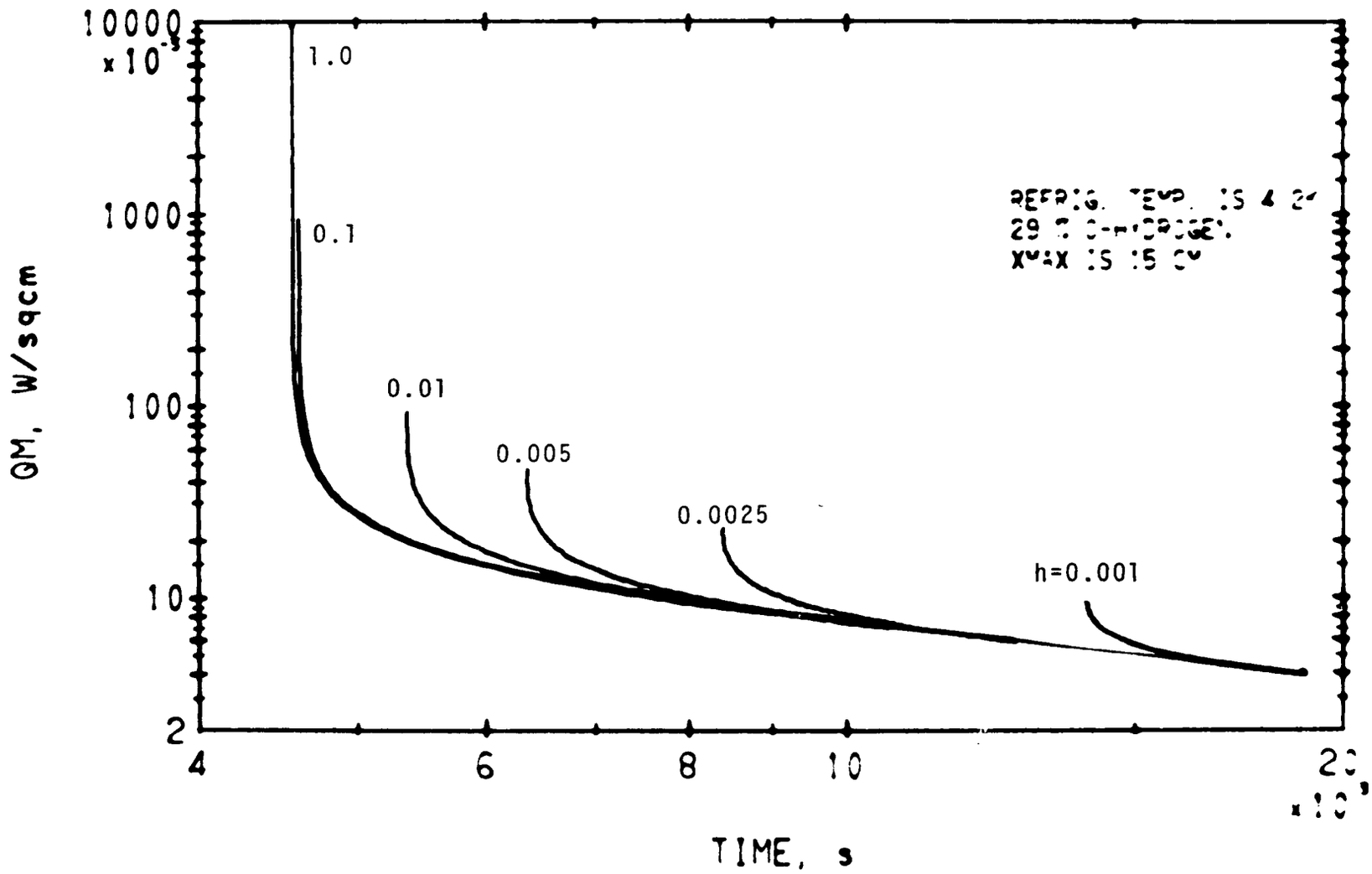

216

01/16/72

LINEAR FREEZING

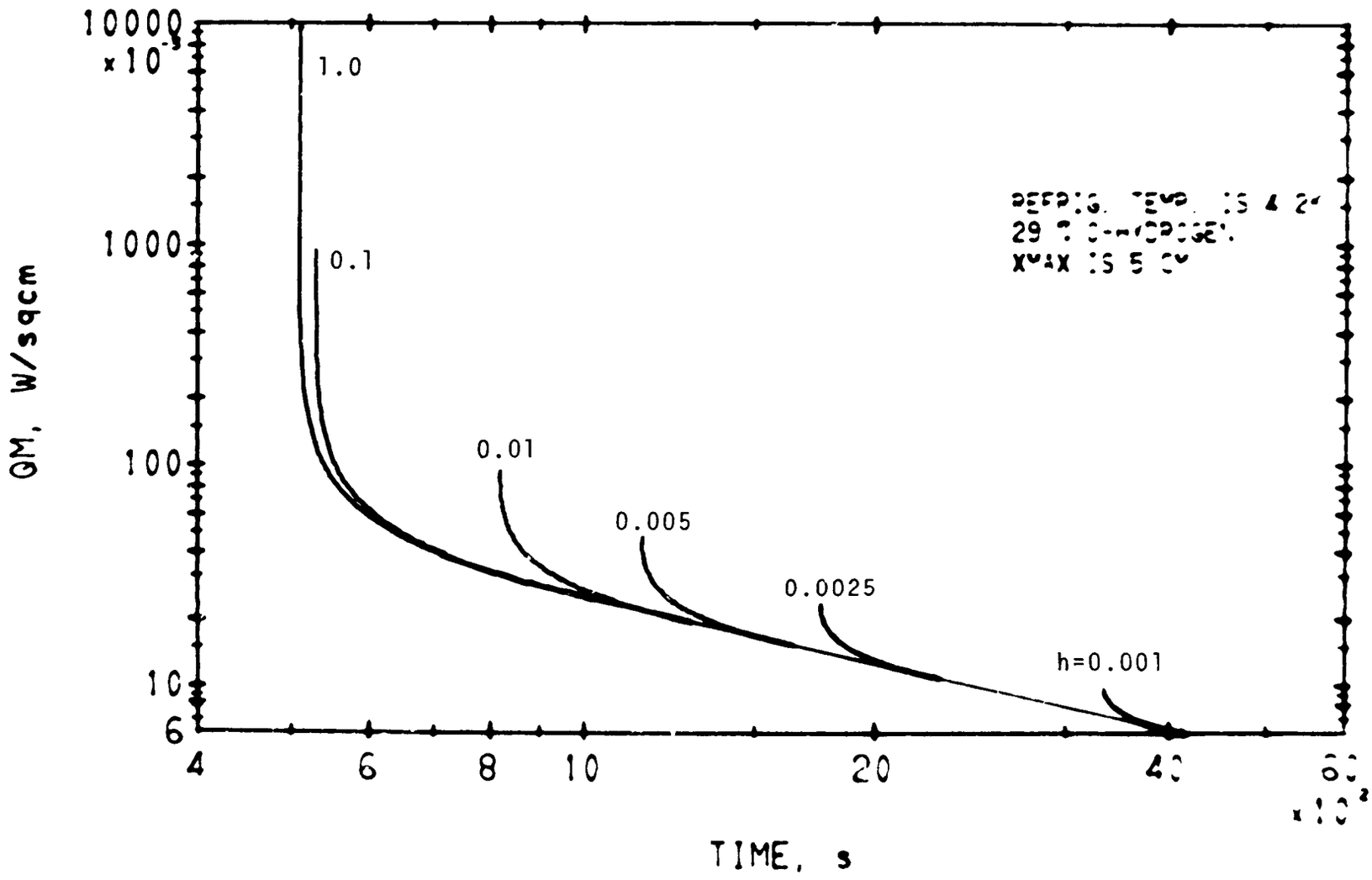

217

01/16/72

LINEAR FREEZING

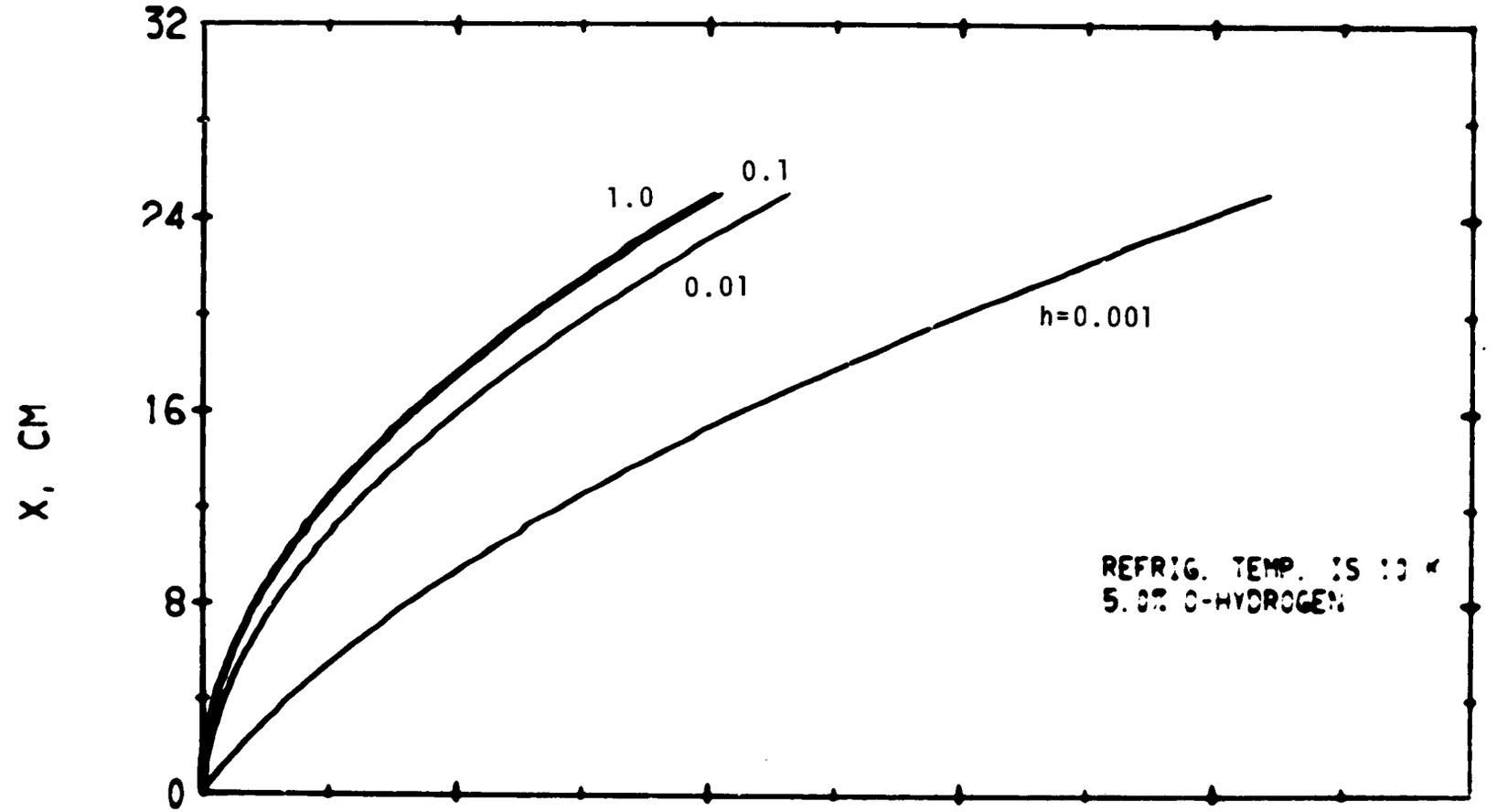

01/12/72

LINEAR FREEZING

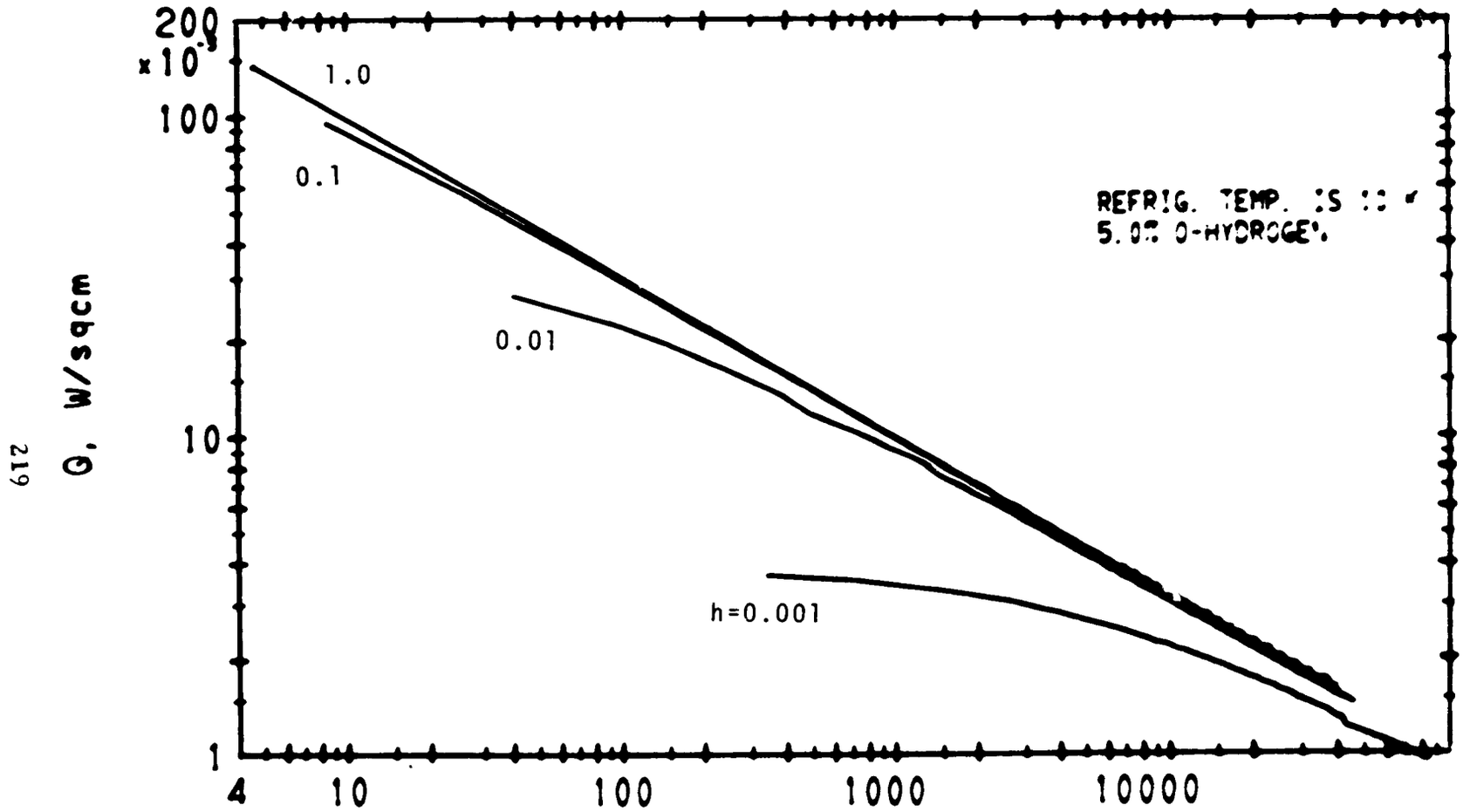

612

01/12/72

LINEAR FREEZING

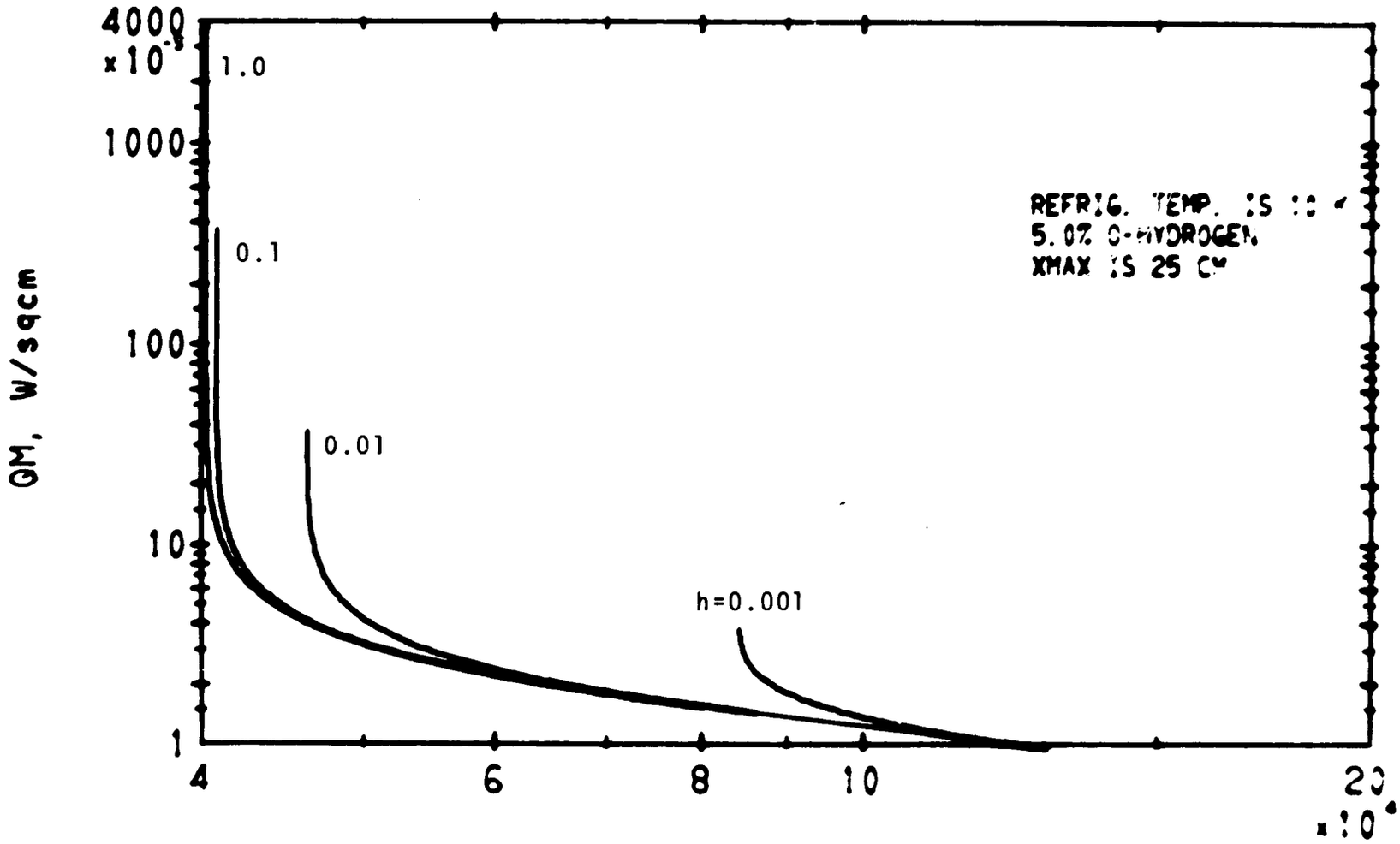

220

01/18/72

LINEAR FREEZING

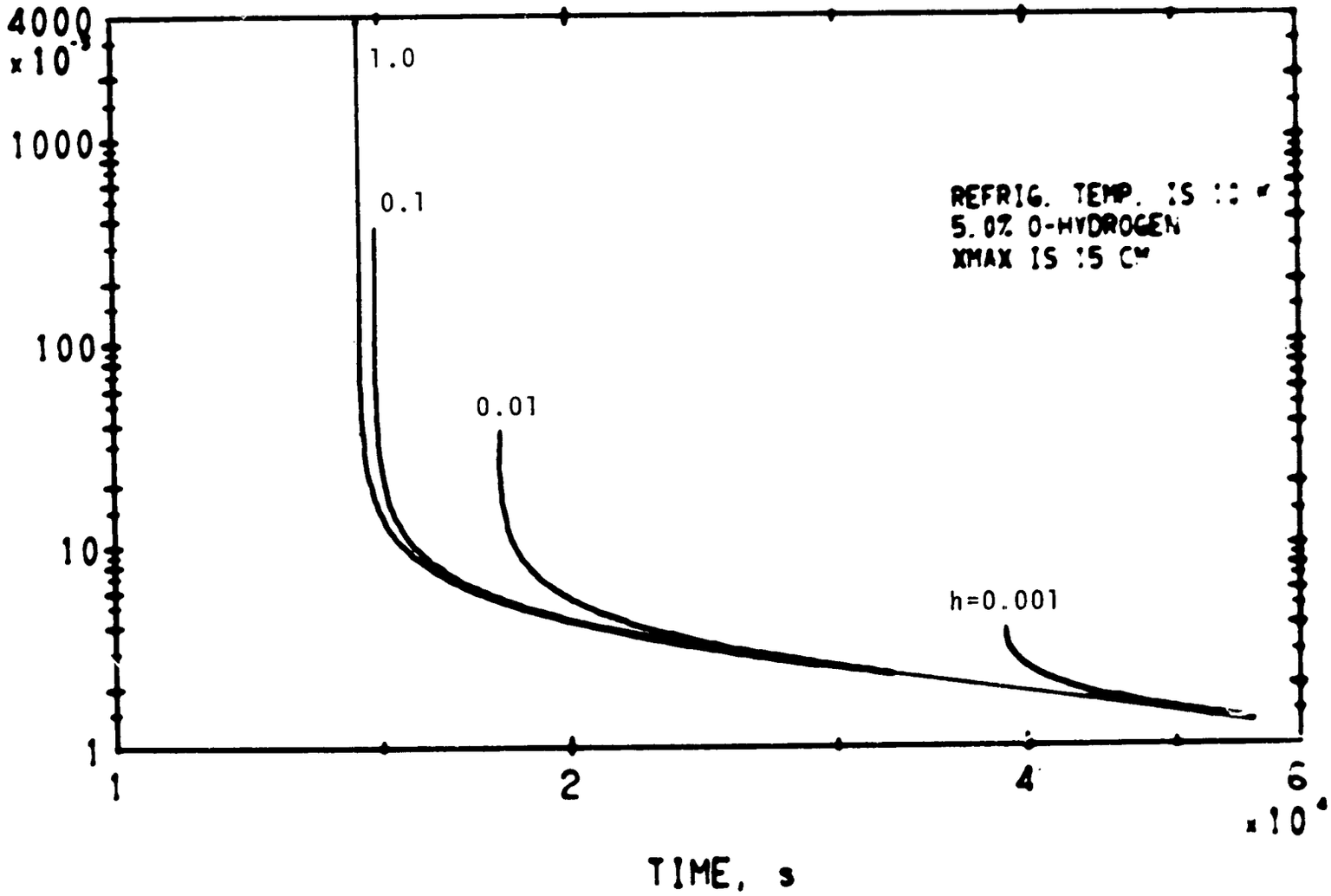

01/12/72

LINEAR FREEZING

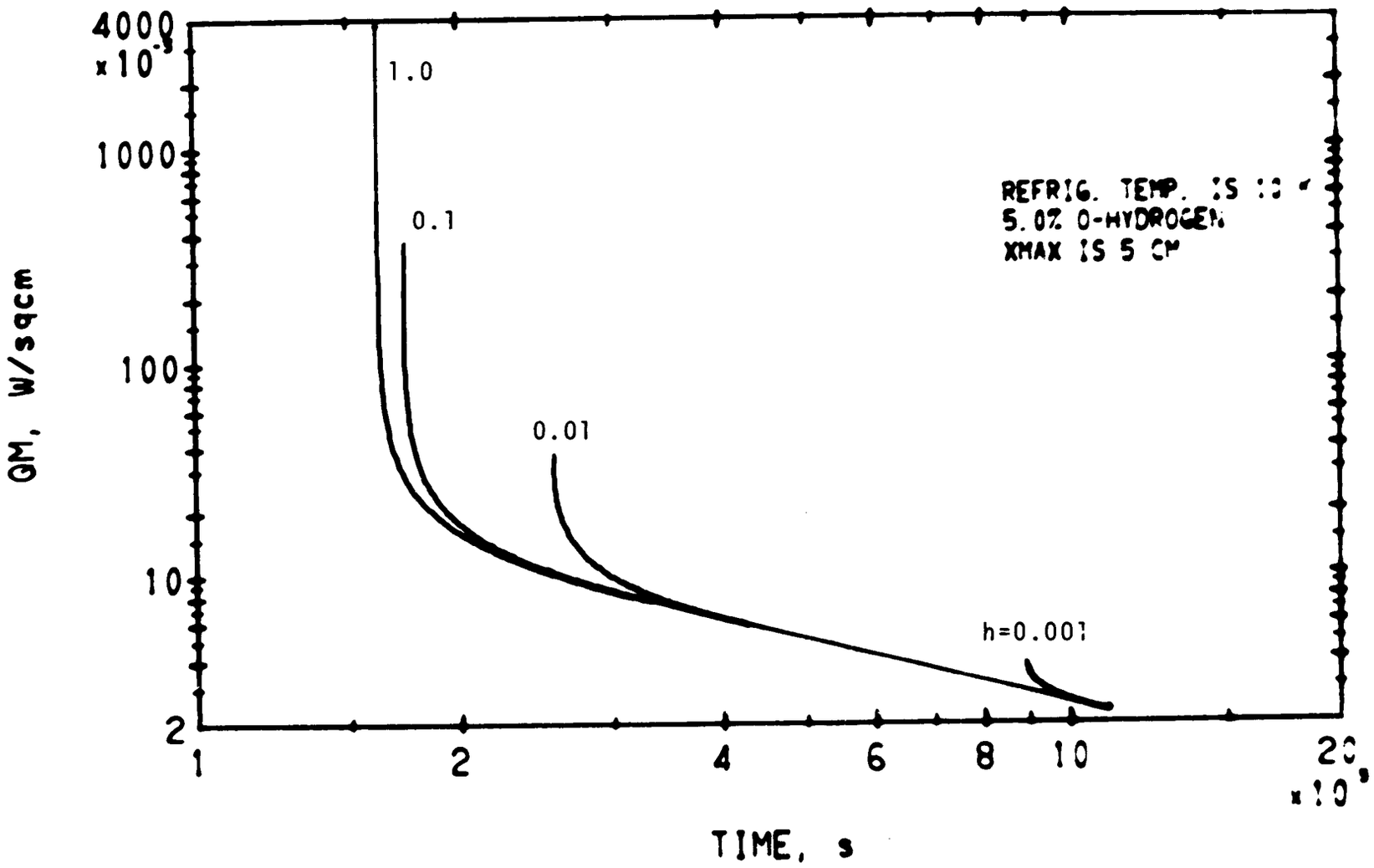

LINEAR FREEZING

01/12/72

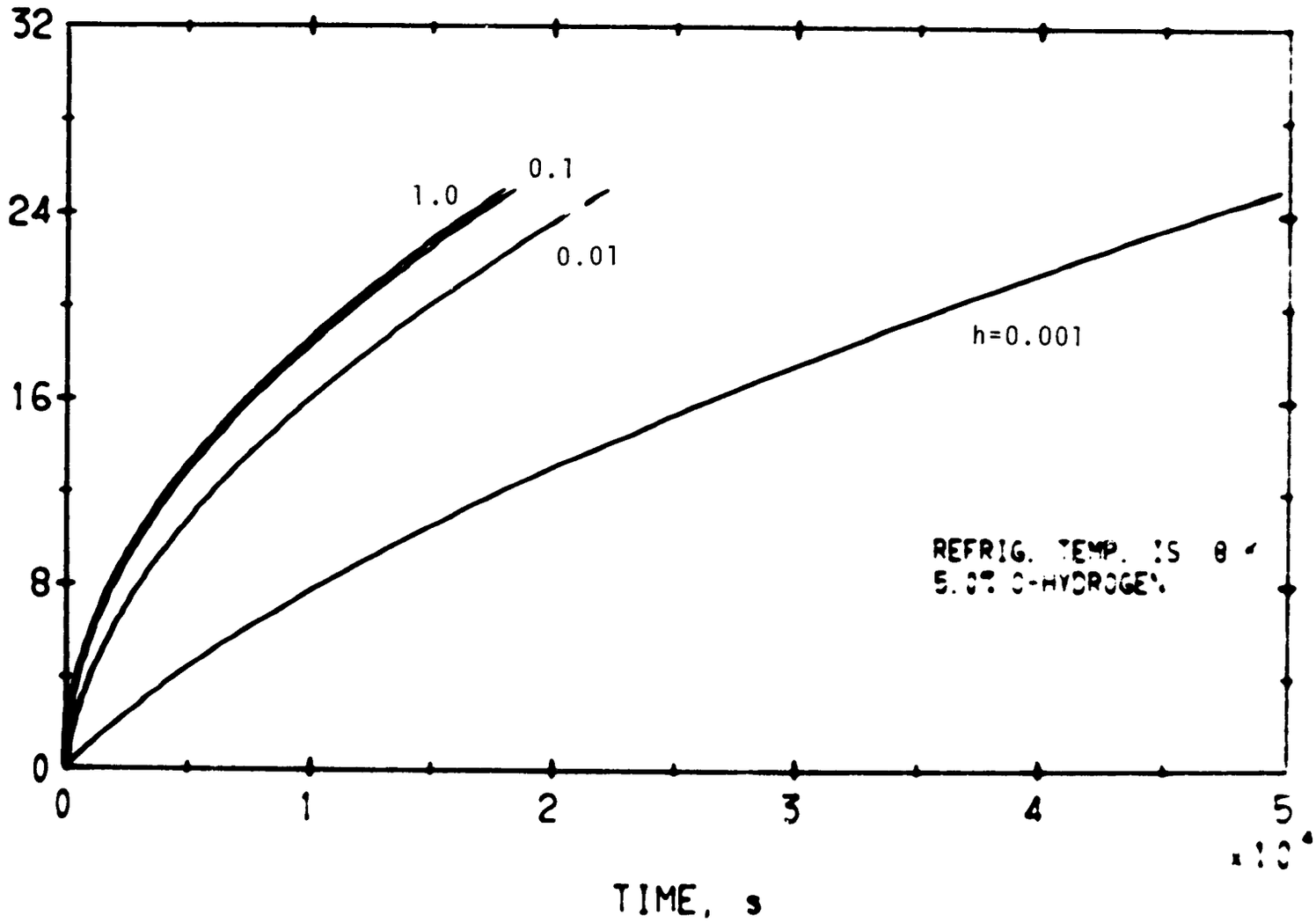

01/12/72

LINEAR FREEZING

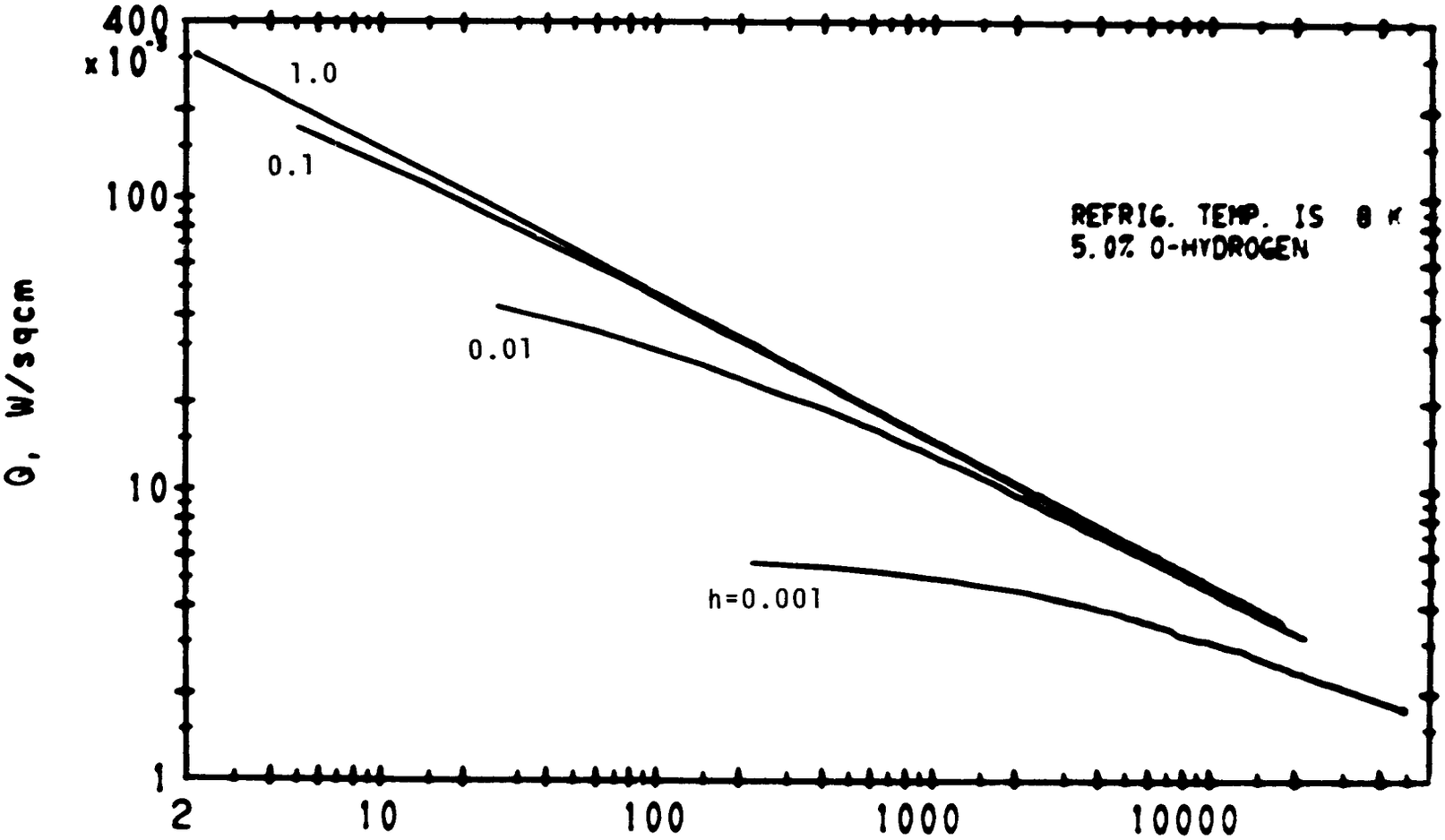

LINEAR FREEZING

01/18/72

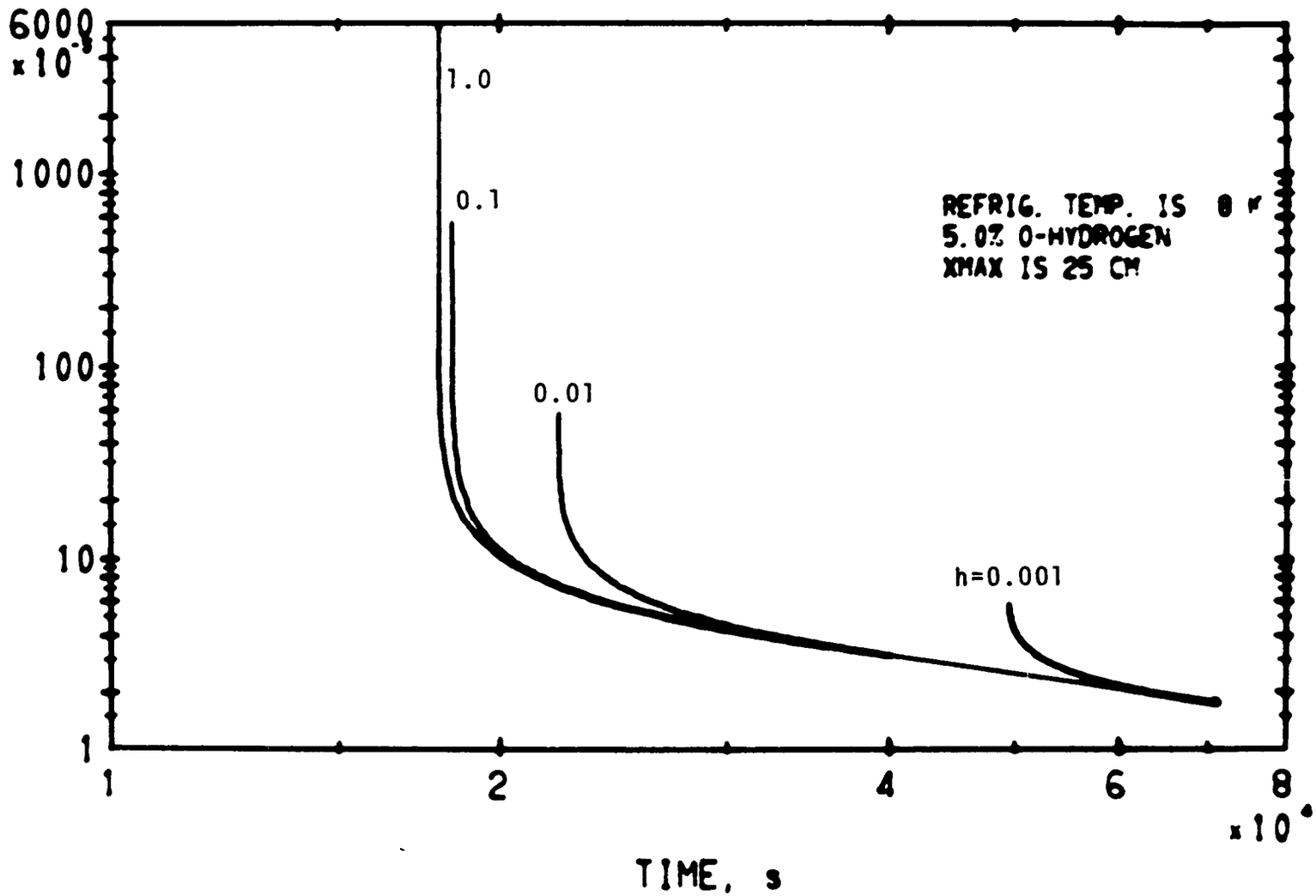

01/12/72

LINEAR FREEZING

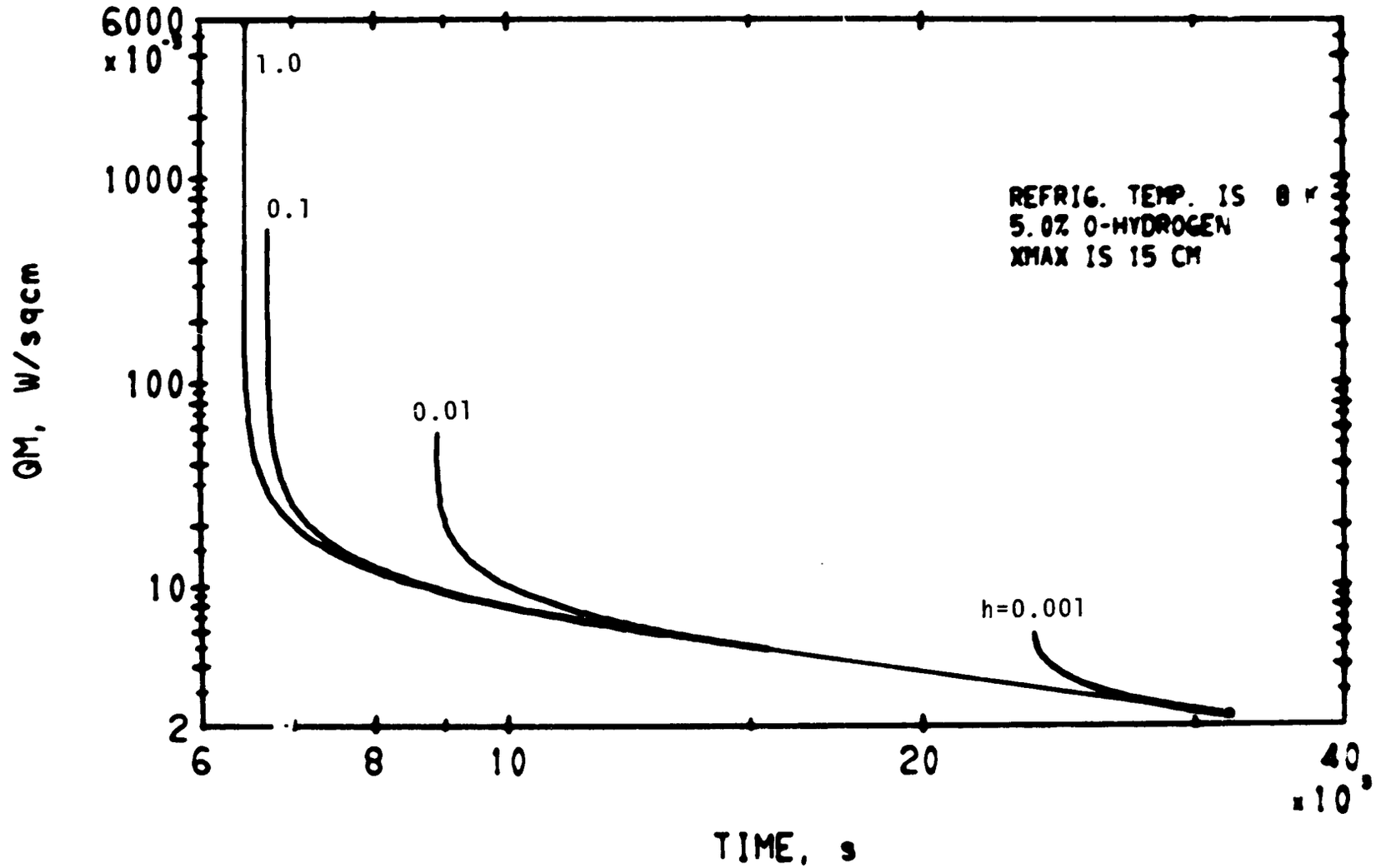

01/12/78

LINEAR FREEZING

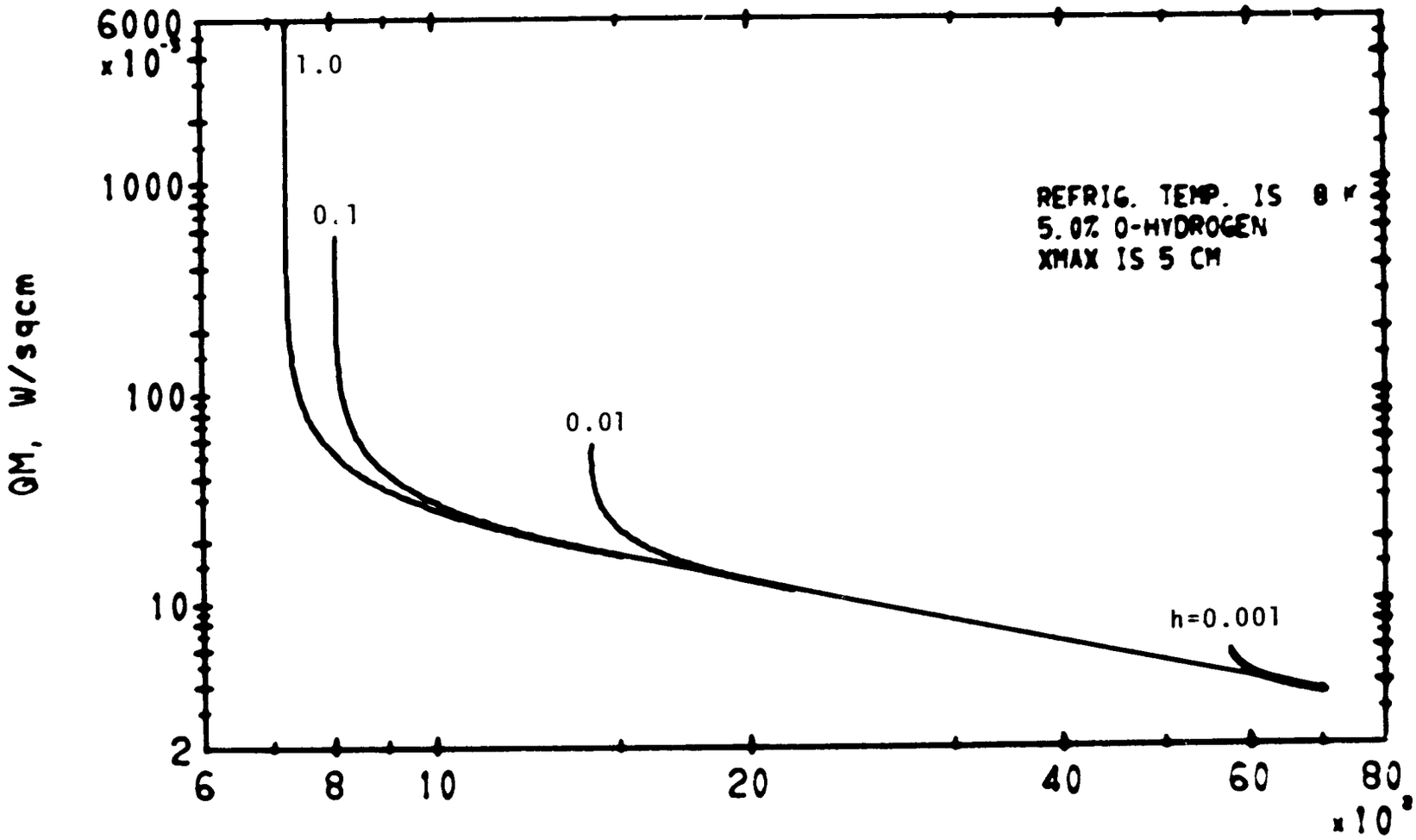

01/12/78

LINEAR FREEZING

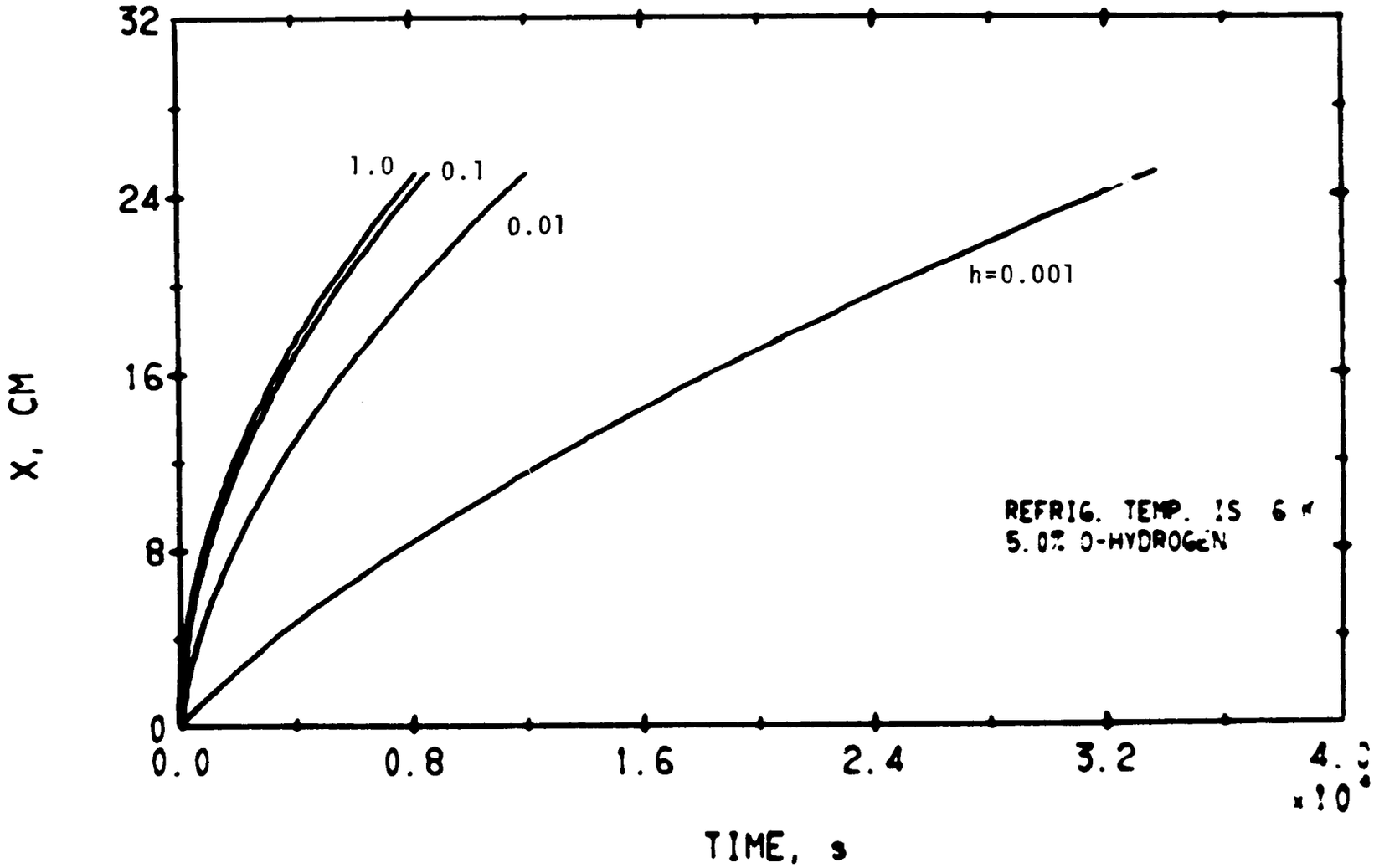

01/12/72

LINEAR FREEZING

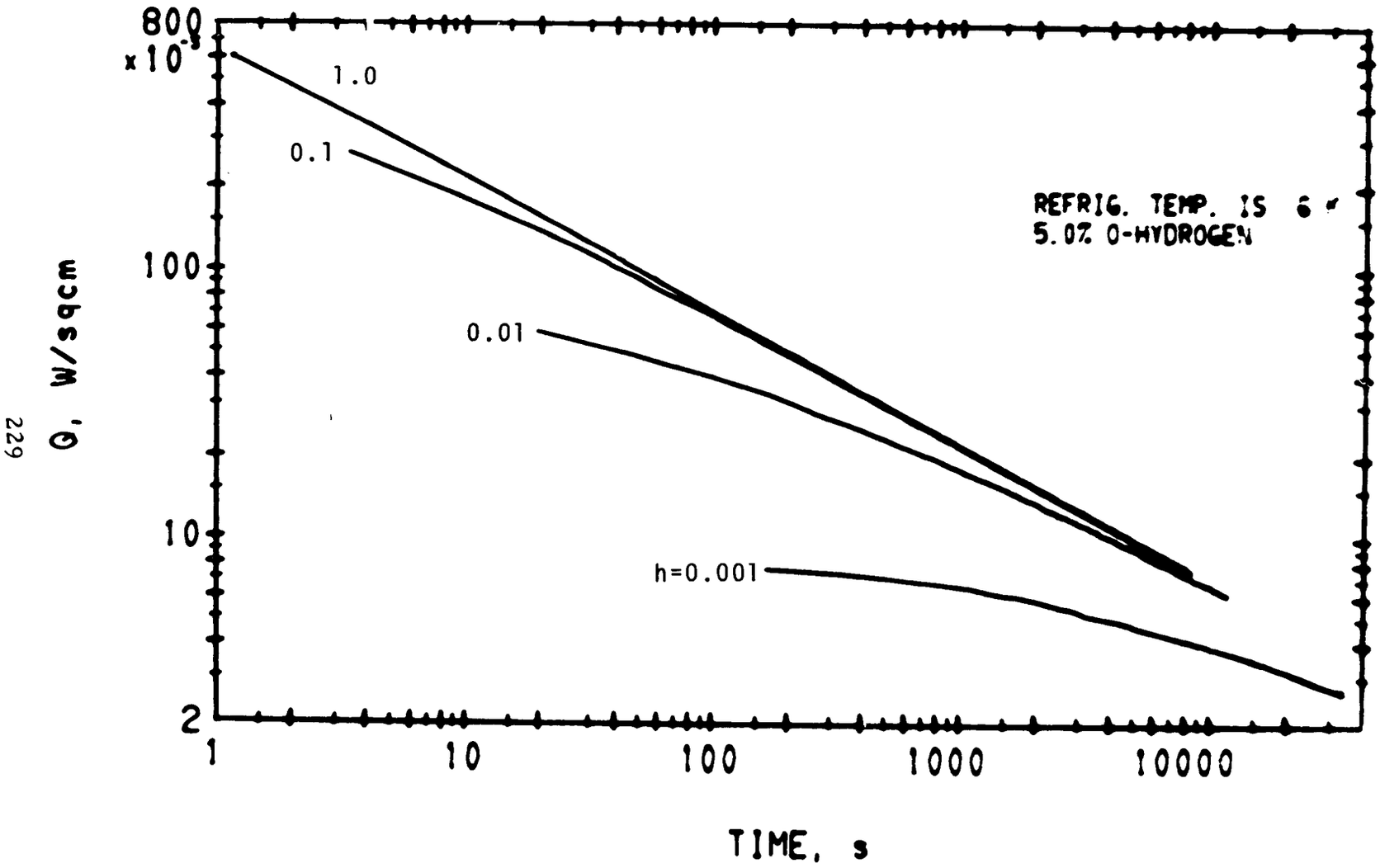

01/12/72

LINEAR FREEZING

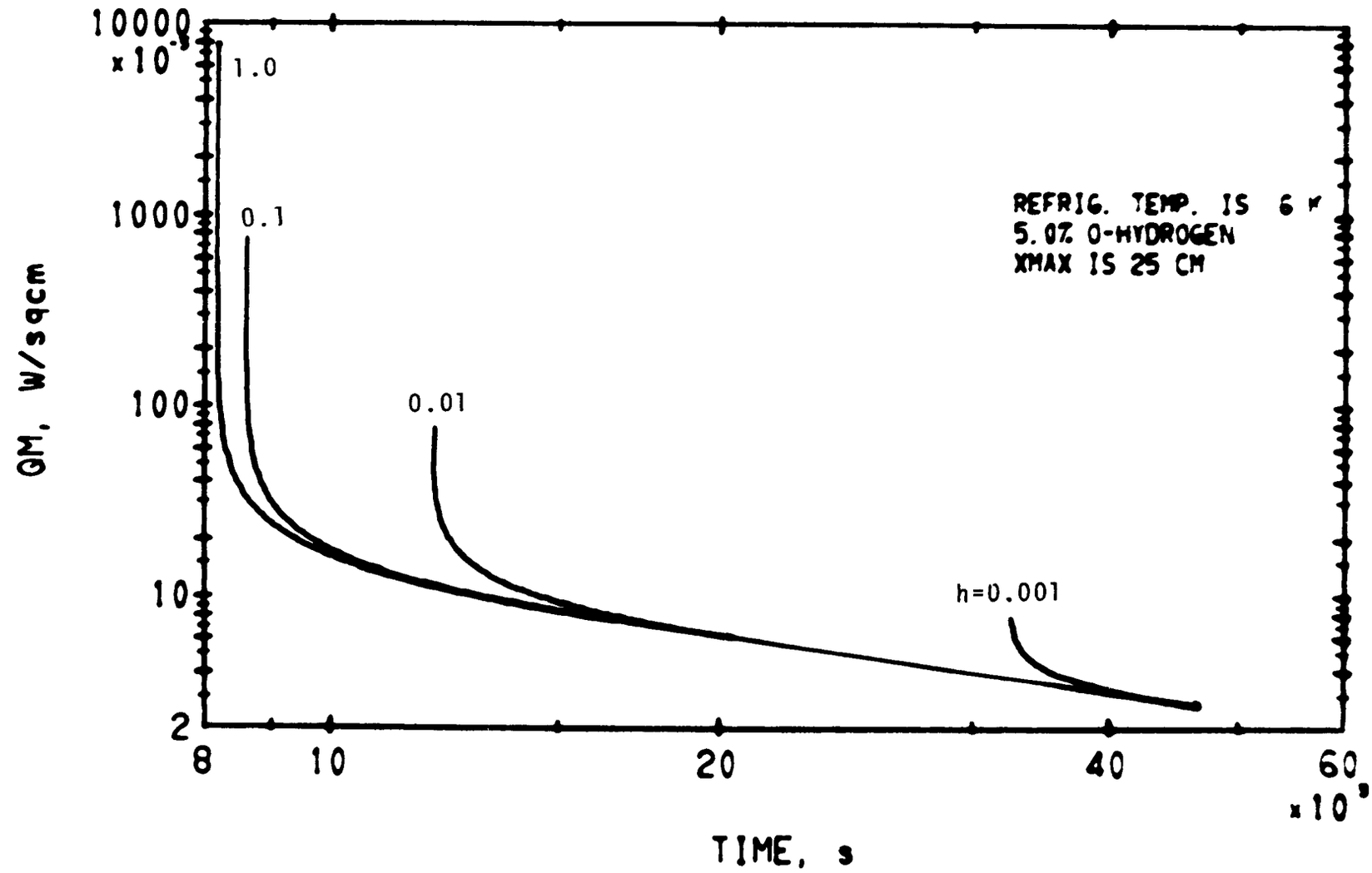

01/18/78

LINEAR FREEZING

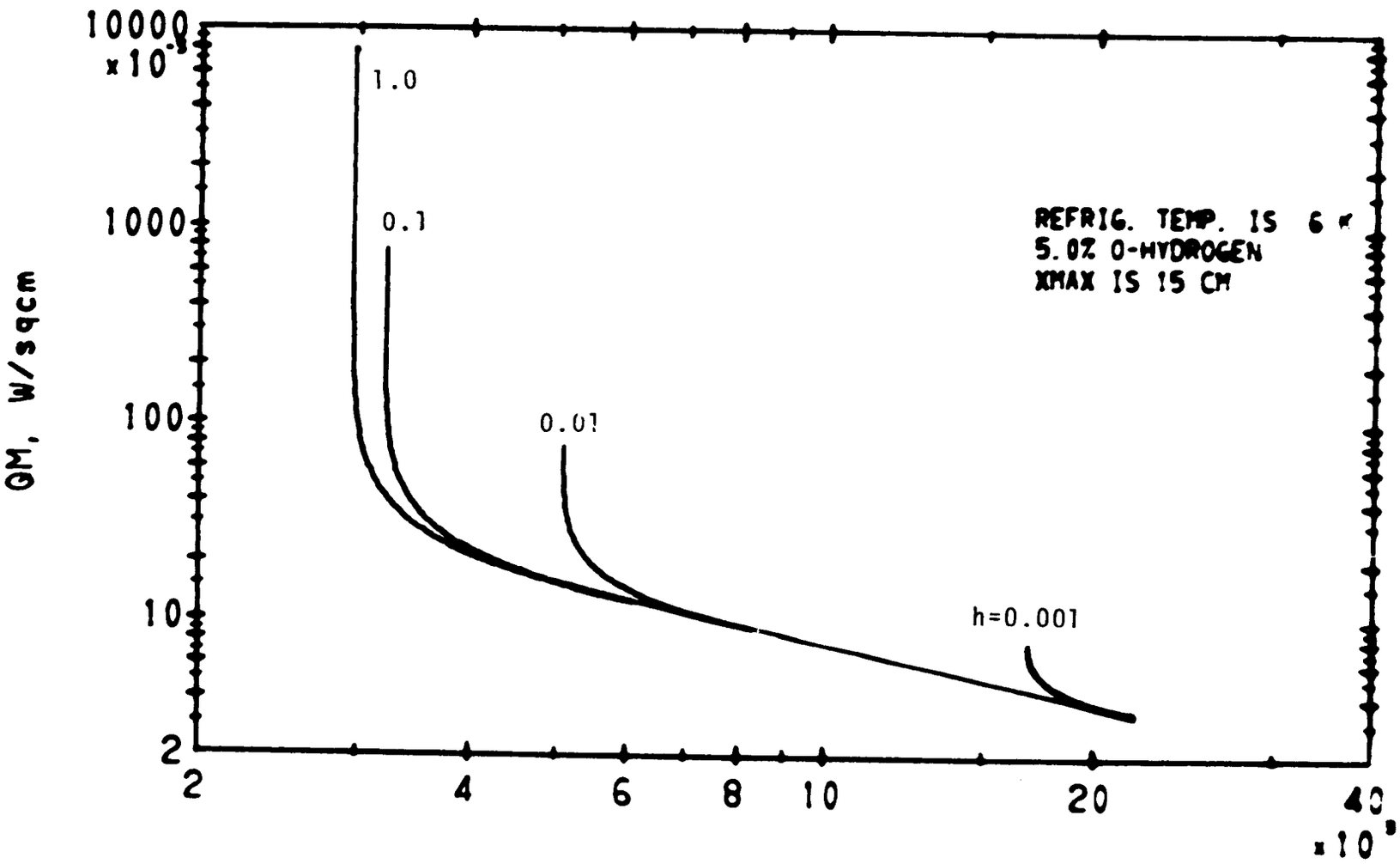

01/12/78

LINEAR FREEZING

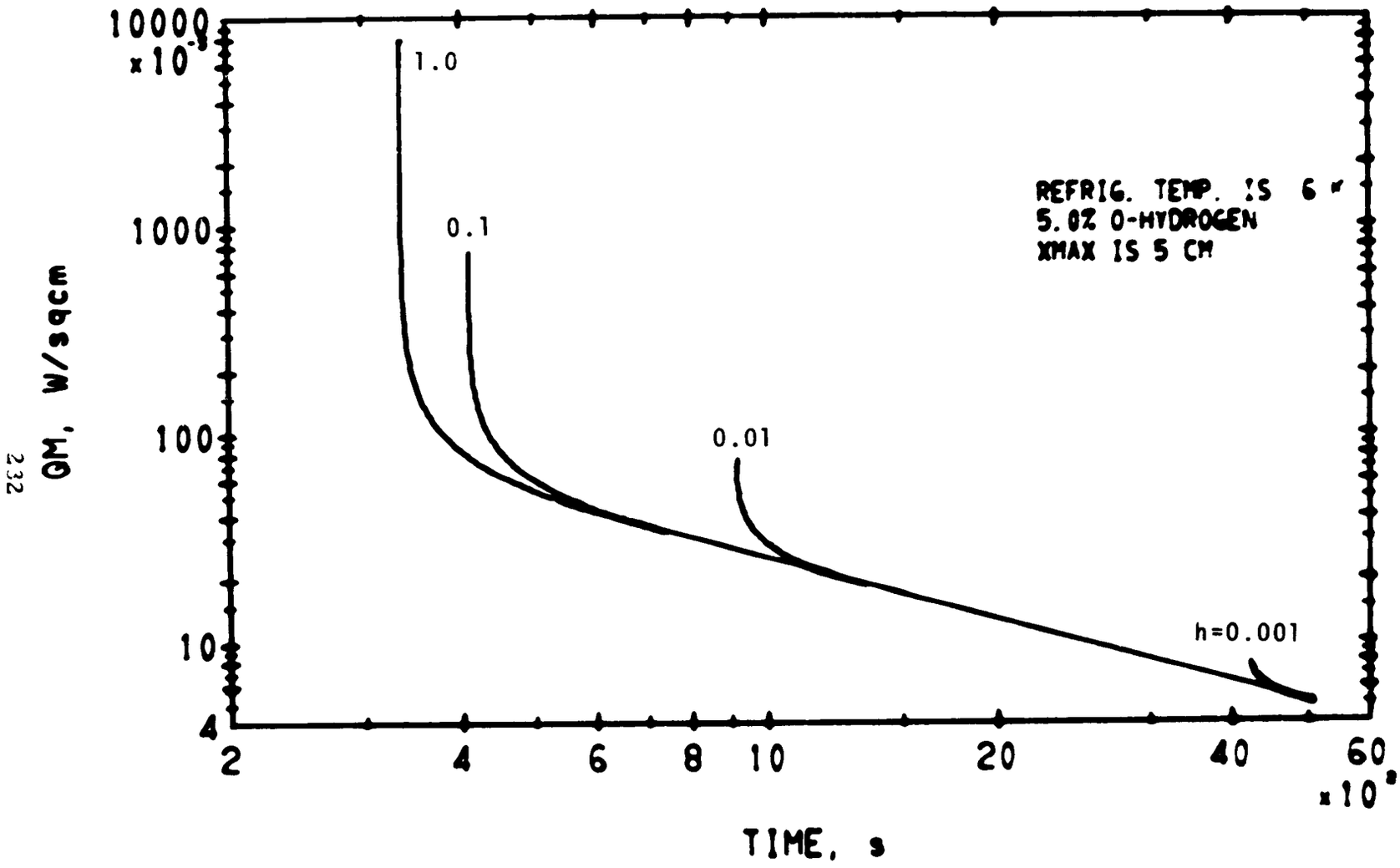

01/12/78

LINEAR FREEZING

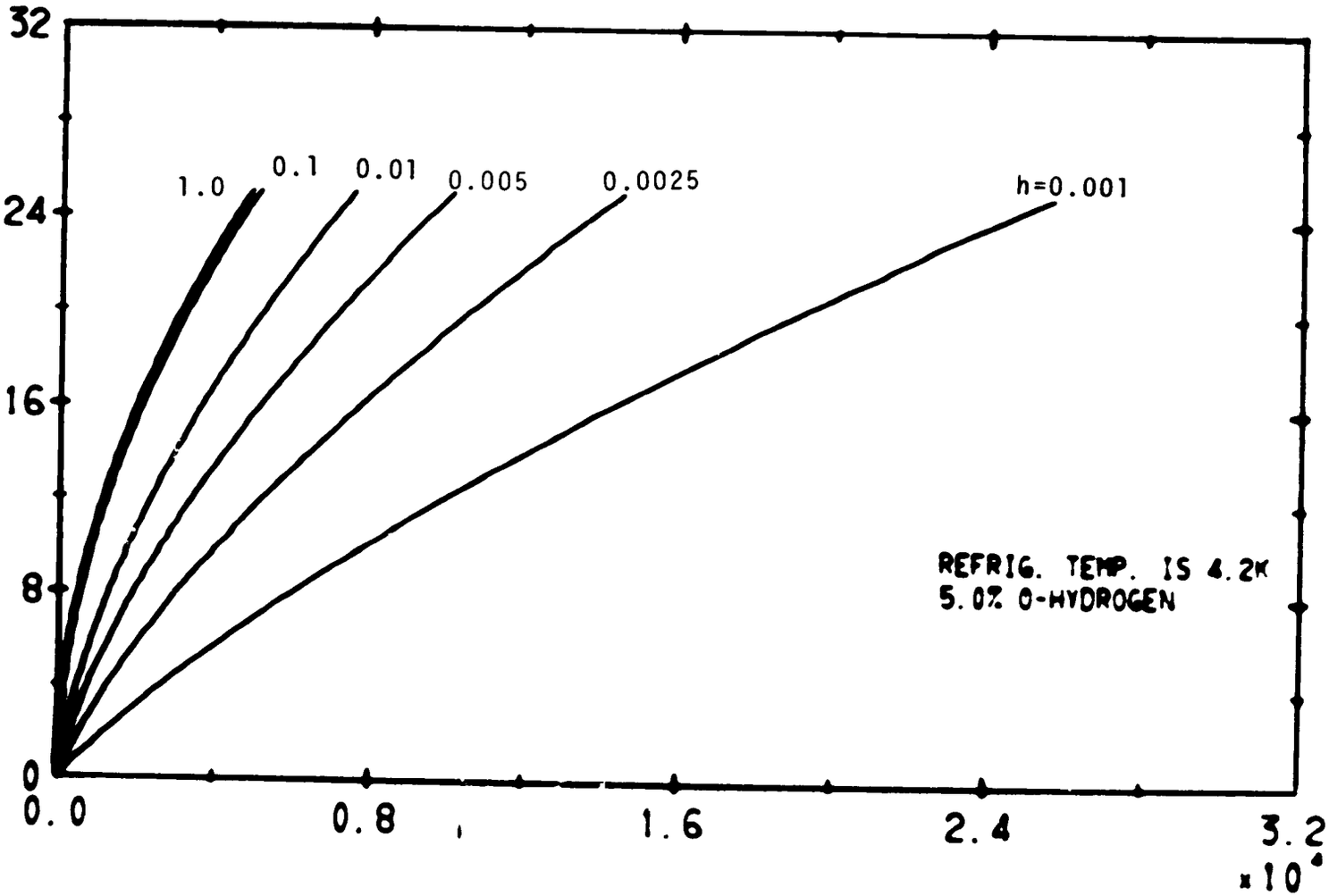

01/12/72

LINEAR FREEZING

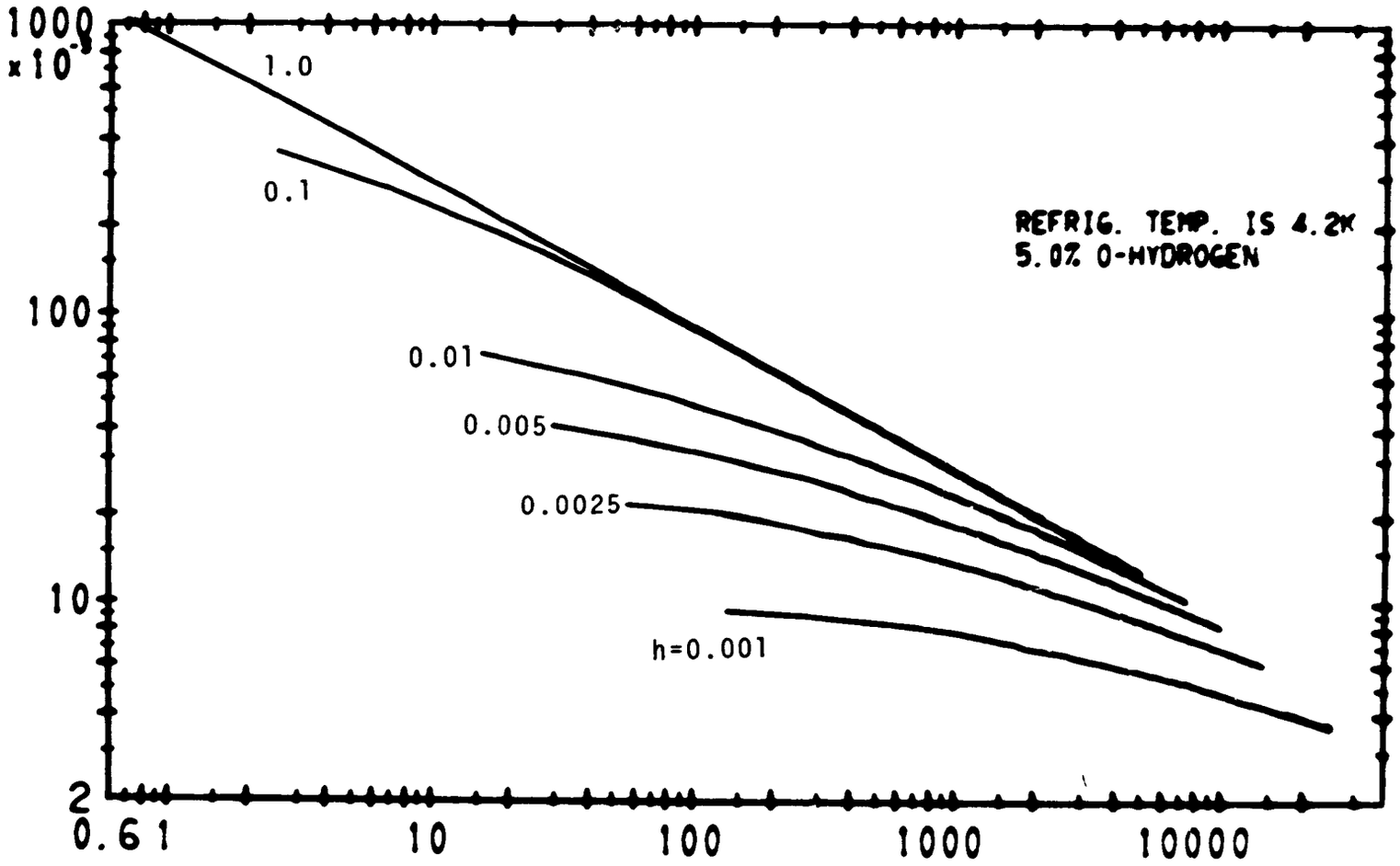

01/12/72

LINEAR FREEZING

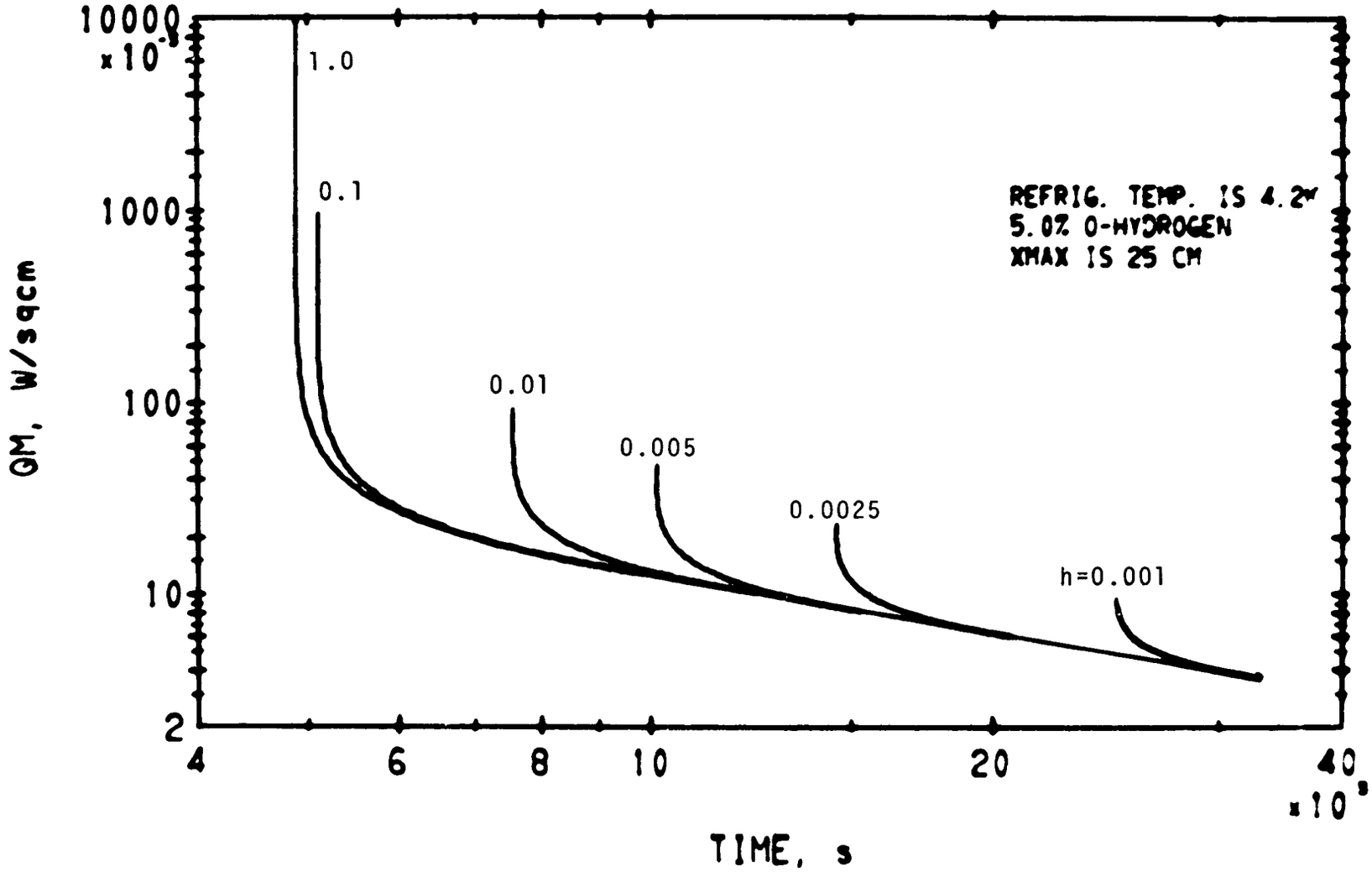

01/12/72

LINEAR FREEZING

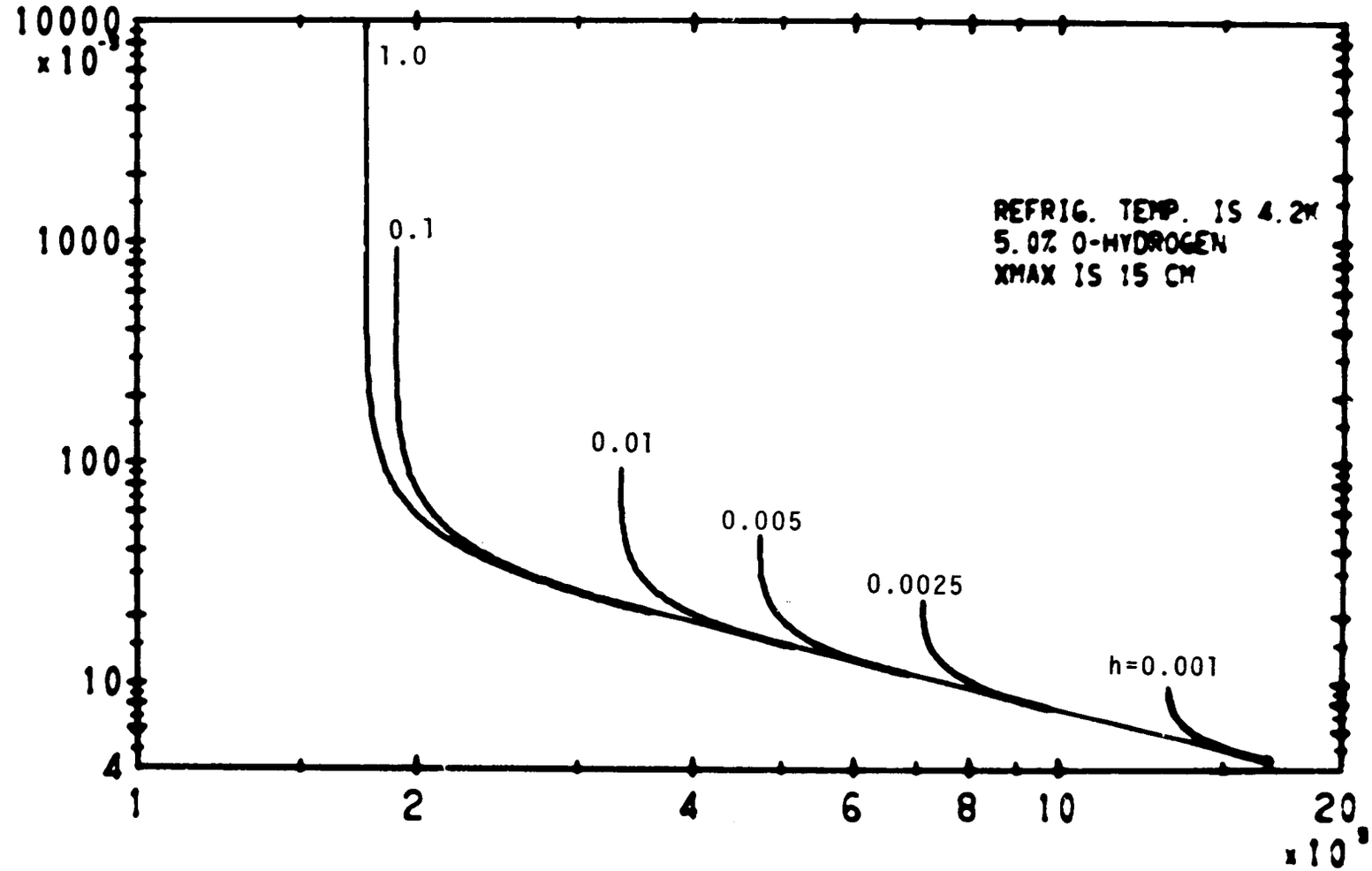

01/12/72

LINEAR FREEZING

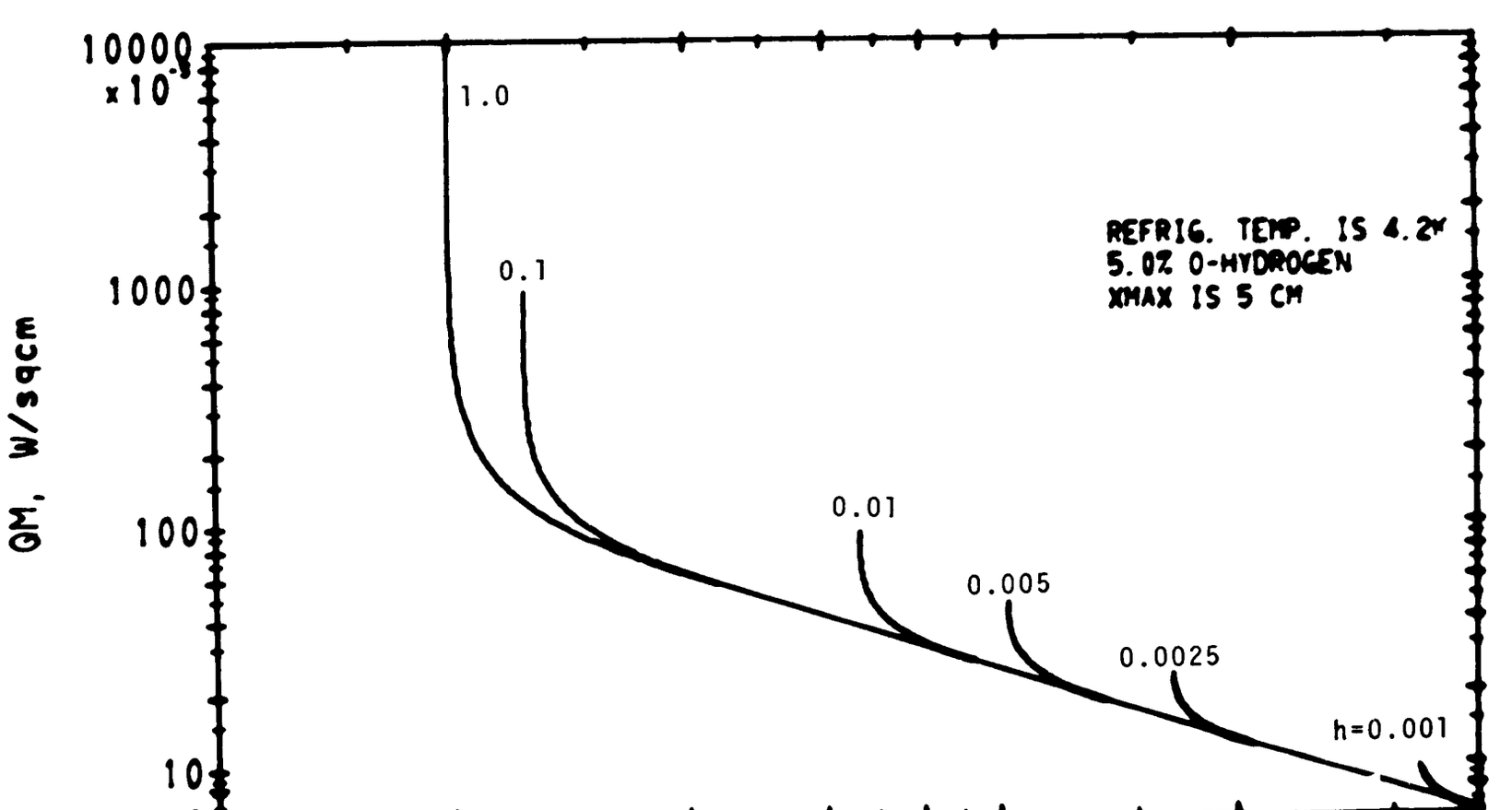

01/12/72

LINEAR FREEZING

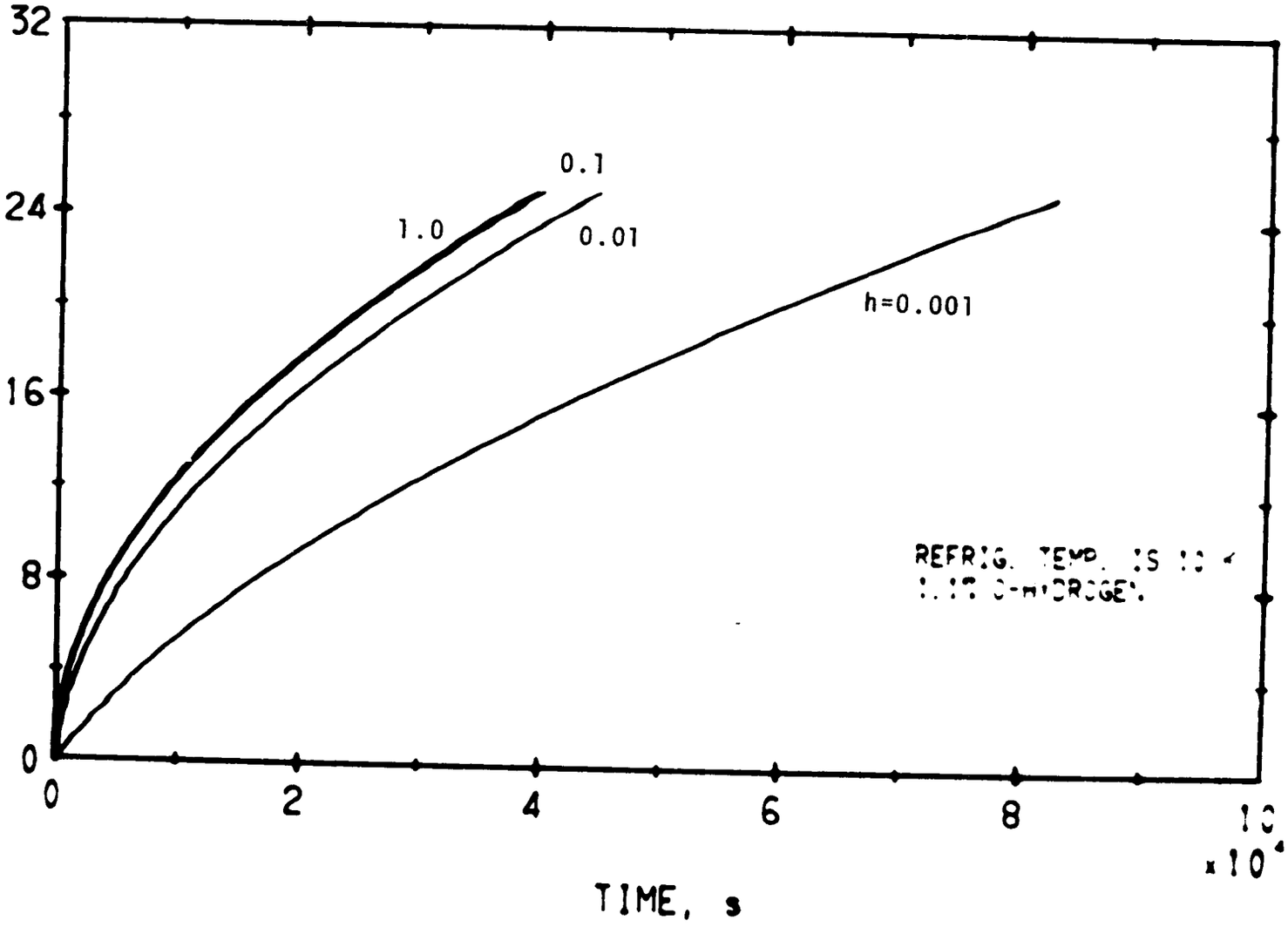

61/11/72

LINEAR FREEZING

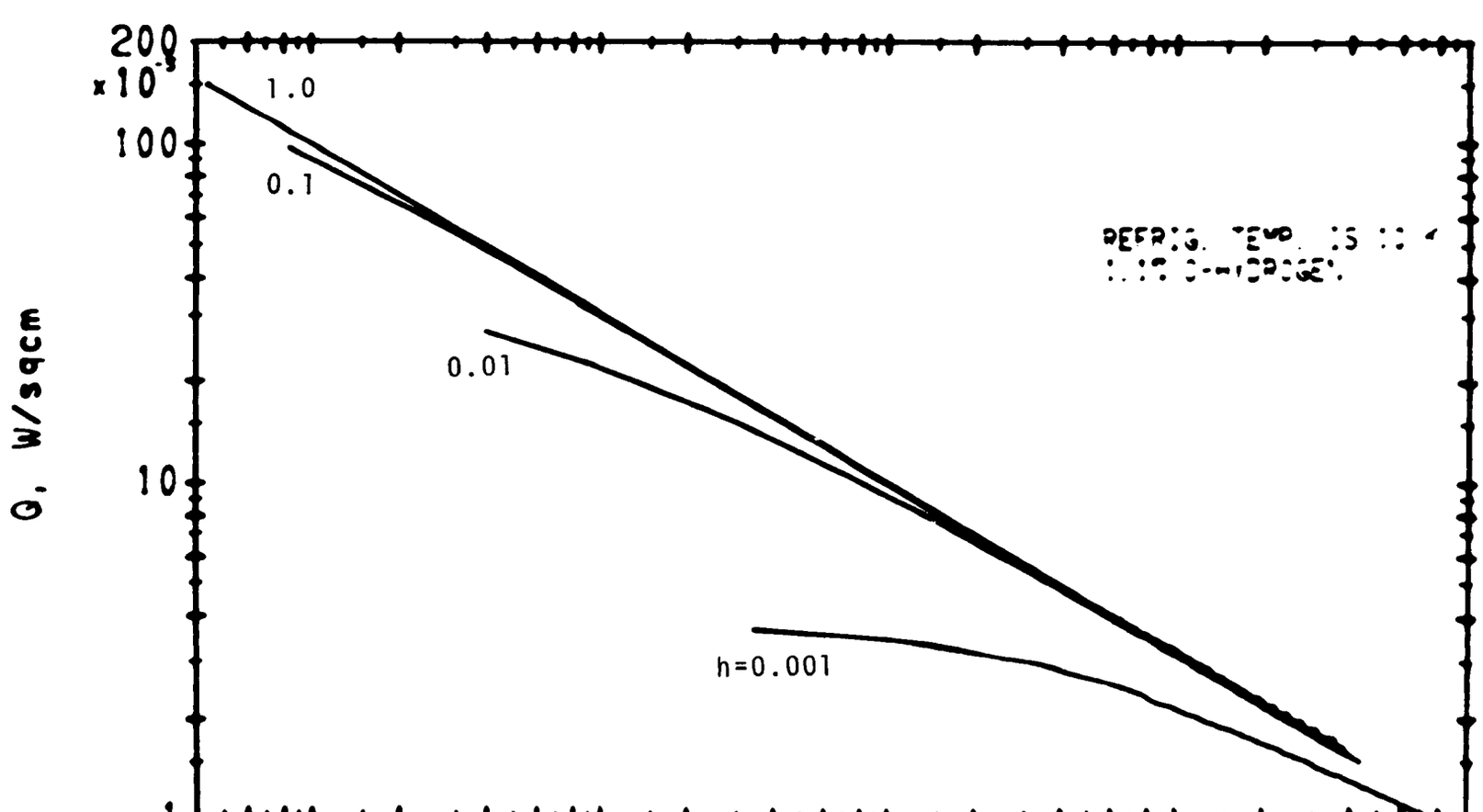

01/11/72

LINEAR FREEZING

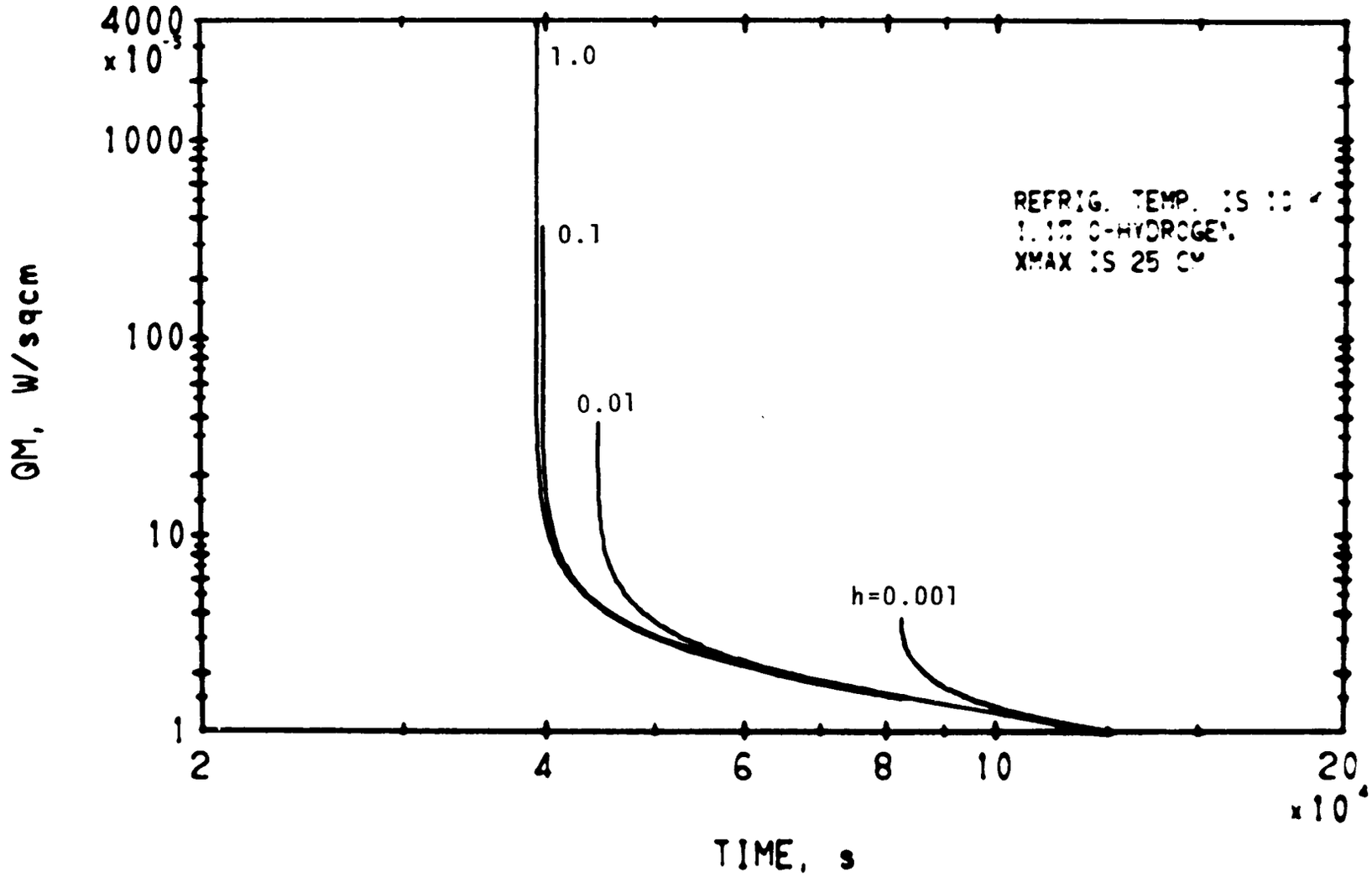

01/11/72

LINEAR FREEZING

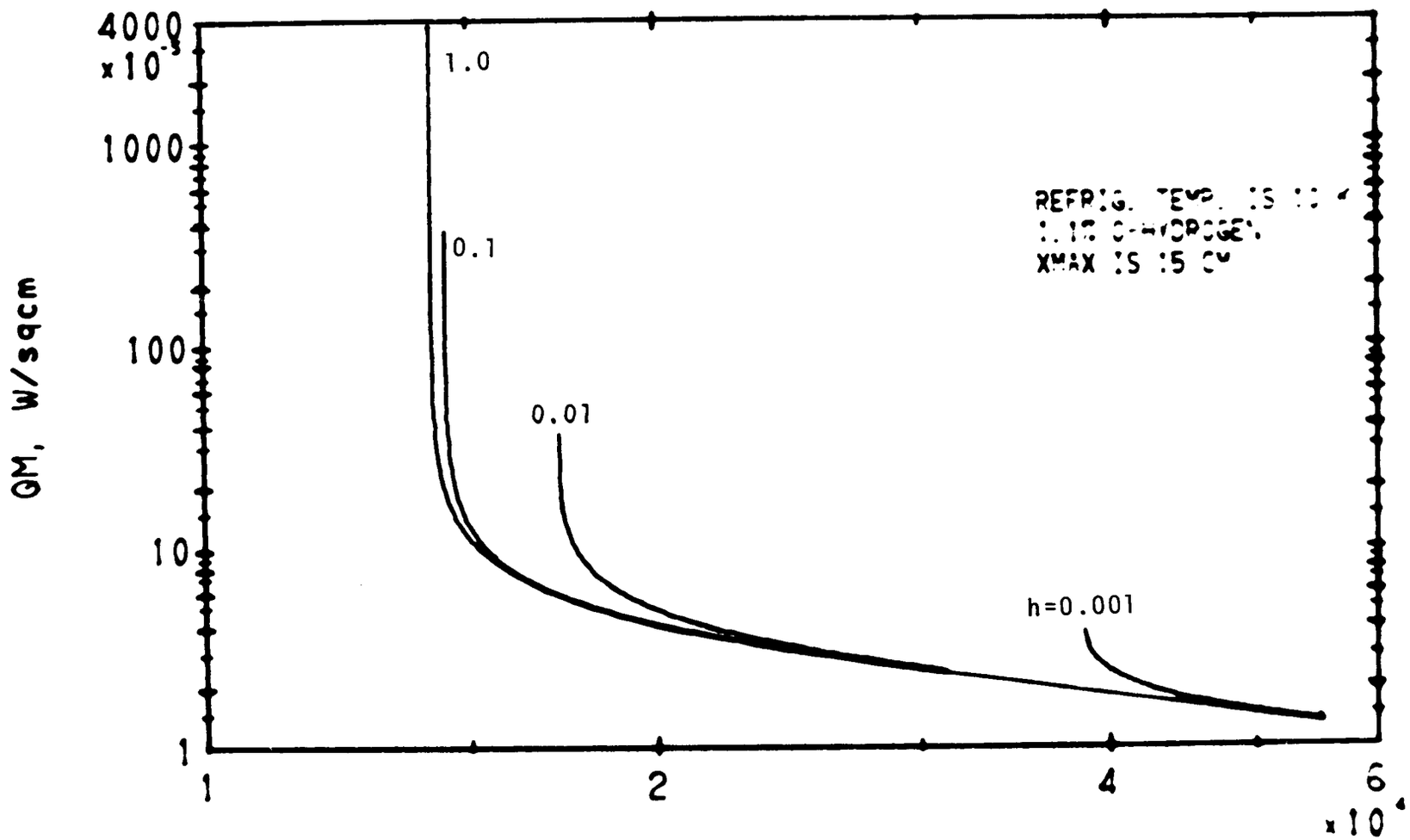

LINEAR FREEZING

01/11/72

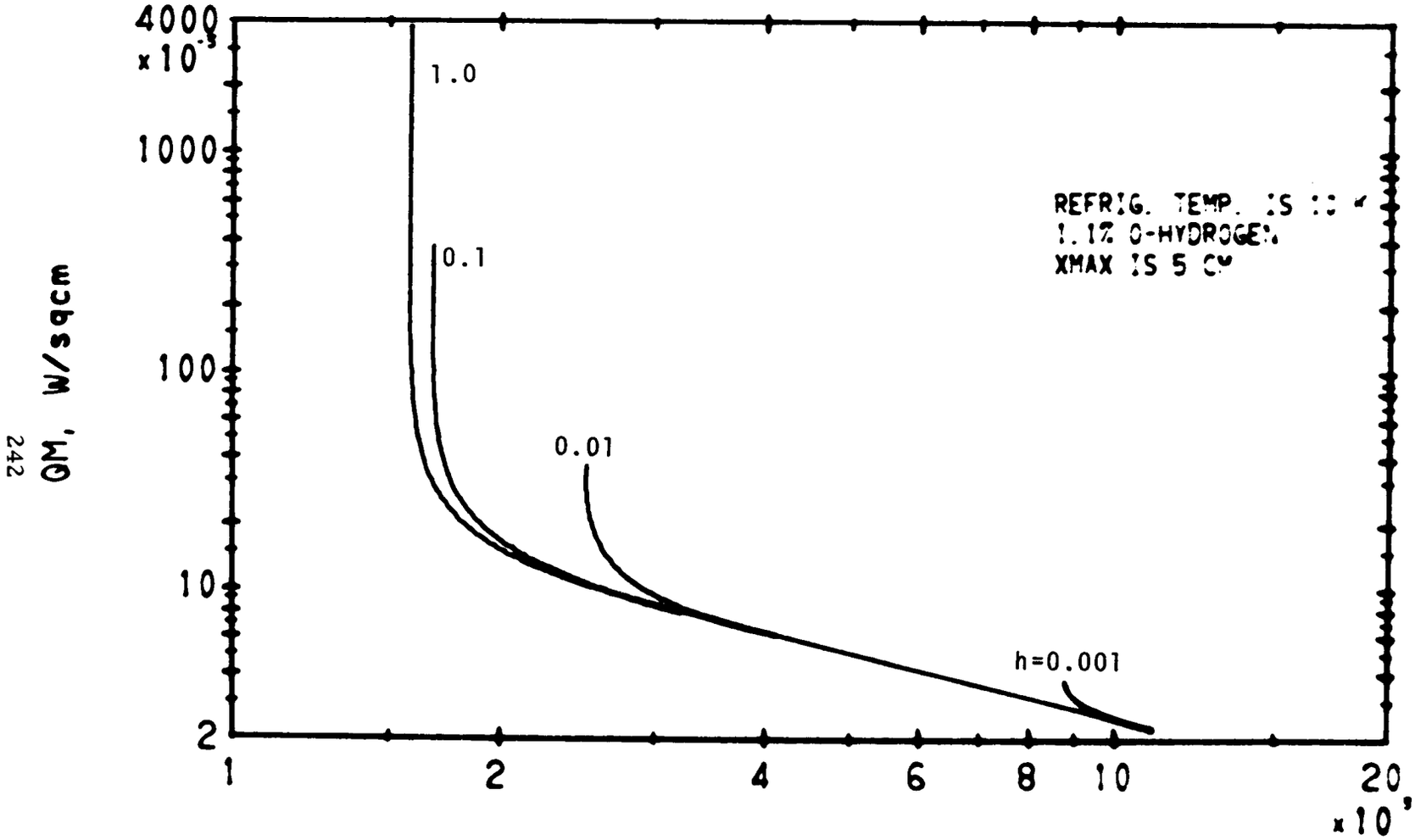

61/11/72

LINEAR FREEZING

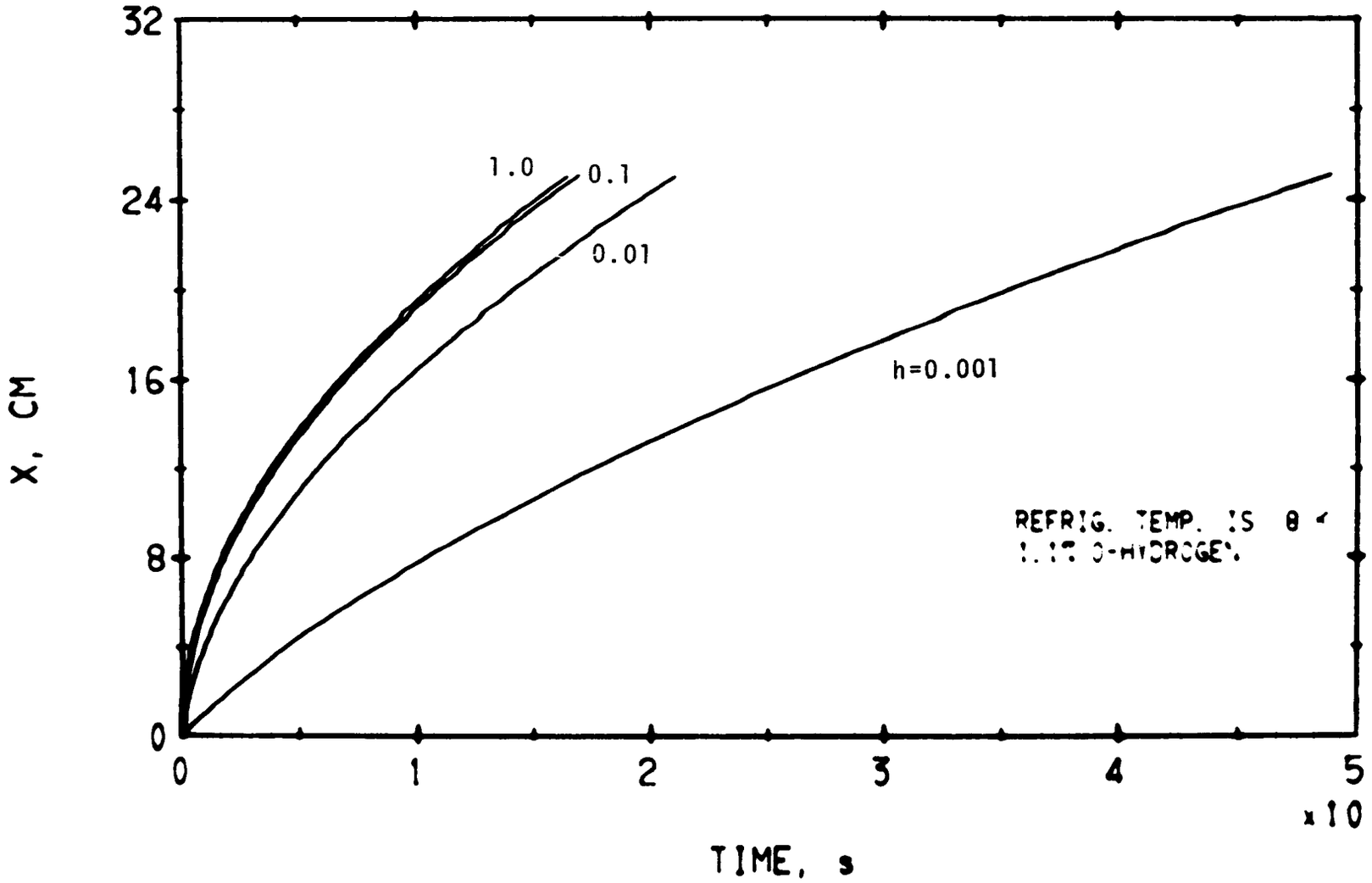

61/11/72

LINEAR FREEZING

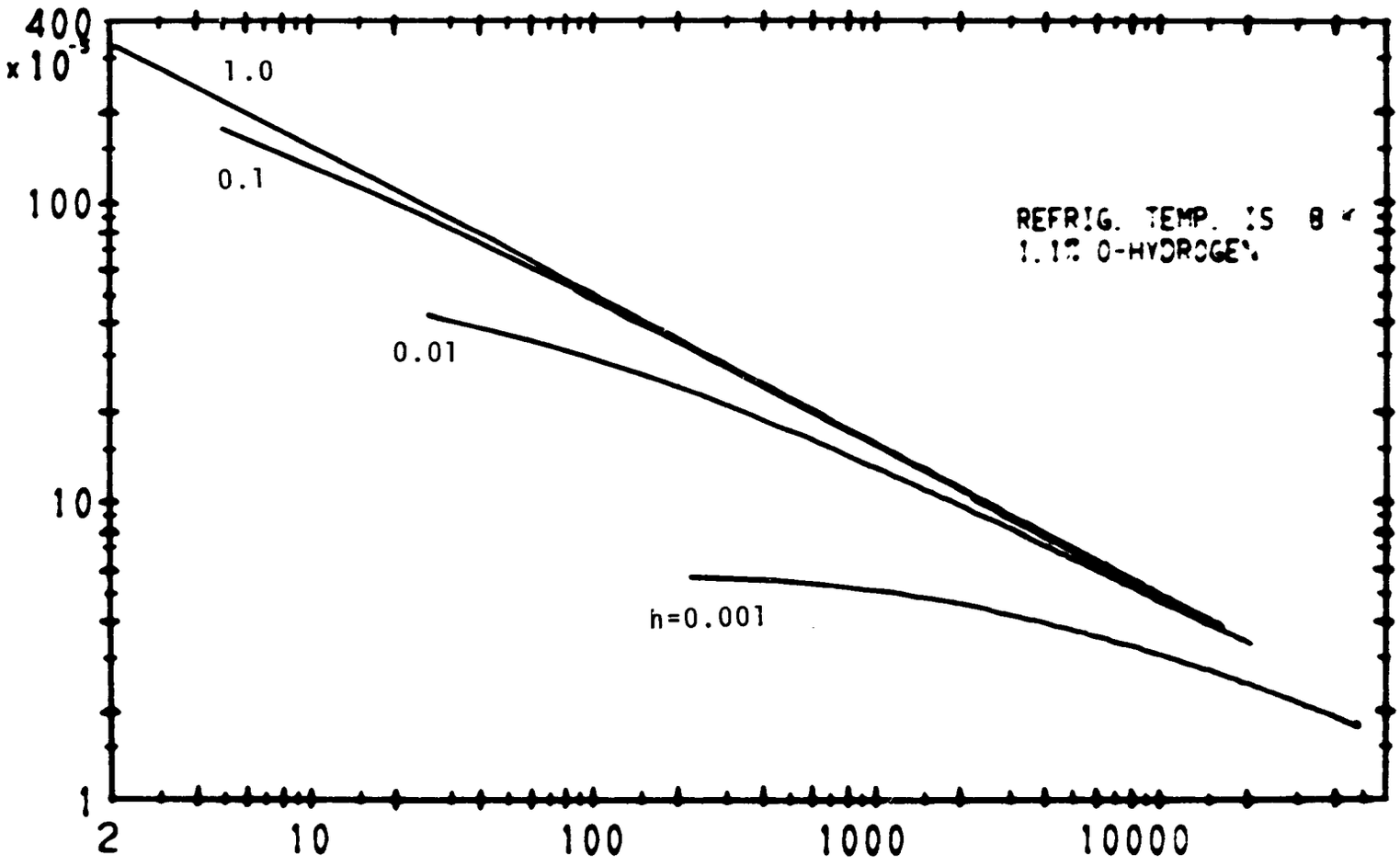

01/11/72

LINEAR FREEZING

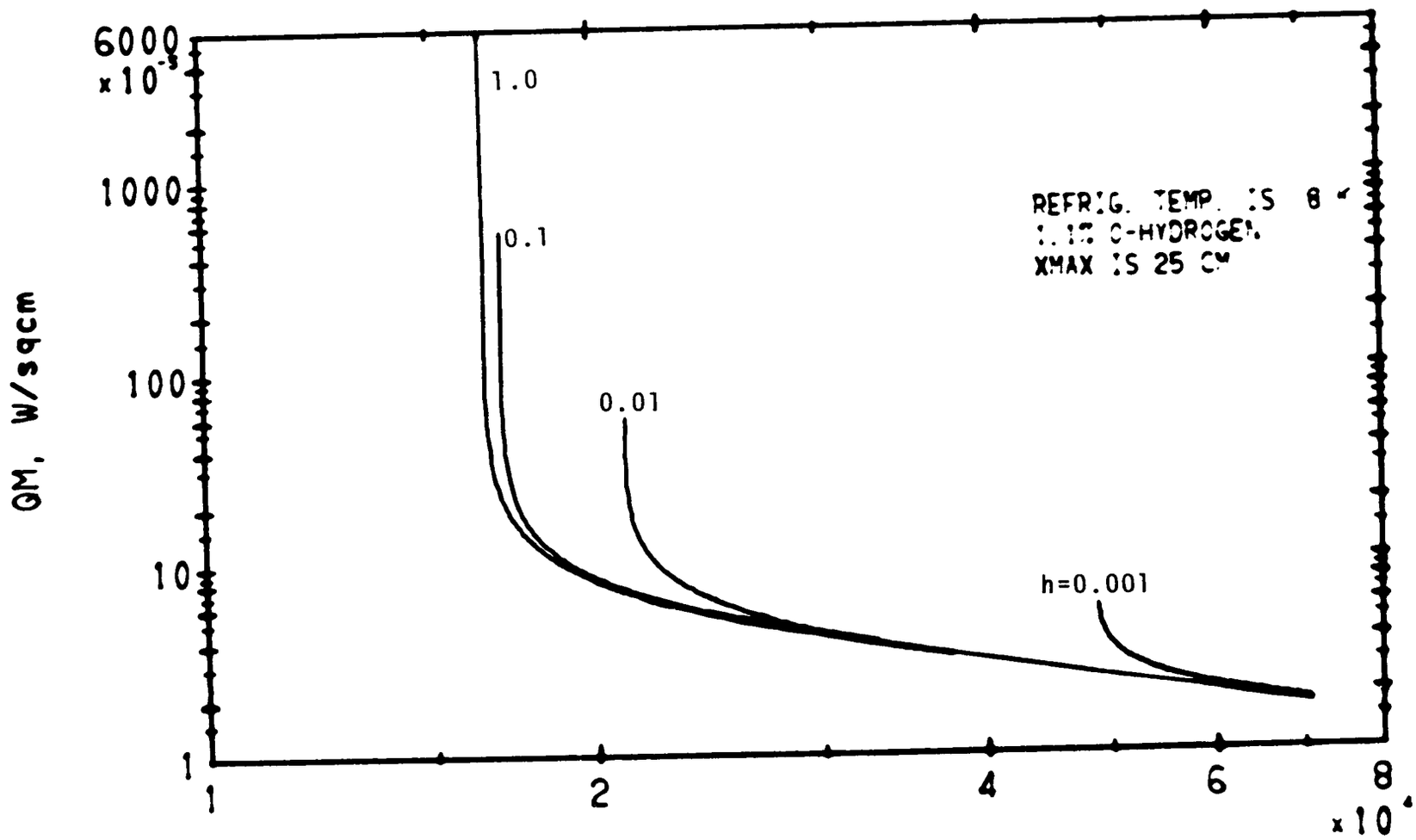

LINEAR FREEZING

81/11/72

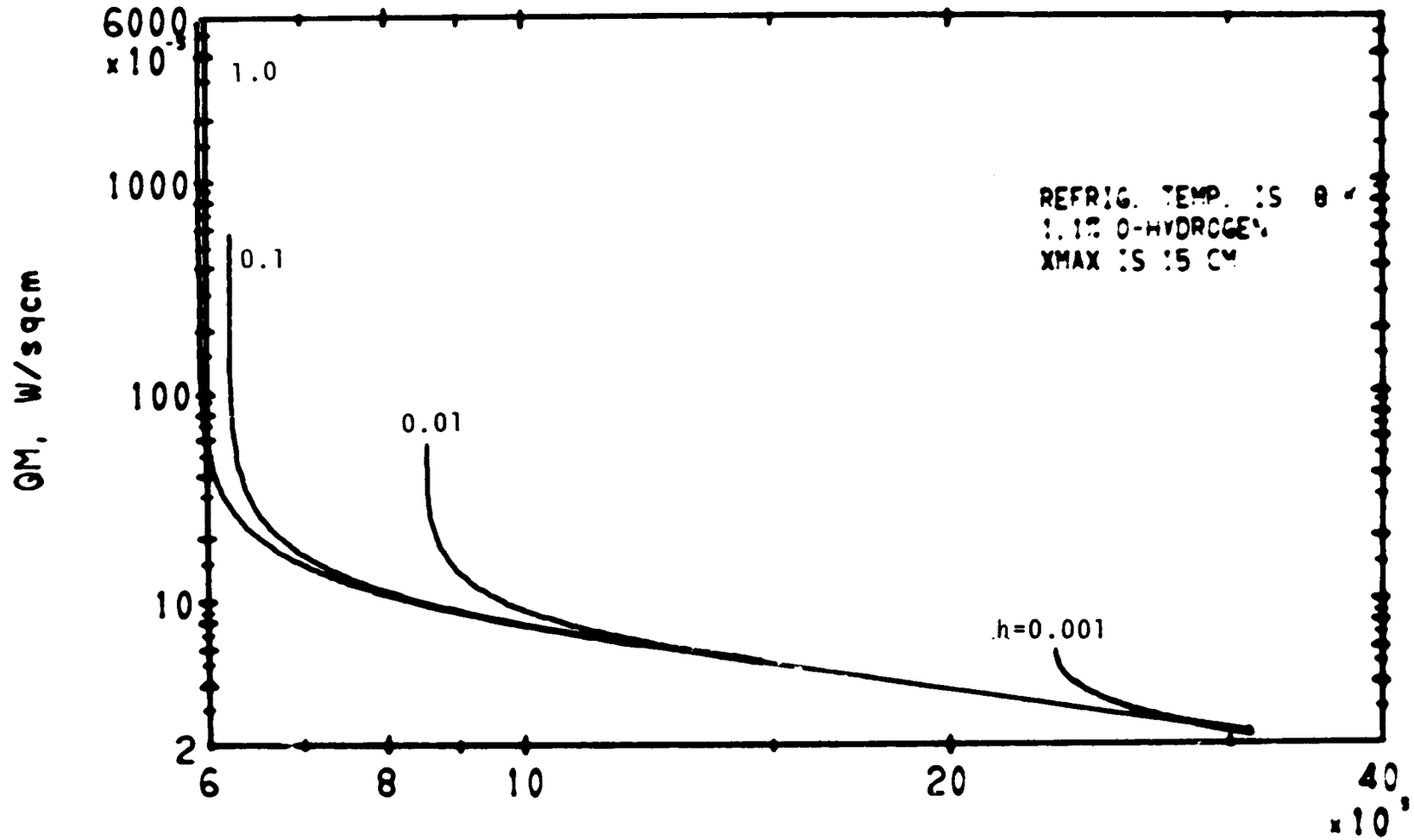

01/11/72

LINEAR FREEZING

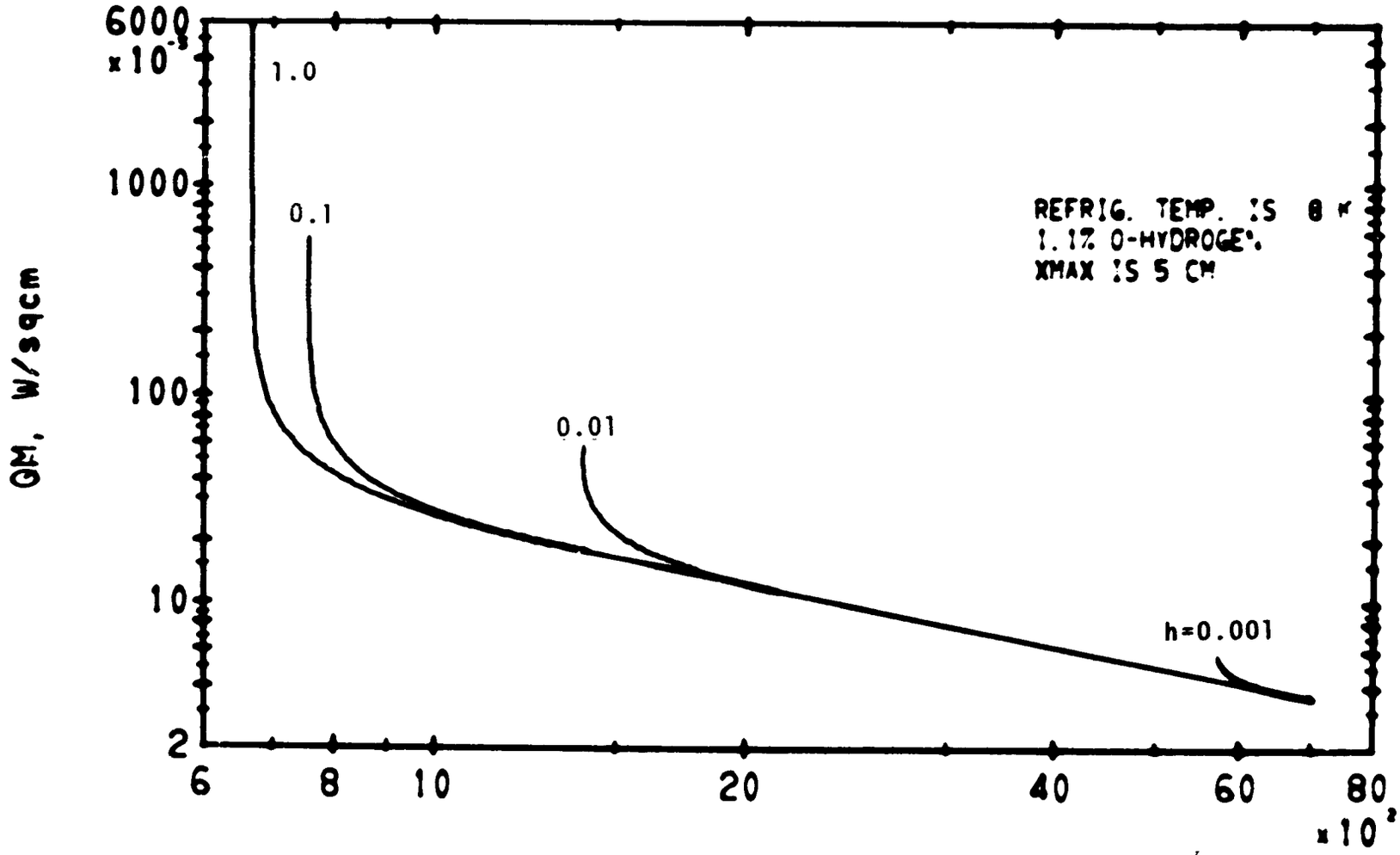

01/11/72

LINEAR FREEZING

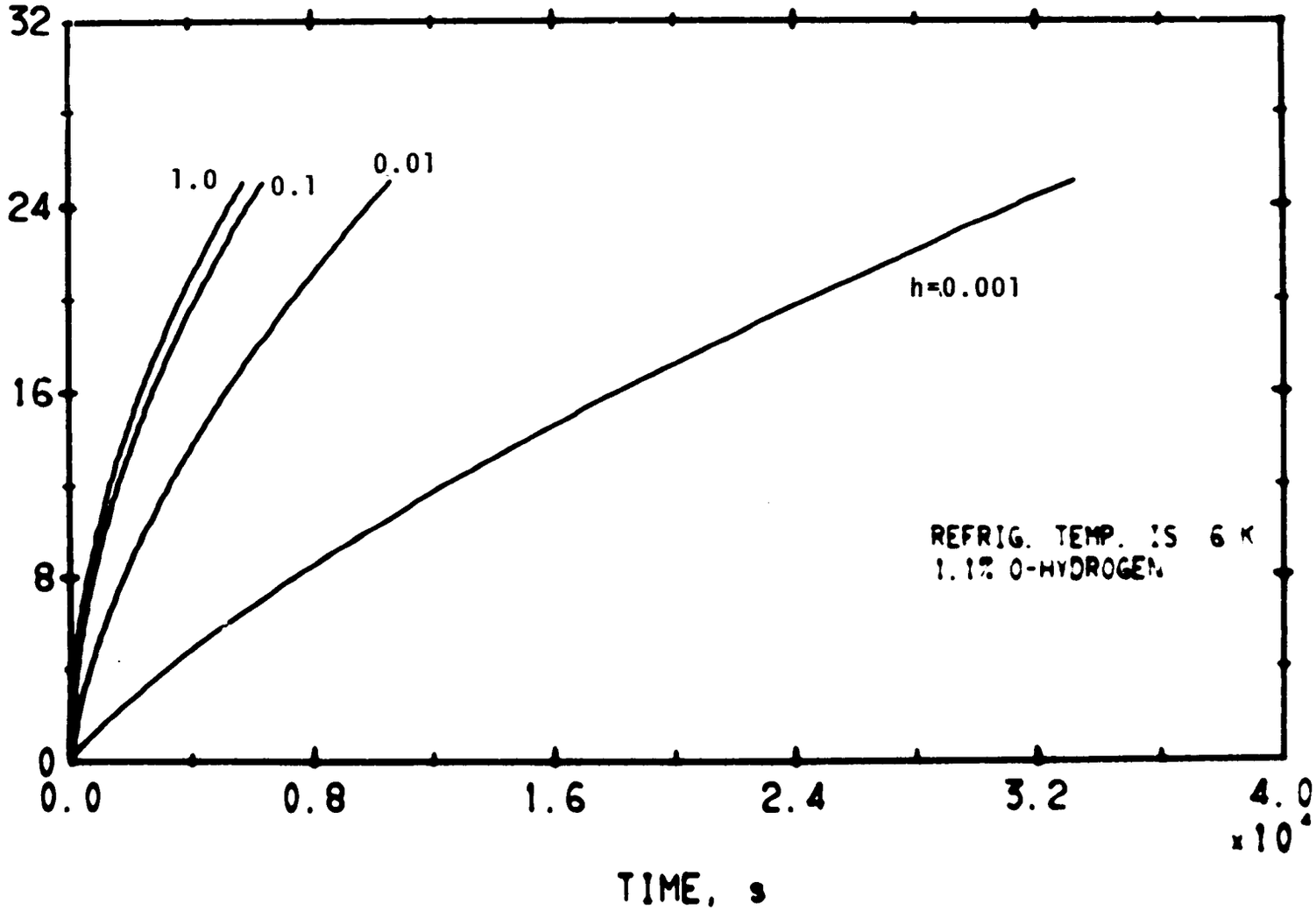

01/11/72

LINEAR FREEZING

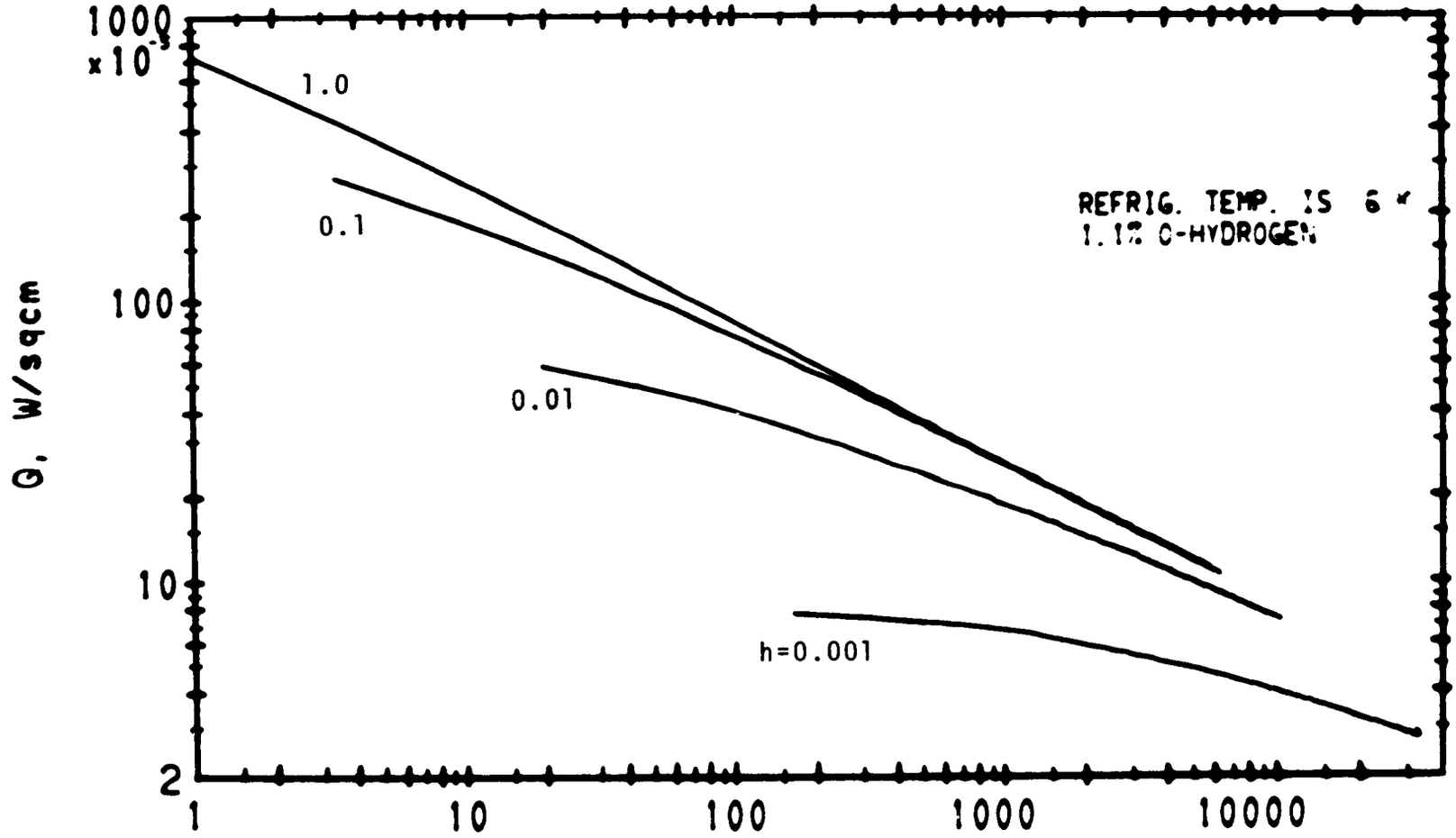

01/11/72

LINEAR FREEZING

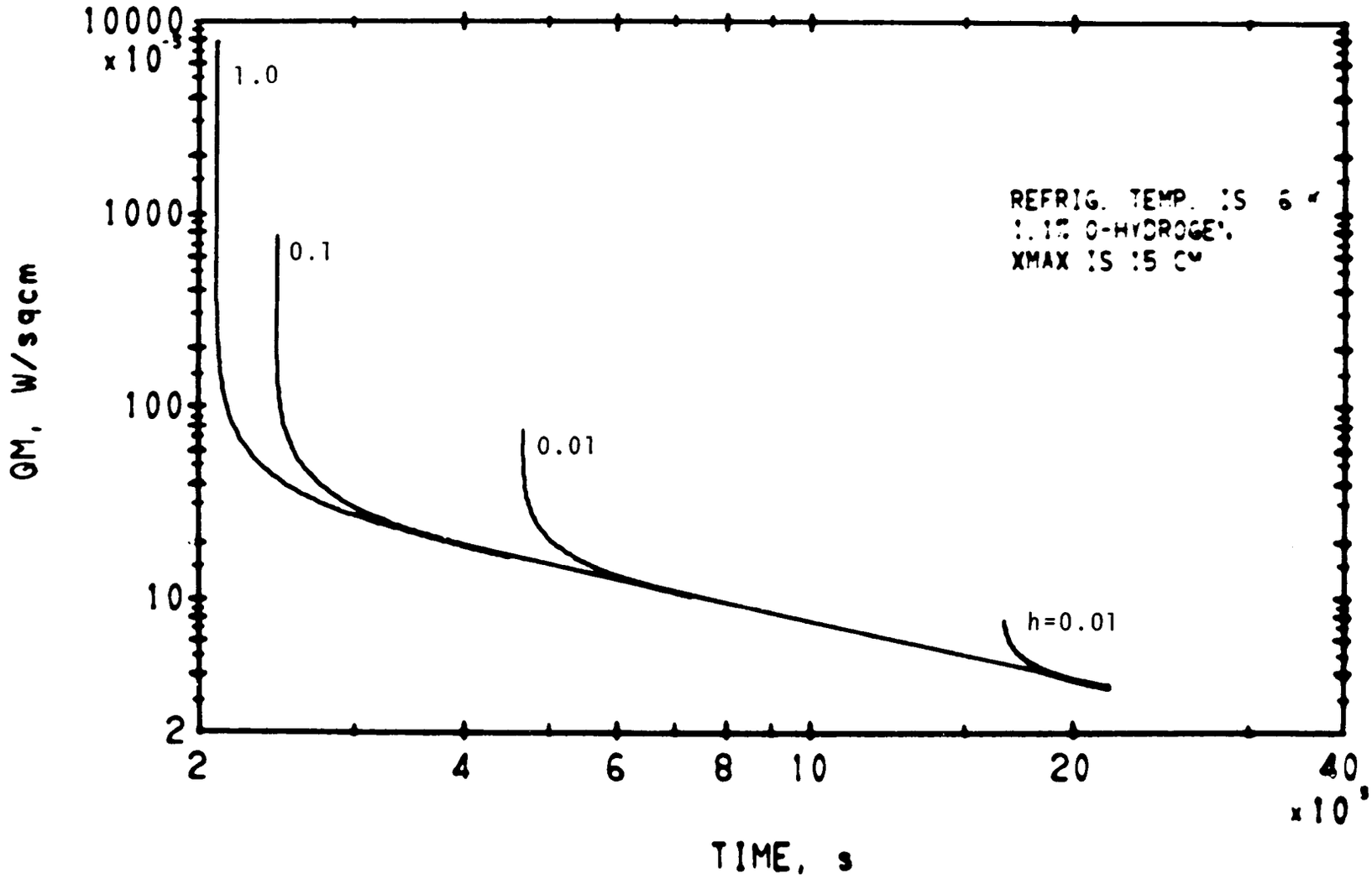

81/11/72

LINEAR FREEZING

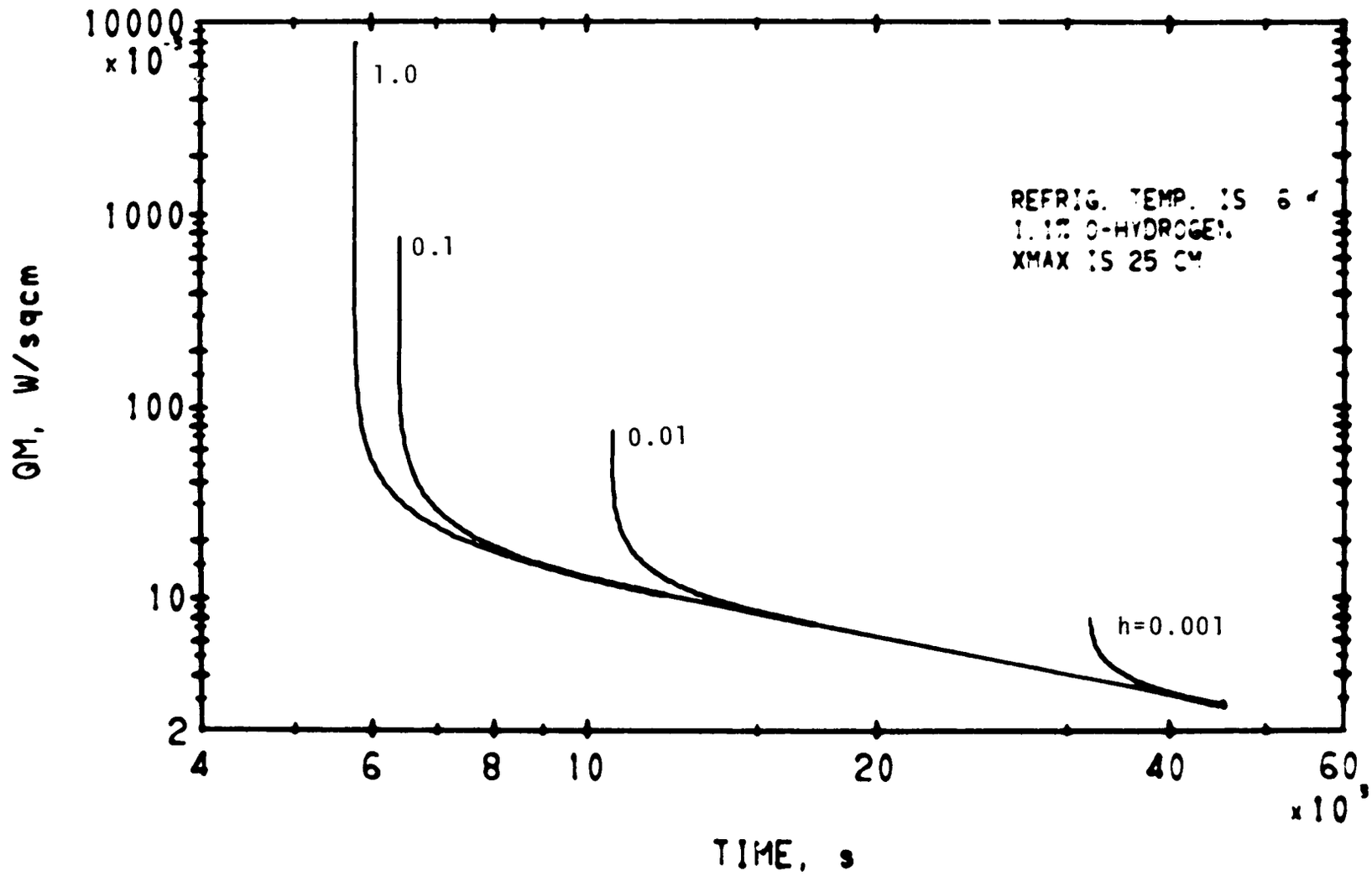

01/11/72

LINEAR FREEZING

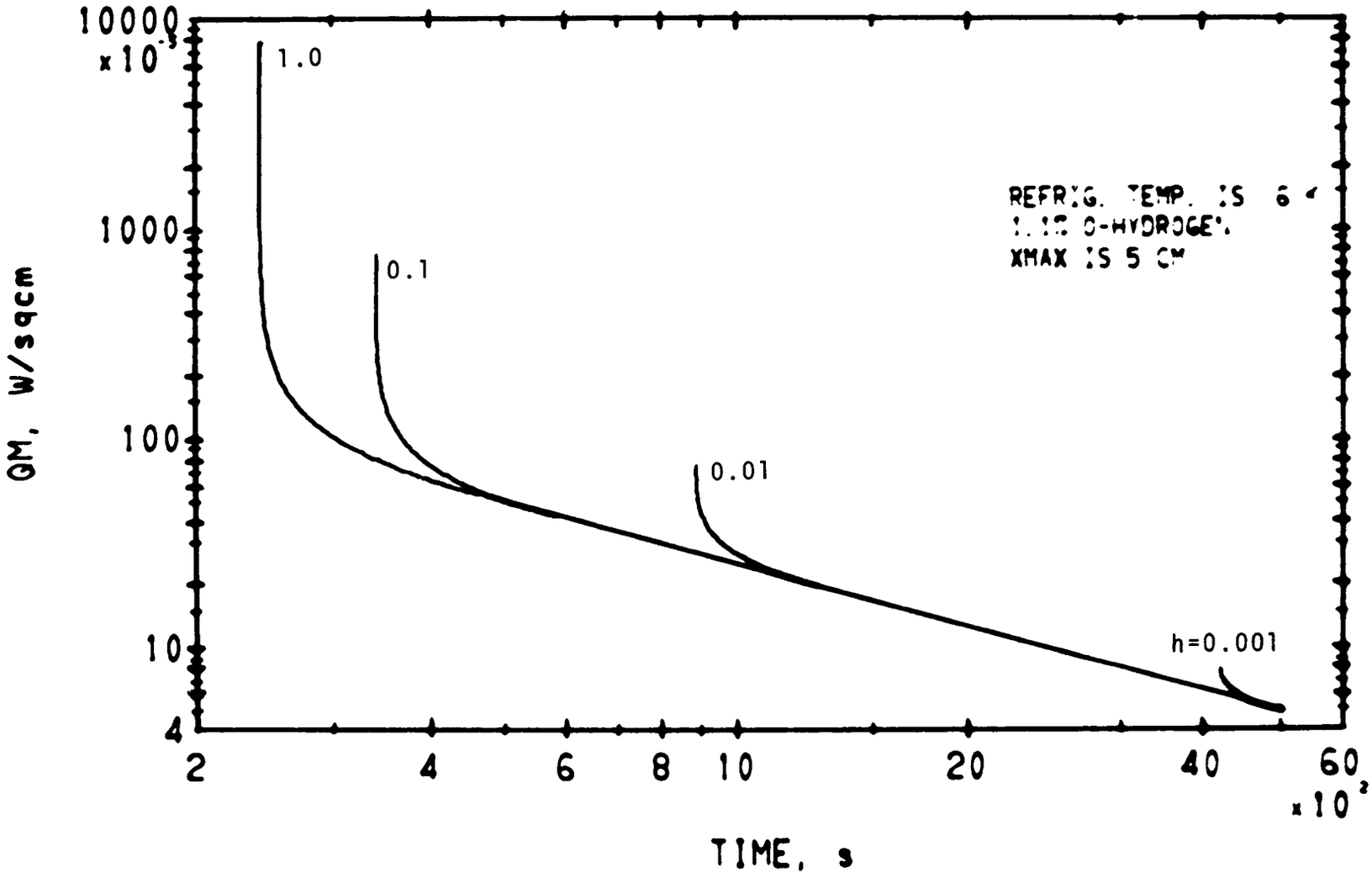

01/11/72

LINEAR FREEZING

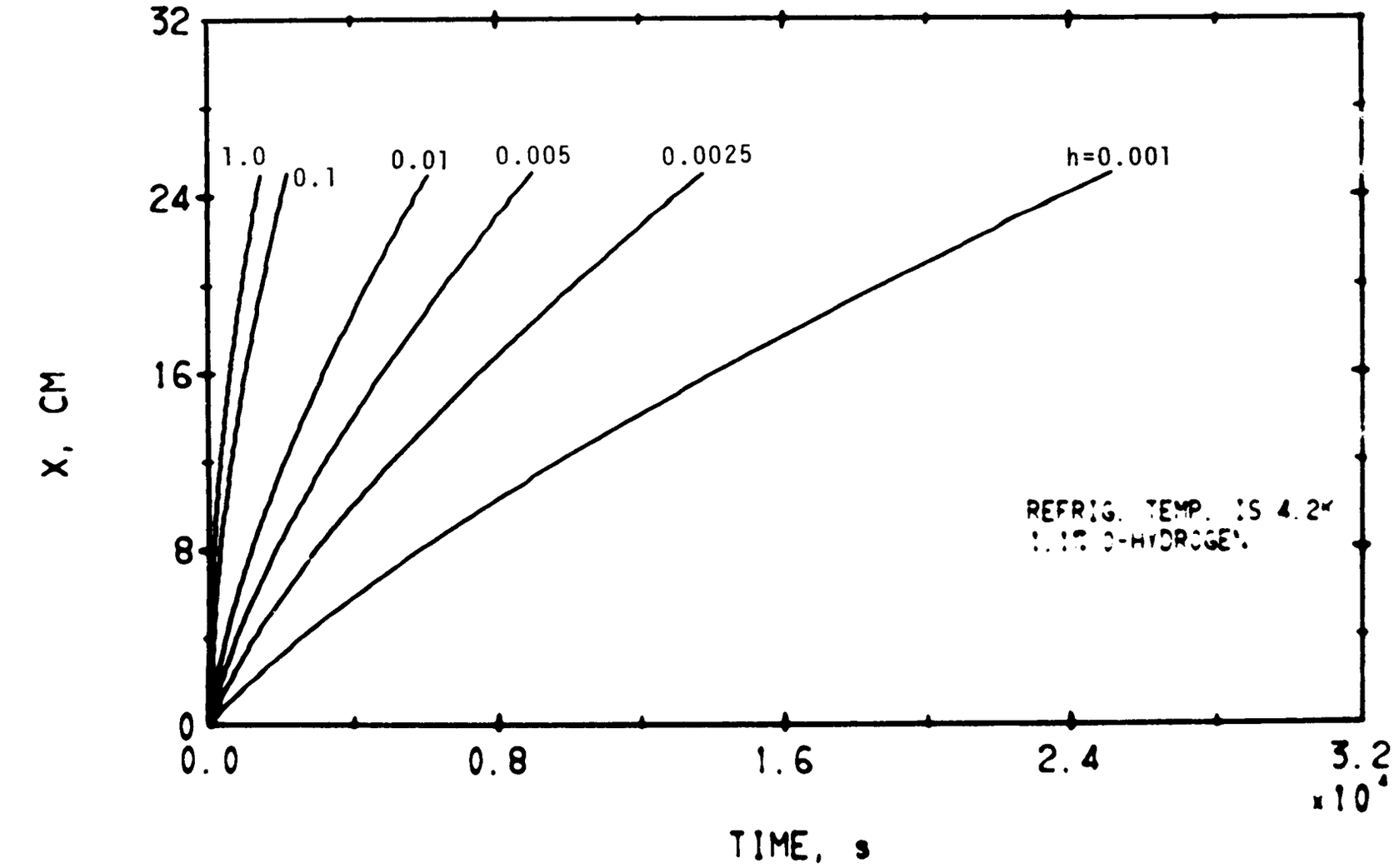

LINEAR FREEZING

01/11/72

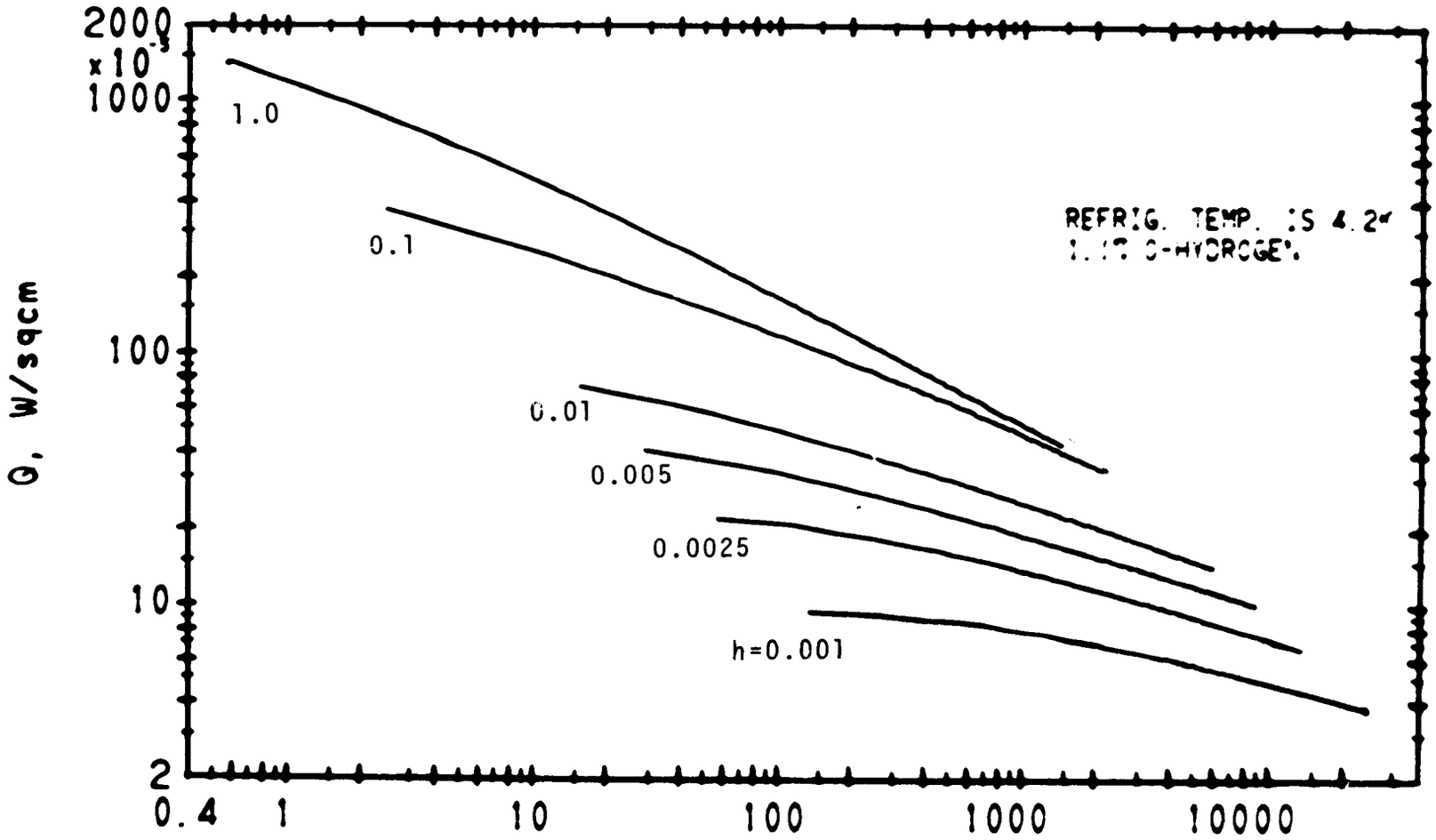

01/11/72

LINEAR FREEZING

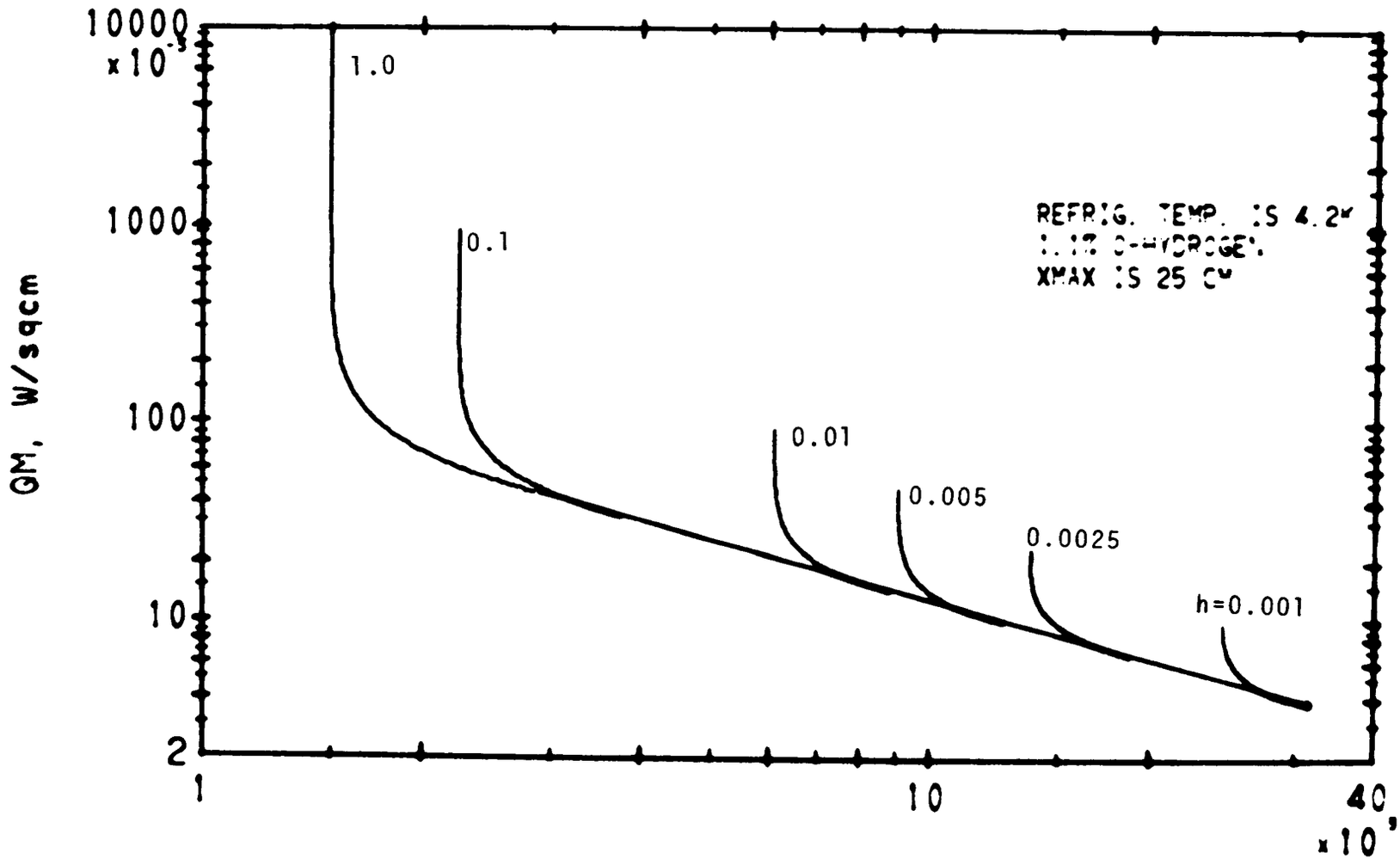

81/11/72

LINEAR FREEZING

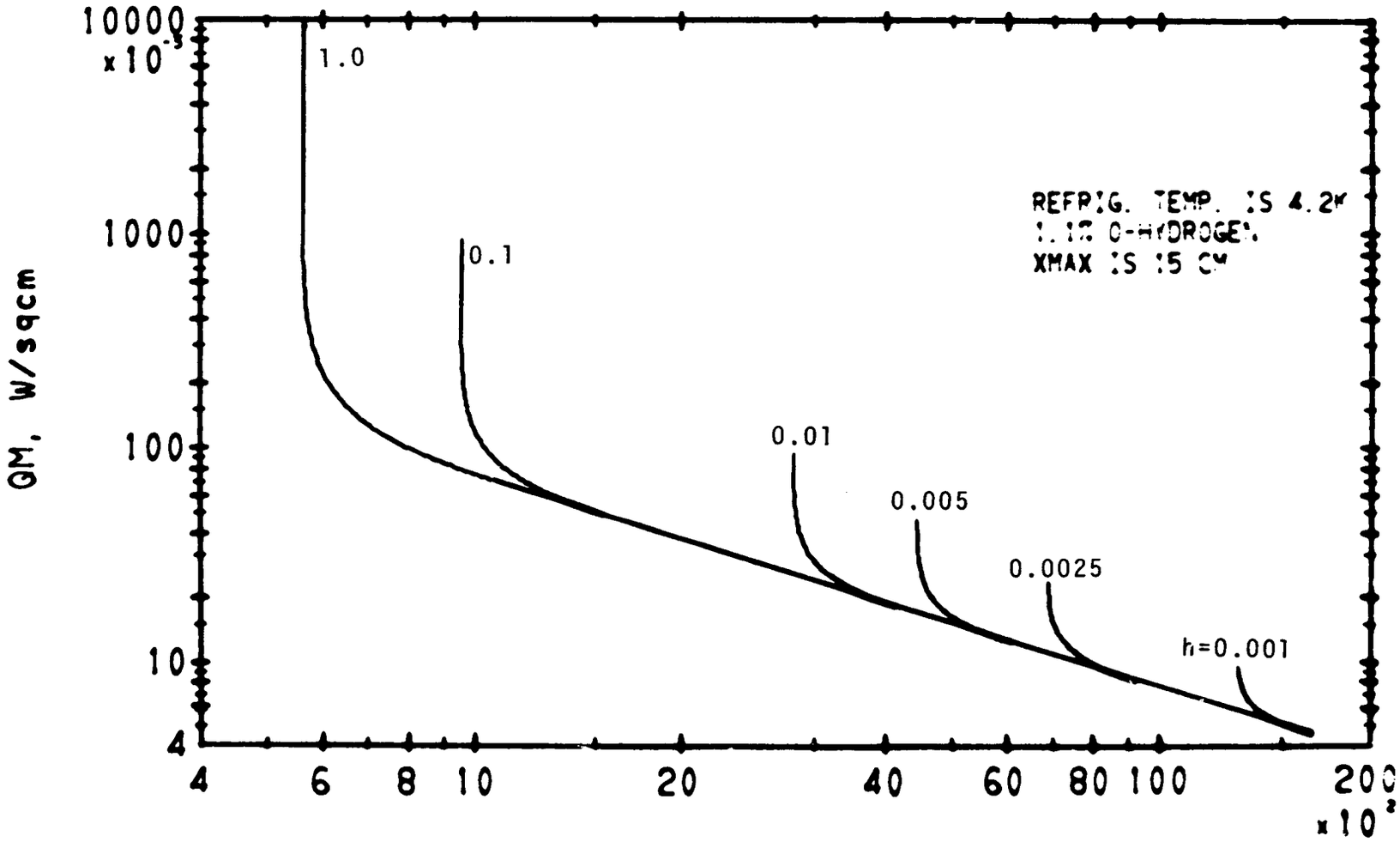

01/11/72

LINEAR FREEZING

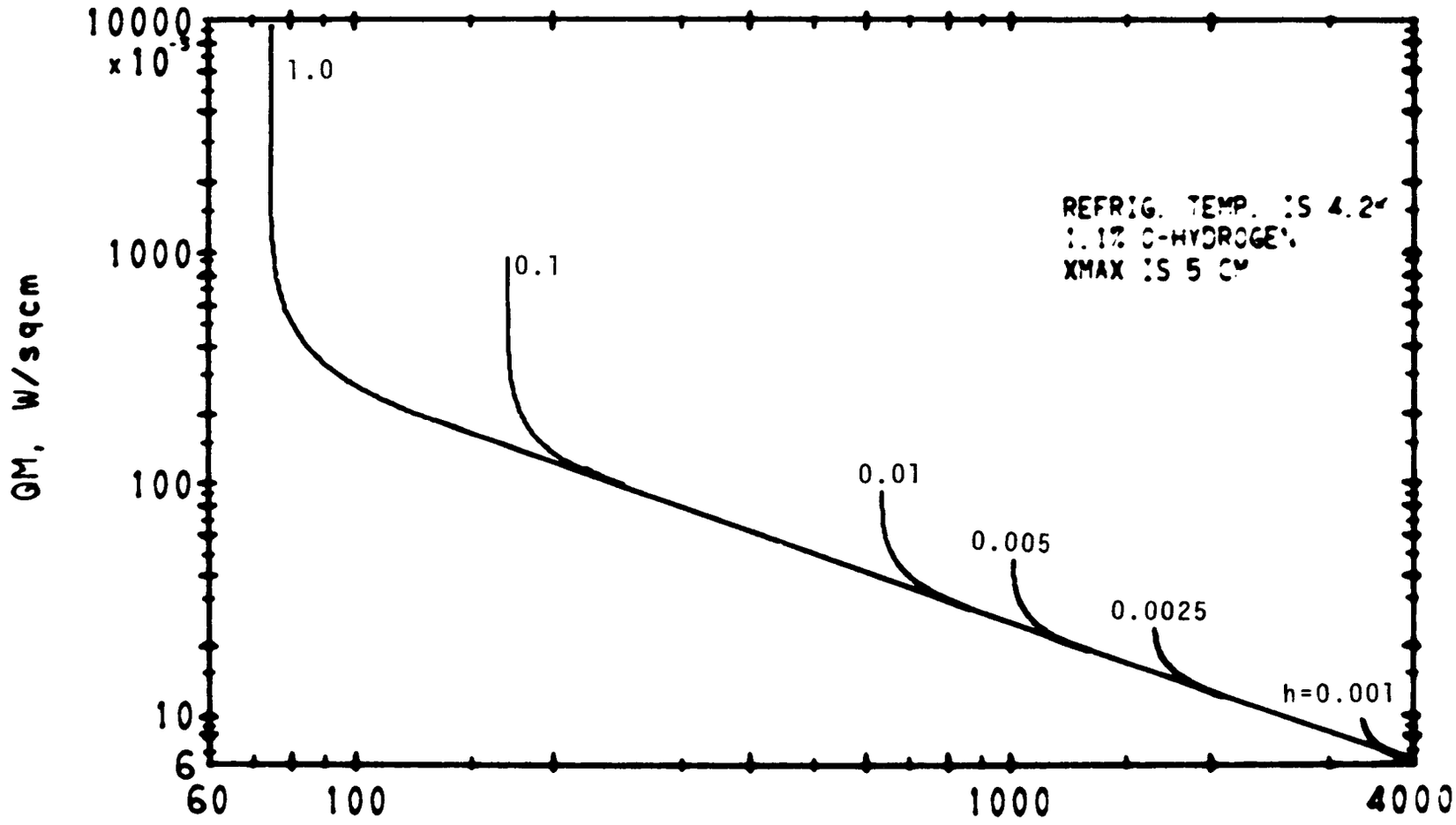

LINEAR FREEZING

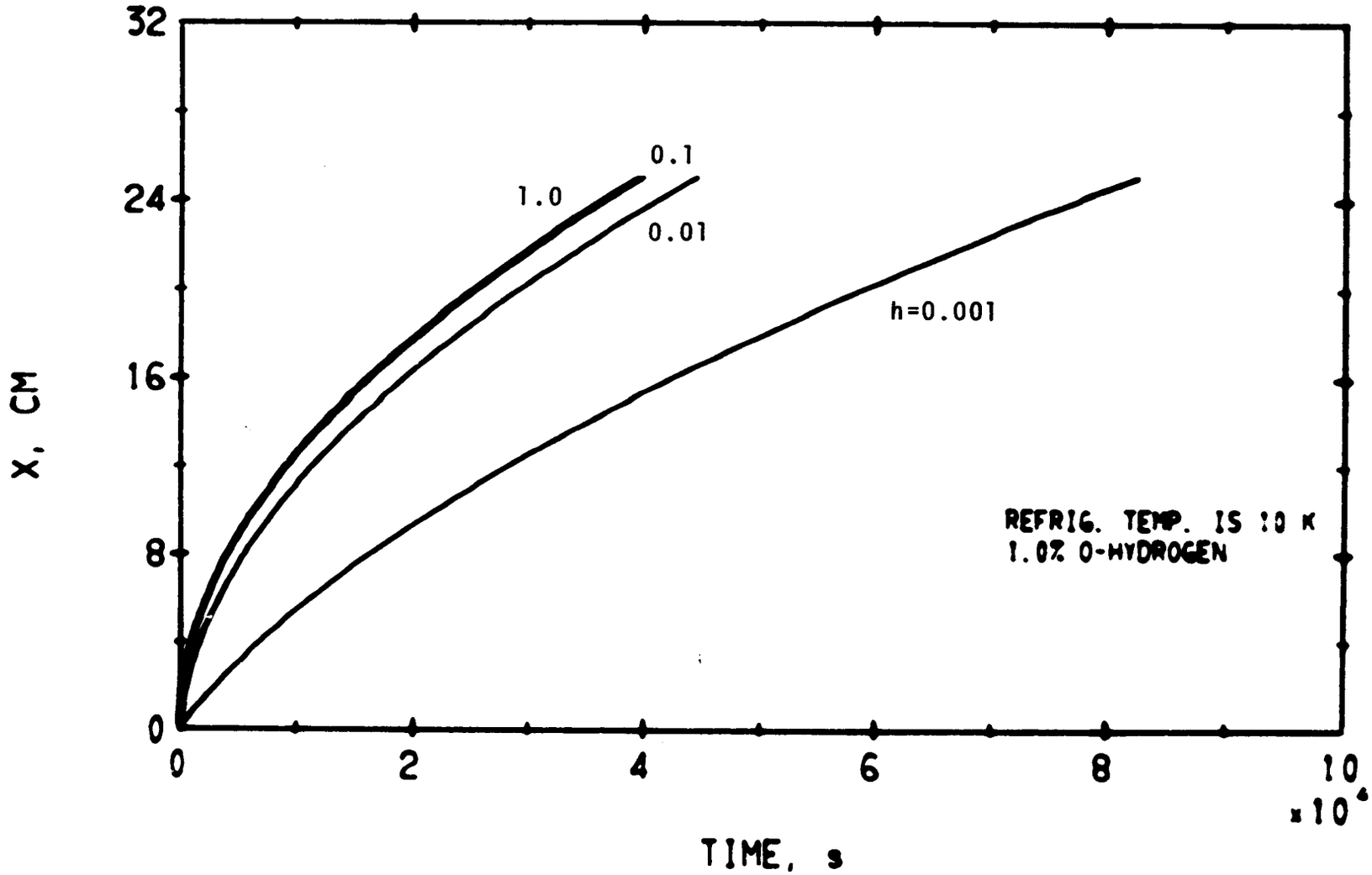

01/15/72

LINEAR FREEZING

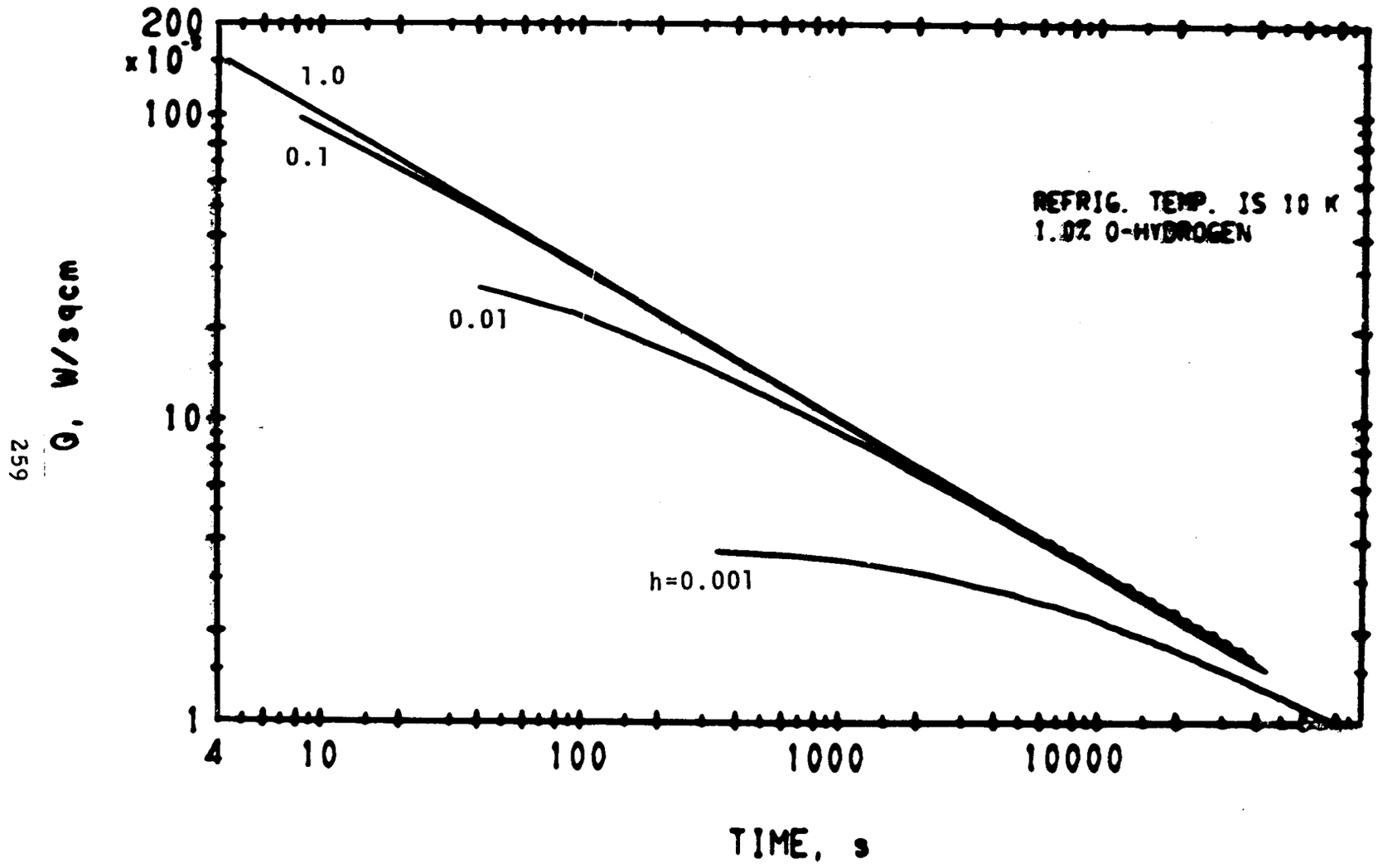

01/15/72

LINEAR FREEZING

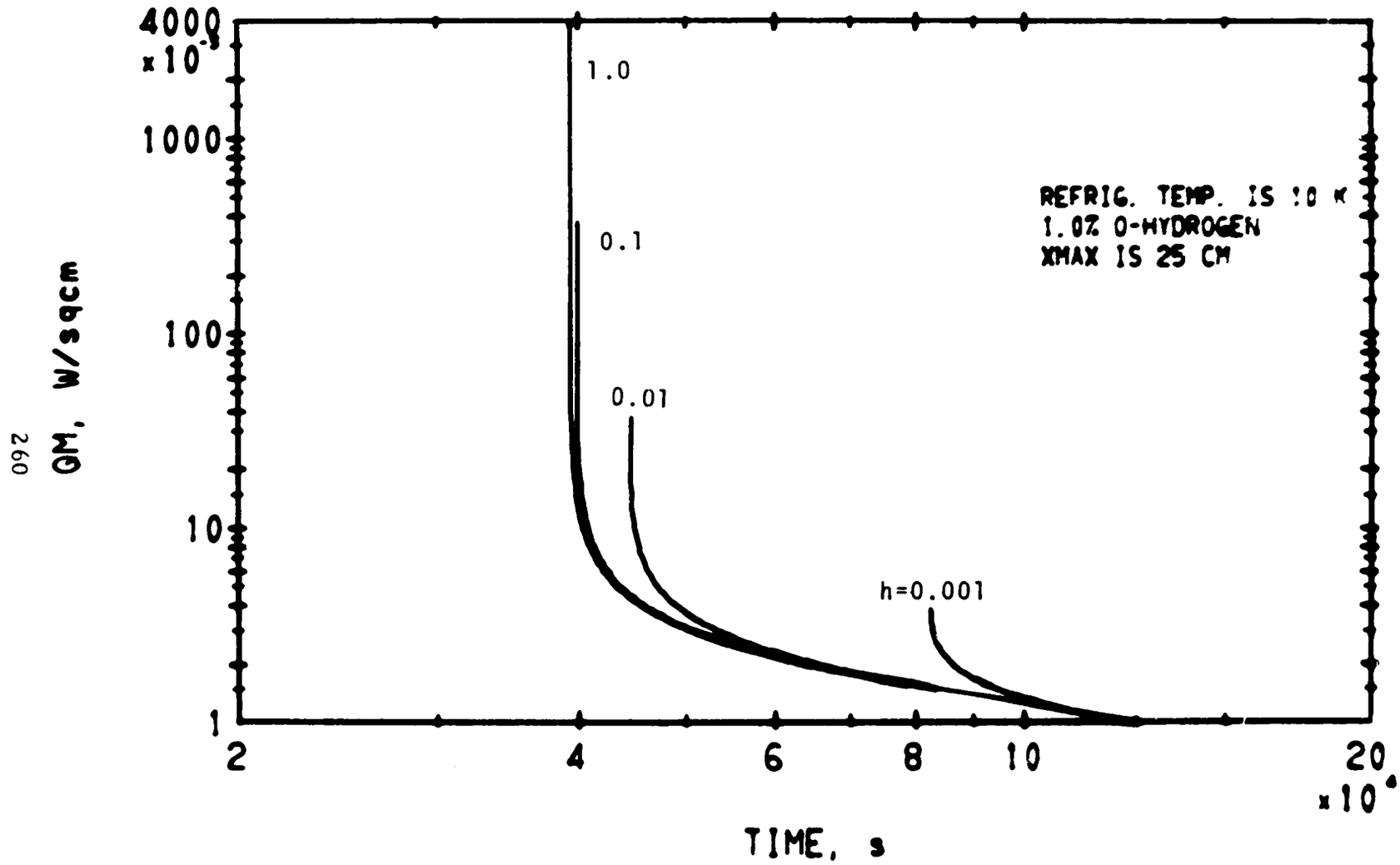

01/18/72

LINEAR FREEZING

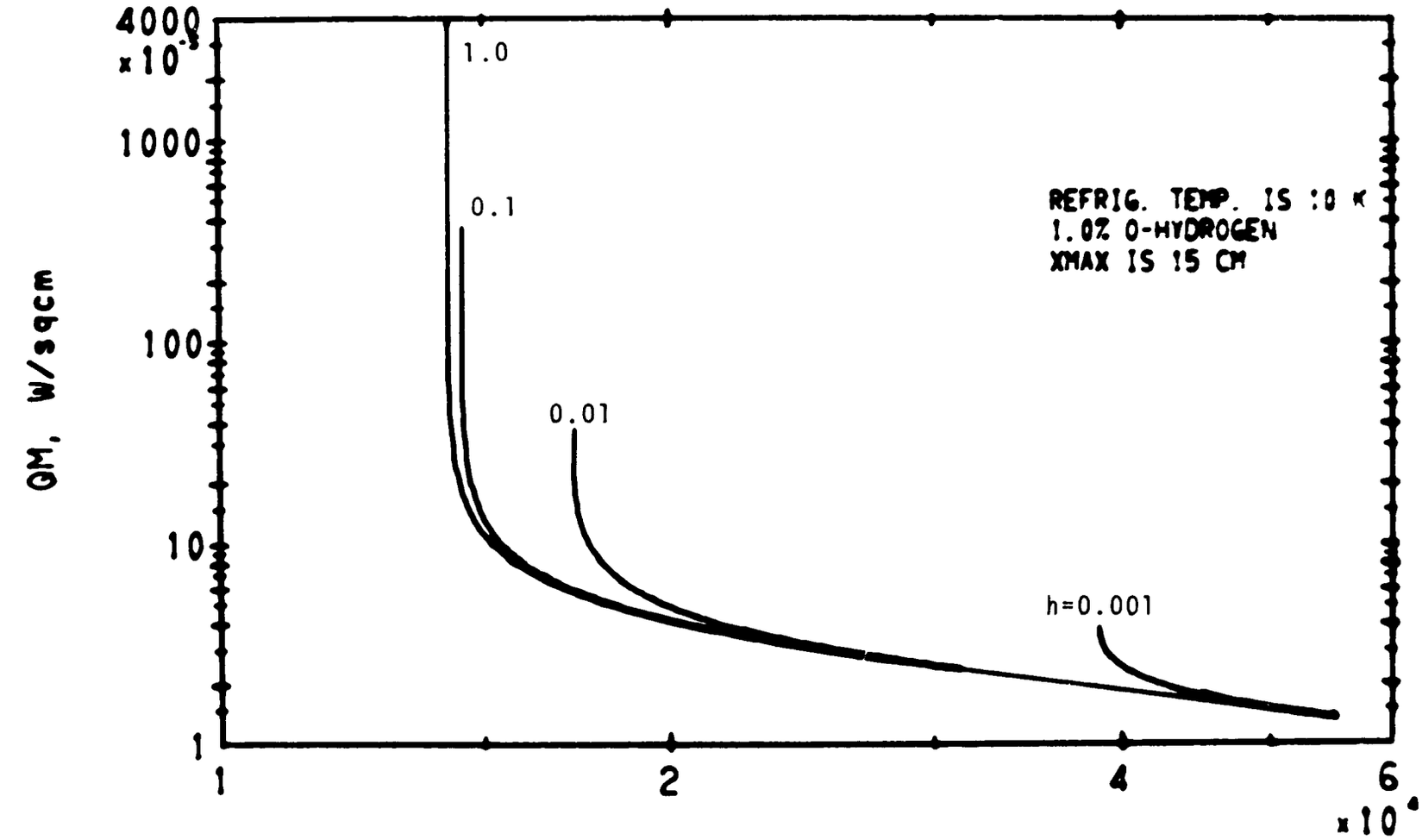

192

01/15/72

LINEAR FREEZING

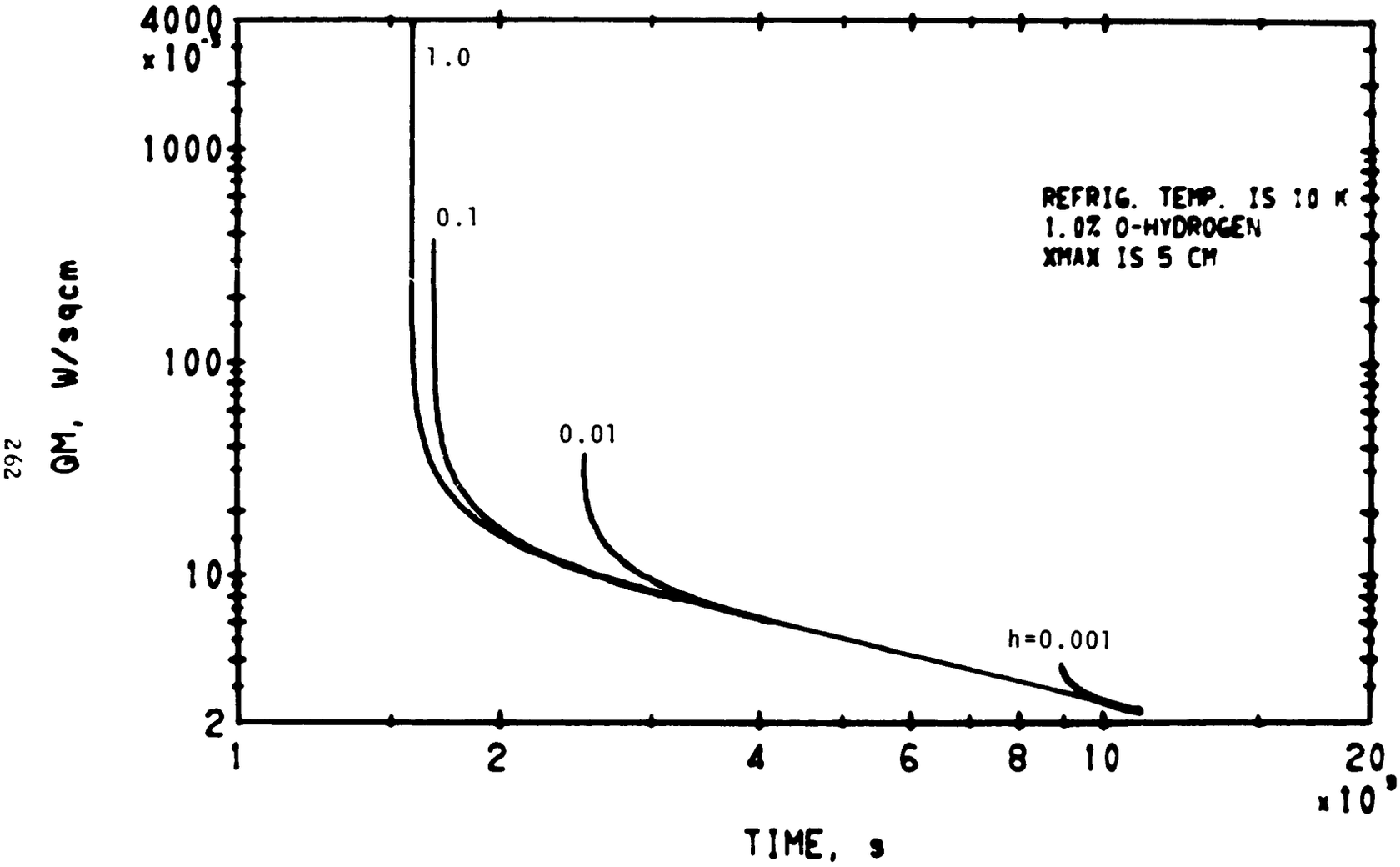

01/18/72

LINEAR FREEZING

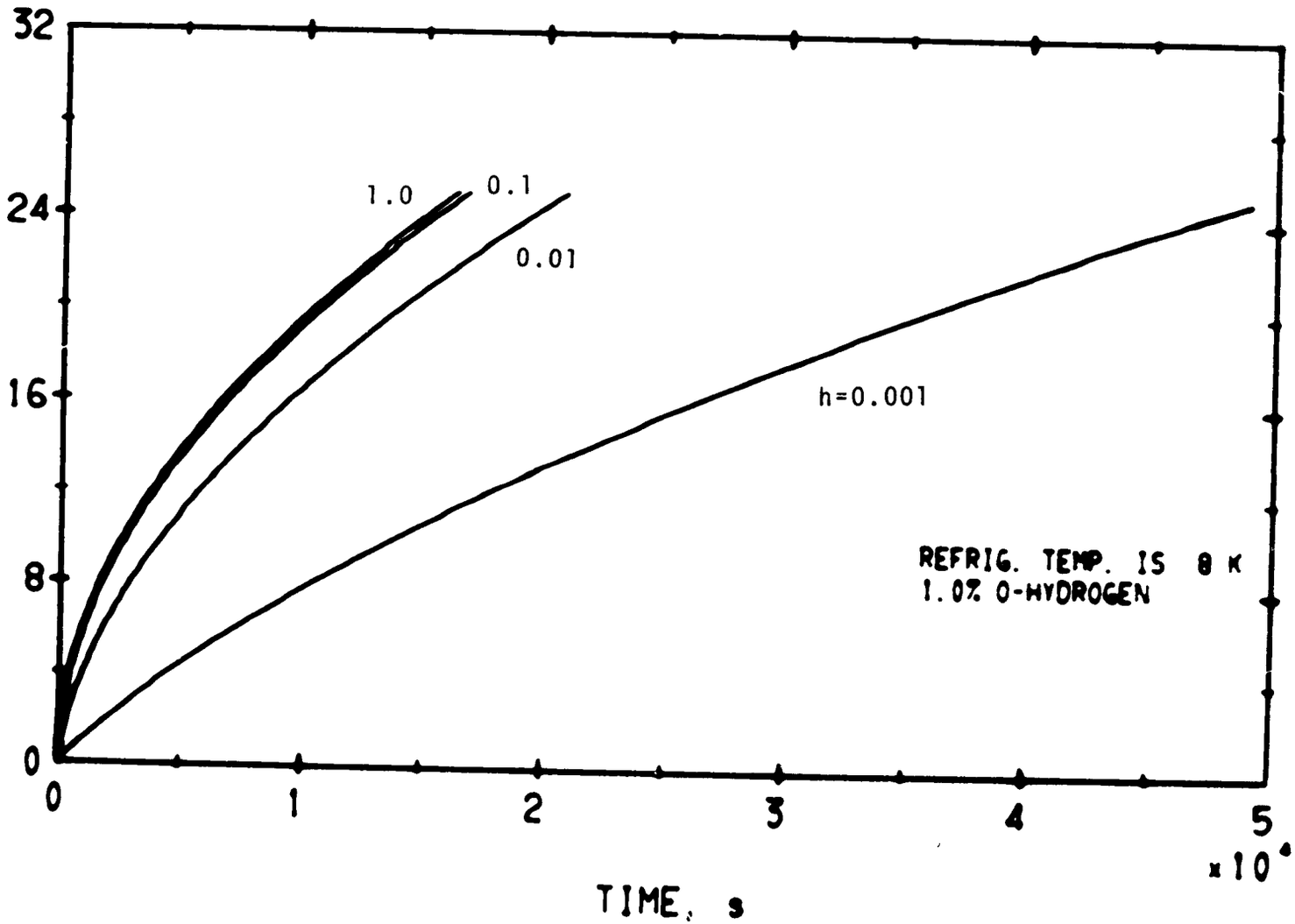

01/15/72

LINEAR FREEZING

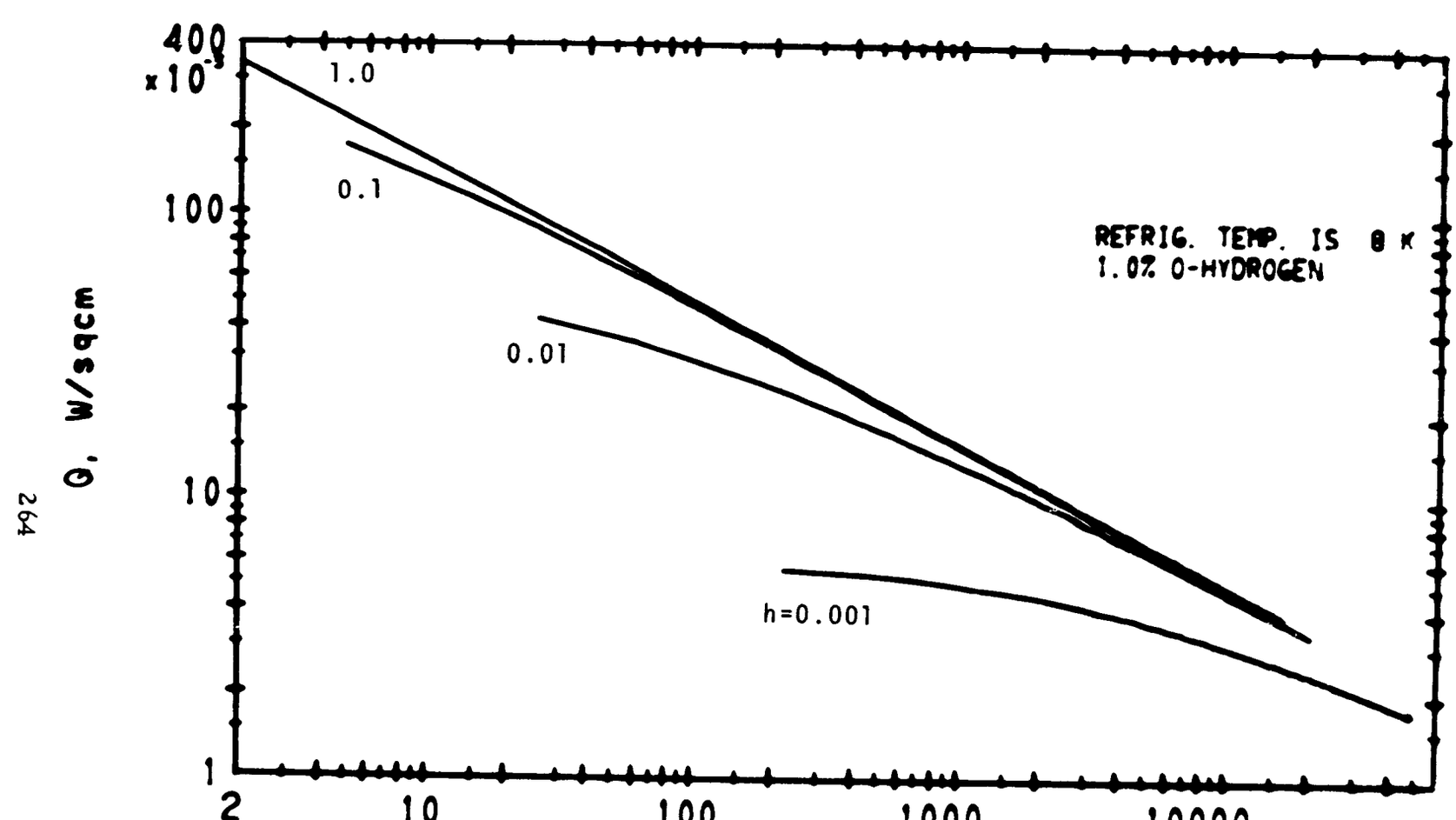

01/15/72

LINEAR FREEZING

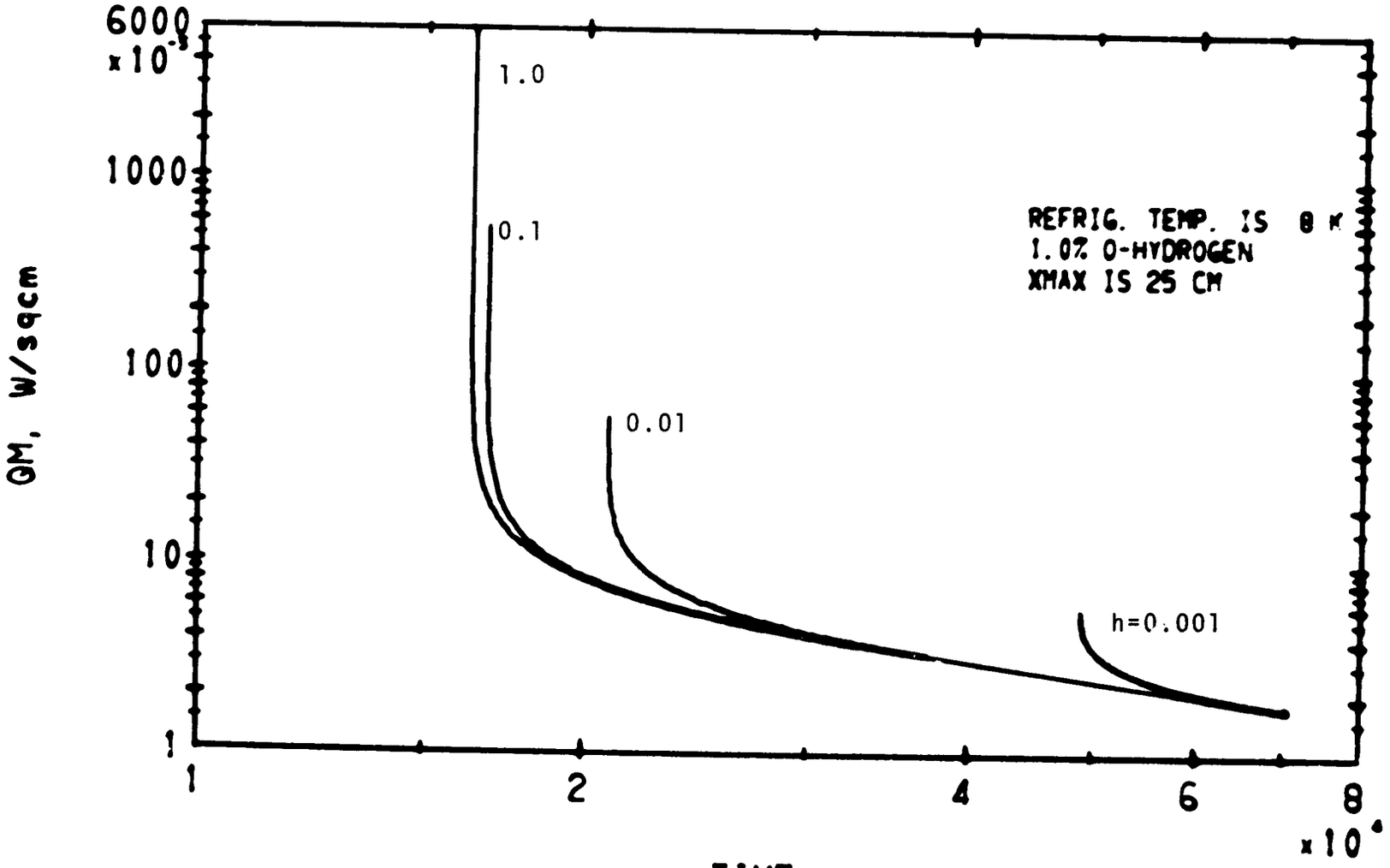

01/18/72

LINEAR FREEZING

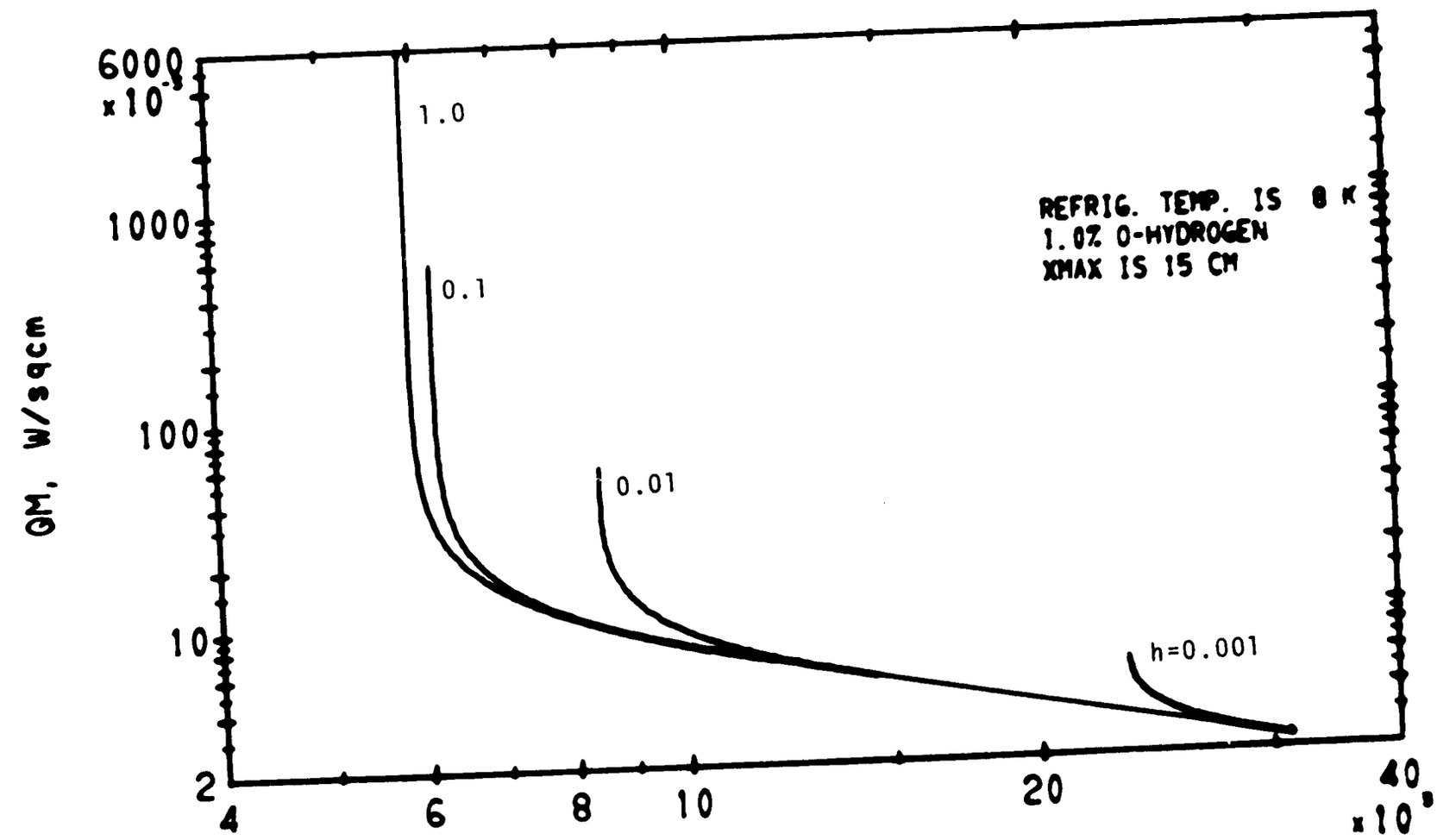

LINEAR FREEZING

01/15/72

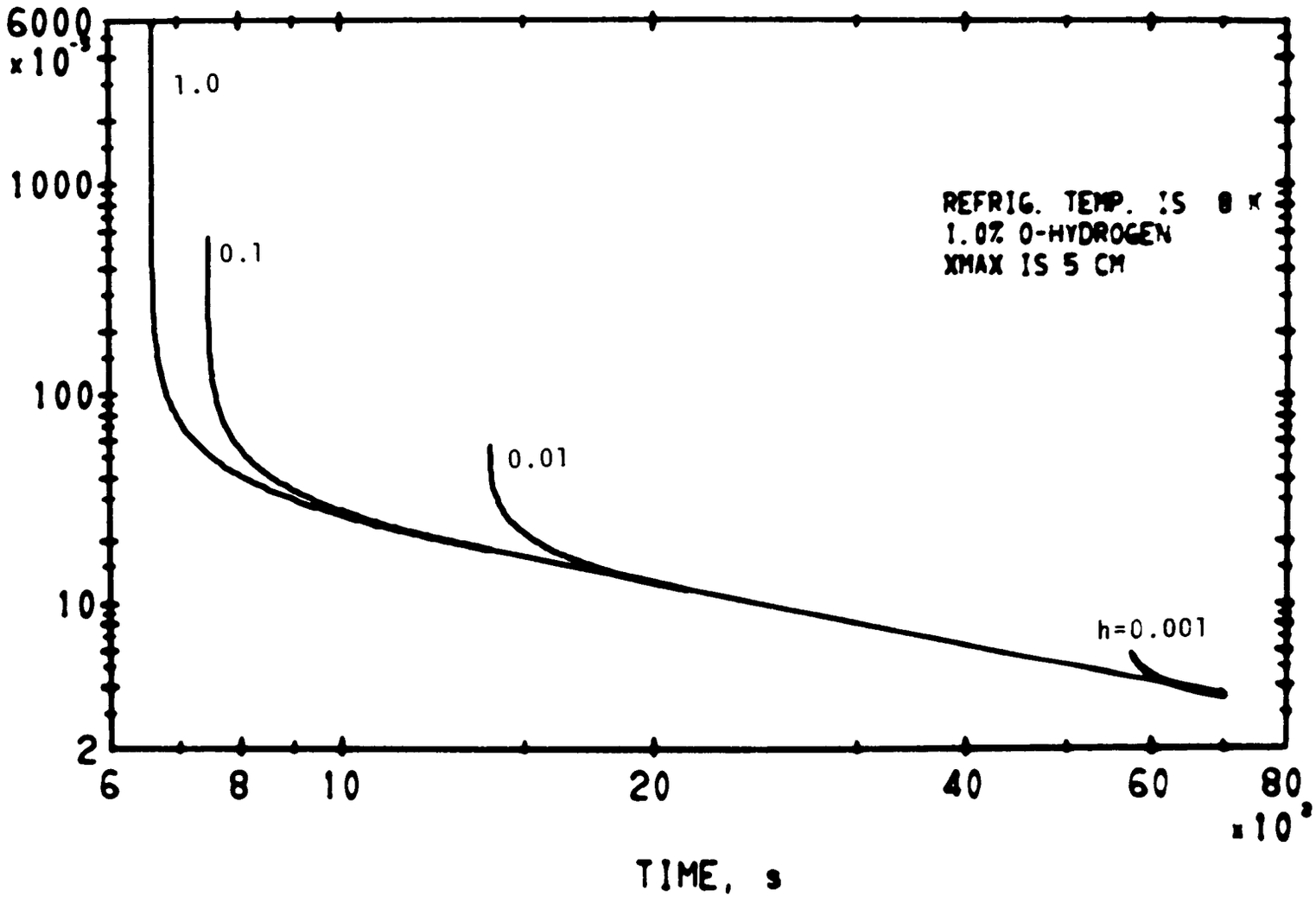

01/15/78

LINEAR FREEZING

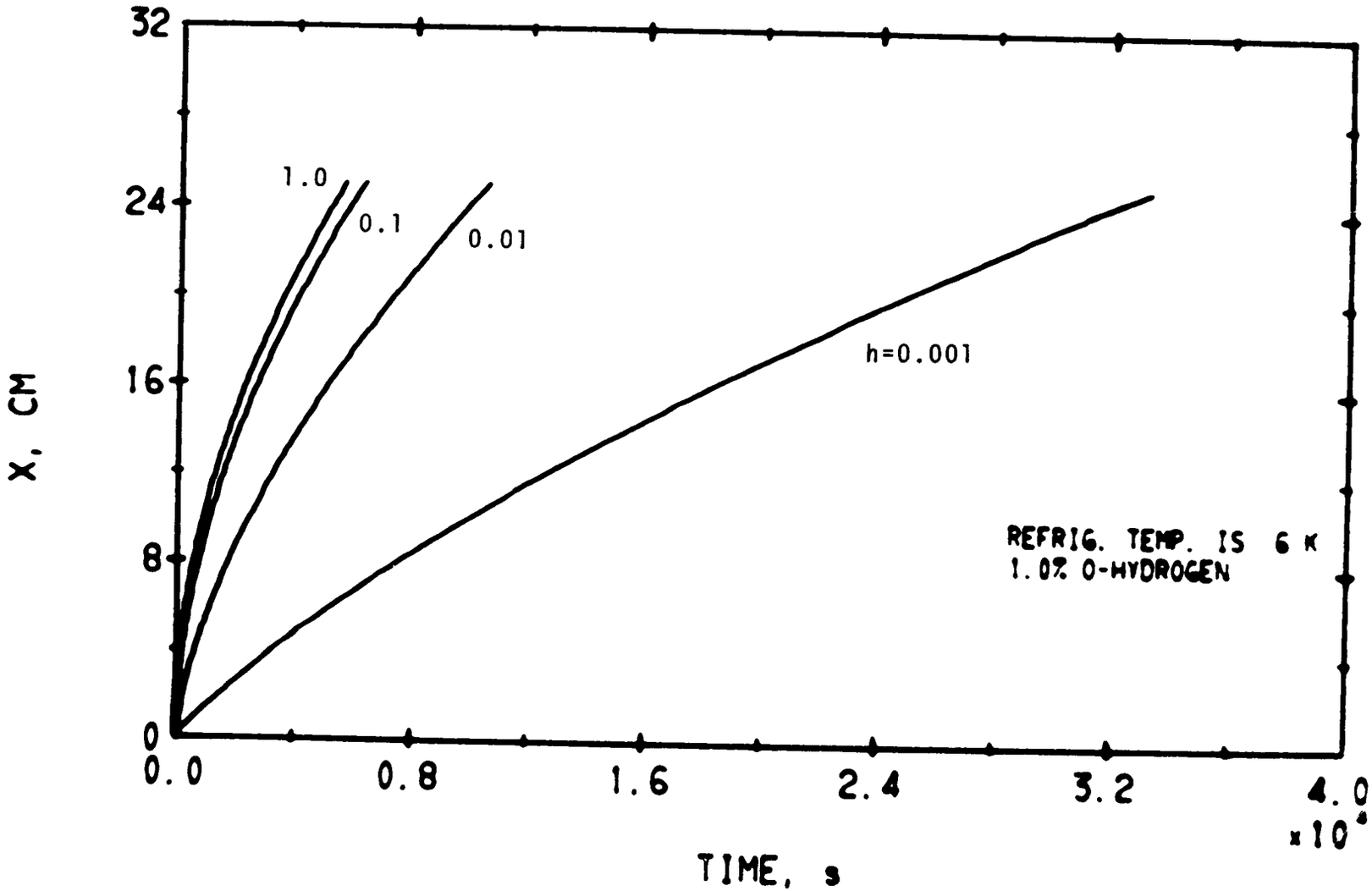

01/15/72

LINEAR FREEZING

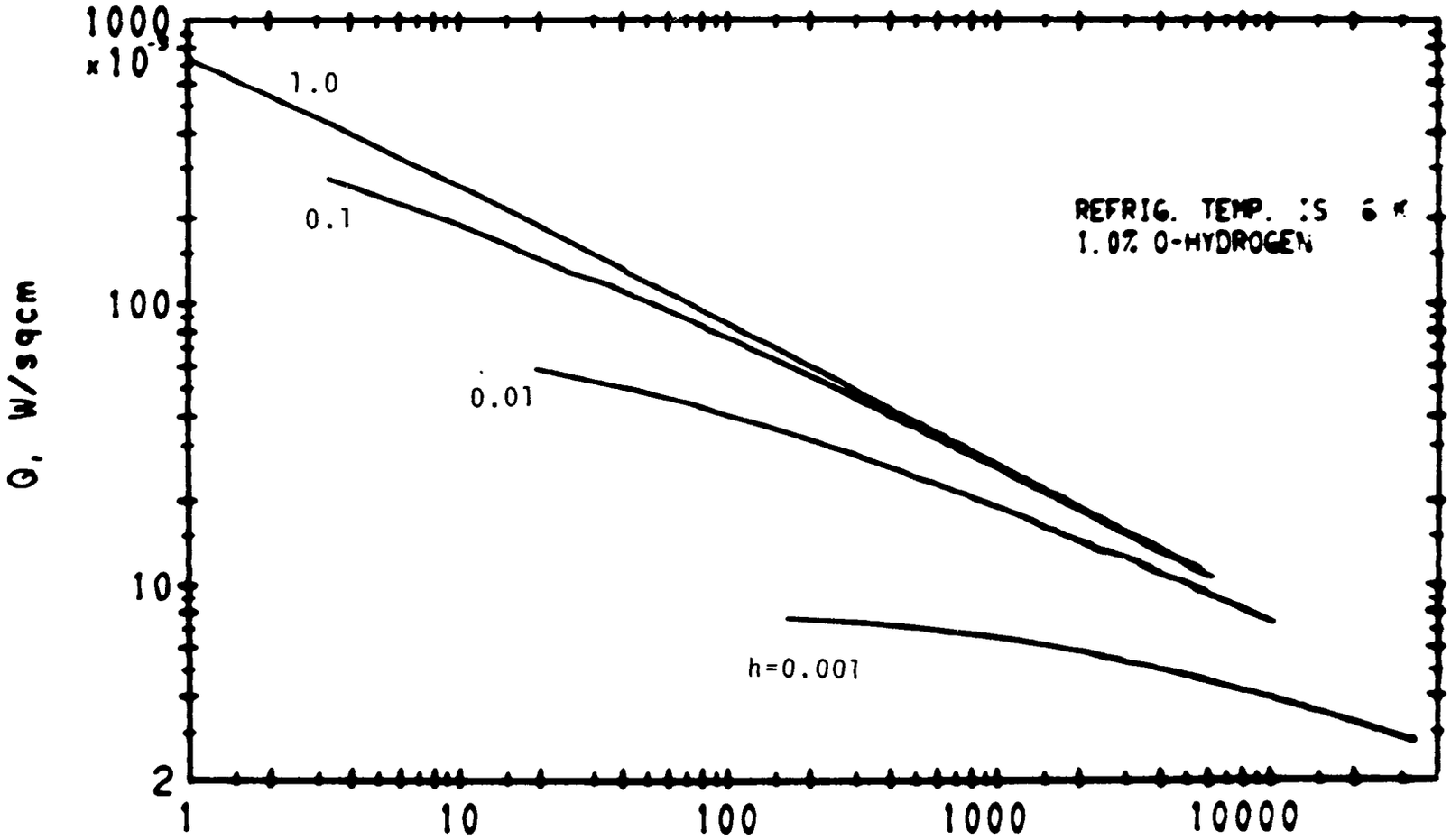

01/15/72

LINEAR FREEZING

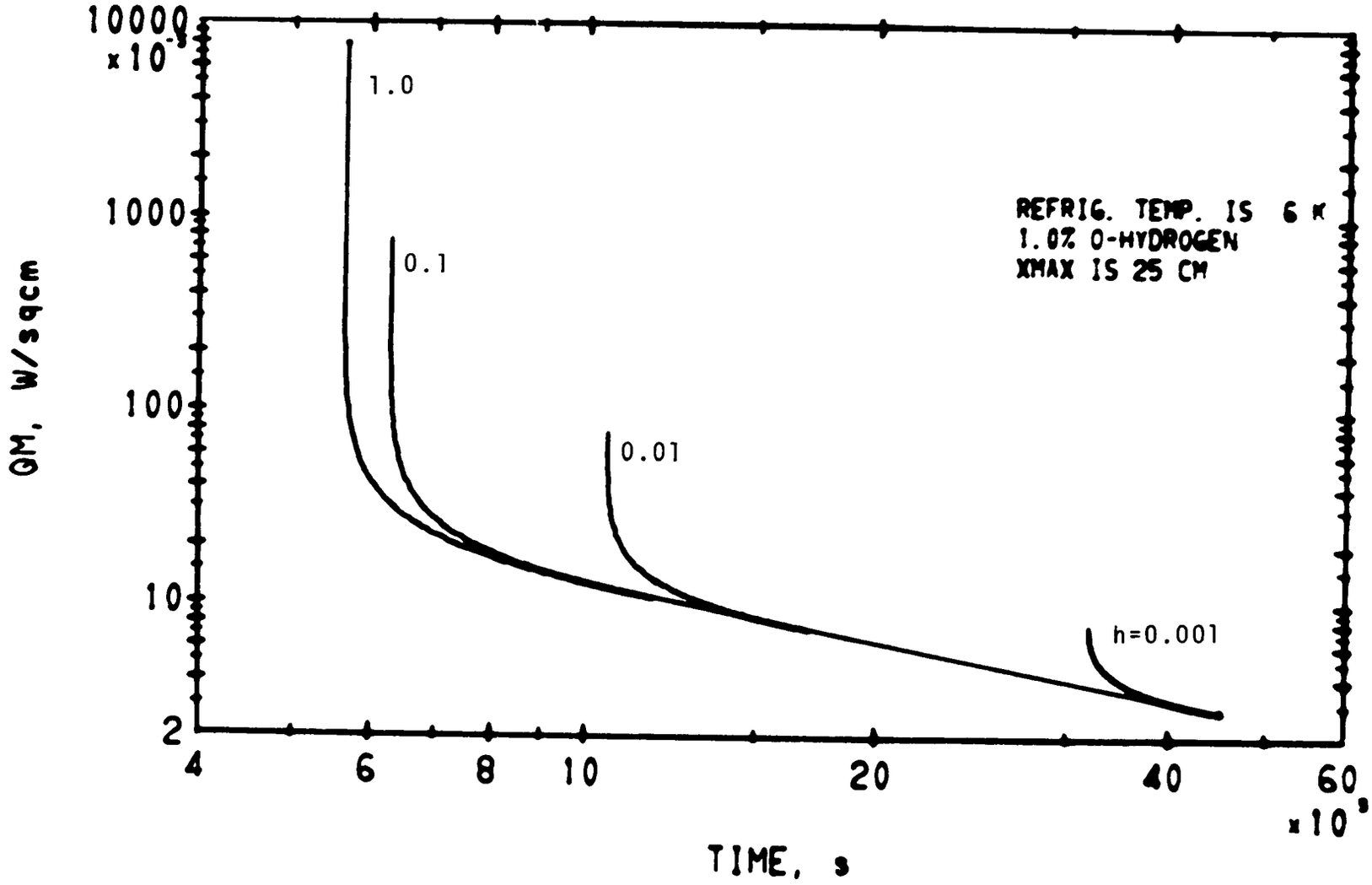

LINEAR FREEZING

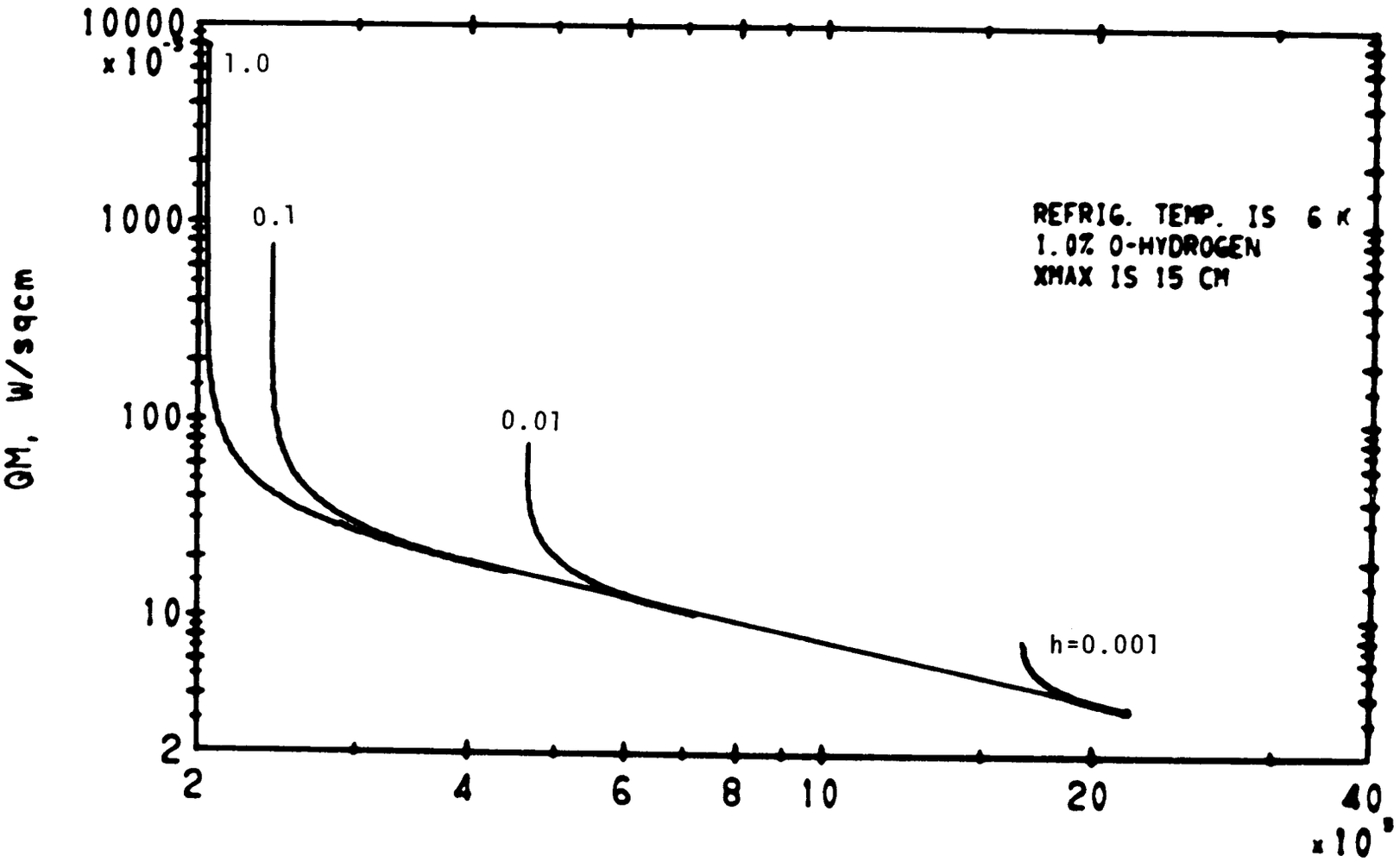

01/15/72

LINEAR FREEZING

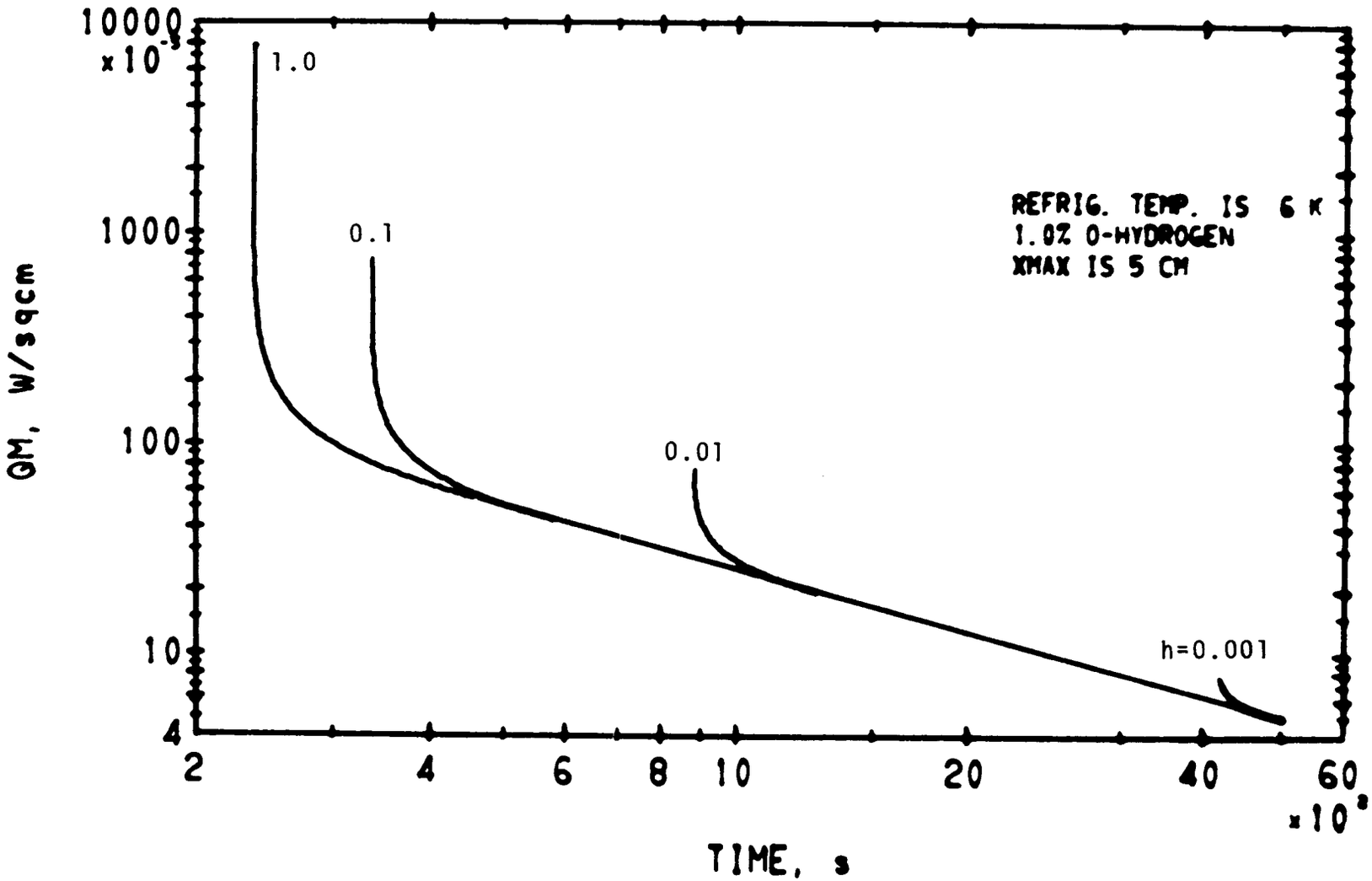

01/15/72

LINEAR FREEZING

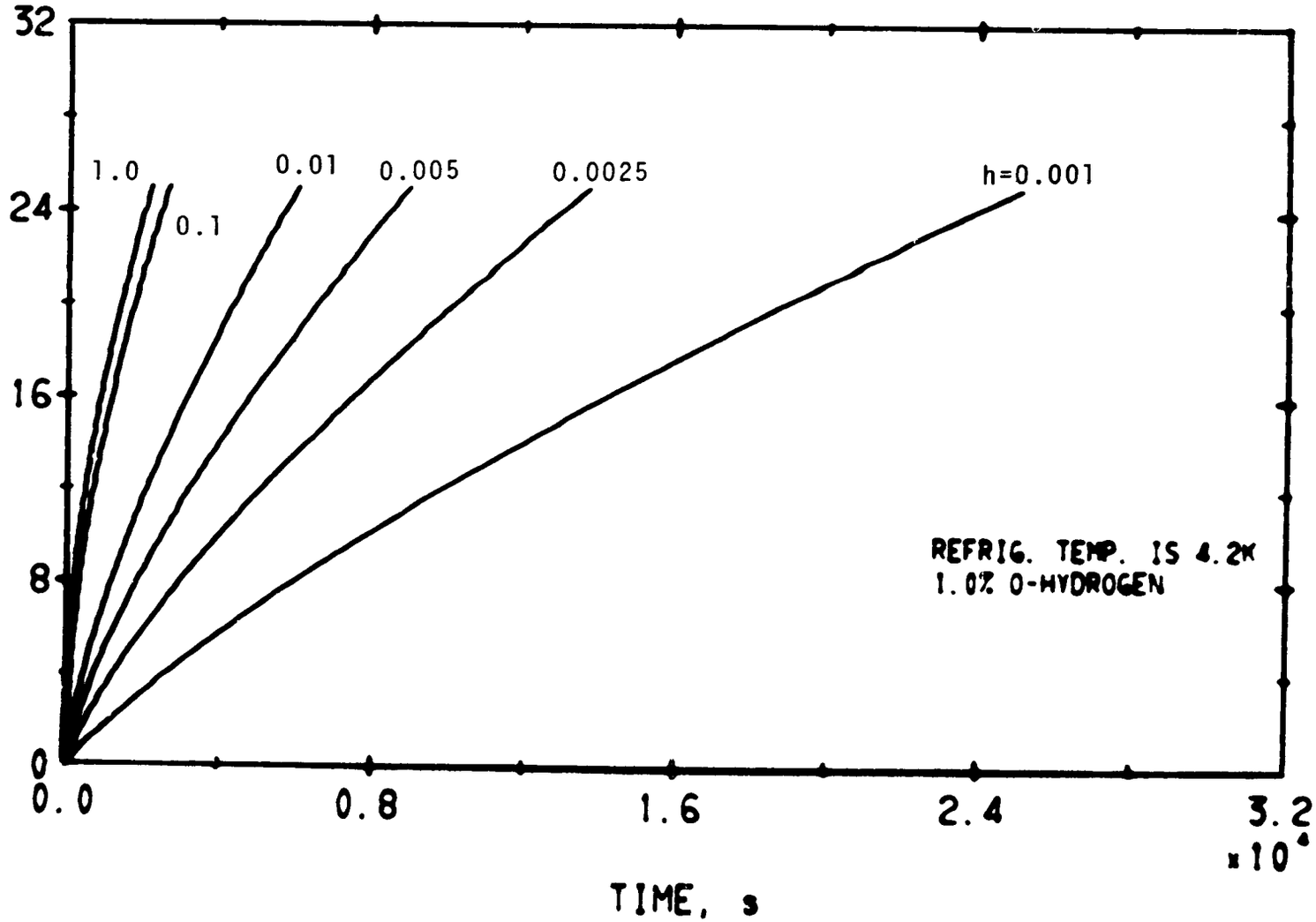

LINEAR FREEZING

01/18/72

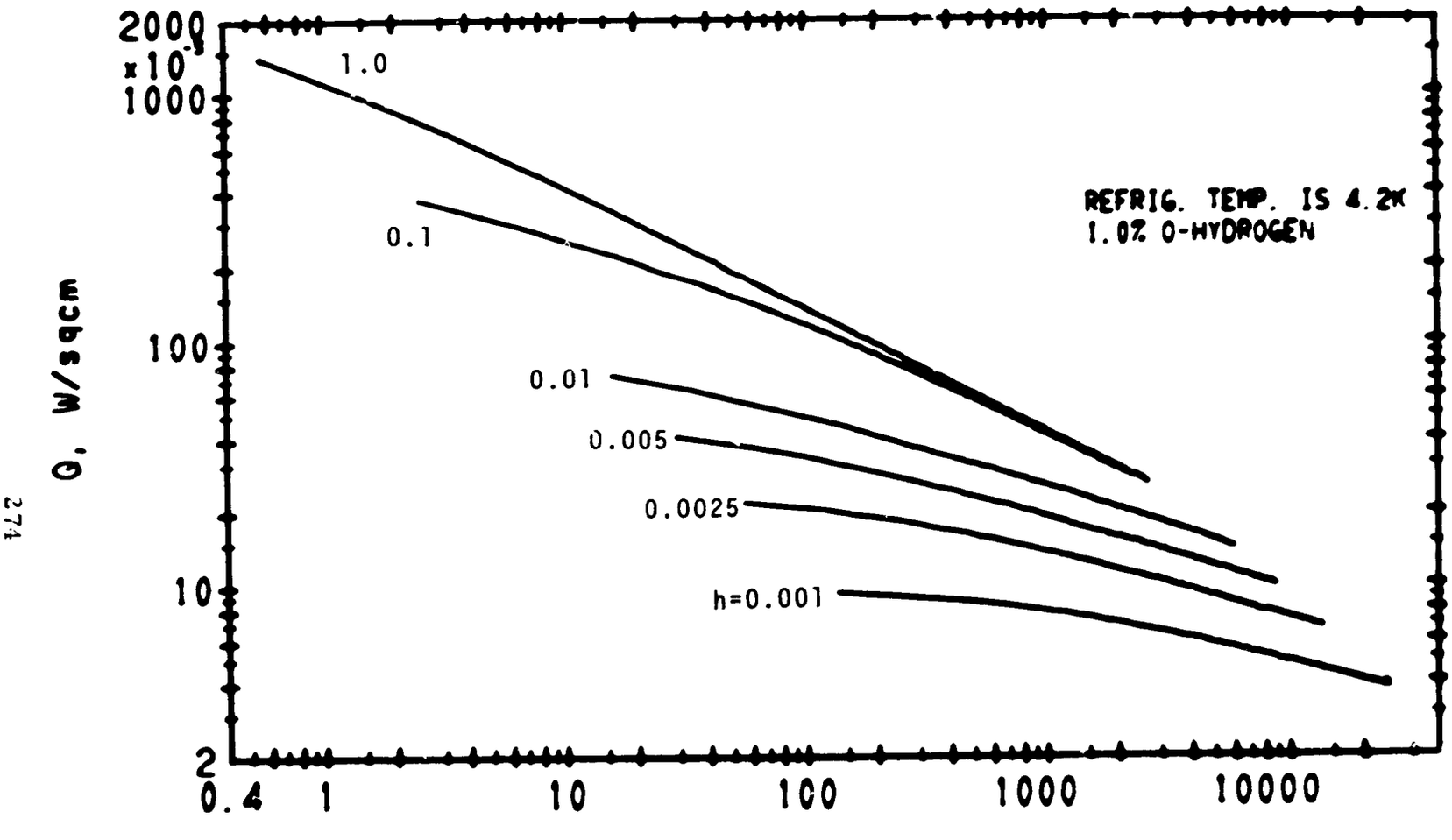

01/18/72

LINEAR FREEZING

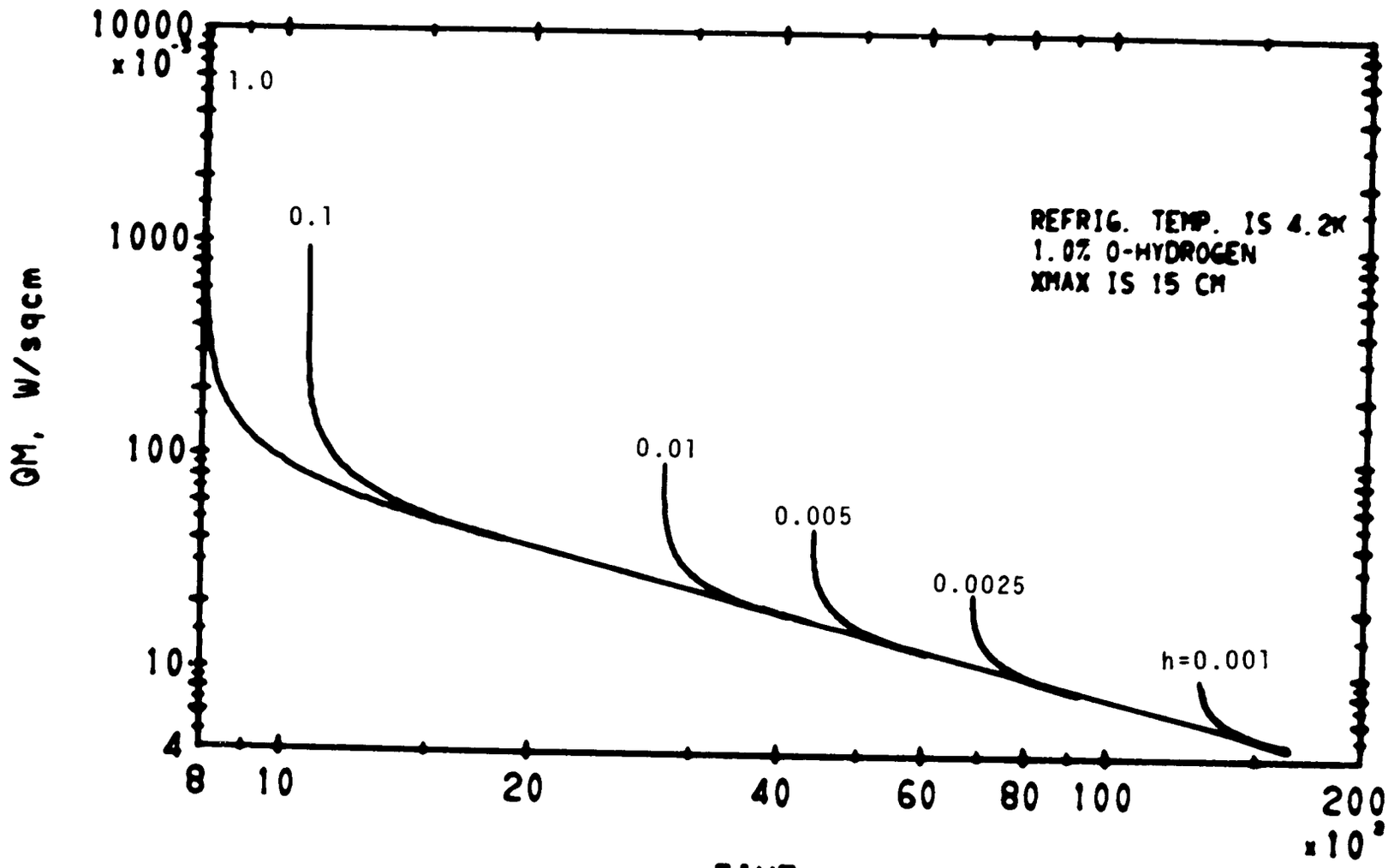

LINEAR FREEZING

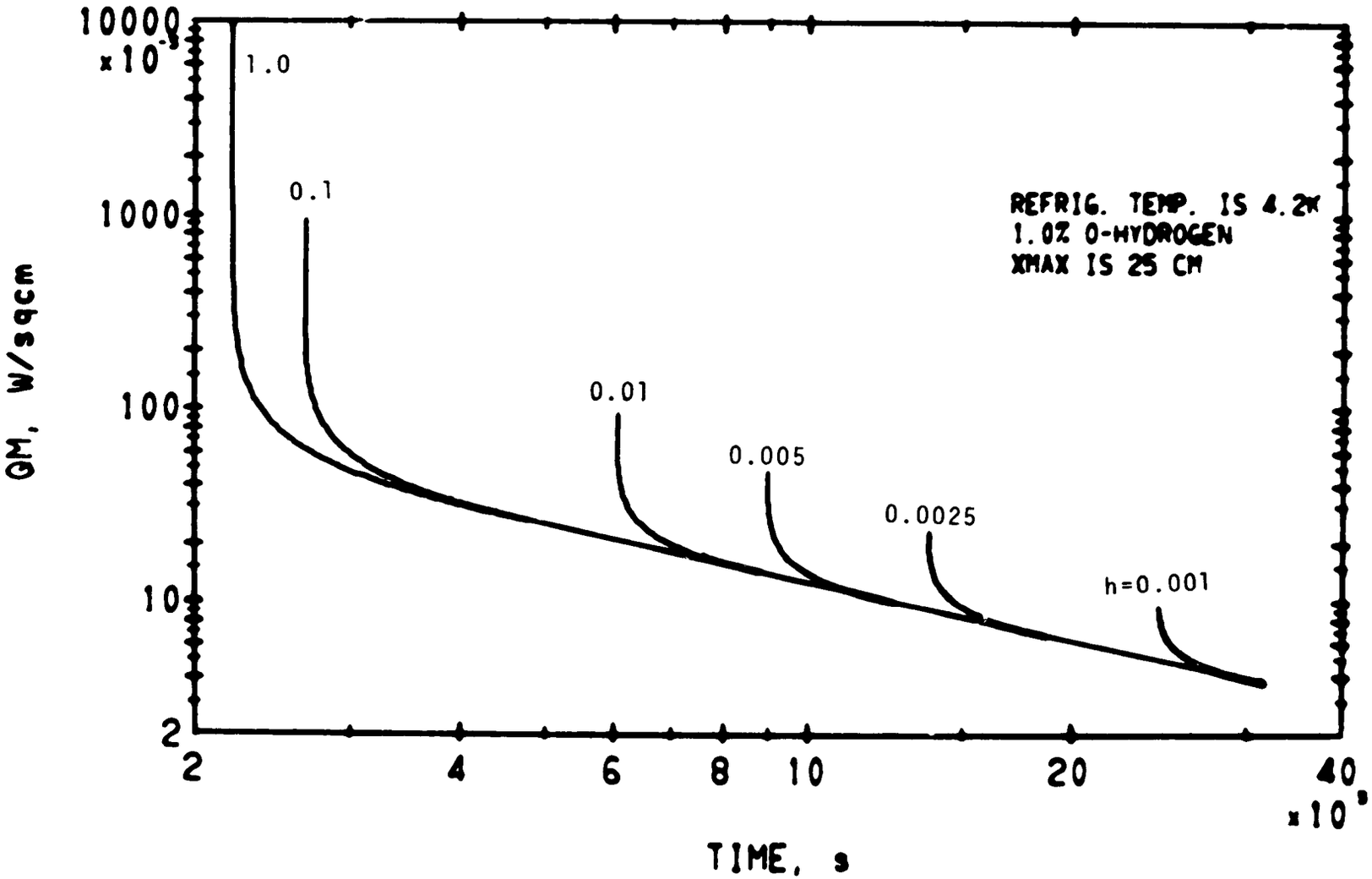

01/18/72

LINEAR FREEZING

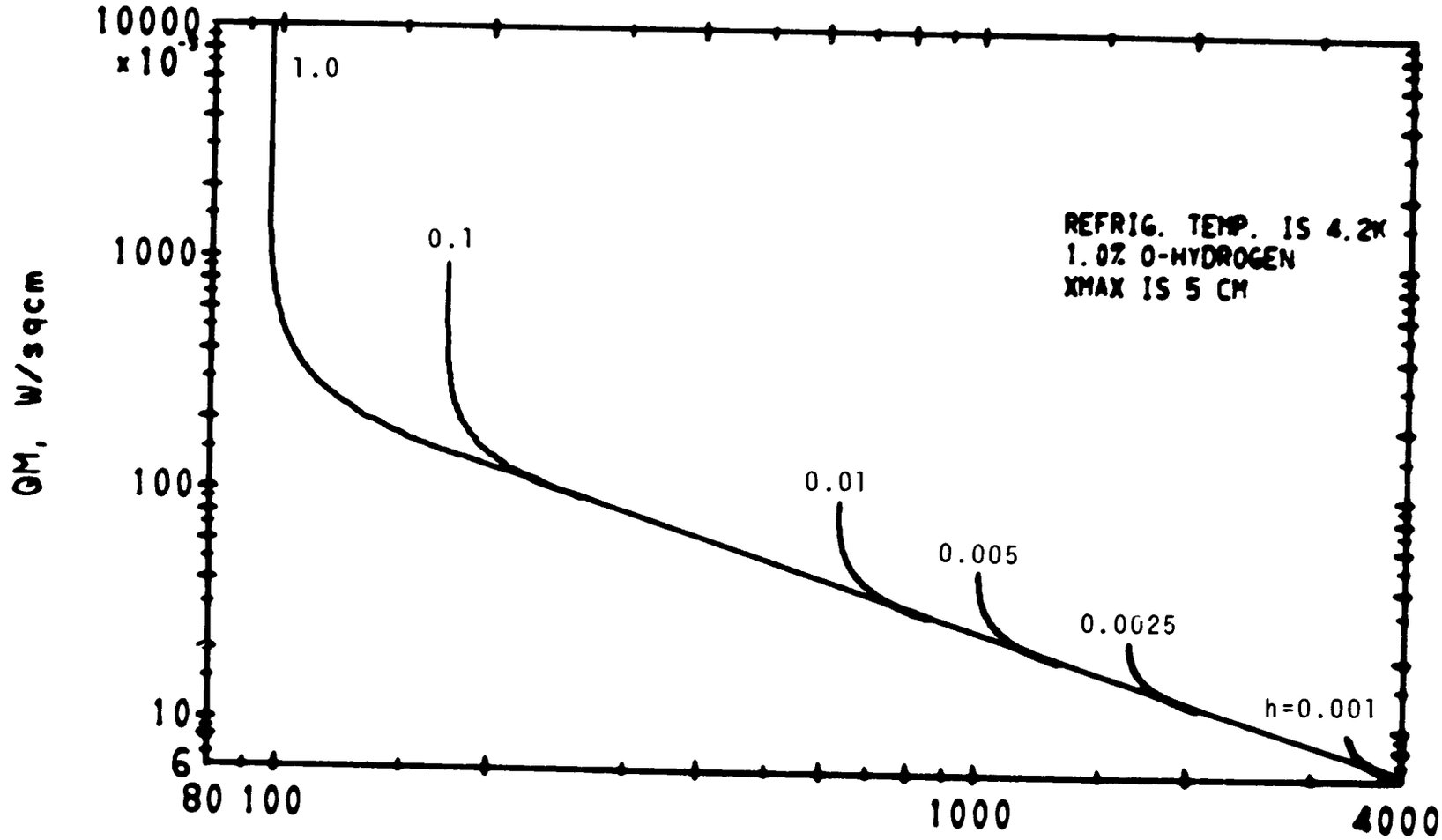

LINEAR FREEZING

01/18/72

END

DATE

FILMED

DEC 23 1974